

STATUS OF THESIS

Title of thesis

ENVIRONMENTAL LOAD FACTORS AND SYSTEM
STRENGTH EVALUATION OF JACKET PLATFORMS IN
OFFSHORE MALAYSIA

I ZAFARULLAH NIZAMANI

hereby allow my thesis to be placed at the information Resource Center (IRC) of Universiti Teknologi PETRONAS (UTP) with the following conditions:

1. The thesis becomes the property of UTP
2. The IRC of UTP may make copies of the thesis for academic purposes only.
3. This thesis is classified as

Confidential

Non-confidential

If the thesis is confidential, please state the reason:

The contents of the thesis will remain confidential for _____ years.

Remarks on disclosure:

Endorsed by

Signature of Author

Signature of Supervisor

Permanent address:

P.O.Tando Qaiser, Via Tando Jam,
District Hyderabad, Sindh, Pakistan.

Name of Supervisor

Prof. Dr.Kurian V. John

Date: _____

Date: _____

UNIVERSITI TEKNOLOGI PETRONAS

ENVIRONMENTAL LOAD FACTORS AND SYSTEM STRENGTH
EVALUATION OF JACKET PLATFORMS IN OFFSHORE MALAYSIA

by

ZAFARULLAH NIZAMANI

The undersigned certify that they have read, and recommend to the Postgraduate Studies Programme for acceptance this thesis for the fulfillment of the requirements for the degree stated.

Signature: _____

Main Supervisor: Professor. Dr.Kurian.V.John

Signature: _____

Co- Supervisor: Associate Professor Ir. Dr. Mohd Shahir Liew

Signature: _____

Head of Department: Associate Professor Ir. Dr. Mohd Shahir Liew

Date: _____

ENVIRONMENTAL LOAD FACTORS AND SYSTEM STRENGTH
EVALUATION OF JACKET PLATFORMS IN OFFSHORE MALAYSIA

by

ZAFARULLAH NIZAMANI

A Thesis

Submitted to the Postgraduate Studies Programme

as a Requirement for the Degree of

DOCTOR OF PHILOSOPHY

CIVIL ENGINEERING DEPARTMENT

UNIVERSITI TEKNOLOGI PETRONAS

BANDAR SRI ISKANDAR

PERAK

JUNE 2013

DECLARATION OF THESIS

Title of thesis

ENVIRONMENTAL LOAD FACTORS AND SYSTEM
STRENGTH EVALUATION OF JACKET PLATFORMS IN
OFFSHORE MALAYSIA

I ZAFARULLAH NIZAMANI

hereby declare that the thesis is based on my original work except for quotations and citations which have been duly acknowledged. I also declare that it has not been previously or concurrently submitted for any other degree at UTP or other institutions.

Witnessed by

Signature of Author

Signature of Supervisor

Permanent address:

P.O.Tando Qaiser, Via Tando Jam, District
Hyderabad, Sindh, Pakistan

Name of Supervisor

Professor Dr. Kurian V. John

Date : _____

Date : _____

DEDICATION

Thanks are first due to Allah almighty for his mercy, gift of knowledge and for making this degree possible.

Author dedicates this dissertation to:

The cherishing memory and Prayers of my Mother,

Support of my Father,

Sincere wishes of Brother & Sister,

Sacrifices of my wife & Sons.

ACKNOWLEDGEMENTS

This thesis has been made possible by Allah subhan hoo wa taala, the Most Gracious and the Most Merciful. I would like to thankfully acknowledge the guidance of Professor Dr. Kurian. V. John for his knowledge sharing and expert supervision which made this research possible. Thank are also due for guidance at critical juncture during my research to my co-supervisor Associate Professor Dr. Mohd. Shahir Liew. Sincere encouragement from Associate Professor Dr. Narayanan Sambu Potty, whose guidance at initial stage was very helpful in building basics of my research. The information shared by Dr. Paul Frieze of PAFA, Howard Lawes and Dr. R.V. Ahilan of GL Noble Denton, Che Wahab Abdullah is duly acknowledged. I would like to thank my colleagues Ir. M Mubarak B A Wahab and Nelson Julio Cossa who were encouraging and supportive during this period of trial. My deepest appreciation goes to Universiti Teknologi PETRONAS for its graduate assistantship scheme without this it would not have been possible for me to complete the study and acquire degree the ultimate aim.

ABSTRACT

API (WSD) and ISO 19902 (LRFD) codes are being used nowadays for design of Jacket platforms all over the world. ISO LRFD code is a probabilistic code which takes into account the uncertainties of material and loads and thus enables an economical design. This advantage is not available for API WSD code. The sustainable development of physical structures depend not only on reliability of structures but also on cost saving. Thus it is high time for Malaysia to adopt ISO code with local environmental load factors. ISO load factors are based on calibration of the Gulf of Mexico and North Sea environment. In this study, three offshore regions of Malaysia have been taken separately. The probabilistic uncertainty models for resistance and loads for local conditions were determined. Resistance uncertainty was evaluated using data collected from fabrication yard in Malaysia. Geometrical and material variations were statistically analysed from this data using probability distributions. Uncertainty model for nine component stresses and eleven joint stresses were analysed using MATLAB and statistical distributions. Environmental load uncertainty model included wave, wind and current parameters. The platform specific and regional data were used for the analysis. The extreme distributions i.e. Weibull and Gumbel were fitted for the analysis and their parameters were evaluated. SACS software was used to find the component stresses. Morrison equation was used for application of wave load and BOMEL and Heideman's equations were used to find the response from the stresses. Extreme conditions of 100 year loads were used to find the reliability. Seven code equations were used to find the component reliability. The member selection for reliability analysis was based on diameter, thickness and slenderness ratios. Component and joint reliability was found through FORM method of reliability using MATLAB code. Target reliability was based on API WSD code. Environmental Load Factor was selected based on reliability which was higher than the target reliability. Codes define three types of Joints, K, T/Y and X in Jacket platforms. Environmental load factor of 1.25 is proposed for components and 1.27 is proposed for joints in this study for offshore Malaysia as compared to 1.35 recommended by ISO 19902 and API LRFD codes. Codes use component and joint based environmental load factors only. It was found necessary to evaluate the system

based approach for the load factor. ISO requires that to assess the strength of structure for extension of life, change in load or resistance of Jacket, 10,000 year load should be applied and Jacket strength evaluated. API and ISO code require that they should be checked against probability of failure of 10^{-4} . Here, the probability of failure was determined and it was updated by applying the Bayesian updating technique.

ABSTRAK

Kod API (WSD) dan ISO 19902 (LRFD) adalah digunapakai pada masa kini di serata dunia untuk rekabentuk struktur Jacket. Kod ISO LRFD adalah kod kebarangkalian yang mengambilkira ketidaktentuan bahan dan beban dan dengan itu membolehkan reka bentuk yang ekonomi. Kelebihan ini tidak didapati pada kod API WSD. Pembangunan mampan struktur fizikal bergantung bukan sahaja kepada kebolehpercayaan struktur tetapi juga pada penjimatan kos. Oleh itu, sudah tiba masanya bagi Malaysia untuk menerima pakai kod ISO dengan faktor beban alam sekitar tempatan. Faktor beban ISO adalah berdasarkan penentukuran Teluk Mexico dan persekitaran Laut Utara. Dalam kajian ini, tiga kawasan luar pesisir pantai Malaysia telah diambilkira secara berasingan. Model ketidakpastian kebarangkalian untuk rintangan dan beban untuk keadaan tempatan telah ditentukan. Ketidakpastian rintangan telah dinilai menggunakan data yang dikumpul dari kawasan fabrikasi di Malaysia. Variasi geometri dan bahan telah dianalisa secara statistik daripada data ini menggunakan taburan kebarangkalian. Model ketidakpastian untuk sembilan tegasan komponen dan sebelas tegasan sendi telah dianalisa menggunakan MATLAB dan pengagihan statistik. Model ketidakpastian beban alam sekitar adalah termasuk parameter ombak, angin dan arus. Data platform tertentu dan serantau telah digunakan untuk analisis. Pengagihan melampau iaitu Weibull dan Gumbel telah digunakan untuk analisis dan parameter masing-masing telah dinilai. Perisian SACS telah digunakan untuk mencari tegasan komponen. Persamaan Morrison telah digunakan untuk aplikasi beban ombak dan persamaan BOMEL dan Heideman telah digunakan untuk mencari tindakbalas dari tegasan. Keadaan Terlampau dari beban 100 tahun telah digunakan untuk mencari kebolehpercayaan. Tujuh persamaan kod telah digunakan untuk mencari kebolehpercayaan komponen. Pemilihan ahli komponen untuk analisis kebolehpercayaan adalah berdasarkan kepada diameter, ketebalan dan

nisbah kelangsingan. Kebolehpercayaan komponen dan sendi telah didapati melalui kaedah kebolehpercayaan FORM menggunakan kod MATLAB. Kebolehpercayaan Sasaran adalah berdasarkan kepada kod API WSD. Faktor alam sekitar telah dipilih berdasarkan kebolehpercayaan yang lebih tinggi daripada kebolehpercayaan sasaran. Kod menentukan tiga jenis sendi, iaitu K, T / Y dan X di platform Jaket. Faktor beban alam sekitar sebanyak 1.25 dan 1.27 adalah dicadangkan bagi komponen dan sendi, masing-masing, dalam penyelidikan ini untuk luar pesisir Malaysia, berbanding dengan 1.35 yang disyorkan oleh Kod ISO 19902 dan API LRFD. Kod menggunakan faktor beban alam sekitar berasaskan komponen dan sendi sahaja. Telah didapati ada keperluan untuk menilai pendekatan berasaskan sistem untuk faktor beban. ISO menekankan bahawa untuk menilai kekuatan struktur bagi lanjutan usia, perubahan dalam beban atau rintangan Jaket, beban 10,000 tahun hendaklah digunakan dan kekuatan Jaket dinilai. Kod API dan ISO menghendaki supaya ianya perlu diperiksa terhadap kebarangkalian kegagalan pada 10^{-4} . Di sini, kebarangkalian kegagalan telah ditentukan dan ianya telah dikemaskini dengan menggunakan Teknik Bayesian Updating.

In compliance with the terms of the Copyright Act 1987 and the IP Policy of the university, the copyright of this thesis has been reassigned by the author to the legal entity of the university,

Institute of Technology PETRONAS Sdn Bhd

Due acknowledgement shall always be made of the use of any material contained in, or derived from, this thesis.

© ZAFARULLAH NIZAMANI, 2013

Institute of Technology PETRONAS Sdn Bhd

All rights reserved

TABLE OF CONTENTS

DECLARATION OF THESIS	iv
DEDICATION.....	v
ACKNOWLEDGEMENTS	vi
ABSTRACT	vii
ABSTRAK	ix
LIST OF TABLES	xxii
LIST OF FIGURES	xxvii
DEFINITIONS	xlii
NOTATIONS	xliii
LIST OF ABBREVIATION.....	xlix
CHAPTER 1 INTRODUCTION.....	1
1.1 Introduction	1
1.2 Overview	2
1.3 Problem Statement	3
1.3.1 Problem Background.....	4
1.3.2 Problem Motivation.....	6
1.3.3 Problem Description.....	6
1.3.4 Previous Work and Limitation of Existing Studies.....	7
1.3.5 Justification of the Research	7
1.4 Aim and Scope of the Present Work.....	8
1.4.1 Research Objectives	9
1.4.2 Limitations	10
1.4.3 Key Assumptions	10
1.5 Design Philosophy	12
1.5.1 Research Methodology	13
1.5.2 Critical Appraisal	14
1.6 Originality and Research Contributions.....	15
1.7 Outline of the Thesis	16
CHAPTER 2 LITERATURE REVIEW	18
2.1 Introduction	18
2.2 History of Code Development.....	19
2.2.1 History of Offshore Oil Production.....	19

2.3	LRFD and WSD Codes of Practice.....	20
2.3.1	API RP2A- WSD.....	20
2.3.2	API RP2A- LRFD / ISO 19902.....	22
2.3.3	Benefits of Limit State Design Code	23
2.3.4	Safety Factor.....	24
2.3.5	Jacket Platform Design in Malaysia	25
2.4	Uncertainty.....	25
2.4.1	Basic Uncertainty.....	26
2.4.2	Sources of Uncertainty.....	28
2.4.2.1	Natural.....	28
2.4.2.2	Statistical Uncertainty	28
2.4.2.3	Human Mistakes	28
2.4.3	Parameters of Uncertainty.....	29
2.4.3.1	Random Variables.....	29
2.4.3.2	Bias	29
2.4.3.3	Return Period	30
2.4.3.4	Distribution Types	30
2.4.4	Types of Resistance Uncertainty	30
2.4.4.1	Geometrical and Material	30
2.4.4.2	Physical Stress Model	31
2.5	Previous Work Done on Resistance Uncertainty	32
2.5.1	Material Uncertainty	34
2.5.2	Characteristic Resistance	34
2.5.3	Geometric Uncertainty.....	34
2.5.4	Resistance Model Uncertainty.....	35
2.5.4.1	Single Stresses	35
2.5.4.2	Double Stresses.....	36
2.5.4.3	Three Stresses	36
2.5.5	Critical Review of Resistance Uncertainty	36
2.6	Load Uncertainty.....	37
2.6.1	Load Uncertainty Parameters	37
2.6.1.1	Characteristic Load	37
2.6.1.2	Return Period Probability	38
2.6.2	Statistical Data Uncertainty for Environmental Load.....	38

2.6.2.1	Collection of Data	40
2.6.2.2	Weibull Distribution	41
2.6.2.3	Gumbel Distribution	41
2.6.2.4	Wave	42
2.6.2.5	Current	42
2.6.2.6	Wind	43
2.6.2.7	Environmental Load Modelling Uncertainty	44
2.6.3	Environmental Load Modelling of Jacket Response.....	44
2.6.3.1	Environmental Load Uncertainty Model	44
2.6.4	Dead Load.....	45
2.6.5	Live Load.....	45
2.7	Critical Analysis of Load Uncertainty	45
2.8	Structural Reliability	46
2.8.1	Reliability Levels	47
2.8.2	Parameters of Structural Reliability	48
2.8.2.1	Limit State.....	48
2.8.2.2	Reliability Index	48
2.8.2.3	Probability of Failure.....	50
2.8.2.4	Target Reliability.....	51
2.8.3	Review of Structural Reliability Methods	53
2.8.3.1	First Order Second Moment (FOSM) Method	54
2.8.3.2	First Order Reliability Method (FORM).....	54
2.8.3.3	Simulation Techniques like Monte Carlo Simulation (MCS)	55
2.9	Component Reliability and Previous Work.....	56
2.9.1	Resistance Factor.....	57
2.9.2	Component Reliability Index-Critical Review	57
2.10	Joint Reliability and Previous Work.....	57
2.10.1	Joint Reliability Index- Critical Review	58
2.11	Reliability and Environmental Load Factor	58
2.11.1	Code Calibration	60
2.12	Non-Linear Collapse Analysis.....	60
2.13	System Reliability and Reserve Strength Ratio (RSR)	61
2.13.1	Previous Work on System Reliability and Load Factors.....	63
2.13.2	System Based Environmental Load Factor-Critical Review	64

2.14	Assessment of Jacket	64
2.14.1	Bayesian Updating and Probability of Failure	65
2.14.2	Damaged Structural Members.....	67
2.14.3	Critical Review of Updating of Probability of Failure	67
2.15	Chapter Summary.....	67
CHAPTER 3 RESEARCH METHODOLOGY.....		68
3.1	Introduction.....	68
3.2	Resistance Uncertainty	69
3.2.1	Collection of Data for Resistance Parameters	70
3.2.2	Statistical Analysis of Geometric and Material Variables	72
3.2.2.1	Resistance Variables taken from Literature.....	73
3.2.3	Component and Joint Stress Model Uncertainty	74
3.2.3.1	Case Study: Axial Tension Model Uncertainty	76
3.3	Load Uncertainty.....	77
3.3.1	ISO and Metocean Criteria.....	77
3.3.1.1	Method 1	78
3.3.1.2	Method 2	78
3.3.1.3	Method 3	78
3.3.2	Environmental Load Uncertainty Parameters	79
3.3.2.1	Climate	79
3.3.2.2	Design Wave.....	80
3.3.2.3	Current.....	81
3.3.2.4	Wind.....	81
3.3.3	Data Collection for Environmental Load Parameters	82
3.3.4	Statistical Analysis of Environmental Load Parameters.....	82
3.3.4.1	Extrapolation of Wave, Wind and Current	83
3.3.5	Weibull Distribution	83
3.3.5.1	Extrapolation of Significant Wave Height (Weibull Distribution): Case Study of PMO Platform.....	83
3.3.5.2	Weibull Shape Factor.....	84
3.3.5.3	Weibull Scale Factor	85
3.3.5.4	Weibull Mean	85
3.3.5.5	Weibull Standard Deviation	85
3.3.6	Gumbel Distribution	86

3.3.6.1	Extrapolation of Significant Wave Height (Gumbel Distribution): Case Study of PMO Platform	86
3.3.6.2	Gumbel Scale Parameter.....	87
3.3.6.3	Gumbel Location Parameter	87
3.3.6.4	Gumbel Mean.....	87
3.3.6.5	Gumbel Standard Deviation.....	87
3.3.7	Environmental Load for SACS	88
3.3.7.1	SACS Modelling of Jacket.....	88
3.4	Structural Reliability	89
3.4.1	FORM.....	91
3.4.1.1	First Order Second Moment Method (FOSM)	91
3.4.1.2	Hasofer and Lind Reliability Index	92
3.4.1.3	Hasofer- Lind and Rackwitz- Fiessler Method (HL-RF).....	94
3.4.2	Monte Carlo Simulations for Determination of Probability of Failure	95
3.4.3	Selection of Jacket Platforms for Reliability Analysis.....	96
3.4.4	SACS Analysis.....	99
3.4.5	Load Ratios	99
3.4.6	Soil Conditions Effect on Component and Joint.....	100
3.5	Component Reliability	101
3.5.1	Single Stresses Case Study: Axial Tension	104
3.6	Joint Reliability.....	105
3.6.1	Target Reliability.....	105
3.7	Environmental Load Factor.....	106
3.8	Resistance Factor	106
3.9	System Reliability Based Environmental Loads	107
3.9.1	SACS Collapse Module.....	107
3.9.2	Collapse Analysis of Jacket	109
3.9.3	SACS Jacket Model for Push Over Analysis.....	109
3.9.4	SACS Jacket Model for Push Over Analysis.....	110
3.9.5	Wave and Current Loads in Malaysia	111
3.9.6	Curve Fitting	112
3.9.7	Safety Factor for Jacket System: API WSD and ISO 19902.....	113

3.9.8	Limit State Function for System Environmental Loading	115
3.9.9	Target System Probability of Failure.....	115
3.10	System Based Environmental Load Factor.....	116
3.11	Assessment of Jacket Platform	116
3.11.1	Uncertainty Model for Resistance and Load.....	117
3.11.2	Bayesian Updating of Probability of Failure-Intact Structure.....	119
3.11.3	Bayesian Updating of Probability of Failure-Damaged Structure...	121
3.12	Chapter Summary.....	121
CHAPTER 4 UNCERTAINTY MODELLING OF RESISTANCE AND LOAD ..		122
4.1	Introduction.....	122
4.2	Load Factor and Uncertainty	123
4.3	Resistance Uncertainty	123
4.4	Statistical Properties of Fundamental Variable for Resistance.....	123
4.4.1	Geometric Properties	124
4.4.2	Material Properties.....	128
4.5	Probabilistic Model Stresses used in ISO Code 19902	130
4.5.1	Component Stresses.....	131
4.5.1.1	Single Stresses	131
4.5.1.2	Two Stresses	135
4.5.1.3	Three Stresses	137
4.5.2	Joint Stresses	139
4.5.2.1	K- Joint.....	140
4.5.2.2	T/Y - Joint	142
4.5.2.3	X- Joint.....	144
4.6	Load Uncertainty.....	147
4.6.1	Wave Load Models	148
4.6.1.1	PMO Region.....	149
4.6.1.2	SBO Region.....	151
4.6.1.3	SKO Region.....	153
4.6.1.4	GULF OF MEXICO (GOM) and NORTH SEA (NS).....	155
4.6.2	Wind load model.....	157
4.6.2.1	PMO Region.....	158
4.6.2.2	SBO Region.....	160
4.6.2.3	SKO Region.....	162

4.6.2.4	GULF OF MEXICO (GOM) and NORTH SEA (NS)	164
4.6.3	Current Load Model	166
4.6.3.1	PMO Region	166
4.6.3.2	SBO Region	169
4.6.3.3	SKO Region	170
4.6.3.4	GULF OF MEXICO (GOM) and NORTH SEA (NS)	172
4.7	Chapter Summary	174
CHAPTER 5 COMPONENT RELIABILITY AND ENVIRONMENTAL LOAD		
FACTOR	176
5.1	Introduction	176
5.2	Selection of Members	176
5.3	Component Target Reliability	177
5.4	Component Reliability Analysis	178
5.4.1	Code Stresses	178
5.4.1.1	Single Stresses	179
5.4.1.2	Combined Two Stresses	181
5.4.1.3	Combined Three Stresses	183
5.4.2	Sensitivity Analysis	184
5.4.3	Effect of Variation of Environmental Load Factor	185
5.4.4	Effect of Column Slenderness Ratio	189
5.4.5	Calibration Points for Jackets	190
5.4.6	Selection of Environmental Load Factor	192
5.4.7	PMO Platform	192
5.4.8	SBO Platform	195
5.4.9	SKO Region	198
5.4.9.1	SKO1 Platform	198
5.4.9.2	SKO2 Platform	201
5.5	All Regions and all Components Combined Result	204
5.6	Resistance Factor	205
5.6.1	Axial Tension	206
5.6.2	Axial Compression	206
5.7	Chapter Summary	207

CHAPTER 6 JOINT RELIABILITY ANALYSIS AND ENVIRONMENTAL LOAD	
FACTOR.....	209
6.1 Introduction.....	209
6.2 Selection of Joints	209
6.2.1 K- Joints	210
6.2.2 T/Y Joints	212
6.2.3 X- Joints	214
6.3 Beta Factor (β) Effects (d/D) on Reliability Index.....	217
6.3.1 K- Joints	217
6.3.2 T/Y Joints	218
6.3.3 X- Joints	220
6.4 Gamma Factor (γ) Effects (D/2T)	222
6.4.1 K- Joints: Tension / Compression.....	223
6.4.2 T/Y Joints	224
6.4.3 X- Joints	226
6.5 Variation of Environmental Load Factor.....	228
6.6 Calibration of API (WSD) and ISO (LRFD) Reliability Index	230
6.7 Environmental Load Factor	232
6.7.1 PMO Region Platform	232
6.7.2 SBO Region Platform	235
6.7.3 SKO Region	237
6.7.3.1 SKO1 Platform	237
6.7.3.2 SKO 2 Platform	239
6.8 All Regions and all Joints Combined Result	241
6.9 Chapter Summary.....	243
CHAPTER 7 SYSTEM RELIABILITY BASED ENVIRONMENTAL LOADING	
AND EXTENSION OF LIFE OF JACKET PLATFORMS	244
7.1 Introduction.....	244
7.2 System Strength Reliability	245
7.2.1 Wave and Current	245
7.2.2 Curve Fitting.....	248
7.2.3 Selection of RSR for Jackets in Malaysia	252
7.3 System Environmental Load Factor	254

7.4	Collapse Analysis of Jacket.....	265
7.4.1	Wave Effect on Collapse Load	265
7.4.2	Directional base shear.....	268
7.4.3	Wave Directional Effects on Collapse Base Shear	270
7.4.4	System Redundancy	275
7.5	Updating the Probability of Failure	275
7.5.1	Sensitivity Analysis	275
7.5.1.1	Effect of Load Uncertainty Model.....	275
7.5.1.2	Probability of Failure and RSR Sensitivity.....	279
7.5.1.3	Effect of Model Uncertainty of Environmental Load on Probability of Failure	282
7.5.2	Bayesian Updating the Probability of Failure.....	285
7.5.3	Bayesian Updating Probability of Failure with Damaged Members.....	289
7.6	Chapter Summary	297
CHAPTER 8 CONCLUSIONS AND RECOMMENDATIONS.....		299
8.1	Summary	299
8.1.1	Uncertainty.....	299
8.1.1.1	(a) Resistance Uncertainty	299
8.1.1.2	(b) Environmental Load Uncertainty.....	300
8.1.2	Load Factors.....	300
8.1.2.1	Component Reliability and Environmental Load Factor	300
8.1.2.2	Joint Reliability and Joint based Environmental Load Factor.....	301
8.1.2.3	System Based Environmental Load Factor	301
8.1.3	Bayesian Updating of Probability of Failure for Reassessment	302
8.2	Future Work.....	302
8.2.1	Time Variant Reliability	302
8.2.2	Accidental Limit State	303
8.2.3	Operational Condition Reliability	303
8.2.4	Structural Reliability of Floaters	303
8.2.5	Environmental Load Parameter Modelling.....	303
8.2.6	Reassessment of Jacket.....	303
8.2.7	Bayesian Updating due to Change of Conditions	304
8.2.8	Reliability of Offshore Mooring Foundations:	304

REFERENCES.....	305
LIST OF PUBLICATIONS	317
APPENDIX A	321
APPENDIX B	325
APPENDIX C	327
APPENDIX D	343
APPENDIX E.....	344
APPENDIX F.....	348
APPENDIX G	351

LIST OF TABLES

Table 1.1: Load factors used for Calculating the Internal Forces.....	4
Table 1.2: Environmental Load Factors	15
Table 2.1: Uncertainties in Model Predictions	31
Table 2.2: Model Uncertainty for Mediterranean Sea using API WSD 18 ED.....	32
Table 2.3: Resistance Uncertainties for Jacket Platforms	33
Table 2.4: Probability of Failure and Reliability Index Relationship	49
Table 2.5: Indicative Target Reliability	52
Table 2.6: Probability of Failure Recommended for NS Jackets	52
Table 3.1: Details of Selected Platforms for Resistance Uncertainty	70
Table 3.2: Variability of Material Properties as shown in as Mill Test Report.....	71
Table 3.3: Statistical Parameters taken from Literature.....	73
Table 3.4: Water Depths ranges for Platforms in Malaysia	80
Table 3.5: Maximum and Critical Values of Significant Wave Height.....	80
Table 3.6: Ratio of H_{max} / H_s for Platforms in Offshore Malaysia & GOM.....	81
Table 3.7: Current at Surface (Maximum / Critical Directions).....	81
Table 3.8: Variation of Wind Speed in Platform at Specific Locations.....	82
Table 3.9: Environmental Load Parameters (Wind, Wave & Current),.....	83
Table 3.10: Cumulative Distribution Function (CDF)-Weibull Distributions	84
Table 3.11: Cumulative Distribution Function (CDF)-Gumbel Distributions	86
Table 3.12: Platform-Weibull Distribution Parameters	88
Table 3.13: Details of Selected Platforms for Reliability Analysis	96
Table 3.14: Random Variable Used to Find the Reliability Index	97
Table 3.15: Dead, Live and Environmental Load Ratios	100

Table 3.16: Load Coefficients for K-Joint.....	101
Table 3.17: Load Coefficients for T/Y-Joint	101
Table 3.18: Load Coefficients for X-Joint.....	101
Table 3.19: Geometry Groups for Component Reliability Analysis.....	102
Table 3.20: Geometry Groups for Joint Reliability Analysis	105
Table 3.21: Basic Details of Jackets Considered for System Analysis	110
Table 3.22: Uncertainty Factors used for Limit State Equation.....	117
Table 4.1: Angle Variations Measured Using Fig. 4.1	125
Table 4.2: Statistical Variation in Geometry of Tubular Component and Joints	126
Table 4.3: Statistical Variation in Yield Strength	129
Table 4.4: Resistance Model Uncertainty for Single Stress	132
Table 4.5: Resistance Model Uncertainty for Combined Two Stresses	136
Table 4.6: Resistance Model Uncertainty under Combined Three Stresses.....	138
Table 4.7: Resistance Model Uncertainties of K-Joint.....	140
Table 4.8: Resistance Model Uncertainties of T/Y - Joint Strength	142
Table 4.9: Resistance Model Uncertainties of X-Joint Strength.....	145
Table 4.10: Return Period and Significant Wave (m) -Weibull Distribution- PMO	150
Table 4.11: Return Period and Significant Wave (m)-Gumbel Distribution- PMO	151
Table 4.12: Return Period and Significant Wave (m)-Weibull Distribution- SBO	152
Table 4.13: Return Period and Significant Wave (m)-Gumbel Distribution- SBO	153
Table 4.14: Return Period and Significant Wave (m)-Weibull Distribution- SKO	154

Table 4.15: Return Period and Significant Wave (m), Gumbel Distribution at SKO	155
Table 4.16: Return Period and Significant Wave (m), Weibull at GOM and NS	156
Table 4.17: Return Period and Significant Wave (m), Gumbel at GOM and NS	157
Table 4.18: Return Period and Wind Speed (m/s), Weibull Distributions at PMO	158
Table 4.19: Return Period and Wind Speed (m/s), Gumbel Distribution at PMO	159
Table 4.20: Return Period and Wind Speed (m/s), Weibull Distribution at SBO	160
Table 4.21: Return Period and Wind Speed (m/s), Gumbel Distribution at SBO	161
Table 4.22: Return Period and Wind Speed (m/s), Weibull Distribution at SKO	162
Table 4.23: Return Period and Wind Speed (m/s), Gumbel Distribution at SKO	163
Table 4.24: Return Period and Wind Speed (m/s), Weibull at GOM and NS	164
Table 4.25: Return Period and Wind Speed (m/s), Gumbel at GOM and NS	165
Table 4.26: Return Period & Current Speed (m/s), Weibull Distribution at PMO	167
Table 4.27: Return Period & Current Speed (m/s), Gumbel Distribution at PMO	168
Table 4.28: Return Period & Current Speed (m/s), Weibull Distribution at SBO	169
Table 4.29: Return Period & Current Speed (m/s), Gumbel Distribution at SBO	170
Table 4.30: Return Period & Current Speed (m/s), Weibull Distribution at SKO	171
Table 4.31: Return Period & Current Speed (m/s), Gumbel Distribution at SKO	171

Table 4.32: Return Period & Current Speed (m/s), Weibull at GOM and NS....	172
Table 4.33: Return Period & Current Speed (m/s), Gumbel at GOM and NS....	173
Table 5.1: Member Selection for Calibration - Slenderness Ratio and d/t Ratio	177
Table 5.2: ISO Target Reliability	178
Table 5.3: Reliability Index against Different Environmental Load Factors.....	178
Table 5.4: Sensitivity Analysis of Random Variables Axial Tension.....	185
Table 5.5: Reliability Index for Jacket Members.....	190
Table 5.6: API (WSD) Target Reliability and ISO (LRFD) Reliability.....	205
Table 6.1 Joint Selected for Calibration	209
Table 6.2: ISO Reliability Index for K- Joints.....	211
Table 6.3: ISO Reliability Index for T/Y- Joints	214
Table 6.4: ISO Reliability Index for X- Joints.....	216
Table 6.5: Joints Reliability Index Under Stresses - ISO 19902 Code	230
Table 6.6: Joints Reliability Index Under Stresses - API RP2A WSD Code	231
Table 6.7: (WSD) Target Reliability and ISO (LRFD) Reliability for Joints	242
Table 7.1: Parameters of Wave and Current for System Reliability	251
Table 7.2: RSR and System Redundancy at Platform PMO.....	252
Table 7.3: RSR and System Redundancy at Platform SBO	252
Table 7.4: RSR and System Redundancy at Platform SKO1	253
Table 7.5: RSR and System Redundancy at Platform SKO2	253
Table 7.6: RSR and System Redundancy at Platform SKO2a.....	253
Table 7.7: Design and Updated Probability of Failure.....	286
Table 7.8: Reduced Capacity for PMO Jacket with Damaged Members.....	289
Table 7.9: Reduced Capacity for SBO Jacket with Damaged Members.....	290
Table 7.10: Reduced Capacity for SKO1 Jacket with Damaged Members.....	292

Table 7.11: Reduced Capacity for SKO2 Jacket with Damaged Members	294
Table 7.12: Reduced Capacity for SKO2a with Damaged Members	295
Table 7.13: Probability of Failure of Jacket with Damaged Members	297

LIST OF FIGURES

Figure 1.1: Wave Theory used in SACS for Analysis of Jacket Platform.....	12
Figure 1.2: Benefits of Standard Codes.....	13
Figure 2.1: Types of Uncertainties	25
Figure 2.2: Exceedance Probability Curve for Wave Height in GOM.....	27
Figure 2.3: Development of Storm growth, Peak and Decay	39
Figure 2.4: Straight Line Representation of Distribution Function.....	40
Figure 2.5: Normal Distribution of Load and Resistance.....	47
Figure 2.6: Relationship between Safety Index and Probability of Failure.....	49
Figure 2.7: Acceptance Criteria for Ductile Jacket Platform at Different Safety Levels.....	53
Figure 2.8: Variation of W_e/G ratio with Reliability Index for Axial Tension	59
Figure 2.9: Variation of Reliability Index with Varying W_e/G	60
Figure 2.10: System RSR with respect to W_e/G ratios for axial Compression at NS Jacket	63
Figure 2.11: Reliability Index against Environmental Load Factors	64
Figure 2.12: Bayesian Updating of Probability of Failure for Jacket at NS.....	66
Figure 3.1: Variability of Diameter	71
Figure 3.2: Fabrication yard in Malaysia.....	72
Figure 3.3: Flow chart for Resistance Model Uncertainty.....	75
Figure 3.4: Surface Fitting Validation for SBO Platform.....	89
Figure 3.5: Reliability Index due to Cornell Probability of Limit State.....	90
Figure 3.6: Reliability Index Representation	94
Figure 3.7: Representation of Failure Surface from X-Space to U-Space	94
Figure 3.8: Jacket Platform at PMO.....	97

Figure 3.9: Jacket Platform at SBO	98
Figure 3.10: Jacket Platform at SKO (SKO1)	98
Figure 3.11: Jacket Platform at SKO (SKO2)	99
Figure 3.12: Flow Chart for Component and joint Reliability	103
Figure 3.13: Flow Chart for System Reliability	113
Figure 3.14: Flow Chart for Finding Probability of Failure.....	118
Figure 3.15: Flow Chart for Bayesian updating of Probability of Failure	120
Figure 4.1: Angle Variations	124
Figure 4.2: Probability Density Function for Brace diameter < 1000 mm	126
Figure 4.3: Probability Density Function for Leg diameter > 1000 mm	127
Figure 4.4: Probability Density Function for Thickness Variation.....	127
Figure 4.5: Probability Density Function for Angle Variation.....	128
Figure 4.6: Probability Density Function for Yield Strength	129
Figure 4.7: Probability Density Function for Tensile Strength	130
Figure 4.8: Probability Density Function for Elongation.....	130
Figure 4.9: Probability Density Function for Tension	132
Figure 4.10: Probability Density Function for Column Buckling	133
Figure 4.11: Probability Density Function for Local Buckling.....	133
Figure 4.12: Probability Density Function for Bending.....	134
Figure 4.13: Probability Density Function for Shear	134
Figure 4.14: PDF for Hydrostatic Pressure (Hoop Buckling)	135
Figure 4.15: Probability Density Function for Tension and Bending.....	136
Figure 4.16: PDF for Compression and Bending (Column Buckling)	137
Figure 4.17: PDF for Compression and Bending (Local Buckling)	137
Figure 4.18: PDF for Tension, Bending and Hydrostatic Pressure.....	138

Figure 4.19: PDF for Compression, Bending and Hydrostatic Pressure (Column Buckling).....	139
Figure 4.20: PDF for Compression, Bending and Hydrostatic Pressure (Local Buckling).....	139
Figure 4.21: Probability Density Function-K-Joint Tension / Compression	141
Figure 4.22: Probability Density Function for K-Joint IPB.....	141
Figure 4.23: Probability Density Function for K-Joint OPB	142
Figure 4.24: Probability Density Function for T/Y-Joint Axial Tension	143
Figure 4.25: Probability Density Function for T/Y-Joint Axial Compression ...	143
Figure 4.26: Probability Density Function for T/Y-Joint IPB	144
Figure 4.27: Probability Density Function for T/Y-Joint OPB.....	144
Figure 4.28: Probability Density Function for X-Joint Axial tension.....	145
Figure 4.29: Probability Density Function for X-Joint Axial Compression.....	146
Figure 4.30: Probability Density Function for X-Joint IPB.....	146
Figure 4.31: Probability Density Function for X-Joint OPB	147
Figure 4.32: Extrapolation of Significant Wave Height (Weibull at PMO).....	150
Figure 4.33: Extrapolation of Significant Wave Height (Gumbel at PMO).....	151
Figure 4.34: Extrapolation of Significant Wave Height (Weibull at SBO).....	152
Figure 4.35: Extrapolation of Significant Wave Height (Gumbel at SBO).....	153
Figure 4.36: Extrapolation of Significant Wave Height (Weibull at SKO).....	154
Figure 4.37: Extrapolation of Significant Wave Height (Gumbel at SKO).....	155
Figure 4.38: Extrapolation of Significant Wave Height, Weibull- GOM and NS	156
Figure 4.39: Extrapolation of Significant Wave Height, Gumbel at GOM and NS	157
Figure 4.40: Extrapolation of Wind Speed -(Weibull at PMO).....	159

Figure 4.41: Extrapolation of Wind Speed -(Gumbel at PMO).....	160
Figure 4.42: Extrapolation of Wind Speed -(Weibull at SBO)	161
Figure 4.43: Extrapolation of Wind Speed -(Gumbel at SBO)	162
Figure 4.44: Extrapolation of Wind Speed -(Weibull at SKO)	163
Figure 4.45: Extrapolation of Wind Speed (Gumbel at SKO)	164
Figure 4.46: Extrapolation of wind speed -(Weibull at GOM and NS).....	165
Figure 4.47: Extrapolation of Wind Speed, (Gumbel at GOM and NS).....	166
Figure 4.48: Extrapolation of Current Speed (Weibull at PMO).....	167
Figure 4.49: Extrapolation of Current Speed (Gumbel at PMO).....	168
Figure 4.50: Extrapolation of Current Speed (Weibull at SBO)	169
Figure 4.51: Extrapolation of Current Speed (Gumbel at SBO)	170
Figure 4.52: Extrapolation of Current Speed (Weibull at SKO)	171
Figure 4.53: Extrapolation of Current Speed (Gumbel at SKO)	172
Figure 4.54: Extrapolation of Current Speed (Weibull at GOM and NS).....	173
Figure 4.55: Extrapolation of Current Speed (Gumbel at GOM and NS).....	173
Figure 5.1: Variation of W_e/G ratio Vs Reliability Index for Components in Axial Tension for API WSD, ISO (MS) and ISO LRFD Codes at SKO1	180
Figure 5.2: Variation of W_e/G ratio Vs Reliability Index for Components in Compression for API WSD, ISO (MS) and ISO LRFD Codes at SKO1	180
Figure 5.3: Variation of W_e/G ratio Vs Reliability Index for Components in Bending for API WSD, ISO (MS) and ISO LRFD Codes at SKO1	181
Figure 5.4: Variation of W_e/G ratio Vs Reliability Index for Components in Tension & Bending for API WSD, ISO (MS) and ISO LRFD Codes at SKO1 ..	182
Figure 5.5: Variation of W_e/G ratio Vs Reliability Index for Components in Compression & Bending for API WSD, ISO (MS) and ISO LRFD Codes at SKO1	182

Figure 5.6: Variation of W_e/G ratio Vs Reliability Index for Components in Tension, Bending & Hydrostatic Pressure for API WSD, ISO (MS) and ISO LRFD Codes at SKO1	183
Figure 5.7: Variation of W_e/G ratio Vs Reliability Index for Components in Compression, Bending & Hydrostatic Pressure for API WSD, ISO (MS) and ISO LRFD Codes at SKO1	184
Figure 5.8: Variation of Reliability Index Vs W_e/G for Axial Tension (Leg) Using ISO code for Different Values of Environmental Load Factor (γ).....	185
Figure 5.9: Variation of Reliability Index Vs W_e/G for Compression (Leg) Using ISO code for Different Values of Environmental Load Factor (γ).....	186
Figure 5.10: Variation of Reliability Index Vs W_e/G for Bending (Leg) Using ISO code for Different Values of Environmental Load Factor (γ).....	186
Figure 5.11: Variation of Reliability Index Vs W_e/G for Tension & Bending (Leg) Using ISO code for Different Values of Environmental Load Factor (γ)	187
Figure 5.12: Variation of Reliability Index Vs W_e/G for Compression & Bending (Leg) Using ISO code for Different Values of Environmental Load Factor (γ).	187
Figure 5.13: Variation of Reliability Index Vs W_e/G for Tension, Bending & Hydrostatic Pressure (Leg) Using ISO code for Different Values of Environmental Load Factor (γ).....	188
Figure 5.14: Variation of Reliability Index Vs W_e/G for Compression, Bending & Hydrostatic Pressure (Leg) Using ISO code for Different Values of Environmental Load Factor (γ).....	188
Figure 5.15: Variation of Reliability Index Vs W_e/G for Combined Stresses (Leg) Using ISO code for Different Values of Environmental Load Factor (γ)	189
Figure 5.16: Column Slenderness Vs Reliability Index for Various W_e/G Ratios	189
Figure 5.17: Calibration of Jacket Members Under ISO for all Types of Model Stresses with W_e/G ratios Vs ISO Reliability Indices	191
Figure 5.18: Calibration of Jacket Members Under API WSD for all Types of Model Stresses with W_e/G ratios Vs API WSD Reliability Indices.....	191
Figure 5.19: Reliability Index Vs Environmental Load Factor for HP at PMO Using ISO 19902 and API WSD.....	193

Figure 5.20: Reliability Index Vs Environmental Load Factor for HD at PMO Using ISO 19902 and API WSD	193
Figure 5.21: Reliability Index Vs Environmental Load Factor for VD at PMO Using ISO 19902 and API WSD	194
Figure 5.22: Reliability Index Vs Environmental Load Factor for Leg at PMO Using ISO 19902 and API WSD	194
Figure 5.23: Reliability Index Vs Environmental Load Factor for Component at PMO Using ISO 19902 and API WSD	195
Figure 5.24: Reliability Index Vs Environmental Load Factor for HP at SBO Using ISO 19902 and API WSD	196
Figure 5.25: Reliability Index Vs Environmental Load Factor for HD at SBO Using ISO 19902 and API WSD	196
Figure 5.26: Reliability Index Vs Environmental Load Factor for VD at SBO Using ISO 19902 and API WSD	197
Figure 5.27: Reliability Index Vs Environmental Load Factor for Leg at SBO Using ISO 19902 and API WSD	197
Figure 5.28: Reliability Index Vs Environmental Load Factor for Component at SBO Using ISO 19902 and API WSD	198
Figure 5.29: Reliability Index Vs Environmental Load Factor for HP at SKO1 Using ISO 19902 and API WSD	199
Figure 5.30: Reliability Index Vs Environmental Load Factor for HD at SKO1 Using ISO 19902 and API WSD	199
Figure 5.31: Reliability Index Vs Environmental Load Factor for VD at SKO1 Using ISO 19902 and API WSD	200
Figure 5.32: Reliability Index Vs Environmental Load Factor for Leg at SKO1 Using ISO 19902 and API WSD	200
Figure 5.33: Reliability Index Vs Environmental Load Factor for Component at SKO1 Using ISO 19902 and API WSD	201
Figure 5.34: Reliability Index Vs Environmental Load Factor for HP at SKO2 Using ISO 19902 and API WSD	202

Figure 5.35: Reliability Index Vs Environmental Load Factor for HD at SKO2 Using ISO 19902 and API WSD.....	202
Figure 5.36: Reliability Index Vs Environmental Load Factor for VD at SKO2 Using ISO 19902 and API WSD.....	203
Figure 5.37: Reliability Index Vs Environmental Load Factor for Leg at SKO2 Using ISO 19902 and API WSD.....	203
Figure 5.38: Reliability Index Vs Environmental Load Factor for Component at SKO2 Using ISO 19902 and API WSD.....	204
Figure 5.39: Reliability Index Vs Environmental Load Factor for Jacket Platforms in Malaysia at SKO2 Using ISO 19902 and API WSD	205
Figure 5.40: Reliability Index Vs Environmental Load Factor for Jacket Platforms in Malaysia Using ISO 19902 and API WSD Axial Tension Resistance Factor for Components	206
Figure 5.41: Reliability Index Vs Environmental Load Factor for Jacket Platforms in Malaysia at SKO2 Using ISO 19902 and API WSD Axial Compression Resistance Factor for Components.....	207
Figure 6.1: Variation of W_e/G ratio Vs Reliability Index for K-Joint-Tension / Compression for API WSD, ISO-MS and ISO LRFD Codes at SKO1	210
Figure 6.2: Variation of W_e/G ratio Vs Reliability Index for K-Joint- IPB for API WSD, ISO-MS and ISO LRFD Codes at SKO1	211
Figure 6.3: Variation of W_e/G ratio Vs Reliability Index for K-Joint- OPB for API WSD, ISO-MS and ISO LRFD Codes at SKO1	211
Figure 6.4: Variation of W_e/G ratio Vs Reliability Index for T/Y-Joint in Tension for API WSD, ISO-MS and ISO LRFD Codes at SKO1	212
Figure 6.5: Variation of W_e/G ratio Vs Reliability Index for T/Y-Joint in C for API WSD, ISO-MS and ISO LRFD Codes at SKO1	213
Figure 6.6: Variation of W_e/G ratio Vs Reliability Index for T/Y-Joint in IPB for API WSD, ISO-MS and ISO LRFD Codes at SKO1	213
Figure 6.7: Variation of W_e/G ratio Vs Reliability Index for T/Y-Joint in OPB for API WSD, ISO-MS and ISO LRFD Codes at SKO1	214
Figure 6.8: Variation of W_e/G ratio Vs Reliability Index for X-Joint in Tension for API WSD, ISO-MS and ISO LRFD Codes at SKO1	215

Figure 6.9: Variation of W_e/G ratio Vs Reliability Index for X-Joint in Compression for API WSD, ISO-MS and ISO LRFD Codes at SKO1	215
Figure 6.10: W_e Variation of W_e/G ratio Vs Reliability Index for X-Joint in IPB for API WSD, ISO-MS and ISO LRFD Codes at SKO1	216
Figure 6.11: Variation of W_e/G ratio Vs Reliability Index for X-Joint in OPB for API WSD, ISO-MS and ISO LRFD Codes at SKO1	216
Figure 6.12: Effect of β ratio on Reliability Index, K-Joint in Tension / Compression at SKO1	217
Figure 6.13: Effect of β on Reliability Index of K-Joint in IPB at SKO1	218
Figure 6.14: Effect of β on reliability index of K-Joint in OPB at SKO1	218
Figure 6.15: Effect of β on Reliability Index of T/Y Joint in Tension at SKO1 ..	219
Figure 6.16: Effect of β on Reliability Index of T/Y Joint in Compression at SKO1	219
Figure 6.17: Effect of β on Reliability Index of T/Y Joint in IPB at SKO1	220
Figure 6.18: Effect of β on Reliability Index of T/Y Joint in OPB at SKO1	220
Figure 6.19: Effect of β on Reliability Index of X Joint Tension at SKO1	221
Figure 6.20: Effect of β on Reliability Index of X Joint in Compression at SKO1	221
Figure 6.21: Effect of β on Reliability Index of X Joint in IPB at SKO1	222
Figure 6.22: Effect of β on Reliability Index of X Joint in OPB at SKO1	222
Figure 6.23: Effect of γ on Reliability Index, K Joint Tension and Compression at SKO1	223
Figure 6.24: Effect of γ on Reliability Index of K Joint in IPB at SKO1	224
Figure 6.25: Effect of γ on Reliability Index of K Joint in OPB at SKO1	224
Figure 6.26: Effect of γ on Reliability Index of T/Y Joint in Tension at SKO1 ..	225
Figure 6.27: Effect of γ on Reliability Index of T/Y Joint in Compression at SKO1	225
Figure 6.28: Effect of γ on Reliability Index of T/Y Joint in IPB at SKO1	226

Figure 6.29: Effect of γ on Reliability Index of T/Y Joint in OPB at SKO1.....	226
Figure 6.30: Effect of γ on Reliability Index of X Joint in Tension at SKO1	227
Figure 6.31: Effect of γ on Reliability Index of X Joint in Compression at SKO1	227
Figure 6.32: Effect of γ on Reliability Index of X Joint in IPB at SKO1.....	228
Figure 6.33: Effect of γ on Reliability Index of X Joint in OPB at SKO1	228
Figure 6.34: Variation of Reliability Index Vs W_e/G for K Joint Using ISO code for Different Values of Environmental Load Factor (γ).....	229
Figure 6.35: Variation of Reliability Index Vs W_e/G for T/Y Joint Using ISO code for Different Values of Environmental Load Factor (γ).....	229
Figure 6.36: Variation of Reliability Index Vs W_e/G for X Joint Using ISO code for Different Values of Environmental Load Factor (γ).....	230
Figure 6.37: Calibration of Jacket Joint Under ISO for all Types of Model Stresses with W_e/G ratios Vs ISO Reliability Indices	231
Figure 6.38: Calibration of Jacket Joint Under API WSD for all Types of Model Stresses with W_e/G ratios Vs API WSD Reliability Indices	232
Figure 6.39: Reliability Index Vs Environmental Load Factor for K Joint at PMO Using ISO 19902 and API WSD.....	233
Figure 6.40: Reliability Index Vs Environmental Load Factor for T/Y Joint at PMO Using ISO 19902 and API WSD.....	233
Figure 6.41: Reliability Index Vs Environmental Load Factor for X Joint at PMO Using ISO 19902 and API WSD.....	234
Figure 6.42: Reliability Index Vs Environmental Load Factor for All Joints at PMO Using ISO 19902 and API WSD.....	234
Figure 6.43: Reliability Index Vs Environmental Load Factor for K Joint at SBO Using ISO 19902 and API WSD.....	235
Figure 6.44: Reliability Index Vs Environmental Load Factor for T/Y Joint at SBO Using ISO 19902 and API WSD	236
Figure 6.45: Reliability Index Vs Environmental Load Factor for X Joint at SBO Using ISO 19902 and API WSD.....	236

Figure 6.46: Reliability Index Vs Environmental Load Factor for All Joints at SBO Using ISO 19902 and API WSD	237
Figure 6.47: Reliability Index Vs Environmental Load Factor for K Joint at SKO1 Using ISO 19902 and API WSD	238
Figure 6.48: Reliability Index Vs Environmental Load Factor for T/Y Joint at SKO1 Using ISO 19902 and API WSD	238
Figure 6.49: Reliability Index Vs Environmental Load Factor for X Joint at SKO1 Using ISO 19902 and API WSD	239
Figure 6.50: Reliability Index Vs Environmental Load Factor for All Joints at SKO1 Using ISO 19902 and API WSD	239
Figure 6.51: Reliability Index Vs Environmental Load Factor for K Joint at SKO2 Using ISO 19902 and API WSD	240
Figure 6.52: Reliability Index Vs Environmental Load Factor for T/Y Joint at SKO2 Using ISO 19902 and API WSD	240
Figure 6.53: Reliability Index Vs Environmental Load Factor for X Joint at SKO2 Using ISO 19902 and API WSD	241
Figure 6.54: Reliability Index Vs Environmental Load Factor for All Joint at SKO2 Using ISO 19902 and API WSD	241
Figure 6.55: Reliability Index Vs Environmental Load Factor for All Joint for All Platforms Using ISO 19902 and API WSD	242
Figure 7.1: Base Shear against Wave Heights and Current Speed at PMO	246
Figure 7.2: Base Shear against Wave Heights and Current Speed at SBO	246
Figure 7.3: Base Shear against Wave Heights and Current Speed at SKO1	247
Figure 7.4: Base Shear against Wave Heights and Current Speed at SKO2	247
Figure 7.5: Base Shear against Wave Heights and Current Speed at SKO2a	248
Figure 7.6: Curve Fitting Model for Platform ‘PMO’	249
Figure 7.7: Curve Fitting Model for Platform ‘SBO’	249
Figure 7.8: Curve Fitting Model for Platform ‘SKO1’	250
Figure 7.9: Curve Fitting Model for Platform ‘SKO2’	250

Figure 7.10: Curve Fitting Model for Platform ‘SKO2a’.....	251
Figure 7.11: Variation of Reliability Index Vs We/G Ratio Using ISO 19902 code for Different Environmental Load Factors (γ_w) at PMO	255
Figure 7.12: Variation of Reliability Index Vs We/G Ratio Using ISO 19902 code for Different Environmental Load Factors (γ_w) at SBO	255
Figure 7.13: Variation of Reliability Index Vs We/G Ratio Using ISO 19902 code for Different Environmental Load Factors (γ_w) at SKO1	256
Figure 7.14: Variation of Reliability Index Vs We/G Ratio Using ISO 19902 code for Different Environmental Load Factors (γ_w) at SKO2	256
Figure 7.15: Variation of Reliability Index Vs We/G Ratio Using ISO 19902 code for Different Environmental Load Factors (γ_w) at SKO2a	257
Figure 7.16: Effect of γ_w on Reliability Index against We/G ratio of 0.5,1, 2.5 at PMO.....	258
Figure 7.17: Effect Effect of γ_w on Reliability Index against We/G ratio of 0.5,1, 2.5 at SBO	258
Figure 7.18: Effect of γ_w on Reliability Index against We/G ratio of 0.5,1, 2.5 at SKO1	259
Figure 7.19: Effect of γ_w on Reliability Index against We/G ratio of 0.5,1, 2.5 at SKO2	259
Figure 7.20: Effect of γ_w on Reliability Index against We/G ratio of 0.5,1, 2.5 at SKO2a.....	260
Figure 7.21: Reliability Index Vs We/G ratios with $\gamma_w=1.10$ and Target Reliability at PMO.....	260
Figure 7.22: Reliability Index Vs We/G ratios with $\gamma_w=1.10$ and Target Reliability at SBO.....	261
Figure 7.23: Reliability Index Vs We/G ratios with $\gamma_w=1.10$ and Target Reliability at SKO1.....	261
Figure 7.24: Reliability Index Vs We/G ratios with $\gamma_w=1.10$ and Target Reliability at SKO2.....	262
Figure 7.25: Reliability Index Vs We/G ratios with $\gamma_w=1.10$ and Target Reliability at SKO2a.....	262

Figure 7.26: Reliability Index Vs Environmental Load Factor, $W_e/G = 1$ at PMO	263
Figure 7.27: Reliability Index Vs Environmental Load Factor, $W_e/G = 1$ at SBO	263
Figure 7.28: Reliability Index Vs Environmental Load Factor, $W_e/G = 1$ at SKO1	264
Figure 7.29: Reliability Index Vs Environmental Load Factor, $W_e/G = 1$ at SKO2	264
Figure 7.30: Reliability Index Vs Environmental Load Factor, $W_e/G = 1$ at SKO2a	265
Figure 7.31: Collapse Base Shear against H_{max} for PMO.	266
Figure 7.32: Collapse Base Shear against H_{max} for SBO	266
Figure 7.33: Collapse Base Shear against H_{max} for SKO1	267
Figure 7.34: Collapse Base Shear against H_{max} for SKO2	267
Figure 7.35: Collapse Base Shear against H_{max} for SKO2a	268
Figure 7.36: Collapse Base Shear against Wave Direction at PMO	268
Figure 7.37: Collapse Base Shear against Wave Direction at SBO	269
Figure 7.38: Collapse Base Shear against Wave Direction at SKO1	269
Figure 7.39: Collapse Base Shear against Wave Direction at SKO2	270
Figure 7.40: Collapse Base Shear against Wave Direction at SKO2a	270
Figure 7.41: Collapse Base Shear against H_{max} Wave with Varying Currents for PMO for 0 Degree	271
Figure 7.42: Collapse Base Shear against H_{max} Wave with Varying Currents for PMO for 45 Degree	271
Figure 7.43: Collapse Base Shear against H_{max} Wave with Varying Currents for PMO for 90 Degree	272
Figure 7.44: Collapse Base Shear against H_{max} Wave with Varying Currents for PMO for 135 Degree	272

Figure 7.45: Collapse Base Shear against H_{max} Wave with Varying Currents for PMO for 180 Degree	273
Figure 7.46: Collapse Base Shear against H_{max} Wave with Varying Currents for PMO for 225 Degree	273
Figure 7.47: Collapse Base Shear against H_{max} Wave with Varying Currents for PMO for 270 Degree	274
Figure 7.48: Collapse Base Shear against H_{max} Wave with Varying Currents for PMO for 315 Degree	274
Figure 7.49: Variation of Load Model Uncertainty on Resistance Model Uncertainty at PMO.....	276
Figure 7.50: Variation of Load Model Uncertainty on Resistance Model Uncertainty at SBO.....	277
Figure 7.51: Variation of Load Model Uncertainty on Resistance Model Uncertainty at SKO1	277
Figure 7.52: Variation of Load Model Uncertainty on Resistance Model Uncertainty at SKO2	278
Figure 7.53: Variation of Load Model Uncertainty on Resistance Model Uncertainty at SKO2a.....	278
Figure 7.54: Variation of Load Model Uncertainty and RSR on Probability of Failure, with $\beta=0.10$ at PMO	279
Figure 7.55: Variation of Load Model Uncertainty and RSR on Probability of Failure, with $\beta=0.10$ at SBO	280
Figure 7.56: Variation of Load Model Uncertainty and RSR on Probability of Failure, with $\beta=0.10$ at SKO1	280
Figure 7.57: Variation of Load Model Uncertainty and RSR on Probability of Failure, with $\beta=0.10$ at SKO2	281
Figure 7.58: Variation of Load Model Uncertainty and RSR on Probability of Failure, with $\beta=0.10$ at SKO2a	282
Figure 7.59: Effect of Wave Heights and Load Model Uncertainty on Probability of Failure at PMO.....	283

Figure 7.60: Effect of Wave Heights and Load Model Uncertainty on Probability of Failure at SBO	283
Figure 7.61: Effect of Wave Heights and Load Model Uncertainty on Probability of Failure at SKO1	284
Figure 7.62: Effect of Wave Heights and Load Model Uncertainty on Probability of Failure at SKO2	284
Figure 7.63: Effect of Wave Heights and Load Model Uncertainty on Probability of Failure at SKO2a	285
Figure 7.64: Effect Wave Heights and RSR on Updated Probability of Failure at PMO	286
Figure 7.65: Effect Wave Heights and RSR on Updated Probability of Failure at SBO	287
Figure 7.66: Effect Wave Heights and RSR on Updated Probability of Failure at SKO1	287
Figure 7.67: Effect Wave Heights and RSR on Updated Probability of Failure at SKO2	288
Figure 7.68: Effect Wave Heights and RSR on Updated Probability of Failure at SKO2a	288
Figure 7.69: Effect of Wave Heights and Collapse Ratio on Updated Probability of Failure with Damaged Members and RSR of 1.5 at PMO.....	289
Figure 7.70: Effect of Wave Heights and Collapse Ratio on Updated Probability of Failure with Damaged Members and RSR of 2.0 at PMO.....	290
Figure 7.71: Effect of Wave Heights and Collapse Ratio on Updated Probability of Failure with Damaged Members and RSR of 1.5 at SBO.....	291
Figure 7.72: Effect of Wave Heights and Collapse Ratio on Updated Probability of Failure with Damaged Members and RSR of 2.0 at SBO.....	292
Figure 7.73: Effect of Wave Heights and Collapse Ratio on Updated Probability of Failure with Damaged Members and RSR of 1.5 at SKO1	293
Figure 7.74: Effect of Wave Heights and Collapse Ratio on Updated Probability of Failure with Damaged Members and RSR of 2.0 at SKO1	293

Figure 7.75: Effect of Wave Heights and Collapse Ratio on Updated Probability of Failure with Damaged Members and RSR of 1.5 at SKO2 294

Figure 7.76: Effect of Wave Heights and Collapse Ratio on Updated Probability of Failure with Damaged Members and RSR of 2.0 at SKO2 295

Figure 7.77: Effect of Wave Heights and Collapse Ratio on Updated Probability of Failure with Damaged Members and RSR of 1.5 at SKO2a 296

Figure 7.78: Effect of Wave Heights and Collapse Ratio on Updated Probability of Failure with Damaged Members and RSR of 2.0 at SKO2a 296

DEFINITIONS

Bias	Mean value/ nominal value
COV	Coefficient of Variation (Standard deviation by Mean)
Factor of safety	Ratio of resistance to stress (load)
Limit state	Boundary between safe and unsafe region
Load factor	Nominal load effects are multiplied by a γ factor to cater the uncertainties and excessive loads
Mean coefficient	Mean of bias values
Nominal strength	calculated from section properties like yield strength
Random variable	It has no fixed value and it is evaluated by using the characteristic distribution and its parameters.
Reliability (1- P_f)	Complement of failure probability. Probability that the Jacket will perform as desired for intended design life.
RSR	$\frac{\text{Ultimate Base Shear at Collapse}}{\text{Design Environmental Load (Base Shear)}}$
Resistance factor	Nominal strength or resistance is multiplied by a ϕ factor to cater for uncertainties in strength
Return Period	Return Period= $\frac{1}{p_f}$, Average period of time which is passed between occurrences of events at the site.
Safety index	Mean Safety Margin / Uncertainty Level
Significant wave height	Mean of highest 1/3 of all waves present in wave train
Standard deviation	(SD) Square root of variance
Standard normal space	Space of normally distributed random variables with zero mean values and unit standard deviation and zero correlation coefficients.
System redundancy	$\left[\frac{\text{Design Collapse Load}}{\text{Peak Collapse Load}} \right] + 1$

NOTATIONS

A	Cross-sectional area, activity factor for Jacket
A_i	Variable area of tubular member, load uncertainty model
A_n	Nominal area of tubular member
a_1, a_2, a_3	Load coefficient
B_i	Resistance model uncertainty
C	Critical elastic buckling coefficient
$C_{m,y}, C_{m,z}$	Moment reduction factors corresponding to the member y and z axes
C_x	Elastic critical buckling coefficient
d	Water depth, Brace outside diameter, dead load ratio
D	Outside diameter of member, random dead load
D_l	Dead load, gravity load
E	Young's Modulus of elasticity
E_l	Environmental load
f_a	Absolute value of acting axial stress
f_b	Absolute value of acting resultant bending stress
f_c	Representative axial compressive strength
f_e	Smaller of Euler buckling strength in Y-Z directions
F_h	Absolute value of hoop compression stress
F_{hc}	Critical hoop stress
f_{he}	Representative elastic critical hoop buckling strength
f_{xe}	Representative elastic local buckling strength
FS	Factor of Safety
F_t	Allowable tensile stress
f_t	Representative axial tensile strength,
f_{ti}	Variable tensile strength
f_{tn}	Nominal tensile strength
F_y	Yield strength

F_{yi}	Random yield strength
F_{yn}	Nominal yield strength
$f_{e,y}, f_{e,z}$	Euler buckling strengths corresponding to member y and z axes.
f_{xe}	Representative elastic buckling coefficient
f_{yb}	brace yield strength
f_{yc}	Representative local buckling strength
f_{yc}	yield strength of chord member or (0.8 of tensile strength)
$f_x(X)$	Probability density function (PDF) of variable X at a value of x
$G(x)$	Performance / Limit state function. $G(x)=0$, Limit state surface with respect to design value of x
g	Acceleration due to gravity, gap between braces
H	Maximum wave height
H_d	Design wave height
H_{max}	Maximum wave height
$H_{max(des)}$	Design wave height (100 year)
H_R	Wave height which gives RSR of 1.0
H_{var}	Random wave height
I	Moment of Inertia of cross-section
ICSF	Implicit code safety factor
K	Effective length factor
K_y, K_z	Effective length factor for y and z directions
L	Wave length or Component span, random live load
L_l	Live Load
l	Unbraced length, live load ratio
L_y, L_z	Un braced lengths in y and z directions
M	Bending moment due to factored actions
M_a	allowable capacity for brace bending moment
M_c	Bending force in chord member
MF	Material factor
M_p	Plastic moment strength of chord

M_{uj}	Joint Bending Moment
M_y	Elastic yield moment
N	Total number of simulation
N_f	Number of failures
n	Platform life in years
n_p	Average number of people on Jacket
P	Return period probability
p	Annual probability that the event will not occur
P_a	allowable capacity for brace axial load
P_c	axial force in chord member
P_d	Gravity load proportion
P_f	Probability of failure
P_{fn}	Target probability of failure
P_s	Probability of survival
P_w	Environmental load proportion
P_{uf}	Updated probability of failure
P_{uj}	Joint Axial Strength
P_y	Yield strength of chord, Axial strength due to yielding , $P_y=A \times f_y$
P_{ult}	Ultimate load
Q	Load
\bar{Q}	Mean load
Q_e	100 year design load
Q_1	Large value of Q
Q_i	Nominal load
Q_f	Chord force factor, base shear (damaged state)
Q_u	Strength factor
R	Resistance effect
\bar{R}	Mean resistance
R_1	Low value of resistance R
R_n	Nominal resistance

R_{ult}	Ultimate resistance of Jacket
r	Radius of Gyration $r = \sqrt{I/A}$
SR	System redundancy
T	Chord wall thickness
t	Wall thickness of member, brace wall thickness
t_l	Design life of Jacket
S	Strength given by code Equation
T_{app}	Apparent wave period
T_p	Peak period
T_z	Mean zero-crossing period and is assumed to equal to $T_p/1.4$
u	Current speed
V_c	Current speed
v_r	COV of resistance
V_{pf}	COV of failure probability
v_q	COV of load
Var (x)	Variance of x
ν	Poisson's ratio =0.3
W	Load effects, random environmental load
w	Environmental load ratio
W_e	Environmental load ratio
W_f	Warning factor for sudden failure
x^*	Design point
X	Random variable
X_m	Resistance model uncertainty
X_w	Load model uncertainty
z	Safety margin
Z	Theoretical value of plastic section modulus of component
Z_e	Elastic section modulus, $Z_e = \frac{\pi}{64} [D^4 - (D - 2t)^4] / (D/2)$

Z_P	Plastic section modulus, $Z_p = \frac{1}{6}[D^3 - (D - 2t)^3]$
γ_D	Dead Load factor
γ_d	Gravity load factor
γ_L	Live Load factor
γ_R	Resistance factor
γ_W	Environmental Load factor
ϕ	Material strength safety factor
γ_i	Loadfactor
$\gamma_{R,t}$	Partial resistance factor for axial tensile strength ($\gamma_{R,t}=1.05$)
μ	Mean
μ_g	Mean of limit state function
μ_Q	Mean load
μ_R	Mean resistance
μ_s	Social criteria factor
σ	Standard deviation
σ_b	Bending stress due to forces from factored actions; when $M > M_y$, σ_b is to be considered as an equivalent elastic bending stress $\sigma_b=M/Z_e$
$\sigma_{b,y}, \sigma_{b,z}$	$\sigma_{b,y}$ = Bending stress about member y-axis or z-axis (in plane) due to forces from factored actions
σ_c	Axial compressive stress due to forces from factored actions
σ_g	Standard deviation of limit state function
σ_h	Hoop stress due to forces from factored hydrostatic pressure
σ_Q	Stand deviation of load
σ_R	Stand deviation of resistance
σ_t	Axial tensile stress due to forces from factored actions
σ_{ti}	Variable tensile stress
σ_{tn}	Nominal tensile stress
γ_c	Compression resistance factor
γ_d	Gravity load factor
γ_w	Environmental load factor

$\gamma_{R,b}$	Partial resistance factor for bending strength, $\gamma_{R,b} = 1.05$
$\gamma_{R,c}$	Partial resistance factor for axial compressive strength, $\gamma_{R,c} = 1.18$
γ_{Rq}	yield strength factor (1.05)
λ	Column slenderness parameter
λ_{ult}	Factor which increases until collapse
θ	Angle between brace and chord
β	Reliability index
Φ	Cumulative distribution function for the standard normal variables

LIST OF ABBREVIATION

AASHTO	American Association of State Highway and Transportation Officials
ACI	American Concrete Institute
AISC	American Institute of Steel Construction
API RP2A (WSD)	American Petroleum Institute-Recommended Practice (Working Stress Design)
API RP2A (LRFD)	American Petroleum Institute-Recommended Practice (Load and Resistance Factor Design)
BOMEL	Company name
CDF	Cumulative Distribution Function
COV	Coefficient of Variation
DNV	Det Norske Veritas (Norwegian Certifying Authority)
DSF	Damaged Strength Factor
FERUM	Compiler based on FORM Method of Reliability
FORM	First Order Reliability Method
GOM	Gulf of Mexico
H_{max}	Maximum wave height
IPB	In-Plane Bending
ISO 19902	International Standard Organization code for (Petroleum and natural gas industries -Fixed steel offshore structures)
ISO LRFD (MS)	Environmental load factor from this study (Malaysian study)
LRFD	Load and Resistance Factor Design
LSD	Limit State Design
MC	Mean Coefficient
MCS	Monte Carlo Simulation
MS	Malaysian Study (This Research)
M-S	March-September
NE	North East

N-M	November to March
NPD	Norwegian Petroleum Directorate
NS	North Sea
NW	North West
OPB	Out Plane Bending
OTC	Offshore Technology Conference
PAFA	Company name
PDF	Probability Density Function
PF	Probability of Failure
PMO	Peninsular Malaysia Operation
PTS	PETRONAS Technical Standard
RSR	Reserve Strength Ratio
S	South
SACS	Structural Analysis Computer Software
SBO	Sabah Operation
SF	Safety Factor
SKO1	Sarawak Operation (Platform No. 1)
SKO2	Sarawak Operation (Platform No. 2-Fixed at Mud line)
SKO2a	Sarawak Operation (Platform No. 2 with Pile Soil Foundation)
SNS-NNS	Southern North Sea, Northern North Sea
SP	Statistical Parameters
SW	South West
UPF	Updated Probability of Failure
VC	Variation Coefficient
We/G	Environmental Load to Gravity Load Ratio
WSD	Working Stress Design

CHAPTER 1 INTRODUCTION

1.1 Introduction

Structural design methodology of civil engineering design codes has changed from allowable stress design to limit state (load and resistance factor) design. Working Stress Design (WSD) method uses safety factors without taking into consideration the uncertainties and it assumes that all variables are deterministic. Thus safety of platform is achieved by WSD through the use of a factor of safety against the inherent uncertainties of load and resistance. For allowable stress design, safety of structure is achieved by the use of a safety factor against the uncertainties of load using some arbitrary experience and judgment like 1/3 decrease for allowable stresses. This method provides no knowledge about effects of various random variable parameters on the safety of Jacket platform. The probabilistic codes for limit state design take into account the uncertainties of material and load. Load and resistance factor design (LRFD) code has safety factors which take into consideration load and resistance uncertainties separately. This code provides safety factors for load i.e. dead, live and environmental load separately. For resistance, tension, compression, bending, shear and hydrostatic stresses are provided with resistance factors separately.

Jacket platform acts as base for overall structure which is used to extract hydrocarbon from oceans. They are suitable for shallow and intermediate water depth (<150 m). There are about 250 Jacket platforms currently operating in offshore Malaysia and any research on the reliability of Jacket platforms will be very much useful for the oil and gas industry. The main offshore regions in Malaysia have been classified in this study as Peninsular Malaysia Operation (PMO), Sabah Operation (SBO) and Sarawak Operation (SKO).

1.2 Overview

According to Ferguson [1], the development of LRFD is highlighted by the load types i.e. components which are dominated by environmental loads are treated conservatively by LRFD but WSD penalises those governed by gravity loads. Thus LRFD method is being utilized nowadays for the further development of research based design codes. The LRFD codes of practice are component and joint reliability based design standards. Structural reliability analysis is based on theory of limit state or failure state. The reliability based structures are designed so that their reliability is always higher than the target reliability i.e. minimum specified by the well established standards. Component and joint reliability is used to find environmental load and resistance factors for Jacket platform. ISO 19902 code specifies the environmental load and resistance factors for the component and joint using Gulf of Mexico (GOM) and North Sea (NS) calibration.

Uncertainties in capacity or member strength occur due to material or geometric variability. Effective utilisation of component, joint and overall system of Jacket platform is achieved by taking into consideration the uncertainty of material and load. Material uncertainties are used to measure statistical spread, evaluated by using the data from fabrication yard and mill test reports. This is due to limitation in engineering theories to predict the component and system response and capacity. The characteristics of structural design are also dependent on load uncertainties which are more specifically related to environmental loads. Physics of ocean wave influence the Jacket design load and its influence varies for different regions of the world [2]. Factor of safety are used for these uncertainties and provide the increased safety margins against future structural damage or deterioration [3] or an addition of scope of work.

The limit state defines the failure or safe region for the member, the failure can be a single or combined failure mode like compression or compression plus bending. These models of limit state are also prone to uncertainty [4]. A component fails when it is not capable to resist the loads and the failure occurs due to yielding, deflection or

buckling. Component failure occurs due to failure of one member like braces and legs. In case of joints, the failure modes may be axial, in-plane bending or out-plane bending.

Environmental load factors are based on characteristic values of the random variables. LRFD is considered better representative of the situation on the ground, with actual variations taken into consideration. It has safety factors on both load and resistance side of limit state Equations. This represents uncertainty more realistic during the design practice as compared to working stress design method. The safety factors play major role for avoiding a case of failure of Jacket platform. At present the environmental load factors being used by API and ISO are based on calibration of extreme environments such as in (GOM) and North Sea (NS). They need to be more representative for the regions of less severe environment such as offshore Malaysia. The resistance factors established by API and ISO are dependent on load factors. If environmental load factors are changed the resistance factor are checked using new load factors.

Jacket platforms are designed as per component and joint based design codes and the end product is structural system [4]. The component and joint reliability cannot be optimised without taking into account the overall impact on the system reliability. Here four platforms were analysed using push over analysis and depending upon the base shear, Reserve Strength Ratios (RSR) were determined. The environmental load factor should be less than that achieved for component and joint due to ductile behaviour of Jacket. Due to change of load and resistance conditions or when extension of service life is being considered, probability of failure of Jacket is evaluated as per ISO guidelines. For the reassessment purpose the probability of failure is updated by using the Bayesian updating.

1.3 Problem Statement

The semi probabilistic codes, API LRFD and ISO 19902 have environmental load and resistance factors based on calibration in GOM or North Sea as shown in Table 1.1. These are the areas of hurricanes (typhoons in Pacific Ocean) and severe winter

storms respectively. Structural safety requires that, required strength (R) should be greater than the design loads (Q). The uncertainties of load and resistance considered were based on the local conditions of these regions. To cater for the requirements for other regions of the world it is necessary to develop local factors considering their own geographical environment. This was the reason the probabilistic evaluation of environmental loads have been done recently in China and Indonesia [5], [6] to check the influence of LRFD code. Therefore it is high time that this issue should be looked into for offshore Malaysia. Malaysia lies within 7 degrees north from equator which is considered to be safe against extreme storms. Using local geographical and fabrication uncertainties, this work proposes the modified environmental load factors for components and joints. The reassessment of platforms as per requirement of ISO and API nowadays is based on evaluating probability of failure of 10,000 year return period of load. There is a need to update this probability of failure considering probability of survival using Bayesian updating.

Table 1.1: Load factors used for Calculating the Internal Forces [7]

Governing Conditions	Partial Action Factors		
	γ_D	γ_L	γ_W
Operating	1.3	1.3	1.0
Extreme	1.1	1.1	1.35

1.3.1 Problem Background

An efficient design of a structure needs a balance between material and risk cost [8]. Platforms are designed to resist three kinds of loads to which they are subjected namely: a) Environmental loads i.e. wave, currents and wind, b) Dead loads i.e. weight of structure, and c) Live loads i.e. weight of consumable supplies and fluids in pipes and tanks. API RP2A WSD forms the basis of offshore steel Jacket platform design all over the world and has proved to be accepted design standard since it was first issued in 1969 [9]. WSD is based on factor of safety which is derived from working stress design theory and reduces the ultimate resistance strength to allowable stress for safe design. In WSD, minimum resistance is based on test results of yield strength and for load it is based on past experience, thus safety factor was inherent in these codes though not apparent. Since the loads/resistances are varying, the

assumptions used in WSD design process i.e. a single factor of safety for all load combinations cannot maintain a constant level of structural safety [10].

WSD and LRFD codes differ essentially in that LRFD uses more factors of safety which produces more uniform safety levels [9], [11]. In modern day structural design, LRFD codes have replaced WSD codes like AISC, API, ACI and AASHTO. The load and resistance factors in LRFD need to be checked for site specific conditions due to change of geography and material fabrications. Thus LRFD method brings out regional differences in variation to design based on extreme and operating conditions. This is more relevant in case of offshore structures where the environmental loads are much varying in nature and are most of the times not normally distributed. This results in variability of loads and affects the structural reliability, measured by reliability index (β).

API and ISO code use GOM and North Sea, geographical environmental parameters for calibration with severe environmental conditions. When this code is used for design of Jacket platforms in less severe environment the design becomes uneconomical. API RP2A WSD is the design code in practice for design of offshore Jacket platforms in Malaysia. PETRONAS Technical Standards (PTS) provides necessary input with regard to metocean parameters for offshore Malaysia [12]. Therefore design environment criteria for platforms in South East Asia is taken based on GOM criteria and thus there is amplification of 60% during platform design due to scarcity of data [13]. High environmental load factors used in this region, due to short lead time between discovery of hydrocarbon and platform design, can result in waste of economical resources. Due to these factors it is extremely essential that actual environmental load factors should be ascertained for this region using component, joint and system reliability.

The change of loading and resistance conditions and need for extension of life of Jacket currently requires checking for probability of failure of 10^{-4} . This method considers only failure probabilities and thus if a Jacket cannot take a load of this magnitude, re-strengthening is required which may incur huge cost. If probability of survival is also included in this analysis, the re-strengthening may not even be required.

1.3.2 Problem Motivation

It has been accepted worldwide, that LRFD method is not only more reliable but also allows the environmental load factors, to be established based on geographical locations [7], [9], [14], [15], [16], [17]. The critical part in structural design of members is assigning the properly evaluated environmental load and resistance factors. The motivation for the present study has come from the need to establish the load factors for Jacket platforms in Malaysia keeping in view the local environmental and fabrication consideration. Such factors can contribute for ISO 19901 and 19902 regional annex in particular and offshore industry in general for the efficient design of Jacket platforms in offshore Malaysia.

Bayesian updating has been suggested by Ang, Nowak and many other authors [18], [19]. This is a useful tool where low probability of failure is of importance. It considers probability of failure by taking into consideration probability of survival. Its benefit for Jacket platforms have been highlighted in a recent work in North Sea [20].

1.3.3 Problem Description

Proper evaluation of metocean parameters is still being investigated in GOM and North Sea, so that their prediction can be made effectively. The metocean data being used has still large coefficient of variation (COV) in GOM and North Sea. The metocean data bank in Malaysia is still in its infancy. ISO 19901 is blank with regard to variables of environmental load parameters for South China Sea. The code proposes that data should be collected by each country itself. There is a great need not only to analyse this data but also to check the environmental load factor. To evaluate the component and joint environmental load factors for Malaysia, we have to find seven types of component stresses and four types of joint stresses specified by API and ISO codes.

Bay's theorem is very useful for updating of probability of failure using probability of survival. When we apply the environmental load on Jacket platform, the responses can be determined. Using these responses, the probability of failure could be

evaluated. If this load is higher than what ISO code recommends, and if the Jacket can still survive, this information could be used to find updated probability of failure.

1.3.4 Previous Work and Limitation of Existing Studies

The load factors have been evaluated in GOM, North Sea and work on establishing metocean parameters is still in progress in this area, as more data becomes available [21]. The work in two region of Jawa and Makassar (Indonesia) has also been reported [6]. In China, Duan et al. [22], has done research on developing combinations of environmental load factors for China. Sakrit [23] has done reliability analysis of Jacket platforms in Gulf of Thailand using onshore data. The work on reliability index for Jacket platforms is reported in PMO region of Malaysia [24], [25]. There is a need for an extensive study covering all the three regions of Malaysia to determine the environmental load factors for components, joints and system.

Offshore industry practice for reassessment of Jacket is based on finding probability of failure of Jacket using ISO and API code requirement. An extrapolated 10^4 years environmental load is applied and probability of failure is calculated. If this probability of failure gives a return period less than 10,000 years, modifications or re-strengthening of Jacket is required. This method can be improved if not only probability of failure is considered but also probability of survival is taken into consideration. When both are combined, the probability of failure decreases considerably at higher loads [20]. The application of Bayes theorem has only recently been finding application for reliability analysis. Bayesian updating of probability of failure on Jacket platforms in this region has never been conducted and there is a need to conduct this study to avoid costly modifications.

1.3.5 Justification of the Research

The justification for finding environmental load factors for Jacket platforms for Malaysia can be attributed to the following reasons. The main justification came from the ISO 19900-1 which says that for each geographic region, environmental load factor should be evaluated specifically for that region. ISO 19902 clause A.9.9.3.3

reports that, “for structures with the same geometrical and structural properties, harmonization in safety levels (as are in GOM), hence requires location dependent partial action factors”. Environmental load factors have been determined for GOM, Northern North Sea, Southern North Sea, Central North Sea, China, Mediterranean Sea, Australia, Gulf of Guinea and they should be determined for regional environmental conditions [2], [9], [26], [27]. Though many studies have been conducted on the efficiency of different codes with regard to the load factors, still work is under progress in many parts of world [21]. In GOM, Graff et al. [14], showed that 19% i.e. 5500 tons would be saved on total weight of Jacket of 27,800 tons of steel. Thomas and Snell found reduction of weight of Jacket by 0.75% at one particular level by using LRFD method in North Sea [28]. The cost of Jacket could be saved by 15% if change of location dependent LRFD load factors is applied [6] in Java sea where Jackets are not dominated by wave loads but by gravity loads. In the light of above facts, it becomes very essential to research on environmental load factors for Jacket platforms in offshore Malaysia region.

Most of Jacket platforms in Malaysia have already completed their design life or will soon be completing. The reassessment will be required for extension of life, and ISO code requires a load with a return period of 10^4 should be applied and Jacket strength evaluated. Only probability of failure is considered in present day assessment which may show that Jacket cannot take a required load. If Bayes theorem for updating of probability of failure is applied for the same Jackets it gives us reduced probability of failure at higher loads and thus modification work can be avoided.

1.4 Aim and Scope of the Present Work

The scope of work consisted of developing uncertainty models for resistance and load. The first part was to collect data on resistance and environmental load parameters. This included site visits for data collection from a fabrication yard in Malaysia which were statistically analysed to determine their statistical properties. For next stage, environmental load data i.e. wave, current and wind was collected and statistically analysed. Extrapolations of load variables for all three regions of Malaysia were made to find the strength of Jacket platforms. The reliability and

probability of failure was found based on First Order Reliability Method (FORM). The component and joint reliability was determined, followed by system reliability. Subsequently environmental load factors, based on component, joint and system reliability were determined. Probability of failure was updated based on Bayesian updating technique using Monte Carlo simulation.

Platform designed by API RP2A WSD and representing all the three regions were analysed in this study. Platforms with four and six number of legs and with different water depths were selected. Availability of SACS model was considered essential so that actual resistance and load effects should be evaluated. SACS loading models were changed as per the requirements of this study.

1.4.1 Research Objectives

The research objectives are to evaluate the environmental load factor for Jacket platforms in Malaysia using component, joint, system reliability analysis and to check the methodology for extension of Jacket life. Following are the main objectives of this research.

1 (a) To determine the geometric, material and model uncertainties to be used for calculation of resistance uncertainty. This was used for the analysis of component, joint and system reliability evaluation of Jacket platforms in all the three regions of offshore Malaysia.

1 (b) To determine the wave, wind and current uncertainties, to be used for calculation of load uncertainty. This will be used for analysis of component, joint and system load evaluation of Jacket platforms in all the three regions of offshore Malaysia.

2 To propose environmental load factors, to be used for the design of Jacket platforms in all three regions of offshore Malaysia. These factors are to be determined based on the reliability index calculated for component, joint and system analysis.

3 To propose improved calculation of probability of failure during reassessment of platforms with a view to extend service life without any modification. It will also be

applicable to change of loading conditions or damage to the platform members. This will help us to extract the remaining hydrocarbons available at the site.

1.4.2 Limitations

Environmental load considered was based on 10 and 100 year omnidirectional maximum values. Loads such as earthquake, boat impact and corrosion were not considered in this study. Dynamic analysis was not considered because Jacket platforms, in shallow water depth i.e. less than 100 m, (which is the case in Malaysia) are stiff in nature. It is required when natural period of vibration exceeds 3 seconds such as deepwater platforms (>300 m) [29], [30]. During the extreme storm conditions, dynamic nature of loads does not play a major role for ultimate limit state performance for Jacket platforms [31]. Fixed steel Jacket platforms response to environmental loading is basically quasi-static. This is due to the reason that Jackets are structurally rigid and natural period of vibration are short. Structures respond to the repetition of wave loads as though they were a series of static loads acting on the Jacket [32]. This comprises the space frame slender tubular which do not influence the gross characteristics of incident waves i.e. no wave diffraction [33]. Four platforms were selected for reliability analysis in this study. The same numbers were used for research elsewhere [26]. This research covered only four out of 250 platforms from three regions of Malaysia, this was due to non-availability of data for other platforms. The increase of data points may reduce epistemic uncertainty, to cater this W_e/G ratio ranging from 0.1-40 is used. For system load factors minimum RSR i.e. range of 1.5 to 2.25 is used to find optimised load factors as suggested by ISO 19902 and API 21st edition, this will cover all types of geometry of Jackets and topsides. Cost benefit analysis was not made in this study.

1.4.3 Key Assumptions

- i) Data collected for uncertainty of resistance is from one representative fabrication yard in Malaysia.

- ii) Four platforms are considered for the calibration representing each region of offshore Malaysia. For GOM and NS the number of platforms considered for calibration are three (3) and six (6) respectively [10].
- iii) Primary members are selected for component reliability analysis which includes leg, diagonal, external horizontal at periphery and internal horizontal bracing.
- iv) In this study only ultimate limit state is considered in consistency with ISO, API LRFD and NPD (Norwegian Petroleum Department).
- v) Like API WSD and API LRFD [1], omnidirectional wave, wind and current values are used for this study.
- vi) 100 year load return period for environmental loads is considered for calibration of Jackets as per guidelines used by API and ISO.
- vii) Stoke's 5th order wave Equations (1.1) and (1.2) were used for the selection of wave theory as can be seen from cross lines superimposed in Figure 1.1 [34].

$$H/(gT_{app}^2) = 9.7/(9.81 \times 10.8^2) = 0.01 \quad (1.1)$$

$$d/(gT_{app}^2) = 61/(9.81 \times 10.8^2) = 0.05 \quad (1.2)$$

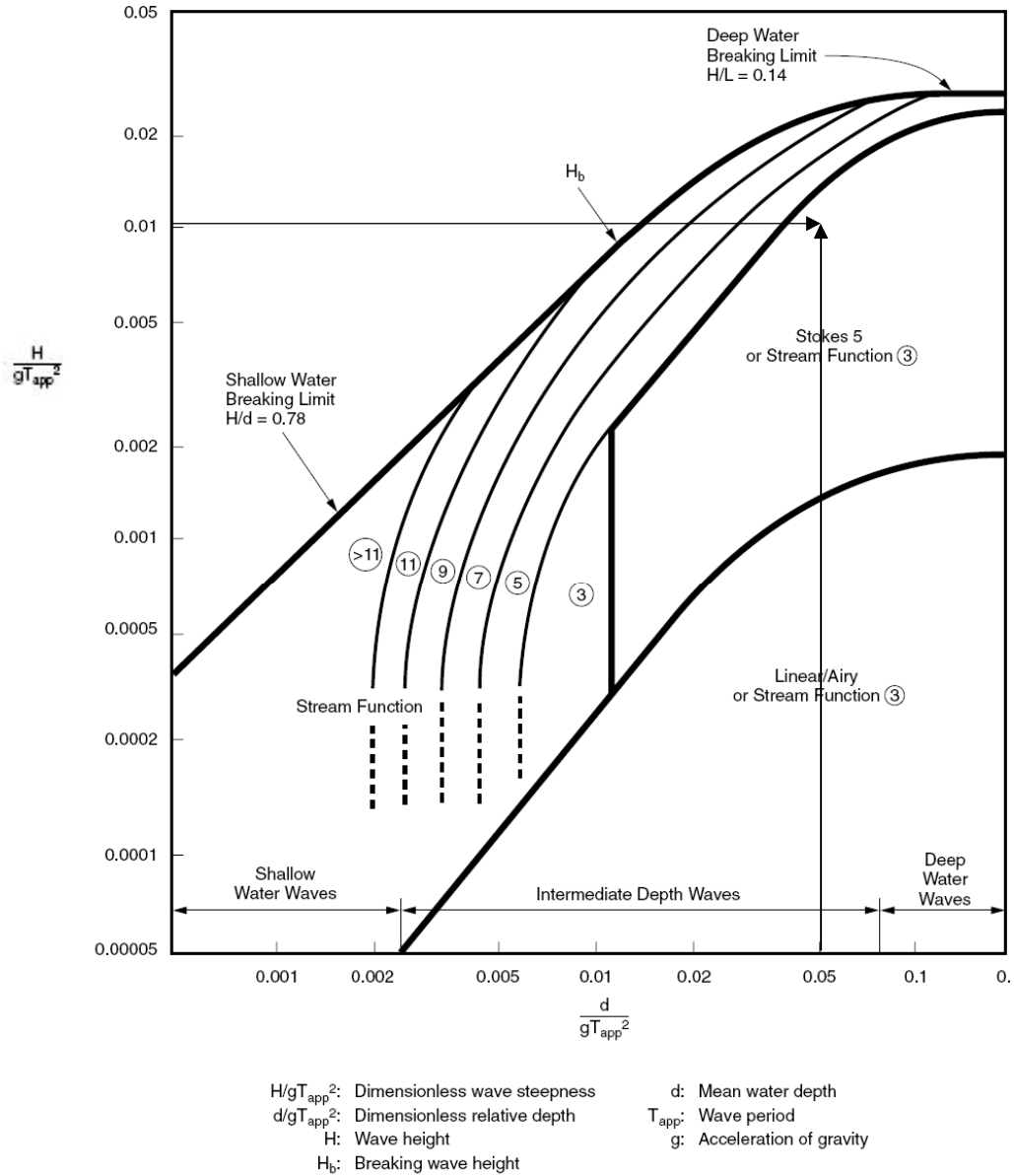


Figure 1.1: Wave Theory used in SACS for Analysis of Jacket Platform [34].

1.5 Design Philosophy

The sustainable development of physical structures depend not only on reliability of structures but also on cost saving. The design uncertainties need to be taken into consideration, when dealing with a balance between safety of structures, purpose and its cost as shown in Figure 1.2. Codes for structural design go through changing process and whenever a new finding is reported and verified, it is incorporated in the

code. API Working stress method is now being replaced by a more robust and logical, limit state design, a probability based method as other codes have already shifted to LRFD. With use of probability, the determination of effects of random variable can be quantified more robustly. Jacket platform is optimised to achieve maximum reliability by using minimum material [35]. Load and Resistance factors are derived so that the structure designed by means of the planned provisions will be at the predefined target level [36]. The advantage of this method is that the latest knowledge can be incorporated into the code, whereas this was not possible for working stress method.

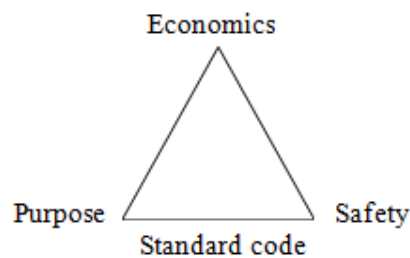


Figure 1.2: Benefits of Standard Codes.

1.5.1 Research Methodology

The randomness with respect to load and uncertainty in structural material requires stochastic/probabilistic methods for analysis. The load and resistance model uncertainties lead us to a safety factor which can cater for these uncertainties and thus a safe structure. W.Wang reports that Freudenthal is the first researcher who came up with statistical approach using structural reliability analysis for design of structures [37]. The reliabilities are found for working stress method (implicit reliability) as well as load and resistance factor design method. Using reliability based methods safety indices are computed for the ultimate limit state. This will be used as a base for evaluation of load factors for this region.

Statistics for resistance include the characteristics of material and geometrical properties. Variability in resistance parameters was found through fitting of it based on probability distribution. The data for resistance was collected from one offshore fabrication yard and for environmental loads the data available from specific

platforms design was used. Statistical parameters (mean, standard deviation, coefficient of variation etc) were obtained for geometrical and material properties. Statistical parameters for environmental loads i.e. wind, wave and current were also evaluated. Statistical modelling of load and resistance with their respective distribution parameters were developed from the available data and compared with data in literature review. Using FORM reliability analysis, the reliability index was determined for component, joint and overall system, which was used for determination of the environmental load factors. To check the extension of life, ISO and API require Jacket should be checked against a load of 10,000 year return period. This was done for all four platforms. Then Bayesian updating technique is used in which first Jacket were preloaded to find the minimum RSR values. This load which gives minimum RSR was used to find the updated probability of failure. This was made for intact and damaged members of Jacket.

1.5.2 Critical Appraisal

WSD and LRFD codes have prominent differences. The WSD considers the uncertainties related to the load and resistance by providing safety factor using judgement and reduction of yield strength to allowable strength. LRFD has the provision to deal with the uncertainties and variations coming from the load and resistance by using random variable statistics. Jacket platforms have to face crucial loading effects, which require proper estimation of loads and design. To cover this aspect WSD is found to be uneconomical and LRFD as efficient.

LRFD results in uniform component and joint safety indices than WSD, for wide range of water depths, loads and platform configurations. It results in lighter Jackets for cases when environmental load to gravity load ratio is low i.e. (shallow water depths, static loading). Heavier Jackets will result where environmental load to gravity load is higher and load and resistance uncertainties are high (deepwater and dynamic loadings) [10]. LRFD provides higher and more consistent safety levels. Environmental load factors based on data for six geographical regions are presented in Table 1.2. The Table clearly shows that the load factors differ according to their environmental conditions [38]. Offshore industry of Malaysia follows the load factors

based on calibration of GOM and North Sea which are considerably higher for this region due to mild weather conditions of Malaysia. It is clear that different regions have different environmental loads and the same can be evaluated for offshore Malaysia.

Table 1.2: Environmental Load Factors [6], [9], [38]

Region	Load factor
Gulf of Mexico	1.35
Central & South North Sea	1.18
Northern North Sea	1.25
NW Australia	1.36
Indonesia	1.0
Mediterranean Sea	1.30

ISO and API require evaluation of probability of failure using 10^4 return period loads for reassessment and extension of life. If we could include results not only from probability of failure but also from probability of survival then a difference is seen in reduction of probability of failure and which have been recommended by researchers [20].

1.6 Originality and Research Contributions

Resistance uncertainty of geometric and material variables for Jacket platforms was determined and this has not been available in this region. Resistance model uncertainty has also not been reported in this region before. The site specific load data for three regions was used to model the load uncertainty variables which have not been reported in previous studies. The reduction in environmental load means a significant reduction of loads which can contribute in reduction of cost of construction. Component, joint and system based load factors proposed have also not been reported for this region previously. Results of this research can be the basis for proposed changes in the provisions of structural design for environmental load factors for this region.

Updating of Jackets reported in unpublished reports from this region are based on finding probability of failure of 10^4 years load. The updating of probability of failure

using Bayesian updating has been reported only in some cases all over the world yet no work has been reported from this region.

1.7 Outline of the Thesis

The thesis is organized into eight chapters which are briefly outlined below:

Chapter one gives an overview of the problem statement, objectives and scope of the work. Reasons are outlined for the justification of this research and brief methodology, critical assessment and outcome of this research are mentioned.

Chapter two discusses the literature review, which forms the basis for this research. The chapter gives a review and summary of the past work done on the given objectives. This Chapter serves as the background for this thesis and also includes critical reviews for the objectives outlined in Chapter one.

Chapter three discusses the research methodology of this study. This covers the statistical analysis made for the resistance variables and load variables. Determination of probability distributions and their parameters for resistance and loads has been explained. Methods used to find the reliability index in this thesis like FORM and Monte Carlo are discussed. Determination of environmental load factors based on component, joints and system reliability are explained. Methodology for Bayesian updating of probability of failure using probability of survival has been outlined.

Chapter four deal with statistical analysis of uncertainty of resistance and load variables. It discusses the statistical features of uncertainty of material resistance and load. Uncertainty of structural characteristics of steel (geometry and material properties) and uncertainty in environmental load was used to find the statistical properties. ISO uncertainty mathematical models were used to find the model uncertainty of component and joint stresses. Probabilistic models for reliability were developed which were used for reliability analysis.

Chapter five deals with the determination of environmental load using component reliability analysis. Members were selected using diameter, thickness and slenderness

ratios. In this chapter component reliability was evaluated for primary members of Jacket i.e. leg, horizontal brace at periphery, horizontal diagonal and diagonal brace members under seven different types of stresses. The environmental load factor was determined using component reliability for four platforms.

Chapter six deals with determination of environmental load using joint reliability analysis. Joints were selected using chord and brace diameter ratios. For joint reliability K, T/Y and X joints were analysed for axial tension, axial compression, in-plane bending and out-plane bending stresses. The environmental load factor was determined using joint reliability for four platforms.

Chapter seven, deals with system reliability and environmental load factor. RSR was used to find the system reliability and the system based environmental load factor. Probability of failure was determined for Jacket platform as per design load and at return period of 10^4 year load. Bayesian updating was used to find probability of failure along with probability of survival at much higher loads for intact and damaged members.

Chapter eight concludes the dissertation with summary of research performed and shows the major findings and achievements of this research. At the end recommendations are made for the areas where this research can lead to for future research.

CHAPTER 2 LITERATURE REVIEW

2.1 Introduction

Risk and safety are two intertwined words. For Jacket platforms safety can be achieved by management of hazards produced by rare events of wave, wind and currents. Material strength of tubular components and joints plays significant role against risk. Structural design is based on load and resistance which are random in nature. The case of offshore Jacket platforms needs special importance, because it deals with loads which are not simple random variable. Environmental load are not like live loads acting on land based structure but are more severe due to unpredictable weather conditions. This environmental load can act with unexpected severity on offshore structures. The resistance can also be reduced due to sudden damage to Jacket. Thus probabilistic techniques are required for estimating the design loads and resistance. This study highlights the reliability analysis of Jackets and significance of different structural and load variables including their respective uncertainties influencing the safety of Jackets.

After treating the uncertainty of resistance and load the issue of structural reliability is dealt with for three areas i.e. component, joint and system. Reassessment of Jacket platforms requires that platform must sustain a load of 10,000 years. Finally minimum RSR values are looked into along with Bayesian updating of probability of failure is also discussed.

2.2 History of Code Development

Offshore platforms are only 65 years old and are fairly new compared to other types of civil engineering structures. The first steel platform was installed in Gulf of Mexico (GOM) in 1947. American Petroleum Institute (API) was the first to publish the code for offshore Jacket platforms namely API RP2A WSD in 1969. This code has been updated throughout these years until recently an errata was issued for 21st edition in March, 2008. It was followed by DNV in Norway and separate guidelines for United Kingdom. Canada and Australia published their own codes for offshore platform design. API LRFD was published in 1993 with errata in 2003 and has not yet been revised. LRFD format of code are probability based code. For API RP2A LRFD code development the target reliability was based on API WSD. The target reliability for a probabilistic code is based on the reliability of platforms designed by existing codes, personal judgement and the safety requirement. ISO 19902 was published in 2007 and is the most updated LRFD code available for steel Jacket platform design today. The hydrocarbon exploring companies like Shell and PETRONAS have developed their own technical standards with respect to geographically specific regions [39], [12]. These standards refer to API RP2A WSD or ISO 19902 for the detailed design and assessment. API WSD is still in practice in most parts of the world due to non availability of regional environmental load factors presented in ISO 19902.

2.2.1 History of Offshore Oil Production

The ever increasing demand for oil and gas has forced engineers to go for offshore exploration, specifically during the energy crises of 1970's. Prior to 1947 offshore Jacket model, most of offshore operations were based on wooden piled decks, connected to shores through trestles [40]. In 1947, Kerr Mcgee-Phillips-Stanolind group used 22 piles to support a drilling deck in Gulf of Mexico in 6.1 m water depth opened a new chapter in marine soil operations. Jacket piles were driven through vertical legs and acted as anchors. Today Jacket platforms in water depth of more than 300 m, are built to withstand the huge forces of nature such as hurricanes and

typhoons [32]. The demand for more hydrocarbons has forced us to go into ever deeper ocean waters with hostile environment for exploration and production. Nowadays offshore structures taller than the Eiffel tower are designed to withstand extremely rare waves of more than 30 m high, collision with ships, scour at mud line, earthquakes or other environmental hazards [41].

Brunei in 1929 became the first country in South East Asia to produce hydrocarbons [13]. In 1992 there were 65 number of platforms in Baram delta Sarawak and 120 in rest of Malaysia [13]. For offshore Malaysia, Baram delta is the biggest and have platforms with integrated drilling, production and quarters facilities [13]. This figure reaches today to 249 platforms in offshore Malaysia.

2.3 LRFD and WSD Codes of Practice

Structural design codes provide a set of minimum technical guideline for satisfactory design. They also provide a path for research findings to create their way into practice of this field [42]. The LRFD method treats the load according to their types and the loads dominated by environment are treated appropriately. Structural design depends on uncertainties which come from environmental loads and resistance of material. The geographical variation of environmental load is so much that ISO 19902 has reported that due to uncertainty of load and resistance load factors should be ascertained in each region separately. Appendix A shows the numerical comparison between API WSD, API LRFD and ISO codes.

2.3.1 API RP2A- WSD

API WSD uses safety factor which is same for all types of loads, whereas API LRFD and ISO use different factors based on each type of stresses. WSD code safety factors have been found empirically [26]. In WSD allowable stresses are either expressed implicitly as a fraction of yield stress or buckling stress or by applying a safety factor on critical buckling stress [43]. WSD strength of component or joint can be evaluated by using Equation (2.1),

$$\frac{R}{FS} \geq D_l + L_l + E_l \quad (2.1)$$

Where, R= resistance effect, FS = factor of safety, D_l = dead load, L_l = live load E_l = environmental load. WSD method is based on safety factor provided only to the resistance of the material without considering the uncertainties related to the loads as shown in Equation (2.2),

$$Q < \phi R \quad (2.2)$$

Where Q = load and ϕ = material strength safety factor and it covers the randomness of material and load. This safety factor theory is based on the assumed concept that probability distributions of Q and R exist but not known [44]. Thus a large value of load $Q = Q_1$ is taken and low value of resistance $R=R_1$ is taken (allowable yield strength is less than the specified yield strength of steel), the factor of safety takes into consideration the uncertainties as shown in Equation (2.3),

$$FS=R_1/Q_1 \quad (2.3)$$

Where R_1 and Q_1 are resistance and load typical values. If $Q_1 < R_1$ i.e. if load is smaller than resistance, structure is safe but if $Q_1 > R_1$, then it means failure of structure. So to avoid any damage to structure, safety factor is provided in advance at design stage.

In working stress, design resistance is divided by a factor of safety but LRFD takes into consideration the inherent natural uncertainties in applied action and resistance of components [1]. Due to this discrepancy LRFD method of design has been introduced to replace WSD. In the limit state design these uncertainties of load and resistance are considered more realistically by using reliability analysis methods. The drawbacks of WSD code has been outlined by Brand et al [45], it is excessively conservative and does not provide engineer any insight of degree of risk or design safety of Jacket. It has no risk balanced capabilities and there is little justification for safety factors. Bilal reports that uncertainty using deterministic factors of safety, could lead to inconsistent reliability levels and may produce over design. WSD does not provide insights into the effects of individual uncertainties and real safety margins [46]. The main disadvantages of deterministic measure are shown below:

- i) Structural model uncertainty
- ii) Uncertainty of external loads

- iii) Human error

2.3.2 API RP2A- LRFD / ISO 19902

The first code using limit state design based on probabilistic analysis was formulated by Canada for cold formed steel members in 1974 [47]. Denmark and Norwegian Certifying Authority, DNV was the first to introduce the limit state design code for Jacket platform which was published in 1977 [1], [11], [22], [48]. In 1993, API RP2A-LRFD, was published and it has been updated by ISO 19900 series of codes for offshore structures. In this method, resistance and load are factored using uncertainty. This type of design is described as balanced design as it provides a balanced allocation of resources [49]. LRFD provides a safe and economically efficient way of designing Jackets to different environmental load conditions. It is also able to incorporate regional and geographical conditions in the design. Instead of factor of safety we use load and resistance factor. In LRFD, the load combination Equation is shown in Equation (2.4),

$$\phi R_n \geq \gamma_D D_l + \gamma_L L_l + \gamma_w E_l \quad (2.4)$$

Where, R_n = nominal resistance, γ_D = dead load factor, D_l = Nominal dead load, γ_L = live load factor, L_l = Nominal live load, γ_w = environmental load factor, E_l = Nominal environmental load (100 year extreme). LRFD format can be represented in more general way in Equation (2.5),

$$\phi R = \sum_{i=1}^n \gamma_i Q_i \quad (2.5)$$

Where R = characteristic / nominal value of resistance, Q_i = characteristic or nominal value of load, ϕ = resistance factor (for uncertainty in stress), γ_i = load factor (for uncertainty in load), n = number/ type of load components (Gravity load and environmental load).

The work for finding load and resistance factors for different offshore regions has made much progress such as North Sea, Mediterranean Sea, Canada , Australia, South China Sea, Bohai Sea and Gulf of Guinea. API RP2A LRFD has been adopted for use in the North Sea, UK sector after an initial transition period during which appropriate load factors were developed. Large majority of platforms installed in the

UK sector after 1995 were also designed using the LRFD format in preference to the WSD [8], [48]. The effect of load variables is significant in different regions of world depending on geography. Specifically the regions near equator, where climate is mild and there is less chance of rare events occurring significantly.

2.3.3 Benefits of Limit State Design Code

LRFD approach provides logical thinking while designing the structures i.e. it considers the uncertainties of resistance and load. Semi-probabilistic approach simplifies the design process. Safety factor calculation remains deterministic one, but load and resistance factors are established depending on the requirement of structures whose reliability is chosen in advance. Nominal load and resistance values can be same in WSD and LRFD codes. LRFD code takes factors which are chosen taking into consideration uncertainty in relation to action and resistance i.e. spread of values, insufficient data. We can derive resistance and load factors by using probabilistic methods design criteria. Factors are adjusted with a uniform degree of reliability to all structural elements in a given class of structure [44]. For instance, each type of stress can be dealt accordingly like axial compression or axial tension. Furthermore as more test data on variables become available, these factors can be modified as per the updated statistical parameters of random variables.

Dead, live and environmental loads are treated separately using probabilistic methods and each type of load is taken after making statistical analysis. These factors can be increased in case of structures which are at high risk like nuclear power plants or offshore structures but can be decreased for low risk structures. WSD uses same factors for both types of structures. The benefits of LRFD can be outlined below:

- i) It gives superior consistency in the reliability of offshore Jacket platforms.
- ii) LRFD has efficient utilization of materials compared to factor of safety design method i.e. WSD.
- iii) Randomness and uncertainties can be taken care off more specifically.

iv) Platforms can be designed as per the actual requirements of operator i.e. specific for certain location, type and life span.

v) This is based on logical interpretation of new research.

vi) Since deck is designed using AISC (2005) which is reliability based design code, it is logical that Jacket should also be designed using LRFD code.

vii) LRFD provides incentives for research with regard to uncertainties, which take part for determination of partial load factors.

2.3.4 Safety Factor

Any structure designed and built with latest knowledge cannot claim to be free from chance of failure. The safety factor is used to give allowance for variation of material and load uncertainties of Jacket platforms. Optimal safety margin for design of Jacket may be observed as problem which involves trade-off between cost and acceptable failure probability [18]. It is a known fact that design involves many uncertainties which are not clear at the time of design. Thus the structural engineer uses probabilistic reasoning for design of structure. The selection process of partial safety factors is called code calibration [50]. The calibration of safety factor is done in such a way that large safety factor is provided in presence of large uncertainties whereas small safety factor is provided in small uncertainties. Code developers assume certain values for basic parameters, which are expected to cover for the uncertainties involved with the material properties during the entire life of the structure. Based on these uncertainties, the model Equations are developed which contain some factors. These are called factors of safety in WSD and load and resistance factors in limit state design and provide a high level of assurance that the structure will perform satisfactorily. This is defined as ratio of expected strength of response of Jacket to expected applied loads [51].

Despite all these safety factors, due to some unforeseen load condition, some member resistance problem may cause the failure of structure [44]. Structural failures demonstrate that however the design is considered safe still accident happen.

Offshore accidents cause not only loss of lives but also produce economic losses and environmental catastrophe.

2.3.5 Jacket Platform Design in Malaysia

In Malaysia API RP2A WSD is used by offshore design and fabrication industry along with PETRONAS technical standard (PTS), for local environmental load parameters. Soon ISO 19902 code will be used to design the Jackets platform with an environmental load factor of 1.35. The application of environmental load factors which is optimised for GOM offshore region and materials, may be not be reasonable for Malaysian waters [52]. The calibration of load factor has never been done so far in this region.

2.4 Uncertainty

Load and resistance are considered as random variables. The main uncertainties deal with the tolerance to which structural members are built and the loads and environmental conditions to which they will be exposed throughout their life [41]. This variation is stated by the probability distribution function and their correlation function if it is considered. In this study random variables are treated as independent and no correlation is taken into consideration. Figure 2.1 shows the types of uncertainty used for reliability analysis.

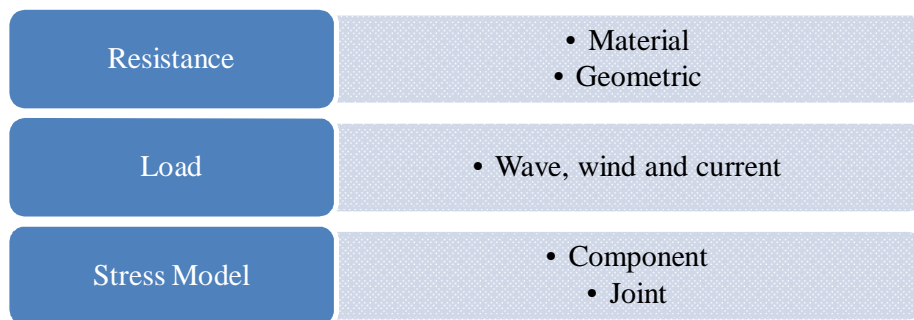


Figure 2.1: Types of Uncertainties

2.4.1 Basic Uncertainty

Modelling of uncertainty is based on the mean (central tendency), the variance (dispersion about the mean) and probability distribution functions [53]. Structural reliability is based on the theory of probability and its treatment to different uncertainties whose role is dominant as far as behaviour of structure is concerned. These uncertainties, if not treated properly, may cause failure, collapse or damage to structure which may become unserviceable and threat to environment. These problems can only be solved by introducing the probability to account for the risks involved in the uncertain design of offshore Jacket platforms. Uncertainties are dealt with by taking into consideration random variable parameters of load and resistance. Uncertainty modelling is the first important step for the reliability analysis for the Jacket platforms. The reliability analysis is significantly dependent and very susceptible to uncertainty modelling [54].

Structural analysis calculations of offshore platforms are also subject to uncertainties. Uncertainties are analysed based on how much basic information is available about that random variable parameter [35]. Modelling uncertainties are introduced by all physical models used to predict the load effects and the structural response [55]. The results are based on geometric and material variability. Equation (2.6) defines the risk and probability of failure of structure. Probabilistic calculation techniques enable these uncertainties to be taken into account. They provide a probability that it will resist the load, (probability that it will not resist the load known as the failure probability of the member) which characterizes its reliability.

$$\text{Risk} = 1 - \text{Reliability} \quad (2.6)$$

Jacket will fail if strength is less than the applied load and probability of failure is shown by Equation (2.7),

$$P_f = \text{Resistance (strength)} < \text{Load} \quad (2.7)$$

Uncertainty reflects lack of information it could be on the load side or on resistance side [56]. Uncertainties deal with how much load we shall consider for

design (loading) and how much load a structure can withstand (resistances). We do not know how big are the largest waves the Jacket will be exposed to throughout the expected design life of the Jacket. This will depend on the geographic location and the design life of Jacket. For instance, in GOM, chances of rare event occurring within expected design life will be higher than in Malaysia. This extreme and rare wave height for design is assumed to occur once every 100 years thus it has a probability of 0.01 of occurrence in a given year. Figure 2.2 shows the exceedance probability curve for wave height at GOM site up to 10,000 years.

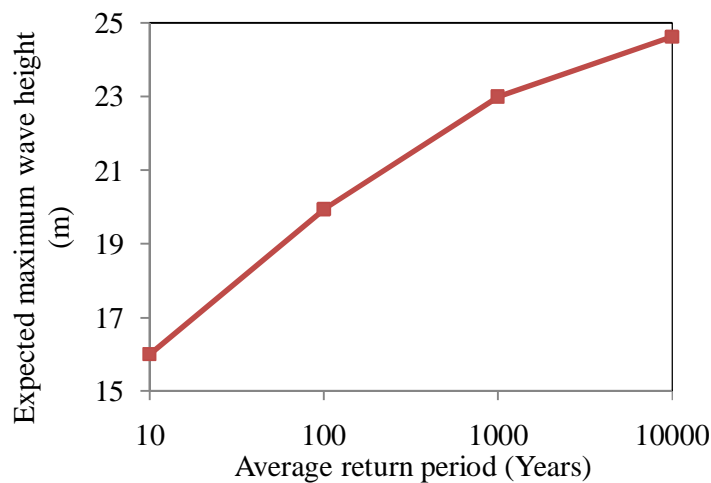


Figure 2.2: Exceedance Probability Curve for Wave Height in GOM [57]

Probabilistic calibration is done to find safety factors in a balanced manner. This takes into consideration the sources of uncertainty in environmental loads and material resistance [58]. Failure of structures has shown us that it is impossible to build a risk free structure. This is due to the nature of extreme environmental loads and uncertainty in material, fabrication, construction, human error and structural analysis of Jacket platforms [3]. Failure of ocean structures has huge impact on oil industry. Such failures have catastrophic effect on the industry. The notable ones are Alexander Kielland (Norway-1980), Ocean ranger (Canada-1985), Piper Alpha (North Sea, UK 1988) Petrobras -36 (Brazil 2001), Deepwater horizon (USA 2011). The failure mode of above five structures was fatigue, buoyancy control system

failure, natural gas fire, buoyancy control system failure and explosion and fire respectively.

2.4.2 Sources of Uncertainty

Uncertainty determination is based on computational tools. This enables the determination of analytical results by determining the component and joint safety, subjected to the uncertain variable loads and resistances during design [35]. There are many sources of uncertainty which are defined below:

2.4.2.1 Natural

This comes from randomness of loads and material resistance and is difficult to control. An example is the tsunami which hit Japan in 2011. Natural and inbuilt randomness of environmental loads and earthquake, which are acting on the structure like wave, wind and current contain uncertainty of time, period, interval magnitude, parameters (height, direction). The Jacket may be exposed to 100 year wave height during its service life. Deterministic calculations verify that each member of the structure can withstand the hundred year wave. The material uncertainty includes yield strength, ductility and elongation. These can be due to operating i.e. fatigue or extreme environmental i.e. storm or extreme natural calamity i.e. earthquake [35].

2.4.2.2 Statistical Uncertainty

This type of uncertainty is related to statistical modelling of distribution of the random parameters [13], [49]. If number of data points are increased this type of uncertainty is reduced.

2.4.2.3 Human Mistakes

This type of uncertainty depends on knowledge of person designing the structure, construction and operation of the structure like piper alpha disaster in 1988 caused by

communication gap between platform operators. Statistical analysis of failure show that 90% of these failures are due to human errors [47].

2.4.3 Parameters of Uncertainty

Variability of member resistance and environmental load parameters can be found through collection of data and fitting of it using probability distribution. Statistical parameters (mean, standard deviation, coefficient of variation etc) can be obtained for the random variables.

2.4.3.1 Random Variables

For structural design, it is extremely important to evaluate the probability of failure and safety levels of a Jacket, especially in the event when variables are random. The variables used for reliability analysis for Jacket platforms are geometric, material properties and loads suggested in literature and are not considered as deterministic [59]. The structural safety is shown by two independent properties i.e. Load effect forces (moments, axial, and shear forces) acting on the structure or its components due to applied forces and strength or resistance, both are random variables. In the case of load effects, these are the forces caused by man, material and nature, and for the case of resistance these are due to the mechanical and geometrical properties of material.

2.4.3.2 Bias

Bias is defined as a ratio of actual capacity to calculated capacity [60]. It can also be defined as mean value over nominal value. It will always be there for geometric variables. For resistance variables mean bias is found by average of measured values against the actual test results or dimension provided by design engineer. If mean value is not equal to 1.0 it shows that it has a bias in the model [61]. Some risk of bias of the analysis will be there always when using computational models, which can define safe and unsafe platforms [62].

2.4.3.3 *Return Period*

API and ISO objectives are defined and report that offshore structures should have ability to withstand the 100 year storm load. The environmental loads acting on the structure are random variables. This makes the reliable estimation of offshore loads for their design life difficult. Random nature of offshore environment can only be estimated by taking into consideration return period of probabilistic models of environmental loads. For Jacket design it is 100 years and for reassessment and life extension it is 10,000 years. In North Sea with 100 year wave the 10 year return period of current have been used as further explained in 3.3.1.

2.4.3.4 *Distribution Types*

Type of distributions for random variables is an important factor for reliability analysis. For rare events the extreme types of distributions are used and for geometric and material resistance, commonly normal or lognormal distributions have been used in literature. Distribution and their parameters are compulsory tools for level III reliability.

2.4.4 Types of Resistance Uncertainty

2.4.4.1 *Geometrical and Material*

This uncertainty relates to the randomness due to geometrical and material variations. This is related to straightness, diameter, thickness, length, yield strength, elongation and tensile strength. Birades et al.[26] take diameter, thickness, young's modulus and yield strength variables for material uncertainty. This type of uncertainty can be dealt properly with the application of controlled manufacturing and fabrication by using international standards and quality control. Many researchers have been working on resistance uncertainty, such as [3], [63] ,[64], [65]. Material properties used for assessment should be estimated using actual material properties of existing structures [66]. But still there are minor but important variations remain between characteristic

values mentioned on structural drawings and fabricated Jacket components placed at site as shown in Chapter 3.

2.4.4.2 *Physical Stress Model*

Model uncertainty is due to deviation of material strengths, from component or joint stress biases, with respect to actual strength acquired from tests results [58]. This type of uncertainty accounts for possible deviation of model assumptions of the resistance of a given section from the actual resistance of geometrical properties. The load model may also show variation due to natural variation in loads. This type of uncertainty is related to shortage of knowledge, information or unavailability of software. These can be reduced by applying the more detailed methods as shown by [49]. Norwegian regulation mentions, “Design loading effects and design resistances are computed by using deterministic computational models. These models shall aim at giving expected average values without introducing any increase or reduction in safety. The uncertainty of the computational models being included in the partial coefficients [62]. Table 2.1 shows the stress model uncertainty considered in this research.

Table 2.1: Uncertainties in Model Predictions

Component		Joint
Tension	Tension and Bending	Tension
Compression Column Buckling	Compression (Column Buckling) and Bending	Compression
Compression Local Buckling	Compression (Local Buckling) and Bending	In-plane bending
Shear	Tension and Bending and Hydrostatic pressure	Out-plane bending
Bending	Compression (Column Buckling) , Bending and Hydrostatic pressure	-
Hydrostatic	Compression (Local Buckling) and Hydrostatic Pressure	-

Table 2.2: Model Uncertainty for Mediterranean Sea using API WSD 18 ED [9].

Tubular member		X_m	COV
Tension and Bending		1.093	0.058
Compression (Column Buckling) and Bending		1.075	0.053
Compression (Local Buckling) and Bending		1.222	0.064
Hydrostatic		0.99	0.095
Tension and Bending and Hydrostatic Pressure		1.018	0.106
Compression (Local Buckling) and Hydrostatic Pressure		1.082	0.104
Joints			
K	Tension / Compression	1.32	0.028
	IPB	1.185	0.183
	OPB	1.113	0.179
T/Y	Tension	2.207	0.401
	Compression	1.306	0.291
	IPB	1.296	0.328
	OPB	1.388	0.354
X	Tension	2.159	0.546
	Compression	1.145	0.144
	IPB	1.595	0.250
	OPB	1.147	0.250

Table 2.2 shows the model uncertainty (X_m) based on Mediterranean Sea. It should be remembered here that it is based on API RP 2A WSD 18th Ed. There have been large changes in API RP 2A 21st Ed. published in 2008 particularly for joint models.

2.5 Previous Work Done on Resistance Uncertainty

ISO 19902 Clause 7.7.4 requires that the test / measured data should be validated by simulation for the resistance of material taking into account the structural behaviour variability of material [7]. DNV report 30.6 recommends that for resistance model, normal distribution should be considered for the reliability analysis of Jacket platforms [61]. The difference between strength and load variable is highlighted by the fact that strength variable is considered unsuitable if its value is less than the mean value as it may cause failure. For model Equations the mean value should be greater than 1.0 which shows the conservativeness of code Equations and usually normal distribution is assumed for it [67]. The load variable is unsuitable, if it is greater than its mean value which can cause failure. Previous studies on resistance of material

have been made by many authors [38], [50], [63], [68], [22], [69] No information is available about any similar study conducted in Malaysia.

Structural design strength is based on characteristic values of basic random variables of resistance. The behaviour of these variables of strength may vary in such a way that they become unsafe during any time of their design life. Structure can fail if the characteristic value of load exceeds the characteristic load carrying capability. Uncertainty determination is based on computational tools available at hand. This enables correct analysis by determining the component safety, subjected to the uncertain variable loads and resistances during design [35]. Generally load tends to increase with time whereas resistance tends to decrease with time. Thus uncertainty of load and resistance increases with time [70]. Ellingwood says that the result of uncertainty is risk, which is defined as ‘the product of the probability of failure and costs associated with failure of structure’ [71]. High probability of failure means low reliability thus cost of failure will be high. These problems can only be solved by introducing the probability into account for the risks involved for the uncertain design of offshore Jacket platforms.

The strength of Jacket depends on the variability of its components from which the member is built. The primary members of Jacket are piles, legs, horizontal periphery braces, horizontal internal braces and vertical diagonal braces. Jacket members are in seven different types of stresses and joints are in four types of stresses. Code provides Equations to find these stresses based on resistance of random variables from which members are fabricated. Table 2.3 shows the uncertainties related to offshore Jacket platforms. Here in this study, material and geometric uncertainties are discussed, due to their relevance to ultimate limit state design. This is the most significant limit state design as compared to other types of limit states.

Table 2.3: Resistance Uncertainties for Jacket Platforms

Types of Resistance uncertainty	Example
Material uncertainty	Yield strength, modulus of elasticity, elongation, tensile strength
Geometric uncertainty	Diameter, thickness
Fatigue uncertainty	Degradation of material
Corrosion uncertainty	Degradation of material

The probability of failure can be updated if changes in COV have been known i.e. after the design of Jacket members or joints. This can be from material tests results or actual geometrical properties statistical analysis. For instance at design stage the COV taken was 0.15 but when actual material test report was issued and it becomes known that the actual COV was 0.1. Using the reliability analysis new probability of failure can be determined [56]. In this study fatigue and corrosion uncertainty are not discussed further. In this research fatigue and corrosion uncertainty are not discussed further.

2.5.1 Material Uncertainty

Materials like steel have variability due to construction practices. The basic strength or resistance uncertainty includes yield strength, elastic modulus (Young's modulus). ISO takes yield strength distribution for North Sea as log normal. Bias of 1.127 and standard deviation of 0.057 was achieved in the study [69]. Duan takes yield strength distribution for China as normal, with a bias of 1.0 and COV of 0.05 was achieved in the study [22].

2.5.2 Characteristic Resistance

Characteristic resistance should have low probability of being exceeded at any specified design life of Jacket. It is defined as that value below which not more than 5% of the test results of large number of test would fall [72] or it is 0.05 fractile of a lower end of normal distributions [73], [74]. Characteristic strength should be equal to guaranteed yield strength but shall not exceed 0.8 times the guaranteed tensile strength [62] or minimum of upper yield strength. Characteristic value of geometric quantity are the dimensions specified by the design engineer [73].

2.5.3 Geometric Uncertainty

The structure can fail due to resistance failure from variation in dimension and fabrication errors. The geometrical uncertainties include diameter, thickness and length and effective length factor. ISO reports following results for statistical

properties of geometry of tubular members [69]. Normal Distribution was taken for diameter, thickness, length and effective length factor for leg and brace. Mean bias of 1.0 and COV of 0.0025 was achieved for diameter. Mean bias of 1.0 and COV of $(0.004+0.25/T)$ was achieved for thickness. Mean bias of 1.0 and COV of 0.0025 was achieved for length. Mean bias of 1.1 and standard deviation of 0.0935 was achieved for effective length factor for leg member. For braces the mean bias was achieved as 0.875 and COV of 0.097. Further details can be found in Table 4.2.

2.5.4 Resistance Model Uncertainty

The modelling uncertainty is predicted from the ISO code Equations. Seven component stresses and four joint stresses for each joint types are modelled for resistance. The uncertainty model for resistance (X_m) is shown by Equation (2.8),

$$X_m = \frac{\text{Actual Resistance}}{\text{Predicted Resistance}} \quad (2.8)$$

This model uncertainty depends on the statistical parameters for basic variables i.e. diameter, thickness, yield strength, modulus of elasticity. The detailed results from literature are shown in Table 4.4-4.6.

2.5.4.1 Single Stresses

The variation of model uncertainty for single stress has been reported by ISO and BOMEL [7, 69]. Mean bias for tensile strength was achieved as 1.0 with standard deviation of 0.0. For column buckling strength, from experimental tests results it was found to be with a bias of 1.057, COV of 0.041 and standard deviation of 0.043. For local buckling, mean bias was 1.065 standard deviation of 0.073 and COV of 0.068. For bending the experimental bias was reported to be 1.109, COV was 0.085 and standard deviation was 0.094. The experimental bias for hoop buckling was found to be 1.142 and COV was 0.124 and standard deviation was 0.1416.

2.5.4.2 *Double Stresses*

The variation of model uncertainty for two combined stresses have been reported by ISO and BOMEL [7, 69]. For tension and bending the bias was found to be 1.109 and standard deviation was 0.094. For compression and bending the experimental bias for compression (local buckling) and bending was found to be 1.246, COV was 0.067 and standard deviation of 0.084. For compression (column buckling) mean bias was 1.03, COV was 0.082 and standard deviation was 0.084.

2.5.4.3 *Three Stresses*

The variation of model uncertainty for three combined stresses have been reported by ISO and BOMEL [7], [69], [75]. For tension, bending and hydrostatic pressure the experimental bias for axial tension, bending and hydrostatic pressure was found to be 1.075, COV was 0.098 and standard deviation was 0.105. For compression, bending and hydrostatic pressure the experimental bias for compression (short column), bending and hydrostatic pressure was found to be 1.199 and COV was 0.134 and standard deviation was 0.161. The experimental bias for compression (long column), bending and hydrostatic pressure was found to be 1.197, COV was 0.091 and standard deviation was 0.109.

2.5.5 Critical Review of Resistance Uncertainty

Safety and risk are associated concepts though different in character i.e. risk is quantifiable but safety is not, it is something to be achieved or assured [76]. The safety of Jacket platforms can be assured within risk management by considering the hazards to which they are subjected. It is emphasised by ISO code that resistance modelling has to be done for each geographic region. Studies based on ISO and China report that the geometrical variables were normally distributed. The yield strength distribution was found to be log-normal for ISO in North Sea but Det Norske Veritas (DNV) in one of its reports takes it as Normal. Study made in China reported it to be normal. The difference in variables was not much high, as was expected due to quality control on fabrication and manufacture of materials nowadays. Literature

on resistance uncertainty was not available in Malaysia and therefore this issue will be dealt in this study. The influence of yield strength and model uncertainty on reliability analysis has been emphasised by many researchers working in this area.

2.6 Load Uncertainty

Proper evaluation of load is the most important step for the design of structure. Sustainable development requires structural robustness of Jacket platforms against extreme environmental events. Environmental load uncertainty, considered safe during design of a Jacket platform may become unsafe during one hurricane event in GOM. This was experienced during hurricane Ivan in 2004. Reliability analysis of Jacket platforms require load models should be based on probability distribution due to random nature of loads. The variability of load is considered random in nature and during reliability analysis, probability distribution and its parameters are used instead of a deterministic value.

Extreme value distributions i.e. Fretchet, Weibull and Gumbel, are three theoretical distributions which are commonly applied to model load uncertainty parameters.[77] These distributions are formulated for the maximum, of an infinite number of events. It is easy to apply them as they represent the maximum load intensity to capture the tail characteristics of these distributions. Many researchers have selected the Weibull distribution for environmental load uncertainty [78], [79],[80].

2.6.1 Load Uncertainty Parameters

There are two basic approaches to find the environmental load factor parameters i.e. energy spectral density and statistical analysis method [34]. Here in this study the second approach has been adopted.

2.6.1.1 Characteristic Load

Characteristic value is taken as the most probable extreme value with a specified return period. The characteristic value of environmental load for extreme conditions

is defined as the most probable largest value in a period of 100 years [62]. The nominal value is the value of random variable which has a probability of not being exceeded during reference period of 100 years as prescribed by ISO 19902. It is the maximum value corresponding to load effect with a standard probability of exceedance. It is the fractile in upper end of normally distributed function of load [74]. Primary environmental loads for fixed Jackets include waves, wind and currents but most of time waves, are the dominating load effect [62], [81].

2.6.1.2 Return Period Probability

Return period probability is shown in Equation (2.9),

$$P = 1 - p^n \quad (2.9)$$

Where, n = platform life in years (30 years), p = annual probability that the event will not occur. Probability of occurrence of an event in 100 years is given by,

$$1/100 = 0.01$$

A return period of 100 years means an annual probability of occurrence of 0.01 or probability of non-occurrence of 0.99

$$P = 1 - (0.99)^{30} = 0.26 \text{ or } 26\%$$

Probability that it will experience at least one event with a return period of 100 years during its life is 26%.

2.6.2 Statistical Data Uncertainty for Environmental Load

Environmental loads vary significantly due to uncertainty of wind, wave and current. Environmental loads are highly variable and the Jacket may fail from overloading effects as they sometime may be more than the design loads. The COV of extreme environmental loading for North Sea is 65% and GOM is 77% [28]. The intense tropical cyclones (typhoons) in the Pacific Ocean create governing extreme conditions in this area. Storm is termed as three phase progress of severe sea involving a development, a peak and decay phase as shown in Figure 2.3. The total duration may be between 12-39 hours of sea state, characterised by development phase i.e. growth (0-18) hrs, a peak duration of 3 hrs (18-21) and subsequent decay phase duration of 21

to 39 hrs i.e. 18 hrs [14], [82], [83]. The wave is the dominant load here along with gravity loads. The effects of any load which are less than 10% of the effects of any other type of load may be ignored like wind loads [84].

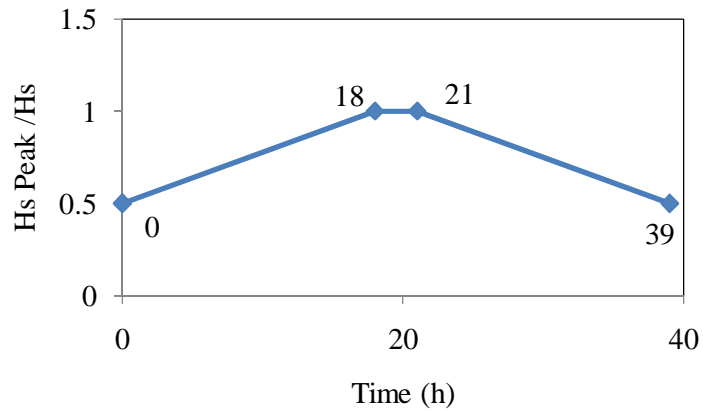


Figure 2.3: Development of Storm growth, Peak and Decay [82] [83]

The extrapolation of probabilistic models is based on distribution functions plotted in straight ascending lines. The wind speed, wave height, time period and current speed are plotted against the return period. Straight line is fitted to the plotted data and it is extended beyond the available data to acquire the estimation of extreme values for the desired return periods as shown in Figure 2.4. This straight line based on fit to the data, may be subject to some errors on uncertainty of extrapolation [79]. The errors can only be decreased by increasing the data points with extended time period.

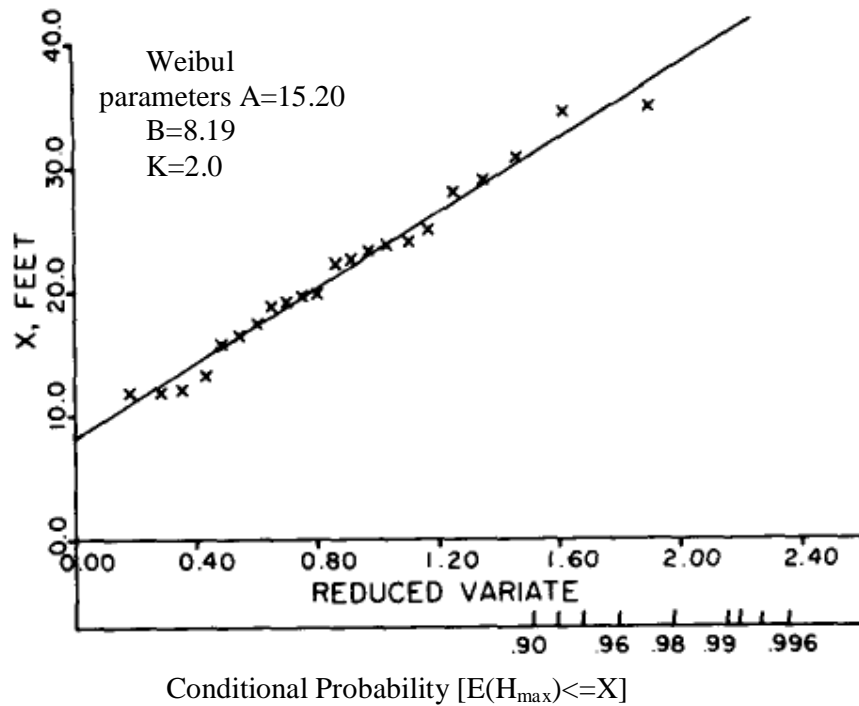


Figure 2.4: Straight Line Representation of Distribution Function [79]

2.6.2.1 Collection of Data

ISO code points out that the statistics of long-term estimation of metocean parameters requires that the individual number of storms used for the statistical analysis must be statistically independent. Wave height taken at hourly rate depends on the wave height of the previous hour. Thus situation of independence of wave is not achieved. To produce independent data points, only numbers of storms are considered for the statistical analysis. Collection of data for wave height is made in two steps:

- i) Long term statistics is based on the highest significant wave height and its associated period. The data are taken from storm data. It is taken for average of 20 minute time periods, and recorded after 3 hour intervals.

ii) Short term statistics uses expected amplitude of highest wave. Such an extreme sea state is estimated, from assumption of linearity. Thus the higher peaks are taken as Rayleigh distributed.

2.6.2.2 Weibull Distribution

Weibull 2-parameter distribution is an extreme value distribution. It is used to capture the variability of rare event which may occur once during the return period. The variable x , has the CDF as shown in Equation (2.10),

$$F(x; a, b) = 1 - \exp\left[-\left(\frac{x}{a}\right)^b\right] \quad (2.10)$$

Parameters a = scale and b = shape, $F(x; a, b)$ =Cumulative Distribution Function (CDF) of variables a , b . Their linear form can be shown by taking the natural logs twice of CDF of Equation (2.9) in $x_{(i)}$, Equation (2.11) [85] shows that,

$$\ln\{-\ln[1 - F(x_{(i)})]\} = -b \ln(a) + b \ln(x_{(i)}) \quad (2.11)$$

The plotting of $\ln\{-\ln[1 - F(x_{(i)})]\}$ against the data $x_{(i)}$ results in a straight line, if the data came from Weibull distribution. The parameter “ a ” is found from intercept and “ b ” by slope of straight line. The slope corresponds to shape and intercept to scale parameters. Scale parameters, scale the model ‘F’ on the measurement axis. This parameters show the horizontal stretching or contracting of the model ‘F’. They are shown always in the following form as “ a ” in $\frac{x-b}{a}$. The shape parameter determines the basic shape of function ‘F’, gives a measure of dispersion. This parameter does not relate to x in a set arrangement common to all models ‘F’ [85].

2.6.2.3 Gumbel Distribution

The Gumbel distribution variable x , has the CDF as shown in Equation (2.12),

$$F(x; c, d) = \exp\left\{-\exp\left[-\frac{x-c}{d}\right]\right\} \quad (2.12)$$

Parameters c =location and d =scale. Their linear form can be shown by taking the natural logs twice of CDF as shown in Equation (2.13) in $x_{(i)}$, [85]

$$-\ln\{-\ln[F(x_{(i)})]\} = -d(c) + d(x_{(i)}) \quad (2.13)$$

The plotting of $-\ln\{-\ln[F(x_{(i)})]\}$ against the data $x_{(i)}$ results in a straight line, if the data came from Gumbel distribution. The parameter “d” is found from intercept and “c” by slope of straight line. The slope corresponds to location and intercept to scale parameters. Location parameters locate the model F on its measurement axis. They are identified by their relation to x in the function ‘F’, i.e. (x-c) in (2.12). Scale parameters, scale the model ‘F’ on the measurement axis. This parameter shows the horizontal stretching or contracting of the model ‘F’ [85].

2.6.2.4 *Wave*

The primary parameter in the classification of sea states is the wave height, which is calculated from peak to trough. The actual selection of design wave height, to be used for specific platforms design is a matter of engineering knowledge and judgement. Jacket platforms are inherently more sensitive to waves than current and winds [80], [86], [87]. This is due to peak response always occur at the time of maximum wave height [86], [88]. During a conventionally short time period of 20 min for a sea state to be regarded as statistically stationary, the most important measure is significant wave height, which is a average wave height of highest one-third of the waves. Only wave parameters were taken into consideration for calibration of environmental load factor for API RP 2A LRFD. Mean bias and COV was set up as 0.70 and 37% [7]. This was same as for wind, therefore only wave was considered for reliability analysis. Weibull distribution fits well with significant wave height [89]. Design wave height is obtained by multiplying the significant wave height by a factor in range of 1.8-2.0 [90].

2.6.2.5 *Current*

Currents can play significant role in total forces acting on Jacket platform. Current refers to motion of water which arises from sources other than surface waves. Tidal currents arise from astronomical forces and wind- drift currents arise from drag of local wind on water surface [91]. When extreme waves along with super-imposed current occur in same direction velocities from both can combine and produce large

wave pressure [52]. Independence of wave should be assumed because there is no reason to believe that extreme wave will occur at the same time as extreme current [26]. The maximum wave height and maximum current occurred only once simultaneously out of 38 storms in North Sea [92].

This current load may never reach the probability of failure of 10^{-1} in the region of Malaysia. During storm conditions, current give rise to horizontal structural forces equal to 10% of the wave induced forces [93]. Even in Norwegian continental shelf, current load experienced is not higher than 10 year load with yearly probability of exceedance of 10^{-1} [94]. That is the reason why ISO code considers 1-5 years time period for operational conditions for South China Sea instead of 1 year as is considered for Gulf of Mexico or North Sea. In North Sea, the current speed used for design of offshore Jacket platform is of 10 year maximum with associated 100 year design wave [95].

2.6.2.6 *Wind*

During storm conditions wind could have significant effect on design of Jacket platforms and it can induce large forces on exposed parts. The effect of wind force depends on size and shape of structural members and on wind speed. Wind force arises from viscous drag of air on component and from difference in pressure on windward and leeward sides [91]. For Jacket platforms wind load can be modelled as deterministic quantity [96], [97]. Wind force is small part i.e. less than 5-10% of wave force [87], [98]. Wind is measured at 10 m reference height. Wind influences the build up of waves which can take significant time, i.e. many hours. This shows that the short-term variations of wind speed and sea elevation may be considered independently [58]. Wind is responsible for generation of surface waves [99]. Bias and COV for wind was found to be as 0.78 and 37%. This was almost same as wave parameters [7]. Wind was assumed to be 2 parameter Weibull distribution for Northern North Sea [100].

2.6.2.7 Environmental Load Modelling Uncertainty

Environmental load model uncertainty was taken as normal distribution with COV of 0.15 and mean bias value of 1.09 [69].

2.6.3 Environmental Load Modelling of Jacket Response

The environmental load model is necessary for the development of load factor using reliability index. Total wave force on platform equals to square of wave height [101]. Here the responses of Jacket (strength of components) in terms of basic applied loads which govern its behaviour are modelled. This can be represented by stochastic processes or random variables. For the FORM analysis it is necessary to use random variable formulations [102]. Different methods for finding the response of offshore Jackets, subjected to random ocean forces have been widely published [26] [50], [103], [104], [105] and two are shown below. Methods suggested by SHELL for development of load factors for ISO is shown in Equation (2.14) [27], [69], [106].

$$W = aH_{max}^2 + bH_{max} + cV_c^2 + dV_c + e \quad (2.14)$$

Where, W =Load effects, H_{max} = variable annual maximum wave height, V_c = variable current speed, coefficients of a, b, c, d and e are found from curve fit tool of MATLAB. Heidman suggested Equation (2.15) [20],

$$W = a_1(H_{max} + a_2v_c)^{a_3} \quad (2.15)$$

Coefficients of a_1 , a_2 and a_3 were found from curve fit tool of MATLAB, H_{max} = maximum wave height and v_c = current speed. Here a_1 factor depends on the size of load area of Jacket [49].

2.6.3.1 Environmental Load Uncertainty Model

The environmental load model uncertainty (X_w) was used in development of API LRFD and ISO codes. ISO and BOMEL takes it as normal distribution with mean bias of 1.09 and COV of 0.18 [69].

2.6.4 Dead Load

ISO categorizes the dead load into 2 classes. Permanent load action, G_1 , includes self weight of structure and associated equipment. This is self weight part of gravity load. Permanent load action, G_2 , represents the self weight of equipment and other objects that remain constant for long periods of time, but which can change from one mode of operation to another. It is treated as normal random variable. The statistical parameters of bias (mean over nominal) are taken from ISO code. The distribution was considered as normal with mean bias of 1.0 and COV of 0.06 [5] [7], [9], [87], [107], [108]. In South China Sea mean bias was 1.0 and COV of 0.08 has been reported [5], [108].

2.6.5 Live Load

It is the permanently mounted variable load Q_1 and variable action, Q_2 , represent the short duration action. The distribution was considered as normal with mean bias of 1.0 and COV of 0.1. These values were used for calibration of Jacket platforms in GOM and North Sea [7] , [9]. The same values were used for calibration of load and resistance factor design for platforms in China [108] but mean bias of 1.0 and COV of 0.14 was suggested by [5].

2.7 Critical Analysis of Load Uncertainty

The gravity loads and environmental loads both are random variables. The gravity load statistics have been taken from literature in this study. Gravity loads are taken as normal and environmental load are selected as Weibull and Gumbel but Weibull is preferred choice of engineers. The load uncertainty has large COV which influences the probability of failure significantly as will be shown in Chapter 7. The data collection is very important for reducing this uncertainty. Therefore if this uncertainty is to be reduced then more accurate data collection method should be applied.

2.8 Structural Reliability

Reliability is defined as an ability, to achieve a desired purpose of platform under operational and extreme conditions, for its designed life. Structural reliability concept consists of structural safety and resistance, serviceability, durability and robustness [66]. Performance of a platform is measured in terms of reliability index or return period (probability of failure). Calibration of North Sea and GOM LRFD code development was based on six Jacket platforms [10], [109]. Structural reliability can be found for time dependent or independent reliability analysis. In this study time independent reliability is considered.

Before probability based codes were developed, structural codes contained safety criteria based on allowable stress method. Structural system was assumed to act always elastically and inelastic behaviour was never assumed. The risk was catered by reducing the yield strength of member. Actual loads were calculated first and then members were selected so that the allowable member strength remained below certain limit like 66% of yield strength. Thus a factor of safety of 2/3 was always there in the member for extreme load combinations. This factor was based on judgment of code developers. Reliability analysis methods based on probability and statistics, started to gain importance since 1960 under the patronage of CA Cornell, NC Lind and H.S. Ang. It was Cornell who in 1969 proposed second moment reliability index method [110] which was further developed by Hasofer and Lind, who gave a proper format to invariant reliability index [49], [111]. Rackwitz and Fiessler gave an efficient numerical procedure for finding the reliability index by using non-normal probability distributions. Rosenblueth and Turkstra gave load combinations. Moses helped in the development of API LRFD for Jacket platforms on which ISO 19902 code is based [38], [50], [112]. Der Kiuregian developed FERUM software for reliability analysis [113] which is based on FORM reliability analysis method.

For normal distribution the characteristic value used to be taken as 1.645 times standard deviation i.e. an upper value and a lower value for load and resistance as shown in Equations (2.16-2.17). On load and resistance curve the characteristic value is the 0.95 fractile for load and 0.05 for resistance. This shows that on load side 95% of design load will lie below this value. On resistance side only 5% values will be

below the design strength. Equations 2.16 and 2.17 show the load and resistance characteristic values.

$$\text{Characteristic load} = \mu + 1.645\sigma \quad (2.16)$$

$$\text{Characteristic resistance} = \mu - 1.645\sigma \quad (2.17)$$

Where μ = mean of normal distribution and σ = Standard deviation of normal distribution. It is possible to relate the number of standard deviations to probability of occurrence. One standard deviation both side of mean relates to 67% of probability of occurrence and two standard deviations equals to 95% [114].

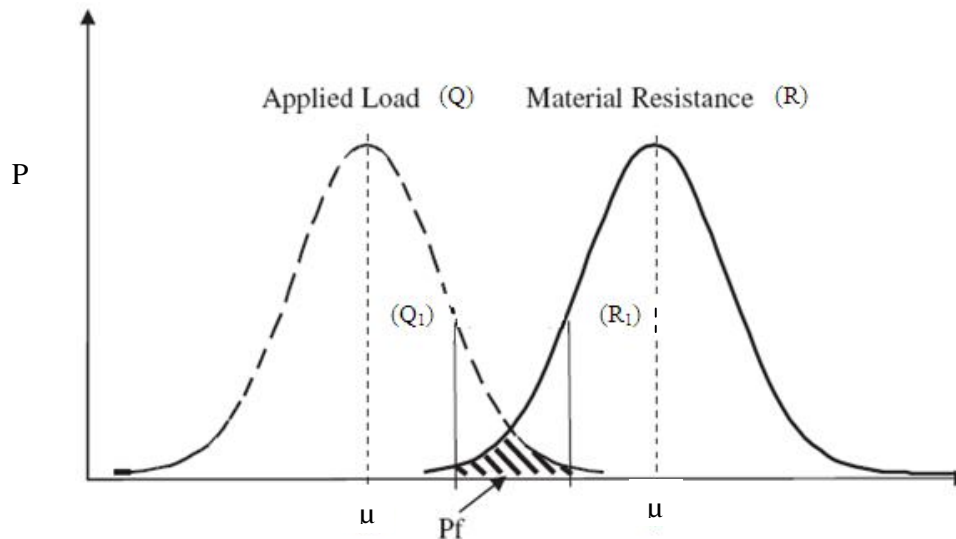


Figure 2.5: Normal Distribution of Load and Resistance [115]

2.8.1 Reliability Levels

Levels are characterised by amount of information about the problem is provided or it is based on how many random variable parameters are being used. If characteristic values are used then it is called level I. If standard deviation and coefficient of correlation are also used then it is termed as level II, and if cumulative distribution function is also used then it is level III [49]. If engineering economic analysis is involved then it is level IV.

2.8.2 Parameters of Structural Reliability

2.8.2.1 *Limit State*

When a structure exceeds a particular limit and the Jacket is unable to perform as desired then at that particular limit it is said that limit state has reached. If that limit state is exceeded then the Jacket is considered unsafe. Conditions separating satisfactory and unsatisfactory states of structure are known as limit state [66]. There are four categories of limit state. The ultimate limit state is concerned with collapse of structure or component and it is necessary that it must have extremely low probability of failure. This limit state is concerned with maximum load carrying capacity of Jacket [74]. The structure must be able to withstand actions and influences occurring during construction and anticipated use in this limit state [66]. The serviceability limit state is related to interruption of normal use of that Jacket, this includes large deflection, excessive vibration, cracks etc. Structure must remain fit for use under expected conditions of serviceability limit state conditions [66]. Fatigue limit state is due to cyclic loading and governs for operational conditions. Accidental limit state is used in consideration of accidental loads. It should maintain integrity and performance of Jacket from local damage or flooding [74].

2.8.2.2 *Reliability Index*

Reliability is a measure of probability of failure of structural member. It is the probability that system will carry out its intended purpose for certain period of time under conditions defined by limit state. This is a truth that it is practically not possible to make a member which does not fail for any kind of load. There will always be some chance or probability that the uncertain load will become large or resistance will be smaller than estimated, which will cause the member failure. It depends on what risks or reliability index value, the related industry is ready to take. For example, if the risks are high, as in offshore industry, higher reliability index or safety index is required but this increases the cost of structure. If risk is low, lower reliability index may also be accepted as in some cases of non important structures.

Table 2.4 shows that as probability of failure decreases the reliability index increases. The same can be shown graphically in Figure 2.5 which shows the reliability index (β) against probability of failure (P_f). Where (β) can be found through Microsoft Excel function, using Equation (2.18),

$$\beta = \text{NORMSINV}(P_f) \quad (2.18)$$

Table 2.4: Probability of Failure and Reliability Index Relationship [58]

β	P_f	Return period
1.28	1×10^{-1}	1 in 100
2.33	1×10^{-2}	1 in 100
3.09	1×10^{-3}	1 in 1000
3.72	2×10^{-4}	1 in 5000
4.26	1×10^{-4}	1 in 10,000
4.75	1×10^{-6}	1 in 1,000,000
5.20	1×10^{-7}	1 in 10,000,000

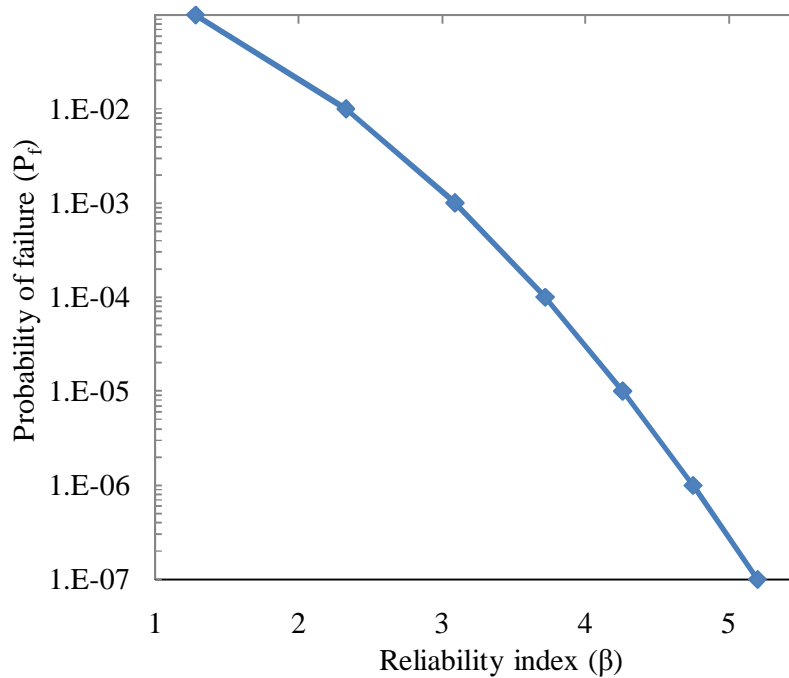


Figure 2.6: Relationship between Safety Index and Probability of Failure [58]

2.8.2.3 Probability of Failure

Risk is defined by probability of occurrence of unfavourable event. There is no risk free design. Risk depends on degree of overlap of load and resistance probability density curves [45]. Optimised design is reached when increase in initial cost is balanced by decrease in expected failure consequence cost [45]. Reliability model defines load and resistance as probabilistic random variables. It is referred as unsatisfactory performance of a component based on particular performance criteria. Platforms in North Sea are designed for a ductility requirement of 10^{-4} /year with a possible annual failure probability of collapse of 10^{-5} , Efthymiou calls this could be 10^{-7} [116]. Annual failure probability is considered for structures where human life is of concern. Where material cost is of importance, design life of structure is considered for failure probability [7], [117]. The preferred safety level for engineering structures is based on loss of life probability due to structural failure. Individual accepted risk is based on death due to failure of structure. In developed countries it is 10^{-4} per year [118].

In reliability based design, an engineer is allowed to select a probability of failure which is proportionate with the failure consequences. This makes design engineer to decide what probability of failure he shall take for a particular Jacket. Thus by this concept, component or joint can be utilised to full capacity. Thus making an economical Jacket such as unmanned Jackets [45]. Structure cannot be designed with 100% surety that it will sustain all types of loads forever i.e. there is no zero risk structural design. If higher safety margins are provided then the load and resistance curves will move further apart thus it will reduce the probability of failure but it will not totally remove load and resistance overlap [45].

The structural failure is shown as Equation (2.19)

$$P_f = P(R < Q) \quad (2.19)$$

Where, P_f = probability of failure and P = probability. Thus probability of survival can be shown by Equation (2.20),

$$P_s = 1 - p_f \quad (2.20)$$

Where, P_s = probability of survival

2.8.2.4 *Target Reliability*

Target reliability for offshore platforms is based on either reliability of platforms designed as per the old code like API WSD or on probability of failure acceptable to society. Here probability of failure is determined based on effects of wave and current loading which are the most severe loading criteria for design of offshore platforms. Target reliability is required for calibration, in order to make sure that certain safety levels are maintained. It is minimum annual average reliability shown as a maximum failure probability for a given safety class, consequence, category and failure types, provided by codes of practice for Jacket design. For setting a value it requires some exercise of engineering judgement [119]. Target reliability is different for manned and unmanned Jacket platforms. For manned platforms, decision is made by required probability of failure, due to environmental loading. It should be small as compared to other high consequences and major risks like fire, explosions and blowouts [33]. There is agreement among researchers that if annual probability of failure due to some cause is less than 1 in 10,000, then it is small in relation to major risks [33]. Assuming that in North Sea during 30 year there are 250 platforms, now platform years will be $(30 \times 250) = 7500$ platform years. Expected number of failures over 30 years period is then $P(a) \times 7500$, [$P(a)$ = annual probability of failure]. Most probable outcome will be zero failures if $[P(a) \times 7500 < 0.5]$, which leads $P(a) < 1$ in 15000 [33].

DNV reports acceptable annual target reliability for redundant Jackets as 3.09 or probability of failure of 10^{-4} [61]. Theophanatos calls selection of target code of API WSD / API LRFD RP 2A / ISO 19902, for selection of target safety index. Separate partial factors are used for load effect types (axial, bending force and hydrostatic etc.) [9]. For Ekofisk area in North Sea target annual probability of failure is 5×10^{-4} (design should make sure a 2000 year return period of collapse limit state) [120]. This target failure probability of 1/2000 per year is chosen as it is consistent with API guidelines for design of new platforms [120]. DNV provides the values for safety index and probability of failure used by the codes. Table 2.5 shows the target reliability for North Sea Jackets.

Table 2.5: Indicative Target Reliability [121]

Limit state	Annual	Lifetime
Ultimate limit state	3.8	4.7
Fatigue limit state	1.5-3.8	-
Serviceability limit state	1.5	3.0

In order to apply reliability methods it is necessary to find components failure function, uncertainty model, probability calculation method and target safety levels [122]. Table 2.6 shows the target reliability in shape of P_f based on consequence of failure of fatalities or economic reasons.

Table 2.6: Probability of Failure Recommended for NS Jackets [122]

Conditions	P_f
Severe consequence i.e. (potential fatalities or significant environmental damage)	4^{-4}
Only economic consequences are involved	1^{-3}

Figure 2.7 shows acceptance criteria for target reliability of Jacket platforms at different safety levels. 1×10^{-4} is used for manned platforms, 1×10^{-3} is used for unmanned platform (high consequence), 2×10^{-3} unmanned platform (low consequence) and 2×10^{-2} closed down platform (ready for removal).

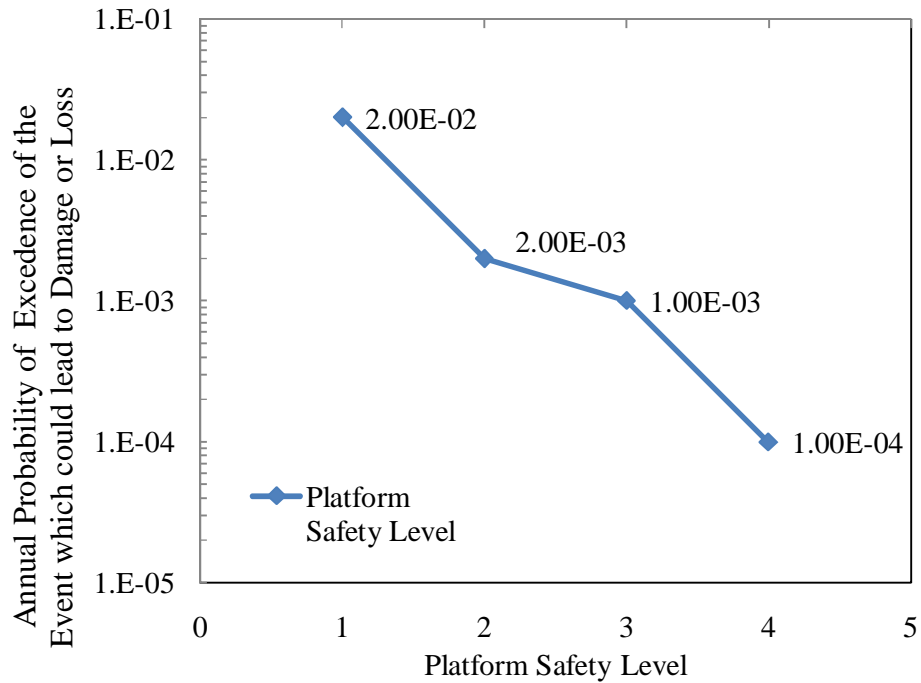


Figure 2.7: Acceptance Criteria for Ductile Jacket Platform at Different Safety Levels [116].

2.8.3 Review of Structural Reliability Methods

There are basically two types of reliability analysis methods i.e. simulation and analytical. The major example for simulation method is Monte Carlo simulation. Monte Carlo simulation is easy to use, robust and accurate by using large number of samples, though it requires large number of analysis for achieving the good quality approximation of low probability of failure. The problem with this simulation technique is that it produces noisy approximation of probability. Analytical methods include moment based methods such as First Order Reliability Method [70]. Cornell, 1969 proposed reliability method i.e. Mean Value First Order Second Moment [123]. It was in 1974 when Hasofer and Lind proposed reliability index using FORM method.

2.8.3.1 First Order Second Moment (FOSM) Method

Probabilistic calibration is done to find safety factors in a balanced manner. It takes into consideration the sources of uncertainty in environmental load and material resistance [58]. This is a level II reliability method. In this, safety is measured by the first and second moments like mean and standard deviation. The method is based on Cornell's theory of reliability measurement given in 1967 [49]. The safety index is based on mean μ and standard deviation σ which are expressed in Equation (2.21).

$$\beta = \frac{\mu}{\sigma} \quad (2.21)$$

Where, β = reliability Index, μ = mean (used to express the central tendency for a random variable in a distribution curve), σ = standard deviation (dispersion of random variable). This means that safety index is the distance in terms of standard deviations. It lies between origin and mean values of margin of safety in distribution curve [49]. Probabilistic calculation techniques enable these uncertainties to be taken into account. Probability distributions characterise the uncertainties associated with mean load (\bar{Q}) and mean resistance (\bar{R}). It is expected that safety factors calibrated for drag-dominated wave loads will be conservative for inertia-dominated load [58]. Equation 2.22 shows the ratio expressed as log-normal distribution. If the coefficients of variation of resistance (v_r) and load (v_q) are less than 30%, the safety index can be calculated by [10],

$$\beta = \text{Ln} (\bar{R}/\bar{Q}) / \sqrt{v_r^2 + v_q^2} \quad (2.22)$$

Where, \bar{R} = mean resistance, \bar{Q} = mean load, v_r = COV of resistance v_q = COV of load.

2.8.3.2 First Order Reliability Method (FORM)

FORM reliability method has been used for reliability analysis of Jackets by many researchers [38], [65], [69]. This is the most significant tool available to find reliability index and widely being followed nowadays to find reliability. The FORM solution provides geometrical interpretation of reliability index as the distance

between origin and design point in standard normal space [61]. The first step is to transform the basic variables which may not be normally distributed into the space of standard normal variables. Thus it is transformation of limit state surface from given space of basic variables to a corresponding limit state surface in standard normal space. Design point is the point on limit state surface which is nearest to origin and is found by optimisation process. This is taken as the most likely failure point. Here limit state surface in standard normal space is approximated by a tangent plane at the design point as shown in Figure 3.5.

2.8.3.3 Simulation Techniques like Monte Carlo Simulation (MCS)

Monte Carlo simulation is another method used to find probability of failure and reliability index. This is an alternative or complementary tool for estimation of probability of failure [61]. Rubinstein, 1981 was the pioneer of Monte Carlo simulation method. It generates large number of random variable (x) samples through the use of random number generator. If the limit state function is implicit the computation requires large number of simulations for exact function evaluation. Accuracy in this technique depends on number of simulations [118]. The sample values of random variables generated are extremely large and number of failures is counted. Thus capacity of computer required to do the analysis is used to be high. The probability of failure can be evaluated by Monte Carlo simulation as shown in Equation (2.23),

$$P_f = \frac{N_f}{N} \quad (2.23)$$

Where, N_f = number of failures, N = total number of simulation. COV of failure probability (V_{pf}) can be evaluated by Equation (2.24),

$$V_{pf} = \frac{1}{\sqrt{P_f \times N}} \quad (2.24)$$

However, there are few problems with this method. In this method, approximation of performance function is used to reduce the computational cost. Random sampling used in this method produces inaccuracy in results [35]. It is because the random numbers generated by the random number generators, which are produced in clusters and not uniformly distributed over the whole design space, may

repeat again. The other problem in this method is that estimated probability of failure depends on sample numbers used for simulation. Therefore if lower order failure probabilities are required the sample numbers needed are higher which increases the cost of computation [35].

2.9 Component Reliability and Previous Work

Component failure occurs due to formation of plastic hinge, member buckling, joint failure due to fatigue cracking or brittle fracture [124]. Component reliability for Jacket platforms have been determined by researchers such as [9], [38], [55], [69], [103], [125]. The work on component reliability has been done in many regions of world including GOM, North Sea, China, Mediterranean Sea and Gulf of Guinea. Failure probability of each component depends on the magnitude of the stresses and corresponding strengths. Strength of tubular component is function of mechanical properties of material, yield strength and dimensional properties. Only the uncertainties in yield strength are of major importance in governing the failure probabilities of tubular legs and brace components [102]. This is due to the fact that leg members have low slenderness ratio. Failure is governed by yield stress and reliability of component can be increased by using steel with high mean yield strength [102]. Jacket design is usually based on elastic skeletal frame analysis. Distribution of stresses is found when it is subjected to design environmental loads.

Individual component stresses are evaluated to make sure that no elements fail against the governing criteria [126]. This type of failure is related to stresses which are produced in member like compression (buckling local or global), bending due to yielding of material and hydrostatic. PAFA reports that gravity load dominates the leg members but environmental load dominates the design of brace members [127]. For buckling, governing design condition is in place extreme environmental condition. This condition is valid for majority of structural components in offshore platforms. Most frequent component found in Jacket platform are tubular members under combined compression and bending with ratio of compression to bending stresses being generally high [58].

2.9.1 Resistance Factor

Resistance of tubular members is multiplied by resistance factor which represents the uncertainty related to prediction of failure mechanism [16]. Resistance factor depends on type of resistance i.e. tension and bending can be predicted more accurately as compared to column buckling. Therefore ISO resistance factor for tension and bending is 1.05 but for compression it is 1.18.

2.9.2 Component Reliability Index-Critical Review

Codes of practice for Jacket design, API WSD and ISO 19902 are both component and joint based design codes. Component reliability for Jacket platforms has been done for ISO code development by BOMEL [69]. Environmental load factor for extreme conditions achieved for North Sea was 1.25. For consistency with GOM calibration, environmental load factor of 1.35 was retained for ISO code. Environmental load factor for component proposed for Mediterranean Sea is 1.30 [9]. Therefore it is high time to evaluate the load factor for offshore Malaysia.

2.10 Joint Reliability and Previous Work

Joint reliability has been determined by researchers such as in GOM, North Sea, China, Mediterranean Sea and Gulf of Guinea [9], [17], [38], [69], [128], [129]. For Jackets, the joints are connected by primary members called chords usually with larger diameter compared to secondary members called braces. In tubular Jacket frame, intersections between main members (chord) and secondary members (brace) are welded together and are called tubular joints [130]. Chord and brace members undergo combined stresses. This is due to hydrostatic pressure and bending moment which arise due to wave and current forces and from load distribution at the nodal points [43]. Joints are the most critical part of truss structure like Jacket. The work on modelling of joint stresses is still very active. With respect to API code, 21st edition published in 2000, the errata published in API 2008 contain many changes in joint design Equations.

Out of all three types of joints K, T/Y and X, the X-type is the most preferred one due to its ductile nature. Capacity and redundancy for ductile redistribution of stresses for an X-braced joint contributes to the reserve strength of structural system which may not be the case for K-Joints. X joint imparts significant ductility, mobilises alternative load paths and gives high frame capacity. Thus ductile behaviour of X braces at failure and brittle behaviour of K-braced frames suggest that different acceptance criteria may be appropriate for redistribution of forces for structural system [126]. That is the reason that X-braced frames are more in new Jackets as compared to old Jackets.

2.10.1 Joint Reliability Index- Critical Review

Joint reliability for Jacket platforms has been done for ISO code development by BOMEL. Joint environmental load factor for extreme conditions achieved for North Sea was 1.25 [69]. For consistency with GOM, load factor of 1.35 was retained in ISO code. In Mediterranean Sea joint environmental load factor proposed was 1.20 [9].

2.11 Reliability and Environmental Load Factor

Bilal [46] reports that primary factors affecting the evaluation of load factor are characterisation of failure modes (limit states), assessing implicit reliability levels in existing design code i.e. API WSD and assigning the target reliability. Target reliability selection is based on calibration of existing code by judgement. Calibration is process of finding reliability levels in components and joints designed using API WSD code [46]. The safety factor in working stress design is evaluated arbitrarily using experience and judgement of designers. Loads are factored on the basis of load uncertainties i.e. the environmental loads have larger safety factor as compared to gravity loads [16]. The design load action is found from characteristic load multiplied by a load coefficient γ . Characteristic loads are same for ultimate and serviceability limit states and only their load coefficients differ. Serviceability limit state takes γ_w value as 1.0 while for ultimate limit state, ISO and API takes γ_w as 1.35 for environmental loads [62]. In structural engineering, useful function of reliability

analysis has been precise in the development of structural codes where the end product has been an optimised set of partial factors [102]. In load and resistance factor design uncertainties are considered objectively by performing reliability analysis taking characteristic values of statistical variables. The environmental load factor can be decided based on target reliability as shown in Figure 2.8. Here target reliability is shown by API WSD and ISO gives us the reliability of new code. The new code reliability index at We/G ratio of 1.0 gives higher reliability as compared to API WSD. This higher reliability will give us the required load factor, as this will contain higher reliability than API WSD which has already proved its robustness at sea.

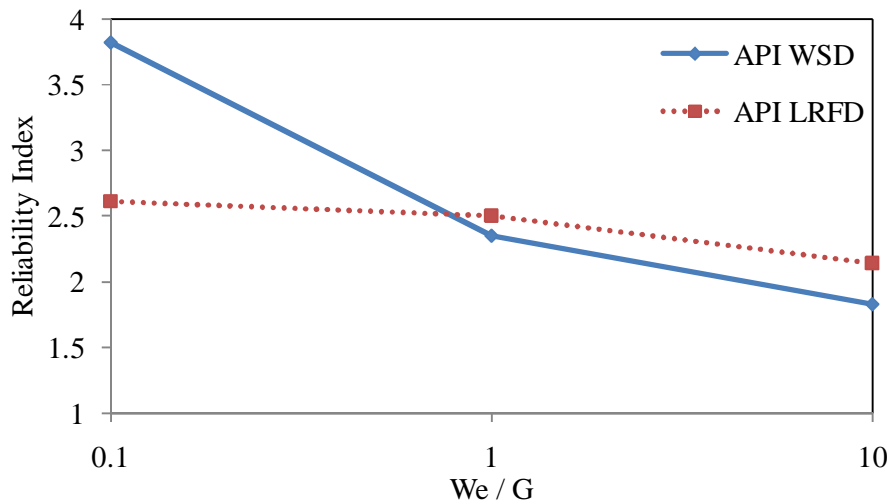


Figure 2.8: Variation of We/G ratio with Reliability Index for Axial Tension [1]

The safety index for LRFD was lower for low environmental to gravity loads ratios and higher for high environmental to gravity load ratios [10]. For Mediterranean Sea the load factors proposed by Theophanatos were based on Figure 2.9.

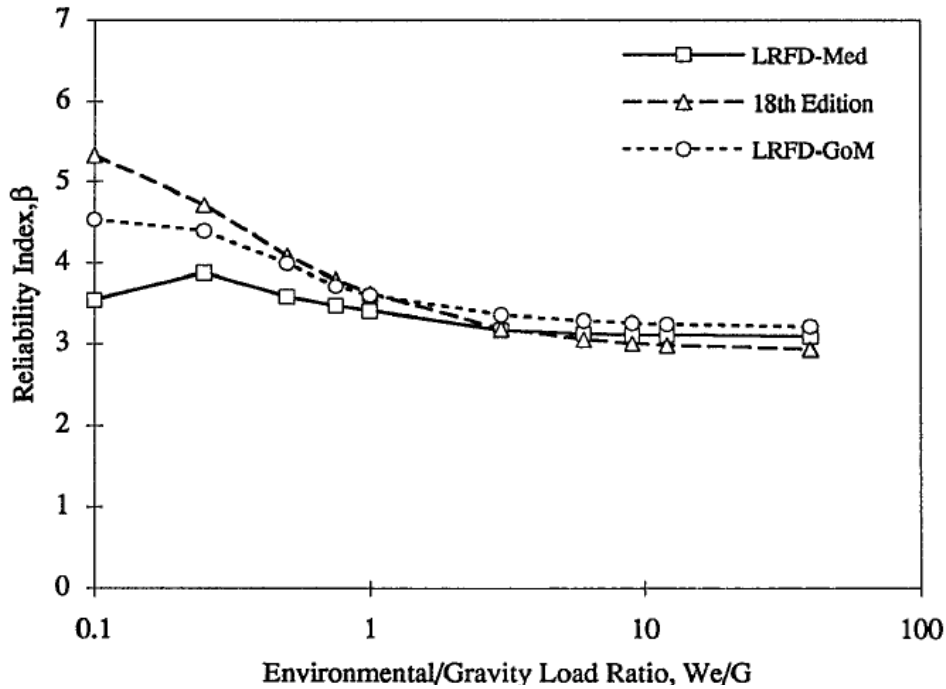


Figure 2.9: Variation of Reliability Index with Varying W_e/G [9]

2.11.1 Code Calibration

There are various methods used for code calibration like judgement, fitting, optimization, or combination of these. Code calibration for ISO is a method to determine the target reliability by decision making or optimization of the load factors or resistance factors [131]. Optimization process is used when it is to be enforced for common level of specific designed structures to that particular target reliability. The target reliability should be selected so that structures designed as per the design codes are homogeneous and independent of material and loading (operational and extreme) conditions [108].

2.12 Non-Linear Collapse Analysis

Progressive collapse is a feature of structural system rather than of an individual component. Structural codes specified element design, without giving consideration to assembly of multi-element structures, till “Ronan Point” disaster in 1968. Structural

collapse brought the consideration of problem of progressive collapse commonly referred as “domino effect” [119]. For ultimate limit state, during linear elastic analysis, strength of structure is considered up to first yield. Due to residual stresses local yielding may occur for loading less than ultimate limit state condition [20]. Ductility of steel makes it possible to redistribute the stresses which make it possible to face some yielding. Structural failure can be explained as full development of yield mechanism. Soreide reports that nonlinear collapse analysis of maximum load criteria simulates the real behaviour of structure during collapse [20]. The allowable stresses are not taken as they used to be in linear elastic analysis but a ratio of design load to collapse strength of structure is evaluated. The work on nonlinear collapse analysis for Jacket platforms has been conducted by [20], [109], [132], [133], [134]. This is currently most popular method of analysis for structural system strength in the presence of extreme loads. Chakrabarti reports that for a Jacket with nonlinear analysis will always give near to or lower than the collapse load compared to linear elastic analysis [20]. Structural Analysis and Computer Systems (SACS) software is used for Jacket analysis. SACS uses its collapse analysis module for nonlinear analysis of Jacket.

2.13 System Reliability and Reserve Strength Ratio (RSR)

System reliability of Jackets in North Sea and GOM has been studied by many researchers [94], [134], [135], [136]. The comparison of system and component reliability provides a measure of effect of redundancy in reliability index [103]. For system reliability assessment it is important to evaluate the likelihood of system failure following first component failure [73]. Structural system reliability has been defined as series and parallel. It is a complex approach for evaluating the system strength in case of nonlinear analytical behaviour. An approximate method has been proposed for Jacket system analysis in North Sea [27]. The structure’s model is developed directly as a system and nonlinear analysis and failure modes are evaluated directly [109]. It is important for economic exploitation of hydrocarbon reserves, from new and old Jackets to understand and realistically predict the ultimate response of Jacket [126]. One clear progress from elastic design to inelastic design is considered to be evolution towards more efficient steel structure design based on

system strength evaluation [132]. Failure of a structure is said to be global collapse i.e. load exceeding the ultimate capacity of the Jacket [122]. System reliability starts with a single member failure but it causes the failure of whole structure. Reliability of Jacket platform depends on performance of components but it is governed by structural system [1]. Reliability of system is product of individual member reliabilities. System reliability is taken higher than component reliability or system probability of failure is taken lower as compared to component probability of failure [137]. The uncertainties in the Jacket loading model are assumed due to wave height for system reliability. The wave period and current speed are taken as deterministic functions of the wave height [97].

If the Jacket has survived the extreme wave loading without any damage, the uncertainty about the strength should be updated and reduced [94]. This will be checked during application of Bayesian updating. The preloading of Jacket at a load level with probability of exceedance of 10^{-5} or less will prove the safety of platform against similar loading conditions if ever to arise. It is very essential to develop a methodology for optimization of loads and resistance. RSR is the ratio of maximum tolerable load as per nonlinear analysis and characteristic design load. The RSR should be determined in all directions and the lowest RSR should be taken as Jacket's RSR [20]. Out of all directions, minimum RSR is used to find the reliability as ISO code is looking for optimised Jacket. The most important RSR value is the lowest, which is related to the weakest direction or extreme environmental loading [27]. Graff and BOMEL have given the methodology for finding RSR based on structural system [27], [138] using North Sea Jacket platforms. Figure 2.10 show RSR against different We/G ratios for North Sea platform calibration. With increasing We/G values RSR was decreasing and high load factor gave high RSR values.

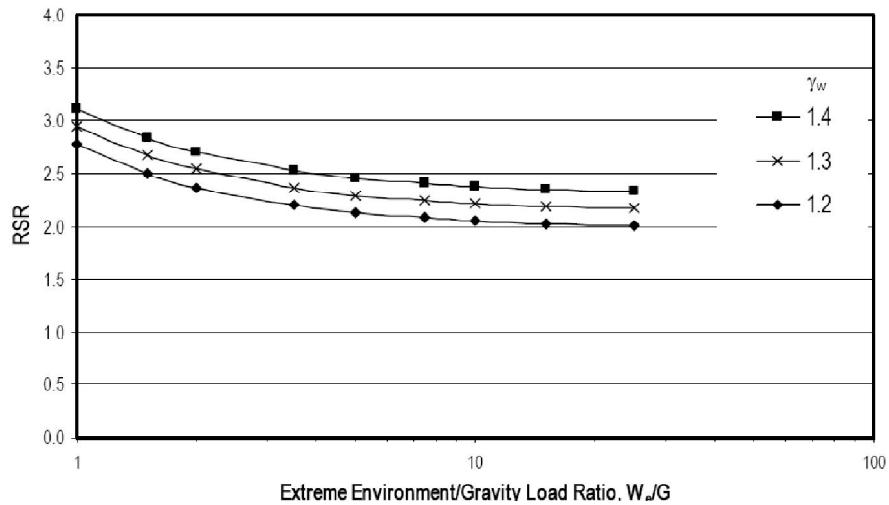


Figure 2.10: System RSR with respect to We/G ratios for axial Compression at NS Jacket [27]

2.13.1 Previous Work on System Reliability and Load Factors

The environmental load factor for North Sea has been proposed by BOMEL based on system reliability [27]. System environmental load factor of 1.25 was achieved for North Sea Jackets. The environmental load factor of 1.35 was suggested due to consistency with GOM. The target probability of failure was set as 3×10^{-5} proposed by Efthymiou [27] for system reliability as reported by BOMEL. Environmental load factor adopted by ISO are based on probability of failure of 3×10^{-5} [27]. The reliability index lies in range of 2.5-5.0, which is higher than component reliability index i.e. 2.5-3.5 of these platforms as suggested also by Moan [137]. Figure 2.11 show results of platforms from North Sea reliability index against load factors are shown for three We/G ratios. The load factor selected here was 1.25 based on notional target reliability of 4.0. Load factor was determined at the point where We/G line crossed the target reliability. This is due to the reason that our target reliability is based on the required safety level. Therefore once this is achieved the load factor will be considered as safe as per the new code.

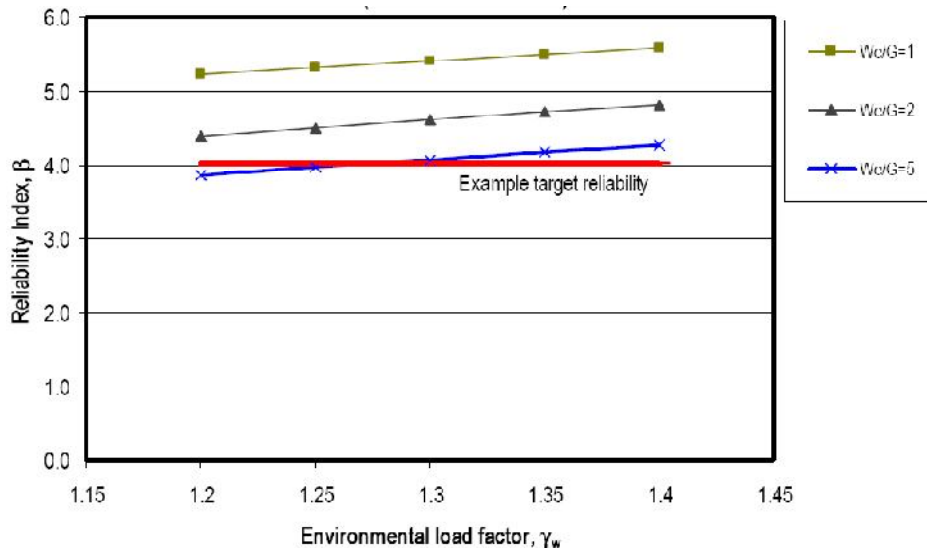


Figure 2.11: Reliability Index against Environmental Load Factors [27]

2.13.2 System Based Environmental Load Factor-Critical Review

During design phase, the lead time is so small that, actual site specific data on environmental load and material are not available with engineer. Therefore once Jacket is installed its probability of failure is evaluated. The API and ISO codes require that, system strength should be checked against environmental load of 10,000 years return period. Jacket platforms are designed using component and joint reliability. Environmental load factor for system only shows the redundancy of Jacket and it is not used during design of Jacket. System based environmental load factor for Jacket has been evaluated by BOMEL [27]. System strength is evaluated by using collapse analysis of Jacket, base shear, wave and current loads. System environmental load factor shows the redundancy available in Jacket.

2.14 Assessment of Jacket

ISO and API code requires that Jacket should be assessed and monitored for any damages throughout its life. Before Jacket reaches the end of its design life, it is assessed whether it can withstand a load of 10,000 year wave return period as per the guidelines of ISO and API. This is a very important step before extension of life is

decided for Jacket. The cost of new Jacket design, fabrication and installation is quite huge. Thus extension of life of Jacket will save a lot of money.

2.14.1 Bayesian Updating and Probability of Failure

Jacket failure due to structural design flaw was 10% of all accidents in offshore industry worldwide [139]. Jacket platforms are designed with limited data available during design phase. This leads to uncertainty for future loads and resistances. The mathematical modelling of the structural design also becomes uncertain in the presence of random uncertainty of load and resistance. The information gathered after the installation of Jacket, is used to extrapolate the extreme environmental event for wave height, wind and current speed. This is where probabilistic design comes into account. Codes of practice for Jacket platforms recommend notional failure probability to assess the effects of variable loads or strength problems. The updating of probability of failure with additional information, collected on material and load can be used in many engineering applications. There could be variations in loading pattern or material problems arising due to severe environmental weather effects from ocean environment after certain time of existence of Jacket under water. It can be due to change of loading pattern, subsidence of Jacket, development of cracks, degradation due to fatigue or any other reason like marine growth [20]. These observations at site can be used to update the probability of failure of Jacket by using the Bayesian method of updating. This will give us foresight about the ductile strength of the Jacket.

Frieze et al. [103], used it for updating RSR for finding bias in push over analysis. Bayes' theorem is used in cases when combined knowledge of statistical and judgmental information is available for updating probabilities based on observed outcomes [19]. This theorem calculates the probability of occurrence of event 'A', which depends on other mutually exclusive and collectively exhaustive event 'B', given that event 'B' has already occurred [140]. When additional information has become available about an existing Jacket, the knowledge implicit in that information may be used to improve the prior estimate of structural probability of failure [70]. Assessment of existing structure becomes real when damages are observed, use of

platform is expected to be changed, deviations from project descriptions are observed, the life time is up to extension beyond what was planned and inspection schedules were planned to be revised [141]. Bayesian updating procedures allow the updating of probability for modeling uncertainty parameters and structural global response [142]. Bay's theorem uses rational approach for incorporating the prior information or judgment into prediction of future behaviour of structures [143].

Figure 2.12 shows the updating probability of failure for Jacket platforms in North Sea. It can be seen that the updated probability of failure decreases with increasing of wave height. This was due to the reason that updating was based on both probability of failure and probability of survival results. Bay's updating is calculated using Monte Carlo simulation.

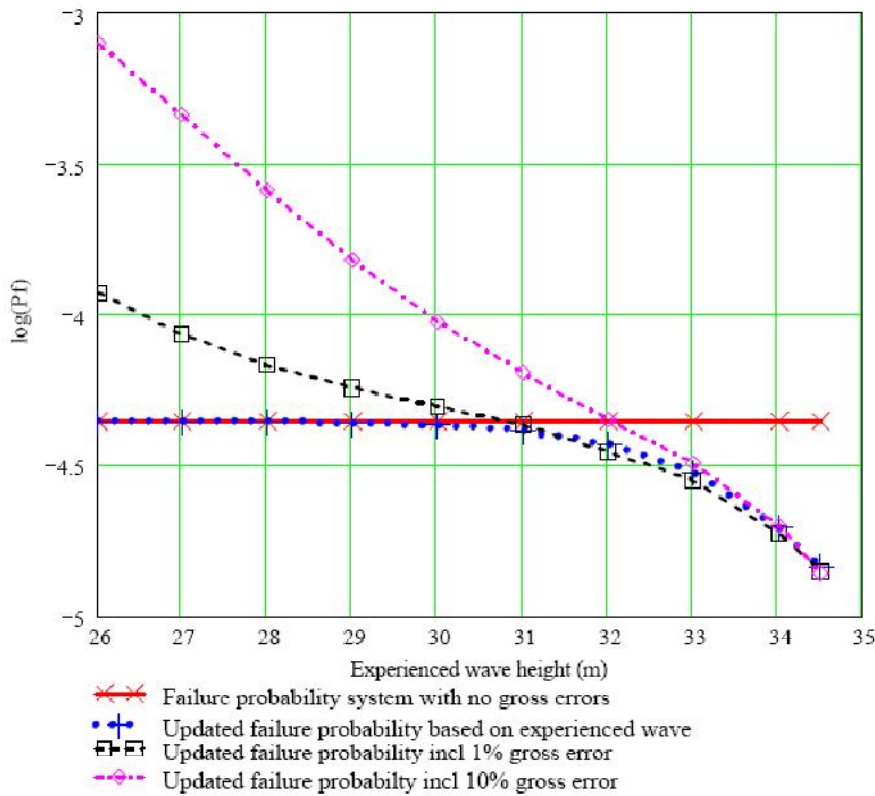


Figure 2.12: Bayesian Updating of Probability of Failure for Jacket at NS [20]

2.14.2 Damaged Structural Members

ISO 19902 clearly allows for existing Jackets to be accepted, with limited damage to individual components, provided that reserve against overall system failure and deformation remain acceptable [7]. Nonlinear collapse analysis approach is used by removing Jacket members and collapse capacity of damaged members is evaluated by Equation (2.25) [133],

$$\text{Damaged Strength Ratio} = \frac{\text{Design load}}{\text{Ultimate collapse capacity}} \quad (2.25)$$

2.14.3 Critical Review of Updating of Probability of Failure

The updating of probability of failure using Bayesian approach has been recommended by [18], [70], [144]. Updating of probability of failure using Bayesian technique has been adopted for Jacket platforms in Norway. For Jacket platform, this has been used by [94], [123], [134], [135], [136]. This method can be used when the design life approaches its end and Jacket is required to be re-evaluated for its strength and extension of Jacket design life.

2.15 Chapter Summary

The critical analysis shows that this topic is extremely important for the hydrocarbon industry of offshore Malaysia. If economics is to be considered as primary importance this study will play some role in future developments of Jacket platform design. The uncertainty models for resistance have never been evaluated in this region. Previous studies load models were treated for one platform only whereas this work attempts to cover platforms from all three regions of offshore Malaysia. The importance of reliability based environmental load factor for component, joint and system show that it should be evaluated and if required modified for this region. The updating of probability of failure also shows its importance with regard to extension of life of Jackets in Malaysia and for some other cases like damaged members. For South China Sea its use has not been reported in any literature.

CHAPTER 3

RESEARCH METHODOLOGY

3.1 Introduction

The reliability theory has evolved from the structural, aerospace and manufacturing industries. This approach considers uncertainty of load and resistance and uses judgement in dealing with the structural problems. It provides a way of quantifying those uncertainties and a way to handle them consistently [41]. There are four types of uncertainties in structural engineering namely aleatory (inherent/ physical randomness), epistemic (statistical/ lack of knowledge), model-related and human error based. The physical randomness is always present in our nature, like wind, wave and current. This inherent randomness is most difficult to forecast. Epistemic uncertainty relates to small number of available data to analyse like yield strength, diameter and thickness of member. This could be improved by the increase of data sets. Model uncertainties are due to our lack of understanding and simplification of the Equation provided by codes for calculating the stresses / forces in the component. Human error uncertainty depends on knowledge of person designing, constructing and operating the Jacket.

The necessary tools for calibration of LRFD are statistics of random variable i.e. mean value, standard deviation and distribution patterns [22]. We need data for analysis of statistical parameters and probability distribution patterns of material (resistance) and environmental load. Probabilistic models are defined for uncertainty, variability and probability distribution functions. These are based on measured data and statistical procedures. After defining basic variables, which have influence on failure of components, joints and system, failure functions are defined for each

one of these in the form of ultimate limit state Equation. Ultimate limit state is used where human life is involved. It also corresponds with maximum load carrying capacity [73]. First Order Reliability Method (FORM) was used to evaluate P_f , for component, joint and system. Environmental load factors γ_w are found so that the factored load has a predetermined probability of being exceeded [36]. Finally system strength is evaluated at design and extrapolated higher load. Bayesian updating is used to update probability of failure using Monte Carlo simulation with intact and damaged Jacket model.

3.2 Resistance Uncertainty

The uncertainty in resistance variable plays a major part in safety, performance and structural behaviour of tubular members. These uncertainties can make variations in resistance that will lead ultimately to significant effect on the reliability analysis of Jacket platforms. The actual strength is always random in nature and it tends to show its behaviour in random way. To measure the uncertainty for reliability analysis, we need to define the basic variables involved in the limit state Equation. These variables are defined by probability/ cumulative density function along with other statistical properties like mean bias, standard deviation and COV. In this study basic random variables were analysed first and their statistical parameters were determined. Then the basic stresses using ISO 19902 code Equations were simulated and their statistical parameters were determined. Once this random behaviour is understood, it makes the task of designer much easier due to reduced uncertainty of material. This study is based on assumption that reliable models of uncertainty can be developed, using limited amount of data. These uncertainty models were used to find the reliability of components, joints and systems using ultimate strength limit state design.

For reassessment of existing platforms, we need to define the actual uncertainties of the material and environmental loads acting at the site. Material uncertainties may change after some time due to degradation of material especially from fatigue and corrosion environment but here in this study this degradation was not considered.

These uncertainties become most important if we want to find probability of failure for operational conditions. Finally, recommendations are made for the statistical characteristics of the random variables to be used for the reliability analysis for ultimate limit state design of Jacket platforms in offshore Malaysia.

3.2.1 Collection of Data for Resistance Parameters

The statistical data for resistance was based on material test report and field measurements at one of the leading ISO certified fabrication yard in Malaysia. The data for this study was collected in 2010 and it was used for statistical modelling. The collected data is based on Jackets which were under construction at the yard. Field data collected include the geometrical parameters i.e. diameter and thickness. The material properties were based on mill test reports for 6 Jacket platforms. The details of these platforms are provided in Table 3.1 covering all three regions of Malaysia.

Thickness of tubular members was obtained through direct measurement of tubular members available at the site and dimensional drawings available at the yard. Diameter variability was obtained using as built drawings. Material strength variation was based on test reports available with the fabricator. Water depth of platforms varied between 53 m – 74 m which is the representative water depth for Jacket platforms in Malaysia. All these platforms were designed and fabricated as per API RP2A WSD code 21st edition, which was the code used for finding the target reliability in this research. These platforms were three and four-legged. The common platforms in this region have 4, 6 and 8 legs. The source material for these platforms was from Japan.

Table 3.1: Details of Selected Platforms for Resistance Uncertainty

Platform	Location	Height (m)	Fabrication Year	No. of legs	Material Source
A	PM	73.40	2009	4	Japan
B	PM	72.00	2009	4	Japan
C	PM	60.40	2007	4	Japan
D	Sarawak	56.70	2005	4	Japan
E	Sarawak	53.60	2008	4	Japan
F	Sabah	55.20	2009	3	Japan

In total, 72 mill tests results were used to measure the variability of material properties of tubular members. For geometric variability, 260 specimens were taken for leg diameter, 113 for brace diameter and 26 for thickness variation. Table 3.2 and Figure 3.1 show the data available at fabrication yard for yield strength variability and diameter variability. Diameter is recorded at four diagonal places in tubular member and its average is used as measured value. Its design value is already mentioned in fabrication drawings. Thus a bias of one member was recorded. All bias values of diameter were then put in Easy fit software to get the mean coefficient and variation coefficient. Figure 3.2 shows a Jacket under construction along with its components at the fabrication yard.

Table 3.2: Variability of Material Properties as shown in as Mill Test Report

Mechanical Test		
Yield Stress (MPa)	Tensile Strength (MPa)	Elongation %
319	475	31
308	471	24
320	475	28
318	471	31
357	505	26

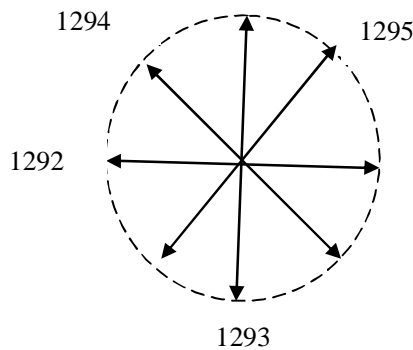


Figure 3.1: Variability of Diameter



Figure 3.2: Fabrication yard in Malaysia

3.2.2 Statistical Analysis of Geometric and Material Variables

This uncertainty relates to the randomness due to geometrical and material variations. They come from diameter of leg and brace, thickness of leg and brace and yield strength. Though this type of uncertainty can be dealt with properly, with the application of quality control using international standards, still there remains some uncertainty. These are defined as errors which are covered by fabrication tolerance limit. These variations between characteristic values mentioned on structural drawings and fabricated component, are due to geometric uncertainty. For instance in the case of diameter, there were four values measured at 90° angle from one another. The average of these four values was taken as measured mean and divided by the characteristic value. The characteristic value was mentioned on the structural drawings. The mean bias of diameter and thickness was calculated by Equation (3.1),

$$\text{Mean bias} = \frac{\text{Measured (average)}}{\text{Nominal/mean}} \quad (3.1)$$

The benefit of this method is that mean bias of any diameter value can be ascertained easily. It is obtained by multiplying any nominal value of variable by its

mean bias. The mean bias values were then statistically analysed and respective distributions were reported for all variables. Tubular members were further divided into leg and brace members. Brace thickness increases as we go down towards mud level [145]. Joint angle was another variable to be used for joint reliability. COV shows the variability in the model. For reliability analysis on resistance model, we must be sure that 95% values taken by the design engineer are higher than that value of actual resistance. Mill test reports were used to find the statistical properties of yield and tensile strength of the tubular members. Same methodology was adopted as mentioned above for statistical analysis of material resistance. As per ISO requirement, the ratio of yield to ultimate tensile strength is shown in Equation (3.2) [63],

$$\frac{\text{Yield Strength}}{\text{Ultimate Tensile Strength}} = \frac{355}{490} = 0.724 < 0.85 \quad (3.2)$$

All variables in this study are assumed to be independently distributed. The data is analysed by using three Goodness of fit test which were Kolmogrov-Smirnov, Anderson Darling and Chi-Square test and the best fit is reported. The distribution types, bias and COV for materials found are used for the reliability analysis of component and joints.

3.2.2.1 Resistance Variables taken from Literature

There were three other resistance variable parameters i.e. length (L) of tubular member, effective length factor K and young's modulus (E). The mean bias and standard deviations and distribution types are shown in Table 3.3.

Table 3.3: Statistical Parameters taken from Literature [69], [146]

Random Variable Parameters	Distribution	Mean Bias	Standard Deviation
Length (L)	Normal	1.0	0.0025
Effective length factor K (leg)	Normal	1.1	0.0935
Effective length factor K (brace)	Normal	0.875	0.097
Young's modulus of Elasticity (E)	Normal	1.0	0.05

3.2.3 Component and Joint Stress Model Uncertainty

The ISO code Equation is used for modelling of stresses as shown in Figure 3.3. High amount of random data was produced using Monte Carlo Simulation. The uncertainty related to prediction of resistance model variability can be calculated using simulation techniques. Monte Carlo simulation was used to generate long simulated data by MATLAB code. In this case, data of 1×10^5 simulations were generated using statistical parameters of random variables, giving reliable outcome without any experiments. Data generated by this simulation was used to find distribution and its parameters. This type of simulation is used when resources are limited and experiments are not possible or extremely difficult. The uncertainty variables as mentioned in 3.2.2 were used to find model uncertainty X_m for nine different stresses for components of Jacket platforms, and four types of stresses for K, T/Y and X joints each.

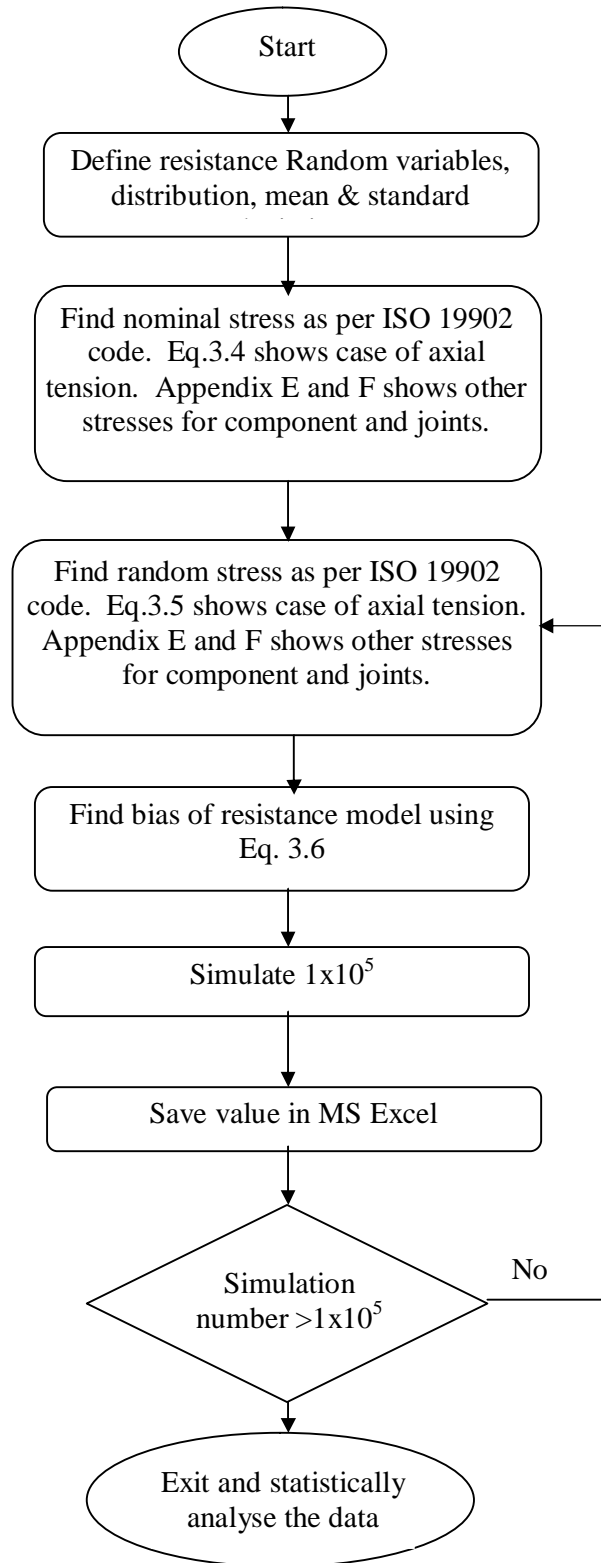


Figure 3.3: Flow chart for Resistance Model Uncertainty

3.2.3.1 Case Study: Axial Tension Model Uncertainty

In this case study model variability of axial tension stress using ISO code is explained. ISO axial tension stress can be found by Equation (3.3),

$$\sigma_t = f_t \times A \quad (3.3)$$

Where, σ_t = tensile stress, f_t = tensile strength, A = area of tubular member. Two main steps were used to find the simulated statistical parameters of the stress of components under axial tension as shown below:

1) Define the nominal values which are used by actual stress model, i.e. F_{yn} , D_n , T_n . Thus in our first part, all input values used will be nominal and deterministic as shown in Equation (3.4),

$$\sigma_{tn} = f_{tn} \times A_n \quad (3.4)$$

Where, σ_{tn} = nominal tensile stress, f_{tn} = nominal tensile strength, A_n =nominal area of tubular member

2) Define the variable values which are used by member or joint stress model, i.e. F_{yi} , D_i , T_i . The biases of mean and standard deviations were defined as variables along with their probability distributions. Thus Equation (3.5) contains input variables based on distribution and its parameters. The output will also be variable, changing each time when analysed.

$$\sigma_{ti} = f_{ti} \times A_i \quad (3.5)$$

Where, σ_{ti} =variable tensile stress, f_{ti} =variable tensile strength, A_i = variable area of tubular member. The limit state Equation for resistance bias using Monte Carlo simulation is shown by Equation (3.6)

$$\text{Resistance Bias} = \frac{\sigma_{tn}}{\sigma_{ti}} \quad (3.6)$$

σ_{tn} = Nominal stress, σ_{ti} = varying stress

The resistance biases will change each time analysis is made due to variable denominator in Equation (3.6) which gave mean bias of axial tension model stresses. Now there were 10^5 simulations which produced as many resistance values due to different variable strengths. These values were statistically analysed using Easy Fit

software. The statistical parameters were taken using best model fit based on statistical test result. This model stress evaluation was done for nine component stresses and eleven joint stresses. The importance of model uncertainty variable can be seen from sensitivity study as shown in Table 5.4.

3.3 Load Uncertainty

For load uncertainty the random variables are wave, wind and current. The nature of environmental load is probabilistic and we need to ascertain the randomness of the load. Two-parameter Weibull and Gumbel distributions were used for the analysis to find the best fit. The authentic available data was in shape of 1, 10, 50 and 100 years return period. Parameters of distribution were determined first, which were used to find mean and standard deviation. From this uncertainty, variables were extrapolated up to 10,000 years which is specified by ISO 19902 and API RP2A for extension of life of existing platforms. Finally the data was compared with data from Gulf of Mexico (GOM), Northern North Sea (NNS), Southern North Sea (SNS) and Central North Sea (CNS).

3.3.1 ISO and Metocean Criteria

Metocean design conditions are extremely important for the design of platform. ISO 19900-1 recommends 3 methods of considering the parameters for design [147]. For the North Sea widely used method to obtain design wave height has involved fitting cumulative distributions to the significant wave heights of successive three hour storm sea state. It is common to neglect both the correlation between consecutive sea states and uncertainty in the extreme environmental load. Through distributions 100 year return period wave is estimated. NPD uses a combination of a wave along with annual probability of exceedence of 10^{-2} and current with an annual probability of exceedance of 10^{-1} . Research for waters outside Europe, USA and Australia propose that considering joint probability for the environmental load parameters reduces the design loads on drag dominated Jacket platforms by 10 to 40 % [147]. This study considers drag wave dominated Jackets because that was the case for steel offshore Jackets for hydrocarbon drilling in Malaysia.

3.3.1.1 *Method 1*

In this method, 100 year return period wave height with associated period, wind and current speeds are taken into consideration. This is suitable for the structures where environmental action is dominated by waves. In this method we need associated current with wave. ISO directs that this wave and current should be from same storm conditions, such type of data was not available. This makes method 1 not possible for this study.

3.3.1.2 *Method 2*

In this method 100 year wave height and period along with the 100 year wind speed and the 100 year current speed are taken into consideration. They should be evaluated by extrapolation of the individual environmental parameters considered independently. When joint probability information for environmental conditions is not available, a conservative estimate of environmental load can be found. Sum of 100 year environmental actions caused by independent extreme values of wind speed, wave height, and period, and current speed were used. This is based on assumption that they act simultaneously and in the same direction. Environmental variables are estimated based on return period of 100 years, using measured or hind cast time series extending over a period of 5 years record. The 100 year wind, wave and current maximum values are assumed to occur at the same time and in the same direction. For Jacket platform, this will lead to design load that will be much more severe than the true 100 year load [147].

3.3.1.3 *Method 3*

Any combination of wave height, period, wind and current speed which results in: a) the global extreme environmental action on the structure with a return period of 100 years, b) a relevant global response of the structure which could be base shear or overturning moment with a return period of 100 years. This method uses associated current speed, wind speed, wave height and significant structural response effects, e.g. base shear and overturning moment. Directional effects of environmental load

parameters and water depth variation from tide and surge are required to be considered.

Though Method 3 is the preferred method by ISO 19901 but due to lack of appropriate data this method could not be used in current study. Since the correlation between wind, wave and current cannot be established due to lack of data, Method 2 was adopted.

3.3.2 Environmental Load Uncertainty Parameters

This study covers three parameters of environmental load acting on Jacket platforms i.e. significant wave height (H_s), wind speed and surface current speed in three regions of offshore Malaysia. In this study four platforms were taken for analysis representing three regions of Malaysia i.e. one from Peninsular Malaysia (PMO), one from Sabah (SBO) and two from Sarawak (SKO1 and SKO2). To find the effect on load uncertainty, the data available for nearby platforms from same region was included in the analysis.

3.3.2.1 Climate

The load produced by extreme storms is important in the design of offshore Jacket platforms. The load is produced by combination of waves, currents and wind, though waves are generally the dominant factor [86]. The type of weather in offshore Malaysia is half-yearly. North East (NE) monsoon during November to March months and half year long South West (SW) monsoon during May to September, the months of October and April are counted as transitional intra monsoon period. The direction of wind is North East towards Peninsular Malaysia. North East to North West towards Sabah and Sarawak region in NE monsoon period. In SW monsoon the wind direction is South- South West. But NE monsoon is more extreme i.e. wave height as well as wind speed are higher. Table 3.4 shows the water depth variations in the region which is quite large. Appendix D shows offshore Malaysia region.

Table 3.4: Water Depths ranges for Platforms in Malaysia

Location	Water depth (m)	
	Minimum	Maximum
PMO	60.0	79.2
SBO	36.9	59.1
SKO	46.0	95.0

3.3.2.2 Design Wave

The South China Sea is the largest sea in the north-west Pacific. It connects to the outside seas through the straits of Taiwan, Luzon, Mindoru, Para Barke, Banka, Gaspar, Karimata and Malaka. This study considers only offshore Malaysia region. Significant wave height is the dominant metocean variable [82]. Present day design methods are based on unidirectional or long-crested waves, where all energy comes from a single direction. Real sea waves are multidirectional- energy comes from many directions simultaneously. The use of unidirectional waves is regarded as conservative factor in design [148]. The direction of wave is NE and NW during N-M monsoon period and S-SW during M-S monsoon period in this region [149]. Wave direction becomes unstable (without any clear prevailing direction) during transition period. The highest significant wave in deepwater South China Sea, during tropical cyclone, is reported as high as 9.5 m [149]. Table 3.5 shows the maximum wave height in three regions. Data is taken from four platforms for reliability analysis. Wave heights used are the highest in their respective regions.

Table 3.5: Maximum and Critical Values of Significant Wave Height

Location	Design wave (H_{max}) with return period of 100 years		Platform specific H_{max} (m)
	Minimum (m)	Maximum (m)	
PMO	4.6	10.9	10.9
SBO	2.3	7.7	7.7
SKO1	3.0	9.9	9.9
SKO2	4.7	11.7	11.7

Table 3.6 shows the relationship between maximum wave height and significant wave height. Ratio lies in between 1.86 - 2.05. In GOM the ratio was 1.93, but ISO gave 1.76 with water depth of 300 m [150].

Table 3.6: Ratio of H_{\max} / H_s for Platforms in Offshore Malaysia & GOM

Area	H_s (m)	H_{\max} (m)	H_{\max}/H_s
PMO	5.3	10.9	2.05
SBO	4.3	7.7	1.79
SKO1	5.2	9.9	1.90
SKO2	6.3	11.7	1.86
GOM (300 m water depth)	14.6	25.8	1.76 (ISO)

3.3.2.3 Current

Stronger currents flow in December and in August near Peninsular Malaysia but they are not as strong as they are near Sabah and Sarawak [149]. 1/7 power law is used to find current at different depths [82], [86]. Table 3.7 shows the comparison between three regions for minimum and maximum currents at critical directions. The current values used in this study were not highest, but it has not much effect on overall reliability as explained in 3.3.1.

Table 3.7: Current at Surface (Maximum / Critical Directions)

Location	Current at surface with return period of 100 years		
	Minimum (m/sec)	Maximum (m/sec)	Platform specific (m/sec)
PMO	0.68	1.50	1.47
SBO	0.66	2.23	0.94
SKO1	0.40	1.80	1.05
SKO2	0.40	1.80	1.2

3.3.2.4 Wind

In South China Sea, waves are mainly controlled by wind field [149]. The wind speed is measured at 10 m above sea level. Strong sustained winds produce severe sea states and both wind and wave loads are high in the event of storm. In open sea waters, the long-term variations of wind speed and sea elevation are highly correlated in the storm event [58]. Wind produces large drag forces on offshore Jacket platforms. Most often, the wind load does not dominate over the wave load in the extreme design conditions [81]. For the Jackets, the wind generates a little part, of the order of 10%, of the sum of extreme load and ISO code reports that sustained wind

speed should be used to compute the extreme global load for design of the Jacket [81]. ISO prefers 10 min mean for global design of the structure and 3 sec gust for design of component. Table 3.8 shows the maximum values prevalent at the specific platforms.

Table 3.8: Variation of Wind Speed in Platform at Specific Locations

Location	3 sec gust with 100 year return period	
	Minimum (m/sec)	Maximum(m/sec)
PMO	29	55
SBO	24	50
SKO1	22	50
SKO2	22	50

3.3.3 Data Collection for Environmental Load Parameters

The data was collected from an offshore working group in Malaysia. There were 20 data sets from PMO region, 11 from SBO region and 22 from SKO region. Available data was in shape of 1, 10, 50, 100 years. In this study, only 10 and 100 year data was taken for analysis. 10 year data was taken because it was more representative of operating conditions of Malaysia. 100 year data was taken as it was maximum processed data available and it was also requirement of ISO and API codes. This formed the basis for the statistical analysis of environmental load parameters.

3.3.4 Statistical Analysis of Environmental Load Parameters

Probability distribution for a random variable shows the uncertainty of the given variable. Many authors have taken extreme value distributions for the wind, wave and current parameters. For extreme conditions, Weibull and Gumbel distributions are the most important distributions as these can capture the rare tail end events better. The reliability analysis results are sensitive to tail of probability distribution. Thus choice of distribution type is always significant and resistance is most of time normally distributed [61]. The bias and COV of environmental loads in different regions are shown in Table 3.9.

Table 3.9: Environmental Load Parameters (Wind, Wave & Current) [22], [38], [151]

Region	BIAS	SD	COV
GOM	0.750	0.216	0.288
Central North Sea	0.861	0.192	0.222
Northern North Sea	0.877	0.165	0.188
NW Australia	0.780	0.257	0.33
China	0.827	0.142	0.172

3.3.4.1 *Extrapolation of Wave, Wind and Current*

Cumulative distribution functions for Weibull and Gumbel distribution were found using the linear model. Two points were used for curve fitting for extrapolation. With two load parameters and their corresponding CDF values of distribution, a linear fit was made in Microsoft Excel. Using linear Equation, along with CDF of 1000 and 10,000 years, the corresponding values were determined for loads. For example, the linear fit for wave height of one platform at PMO, was given as, $0.577x + 4.418$. Here x is the value of corresponding CDF values. This model was used to find the extrapolated values for wave heights, wind and current speed for 1000 year and 10,000 year return periods. Further details are given in sections 3.3.5 and 3.3.6 and in Chapter 4.

3.3.5 **Weibull Distribution**

Here extreme distribution of Type 2 Weibull distribution was used. This type is used where rare events are of interest.

3.3.5.1 *Extrapolation of Significant Wave Height (Weibull Distribution): Case Study of PMO Platform*

In this study, linear extrapolation of Weibull distribution was used as follows. The probability of exceedance and CDF values as per Weibull is shown in Table 3.10. For PMO metocean reports gave 10 year and 100 year significant wave heights as 4.9 m and 5.3 m respectively. The linear Equation for 10 and 100 year values are shown in Equations (3.7-3.8) [85],

$$\ln\{-\ln[1 - F(x_{(i)})]\} = \ln - \{\ln(1 - 0.9)\} = 0.834 \quad (3.7)$$

$$\ln\{-\ln[1 - F(x_{(i)})]\} = \ln - \{\ln(1 - 0.99)\} = 1.527 \quad (3.8)$$

Table 3.10: Cumulative Distribution Function (CDF)-Weibull Distributions

Return Period	Probability of Exceedence	CDF Weibull
10	$\left[1 - \left(\frac{10}{100}\right)\right] = 0.9$	0.834032
100	$\left[1 - \left(\frac{1}{100}\right)\right] = 0.99$	1.52718
1000	$\left[1 - \left(\frac{1}{1000}\right)\right] = 0.999$	1.932645
10,000	$\left[1 - \left(\frac{1}{10000}\right)\right] = 0.9999$	2.2203

Thus 10 and 100 year values of wave height were plotted at vertical axis against CDF of 0.834 and 1.527 on horizontal axis. The trend line Equation was plotted for those two values. Now with trend line Equation and CDF of 1000 and 10,000 years available, the corresponding wave heights were extrapolated. The same method was adopted for wind and current extrapolation. The parameters of Weibull distributions were evaluated as below:

3.3.5.2 Weibull Shape Factor

The shape factor for Weibull distribution was found as follows:

$$\ln(x) = \ln(4.9) = 1.589$$

$$\text{CDF}(10-100) = 0.834 - 1.527 = -0.693$$

$$1.589 - \ln(5.3) = -0.078$$

$$\text{Shape factor (b)} = \frac{-0.693}{-0.078} = 8.8$$

3.3.5.3 Weibull Scale Factor

$$\ln(8.8) = 2.17$$

$$8.8 \times 1.589 = 14.0$$

$$0.834 - 14 = -13.20$$

$$-13.20 / (-8.8) = 1.49$$

$$\text{Scale Factor (a)} = \exp(1.49) = 4.46$$

3.3.5.4 Weibull Mean

Using these parameters mean value was found based on Equation given by [152] as shown in Equation (3.9)

$$\text{Mean } (\mu) = a \times \Gamma\left(1 + \frac{1}{b}\right) \quad (3.9)$$

Where, Γ = gamma function

$$1 + \frac{1}{8.8} = 1.11$$

Now Microsoft excel gamma function is given by:

$$\exp(\text{Gamma Ln}(1.11)) = 0.946$$

$$\text{Mean} = 4.46 \times 0.946 = 4.22$$

3.3.5.5 Weibull Standard Deviation

Using these parameters standard deviation (SD) was found based on Equation given by [152] as shown in Equation (3.10),

$$\text{Standard Deviation}(\sigma) = a \left[\Gamma\left(1 + \frac{2}{b}\right) - \Gamma^2\left(1 + \frac{1}{b}\right) \right]^{1/2} \quad (3.10)$$

$$1 + \frac{2}{8.8} = 1.22$$

$$\text{Exp}(\text{Gamma Ln}(1.22)) = 0.911$$

$$(0.946)^2 = 0.895$$

$$\text{Standard deviation} = 4.46 \times (0.911 - 0.895)^{0.5} = 0.57$$

3.3.6 Gumbel Distribution

3.3.6.1 Extrapolation of Significant Wave Height (Gumbel Distribution): Case Study of PMO Platform

For platform in PMO 10 year and 100 year significant wave heights given in metocean reports were 4.9 m and 5.3 m. The probability of exceedance as per Gumbel is shown in Table 3.11. Linear model of Gumbel distribution is given for 10 and 100 years in Equation (3.11-3.12) [85],

$$-\ln\{-\ln[F(x_{(i)})]\} = -\ln\{-\ln(0.9)\} = 2.25 \quad (3.11)$$

$$-\ln\{-\ln[F(x_{(i)})]\} = -\ln\{-\ln(0.99)\} = 4.60 \quad (3.12)$$

Table 3.11: Cumulative Distribution Function (CDF)-Gumbel Distributions

Return Period	Probability of Exceedence	CDF Gumbel
10	$\left[1 - \left(\frac{10}{100}\right)\right] = 0.9$	2.250367
100	$\left[1 - \left(\frac{1}{100}\right)\right] = 0.99$	4.600149
1000	$\left[1 - \left(\frac{1}{1000}\right)\right] = 0.999$	6.907255
10,000	$\left[1 - \left(\frac{1}{10000}\right)\right] = 0.9999$	9.21029

Thus 10 and 100 year values of wave height were plotted at vertical axis against CDF of 2.25 and 4.60 on horizontal axis. The trend line Equation was plotted for those two values. Now with trend line Equation and CDF of 1000 and 10,000 years available, the corresponding wave heights were extrapolated. The same method was adopted for wind and current extrapolation using Gumbel extrapolation.

3.3.6.2 Gumbel Scale Parameter

$$2.25-4.6= - 2.349$$

$$4.9-5.3= -0.4$$

$$\text{Scale Factor (d)} = \frac{-2.349}{-0.4} = 5.87$$

3.3.6.3 Gumbel Location Parameter

$$5.87 \times 4.9=28.785$$

$$2.25-28.78= - 26.53$$

$$\text{Location factor (c)} = \frac{-26.53}{-5.87} = 4.52$$

3.3.6.4 Gumbel Mean

Using location and scale factors parameters the mean was found from Equation (3.13).

$$\text{Mean}(\mu) = c + \left(\frac{0.57722}{d}\right) \quad (3.13)$$

$$\text{Mean}(\mu) = 4.52 + \frac{0.57722}{5.87} = 4.62$$

3.3.6.5 Gumbel Standard Deviation

Using location and scale parameters standard deviations was found from Equation (3.14).

$$\text{Standard Deviation} (\sigma) = \frac{\pi}{d\sqrt{6}} \quad (3.14)$$

$$\text{Standard Deviation} (\sigma) = \frac{\pi}{5.87\sqrt{6}} = 0.218$$

When both distributions were analysed it was found that Gumbel gave higher mean values as shown in section 4.6. Therefore Weibull distribution was the best fit and thus selected for this study.

3.3.7 Environmental Load for SACS

Table 3.12 contains the platform specific load parameters for selection of input values for finding the environmental load for component and joint reliability. Table 3.12 shows the basic values used for conversion into random input for load values in SACS. Using these values along with Weibull distribution, 50 random values were generated for wave, current and time period using MATLAB. These 50 random load values were used to get 50 stresses from SACS output file for each component and joint. The corresponding 50 component and joint output stresses were produced by SACS analysis using Morrison Equation. These were converted to load model using curve fit tool of MATLAB.

Table 3.12: Platform-Weibull Distribution Parameters

	Parameter	10 year	100 year	Scale	Shape
PMO	H_{max} (m/s)	9.6	10.8	8.33	5.89
	T_p (s)	10.3	10.8	9.73	14.62
	Current (m/s)	0.98	1.10	0.85	6.00
SBO	H_{max} (m/s)	6.8	7.7	5.86	5.58
	T_p (s)	10.6	11.0	18.71	10.14
	Current (m/s)	0.78	0.94	0.62	3.71
SKO1	H_{max} (m/s)	5.5	9.2	2.96	1.35
	T_p (s)	9.7	11	8.34	5.51
	Current (m/s)	0.96	1.05	0.86	7.73
SKO2	H_{max} (m/s)	10.4	11.7	9.03	5.89
	T_p (s)	10.9	11.4	10.33	15.46
	Current (m/s)	1.05	1.20	0.89	5.19

3.3.7.1 SACS Modelling of Jacket

To get environmental load effect for the reliability analysis, 50 stress values for wave, time period and current were found. For statistics of environmental load it is necessary to make component and joint stresses dimensionless, which is acquired by dividing it by 100 year characteristic values [82]. Therefore the output of applied

stresses from SACS were normalised before being used for curve fitting tool of MATLAB. Figure 3.4 shows the normalised stresses and curve fit Equation results. The input for surface fitting was wave height, current and normalised stress values. It can be seen from Figure 3.4 that vertical axis is the normalised joint stresses for one joint. The horizontal axis is the output from curve fit model containing same wave height and current for which stress was achieved.

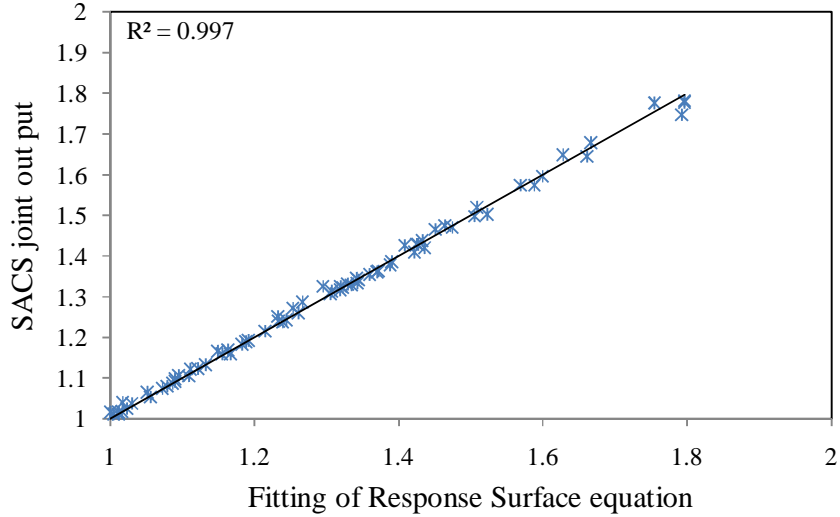


Figure 3.4: Surface Fitting Validation for SBO Platform

3.4 Structural Reliability

When randomness of material or load is low, a deterministic model can be used. In cases when random uncertainty is high, stochastic models containing statistical properties should be used [51]. Safety margin between load and resistance is indicated by limit state in Equations (3.15-3.16),

$$g = R - Q \leq 0 \quad (3.15)$$

Where, g = Limit state function

$$g = R/Q \leq 1 \quad (3.16)$$

Probability of failure is given by Equation (3.17),

$$P_f = P(g < Q) \quad (3.17)$$

Here ($g < 0$) indicates failure region, $g > 0$ safe region and $g = 0$ failure surface, Mean of limit state function is shown as Equation (3.18),

$$\mu_g = \mu_R - \mu_Q \quad (3.18)$$

Where, μ_R = mean resistance, μ_Q = mean load

Standard deviation of limit state function is shown by Equation (3.19),

$$\sigma_g = \sqrt{\sigma_R^2 + \sigma_Q^2} \quad (3.19)$$

Where, σ_R = standard deviation of resistance, σ_Q = standard deviation of load. Reliability index can be found as shown in Equation (3.20) which is based on level II reliability method,

$$\beta = \frac{\mu_g}{\sigma_g} \text{ or } \frac{\mu_R - \mu_Q}{\sqrt{\sigma_R^2 + \sigma_Q^2}} \quad (3.20)$$

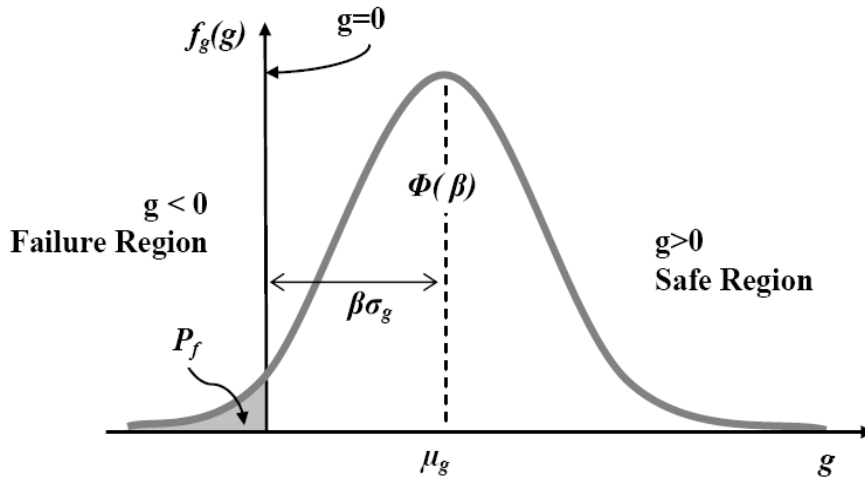


Figure 3.5: Reliability Index due to Cornell Probability of Limit State [51]

In Figure 3.5, probability of failure is represented by the shaded area under the curve which indicates the failure region [51]. Vertical axis shows probability density function and horizontal axis shows failure / success of member. Reliability index is the distance from μ_g to the limit state surface. Reliability index β shows the distance

of mean margin of safety from failure function (g) = 0. Distance is shown by uncertainty parameter of standard deviation.

Common stochastic methods for reliability analysis are based on simulation techniques like Monte Carlo or moment based techniques like FORM. This study did not take into consideration of time variant variables i.e. fatigue and corrosion. FORM and Monte Carlo simulation methods of reliability are used for time invariant random variables [73]. These methods vary with respect to accuracy, required input data, computational effort [153]. The same author reports that reliability can be used as professional criteria for the choice of load and resistance factors.

3.4.1 FORM

Here random variables are defined by first moment (mean) and second moment (coefficient of variation) and type of distribution. Approximating of limit state function is based on reliability based algorithms like FOSM, FORM.

3.4.1.1 First Order Second Moment Method (FOSM)

It is defined by Mean Value First Order Second Moment method (MVFOSM) . First order means, first order expansion of transfer Equation. The main variables are mean and standard deviations only and no distribution is needed. Taylor series expansion is used for the expansion of Equation based on mean value. Considering that our variables are independently distributed , approximate limit state function at mean value is given by Equation (3.21) [51],

$$\tilde{g}(X) \approx g(\mu_x) + \nabla g(\mu_x)^T (X_i - \mu_{x_i}) \quad (3.21)$$

$\mu_x = (\mu_{x_1}, \mu_{x_2}, \dots, \mu_{x_n})^T$, $\nabla g(\mu_x)$ is the gradient of g evaluated at μ_x as shown in Equation (3.22)

$$\nabla g(\mu_x) = \left[\frac{\partial g(\mu_x)}{\partial x_1}, \frac{\partial g(\mu_x)}{\partial x_2}, \dots, \frac{\partial g(\mu_x)}{\partial x_n} \right]^T \quad (3.22)$$

The mean value of limit state function is $\tilde{g}(X)$ as shown in Equation (3.23):

$$\mu_{\tilde{g}} \approx E\{g(\mu_x)\} = g(\mu_x) \quad (3.23)$$

Since $Var[g(\mu_x)] = 0$ and $Var \nabla g(\mu_x) = 0$

The Standard deviation value of limit state function is $\tilde{g}(X)$ as shown in Equations (3.24-3.25),

$$\sigma_{\tilde{g}} = \sqrt{Var \tilde{g}(X)} = \sqrt{[\nabla g(\mu_x)^T]^2 Var(X)} \quad (3.24)$$

$$= \left[\sum_{i=1}^n \left(\frac{\partial g(\mu_x)}{\partial x_i} \right)^2 \sigma_{x_i}^2 \right]^{1/2} \quad (3.25)$$

The reliability index is given by Equation (3.26),

$$\beta = \frac{\mu_{\tilde{g}}}{\sigma_{\tilde{g}}} \quad (3.26)$$

If the limit state Equation is linear this will become same as Equation (3.20). In the case when limit state function becomes nonlinear then approximation is made here by taking the actual limit state function at mean value thus making it linear. Thus Equation (3.26) is named as Mean Value First Order Second Moment method for evaluating reliability index. Here random variables used were mean (first moment) and variance (second moment). There were two drawbacks found in this method. In case of high nonlinearity this method was not suitable. This method fails to be invariant with different mathematical equal Equations of same question.

3.4.1.2 Hasofer and Lind Reliability Index

The above method was improved by Hasofer and Lind (HL) and thus better results were possible for nonlinear cases. Difference between HL and MVFOSM is that this method takes design point (most probable point) as the approximation of limit state function instead of mean value. This method uses iterations to converge. This method also takes distribution into considerations for finding the reliability index. HL

method proposes linear mapping of basic variables into a set of normalised and independent variables (u_i) [51]. The standard normalised random variables for resistance and load are shown in Equation (3.27),

$$\hat{R} = \frac{R - \mu_R}{\sigma_R}, \hat{Q} = \frac{Q - \mu_Q}{\sigma_Q} \quad (3.27)$$

Where, μ_R, μ_Q = mean values of resistance and load, σ_R, σ_Q = standard deviation of resistance and load. Transformation from limit state surface of $g(R, Q)$ in original coordinate system into standard normal coordinate system (\hat{R}, \hat{Q}) is shown in Equation (3.28),

$$\hat{g}(\hat{R}, \hat{Q}) = \hat{R}\sigma_R - \hat{Q}\sigma_Q + (\mu_R - \mu_Q) = 0 \quad (3.28)$$

The shortest distance from origin (\hat{R}, \hat{Q}) in normal coordinate system to failure surface of $\hat{g}(\hat{R}, \hat{Q})$ is equal to reliability index, i.e. $\beta = \hat{O}P^*$ as shown in Figure 3.6. Failure surface for independent and normally distributed variables is nonlinear function is shown in Equation (3.29),

$$g(X) = g(x_1, x_2, \dots, x_n)^T \quad (3.29)$$

Variables are transformed into standard forms by Equation (3.30),

$$u_i = \frac{x_i - \mu_{x_i}}{\sigma_{x_i}} \quad (3.30)$$

Where μ_{x_i}, σ_{x_i} are the mean and standard deviation of x_i . The mean and standard deviation of standard normal distribution are 0, 1. Thus reliability index is shortest distance from origin to failure surface, given by Equation (3.31) as shown in Figure 3.7,

$$\beta = \min(U^T U)^{1/2} \quad (3.31)$$

There are certain limitations in this method i.e. in some cases there is a problem of non-convergence. But the main issue still remained i.e. it considered only normal distributed random variables.

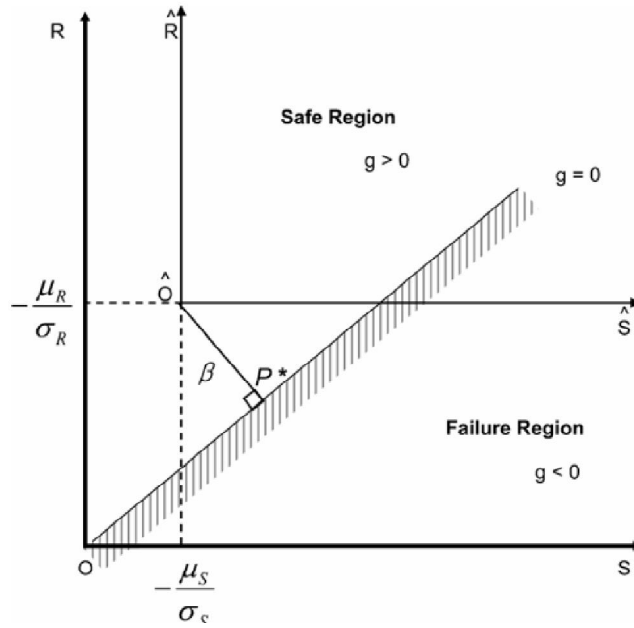


Figure 3.6: Reliability Index Representation [51]

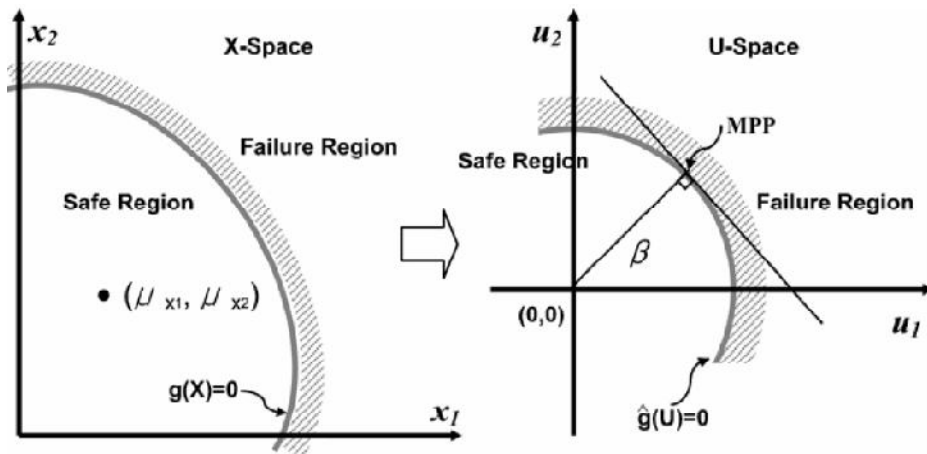


Figure 3.7: Representation of Failure Surface from X-Space to U-Space [51]

3.4.1.3 Hasofer-Lind and Rackwitz-Fiessler Method (HL-RF)

This is extension of HL method and the only difference is that it can take non normal distribution for finding the reliability index. Non-normal distributed variable was transformed into normal space. Using this method, FORM model based on FERUM has been adopted in this study. FERUM is based on MATLAB and was an open

source compiler available from University of California, Berkley [154]. FERUM was used in this study for component, joint and system reliability analysis.

3.4.2 Monte Carlo Simulations for Determination of Probability of Failure

This method is attributed to the research by Neumann and Ulam, in which random behaviour is evaluated using sampling techniques. MCS uses randomly generated sampling sets for uncertain random variables of load and resistance. This is used to find approximate probability of some event, which is the result of a series of probabilistic processes [51]. Following steps are followed here in this method: 1) type of probability distribution function is selected for the particular random variable, 2) samples are generated based on probability density function, 3) limit state function is defined, 4) Using simulation the response is evaluated. This method was used to find probability of failure and for updating of probability of failure using Bayesian updating technique. Probability of failure in Monte Carlo simulation is shown by Equation (3.32)

$$\text{Probability of Failure } (P_f) = \frac{\text{Number of failures}}{\text{Total number of simulations}} \quad (3.32)$$

The Equation (3.33) gives the return period of load [66], using probability of failure,

$$\text{Return Period} = \frac{1}{p_f} \quad (3.33)$$

Monte Carlo simulation uses randomly generated samples as per their probability distributions. Probability of failure is achieved by solving Equation (3.32) for large number of times. It is a ratio of number of samples (failed) i.e. in unsafe region divided by total number of samples of random variable i.e. simulations. The accuracy of this technique depends on number of simulations used in the analysis. The number of simulations used in this study is fixed at 1×10^7 . For each simulation, there was new wave height and new model uncertainty factor for load and resistance. The platform will fail if the load effect (Q) exceeds the resistance of the member (R). The reliability index can be found by Equation (3.34),

$$\beta = \Phi^{-1}(P_f) \quad (3.34)$$

Where, Φ^{-1} = Inverse standard normal distribution. Probability of failure can be found by Equation (3.35),

$$P_f = 1 - \Phi(\beta) \quad (3.35)$$

Φ =Cumulative distribution function for the standardized normal variable

3.4.3 Selection of Jacket Platforms for Reliability Analysis

Offshore Malaysia has three regions and Jacket platforms were selected to represent each region. Two platforms were from Sarawak, one from Sabah and one from Peninsular Malaysia. These platforms were designed as per API RP2A-WSD 21st (current edition). SACS software was used for static linear and nonlinear analyses. The availability of the original SACS model of the platform was compulsory in this study for the calibration. This is because the designed structure has already proved its strength and it could be used for target reliability. The load models used in the original SACS model were necessary for this analysis. The characteristics for selection of platform were based on i.e. varying number of legs, and different water depths. Table 3.13 and Figures 3.8-3.11 show the details of the platforms selected for reliability analysis. Their water depth varies from 42 m to 95 m which represents the range of depths of platforms in offshore Malaysia.

Table 3.13: Details of Selected Platforms for Reliability Analysis

Platform Location	Water Depth (m)	Installation Year	No. of Legs	Design Wave Height (m)
PMO	61.00	2006	4	10.8
SBO	42.80	2007	6	7.7
SKO1	72.40	2003	4	9.9
SKO2	94.8	2008	4	11.7

These Jackets were checked for material and geometrical variability, load effect ratios (axial to bending to hydrostatic) and load type ratios (dead to live to environmental). Load capacities were calculated for the components, joints and overall system. Table 3.14 shows a case study showing the benefits of using mean coefficient and variation coefficient to convert into any required value of mean & standard deviation (SD).

Table 3.14: Random Variable Used to Find the Reliability Index

Factor	Distribution	Initial value	MC	VC	Mean used	SD
Fy	Normal	340	1.230	0.050	418.200	17.000
D	Normal	610	1.001	0.0014	610.610	0.854
T	Normal	25	1.024	0.016	25.600	0.400
d	Normal	610	0.9993	0.0018	609.573	1.098
t	Normal	16	1.024	0.016	16.384	0.256
Angle	Normal	90	1.000	0.050	89.709	4.238
Dead Load	Normal	1.0	1.000	0.060	1.000	0.060
Live Load	Normal	1.0	1.000	0.100	1.000	0.100
Xm (Tension)	Normal	1.26	1.260	0.050	1.260	0.063
Wave Height	Weibull	2.59	2.590	1.060	2.590	1.060
Current	Weibull	0.81	0.810	0.120	0.810	0.120
Xw	Normal	1.0	1.000	0.150	1.000	0.150



Figure 3.8: Jacket Platform at PMO

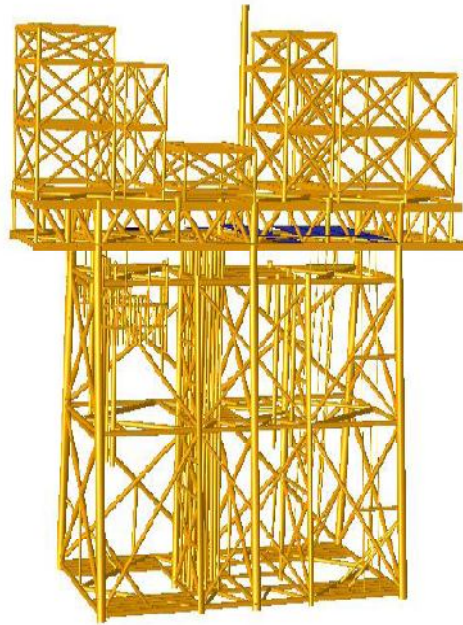


Figure 3.9: Jacket Platform at SBO



Figure 3.10: Jacket Platform at SKO (SKO1)



Figure 3.11: Jacket Platform at SKO (SKO2)

3.4.4 SACS Analysis

SACS is three dimensional space frame software for analysis of Jackets for all loading conditions i.e. dead, live and environmental loads i.e. wind, wave, current. Environmental loads are applied horizontally on the platform. Wind acts mainly on topside and wave and current act on the Jacket members. Wave and current forces on the members are calculated using Morison Equation. SACS analysis was used to find the component stresses, joint stresses and system base shear at design loads and at higher loads.

3.4.5 Load Ratios

In this study, Jacket was divided into different levels and representative members and joints were selected from Jacket. Major gravity loads are supported by legs and braces in vertical plane while horizontal loads (which are variable) are supported by horizontal braces [108]. Loads acting on Jacket vary in their influence. Shallow water Jackets are dominated by gravity load and deepwater Jackets are dominated by

Environmental load (γ_w). The dead, live and environmental load ratios for Jackets are shown in Table 3.15. Gravity load consists dead and live loads. It has been shown that on Jacket platform 70% of gravity load is dead and 30% is live load [69]. In this study load proportions were used to represent the variability of load under which a Jacket can undergo at site. Here load ratios were derived based on total load which was equated to 1.0. Case study of evaluating of load ratio is given in Appendix B. For GOM, load ratios used were in range of 0.3-40 and for North Sea it was between 0.3-12 [151]. Ratios used for Mediterranean Sea has been 0.3 to 12 for extreme conditions and 0.2 to 0.6 for operating conditions [9]. In this research, load ratios 0.1 to 50 were considered for reliability analysis.

Table 3.15: Dead, Live and Environmental Load Ratios

W_e/G	0.1	0.25	0.5	1.0	2.5	5.0	10	25	50
Dead load (d) 70% of G	0.64	0.56	0.47	0.35	0.20	0.12	0.06	0.03	0.01
Live load (l) (30% of G)	0.27	0.24	0.20	0.15	0.09	0.05	0.03	0.01	0.01
Environmental load (w)	0.09	0.20	0.33	0.50	0.71	0.83	0.91	0.96	0.98
Unity check (d+ l+ w=1)	1.00	1.00	1.00	1.00	1.00	1.00	1.00	1.00	1.00

3.4.6 Soil Conditions Effect on Component and Joint

The effect of fixing of Jacket at mud level or providing the effective pile foundations at mud level has been different for component and joint cases and overall system. In this study one platform from Sarawak (SKO2a) was used with pile foundation and SKO2 was fixed at mud level for analysis. Tables 3.16, 3.17 and 3.18 show the coefficients achieved for both cases for SKO2 and SKO2a platform using response fitting. The results show that there was not much difference in coefficients which gave minor difference in reliability index. Therefore reliability analysis was not performed for component and joint of SKO2a platform. For system reliability the coefficients were slightly different and thus it has been calculated in Chapter 7.

Table 3.16: Load Coefficients for K-Joint

K-Joint						
	Stress Type	a ₁	a ₂	a ₃	a ₄	a ₅
K-SKO2	Axial	0.01218	-0.07960	0.10520	-0.06624	0.259
	IPB	0.01652	-0.13650	-0.00648	0.02542	0.388
	OPB	0.05543	-0.91780	-0.02879	0.25140	4.008
K-SKO2a	Axial	0.01216	-0.07914	0.10680	-0.06986	0.258
	IPB	0.01646	-0.13590	-0.00541	0.02542	0.387
	OPB	0.05322	-0.87510	0.005137	0.20830	3.815

Table 3.17: Load Coefficients for T/Y-Joint

T/Y-Joint						
	Stress Type	a ₁	a ₂	a ₃	a ₄	a ₅
T/Y-SKO2	Axial	-0.00407	0.22560	0.2013	-0.4439	-0.3101
	IPB	0.003423	0.02700	0.1224	0.1545	-0.1315
	OPB	0.02387	-0.32660	-0.2178	0.2196	1.5990
T/Y-SKO2a	Axial	-0.00350	0.23100	0.1322	-0.3425	-0.3347
	IPB	0.003422	0.02697	0.1221	0.1550	-0.1314
	OPB	0.02020	-0.26460	-0.1344	0.1385	1.3360

Table 3.18: Load Coefficients for X-Joint

X-Joint						
	Stress Type	a ₁	a ₂	a ₃	a ₄	a ₅
X-SKO2	Axial	0.006135	-0.00264	0.1172	0.02035	0.04043
	IPB	0.002713	0.03073	0.1204	0.19250	-0.15200
	OPB	0.004213	0.009521	0.1619	0.08998	0.01732
X-SKO2a	Axial	0.00613	-0.002620	0.1171	0.02093	0.04001
	IPB	0.002765	0.029820	0.1221	0.19050	-0.14840
	OPB	0.004303	0.008561	0.1582	0.09002	0.01726

3.5 Component Reliability

Jacket platform was divided into different bays. Members were selected based on their location, diameter to thickness variation and slenderness ratio. The primary members are leg and brace. Brace members were further divided into horizontal

periphery, horizontal diagonal and vertical diagonal. Seven component stresses were analysed for each member. For combined stresses, the limit state Equation contained combination ratios for each type of stress. Table 3.19 shows component grouped for one platform and selected for reliability analysis. Similarly, different groups were selected from other regions. Figure 3.12 shows the flow chart of the methodology to evaluate component and joint reliability.

Table 3.19: Geometry Groups for Component Reliability Analysis

Type of Component	Bay	Outer Diameter (mm)	Wall Thickness (mm)	Length (mm)
Horizontal Diagonal	Mid	813	15	3000
	Mid	813	25	21200
Horizontal Brace Periphery	Mid	813	15	7700
	Mid	813	15	9500
Leg	Bottom	1650	25	13100
	Bottom	1200	20	5000
Vertical Diagonal	Top	762	30	7820
	Top	914	20	18521

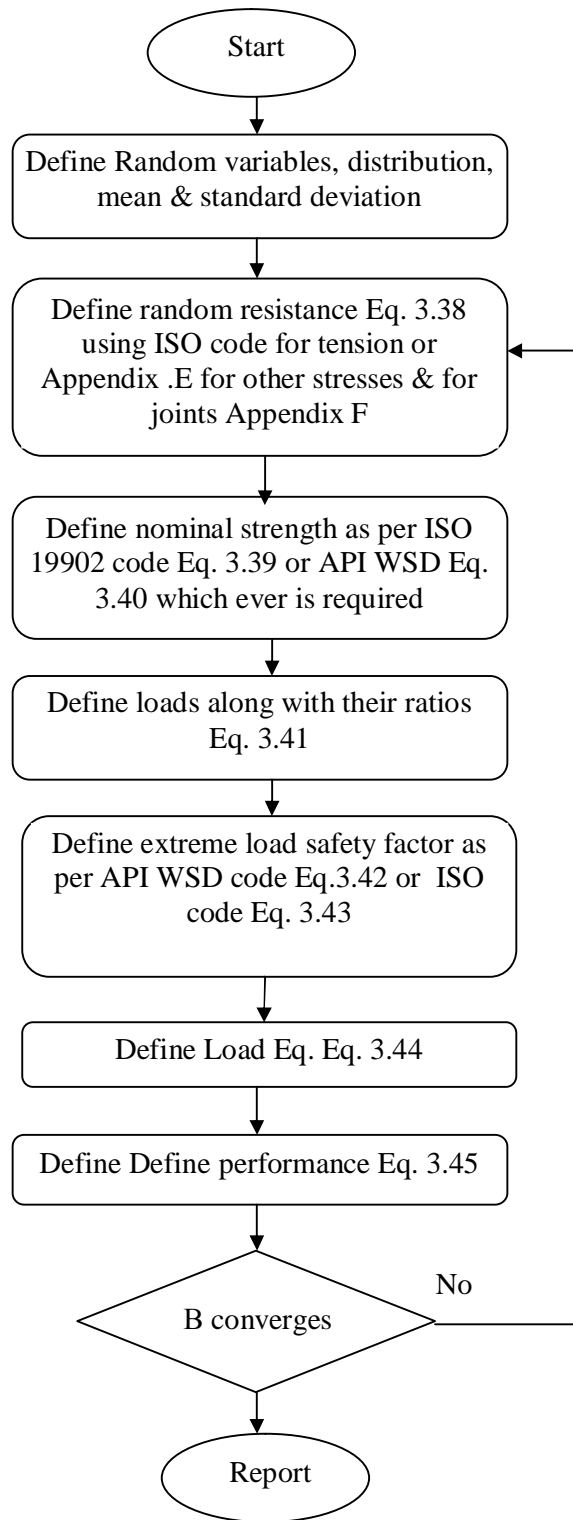


Figure 3.12: Flow Chart for Component and joint Reliability

3.5.1 Single Stresses Case Study: Axial Tension

Code Equation for axial tension provided by ISO and API WSD are shown by Equations (3.36-3.37) respectively.

$$\sigma_t \leq \frac{f_t}{\gamma_{R,t}} \quad (3.36)$$

Where, $\gamma_{R,t}$ = resistance factor, σ_t = tensile stress, f_t = tensile strength

$$F_t = 0.6F_y \quad (3.37)$$

F_t = allowable tensile stress, F_y = yield strength. Reliability analysis provides strength of component using ISO code Equation (3.38)

$$R = f_{yi} \times A_i \times X_m \quad (3.38)$$

Where f_{yi} = random yield strength, A_i = random area of tubular member, X_m = model uncertainty. To find the applied stress, reliability analysis for loading purpose will include Equations (3.39-3.40) for API WSD and ISO respectively,

$$S = f_{yn} \times A_n \quad (3.39)$$

Where, f_{yn} = nominal yield strength and A_n = nominal tubular area

$$S = 0.6 \times F_{yn} \times A_n \quad (3.40)$$

Where, S = strength given by code Equation. Application of load ratios for reliability analysis are given by Equation (3.41),

$$L_r = dD + lL + wW/X_w \quad (3.41)$$

Where, d , l and w are the dead, live and environmental load ratios shown in Table 3.15, D , L , W are the variable uncertain random dead, live and environmental load and X_w = environmental load uncertainty model and in this study it has been taken from study which was conducted for ISO [69]. Normal distribution was considered with mean of 1.0 and standard deviation of 0.15. Parameters of random variables are defined separately in FERUM. The main part of calibration is that we want a component or joint which is fully utilised we need to define factor of safety as per the code. Factor of safety in API WSD for extreme conditions is shown by Equation (3.42)

$$FS(API\ WSD) = \frac{4}{3 \times 1.67} \quad (3.42)$$

The factor of safety in ISO 19902 for extreme conditions is given by Equation (3.43)

$$FS(ISO) = \frac{(1/1.05) \times (D+L+W/X_w)}{(1.1D+1.1L+(1.35 \times W/X_w))} \quad (3.43)$$

Where, FS = factor of safety, 1.05, 1.1, 1.35 are tensile resistance, gravity load and environmental load factors. The actual load applied by API or ISO can be shown as Equation (3.44),

$$L = S \times L_r \times FS \quad (3.44)$$

The limit state Equation becomes, as shown in Equation (3.45),

$$g = R - L \quad (3.45)$$

Same procedure was adopted for all other types of stresses to find the reliability.

3.6 Joint Reliability

There are three types of joints identified by the codes i.e. K, T/Y and X. They are defined by the way loads act on the joint and geometry of the joint. There are four types of stresses tension, compression, in-plane bending and out-plane bending for each joint. The methodology adopted was same as explained in 3.5.1. Table 3.20 shows the groups of geometry considered for reliability from one platform. Similarly different groups of joints were selected from other regions.

Table 3.20: Geometry Groups for Joint Reliability Analysis

Type of Joint	Chord Diameter (mm)	Chord Thickness (mm)	Brace Diameter (mm)	Brace Thickness (mm)	Brace angle (Degrees)
K	1200	40	914	25	90
	813	30	813	25	55
T/Y	711	30	457	25	83
	1200	40	711	15	90
X	813	15	711	12	42
	1200	50	813	30	90

3.6.1 Target Reliability

When Jacket platform designed as per existing code, has proved its strength and reliability, it is considered safe to take the reliabilities of that platform as our target

reliability. In theory, it is said that it should consider minimization of cost of construction, maintenance cost and consequence of failure. Target reliability for components and joints was set as per API WSD reliability and reliability achieved by ISO was compared with WSD. For practical purpose, calibration of factor of safety of new code is done against reliability of in-service Jackets designed. Jackets designed as per the old code are taken as target reliability. Here for each case, ISO and WSD reliabilities were found out separately and then compared to find the environmental load factor, which is explained in Chapter 5. Component target reliability for Jacket legs and braces was set at 3.85 and 3.88 for North Sea [30].

3.7 Environmental Load Factor

When API WSD designed platforms have already survived certain amount of time in rough weather, they have established their robustness in design. Now we can take their reliability as safe against failure and the reliability index higher than API WSD can be taken as safe as API WSD. The reliability found using ISO 19902 and API WSD code were plotted together. Reliability index was determined with different load factors as per ISO code. When the ISO reliability index crossed the target reliability (higher reliability than available reliability) it was taken as the load factor for that member, joint or overall platform. This method is explained in Chapters 5, 6 and 7.

3.8 Resistance Factor

Environmental load factor achieved in this study for components and joints was used to find resistance factor for component stresses. This was necessary so that ISO resistance factors could be assessed and evaluated with new load factors proposed for this region. Two types of stresses were checked here which were axial tension and compression using FORM method.

3.9 System Reliability Based Environmental Loads

Probability of failure for Jacket platform was determined by increasing the wave heights for 10,000 year return period and higher. Wave height was increased so that effect of wave on deck could also be ascertained. The effect of load and resistance model uncertainty and RSR on probability of failure / return period was evaluated. Failure of platform in eight directions was initiated by compression buckling of primary components of Jackets i.e. horizontal and vertical diagonal brace, leg and piles. In this study, the maximum wave height was increased, which increased the applied wave load and corresponding base shear of platform was obtained.

Regression analysis was used to find the coefficients for response surface Equation by converting the wave and current forces into environmental load model by the use of curve fit tool. Probabilities of failure, return periods, safety indices and their COV were obtained against an RSR of 1.5-2.5. For system reliability analysis target probability of failure was taken from literature. SACS collapse module was used for nonlinear analysis of the platform. MATLAB code was used for FORM analysis to find reliability index. Fatigue wear and tear was considered negligible and fatigue limit state was not checked against failure. The system reliability for critical direction was taken as 4.46 in North Sea. The probability of failure at system level should be about an order of magnitude smaller than at component level [30].

3.9.1 SACS Collapse Module

SACS software has collapse module used for nonlinear analysis. This module has its parallel in SESAME software named USFOS. This module includes member buckling with 8 or more hinge points. It also includes evaluation of joint failure due to excessive strain, strain hardening as well as residual stresses. This module includes collapse view which shows progress of failure, gradual plastification and finally collapse mechanism.

It requires main input file to be established before this model is formulated. The primary file is used to define geometry, material and loading properties. The load is defined along with different combinations of operating and extreme conditions.

Extreme loading conditions are used for collapse analysis. One difference between linear and nonlinear analysis in SACS module is the defining of loading conditions. Dead, live and dead loads are combined for loading conditions in linear analysis, but for collapse analysis loads are separately defined. First of all linear analysis is run with all load combinations in eight directions i.e. at each 45 degrees, if Jacket is four, six or eight legs. The combination and direction which gives maximum base shear is selected for collapse analysis.

The next step is the formulation of collapse module which includes different steps to be defined as follows.

- 1) Maximum iterations per load increment
- 2) Number of member segments
- 3) Maximum number of member iterations
- 4) Define deflection tolerance
- 5) Rotation tolerance
- 6) Member deflection tolerance
- 7) Strain hardening ratio
- 8) Maximum ductility allowed
- 9) Load type, number of its increments, start and end load factor. For instance
 - Load type = dead load,
 - Number of its increments=5
 - Start load factor=0
 - End load factor=1

$$\text{Load increment} = \frac{\text{End factor} - \text{Begin factor}}{\text{Number of increments}}$$

Each time load will be increased by $1/5=0.2$ times the actual load, until it reaches to 1.0, this is for dead and live load but end load factor for environmental load is put up to 4 or 5. This is due to the fact that environmental load is increased until failure.

- 10) Defining member groups which are not to be analysed in this module like pipes, conductors etc.

3.9.2 Collapse Analysis of Jacket

Working Stress Design (WSD) is based on linear elastic behaviour of platforms for determination of loads and resistance. Ductility is measured in RSR, which is the main criterion for ultimate strength of platforms. Ultimate capacity of platform can be determined by using nonlinear static push over analysis. In this approach first of all gravity loads i.e. dead and live are applied, followed by increase of environmental loads till failure occurs. Resistance at collapse is represented by Equation (3.46) which provides the push over strength of member [109],

$$R_{ult} = \lambda_{ult} E \quad (3.46)$$

Where, R_{ult} = ultimate resistance of platform, λ_{ult} = factor which is increased until collapse, E = modulus of elasticity

Design codes provide check against ultimate strength as shown in Equation (3.47):

$$\frac{R_{ultimate}}{\gamma_R} \geq \gamma_d D_1 + \gamma_w E_1 \quad (3.47)$$

Where, γ_R = resistance factor, γ_d = gravity load factor, γ_w = environmental load factor, D_1 = gravity load, E_1 = environmental load. The minimum requirement for safe structure from pushover analysis is given by Equation (3.48),

$$\lambda_{ult} \geq \gamma_R \times \gamma_w \quad (3.48)$$

$$\lambda_{ult} \geq 1.18 \times 1.35 = 1.59 \text{ (ISO for compression failure)}$$

The minimum RSR is recommended by ISO and API i.e. 1.58 as per API RP 2A WSD and 1.85 for ISO 19902 codes for high consequence and manned platforms. The minimum RSR range considered in this study were in range of 1.5-2.5 which are considered as reasonable [94]. Here in this analysis, wave load is increased and corresponding RSR is found. The main objective was to find wave height which will give RSR of 1.0 considered as fully optimised Jacket.

3.9.3 SACS Jacket Model for Push Over Analysis

Once this collapse module is defined in SACS pushover analysis is conducted to find reserve strength ratio of Jacket. The Load sequence followed in this analysis is as follows: 1) All Dead load, 2) All live load, 3) Environmental load is increased until

failure is reached. At each load increment base shear is recorded, the first important information to be noted is base shear at 100 year environmental load, second when first member fails and the last is when Jacket collapses completely.

3.9.4 SACS Jacket Model for Push Over Analysis

Platform SACS geometry models were not changed and only load models were changed which was necessary to check the effects of overloading. Table 3.21 gives details of the platforms used for system reliability analysis. Water depth and topside height varies with respect to each region. Jacket length given here covers from bottom of mud line to the top of leg. Design wave was the maximum wave height for that particular platform site for 100 year extreme conditions. Free board for each platform also varied from 10.5 to 16.5 m. The height of topside, excluding helipad deck, has been shown in Table 3.21.

Table 3.21: Basic Details of Jackets Considered for System Analysis

Region (Platform)	Jacket length (m)	Water depth (m)	Design wave height (m)	Free board (m)	Topside height (m)
PMO	78.2	61.7	10.8	16.5	25.7
SBO	53.3	42.8	7.7	10.5	30.5
SKO1	85.7	72.3	9.9	16.5	26.9
SKO2	107.9	94.8	11.7	13.1	21.0

Push Over analysis was based on nonlinear collapse analysis of SACS module. RSR is based on ultimate strength divided by characteristic design load (100 year extreme load). In this analysis gravity and environmental loads were increased from a factor of 0 to 1 in load step of 0.1 and the environmental load is then increased beyond 1 (which is 100 year extreme load) until the collapse of a member/system.

RSR was calculated when first member failed, this is due to the fact that this member has lowest RSR value as per WSD code. We need optimally designed structure for environmental load for Jackets designed as per ISO code, which requires

that member should be checked with minimum RSR. Jackets in this study have 4 and 6 legs and therefore environmental load in 8 directions was used to find the minimum RSR. Maximum design wave was used from all directions. The range of values for RSR, based on failure load to characteristic load i.e. 100 year design load were achieved as 2.0-4.9. For consistency the range of RSR was fixed at 1.50-2.25. Higher values of RSR represented extra safety in Jacket platform and therefore they were not used in this study.

3.9.5 Wave and Current Loads in Malaysia

Platform analysis was made for different wave heights keeping current values constant for one wave height. This was required to find the wave height which would give minimum value of RSR of 1.0 and variability for curve fit was evaluated at this RSR as shown in Figures 7.1-7.5. This was a case of severe environmental load condition for Jacket platforms. Current velocities vary at different heights above mud level in linear stretching profile as proposed by API WSD and ISO 19902 codes. There were three current values i.e. near mud level, at mid level and at surface level. Current speed was fixed in this study for a given wave height.

For platform at PMO region, the wave heights increased in steps of 10.8, 11.3, 11.9, 12.4, 13.0, 13.5, 16.0, and 19.0 m. Design current velocities for 100 years storm conditions at different water depths were 0.57, 1.0, and 1.1 m/s at one meter above mud level, mid water and at surface level respectively. Thus for instance, when a wave of 10.8 m height was analyzed each current speed was used separately for eight directions. Thus 24 analyses were made for each wave height and there were 192 SACS analysis for this platform. For platform at SBO region wave heights considered were 7.7, 8.1, 8.5, 8.9, 9.2, 9.6, 11.6, 13.9, 16.2 and 18.1 m. The 100 year current velocities were 0.68, 0.86 and 0.94 m/s at one meter above mud level, mid water and at surface level respectively. Thus 240 SACS analyses were made for this platform. For platform SKO1 at SKO region wave heights considered were 9.9, 10.4, 10.9, 11.4, 11.9, 12.4, 15, 17.5, 20, 22.5 m. The 100 year current velocities were 0.68, 0.95 and 1.05 m/s at one meter above mud level, mid water and at surface level respectively. Thus 240 SACS analyses were made for this platform. Platform SKO2

at SKO region wave heights considered were 11.7, 12.3, 12.9, 13.5, 14, 14.6, 17.6, 20.5, 23.4 m. The 100 year current velocities were 0.55, 0.95, 1.20 m/s at one meter above mud level, mid water and at surface level respectively. Thus 216 SACS analyses were made for this platform. Same number of separate analysis was made for SKO2a platform to get its response coefficients. Wave height properties in shape of base shear are shown in Figures 7.46-7.53 and Appendix C.

3.9.6 Curve Fitting

The curve fitting for the platforms was made using MATLAB curve fit tool. The custom polynomial Equation for wave and current was defined to get the parametric values for the given coefficients. Response surface fit proposed by Heidman and Efthymiou in Equation (2.15) as shown by E. Gerhard was used to get the load effects from Jacket base shear and wave heights [20]. The coefficients were derived using the least mean square method. Data was analysed at 95% confidence level and coefficient of variance i.e. R^2 value of above 0.90 as shown in Figures 7.6-7.10

3.9.7 Safety Factor for Jacket System: API WSD and ISO 19902

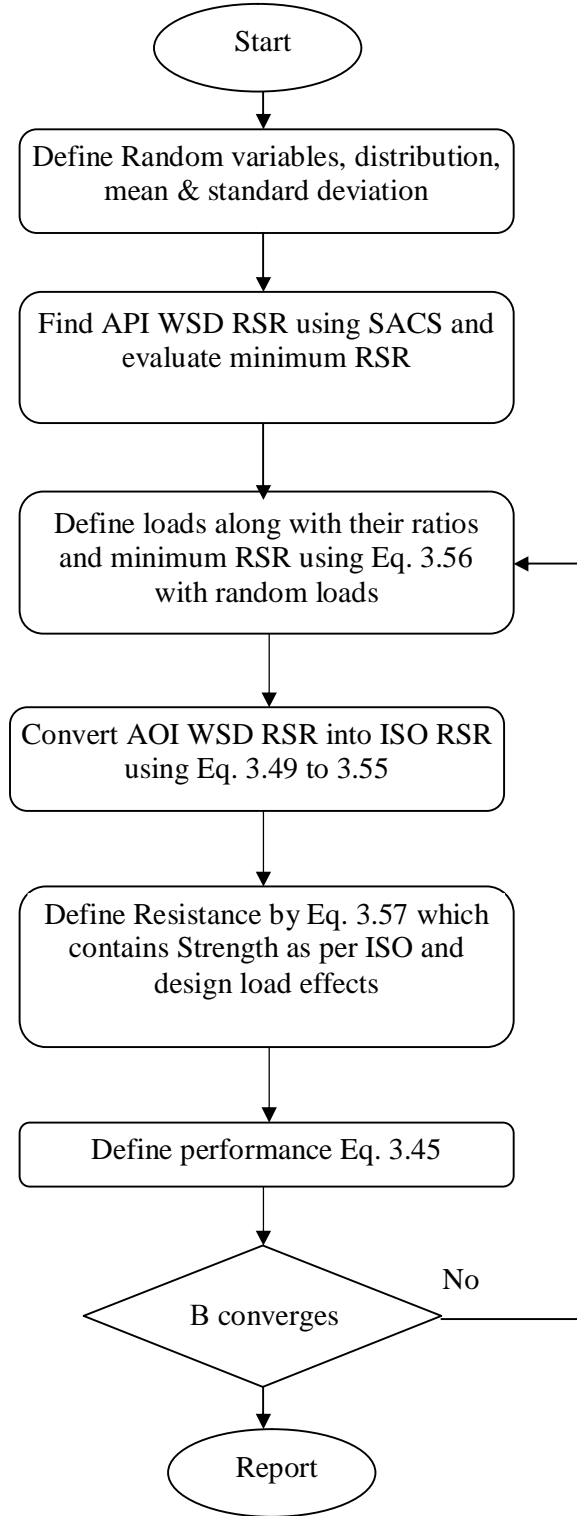


Figure 3.13: Flow Chart for System Reliability

Figure 3.13 shows the flow chart to evaluate the system reliability index. In this section, a relationship is established between API WSD RSR and ISO RSR. This is based on safety factors available with both codes. These safety factors are apparent as well as inherent. Therefore both are highlighted and effects of change of code are explained. The methodology adopted here was used for calibration of ISO code [27]. Design capacity of component in ISO code is given by Equation (3.49),

$$\frac{R}{\gamma_c} \leq (\gamma_d \times P_d + \gamma_w \times P_w) \quad (3.49)$$

Where, P_d = gravity load proportion, P_w = environmental load proportion, γ_c = compression resistance factor, γ_d = gravity load factor, γ_w = environmental load factor. There is a relationship between WSD and ISO RSR. The RSR for ISO code could be found from Equation (3.50),

$$RSR_{ISO} = MOS_{ISO} \times MF \times ICSF \times SR \times P_d P_{w_{ISO}} \quad (3.50)$$

Material factor (MF) is based on the yield strength. In this study it was achieved to be 1.23 as reported in Table 4.2 but making consistency with ISO code it was fixed as 1.15 to be on the lower side. Here it has been taken from ISO code i.e. for grade 345 MPa it has been reported that average material strength is higher by 15% [138]. System redundancy (SR) was based on platform specific values as shown in Tables 7.2-7.6.

The ultimate load can be found using Equation (3.51),

$$P_{ult} = (\gamma_d \times P_d + \gamma_w \times P_w) \times M_F \times ICSF \quad (3.51)$$

The ISO RSR could be shown as Equation (3.52), this will be used in limit state Equation (3.57),

$$RSR = ICSF \times MF \times S_R \quad (3.52)$$

RSR values were also selected using platform specific values as shown in Tables 7.2-7.6. P_d/P_w ratio varies in this study ranging from 0.1-20. In this study the load factor is calibrated as per P_d/P_w ratio of 1.0 which was considered reasonable as per the conditions of offshore [69]. Implicit code safety factor (ICSF) is the difference between applied stresses and strength provided by code Equation (3.53).

$$ICSF = \frac{RSR_{WSD}}{(P_d/P_w) \times SR \times MF \times MOS_{WSD}} \quad (3.53)$$

Safety margin (MOS)_{WSD} were set as reported by code i.e. for extreme conditions there should be one-third increase in the required stresses. Therefore, in this study it has been fixed as 1.32 as also suggested by [20, 27]. For ISO, this safety factor was provided by Equation (3.54),

$$MOS_{ISO} = \left(\frac{\gamma_d \times P_d + \gamma_w \times P_w}{P_d + P_w} \right) \gamma_c \quad (3.54)$$

ISO gravity and environmental load which were used in limit state Equation can be shown in Equation (3.55),

$$P_d P_w_{ISO} = 1 + \left[1 - \left\{ \frac{1}{(MOS_{ISO} \times MF \times ICSF)} \right\} \right] \times \frac{P_d}{P_w} \quad (3.55)$$

3.9.8 Limit State Function for System Environmental Loading

The limit state function for load and resistance for system reliability can be shown by Equations (3.56-3.57):

$$load = RSR_{WSD} \times \left[Dd + Ll + w \left(\frac{a_1(H_{max} + a_2 V_c)^{a_3}}{X_w} \right) \right] \quad (3.56)$$

Where, w =Environmental load ratio

$$Resistance = a_1(H_{max(des)} + a_2 V_c)^{a_3} \times MOS_{ISO} \times P_d P_w_{ISO} \times RSR \times X_w \quad (3.57)$$

$H_{max(des)}$ =Design wave height

3.9.9 Target System Probability of Failure

Notional target failure probability can be determined by using Equations (3.58 and 3.59) [70]. The Equation 3.59 was also used by CIRIA Report 63 [155],

$$Pf_n = 10^{-4} \times \mu_s \times t_l \times n_p^{-1} \quad (3.58)$$

Where, t_l =design life of structure i.e. 30 years (PTS manual), n_p = average number of people at/ near platform = 70; μ_s = social criteria factor (for offshore structures) = 5.0

$$Pf_n = 10^{-5} \times A \times W_f^{-1} \times t_l \times n_p^{-1/2} \quad (3.59)$$

Where, A = activity factor (for offshore structures) = 10.0, W_f = Warning factor for sudden failure =1.0

Failure probability was found to be 2.14×10^{-3} and 3.58×10^{-3} from Equations 3.58 and 3.59 respectively. Efthymiou gave probability of failure of 10^{-4} (reliability index = 4.0). Therefore in this study, Melchers target reliability of 3.58 and Efthymiou target reliability 4.0 were used.

3.10 System Based Environmental Load Factor

The methodology adopted here was based on [20, 27]. System reliability based environmental load factors for offshore Malaysia were determined using calibration of API WSD design code. The given method establishes the relationship between RSR and environmental load factors. The RSR achieved was based on API WSD design code. Therefore it was first converted to RSR ISO code as shown in 3.9.5. Redesign as per ISO code was not selected due to following facts: the actual design was API WSD which has proved its strength and reliability at site. Besides that, API WSD has been in changing process. The erratum was published only in 2008 which incorporate the latest changes of ISO code. The RSR was based on inherent and apparent factors of safety of codes along with redundancy in system. The structural reliability was determined with respect to varying W_e/G ratios and different RSR values within practical range. Therefore lower values of RSR were used in this analysis as they would give optimally designed Jackets. The main aim depended on safety level of WSD and economy of ISO code which makes maximum use of utilization of member.

3.11 Assessment of Jacket Platform

There are many uncertain parameters used in Jacket design. The complete safety of Jacket cannot be guaranteed. Future loading conditions, inability at design stage to accurately get data for material resistance, the simplified code Equations used to predict the load behaviour, and errors and omissions due to human factors [53]. This makes the reliability check even more necessary after the completion of Jacket platform. Design life of Jacket platform in Malaysia has been fixed as 30 years. Even before reaching that age, due to the requirements from insurance and other governmental institutions, the assessment is made mandatory after 3-5 years.

Therefore, once in operation, it becomes necessary to get its probability of failure updated using latest resistance and load conditions. Here in this study, probability of failure was found first at design load, and then it was determined for a return period load of 10,000 years. This was increased to higher values of wave height as explained in 3.9.3. Monte Carlo simulations were used to find the probability of failure for all the platforms.

3.11.1 Uncertainty Model for Resistance and Load

Load model uncertainty, which predicts extreme environmental conditions and transforms the storm condition wave to an individual wave height, is shown by Equation (3.60),

$$L = A_i \times a_1(H_{var} + a_1 \times V_c)^{a_3} \quad (3.60)$$

Where H_{var} = random wave height. Resistance model uncertainty was shown by Equation (3.61),

$$R = B_i \times RSR \times a_1(H_{max} + a_1 \times V_c)^{a_3} \quad (3.61)$$

Where, A_i, B_i are load and resistance model uncertainty parameters and are shown in Table 3.22. The resistance model uncertainty parameters i.e. mean was 1.0 and coefficient of variation (COV) was 0.1 [27] and the COV used by DNV are in range of 0.05-0.1. DNV gives conservative values and therefore Efthymiou' recommended values were taken. For load model uncertainty Haver [94] has given COV of 0.15. RSR values considered were in between 1.5-2.5.

Table 3.22: Uncertainty Factors used for Limit State Equation

Factor	Description	Distribution Parameters	Reference
A_i	Load model uncertainty	Normal distribution $\mu = 1.0, \sigma = 0.15$	[94]
B_i	Resistance model uncertainty	Normal distribution $\mu = 1.0, \sigma = 0.10$	[94]

Thus limit state function can be shown by Equation (3.62),

$$g = B_i \times RSR \times a_1(H_{max} + a_1 \times V_c)^{a_3} - A_i \times a_1(H_{var} + a_1 \times V_c)^{a_3} \quad (3.62)$$

Where, H_{var} = varying wave height as per Weibull distribution parameters

Figure 3.14 shows the flow chart to evaluate probability of failure of Jacket using design load.

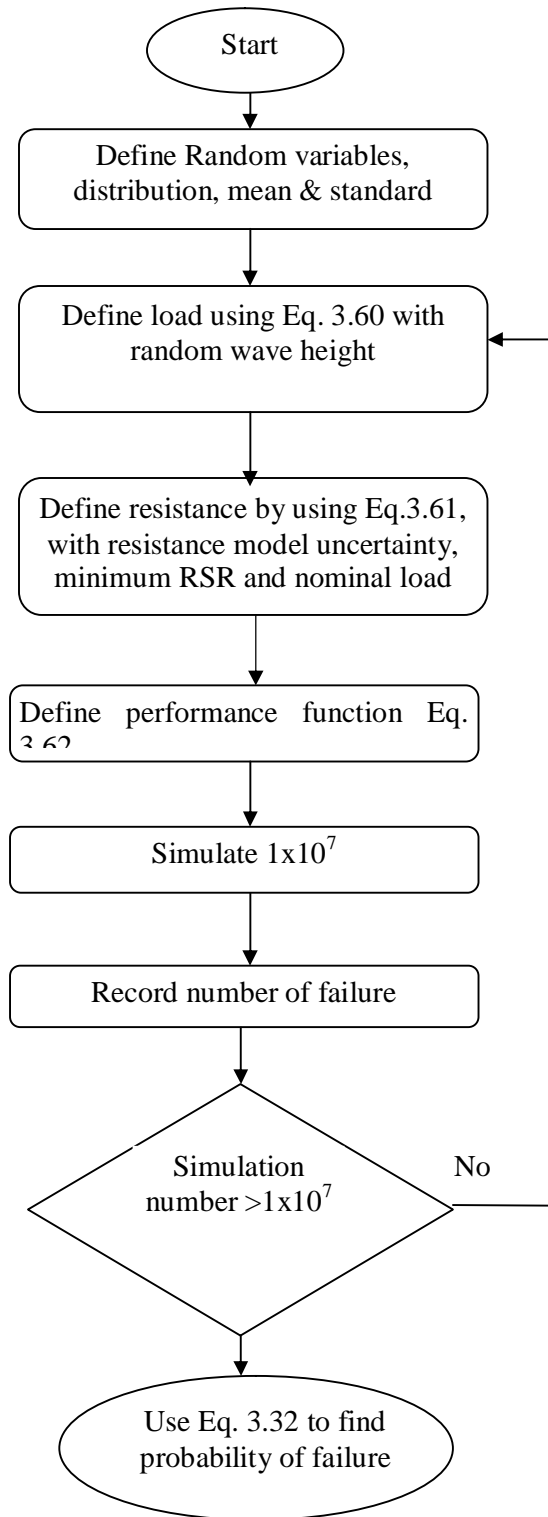


Figure 3.14: Flow Chart for Finding Probability of Failure

3.11.2 Bayesian Updating of Probability of Failure-Intact Structure

The Jacket platform was overloaded with increase in wave height till an RSR value of 1.0 was reached and the corresponding wave was recorded. Using this experience acquired from the Jacket analysis we are confident enough that the platform will be safe against a wave height which produces an RSR of 1.0. This new wave height was used to find the survival probability of platform (P_s), as shown in Equation (3.63),

$$P_s = \frac{\text{Number of Survival}}{\text{Total Number of Simulations}} \quad (3.63)$$

When P_f is evaluated given that P_s is also known then we can find the updated probability of failure (P_{uf}) based on Equation (3.64). Failure probability has already been found using Equation (3.32). The new updated probability of failure was given by Equation (3.64),

$$P_{uf} = P(g < 0 | S > 0) \quad (3.64)$$

$P(g < 0)$ = Probability of failure of limit state function,

$P(S > 0)$ = Probability of survival of limit state function

Thus updated probability of failure (P_{uf}) can be shown by Equations (3.65-3.66),

$$P_{uf} = \frac{P[g(x) < 0 \cap S > 0]}{P[S > 0]} \quad (3.65)$$

$$P_{Uf} = P(g|S)P(S) \quad (3.66)$$

Survival limit state function is given by Equation (3.67),

$$g = B_i \times RSR \times a_1 \times (H_d + a_2 \times V_c)^{a_3} - A_i * a_1 * (H_R + a_2 \times V_c)^{a_3} \quad (3.67)$$

Where, H_d = design wave height, H_R = wave height when RSR = 1.0

Figure 3.15 shows the flow chart to update probability of failure using Bayesian updating technique.

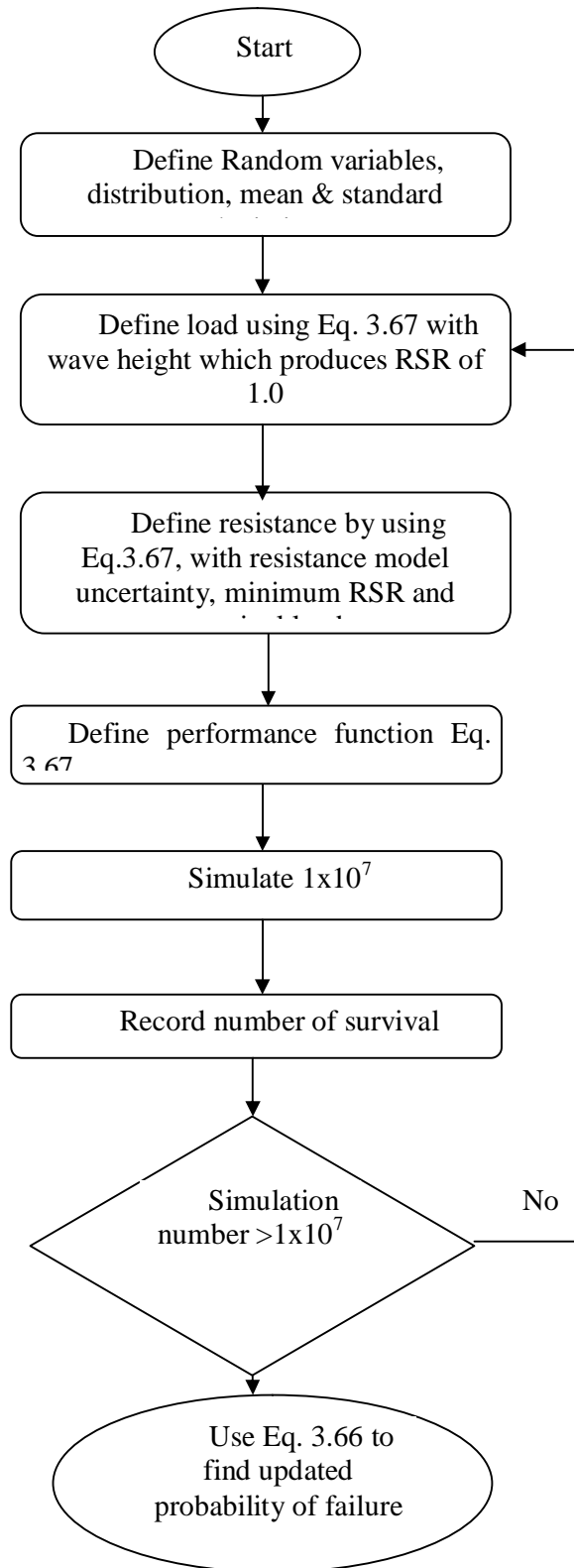


Figure 3.15: Flow Chart for Bayesian updating of Probability of Failure

3.11.3 Bayesian Updating of Probability of Failure-Damaged Structure

The knowledge of increased wave load effect was used to find the Bayesian updated failure probability. When some Jacket members fail, the overall capacity of Jacket could be reduced. This assumption was used by removing three members one by one from each Jacket. At each member failure corresponding base shear was evaluated and its strength was determined as shown in Tables 7.8-7.12. Damaged strength factor is given in Equation 3.68. This reduced capacity was used to find updated probability of failure. The capacity was reduced about 50% in case of three member failures. As this was not acceptable, the probability of failure was determined for two member failures.

$$DSf = \frac{Q_f}{Q_e} \quad (3.68)$$

Where, Q_f = Base shear (damaged state), Q_e = 100 year design load

3.12 Chapter Summary

In this chapter uncertainty models developed for resistance and load were explained. The extreme distribution models of Weibull and Gumbel were outlined with respective mathematical modelling. Structural reliability methods of FORM and Monte Carlo simulation were presented. Typical ISO and API reliability limit state Equation for tension were discussed for uncertainty modeling and reliability analysis. Environmental load factor determination for Jacket platform was discussed using component and joint and system reliability analysis. Jacket assessment for 10,000 years and higher return period load was discussed. Lastly Bayesian updating was explained which is a necessary tool for updating the probability of failure.

CHAPTER 4

UNCERTAINTY MODELLING OF RESISTANCE AND LOAD

4.1 Introduction

Load and resistance in LRFD method are taken as random variables. Uncertainty modelling is the most important step for reliability analysis. The resulting estimates of reliability significantly rely on and are very sensitive to uncertainty modelling [54]. This chapter deals with statistical data analysis for strength and load variables. The random variables are analysed and range of type of distributions, mean values and standard deviations, are discussed. There are two parts for this chapter. One part deals with basic resistance uncertainty of geometry and material properties and ISO component and joint stresses model resistance. The statistical parameters for model resistance were found by using Monte Carlo simulations for component and joint resistance. Easy Fit statistical software was used to analyse and find the probability distributions for resistance variables. The other part deals with environmental load parameters i.e. wind, wave and current. For load it was based on available database record, provided by local industry. Microsoft Excel was used to do the regression analysis for extrapolation of extreme event for sea state parameters i.e. wind, wave and current. Actual data used to find the long return periods was very small and thus extrapolation was made to acquire data for higher return periods. Least square fitting method was used to find cumulative distribution function.

4.2 Load Factor and Uncertainty

Uncertainty of random variable plays a significant role for the determination of reliability index. Load factor is suitable and appropriate means of finding the reliability of structures to meet local geographical requirements [82]. Load factors are produced by code calibration using reliability analysis. The basic input to the reliability analysis for environmental load factors for Jacket platforms was statistical parameters of environmental load and material resistance [82], [156].

4.3 Resistance Uncertainty

The work on resistance variations have been done on onshore and offshore structures in different parts of the world and are available in literature. Here, an effort was made to analyse the data as per existing conditions in Malaysia which was required as per ISO 19902 requirement. There were three steps for this analysis. The first one was to collect the data on random variables. The second step was to make statistical analysis of basic random variables used for design Equations of tubular members and joints. The last step was to use these resistance random variables in ISO 19902 code Equations and get the parameters for the stress uncertainty models which are faced by Jackets. Nine random stresses were modelled using ISO 19902 code for component and four for each type of K, T/Y and X joint. After the analysis, it was compared with other similar studies made in different offshore regions.

4.4 Statistical Properties of Fundamental Variable for Resistance

The basic variables of resistance are geometry and material i.e. thickness, diameter, yield strength and modulus of elasticity. It has been reported that reliability index depends on geometry and material strength for Jacket platforms [157]. The results from this study are compared with studies in ISO 19902 code, GOM, North Sea and China. Here in this study, resistance uncertainty bias was used for statistical analysis. Bias is defined as ratio of actual characteristic value to assumed characteristic value

[58]. Probability density function (PDF) shows the frequency of occurrence of certain parameters. This could be normal distribution with perfectly parabolic curve. Here central tendency will be more and likely occurrence will be at middle of parabola.

4.4.1 Geometric Properties

The uncertainties for geometric properties, considered in this study are the diameter and thickness for legs and braces. These are the basic variables for the reliability analysis. Samples collected for thickness variations were 26, for leg diameter 260 and for brace diameters 113. Measured samples for angles were 85 obtained from as built drawings. Geometrical design and fabrication nowadays are well controlled due to ISO quality control standards. The variations measured were very low for geometrical variables. That was the main reason that distribution was also normally distributed. Figure 4.1 shows the plan of Jacket at a bay showing braces and legs. The chord-braces angles, however accurately they may be connected still, show some variations. Table 4.1 shows the difference in design and actual values for angle on plan one bay of Jacket. This difference is actually covered by tolerance limit provided for each variable by the design codes.

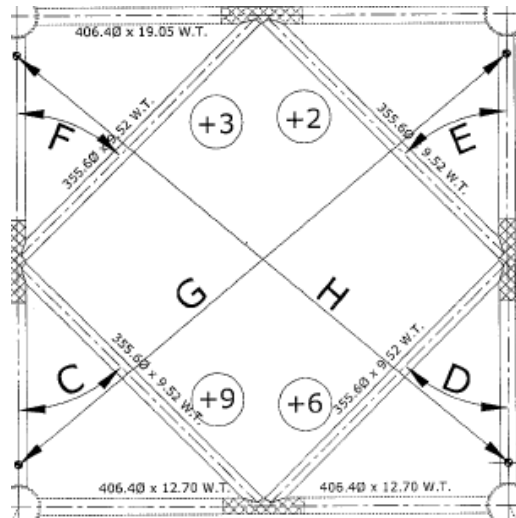


Figure 4.1: Angle Variations

Table 4.1: Angle Variations Measured Using Fig. 4.1

Location	Design Value	Actual	Deviation	Tolerance
C	45°	45.0013	+0.0013	5°
D	45°	44.8958	-0.1042	5°
E	45°	44.8852	-0.1148	5°
F	45°	44.6777	-0.3223	5°

Analysed data is shown in Table 4.2 and Figures 4.2-4.5. Statistical analysis was used to find the parameters of distribution and probability density function based on Goodness of fit tests. Distributions were fitted and the best fit was reported. The results show that the best fit was achieved with normal distribution. Though log-normal curve was also very close to normal but depending on Anderson-Darling and Kolmogorov-Smirnov test results best fit was proposed. Here Weibull distribution came at third place during the applied statistical tests. These three distributions were evaluated out of many others due to recommendation by ISO code [73]. The best distribution fit achieved for China, North Sea (DNV) code and ISO 19902 was also normal. The values matched the results from China and North Sea and GOM. The variation coefficient was very small for diameter and angle except wall thickness which has relatively higher variations. This trend was also present in GOM, North Sea and China. In this study variation in diameter of legs and braces was presented separately, this was done due to difference in leg and brace diameter variations. Angle variation from other sources was not available for comparison.

Table 4.2: Statistical Variation in Geometry of Tubular Component and Joints

Type of Variability	Statistical Parameter	MS		Duan et al., 2005 [22]	BOMEL, 2003 [69]	Adams et al. 1998 [158]
		Leg >1000 mm	Brace <1000 mm	China	ISO	GOM
Diameter (mm)	Distribution	Normal	Normal	Normal	-	Normal
	MC	1.001	0.9993	1.0	1.005	1.0
	VC	0.0014	0.0018	0.0025	0.001	0.0025
Wall Thickness (mm)	Distribution	Normal	Normal	Normal	-	Normal
	MC	1.024		1.0	1.0	1.0
	VC	0.016		0.015-0.050	0.0024+ 0.25/T	0.021
Angle	Normal	-		-	-	-
	MC	0.999		-	-	-
	VC	0.00281		-	-	-

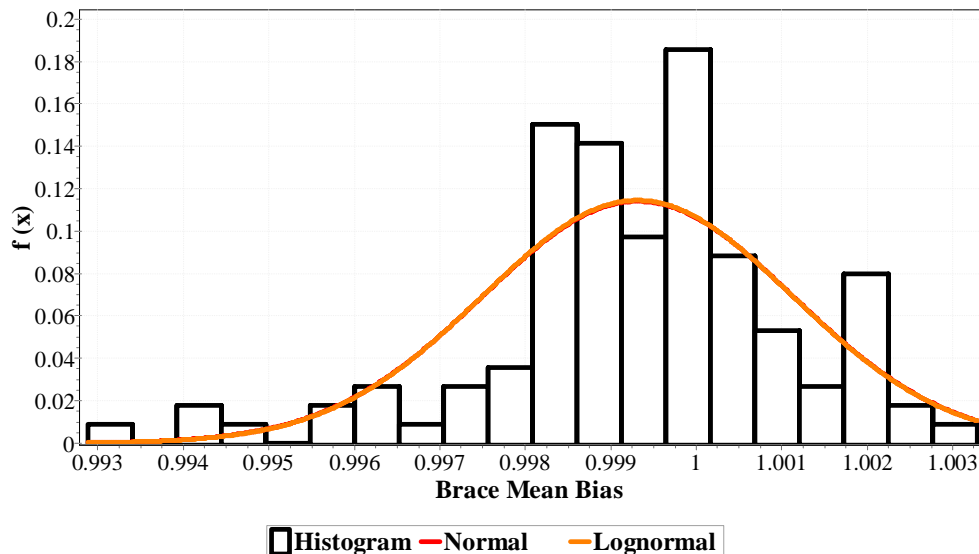


Figure 4.2: Probability Density Function for Brace diameter < 1000 mm

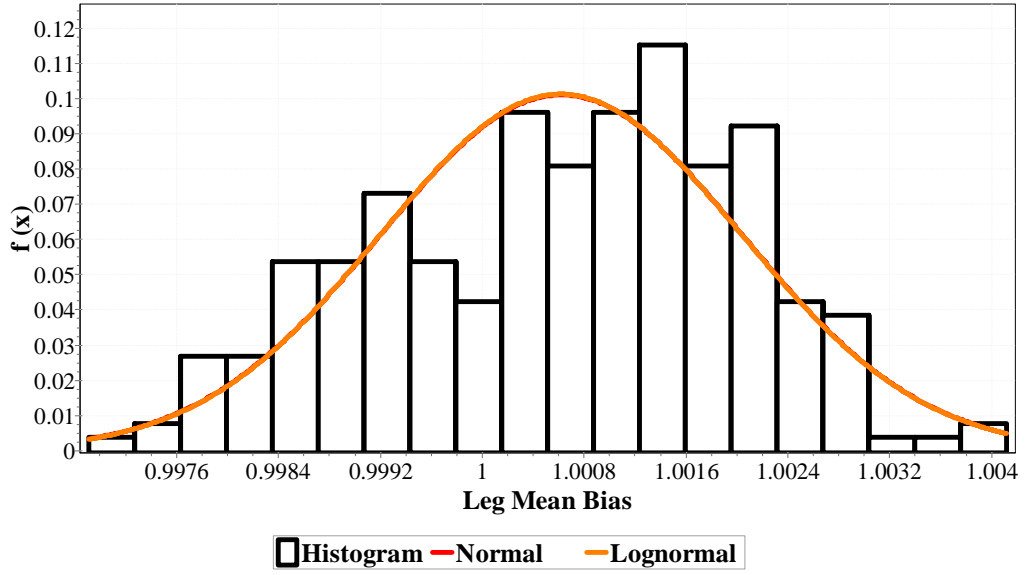


Figure 4.3: Probability Density Function for Leg diameter > 1000 mm

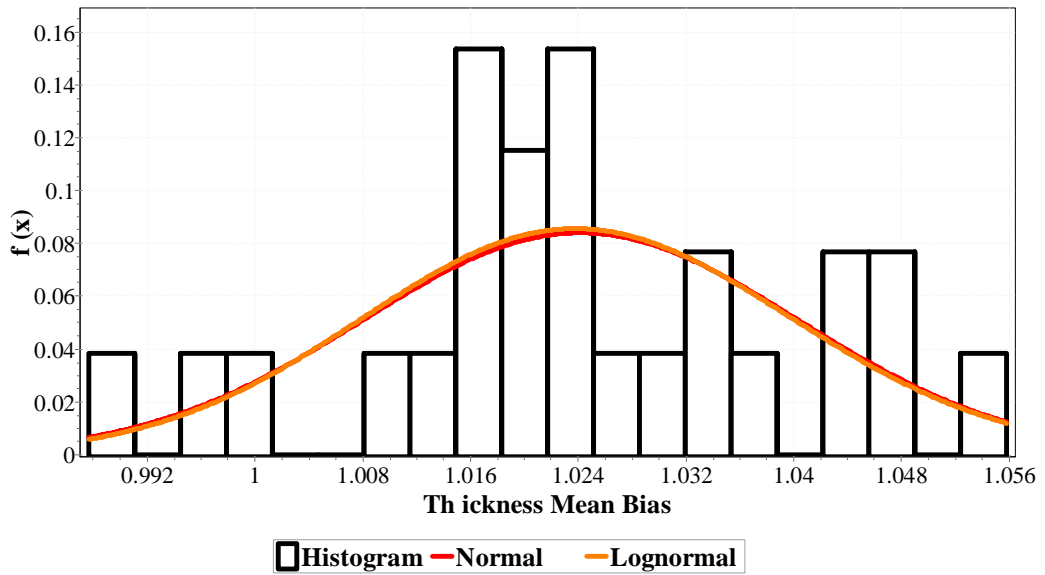


Figure 4.4: Probability Density Function for Thickness Variation

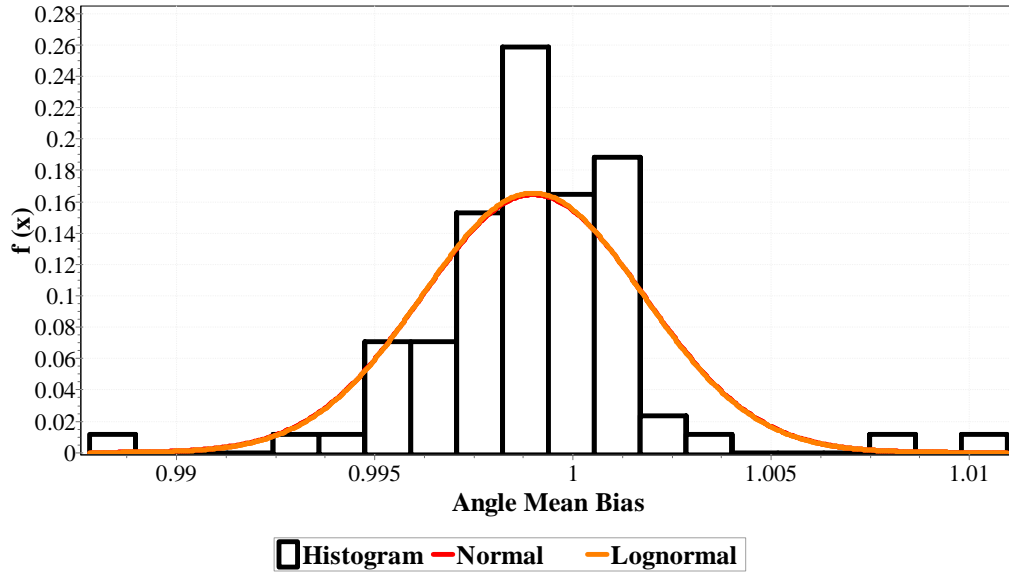


Figure 4.5: Probability Density Function for Angle Variation

4.4.2 Material Properties

It is always assumed that the lower tail of material strength distribution is of important for the evaluation of reliability [159]. Material property uncertainties considered in this study were yield strength, tensile strength and elongation. Table 4.3 and Figures 4.6-4.8 show the statistical parameters and probability density function. The sample size for yield strength obtained from mill certificates were 72 with nominal yield strength of 340, 345 and 355 MPa. Three distributions were fitted and the best fit was reported as per Goodness of fit tests. The analysis shows that the collected data fits with the normal distribution though lognormal was very close and Weibull came at third place. The results achieved in China report normal distribution and from North Sea, DNV Code and ISO 19902 reported Log-Normal, though DNV in another study [61] recommended normal distribution for material strength variable.

Table 4.3: Statistical Variation in Yield Strength

Type of Variability	Statistical Parameter	MS	Duan et al., 2005 [22]	ISO [69]	Adams et al. 1998 [158]
Yield Strength	Distribution	Normal	Normal	Log-Normal	Log-Normal
	MC	1.230	1.12	1.13	1.02-1.09
	VC	0.050	0.05	0.06	-
Tensile Strength	Distribution	Normal	-	-	-
	MC	1.123	-	-	-
	VC	0.039	-	-	-
Elongation	Distribution	Normal	-	-	-
	MC	1.520	-	-	-
	VC	0.090	-	-	-

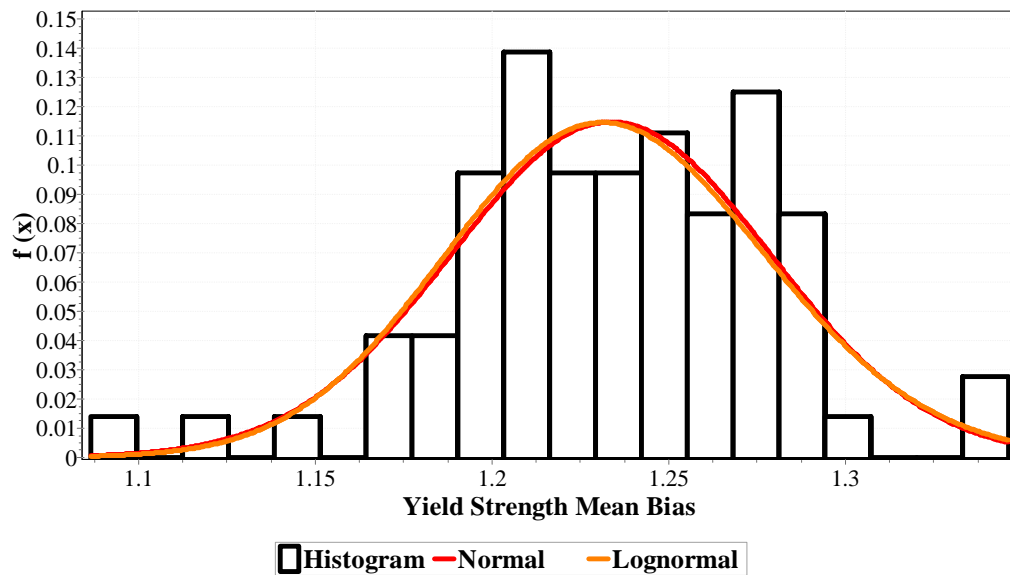


Figure 4.6: Probability Density Function for Yield Strength

For tensile strength, sample size was 72, and mill tests reported characteristic strength of 490 MPa. The best fit was found to be normal distribution; other parameters were mean bias 1.123 and COV 0.039. For elongation, sample size was 70 and characteristic value of 18% - 20% was reported in mill certificates. After analysis the distribution as per Goodness of fit test was found to be normal, with mean bias of 1.52 and COV of 0.09.

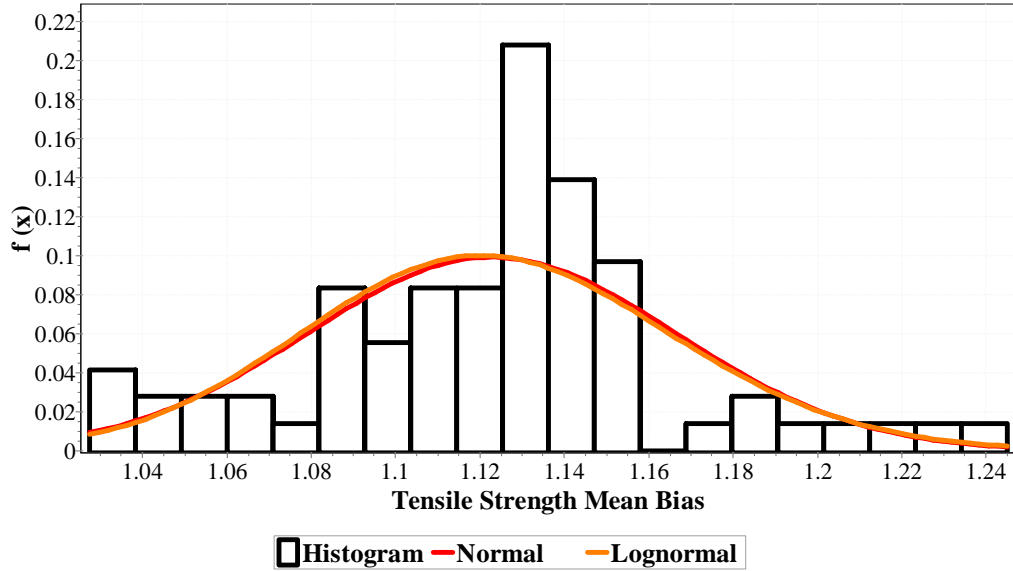


Figure 4.7: Probability Density Function for Tensile Strength

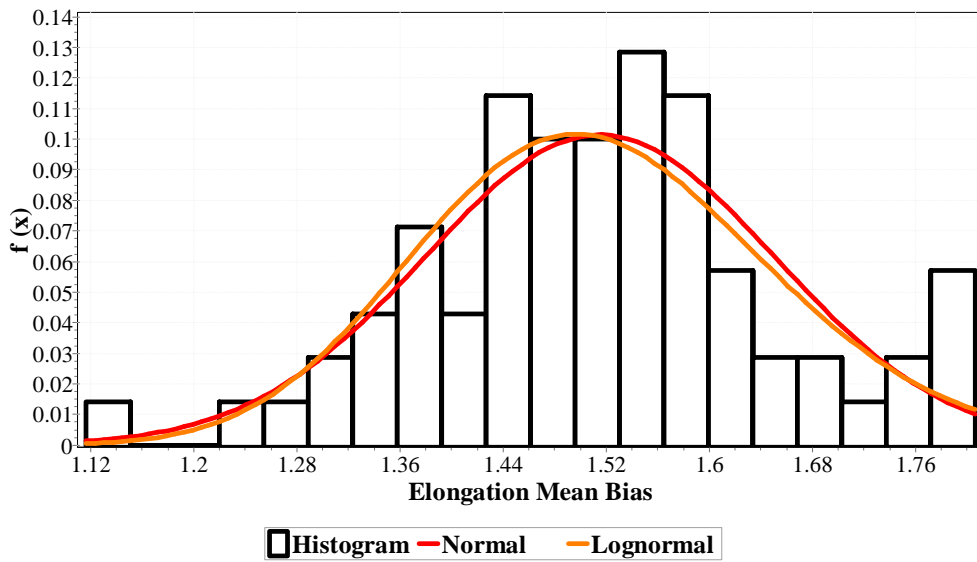


Figure 4.8: Probability Density Function for Elongation

4.5 Probabilistic Model Stresses used in ISO Code 19902

Once basic random variables results are available it was easy to find resistance model uncertainties using ISO 19902 model stress Equations. The model uncertainty (x_m) was determined so that it could be used for reliability analysis of Jacket platforms in offshore Malaysia.

4.5.1 Component Stresses

API RP2A WSD and ISO 19902 code of practice identify nine types of stresses which Jacket members undergo during operating and storm loading conditions. Monte-Carlo simulation was used to find stress variability as it was difficult to find the variability using test modelling. Simulated sample size was fixed at 1×10^5 and the nominal f_y used was 345 MPa. Probability distribution curve again showed that the difference in normal and lognormal was very small as compared to Weibull. The best fit was normal for all types of component stresses.

4.5.1.1 *Single Stresses*

ISO 19902 and API RP2A code identify member stresses, in which Jacket platform undergoes during operation which have been listed in Table 2.1. Table 4.4 and Figure 4.9-4.14 show the statistical properties and probability density function for single stress. Parameters of distribution for geometric and material properties, used in the given Equation were normal. The law of probability says that combined distributions will give the result of normal distribution. BOMEL shows the data reported for North Sea which was incorporated in ISO code. Duan et al.[22] show data analysis for China LRFD. The report of MSL is based on experimental results from tubular members. Result shows minor variation in mean coefficients in this study. The range of mean coefficients was in between 1.13-1.26 for this study, except for hydrostatic where it was 1.59. The given range for ISO was 1.0-1.14, for China it was 1.16-1.32. The variation coefficient was in between 0.05-0.16 for this study. For ISO, it was between 0.0-0.14 and for China it was 0.07-0.12.

Table 4.4: Resistance Model Uncertainty for Single Stress

Types of Stresses	SP	MS	BOMEL ISO, 2003 [69]	Duan et al., 2005 [22]	MSL [160]		BOMEL 2001[75]	Moses, 1995 [50]
					ISO, 2000	WSD, 2000		
Tension	MC	1.26	1.0	1.19	-	-	-	-
	VC	0.05	0.0	0.07	-	-	-	-
Column buckling	MC	1.26	1.05	1.16	1.26	1.16	1.06	1.19
	VC	0.05	0.04	0.12	0.06	0.08	0.05	0.12
Local buckling	MC	1.24	1.07	1.23	1.26	1.40	1.07	-
	VC	0.05	0.07	0.10	0.09	0.08	0.07	-
Bending	MC	1.13	1.11	1.32	1.16	1.43	1.11	1.26
	VC	0.05	0.09	0.11	0.09	0.12	0.10	0.11
Shear	MC	1.26	1.0	1.19	-	-	-	-
	VC	0.05	0.05	0.08	-	-	-	-
Hydrostatic	MC	1.59	1.14	-	1.43	1.85	1.14	1.05
	VC	0.16	0.14	-	0.12	0.12	0.12	0.11-0.15

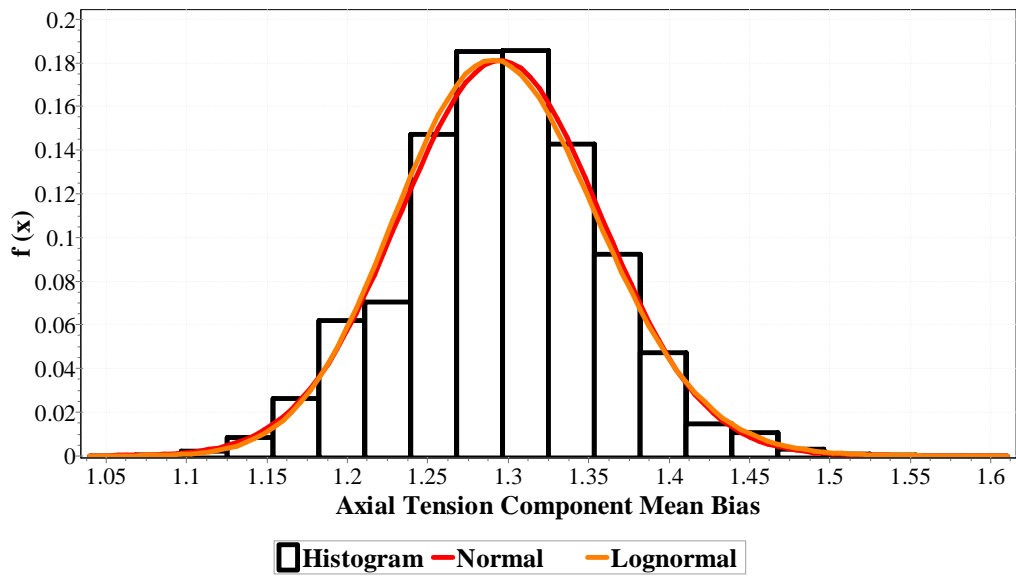


Figure 4.9: Probability Density Function for Tension

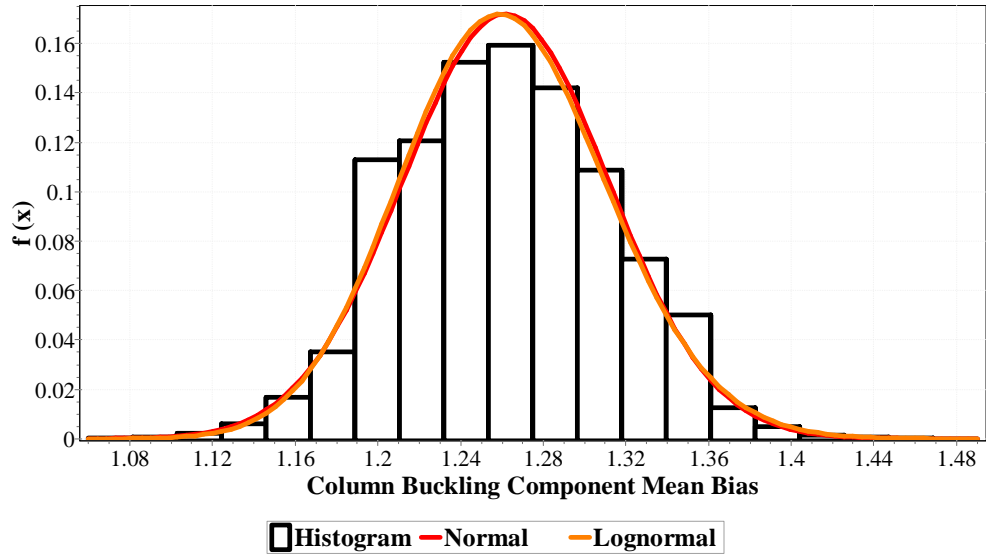


Figure 4.10: Probability Density Function for Column Buckling

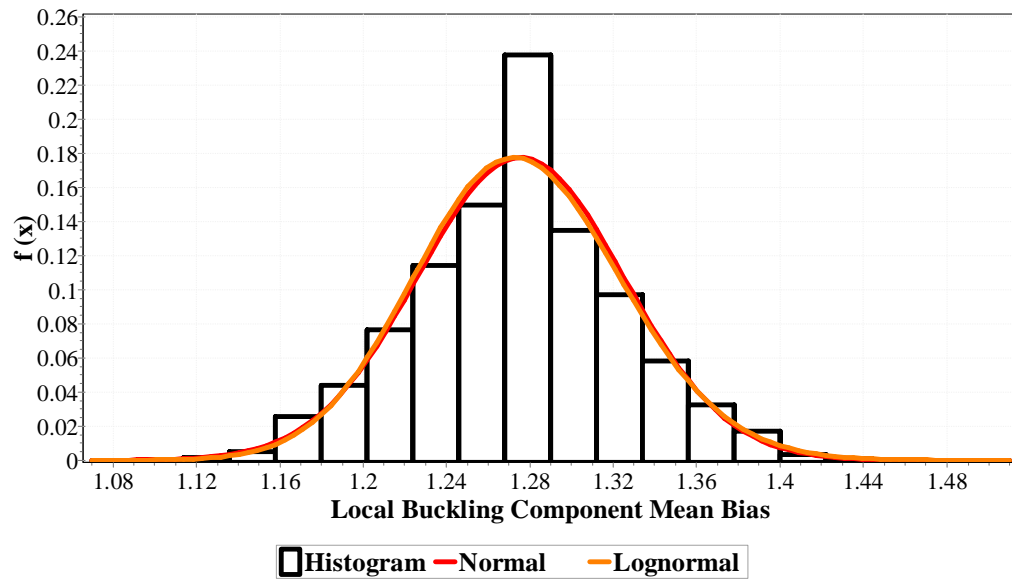


Figure 4.11: Probability Density Function for Local Buckling

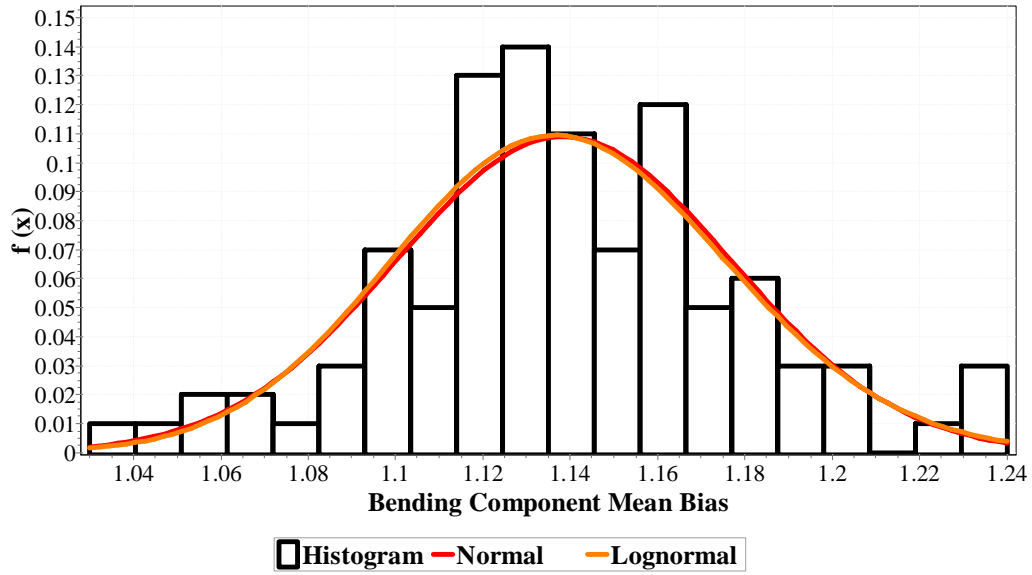


Figure 4.12: Probability Density Function for Bending

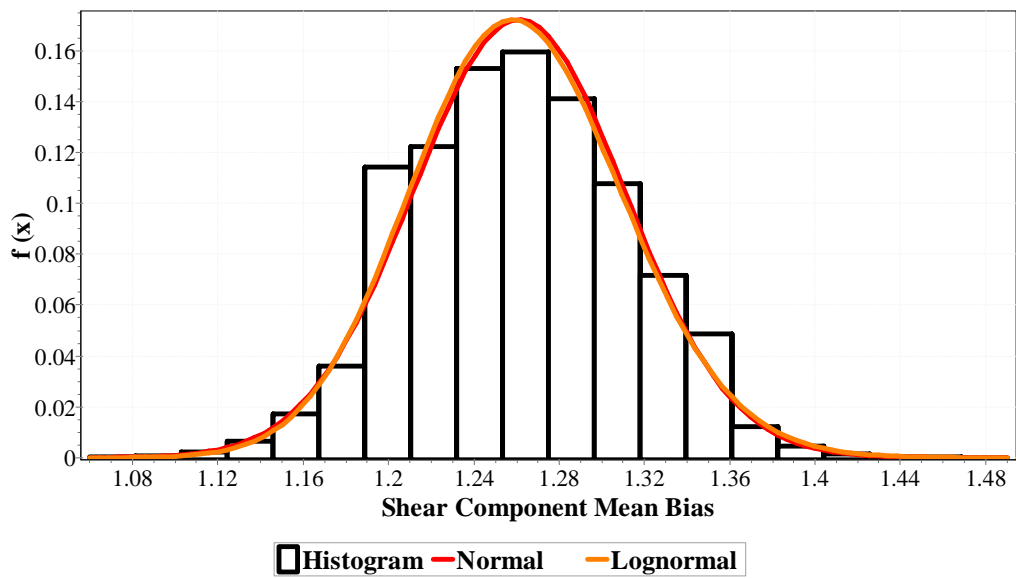


Figure 4.13: Probability Density Function for Shear

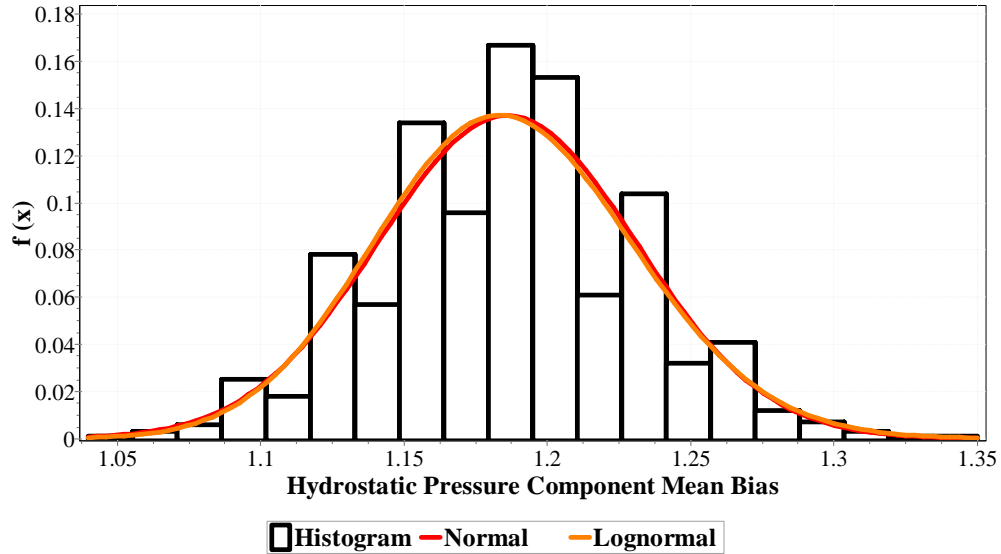


Figure 4.14: PDF for Hydrostatic Pressure (Hoop Buckling)

4.5.1.2 Two Stresses

Table 4.5 and Figures 4.15 - 4.17 show the uncertainty model for the combined two stress code Equations. In this study, the mean values achieved were 1.19 to 1.27. For ISO code the same were in range of 1.03 to 1.25 which was not much different from this study. The standard deviation achieved in this study was in range of 0.047-0.050. The same achieved for ISO code was 0.083-0.094 which shows more variation in the results. This is due to difference in basic random variables used by ISO code. Other reasons such as improved quality of material and fabrication standards introduced in the manufacturing industries in recent years may also have reduced the variability in this study. Due to these reasons, uncertainties were reduced, with less variability in material and in geometry of tubular members. MSL and BOMEL 2001 studies showed similar trend as was shown in this study.

Table 4.5: Resistance Model Uncertainty for Combined Two Stresses

Types of Stresses	SP	MS	ISO [69]	MSL, 2000 [160]			BOMEL, 2001 [75]
				ISO	LRFD	WSD	
TB	MC	1.19	1.11	-	-	-	-
	VC	0.05	0.10	-	-	-	-
CB (Column Buckling)	MC	1.27	1.03	1.14	1.15	1.15	1.03
	VC	0.05	0.08	0.10	0.10	0.09	0.08
CB (Local Buckling)	MC	1.23	1.25	1.41	1.43	1.61	1.25
	VC	0.05	0.08	0.06	0.05	0.11	0.08

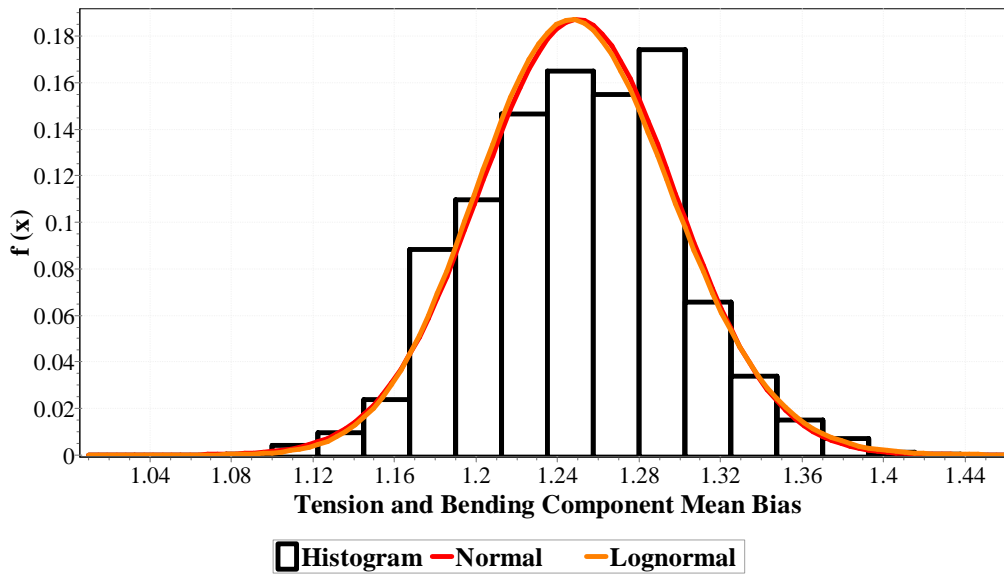


Figure 4.15: Probability Density Function for Tension and Bending

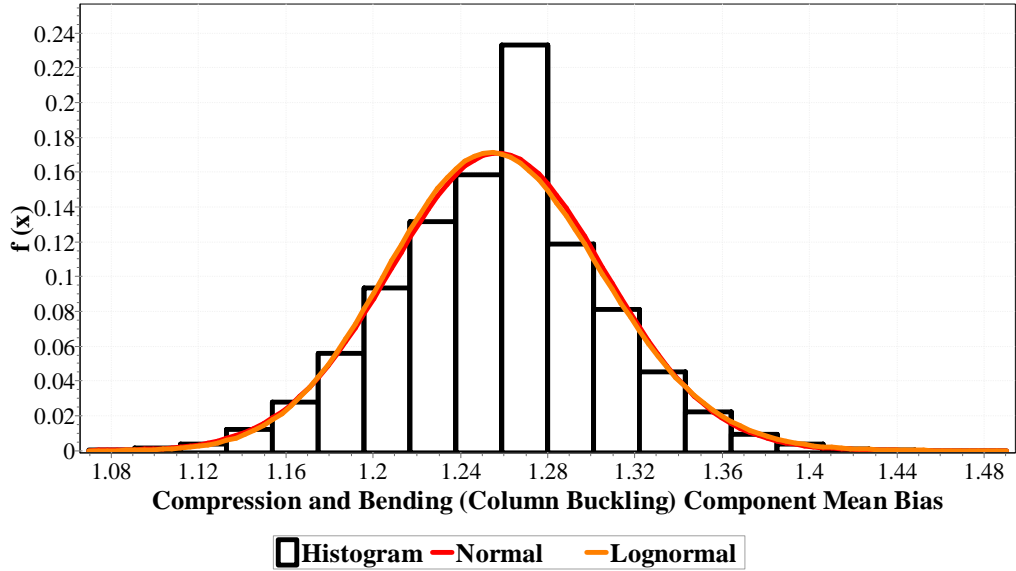


Figure 4.16: PDF for Compression and Bending (Column Buckling)

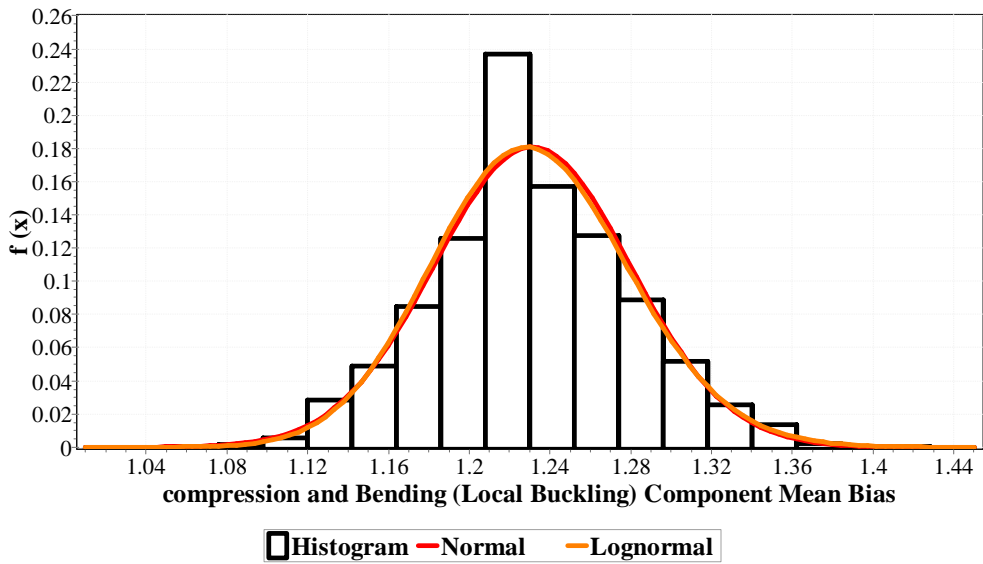


Figure 4.17: PDF for Compression and Bending (Local Buckling)

4.5.1.3 Three Stresses

Table 4.6 and Figure 4.18 - 4.20 show the uncertainty model for the given ISO code Equations. The mean biases achieved for this study were 1.27 - 1.30 and the same for ISO were in the range of 1.08 - 1.20. This shows that mean values for this study are higher by small margin as compared to ISO code. The standard deviation for this

study was 0.05 and for ISO it was 0.11 to 0.16 which was higher than the present study, showing higher variation in ISO data. MSL and BOMEL 2001 showed similar trend with this study. The variability in this study was less than as reported in literature. Thus with less uncertainty, higher reliability can be achieved.

Table 4.6: Resistance Model Uncertainty under Combined Three Stresses

Types of stresses	SP	MS	ISO,2003 [69]	MSL,2000 [160]			BOMEL, 2001 [75]
				ISO	LRFD	WSD	
TBH	MC	1.27	1.08	-	-	-	-
	VC	0.05	0.11	-	-	-	-
CBH (Column Buckling)	MC	1.28	1.20	1.33	1.29	1.43	1.25
	VC	0.05	0.11	0.16	0.12	0.20	0.14
CBH (Local Buckling)	MC	1.30	1.20	1.35	1.36	1.63	1.25
	VC	0.05	0.16	0.19	0.13	0.19	0.14

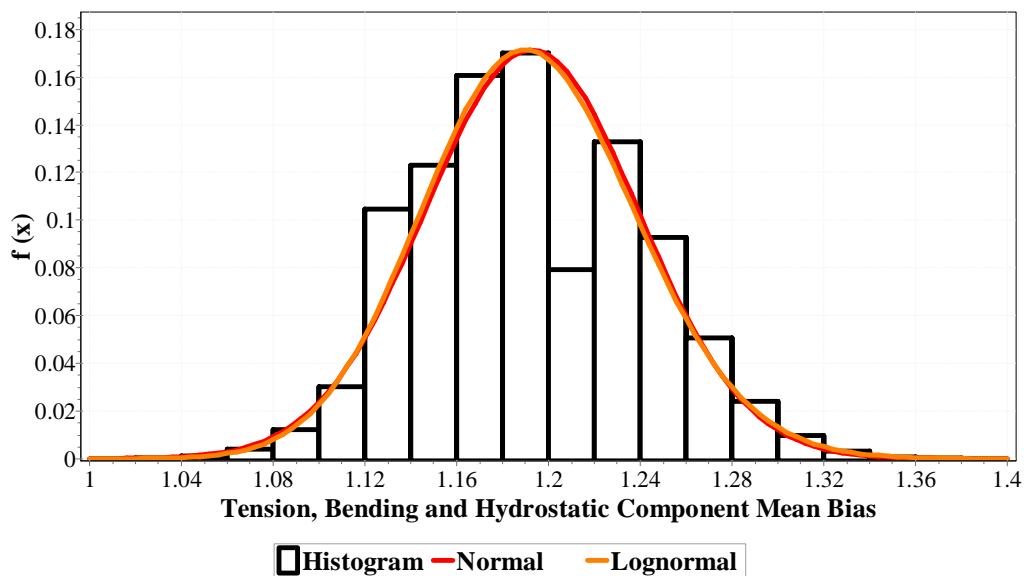


Figure 4.18: PDF for Tension, Bending and Hydrostatic Pressure

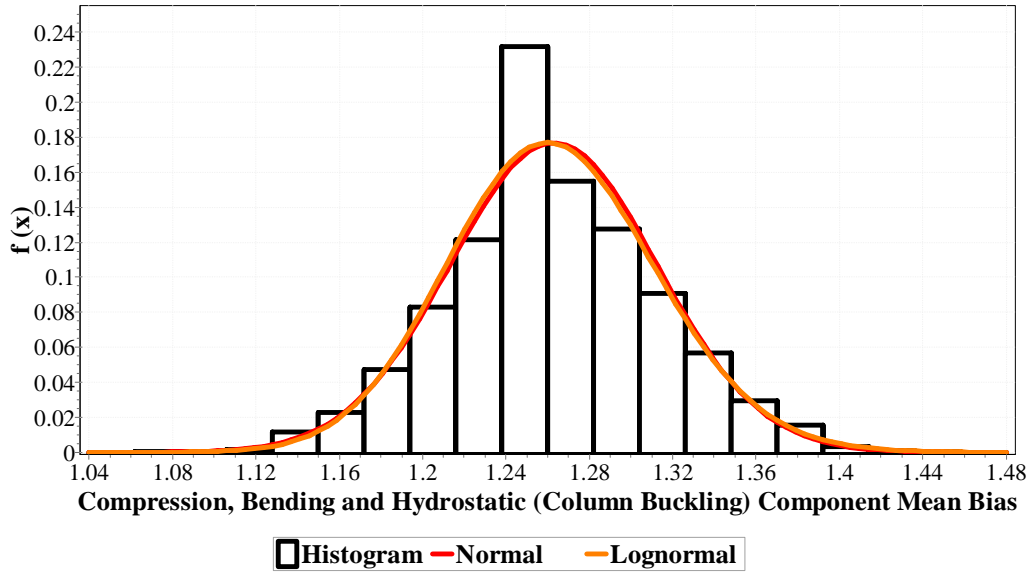


Figure 4.19: PDF for Compression, Bending and Hydrostatic Pressure (Column Buckling)

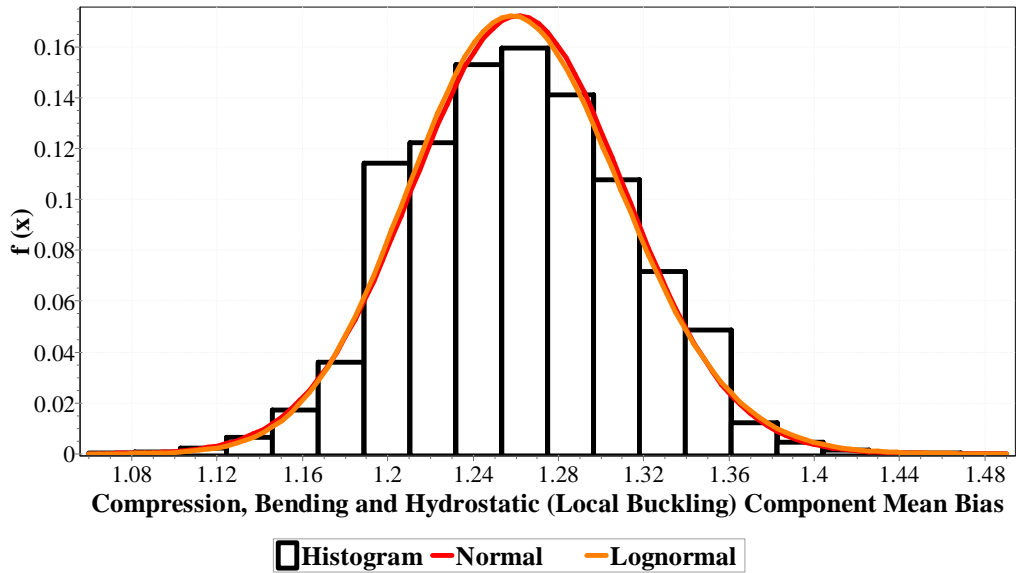


Figure 4.20: PDF for Compression, Bending and Hydrostatic Pressure (Local Buckling)

4.5.2 Joint Stresses

There are three types of joints i.e. K, Y/T and X joints used in Jacket platform as defined by codes of practice. Offshore Jacket design codes identify four types of

stresses under which each joint are subjected at site. Probability distribution curve again showed that the difference in normal and lognormal was very small as compared to Weibull. The best fit was normal for all types of joints and for all stresses. The variability in this study was less than as reported in literature. With less uncertainty, higher reliability can be achieved.

4.5.2.1 K- Joint

Table 4.7 and Figure 4.21-4.23 show the uncertainty model for K joint stress Equations. ISO gives same Equation in case of K- Joint for compression and tension. The mean bias achieved for this study were 1.27-1.29 for all four types of stresses. The same for ISO was in the range of 1.22-1.24 which was based on actual test results reported by MSL. This shows that mean values for this study are higher by small margin as compared to ISO code. The standard deviation for this study was 0.10 and for ISO it was 0.13 to 0.18 which was higher than the present study, showing higher variation in ISO data.

Table 4.7: Resistance Model Uncertainties of K-Joint

Types of stresses	SP	MS	Duan et al., 2006	ISO [69]	Ferguson [1]	MSL [160]	
						ISO (LRFD)	API (WSD)
Tension/ Compression	MC	1.29	1.58	1.23	1.22	1.23	1.7
	VC	0.10	0.23	0.17	0.1	0.17	0.15
IPB	MC	1.27	1.31	1.24	1.29	1.24	1.64
	VC	0.10	0.21	0.13	0.14	0.13	0.15
OPB	MC	1.27	1.14	1.22	1.23	1.22	1.48
	VC	0.10	0.26	0.18	0.16	0.18	0.20

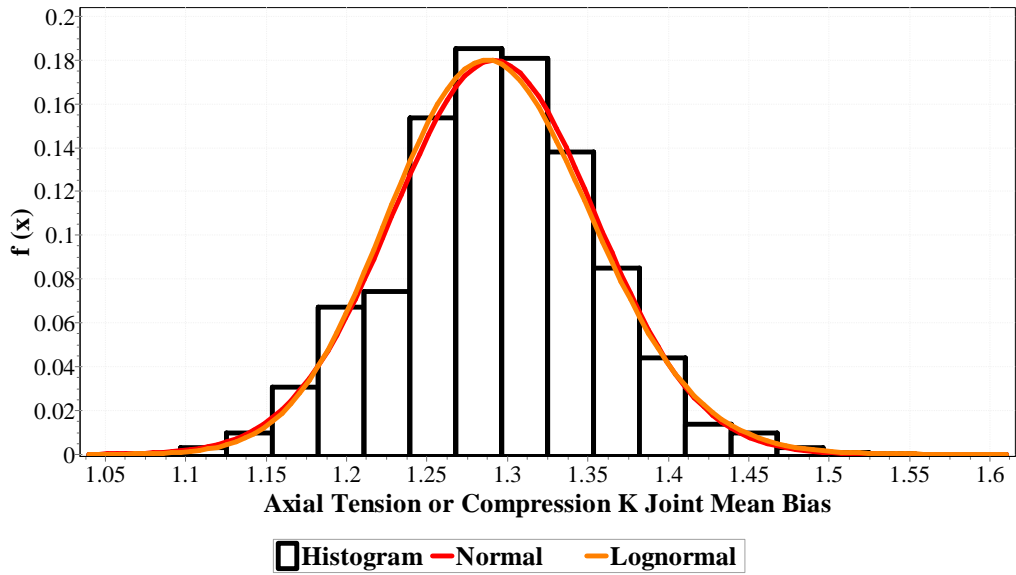


Figure 4.21: Probability Density Function-K-Joint Tension / Compression

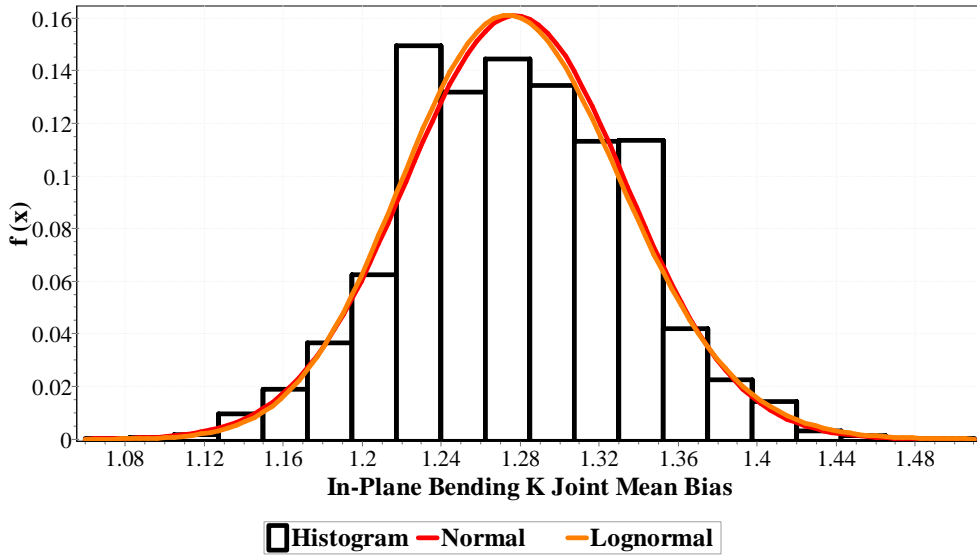


Figure 4.22: Probability Density Function for K-Joint IPB

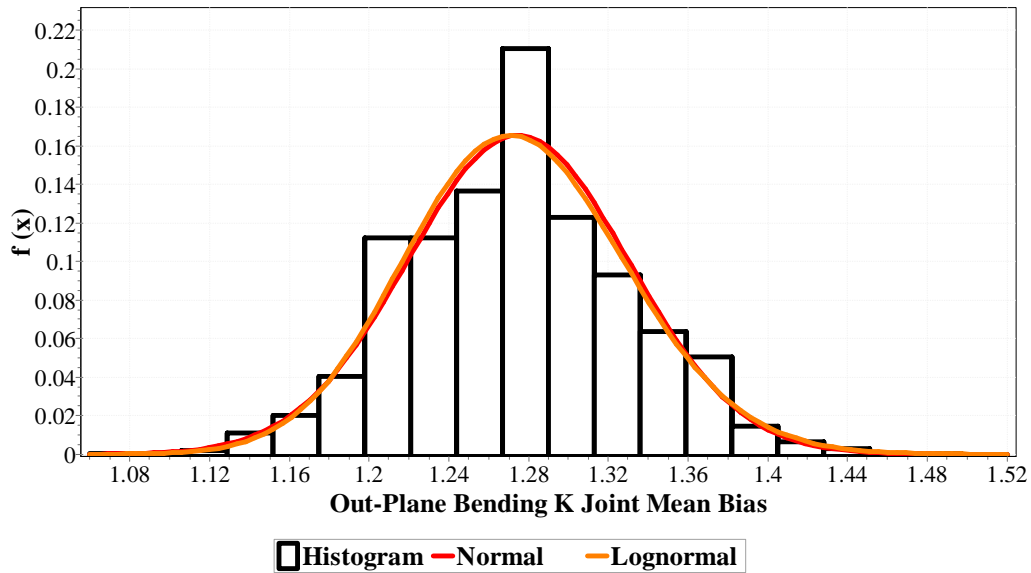


Figure 4.23: Probability Density Function for K-Joint OPB

4.5.2.2 T/Y - Joint

Table 4.8 and Figures 4.24 - 4.27 shows the uncertainty model for T/Y joint stress Equation. The mean bias achieved for this study was 1.27-1.30 for all four types of stresses and the same for ISO were in the range of 1.21-1.71. The standard deviation for this study was 0.10 and for ISO it was 0.13 to 0.41 which was higher than the present study, showing higher variation in ISO data.

Table 4.8: Resistance Model Uncertainties of T/Y - Joint Strength

Types of stresses	SP	MS	Duan et al., 2006	ISO [69]	Ferguson [1]	MSL [160]	
						LRFD	WSD
Tension	MC	1.30	1.53	1.71	1.48	1.70	2.3
	VC	0.10	0.28	0.41	0.43	0.40	0.74
Compression	MC	1.30	1.28	1.27	1.12	1.30	1.4
	VC	0.10	0.21	0.17	0.09	0.16	0.20
IPB	MC	1.28	1.31	1.21	1.29	1.21	1.66
	VC	0.10	0.21	0.13	0.14	0.12	0.25
OPB	MC	1.27	1.14	1.27	1.23	1.27	1.46
	VC	0.10	0.26	0.15	0.16	0.14	0.25

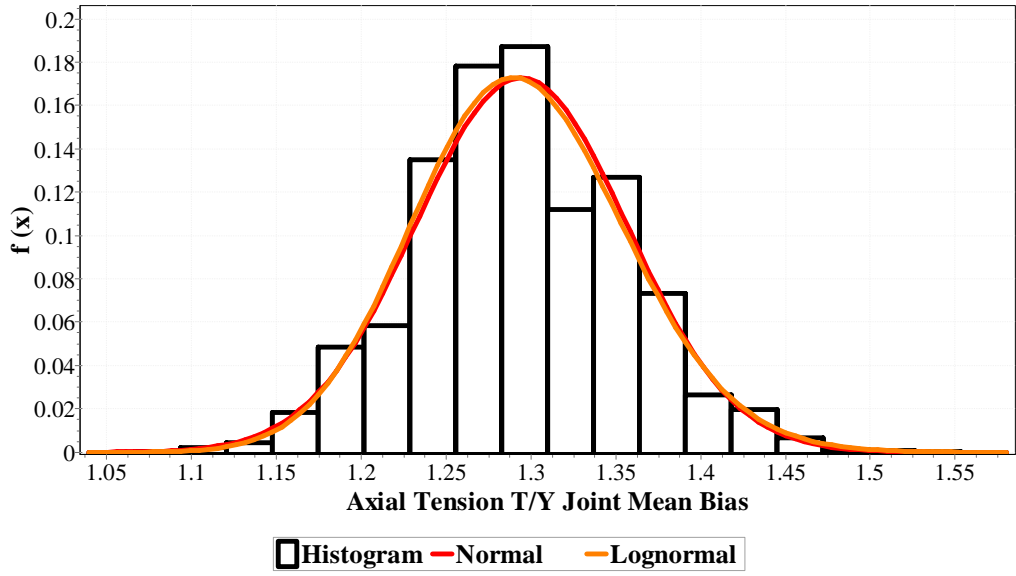


Figure 4.24: Probability Density Function for T/Y-Joint Axial Tension

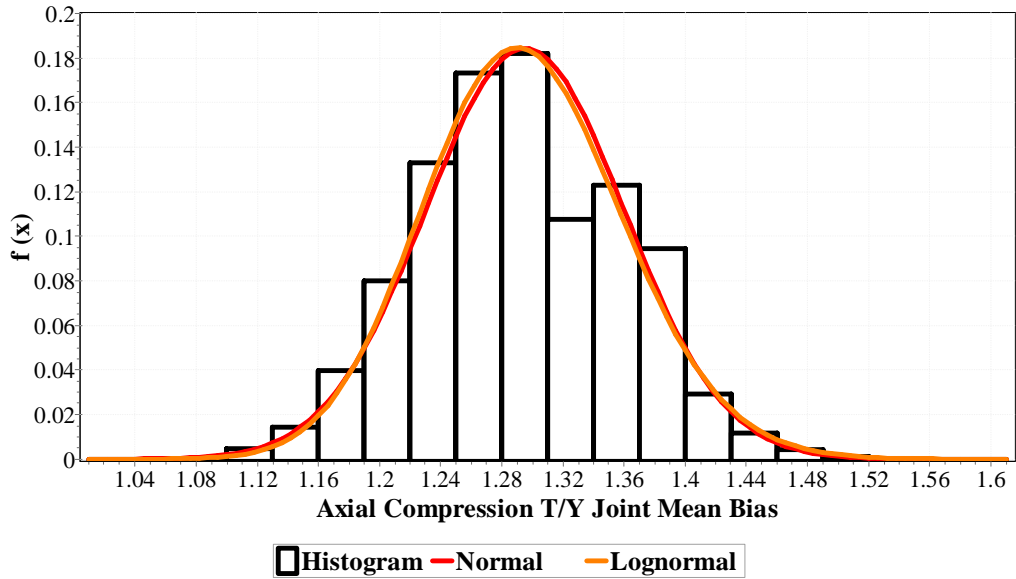


Figure 4.25: Probability Density Function for T/Y-Joint Axial Compression

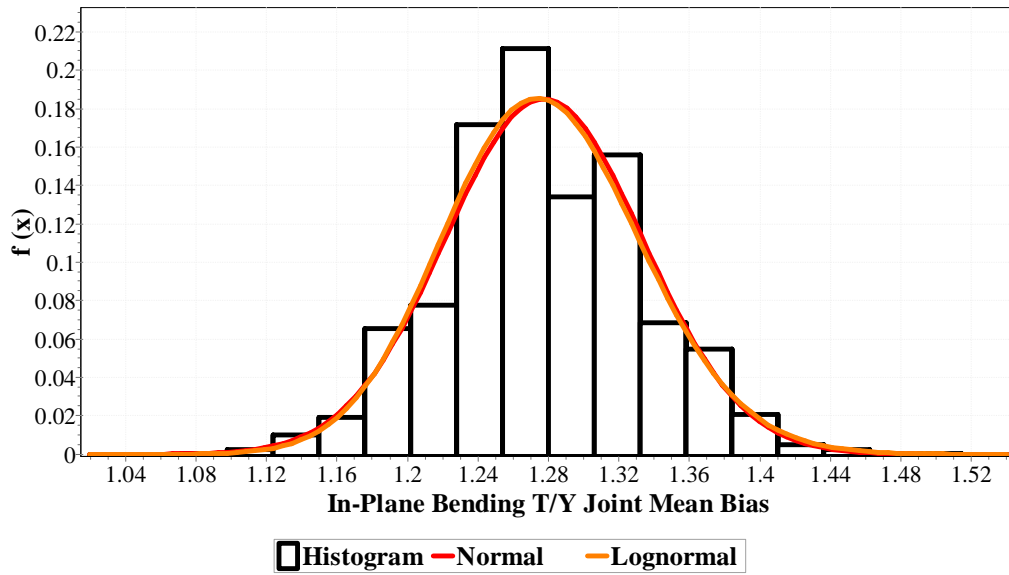


Figure 4.26: Probability Density Function for T/Y-Joint IPB

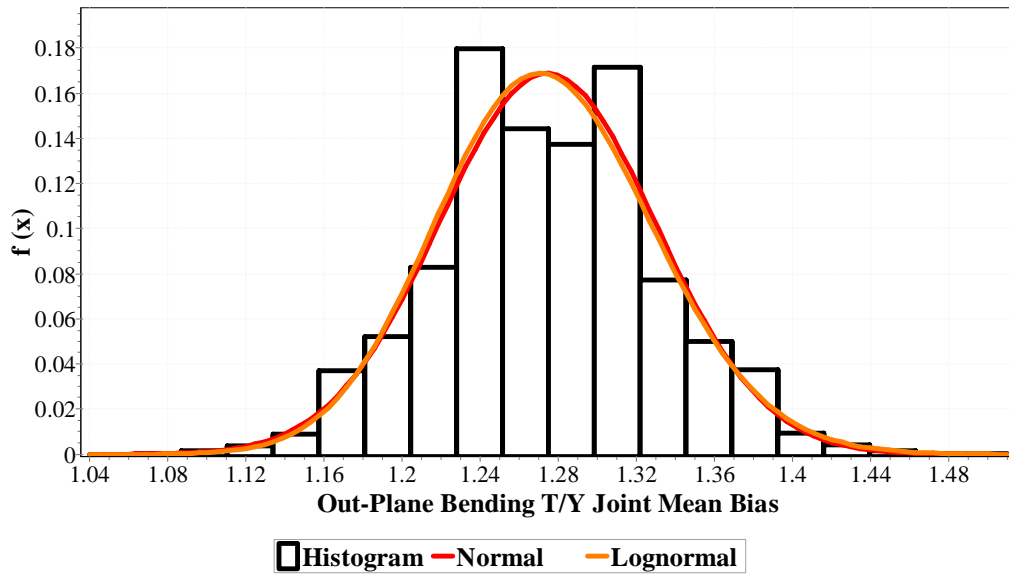


Figure 4.27: Probability Density Function for T/Y-Joint OPB

4.5.2.3 X- Joint

Table 4.9 and Figure 4.28-4.31 show the uncertainty model for X joint stress Equation. The mean bias achieved for this study was 1.24 - 1.28 for all four types of

stresses and the same for ISO was in the range of 1.14 - 1.40. The standard deviation for this study was 0.04 to 0.068 and for ISO it is 0.06 to 0.25 which was higher than the present study, showing higher variation in ISO data.

Table 4.9: Resistance Model Uncertainties of X-Joint Strength

Types of stresses	SP	MS	Duan et al., 2006	ISO [69]	MSL [160]	
					ISO(LRFD)	API (WSD)
Tension	MC	1.24	1.68	1.40	1.4	2.0
	VC	0.04	0.18	0.27	0.25	0.96
Compression	MC	1.29	1.2	1.17	1.2	1.4
	VC	0.07	0.16	0.11	0.10	0.13
IPB	MC	1.28	1.31	1.24	1.23	1.76
	VC	0.06	0.21	0.09	0.09	0.28
OPB	MC	1.28	1.14	1.14	1.13	1.47
	VC	0.06	0.26	0.07	0.06	0.11

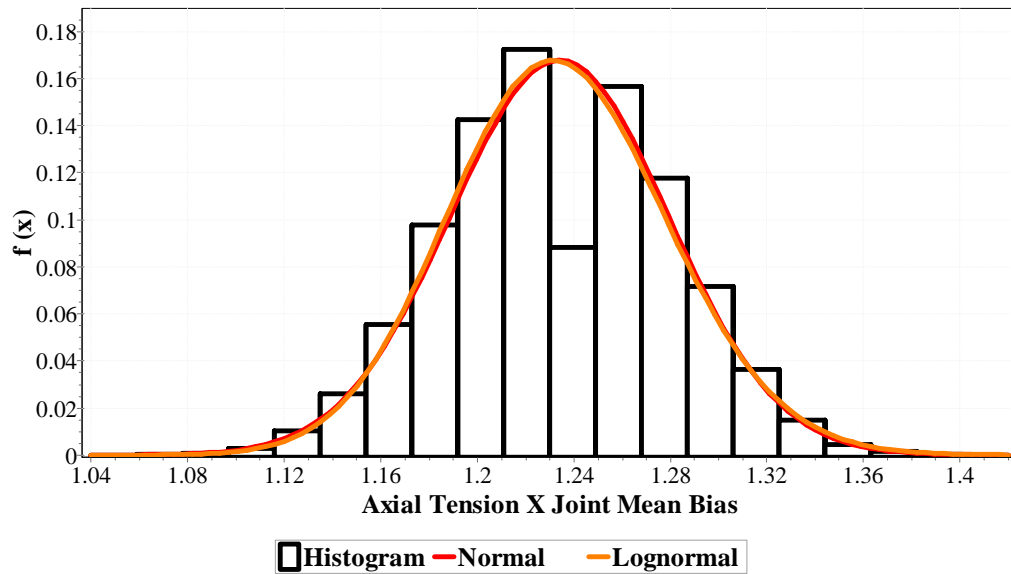


Figure 4.28: Probability Density Function for X-Joint Axial tension

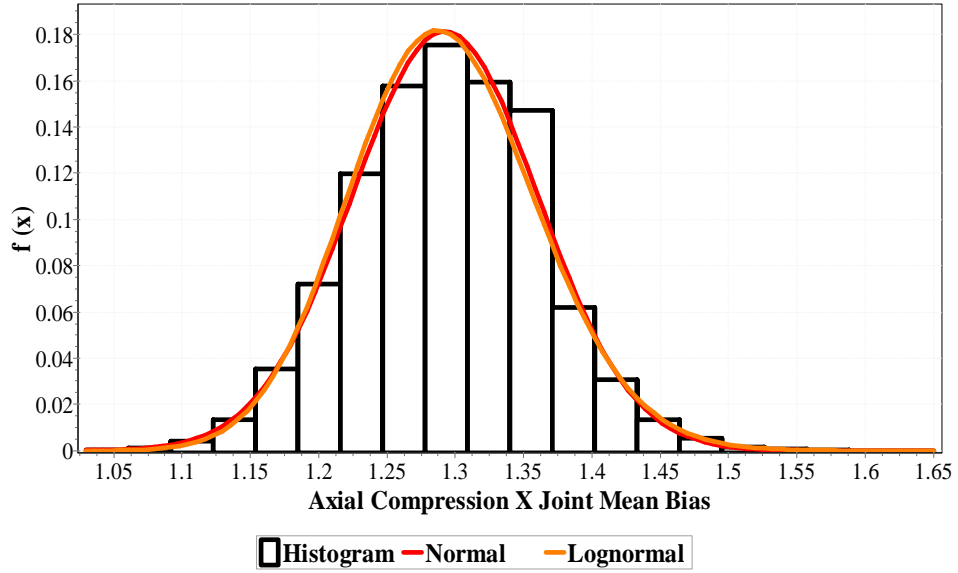


Figure 4.29: Probability Density Function for X-Joint Axial Compression

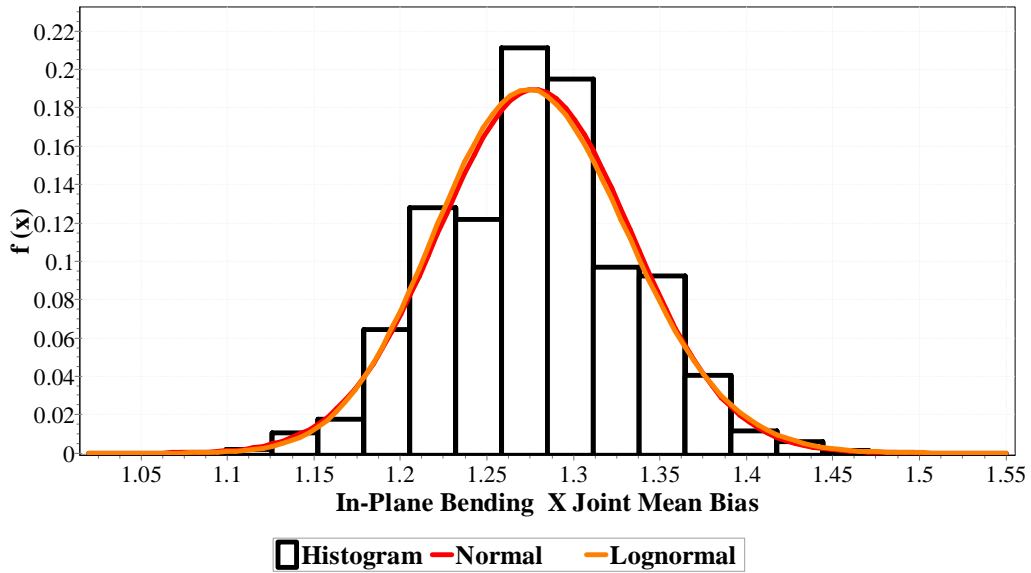


Figure 4.30: Probability Density Function for X-Joint IPB

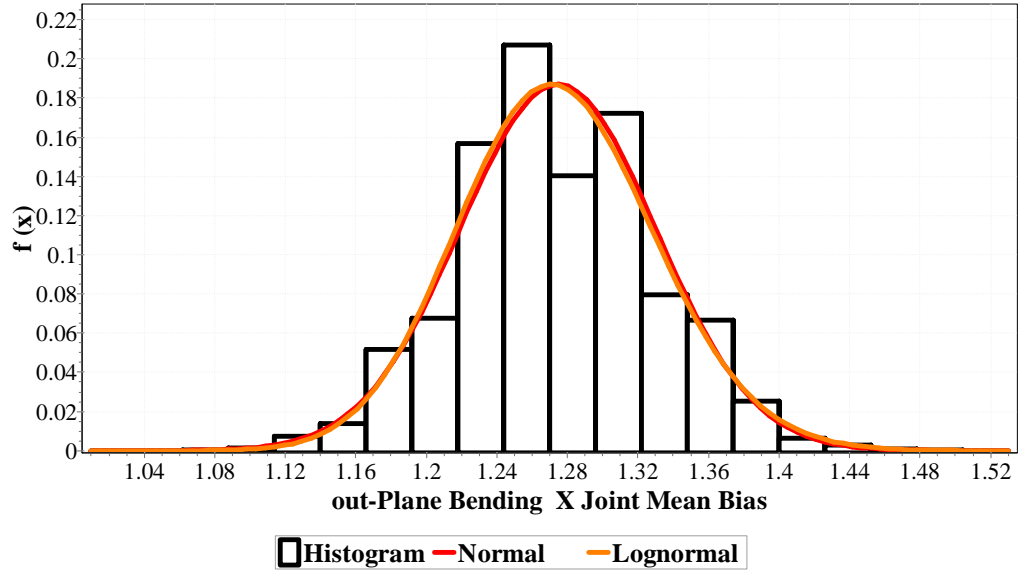


Figure 4.31: Probability Density Function for X-Joint OPB

4.6 Load Uncertainty

Environmental load uncertainty is much higher than the capacity of Jacket or resistance uncertainty [54]. Loads acting on offshore platforms act in different directions. The gravity loads act vertically downward whereas environmental loads (wind, wave and current) act horizontally. For the design of Jacket we need to know the maximum environmental loads ever to act on the structure. This maximum load which can occur at any time during the entire service life of Jacket is the most critical variable to be taken into account during design. ISO and API codes require 100 year extreme conditions of wave for the design of Jacket platforms. One sudden event may even exceed this condition, up to extreme waves of 10,000 years return period. For instance waves in GOM during hurricane Evan were reported to have reached heights of 10,000 years return period. For the platforms designed for return period of 100 years, this makes the task of design engineer very difficult.

Due to these conditions, it was necessary to find the reliability of Jacket component and joint, based on design environmental conditions and for system the applied load was 10,000 years as recommended by ISO 19902. To find the reliability index, we need to have distribution parameters for the random variables for environmental loads

i.e. wave, wind and current. Therefore in this study, first of all, distribution parameters were found using Weibull two parameter and Gumbel distributions. Secondly, the linear model of these distributions was used for extrapolation of data corresponding to 10,000 year return period. Then the parameters of distributions were also found as were explained in 3.3.5. Design criteria for environmental loads are inherently uncertain for the design of Jacket platforms due to variability of climate. The main design parameters for Jacket platforms are based on statistical characteristics of wave, wind and current.

The metocean record from existing platform sites in Malaysia shows that there have been typhoons occurring in this region. In 1983 Percy attacked Sarawak, in 1996 Greg attacked Sabah and in 2001 Vamei attacked Peninsular Malaysia. The Vamei, with a return period of 100-400 years has already been acknowledged as a typhoon. The basic cause for this weather condition is strong wind surges in south-east of PM region. This phenomenon is always prevailing during North-East monsoon months of November-March. Waves generated by typhoons can cause widespread damage on Jacket platforms.

In this study, site specific data for platforms was analysed. Weibull distribution was taken for the wave, wind and current in North Sea [61]. Many authors have used Weibull distribution in preference to Gumbel distribution for environmental load parameters ranging from GOM, North Sea, Arabian Gulf [82], [149], [161], [162], [163]. Statistics of extreme value was acquired through design wave which was based on extrapolating of historical storm value data. The record period is usually very short as compared to the return period selected for probability of exceedence. This recorded period ranges 5-20 years, which makes extrapolation of data extremely important. The extrapolation for GOM has been shown in Figure 2.2.

4.6.1 Wave Load Models

The oceanographic data available for wave height has usually been of short period. From this small amount of data we have to estimate extreme value of tail end of distribution and associated wave uncertainties for the large storm conditions which have extremely small probability of occurrence. Load uncertainty of significant wave

height is of prime importance when evaluating the structural reliability as shown in Chapter 5. COV for annual extreme wave loading was more than 50% in North Sea [54]. Heidman and Weaver report COV of 25% for wave loads [54]. Here due to low mean values predicted by Weibull 2 parameter distribution, it was selected. It fitted well with existing available data.

4.6.1.1 *PMO Region*

Significant wave height defines the characteristic wave height of a random wave. It is the most important parameter of environmental data for offshore Jacket design. Tables 4.10-4.11 show significant wave heights distributed as per Weibull and Gumbel distributions in PMO for 12 platforms. Figure 4.32 - 4.33 shows the extrapolated wave heights based on CDF of respective distributions for PMO.

The coefficient of variation (COV) for wave, distributed as Weibull gave variation between 12% - 29% whereas Gumbel gave COV between 4%-12%. Gumbel gave low COV values for corresponding wave height. The Weibull distribution mean values were lower than those estimated by Gumbel distribution. This was also reported by [164]. The Gumbel model overestimated the chance of large wave heights [164]. Due to this reason, in this study Weibull distribution has been adopted for the reliability analysis of Jacket platforms as it proved to be better fit. The same findings were reported by [152].

Table 4.10: Return Period and Significant Wave (m) -Weibull Distribution- PMO

PM	Return Period in Years				Weibull Distribution Parameters				
	10	10 ²	10 ³	10 ⁴	Scale	Shape	Mean	SD	COV
A	4.9	5.3	5.53	5.70	4.46	8.83	4.22	0.57	0.14
B	4.8	5.2	5.43	5.60	4.36	8.66	4.12	0.57	0.14
C	5.2	5.6	5.83	6.00	4.76	9.35	4.51	0.58	0.13
D	5.5	6.5	7.08	7.50	4.50	4.15	4.09	1.11	0.27
E	5.1	5.5	5.69	5.90	4.66	9.18	4.41	0.58	0.13
F	4.9	5.4	5.69	5.90	4.36	7.13	4.08	0.67	0.17
G	4.3	4.6	4.77	4.90	3.96	10.28	3.78	0.44	0.12
H	5.7	6.8	7.44	7.90	4.61	3.93	4.17	1.19	0.29
I	4.5	4.9	5.13	5.30	4.06	8.14	3.83	0.56	0.15
J	4.4	4.7	4.87	5.00	4.06	10.51	3.87	0.44	0.11
K	4.6	5	5.23	5.40	4.16	8.31	3.93	0.56	0.14
L	4.5	4.8	4.97	5.10	4.16	10.74	3.97	0.45	0.11

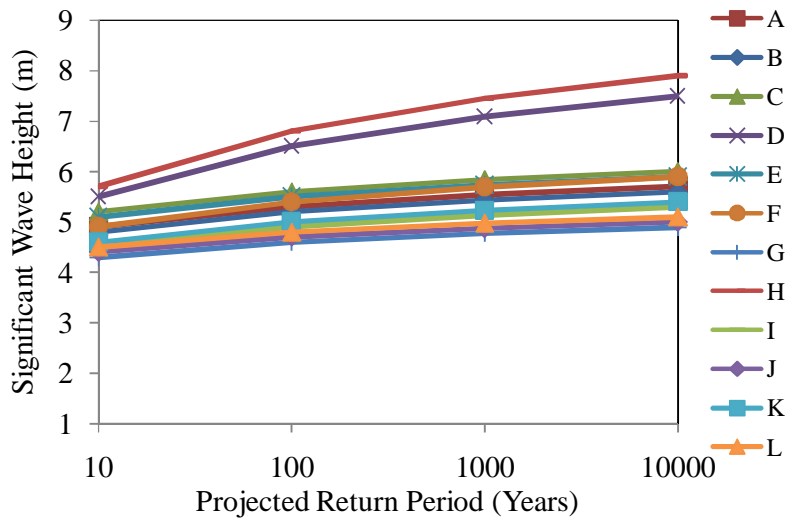


Figure 4.32: Extrapolation of Significant Wave Height (Weibull at PMO)

Table 4.11: Return Period and Significant Wave (m)-Gumbel Distribution- PMO

PM	Return Period in Years				Gumbel Distribution Parameters				
	10	10 ²	10 ³	10 ⁴	Scale	Location	Mean	SD	COV
A	4.9	5.3	5.69	6.08	5.87	4.52	4.62	0.22	0.05
B	4.8	5.2	5.59	5.98	5.87	4.42	4.52	0.22	0.05
C	5.2	5.6	5.99	6.38	5.87	4.82	4.92	0.22	0.04
D	5.5	6.5	7.48	8.46	2.35	4.54	4.79	0.55	0.11
E	5.1	5.5	5.89	6.28	5.87	4.72	4.82	0.22	0.05
F	4.9	5.4	5.89	6.37	4.70	4.42	4.54	0.27	0.06
G	4.3	4.6	4.89	5.18	7.83	4.01	4.09	0.16	0.04
H	5.7	6.8	7.87	8.96	2.14	4.65	4.92	0.60	0.12
I	4.5	4.9	5.29	5.68	5.87	4.12	4.22	0.22	0.05
J	4.4	4.7	4.99	5.28	7.83	4.11	4.19	0.16	0.04
K	4.6	5	5.39	5.78	5.87	4.22	4.32	0.22	0.05
L	4.5	4.8	5.09	5.38	7.83	4.21	4.29	0.16	0.04

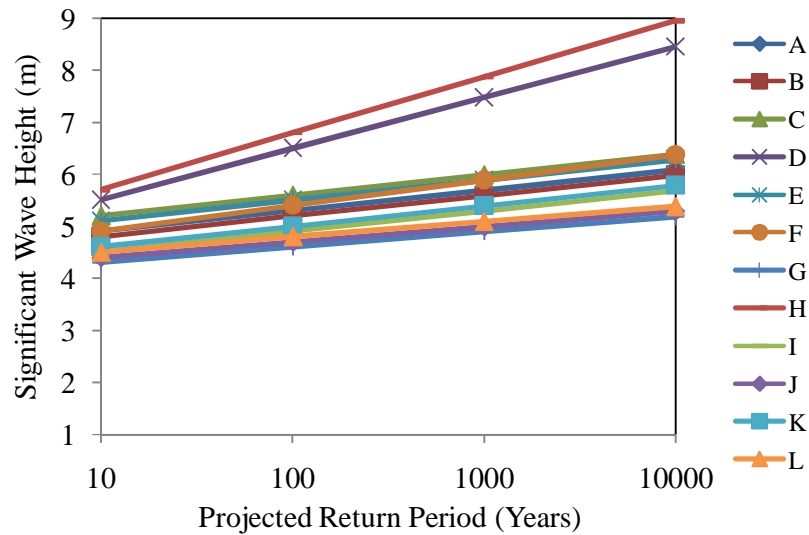


Figure 4.33: Extrapolation of Significant Wave Height (Gumbel at PMO)

4.6.1.2 SBO Region

Table 4.12 shows eight platforms specific data from SBO using Weibull distribution and Table 4.13 shows same platforms using Gumbel distribution. The range of 100 year wave height was 4.4-6.5 m and for 10,000 years it was 4.8 - 8.20 m as per the Weibull distribution shown in Figure 4.34. Gumbel for same 10 and 100 year wave height gave 10,000 return period of 5.27 - 9.83 m as shown in Figure 4.35.

Table 4.12: Return Period and Significant Wave (m)-Weibull Distribution- SBO

SBO	Return Period in Years				Weibull Distribution Parameters				
	10	10 ²	10 ³	10 ⁴	Scale	Shape	Mean	SD	COV
A	4.8	6.5	7.49	8.20	3.33	2.29	2.95	1.37	0.46
B	4.5	5.1	5.45	5.70	3.87	5.54	3.57	0.75	0.21
C	3.5	4.7	5.40	5.90	2.45	2.35	2.18	0.98	0.45
D	3.8	4.3	4.59	4.80	3.27	5.61	3.03	0.62	0.21
E	4.1	5.7	6.63	7.30	2.76	2.10	2.44	1.22	0.50
F	4.5	5.6	6.24	6.70	3.46	3.17	3.10	1.07	0.35
G	3.1	4.4	5.16	5.70	2.03	1.98	1.80	0.95	0.53
H	3.7	4.5	4.97	5.30	2.92	3.54	2.63	0.82	0.31

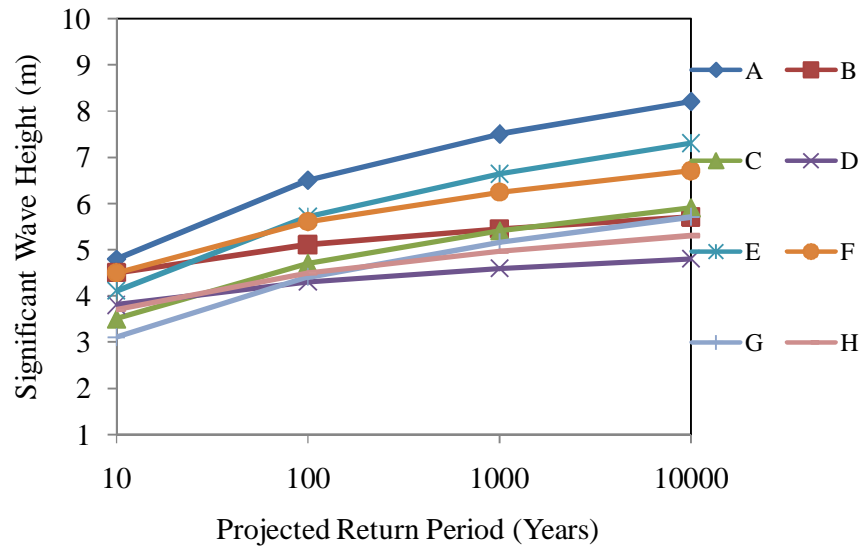


Figure 4.34: Extrapolation of Significant Wave Height (Weibull at SBO)

Table 4.13: Return Period and Significant Wave (m)-Gumbel Distribution- SBO

SBO	Return Period in Years				Gumbel Distribution Parameters				
	10	10 ²	10 ³	10 ⁴	Scale	Location	Mean	SD	COV
A	4.8	6.5	8.16	9.83	1.38	3.17	3.59	0.93	0.26
B	4.5	5.1	5.69	6.27	3.92	3.93	4.07	0.33	0.08
C	3.5	4.7	5.87	7.05	1.96	2.35	2.65	0.65	0.25
D	3.8	4.3	4.79	5.27	4.70	3.32	3.44	0.27	0.08
E	4.1	5.7	7.26	8.83	1.47	2.57	2.96	0.87	0.29
F	4.5	5.6	6.68	7.76	2.14	3.45	3.72	0.60	0.16
G	3.1	4.4	5.67	6.95	1.81	1.86	2.17	0.71	0.33
H	3.7	4.5	5.28	6.06	2.94	2.93	3.13	0.44	0.14

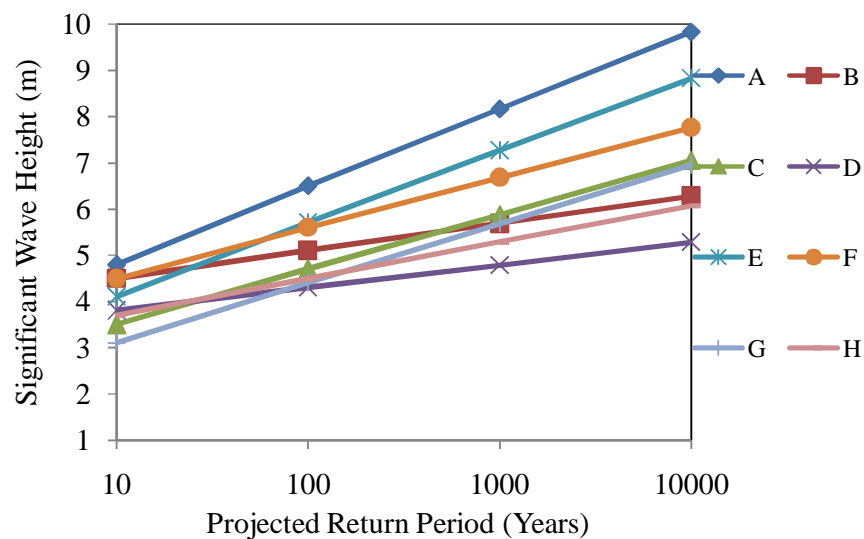


Figure 4.35: Extrapolation of Significant Wave Height (Gumbel at SBO)

4.6.1.3 SKO Region

Table 4.14 shows 13 platforms specific data from SKO using Weibull distribution and Table 4.15 shows same platforms using Gumbel distribution. The range of 100 year wave height was 4.4 - 6.4 m and for 10,000 years it was 5.0 - 8.10 m as per the Weibull distribution as shown in Figure 4.36. The Gumbel for same 10 and 100 year wave height gave 10,000 year return period wave heights of 5.57-9.73 m as shown in Figure. 4.37.

Table 4.14: Return Period and Significant Wave (m)-Weibull Distribution- SKO

SKO	Return Period in Years				Weibull Distribution Parameters				
	10	10 ²	10 ³	10 ⁴	Scale	Shape	Mean	SD	COV
A	4	5.2	5.90	6.40	2.92	2.64	2.59	1.06	0.41
B	4	4.9	5.43	5.80	3.13	3.42	2.82	0.91	0.32
C	4.7	6.4	7.39	8.10	3.24	2.25	2.87	1.35	0.47
D	3.8	4.4	4.75	5.00	3.19	4.73	2.92	0.70	0.24
E	4.2	5.1	6.00	5.63	3.32	3.57	2.99	0.93	0.31
F	4.4	5.1	5.51	5.80	3.68	4.69	3.37	0.82	0.24
G	4.3	4.9	5.65	5.90	3.67	5.31	3.39	0.73	0.22
H	3.8	5.1	5.86	6.40	2.67	2.36	2.36	1.07	0.45
I	4.2	5.1	5.63	6.00	3.32	3.57	2.99	0.93	0.31
J	4.5	5.2	5.61	5.90	3.78	4.79	3.46	0.82	0.24
K	5	5.8	6.27	6.60	4.18	4.67	3.82	0.93	0.24
L	5.6	6.3	6.71	7.00	4.86	5.88	4.50	0.89	0.20
M	4.5	5.3	5.77	6.10	3.70	4.24	3.36	0.90	0.27

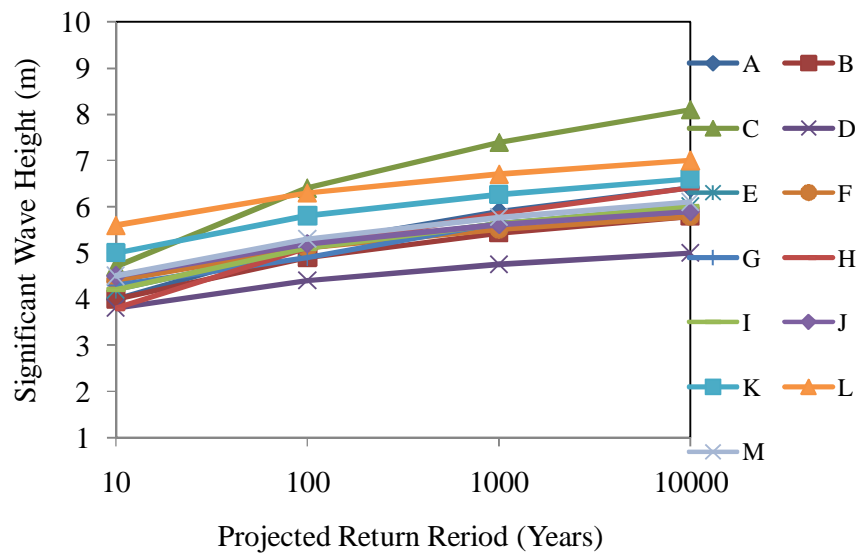


Figure 4.36: Extrapolation of Significant Wave Height (Weibull at SKO)

Table 4.15: Return Period and Significant Wave (m), Gumbel Distribution at SKO

SKO	Return Period in Years				Gumbel Distribution Parameters				
	10	10 ²	10 ³	10 ⁴	Scale	Location	Mean	SD	COV
A	4	5.2	6.37	7.55	1.96	2.85	3.15	0.65	0.21
B	4	4.9	5.78	6.67	2.61	3.14	3.36	0.49	0.15
C	4.7	6.4	8.06	9.73	1.38	3.07	3.49	0.93	0.27
D	3.8	4.4	4.99	5.57	3.92	3.23	3.37	0.33	0.10
E	4.2	5.1	5.98	6.87	2.61	3.34	3.56	0.49	0.14
F	4.4	5.1	5.78	6.46	3.36	3.73	3.90	0.38	0.10
G	4.3	4.9	5.49	6.07	3.92	3.73	3.87	0.33	0.08
H	3.8	5.1	6.37	7.65	1.81	2.56	2.87	0.71	0.25
I	4.2	5.1	5.98	6.87	2.61	3.34	3.56	0.49	0.14
J	4.5	5.2	5.88	6.56	3.36	3.83	4.00	0.38	0.10
K	5	5.8	6.58	7.36	2.94	4.23	4.43	0.44	0.10
L	5.6	6.3	6.98	7.66	3.36	4.93	5.10	0.38	0.07
M	4.5	5.3	6.08	6.86	2.94	3.73	3.93	0.44	0.11

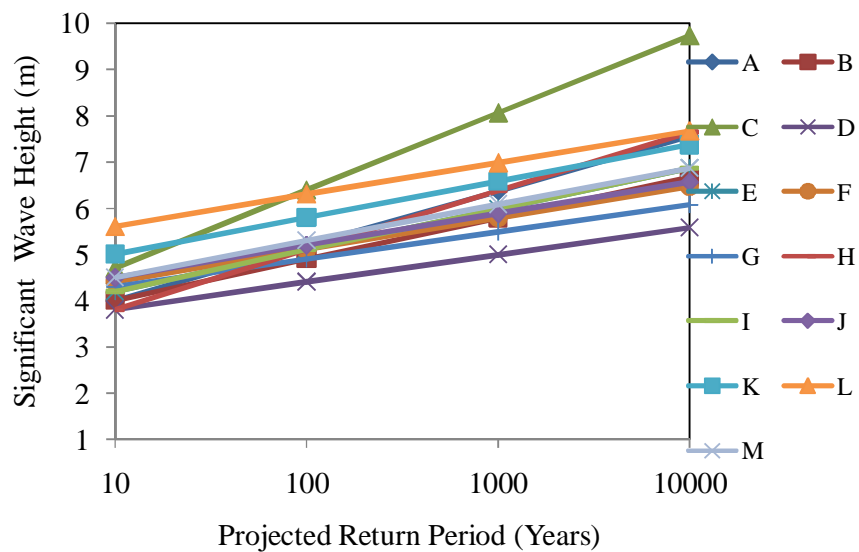


Figure 4.37: Extrapolation of Significant Wave Height (Gumbel at SKO)

4.6.1.4 GULF OF MEXICO (GOM) and NORTH SEA (NS)

The data for GOM and North Sea was acquired from ISO code [147]. Table 4.16 and Figure 4.38 show the Weibull distribution parameters for International waters. The

waves were as high as 14.6 and 16.4 m for 100 years and they were 20.70 and 18.50 m for 10,000 years. The COV was high for GOM with 79% as compared to 29% in North Sea. Table 4.17 and Figure 4.39 show the Gumbel distribution parameters for International waters. For Gumbel the GOM and North -North Sea 10,000 year return period wave gave 26.57 and 20.50 m. Gumbel gave 9 - 80% of COV. The distributions were based on data acquired from ISO 19900-1.

Table 4.16: Return Period and Significant Wave Height (m), Weibull at GOM and NS

	Return Period in Years				Weibull Distribution Parameters				
	10	10 ²	10 ³	10 ⁴	Scale	Shape	Mean	SD	COV
GOM	8.5	14.6	18.17	20.70	4.43	1.28	4.11	3.23	0.79
SNS	7.5	9	9.88	10.50	6.02	3.80	5.44	1.60	0.29
CNS	11.8	13.6	14.65	15.40	9.95	4.88	9.12	2.13	0.23
NNS	14.3	16.4	17.62	18.50	12.13	5.06	11.14	2.52	0.23

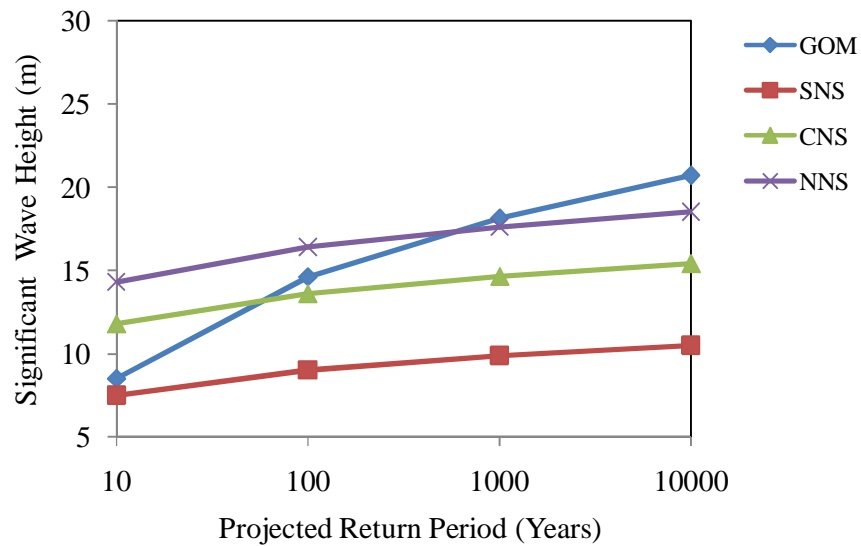


Figure 4.38: Extrapolation of Significant Wave Height, Weibull- GOM and NS

Table 4.17: Return Period and Significant Wave (m),Gumbel at GOM and NS

	Return Period in Years				Gumbel Distribution Parameters				
	10	10 ²	10 ³	10 ⁴	Scale	Location	Mean	SD	COV
GOM	8.5	14.6	20.59	26.57	0.39	2.66	4.16	3.33	0.80
SNS	7.5	9	10.47	11.94	1.57	6.06	6.43	0.82	0.13
CNS	11.8	13.6	15.36	17.13	1.31	10.08	10.52	0.98	0.09
NNS	14.3	16.4	18.45	20.50	1.12	12.29	12.80	1.15	0.09

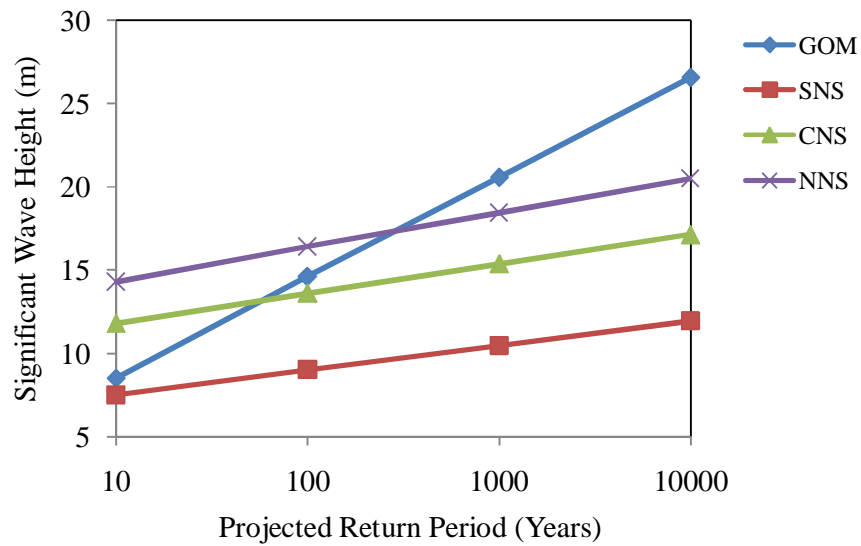


Figure 4.39: Extrapolation of Significant Wave Height, Gumbel at GOM and NS

4.6.2 Wind load model

Wind contributes less than 10% of total base shear under extreme environmental loading. Wind loads contribute comparatively little to the total base shear [54]. Weibull and Gumbel distributions were fitted to the wind load model. Due to low mean values and data fitting well with existing values, 2 parameter Weibull distribution was selected in this study.

4.6.2.1 PMO Region

From many previous studies, it has been shown that two parameter Weibull distributions can fit well for surface wind speed on land and sea [152]. Here in this study hourly mean wind speed was used which was measured at 10 m height. The COV based on Weibull distribution for wind speed was in range of 21 - 93% and for Gumbel distribution was between 8 - 137%. The general tendency was low values of COV for Gumbel. This has been shown in Tables 4.18 - 4.19 and Figures 4.40 - 4.41. Data for ten platforms was analysed from PMO region.

The Gumbel distribution gave higher mean wind values during extrapolation as compared to Weibull distribution. This means that extrapolation based on Gumbel distribution overestimated the wind speed besides that Weibull also gave a better fit. Therefore Weibull model was recommended for the reliability of Jacket platforms in offshore Malaysia.

Table 4.18: Return Period and Wind Speed (m/s), Weibull Distributions at PMO

PM	Return Period in Years				Weibull Distribution Parameters				
	10	10 ²	10 ³	10 ⁴	Scale	Shape	Mean	SD	COV
A	20	33	40.60	45.99	10.95	1.38	10.00	7.31	0.73
B	20	23	24.75	26.00	16.90	4.96	15.51	3.58	0.23
C	22	26	28.33	29.99	17.99	4.15	16.34	4.44	0.27
D	22	34	41.01	45.99	13.03	1.59	11.69	7.51	0.64
E	20	38	51.83	59.30	9.24	1.08	8.97	8.31	0.93
F	22	25	26.75	28.00	18.86	5.42	17.40	3.70	0.21
G	20	34	42.17	47.98	10.56	1.31	9.75	7.53	0.77
H	22	25	26.75	28.00	18.86	5.42	17.40	3.70	0.21
I	21	40	54.83	62.72	9.67	1.08	9.40	8.75	0.93
J	20	28	32.67	35.99	13.34	2.06	11.82	6.02	0.51

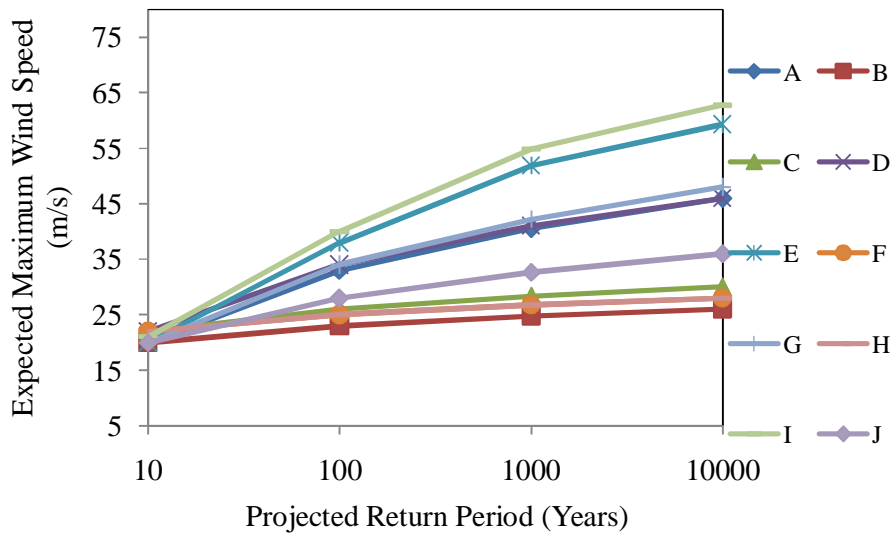


Figure 4.40: Extrapolation of Wind Speed -(Weibull at PMO)

Table 4.19: Return Period and Wind Speed (m/s), Gumbel Distribution at.PMO

PM	Return Period in Years				Gumbel Distribution Parameters				
	10	10 ²	10 ³	10 ⁴	Scale	Location	Mean	SD	COV
A	20	33	45.76	58.50	0.18	7.55	10.74	7.10	0.66
B	20	23	25.93	28.87	0.78	17.13	17.86	1.64	0.09
C	22	26	29.92	33.84	0.59	18.17	19.15	2.18	0.11
D	22	34	45.77	57.53	0.20	10.51	13.46	6.55	0.49
E	20	38	55.67	73.31	0.13	2.76	7.18	9.82	1.37
F	22	25	27.93	30.87	0.78	19.13	19.86	1.64	0.08
G	20	34	47.75	61.47	0.17	6.59	10.03	7.64	0.76
H	22	25	27.93	30.87	0.78	19.13	19.86	1.64	0.08
I	21	40	58.65	77.27	0.12	2.80	7.47	10.37	1.39
J	20	28	35.84	43.68	0.29	12.34	14.30	4.37	0.31

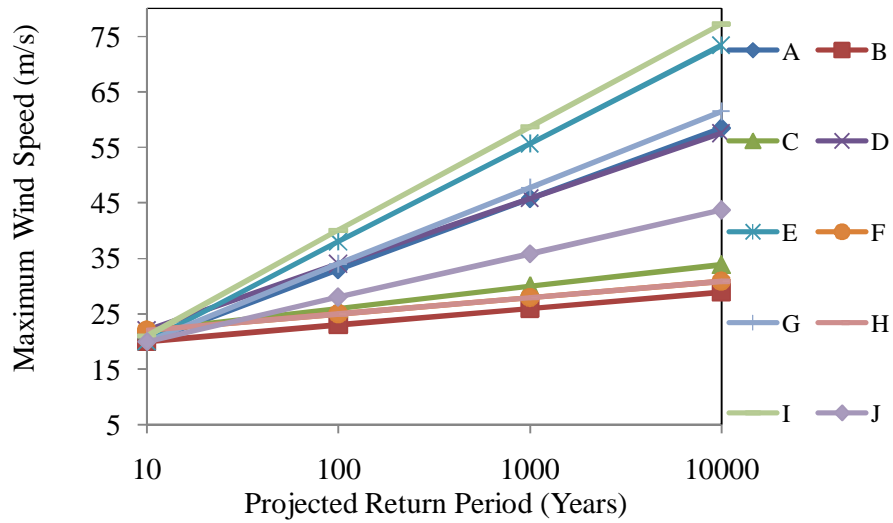


Figure 4.41: Extrapolation of Wind Speed -(Gumbel at PMO)

4.6.2.2 SBO Region

Data for five Jacket platforms from SBO was analysed. Table 4.20 and Figure 4.42 show the result for wind as per the Weibull distribution. The range for 100 years was 29 - 32 m/s. The corresponding 10,000 year values were in range of 33 - 47 m/s. The Gumbel distribution was shown in Table 4.21 and Figure 4.43. The 10,000 year value was shown as 36.84 – 61.42 m/s.

Table 4.20: Return Period and Wind Speed (m/s), Weibull Distribution at SBO

SBO	Return Period in Years				Weibull Distribution Parameters				
	10	10 ²	10 ³	10 ⁴	Scale	Shape	Mean	SD	COV
A	18	31	38.60	43.99	9.36	1.28	8.68	6.86	0.79
B	19	32	39.59	44.99	10.15	1.33	9.33	7.09	0.76
C	25	29	31.33	33.00	20.91	4.67	19.12	4.66	0.24
D	17	32	40.77	47.00	7.94	1.10	7.67	7.01	0.91
E	24	31	35.07	37.97	17.64	2.71	15.69	6.25	0.40

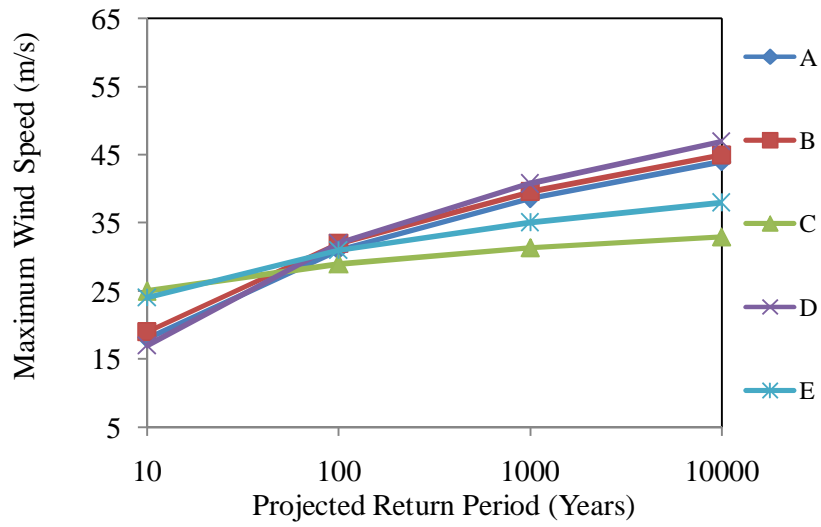


Figure 4.42: Extrapolation of Wind Speed -(Weibull at SBO)

Table 4.21: Return Period and Wind Speed (m/s), Gumbel Distribution at SBO

SBO	Return Period in Years				Gumbel Distribution Parameters				
	10	10 ²	10 ³	10 ⁴	Scale	Location	Mean	SD	COV
A	18	31	43.76	56.50	0.18	5.55	8.74	7.10	0.81
B	19	32	44.76	57.50	0.18	6.55	9.74	7.10	0.73
C	25	29	32.92	36.84	0.59	21.17	22.15	2.18	0.10
D	17	32	46.72	61.42	0.16	2.63	6.32	8.19	1.30
E	24	31	37.87	44.73	0.34	17.30	19.02	3.82	0.20

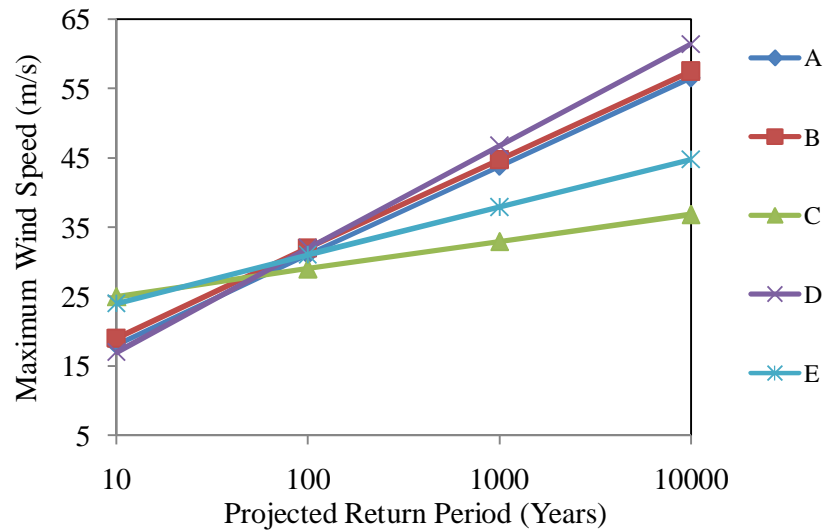


Figure 4.43: Extrapolation of Wind Speed -(Gumbel at SBO)

4.6.2.3 SKO Region

Data for eight Jacket platforms from this region was analysed. Table 4.22 and Figure 4.44 show the result for wind as per the Weibull distribution. The range for 100 years was 20 - 36 m/s. The corresponding 10,000 year values were in range of 22-52 m/s. The Gumbel distribution was shown in Table 4.23 and Figure 4.45. The Gumbel 10,000 year values were in range of 24 - 67 m/s.

Table 4.22: Return Period and Wind Speed (m/s), Weibull Distribution at SKO

SKO	Return Period in Years				Weibull Distribution Parameters				
	10	10 ²	10 ³	10 ⁴	Scale	Shape	Mean	SD	COV
A	19	29	34.84	38.98	11.42	1.64	10.22	6.40	0.63
B	28	33	35.92	38.00	22.98	4.22	20.89	5.58	0.27
C	20	36	45.35	52.00	9.86	1.18	9.32	7.93	0.85
D	19	24	26.92	29.00	14.34	2.97	12.80	4.70	0.37
F	20	32	39.01	43.99	11.36	1.47	10.28	7.09	0.69
G	20	24	26.33	27.99	16.06	3.80	14.52	4.26	0.29
H	18	22	24.33	25.99	14.14	3.45	12.71	4.07	0.32
I	18	20	21.17	22.00	15.86	6.58	14.78	2.63	0.18

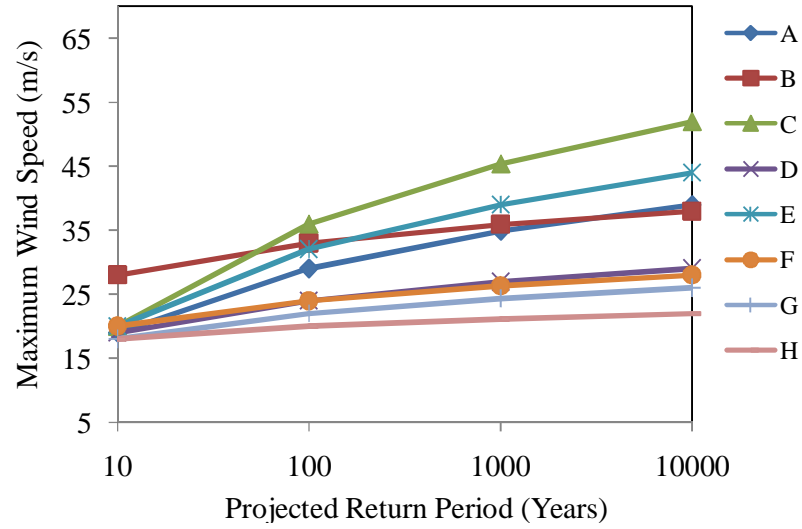


Figure 4.44: Extrapolation of Wind Speed -(Weibull at SKO)

Table 4.23: Return Period and Wind Speed (m/s), Gumbel Distribution at SKO

SKO	Return Period in Years				Gumbel Distribution Parameters				
	10	10 ²	10 ³	10 ⁴	Scale	Location	Mean	SD	COV
A	19	29	38.81	48.61	0.23	9.42	11.88	5.46	0.46
B	28	33	37.90	42.80	0.47	23.21	24.44	2.73	0.11
C	20	36	51.71	67.00	0.15	4.68	8.61	8.73	1.01
D	19	24	28.90	33.80	0.47	14.21	15.44	2.73	0.18
F	20	32	43.78	55.53	0.20	8.51	11.46	6.55	0.57
G	20	24	27.92	31.84	0.59	16.17	17.15	2.18	0.13
H	18	22	25.92	29.84	0.59	14.17	15.15	2.18	0.14
I	18	20	21.96	24.00	1.17	16.08	16.58	1.09	0.07

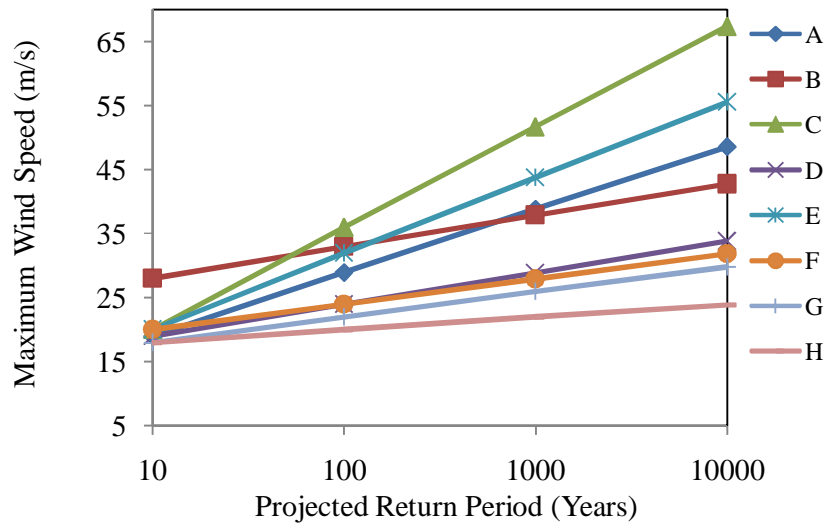


Figure 4.45: Extrapolation of Wind Speed (Gumbel at SKO)

4.6.2.4 GULF OF MEXICO (GOM) and NORTH SEA (NS)

The data from international waters was taken from ISO code [147]. Table 4.24 and Figure 4.46 show the result for wind as per the Weibull distribution. The GOM for 100 years was 46.1 m/s. The corresponding 10,000 year value was 63.79 m/s. For North Sea 100 year wind was in range of 36 - 45 m/s and 10,000 was 40 - 50 m/s. The Gumbel distribution is shown in Table 4.25 and Figure 4.47. The 10,000 year GOM was 81 m/s and for North Sea it was 44 - 55 m/s.

Table 4.24: Return Period and Wind Speed (m/s), Weibull at GOM and NS

	Return Period in Years				Weibull Distribution Parameters				
	10	10 ²	10 ³	10 ⁴	Scale	Shape	Mean	SD	COV
GOM	28.4	46.1	56.44	63.79	15.86	1.43	14.40	10.22	0.71
SNS	32	36	38.33	40.00	27.77	5.88	25.74	5.08	0.20
CNS	34	39	41.92	44.00	28.83	5.05	26.48	6.01	0.23
NNS	40	45	47.92	50.00	34.71	5.88	32.17	6.35	0.20

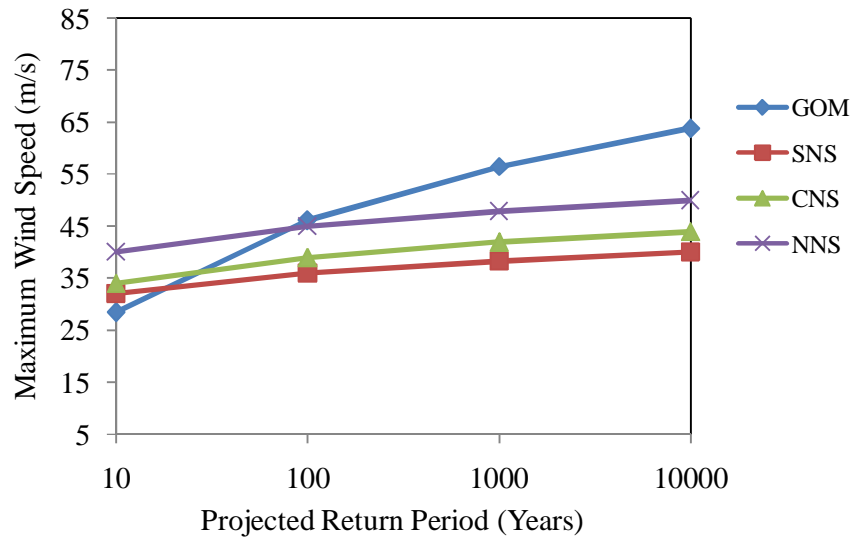


Figure 4.46: Extrapolation of wind speed -(Weibull at GOM and NS)

Table 4.25: Return Period and Wind Speed (m/s), Gumbel at GOM and NS.

	Return Period in Years				Gumbel Distribution Parameters				
	10	10 ²	10 ³	10 ⁴	Scale	Location	Mean	SD	COV
GOM	28.4	46.1	63.47	81.00	0.13	11.45	15.80	9.66	0.61
SNS	32	36	39.92	44.00	0.59	28.17	29.15	2.18	0.07
CNS	34	39	43.90	49.00	0.47	29.21	30.44	2.73	0.09
NNS	40	45	49.90	55.00	0.47	35.21	36.44	2.73	0.07

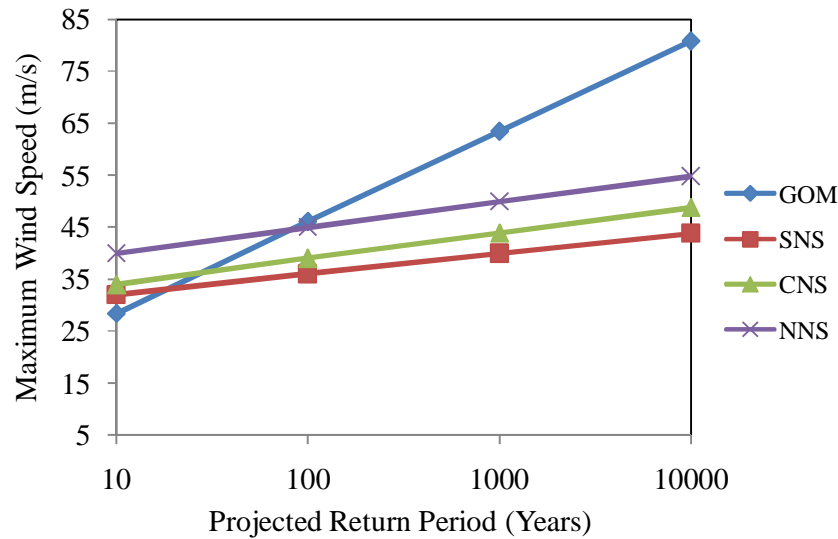


Figure 4.47: Extrapolation of Wind Speed, (Gumbel at GOM and NS)

4.6.3 Current Load Model

Due to low mean value of current and data fitting well with existing Weibull 2 parameter distribution, it was selected for this study.

4.6.3.1 PMO Region

Current data from fifteen platforms was analysed for PMO region. Current distributed as per Weibull distribution gave COV in the range of 15% - 33% and Gumbel distribution gave 6% - 15%. Thus Gumbel distribution has low COV but it gave higher extrapolated mean values. Tables 4.26 - 4.27 give basic current parameter for Weibull and Gumbel. The corresponding extrapolated values are shown in Figure 4.48 - 4.49. The 100 year value lies in range of 1.1-1.5 and 10,000 year Weibull was in range of 1.22 - 1.63. The Gumbel 10,000 year value was in range of 1.33 - 1.84.

Table 4.26: Return Period & Current Speed (m/s), Weibull Distribution at PMO

PM	Return Period in Years				Weibull Distribution Parameters				
	10	10 ²	10 ³	10 ⁴	Scale	Shape	Mean	SD	COV
A	0.98	1.1	1.17	1.22	0.85	6.00	0.79	0.15	0.19
B	1.14	1.25	1.31	1.36	1.02	7.52	0.96	0.15	0.16
C	1.15	1.3	1.39	1.45	0.99	5.65	0.92	0.19	0.20
D	1.15	1.35	1.47	1.55	0.95	4.32	0.86	0.23	0.26
E	1.05	1.2	1.29	1.35	0.89	5.19	0.82	0.18	0.22
F	1.06	1.2	1.28	1.34	0.91	5.59	0.84	0.17	0.21
G	1.05	1.21	1.30	1.37	0.89	4.89	0.81	0.19	0.23
H	1.07	1.2	1.27	1.33	0.93	6.05	0.87	0.17	0.19
I	1.37	1.5	1.57	1.63	1.23	7.65	1.15	0.18	0.15
J	1.1	1.35	1.49	1.60	0.86	3.38	0.77	0.25	0.33
K	1.16	1.37	1.49	1.58	0.95	4.17	0.86	0.23	0.27
L	1.05	1.26	1.38	1.47	0.84	3.80	0.76	0.22	0.29
M	1.12	1.26	1.34	1.40	0.97	5.88	0.90	0.18	0.20
N	1.19	1.34	1.43	1.49	1.03	5.84	0.96	0.19	0.20
O	1.05	1.19	1.27	1.33	0.90	5.54	0.83	0.17	0.21

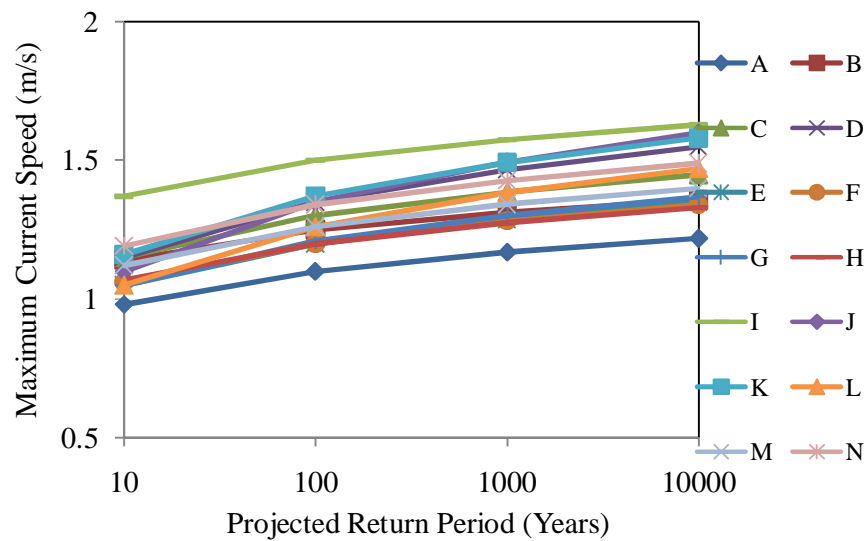


Figure 4.48: Extrapolation of Current Speed (Weibull at PMO)

Table 4.27: Return Period & Current Speed (m/s), Gumbel Distribution at PMO

PM	Return Period in Years				Gumbel Distribution Parameters				
	10	10 ²	10 ³	10 ⁴	Scale	Location	Mean	SD	COV
A	0.98	1.1	1.22	1.33	19.58	0.87	0.89	0.07	0.07
B	1.14	1.25	1.35	1.46	21.36	1.03	1.06	0.06	0.06
C	1.15	1.3	1.44	1.59	15.67	1.01	1.04	0.08	0.08
D	1.15	1.35	1.55	1.74	11.75	0.96	1.01	0.11	0.11
E	1.05	1.2	1.34	1.49	15.67	0.91	0.94	0.08	0.09
F	1.06	1.2	1.33	1.47	16.78	0.93	0.96	0.08	0.08
G	1.05	1.21	1.37	1.52	14.69	0.90	0.94	0.09	0.09
H	1.07	1.2	1.32	1.45	18.08	0.95	0.98	0.07	0.07
I	1.37	1.5	1.62	1.75	18.08	1.25	1.28	0.07	0.06
J	1.1	1.35	1.59	1.84	9.40	0.86	0.92	0.14	0.15
K	1.16	1.37	1.57	1.78	11.19	0.96	1.01	0.11	0.11
L	1.05	1.26	1.46	1.67	11.19	0.85	0.90	0.11	0.13
M	1.12	1.26	1.39	1.53	16.78	0.99	1.02	0.08	0.07
N	1.19	1.34	1.48	1.63	15.67	1.05	1.08	0.08	0.08
O	1.05	1.19	1.32	1.46	16.78	0.92	0.95	0.08	0.08

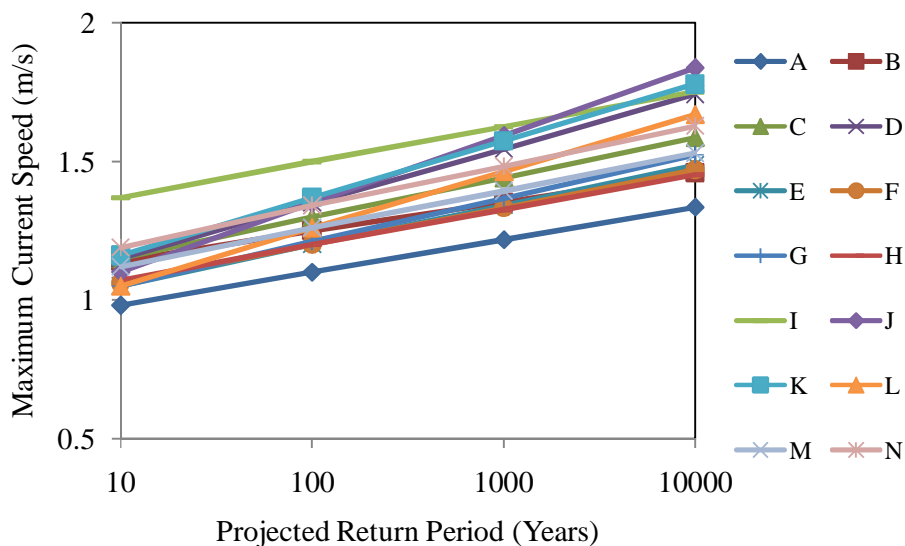


Figure 4.49: Extrapolation of Current Speed (Gumbel at PMO)

4.6.3.2 SBO Region

Current data for six Jacket platforms from SBO was analysed. Table 4.28 and Figure 4.50 show the result for current as per the Weibull distribution. The range for 100 years was 0.87 - 2.23 m/s. The corresponding 10,000 year values were in range of 0.93 - 2.56 m/s. The Gumbel distribution is shown in Table 4.29 and Figure 4.51. The 10,000 year value achieved was 0.98-2.87 m/s.

Table 4.28: Return Period & Current Speed (m/s), Weibull Distribution at SBO

SBO	Return Period in Years				Weibull Distribution Parameters				
	10	10 ²	10 ³	10 ⁴	Scale	Shape	Mean	SD	COV
A	1.9	2.23	2.42	2.56	1.57	4.33	1.43	0.37	0.26
B	0.81	0.87	0.90	0.93	0.74	9.70	0.71	0.09	0.12
C	1.13	1.26	1.33	1.39	0.99	6.37	0.92	0.17	0.18
D	0.78	0.94	1.03	1.10	3.71	0.62	0.56	0.17	0.30
E	1.11	1.26	1.35	1.41	0.95	5.47	0.88	0.19	0.21
F	1.2	1.35	1.44	1.50	1.04	5.88	0.97	0.19	0.20

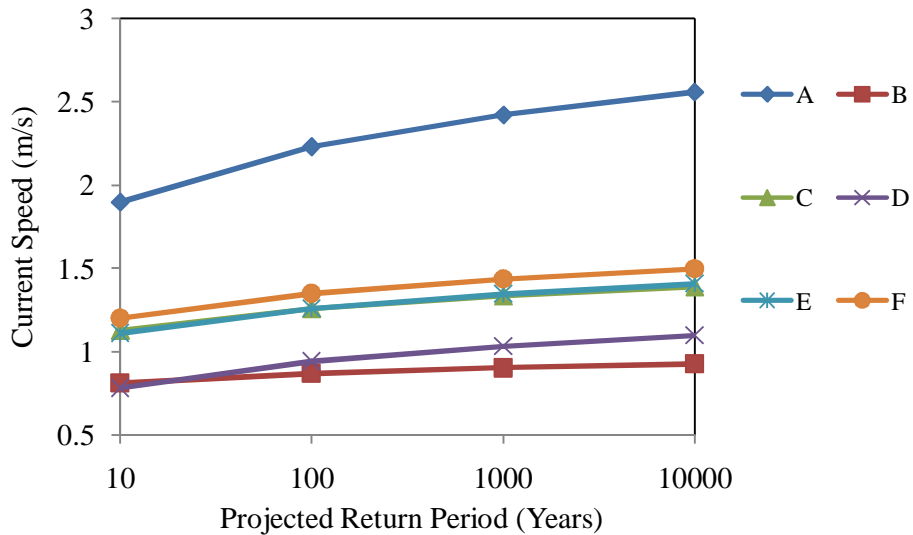


Figure 4.50: Extrapolation of Current Speed (Weibull at SBO)

Table 4.29: Return Period & Current Speed (m/s), Gumbel Distribution at SBO

SBO	Return Period in Years				Gumbel Distribution Parameters				
	10	10 ²	10 ³	10 ⁴	Scale	Location	Mean	SD	COV
A	1.9	2.23	2.55	2.87	7.12	1.58	1.67	0.18	0.11
B	0.81	0.87	0.92	0.98	39.16	0.75	0.77	0.03	0.04
C	1.13	1.26	1.38	1.51	18.08	1.01	1.04	0.07	0.07
D	0.78	0.94	1.10	1.25	14.69	0.63	0.67	0.09	0.13
E	1.11	1.26	1.40	1.55	15.67	0.97	1.00	0.08	0.08
F	1.2	1.35	1.49	1.64	15.67	1.06	1.09	0.08	0.07

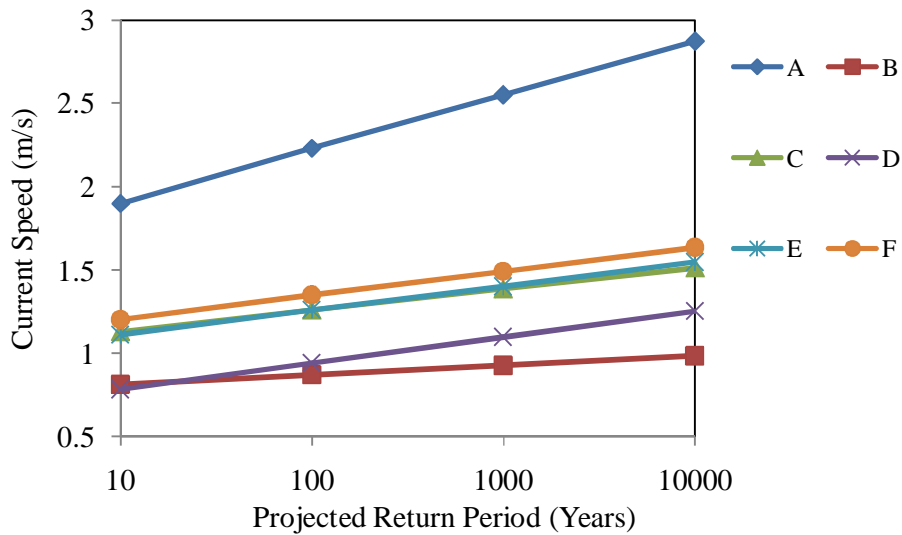


Figure 4.51: Extrapolation of Current Speed (Gumbel at SBO)

4.6.3.3 SKO Region

Current data for nine Jacket platforms from SKO was analysed. Table 4.30 and Figure 4.52 show the result for wind as per the Weibull distribution. The range for 100 years was 1.0 - 1.8 m/s. The corresponding 10,000 year values were in range of 1.14 - 2.10 m/s. The Gumbel distribution is shown in Table 4.31 and Figure 4.53. The 10,000 year value is shown as 1.22 - 2.38 m/s.

Table 4.30: Return Period & Current Speed (m/s), Weibull Distribution at SKO

SKO	Return Period in Years				Weibull Distribution Parameters				
	10	10 ²	10 ³	10 ⁴	Scale	Shape	Mean	SD	COV
A	0.96	1.05	1.10	1.14	0.86	7.73	0.81	0.12	0.15
B	1.5	1.8	1.97	2.10	1.20	3.80	1.09	0.32	0.29
C	1.53	1.74	1.86	1.95	1.31	5.39	1.21	0.26	0.21
D	1.55	1.75	1.87	1.95	1.34	5.71	1.24	0.25	0.20
E	0.87	1	1.07	1.13	0.74	4.98	0.68	0.16	0.23
F	1.1	1.25	1.34	1.40	0.94	5.42	0.87	0.19	0.21
G	0.83	1.21	1.43	1.59	0.53	1.84	0.47	0.26	0.56
H	1.05	1.2	1.29	1.35	0.89	5.19	0.82	0.18	0.22
I	1.3	1.5	1.62	1.70	1.09	4.84	1.00	0.24	0.24

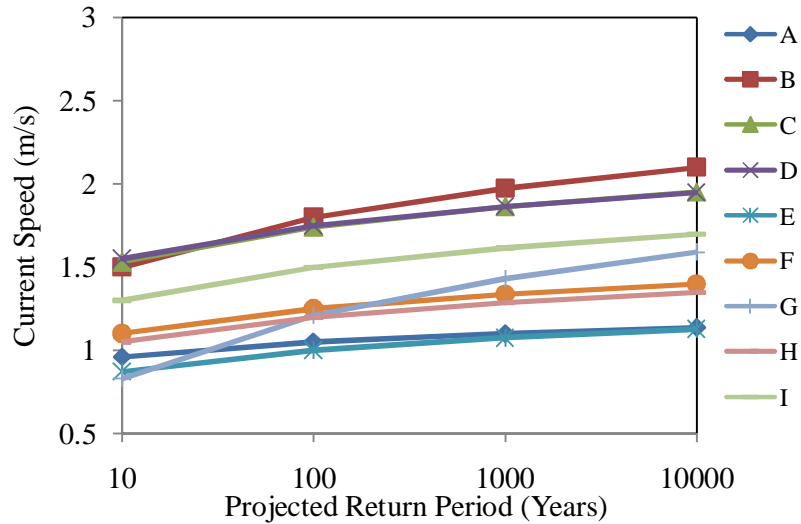


Figure 4.52: Extrapolation of Current Speed (Weibull at SKO)

Table 4.31: Return Period & Current Speed (m/s), Gumbel Distribution at SKO

SKO	Return Period in Years				Gumbel Distribution Parameters				
	10	10 ²	10 ³	10 ⁴	Scale	Location	Mean	SD	COV
A	0.96	1.05	1.14	1.22	26.11	0.87	0.90	0.05	0.05
B	1.5	1.8	2.09	2.38	7.83	1.21	1.29	0.16	0.13
C	1.53	1.74	1.94	2.15	11.19	1.33	1.38	0.11	0.08
D	1.55	1.75	1.95	2.14	11.75	1.36	1.41	0.11	0.08
E	0.87	1	1.12	1.25	18.08	0.75	0.78	0.07	0.09
F	1.1	1.25	1.39	1.54	15.67	0.96	0.99	0.08	0.08
G	0.83	1.21	1.58	1.95	6.18	0.47	0.56	0.21	0.37
H	1.05	1.2	1.34	1.49	15.67	0.91	0.94	0.08	0.09
I	1.3	1.5	1.70	1.89	11.75	1.11	1.16	0.11	0.09

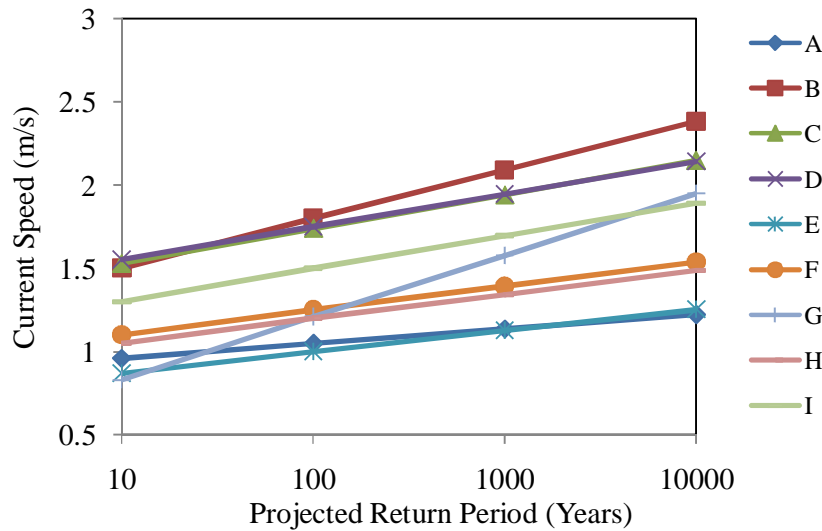


Figure 4.53: Extrapolation of Current Speed (Gumbel at SKO)

4.6.3.4 GULF OF MEXICO (GOM) and NORTH SEA (NS)

The data from international waters was taken from ISO code [147]. Table 4.32 and Figure 4.54 show the result for current as per the Weibull distribution. The GOM for 100 years was 2.3 m/s. The corresponding 10,000 year value was 3.30 m/s. For North Sea 100 year was in range of 0.9-1.3 3 m/s and 10,000 was 1.1-1.41 m/s. The Gumbel distribution is shown in Table 4.33 and Figure 4.55. The 10,000 year GOM was 4.26 m/s and for North Sea it was 1.29-1.49 m/s.

Table 4.32: Return Period & Current Speed (m/s), Weibull at GOM and NS.

	Return Period in Years				Weibull Distribution Parameters				
	10	10 ²	10 ³	10 ⁴	Scale	Shape	Mean	SD	COV
GOM	1.3	2.3	2.88	3.30	0.65	1.21	0.61	0.51	0.83
SNS	1.25	1.33	1.38	1.41	1.16	11.17	1.11	0.12	0.11
NNS	0.7	0.9	1.02	1.10	0.52	2.76	0.46	0.18	0.39

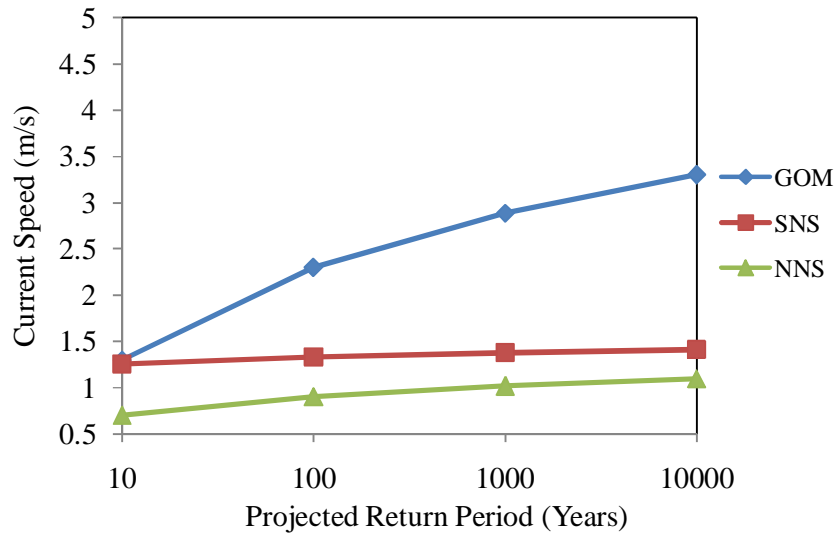


Figure 4.54: Extrapolation of Current Speed (Weibull at GOM and NS)

Table 4.33: Return Period & Current Speed (m/s), Gumbel at GOM and NS.

	Return Period in Years				Gumbel Distribution Parameters				
	10	10 ²	10 ³	10 ⁴	Scale	Location	Mean	SD	COV
GOM	1.3	2.3	3.28	4.26	2.35	0.34	0.59	0.55	0.93
SNS	1.25	1.33	1.41	1.49	29.37	1.17	1.19	0.04	0.04
NNS	0.7	0.9	1.10	1.29	11.75	0.51	0.56	0.11	0.20

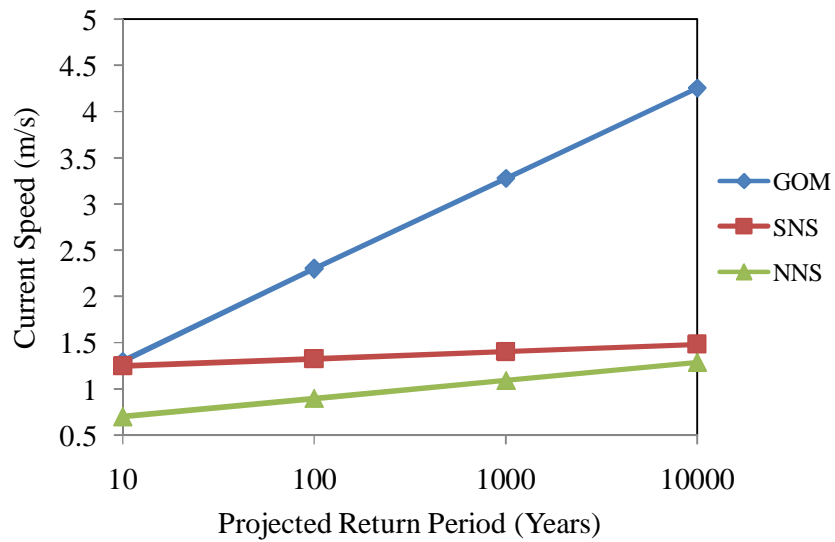


Figure 4.55: Extrapolation of Current Speed (Gumbel at GOM and NS)

4.7 Chapter Summary

To develop reliability models we need to identify the variability in actual tubular members and model stress Equations used by ISO code. Two types of uncertainty parameters were discussed in this chapter i.e. resistance and environmental load. The actual strength of tubular member varies from the characteristic /nominal strength. This is due to the variation in basic variables like material strength and dimensional properties i.e. yield strength, elastic modulus, diameter and thickness. The resistance of Jacket reduces with time period due to effects of ocean environment. This problem is catered by providing certain safety factor while designing the Jacket. The bias and COV evaluated in this study, on the basis of database of actual data, reflected that geometry and material variability existed in Malaysia as was expected. This was also reported in GOM, North Sea and China. The other uncertainty is related to an estimation of parameters for extreme environmental load. This variable load is expected to occur near Jacket platform at any time during its design life time or beyond. The major findings of this Chapter are:

1) Uncertain basic variables i.e. thickness, diameter, yield strength, tensile strength, elongation and angle were modelled based on actual variability in the material available in Malaysia. The standard deviation and mean bias and COV were evaluated and they reported values show similarity between this study and the studies conducted in GOM, North Sea and China. This study shows less variability in basic parameters of resistance uncertainty.

2) Nine ISO code stress Equations for component and eleven for joints were statistically modelled in this research for evaluating model uncertainty. The model Equations recommended by ISO code were used to find the variability of model uncertainty. The uncertainty models achieved in this study were compared with models developed for ISO 19902 and in China. The variation in current study was less than that reported in literature. Using this variability in the reliability model, the offshore Malaysia Jacket will have higher reliability. The results from this research were used for reliability analysis of components and joints using ultimate limit state design of Jacket platforms in Malaysia.

3) The reliability determination requires that distribution parameters should be used for uncertain random variables. There are three parameters of uncertainty for Jacket platforms i.e. wave, wind and current. Here in this study, based on Weibull and Gumbel distributions these parameters were determined using 10 and 100 year values.

4) Gumbel distribution overestimated the parameters of environmental load. Therefore Weibull-two parameter distribution was recommended for the reliability of Jacket platforms in Malaysia.

5) The ISO 19902 requires that reassessment of Jacket platforms should be based on 10,000 year return period. In this study, Weibull and Gumbel distributions were used to find significant wave height, current and wind speed, extrapolations.

CHAPTER 5

COMPONENT RELIABILITY AND ENVIRONMENTAL LOAD FACTOR

5.1 Introduction

Reliability is defined as an ability to fulfil the particular requirements including the design working life of Jacket for which it has been designed [66]. Behaviour of structure can be measured by probability of failure or reliability index. Target reliability of components is found as per API RP2A WSD. Load factors were developed in such a way that the reliability index of Jacket is at predefined target level. The reliability indices of ISO LRFD design for a range of load factors were determined. When ISO load factors were plotted against the corresponding API target reliabilities, the intersection point gave the proposed load factor. The Jacket reliability designed as per new load factors will not only be higher than the target, but also will ensure safer Jacket. This chapter presents the structural reliability analysis of tubular components of four Jacket platforms in Malaysia. This is followed by development of environmental load factors which are not available for offshore Malaysia.

5.2 Selection of Members

The method followed here is based on ISO LRFD 19902 which is explained by BOMEL [69]. Primary members were selected from Jacket for reliability analysis. These members were leg, vertical diagonal and horizontal at periphery and horizontal diagonals. Table 5.1 shows some typical members selected for finding the reliability index. They are selected based on the slenderness $\frac{k X l}{r}$ and diameter to thickness ratio. This table is based on one of the four selected platforms.

Table 5.1: Member Selection for Calibration - Slenderness Ratio and d/t Ratio

Diameter (D) mm	Wall thickness (T) mm	Length (L) mm	K factor	Slenderness %	D/T
1650	25.0	9344	1.0	0.23	66.00
1630	15.0	17500	1.0	0.43	108.7
660	12.7	15370	0.7	0.65	51.97
711	15.0	11000	0.7	0.43	47.40
610	12.7	11800	0.7	0.54	48.03
660	19.0	11940	0.7	0.51	34.74
406	12.7	12000	0.7	0.83	31.97
508	12.7	12400	0.7	0.68	40.00

5.3 Component Target Reliability

Reliability index for offshore Jacket platforms can be taken as minimum lower bounds of safety levels acceptable to the public. Load and resistance factor design requires the development of target reliability levels. Theophanatos et al., 1992 suggested the selection of target reliability using (API WSD /API LRFD / ISO 19902) for the selection of target safety index and separate partial factors for individual component and load effect types to be determined [9]. The best possible safety required for the structure depends on cost of failure of structure [153]. Optimum safety can be determined by minimum expected cost or with maximum utility [111], [153]. The target reliability indices were chosen so that it can give consistent and uniform safety margin for all components.

Primary members are the main element of the Jacket, whose failure may cause serious damage to structure. Target reliability of secondary components can be fixed at a lower value than the primary members. Serviceability limit state (SLS) has a lower level of consequences of failure than ultimate limit states (ULS). For ultimate limit states, calculated reliability indices represent component reliability [111], [153]. Therefore in this study, only ultimate limit state has been considered for finding the reliability index. Tables 5.2 - 5.3 shows the values used for the calibration of ISO code taking into effect of North Sea platforms. Reliability indices are for different Jacket components and load factors [69].

Table 5.2: ISO Target Reliability [50]

Load Effect	API RP2AWS	ISO ($\gamma=1.35$)
	β	β
Compression & Bending	3.49	3.84
Tension & bending (brace)	3.64	3.85
All	3.50	3.85

Table 5.3: Reliability Index against Different Environmental Load Factors [69]

Code		Brace	Brace compression & bending	Leg
API (WSD)		3.70	3.70	3.49
ISO	$\gamma_w=1.20$	3.66	3.69	3.57
	$\gamma_w=1.25$	3.75	3.79	3.66
	$\gamma_w=1.30$	3.84	3.88	3.76
	$\gamma_w=1.35$	3.93	3.97	3.84
	$\gamma_w=1.40$	4.02	4.05	3.94
	$\gamma_w=1.45$	4.11	4.14	4.02

5.4 Component Reliability Analysis

API and ISO are component based design codes. The element is designed and then system is checked using overall system analysis. In this study it was divided into different bays and sub-divided into types of members. SACS software was used for the analysis of Jackets. Though We/G ratios above 10 may not actually occur in this region but still they were included in this study to check effects of higher load. The most pertinent We/G ratio lies in between 0.5-2.0.

5.4.1 Code Stresses

API and ISO codes specify seven types of stresses a component undergoes during its design life. These can be single or two or three combined stresses. Here limit state Equation for seven types were used to find the reliability.

5.4.1.1 *Single Stresses*

Jacket members under pure axial tension were not found during the analysis. For finding reliability against tensile stresses, only those members were selected which were predominantly influenced by axial tensile stresses and with minimum bending stresses. The reliability was determined for the member, to find the effect of API and ISO codes using different environmental to gravity load ratios. The basic Equations for API and ISO were found to be similar i.e. depending on yield strength (F_y) except safety factors. Figure 5.1 shows component reliability of member under axial tension. The ISO LRFD with a load factor of 1.35 gave higher values of reliability as compared to API WSD. This study ISO LRFD (MS) proposes a load factor of 1.25 as shown in Figure 5.39. Here ISO LRFD was plotted with an environmental load factor of 1.35 as given by ISO code. ISO LRFD (MS) stands for this region with a load factor of 1.25. The ratio of W_e/G increases the reliability decreases. It can be seen that with increase of W_e/G ratio, reliability decreases for all cases. The ISO (LRFD) code gave higher values as compared to API (WSD), which shows the consistency of ISO code.

The same trend was observed in case of axial compression as shown in Figure 5.2. Here also the ISO code gave higher reliability index at different W_e/G ratios. It was found that Metocean parameters were more influencing as compared to other variables for this type of stresses.

Figure 5.3 shows reliability for members under isolated bending stress which were not encountered during the Jacket analysis. Here, selected members were those which showed high ratio of bending stresses as compared to axial stress. The results showed the same trend and ISO was again higher as compared to API. ISO_MS comes in between both codes for compression and bending cases as shown in Figure 5.2-5.3. During Jacket analysis compression stress was the only isolated stress present in components out of above three isolated stresses.

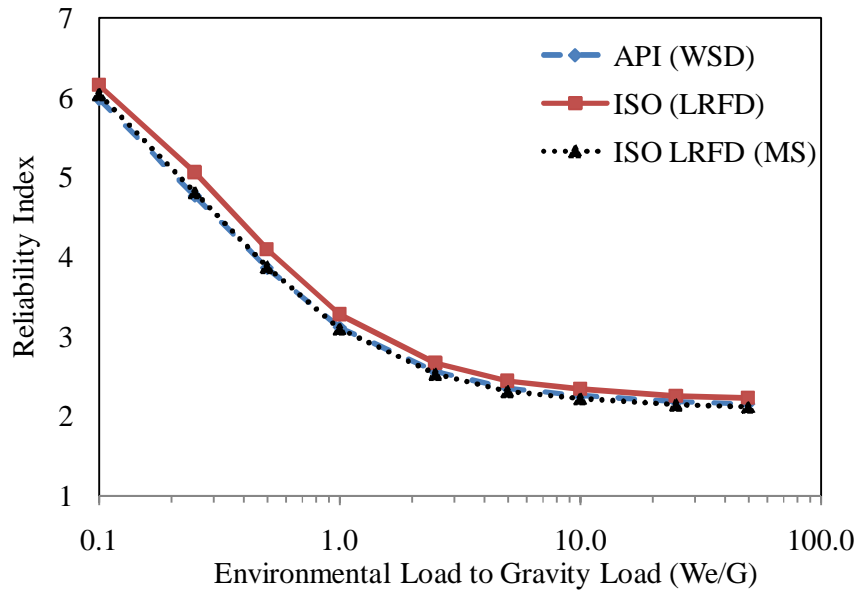


Figure 5.1: Variation of W_e/G ratio Vs Reliability Index for Components in Axial Tension for API WSD, ISO (MS) and ISO LRFD Codes at SKO1

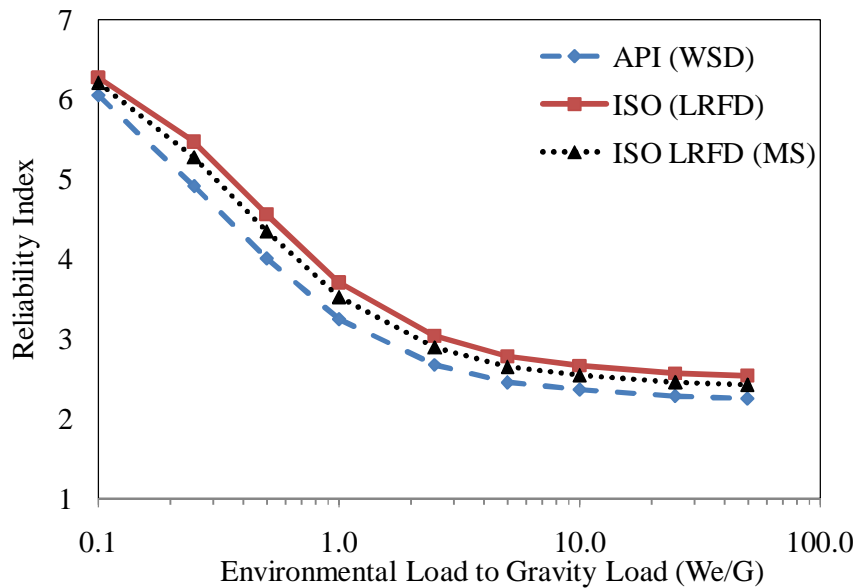


Figure 5.2: Variation of W_e/G ratio Vs Reliability Index for Components in Compression for API WSD, ISO (MS) and ISO LRFD Codes at SKO1

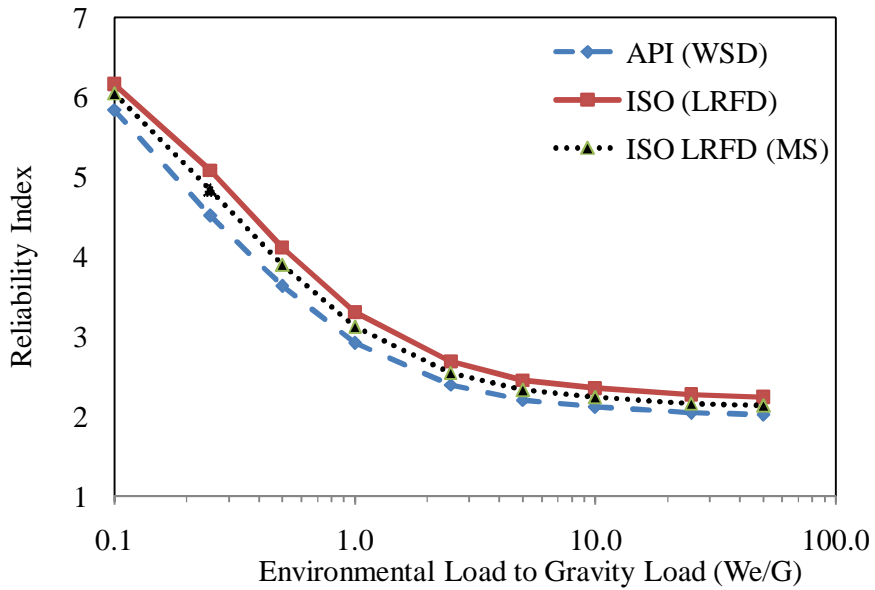


Figure 5.3: Variation of W_e/G ratio Vs Reliability Index for Components in Bending for API WSD, ISO (MS) and ISO LRFD Codes at SKO1

5.4.1.2 Combined Two Stresses

Figure 5.4 and 5.5 are based on reliability of combined two stresses which were found in actual member analysis. The code Equations were similar in API WSD and ISO LRFD but the only difference was in safety factors. The ratio of axial to bending stress used here was 0.5 which was based on actual stresses as explained in Chapter 3. The result shows that the ISO reliability was again higher but in the case of compression and bending both curve were not only close together but at higher gravity load API gave higher values. This study proposes values which are in between the curves with a load factor of 1.25. Combined stresses used for reliability analysis was based on 50% for axial tension / compression and 50% for bending. This was the ratio available from the Jacket and also used for ISO code development [69].

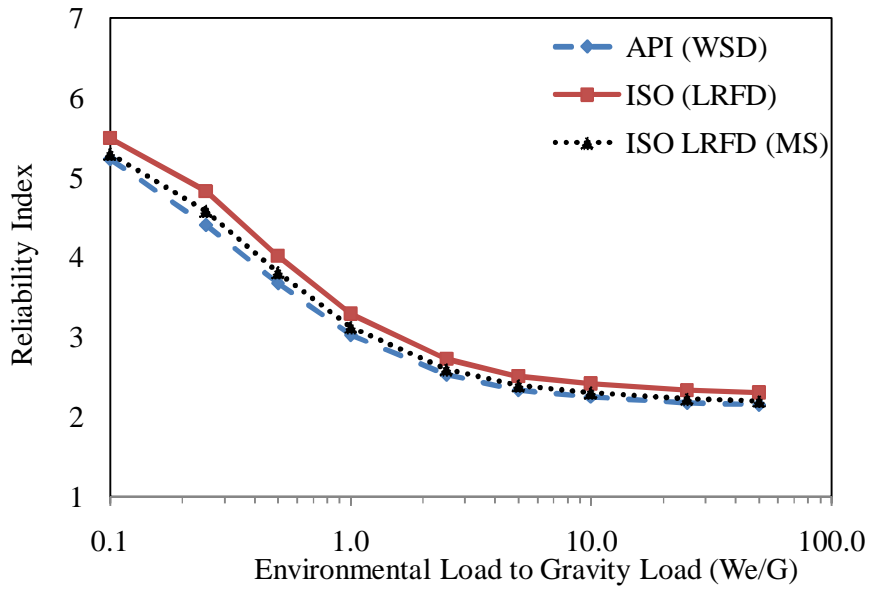


Figure 5.4: Variation of W_e/G ratio Vs Reliability Index for Components in Tension & Bending for API WSD, ISO (MS) and ISO LRFD Codes at SKO1

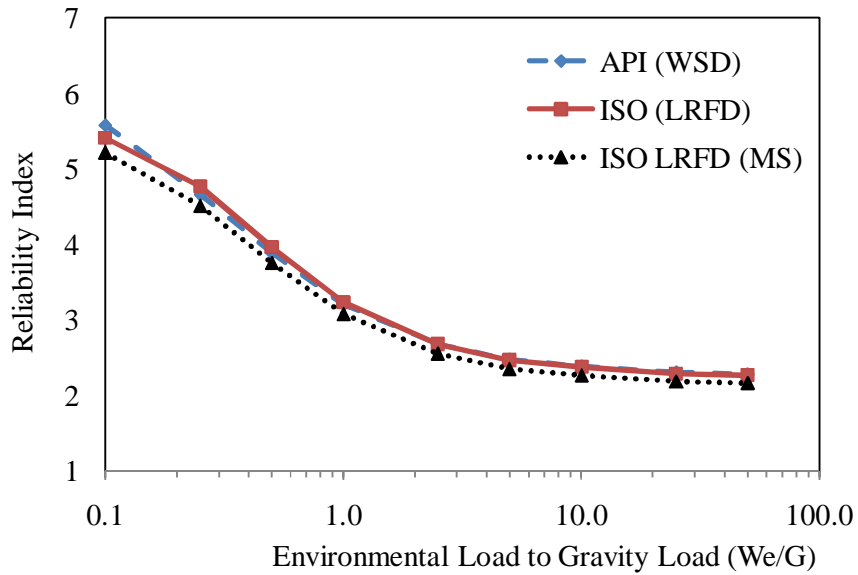


Figure 5.5: Variation of W_e/G ratio Vs Reliability Index for Components in Compression & Bending for API WSD, ISO (MS) and ISO LRFD Codes at SKO1

5.4.1.3 Combined Three Stresses

The ratio for combined three stresses used in this study for axial to bending stress was 0.4 to 0.6. The result in Figures 5.6 - 5.7 show the same trend as was found for ISO. Steepness reduced at higher values of W_e/G as compared to low values. The ISO LRFD value gave higher reliability as compared to API WSD, this study proposes load factor of 1.25. Figure 5.7 shows this study proposed reliability values which are less than the target reliability index but on averaging the results showed that 1.25 was agreed upon. Combined stress ratio used for reliability analysis was based on 40% - 60% for axial tension / compression and bending. This was the ratio available from the Jacket and also used for ISO code development [69].

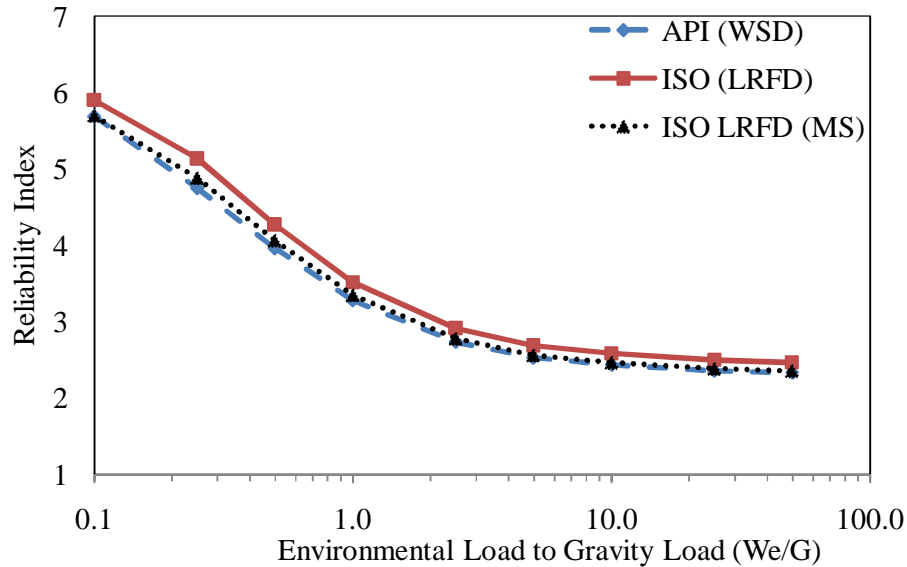


Figure 5.6: Variation of W_e/G ratio Vs Reliability Index for Components in Tension, Bending & Hydrostatic Pressure for API WSD, ISO (MS) and ISO LRFD Codes at SKO1

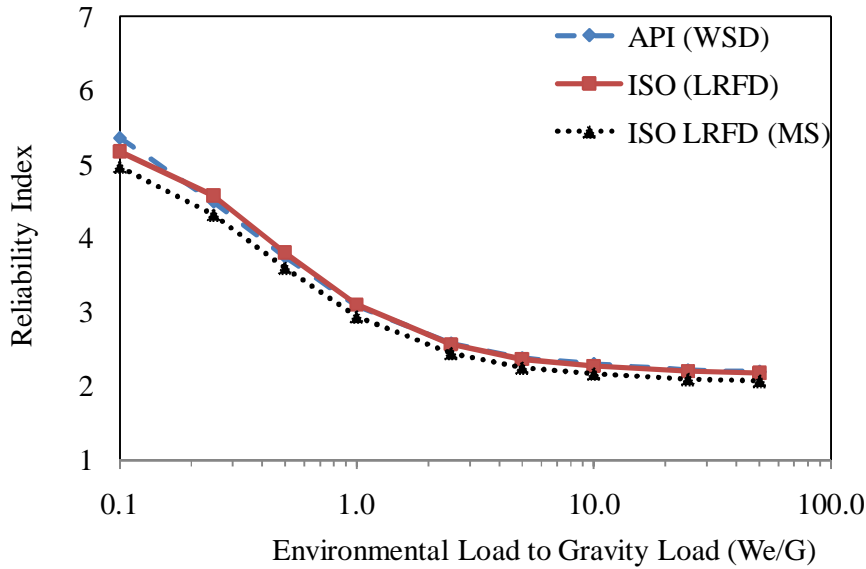


Figure 5.7: Variation of W_e/G ratio Vs Reliability Index for Components in Compression, Bending & Hydrostatic Pressure for API WSD, ISO (MS) and ISO LRFD Codes at SKO1

5.4.2 Sensitivity Analysis

All variables of random input do not have equal influence on reliability index output. Sensitivity analysis can be used to quantify the influence of each basic random variable [59]. Table 5.4 shows the sensitivity index for the variables used in this research. The most important influence was made by significant wave height, current, environmental load model uncertainty, stress model uncertainty and yield strength. This means that these parameters have high weightage for reliability index and geometrical parameters are less sensitive. The same was achieved for study in Mediterranean Sea [16] and for ISO [69]. ISO recommends most sensitive α values for resistance should have value of 0.8 and for load -0.7 [73]. The significant wave height of Malaysian regions is lower as compared to GOM and NS which plays important role in reliability analysis as shown in Table 5.4. Thus comparative target reliability was achieved using a reduced load factor of 1.25. Sensitivity study indicated that environmental load parameters strongly influenced the reliability of Jacket [96].

Table 5.4: Sensitivity Analysis of Random Variables Axial Tension

Basic variable	Reliability Index was achieved at these values of random variables	Sensitivity factor (α)
Yield strength	414.42	-0.1028
Diameter	1855	-0.0036
Thickness	52.15	-0.0378
Significant wave height	4.7	0.8783
Current	0.85	0.1160
Environmental load uncertainty model	0.86	-0.4325
Dead Load	1.0	0.000787
Live Load	1.0	0.0013
Stress model uncertainty	1.24	-0.127

5.4.3 Effect of Variation of Environmental Load Factor

The effect of environmental load to gravity load variations for ISO code Equations is shown in Figures 5.8 - 5.15. This shows variation in reliability index with respect to change in environmental load factors. With high W_e/G ratios the steepness reduced and thus reliability decreased with high W_e/G ratios. Figures 5.8 - 5.15 show clearly that the reliability index follows the same trend in the case of single, two or three stresses. Higher reliability is achieved with increases in load factor.

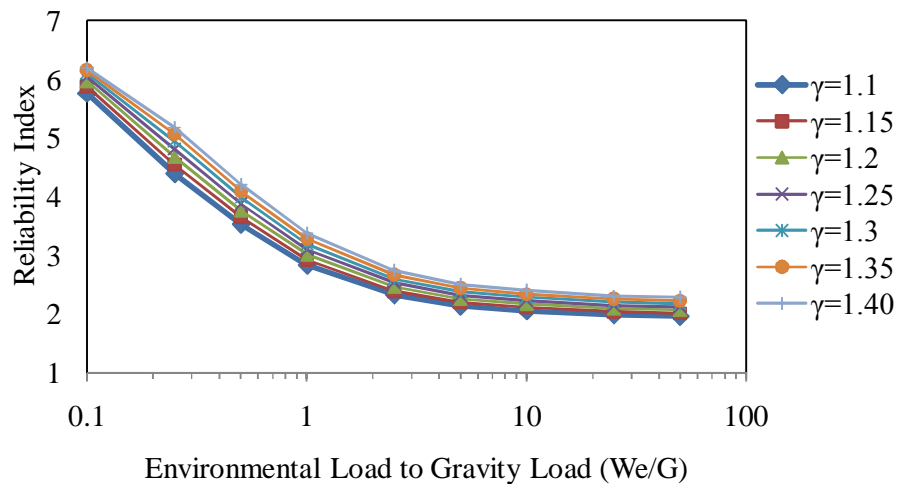


Figure 5.8: Variation of Reliability Index Vs W_e/G for Axial Tension (Leg) Using ISO code for Different Values of Environmental Load Factor (γ)

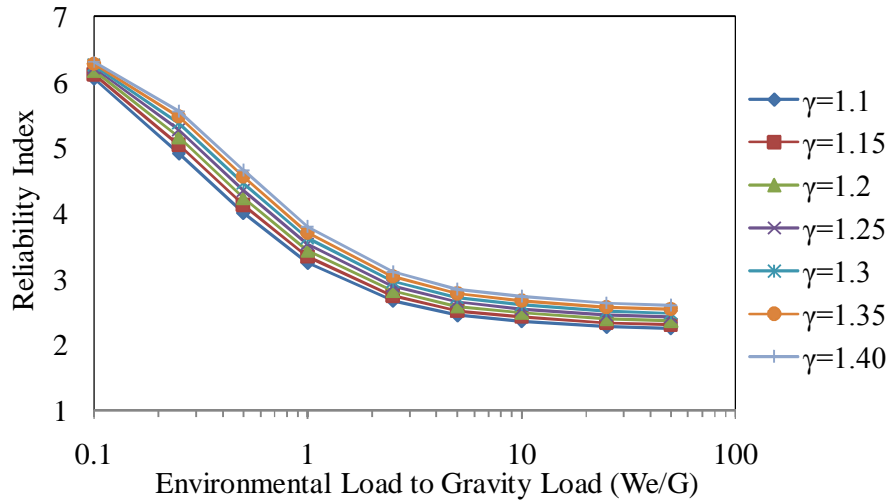


Figure 5.9: Variation of Reliability Index Vs W_e/G for Compression (Leg) Using ISO code for Different Values of Environmental Load Factor (γ)

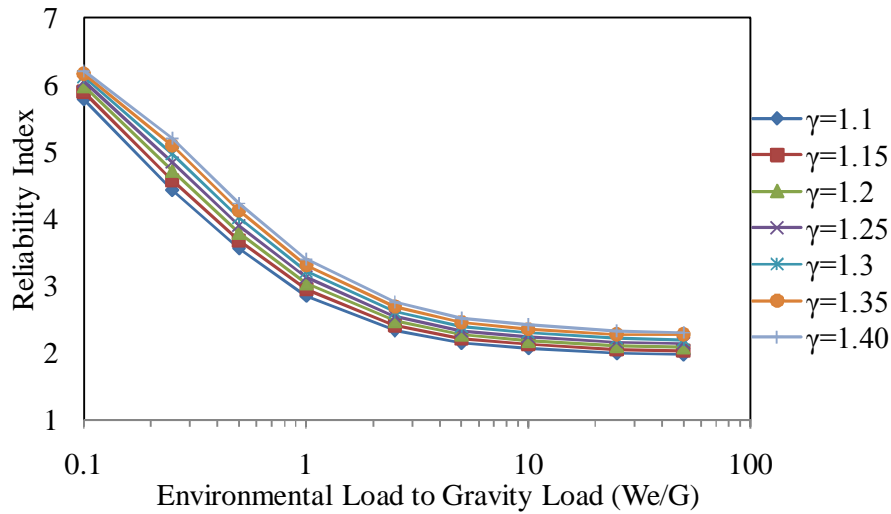


Figure 5.10: Variation of Reliability Index Vs W_e/G for Bending (Leg) Using ISO code for Different Values of Environmental Load Factor (γ)

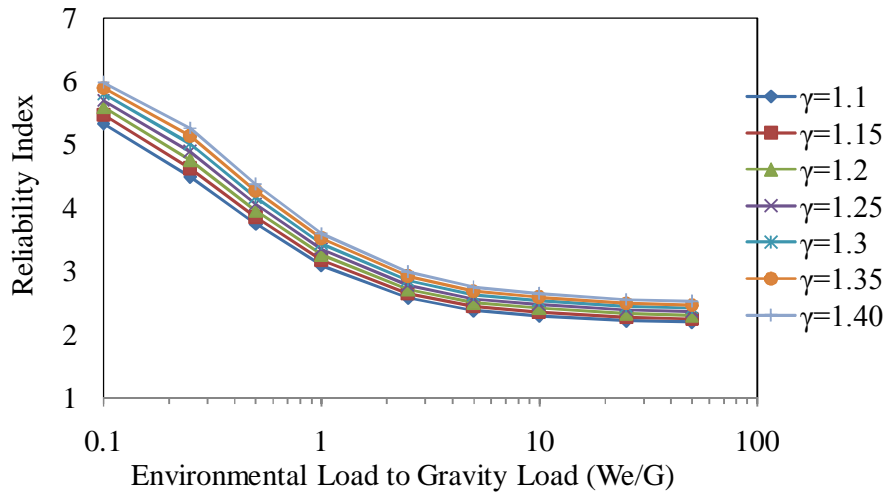


Figure 5.11: Variation of Reliability Index Vs W_e/G for Tension & Bending (Leg) Using ISO code for Different Values of Environmental Load Factor (γ)

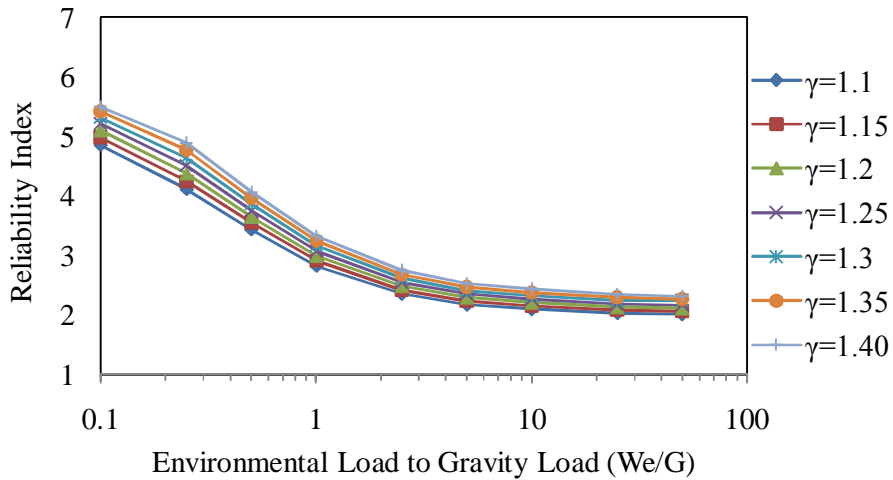


Figure 5.12: Variation of Reliability Index Vs W_e/G for Compression & Bending (Leg) Using ISO code for Different Values of Environmental Load Factor (γ)

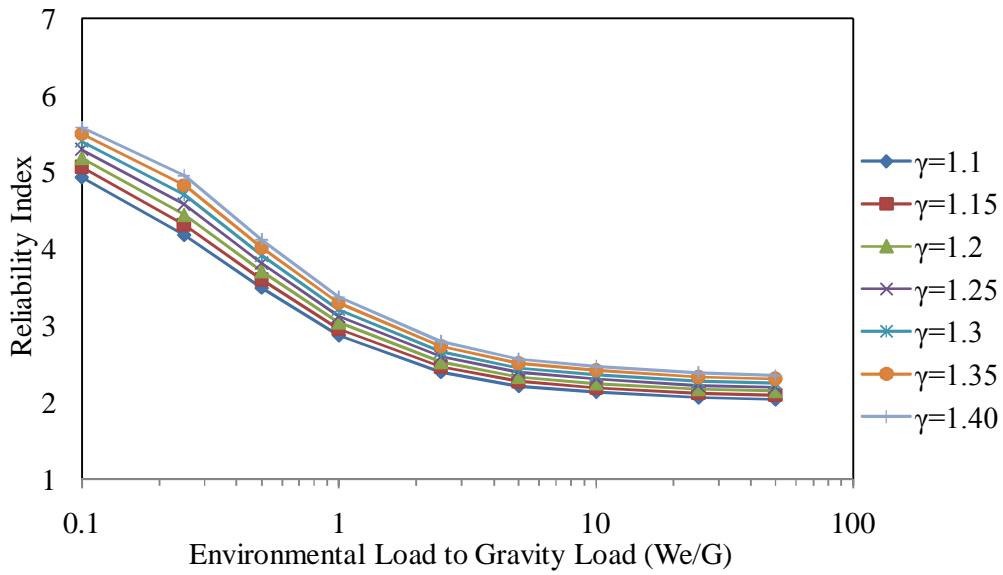


Figure 5.13: Variation of Reliability Index Vs W_e/G for Tension, Bending & Hydrostatic Pressure (Leg) Using ISO code for Different Values of Environmental Load Factor (γ)

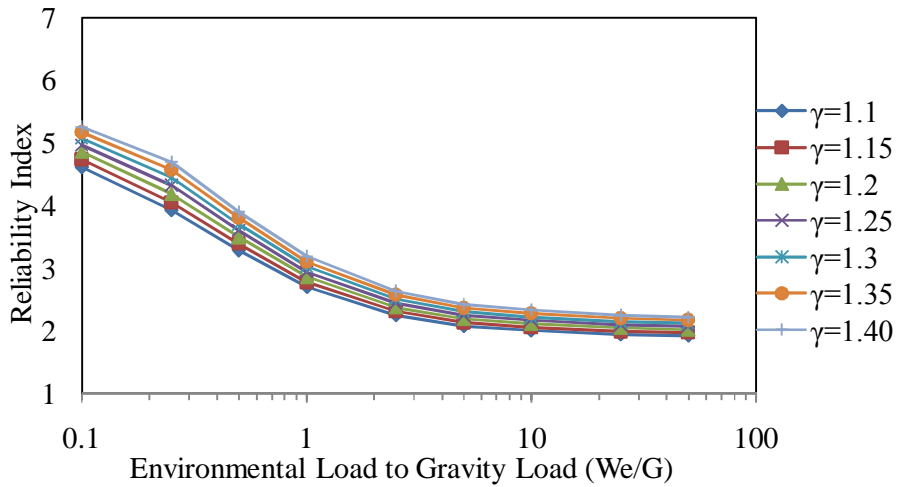


Figure 5.14: Variation of Reliability Index Vs W_e/G for Compression, Bending & Hydrostatic Pressure (Leg) Using ISO code for Different Values of Environmental Load Factor (γ)

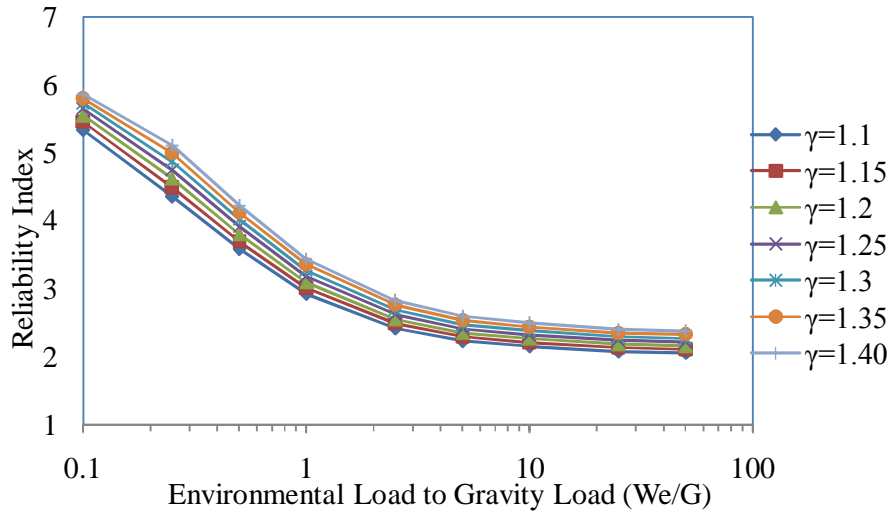


Figure 5.15: Variation of Reliability Index Vs W_e/G for Combined Stresses (Leg) Using ISO code for Different Values of Environmental Load Factor (γ)

5.4.4 Effect of Column Slenderness Ratio

The effect of slenderness on component reliability was not much varying. The variation of reliability index was small with wide range of columns having slenderness ratio in the range of 0.2 - 1.15. Column buckling ISO code Equation was used for the reliability was evaluated with range of W_e/G ratio. Therefore it can be concluded that reliability index was not sensitive to slenderness ratio as shown in Figure 5.16.

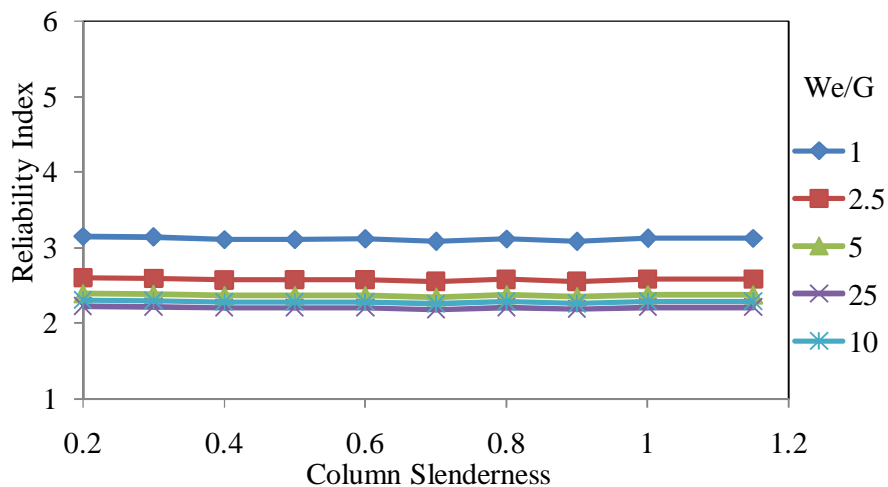


Figure 5.16: Column Slenderness Vs Reliability Index for Various W_e/G Ratios

5.4.5 Calibration Points for Jackets

Calibration points were used to evaluate the effects of component reliability on both codes. It was seen that both codes gave results which were consistent and not much varied. Table 5.5 shows reliability index for this study compared with ISO study. Figures 5.17 - 5.18 shows the calibration points for Jacket members for all types of model stresses. API WSD showed more consistency for all stresses. The calibration points of API are much close together as compared to ISO. The reliability index obtained in this study was comparable with ISO.

Table 5.5: Reliability Index for Jacket Members

Load type	MS		BOMEL [75]	
	ISO (LRFD)	API (WSD)	ISO (LRFD)	API (WSD)
Compression & Bending	3.65	3.82	3.97	3.70
Tension & Bending	4.53	4.09	3.85	3.64
Compression, bending & Hydrostatic	4.25	3.93	4.09	3.80
Tension, bending & Hydrostatic	4.37	3.74	3.72	3.85
Average	4.20	3.90	3.91	3.75

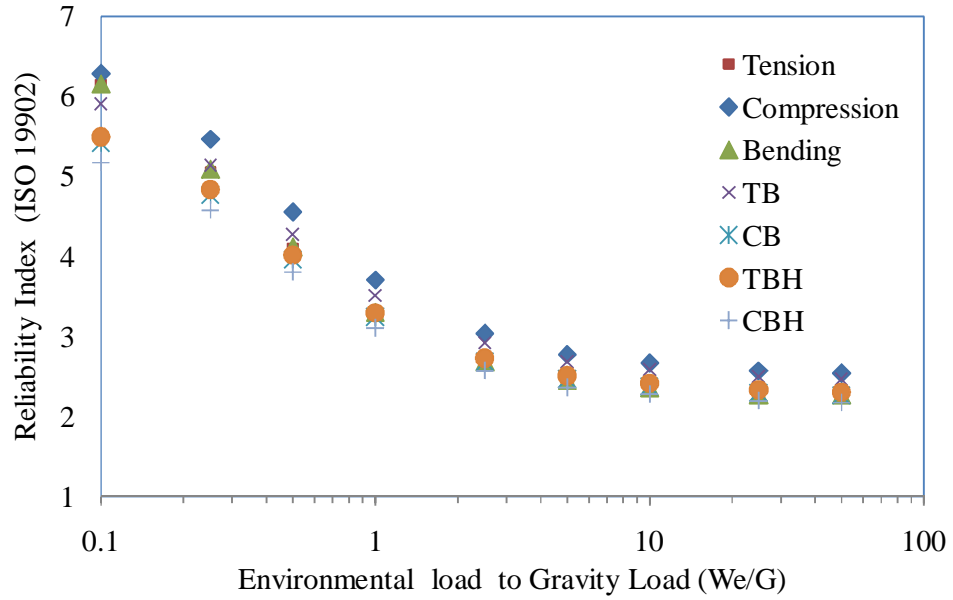


Figure 5.17: Calibration of Jacket Members Under ISO for all Types of Model Stresses with W_e/G ratios Vs ISO Reliability Indices

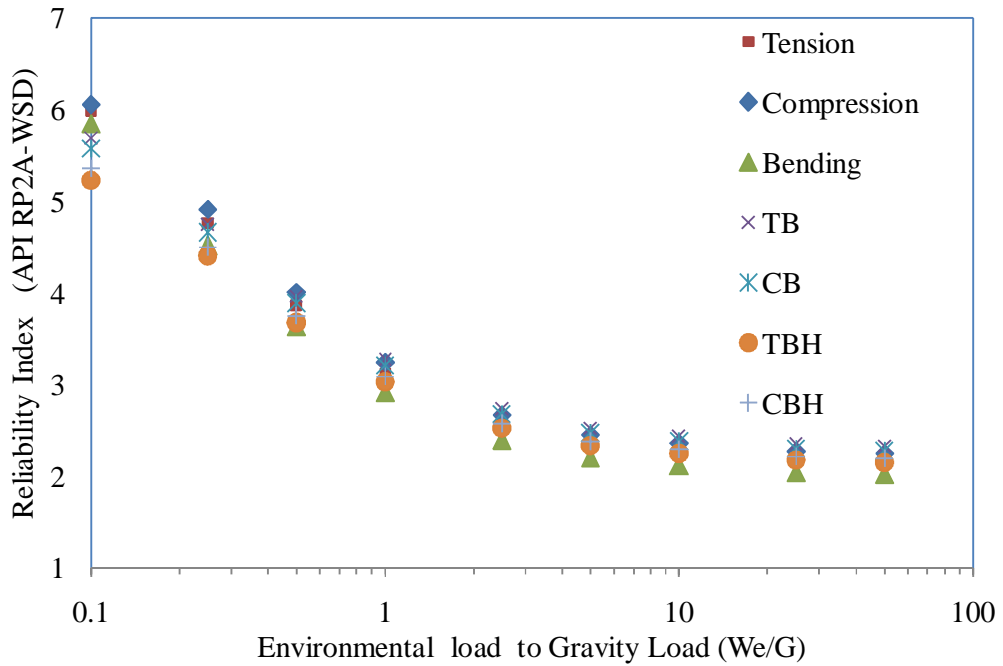


Figure 5.18: Calibration of Jacket Members Under API WSD for all Types of Model Stresses with W_e/G ratios Vs API WSD Reliability Indices

5.4.6 Selection of Environmental Load Factor

Load factors are multiplied with design / characteristic load with an intention so that this new factored load will be higher than the actual load. The criterion for selection of load and resistance factors is the closeness to the target reliability level [111], [153]. The factors must be based on the target reliability which should be equal to or greater than the preselected target reliability, in this case it was API WSD. Here environmental load and resistance factors were calibrated so that the one close to target reliability can be selected. The point where ISO code overtakes the target reliability can be taken as the load factor. API (WSD) and ISO (LRFD) load factors were evaluated at W_e/G ratio of 1.0 as was determined by BOMEL [69]. The variation of load factors was influenced by the sensitivity of random variables as shown in Table 5.4. This method has been tried for finding the load factors using target reliability based on previous code which has proved its robustness or on notional probability of failure. This was done for AISC and ACI 318 codes. Target reliability was based on API WSD which has already proved it to be a reliable code.

5.4.7 PMO Platform

Figures 5.19 - 5.23 show the environmental load factor for the PMO region for all four components of Jacket. Figure 5.19 show the load factor for horizontal periphery brace member with a load factor of 1.20. Horizontal diagonal load factor of 1.27 is shown in Figure 5.20. Figure 5.21 shows vertical diagonal load factor of 1.15 and finally leg members shown in Figure 5.22 have a load factor of 1.25. The averaged load factor for this region was evaluated to be 1.25 as shown in Figure 5.23 with a target API WSD reliability index of 3.59. For the platform at PMO, the horizontal diagonal members were highly stressed. The least stressed members were vertical diagonals. The highest target reliability used was 4.0 for leg members.

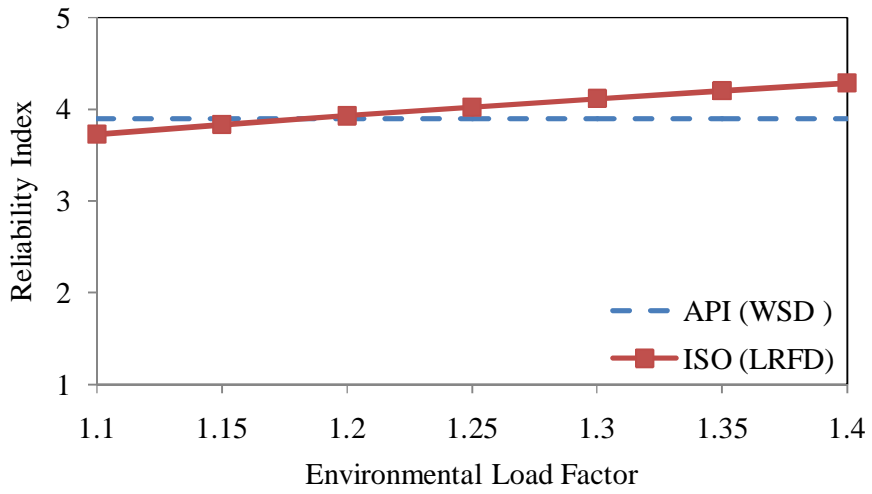


Figure 5.19: Reliability Index Vs Environmental Load Factor for HP at PMO Using ISO 19902 and API WSD

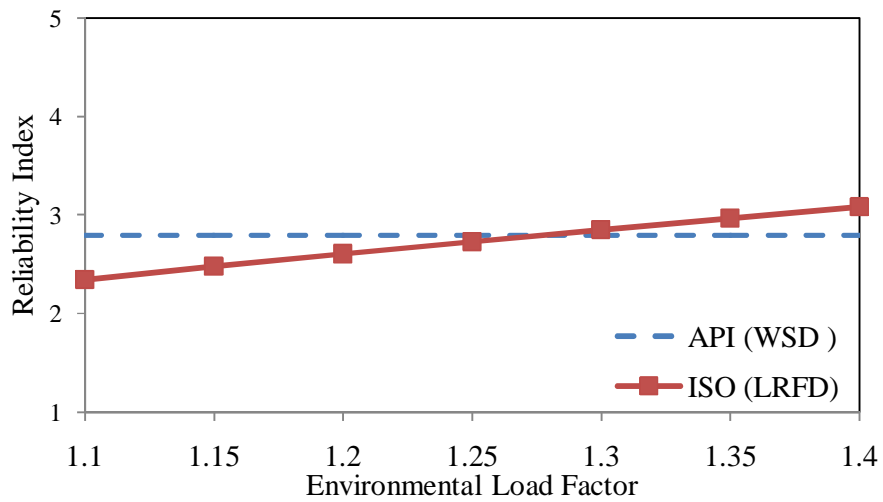


Figure 5.20: Reliability Index Vs Environmental Load Factor for HD at PMO Using ISO 19902 and API WSD

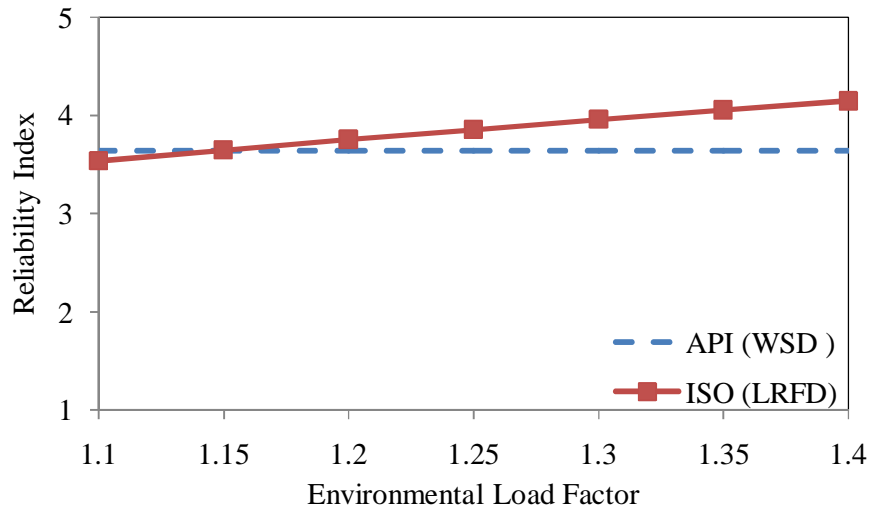


Figure 5.21: Reliability Index Vs Environmental Load Factor for VD at PMO Using ISO 19902 and API WSD

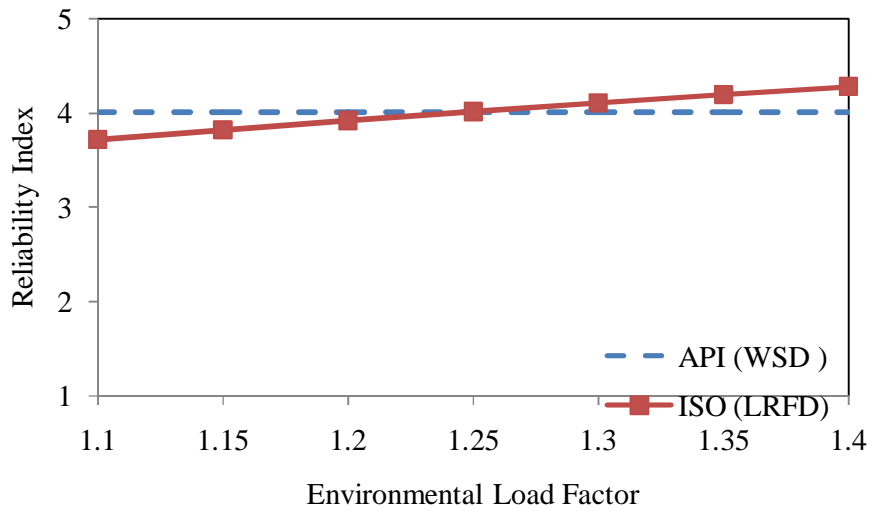


Figure 5.22: Reliability Index Vs Environmental Load Factor for Leg at PMO Using ISO 19902 and API WSD

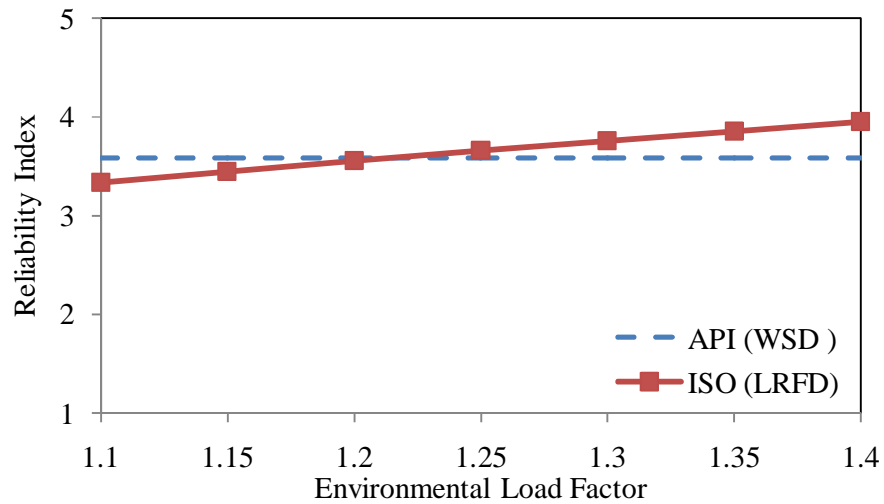


Figure 5.23: Reliability Index Vs Environmental Load Factor for Component at PMO Using ISO 19902 and API WSD

5.4.8 SBO Platform

Figures 5.24 - 5.28 show the environmental load factor for the SBO region for all four types of components of Jacket. Figure 5.24 show horizontal periphery brace member with a load factor of 1.25. Horizontal diagonal load factor of 1.25 is shown in Figure 5.25. Figure 5.26 shows vertical diagonal load factor of 1.25 and finally leg member is shown in Figure 5.27 with a load factor of 1.25. The averaged load factor for this region was evaluated to be 1.27 as shown in Figure 5.28, with average target reliability index of 4.30. The results from this platform were the most consistent among all platforms. This shows members were equally stressed, though the target reliability was different for all members. The highest reliability was found for horizontal diagonal member with target reliability of 6.1 and the lowest was for horizontal brace at periphery. The API WSD target reliability of 4.3 was evaluated for this platform.

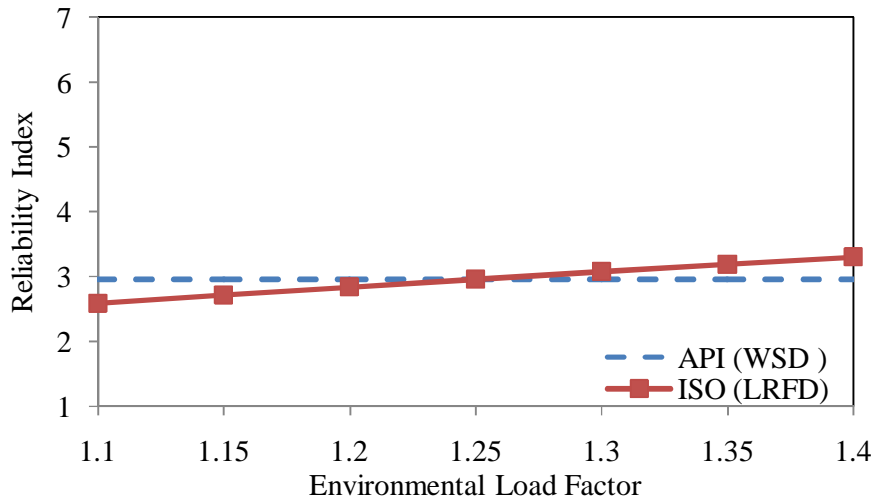


Figure 5.24: Reliability Index Vs Environmental Load Factor for HP at SBO Using ISO 19902 and API WSD

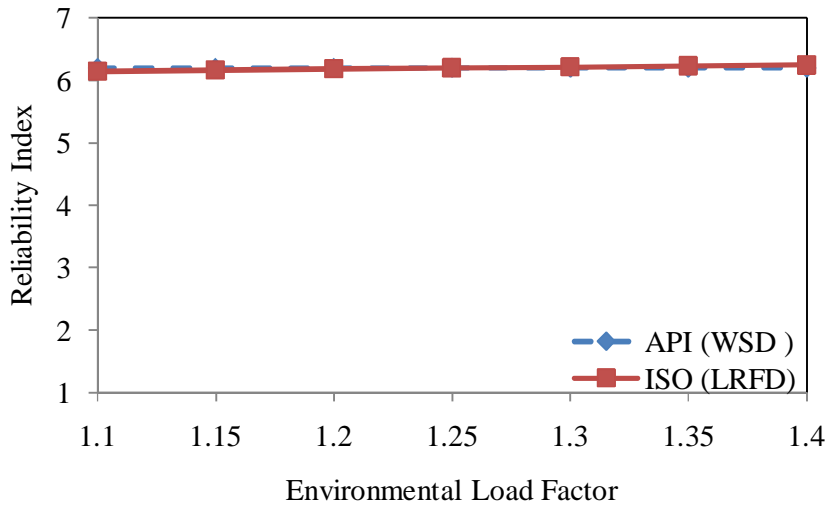


Figure 5.25: Reliability Index Vs Environmental Load Factor for HD at SBO Using ISO 19902 and API WSD

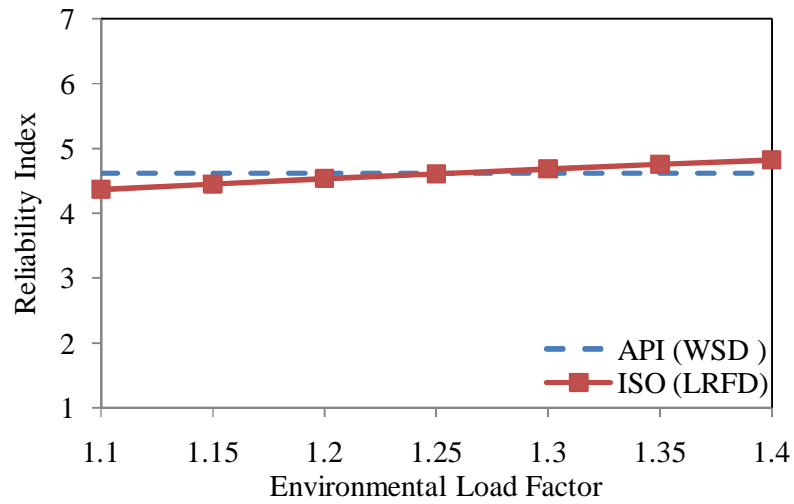


Figure 5.26: Reliability Index Vs Environmental Load Factor for VD at SBO Using ISO 19902 and API WSD

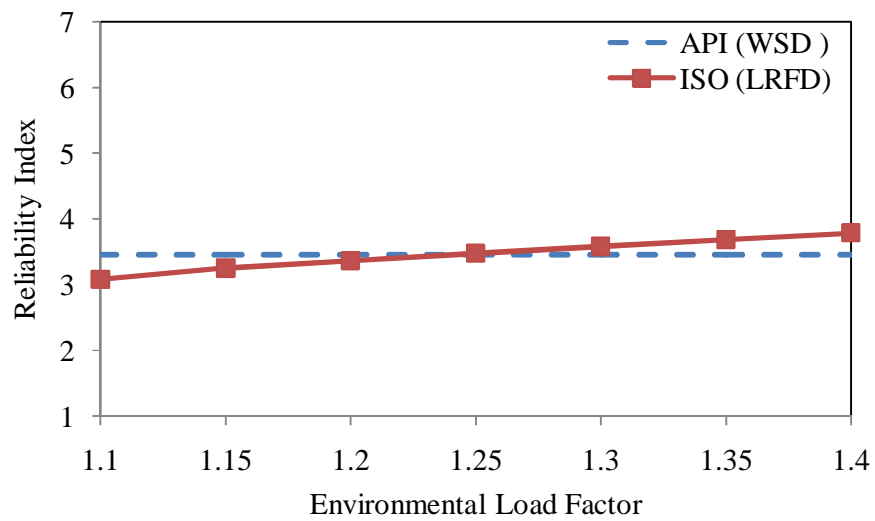


Figure 5.27: Reliability Index Vs Environmental Load Factor for Leg at SBO Using ISO 19902 and API WSD

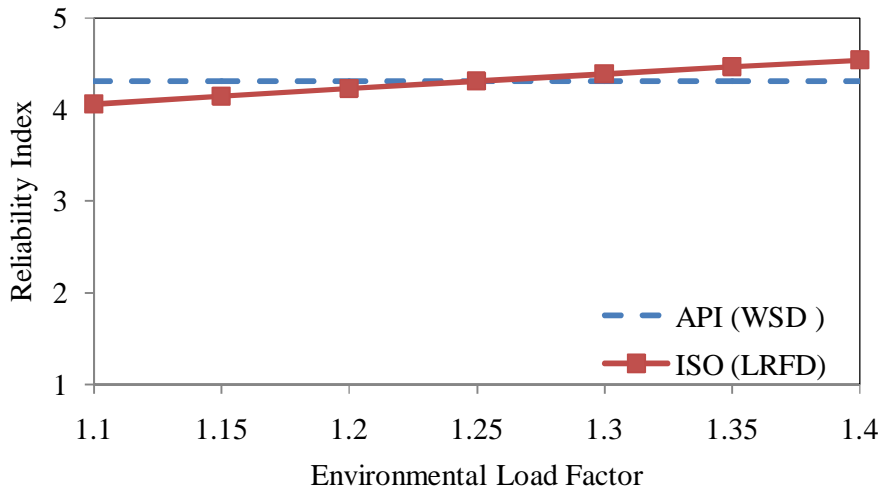


Figure 5.28: Reliability Index Vs Environmental Load Factor for Component at SBO Using ISO 19902 and API WSD

5.4.9 SKO Region

From SKO region two Jackets were selected for analysis and results are presented here.

5.4.9.1 SKO1 Platform

Figures 5.29 - 5.33 show the environmental load factor for the SKO1 Jacket, for all four types of components of Jacket. Figure 5.29 show the horizontal periphery brace member with a load factor of 1.15. Horizontal diagonal load factor of 1.25 was shown in Figure 5.30. Figure 5.31 show vertical diagonal load factor of 1.25 and finally leg members in Figure 5.32 show a load factor of 1.25. The averaged load factor for this region was 1.20 as shown in Figure 5.33. The average target reliability index was 3.17 for this platform in SKO region.

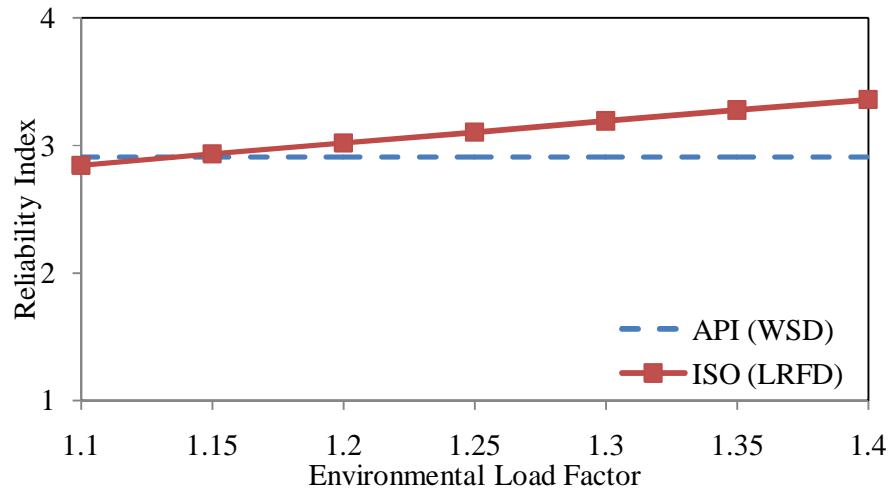


Figure 5.29: Reliability Index Vs Environmental Load Factor for HP at SKO1 Using ISO 19902 and API WSD

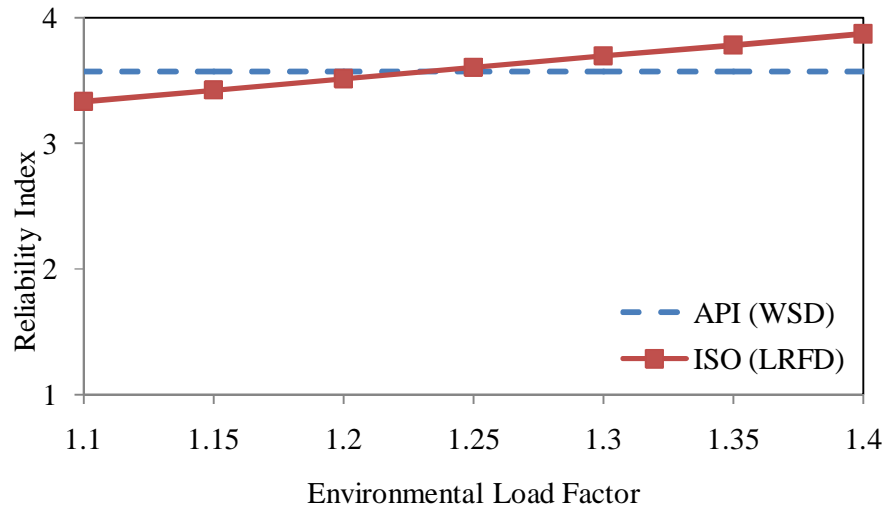


Figure 5.30: Reliability Index Vs Environmental Load Factor for HD at SKO1 Using ISO 19902 and API WSD

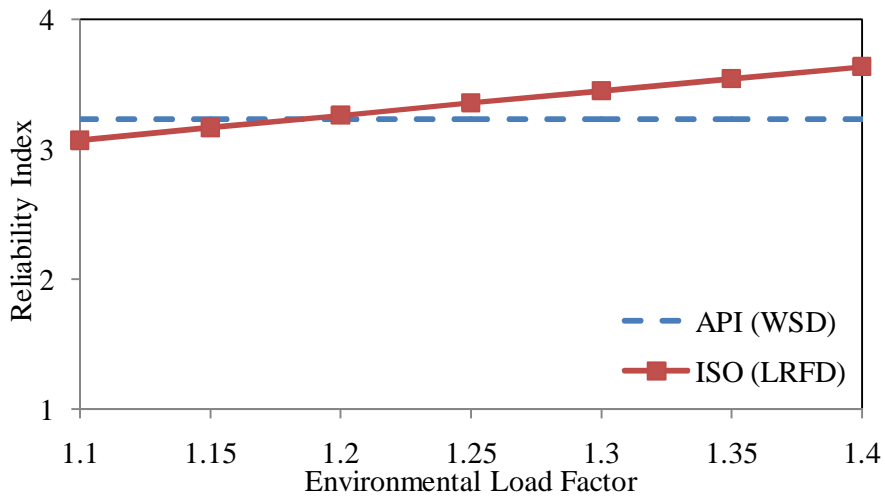


Figure 5.31: Reliability Index Vs Environmental Load Factor for VD at SKO1 Using ISO 19902 and API WSD

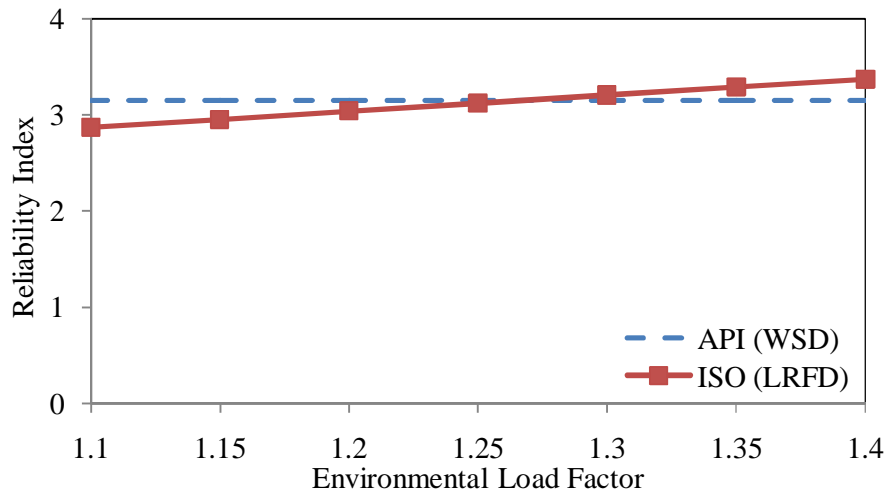


Figure 5.32: Reliability Index Vs Environmental Load Factor for Leg at SKO1 Using ISO 19902 and API WSD

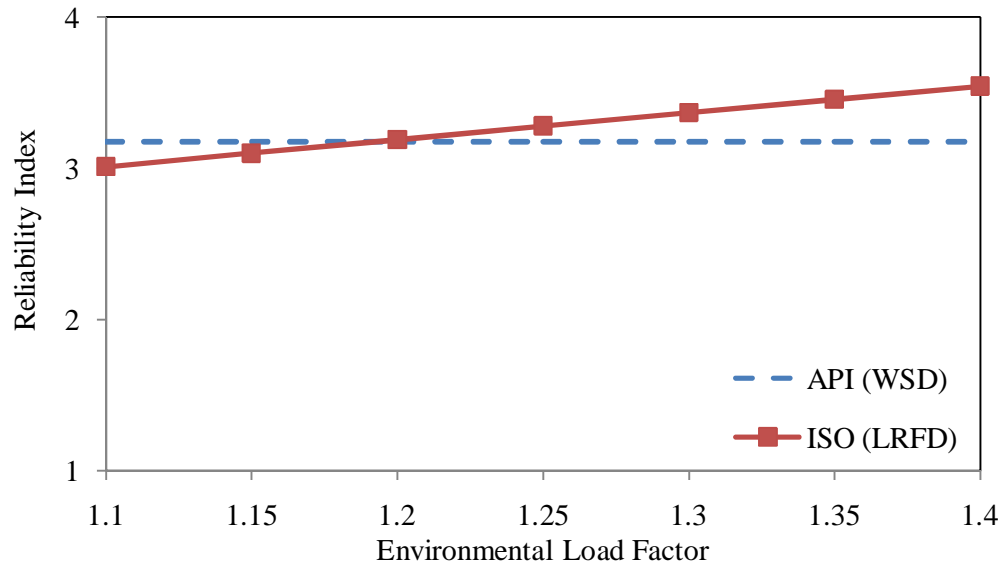


Figure 5.33: Reliability Index Vs Environmental Load Factor for Component at SKO1 Using ISO 19902 and API WSD

For the platform at SKO1, the leg members were highly stressed. The least stressed members were braces at horizontal periphery and vertical diagonals. The target reliability of 3.6 was the highest for horizontal diagonal members.

5.4.9.2 SKO2 Platform

Figure 5.34 - 5.38 show the environmental load factor for SKO2 Jacket, for all four types of components of Jacket were analysed. Figure 5.34 show horizontal periphery brace member with environmental load factor of 1.25. Horizontal diagonal load factor of 1.20 is shown in Figure 5.35. Figure 5.36 show vertical diagonal member with environmental load factor of 1.20 and finally leg members in Figure 5.37 shows a load factor of 1.15. The averaged load factor shown in Figure 5.38 for this Jacket came out to be 1.25. The average target reliability index was 5.08 for this platform. For the platform at SKO2, the horizontal members at periphery and vertical diagonals were highly stressed. The least stressed members were leg members. All members have high target reliability and maximum was found for horizontal members with target reliability of 5.2.

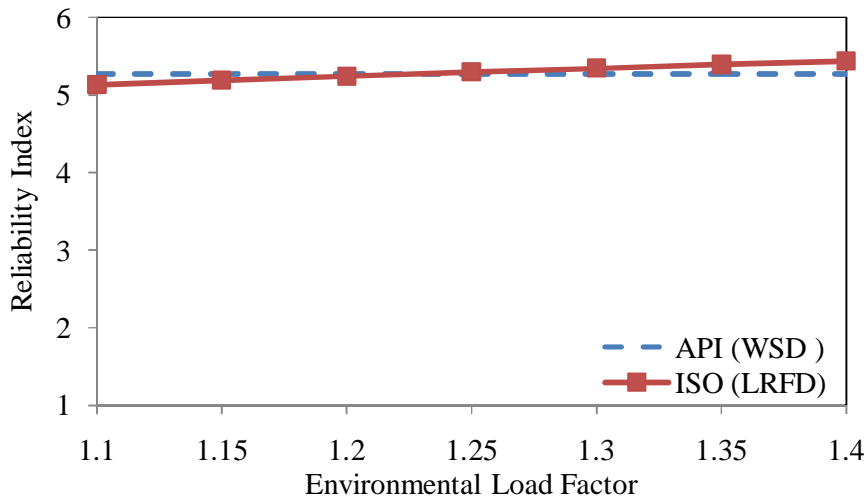


Figure 5.34: Reliability Index Vs Environmental Load Factor for HP at SKO2 Using ISO 19902 and API WSD

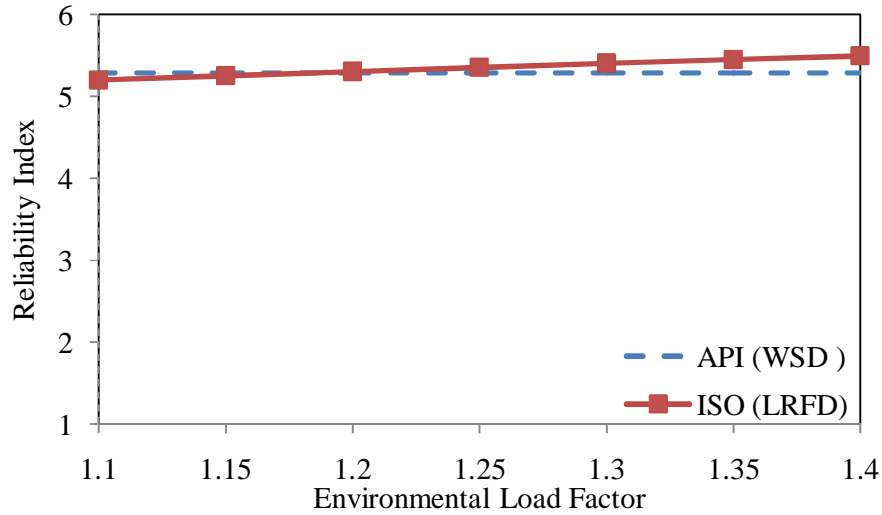


Figure 5.35: Reliability Index Vs Environmental Load Factor for HD at SKO2 Using ISO 19902 and API WSD

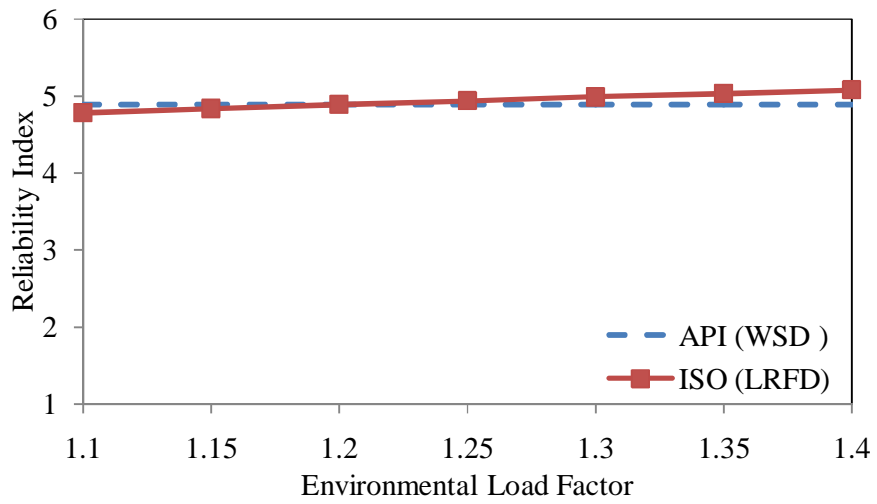


Figure 5.36: Reliability Index Vs Environmental Load Factor for VD at SKO2 Using ISO 19902 and API WSD

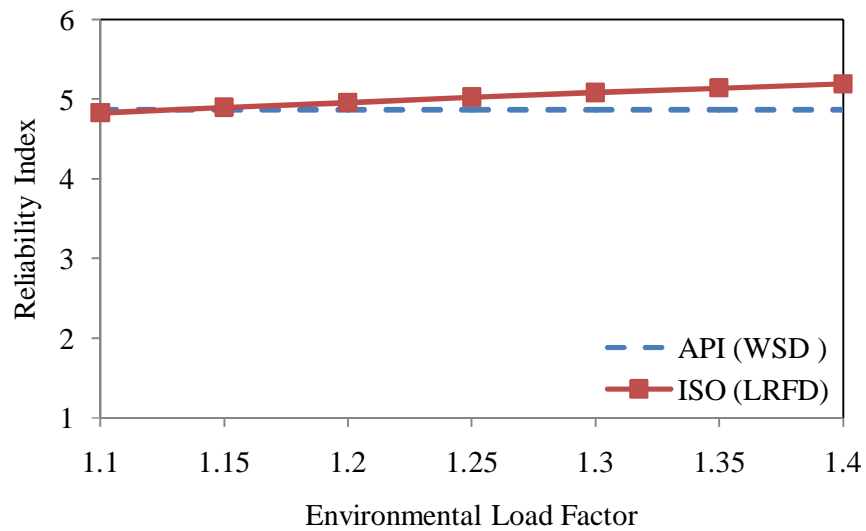


Figure 5.37: Reliability Index Vs Environmental Load Factor for Leg at SKO2 Using ISO 19902 and API WSD

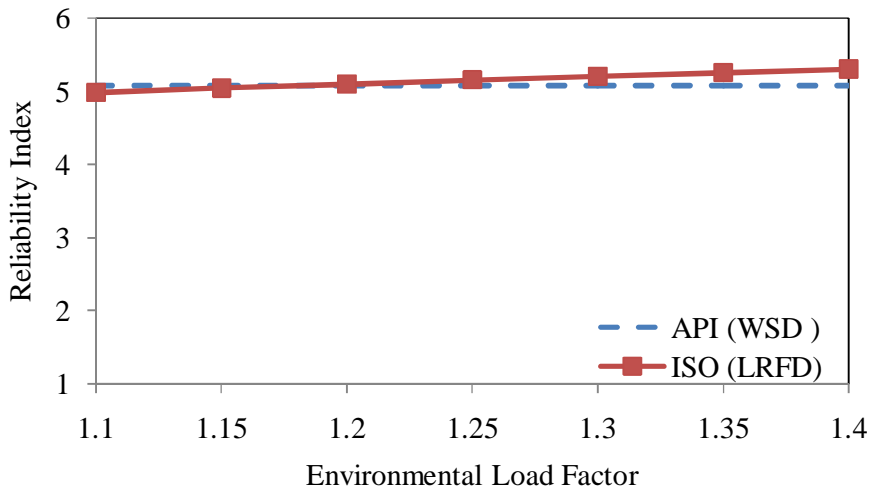


Figure 5.38: Reliability Index Vs Environmental Load Factor for Component at SKO2 Using ISO 19902 and API WSD

5.5 All Regions and all Components Combined Result

When all stress conditions and regions were added and averaged together the environmental load factor for Jacket platform components in Malaysia was 1.25 as shown in Figure 5.39. In Table 1.2 the environmental load factors used in different parts of world has already been shown. This work establishes that the common load factor of 1.35 used by ISO code is on the higher side. Even with reduced load factor reliability of Jacket will be higher as compared to API RP2A WSD code. It is reported that higher the reliability index is, the larger the structural safety margin will be and the more corresponding cost will be and vice versa [165]. Target reliability index used in one study in China was 4.2 [108] and 2.8 also in China from other study [5] but the later uses the Gumbel distribution for environmental load. Table 5.6 shows the target reliability index for Malaysia and reliability index against increasing load factors. These are compared with ISO LRFD code.

Table 5.6: API (WSD) Target Reliability and ISO (LRFD) Reliability

Code		Reliability Index Malaysia	Reliability Index North Sea/GOM [69]
API (WSD)		3.96	3.70
ISO(LRFD)	$\gamma_w=1.10$	3.78	-
	$\gamma_w=1.15$	3.86	-
	$\gamma_w=1.20$	3.95	3.70
	$\gamma_w=1.25$	4.03	3.80
	$\gamma_w=1.30$	4.11	3.88
	$\gamma_w=1.35$	4.19	3.97
	$\gamma_w=1.40$	4.27	4.10

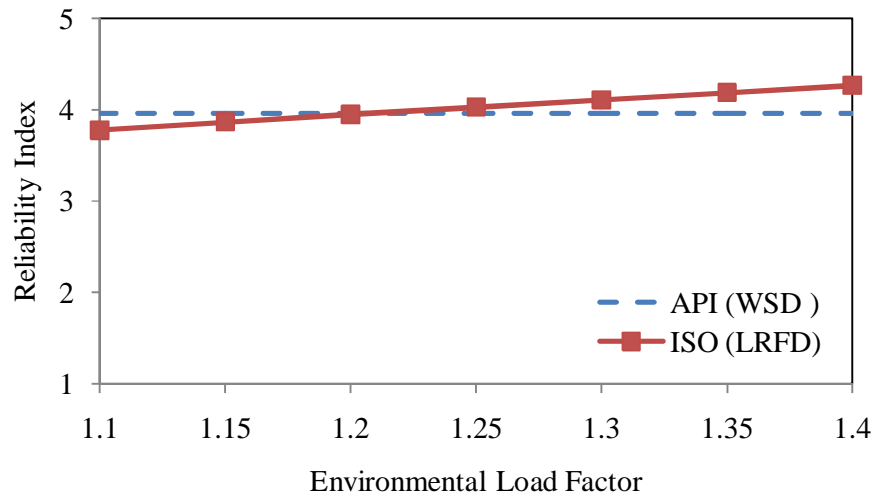


Figure 5.39: Reliability Index Vs Environmental Load Factor for Jacket Platforms in Malaysia at SKO2 Using ISO 19902 and API WSD

5.6 Resistance Factor

The characteristic resistance of tubular members is reduced by the resistance factors. Safety is ensured through common understanding that factored resistance is less than or equal to factored environmental load. Here environmental load factor of 1.25 was used to find the resistance factor of component. Two types of stress conditions were considered here i.e. axial tension and axial compression. The ISO 19902 resistance factors for axial tension and compression are 1.05 and 1.18, which are equal to API RP2A LRFD with a environmental load factor of 1.35 [107].

5.6.1 Axial Tension

The resistance factor for axial tension in ISO code is 1.05. In this study load factor of 1.25 gave equivalent resistance factor of 1.05. Therefore, for axial tension, same resistance factor was suggested to be used for offshore Malaysia as shown in Figure 5.40.

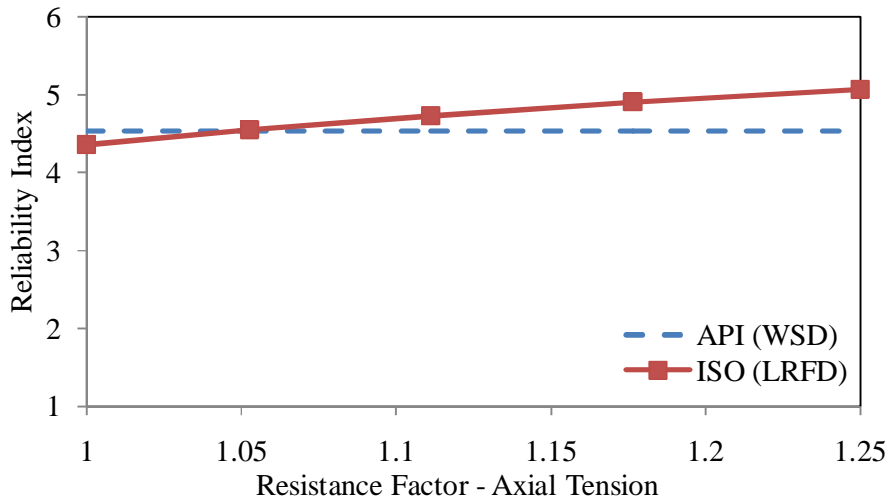


Figure 5.40: Reliability Index Vs Environmental Load Factor for Jacket Platforms in Malaysia Using ISO 19902 and API WSD Axial Tension Resistance Factor for Components

5.6.2 Axial Compression

The resistance factor for axial compression in ISO code is 1.18. In this study load factor of 1.25 gave equivalent resistance factor of 1.18. Therefore, for axial compression, same resistance factor was suggested to be used for offshore Malaysia as shown in Figure 5.41.

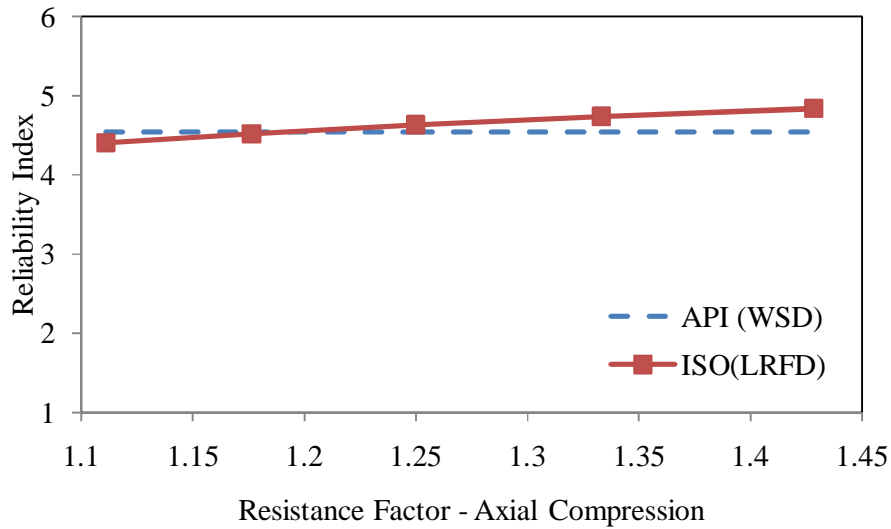


Figure 5.41: Reliability Index Vs Environmental Load Factor for Jacket Platforms in Malaysia at SKO2 Using ISO 19902 and API WSD Axial Compression Resistance Factor for Components

5.7 Chapter Summary

Structural reliability analysis of Jacket platforms provides a rational basis for finding the load and resistance factors for Jacket platforms. The load factor was taken as the value which gives at least similar or higher reliability level as compared to API WSD code. From calibration of both code results it was clear that reliability based ISO LRFD factors can provide uniform safety levels for Jackets in Malaysia. The environmental load factor results obtained are:

- 1) For the platform in PMO region environmental load factor was in range of 1.15 - 1.27. The range of target reliability as per API WSD here was 2.80 to 4.01.
- 2) For the platform in SBO region environmental load factor was in range of 1.23 - 1.27. The range of target reliability as per API WSD here was 2.96 to 6.20.
- 3) For the platform SKO1 in SKO region environmental load factor was in range of 1.15 - 1.26. The range of target reliability as per API WSD here was 2.90 to 3.57.
- 4) For the platform SKO2 in SKO region environmental load factor was in range of 1.14 - 1.24. The range of target reliability as per API WSD here was 4.27 to 5.29.

When above load factors were averaged the outcome was the common environmental load factor for offshore Malaysia was determined to be 1.25. With this modified load factor the resistance factors were checked for the Jacket component. Two cases were considered i.e. axial tension and axial compression. It was found that the resistance factor for axial tension and compression were the same as per ISO 19902 code i.e. 1.05 and 1.18 with new load factor. Thus it can be recommended that with load factor of 1.25 the same resistance factor can be used.

CHAPTER 6

JOINT RELIABILITY ANALYSIS AND ENVIRONMENTAL LOAD FACTOR

6.1 Introduction

To safeguard the structure against uncertainties, safety margins are introduced in design by means of various load and resistance factors. This is due to imprecise knowledge and inherent randomness, in the design parameters. Joint design is an important part for the Jacket platforms. Due to critical nature of joints API and ISO code recommend them to be stronger than components. The joint types are K, T/Y or X joint, they are classified as based on the geometry and loads acting on the member. The joints were analyzed for four types of stresses.

6.2 Selection of Joints

Joints for this study were arranged in groups chosen from the four platforms. They were based on chord diameter and brace diameter ratio, joint types and angle. These different joints were grouped and the representative joints were analysed. Table 6.1 shows selection of joints from one platform.

Table 6.1 Joint Selected for Calibration

Joint Type	Chord diameter (D) mm	Chord Wall thickness (T) mm	Brace diameter (d) mm	Brace Wall thickness (t) mm	Angle (degrees)
K	1854	51	660	19	60
	908	41	604	29	50
T/Y	1880	64	908	41	87
	610	16	610	13	90
X	660	25	660	13	72
	502	22	502	16	83

6.2.1 K- Joints

For axial stresses and in-plane bending ISO LRFD gave higher reliability index values as compared to API WSD. For OPB case it was API WSD which gave higher values. With increase of environmental load the reliability decreased significantly. Figures 6.1-6.3 show the reliability index with respect to increasing W_e/G ratios. The ISO LRFD with a load factor of 1.35 gave higher values of reliability as compared to API WSD. In this study, ISO LRFD (MS) environmental load factor of 1.25 is proposed as shown in Figure 6.55. ISO LRFD was plotted with an environmental load factor of 1.35 as recommended by ISO code. ISO LRFD (MS) stands for this region with a load factor of 1.25. Figures 6.2 - 6.3 shows the proposed reliability values for in-plane and out-plane bending. Table 6.2 show the reliability index for K-joint for one platform. In this study reliability index was found out at environmental load factor of 1.25 and 1.35. Offshore Malaysia values were compared with ISO code values. The environmental load factor of 1.25 gave good results as compared to ISO code values with given target reliability.

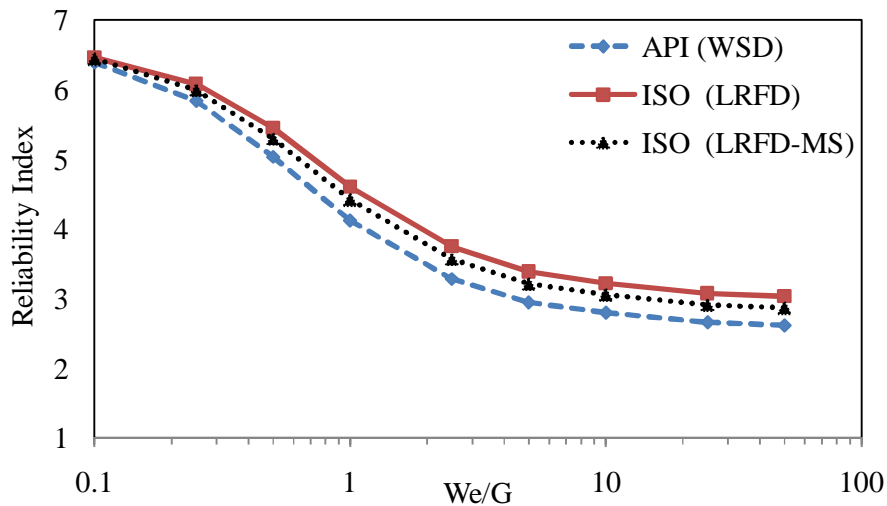


Figure 6.1: Variation of W_e/G ratio Vs Reliability Index for K-Joint-Tension / Compression for API WSD, ISO-MS and ISO LRFD Codes at SKO1

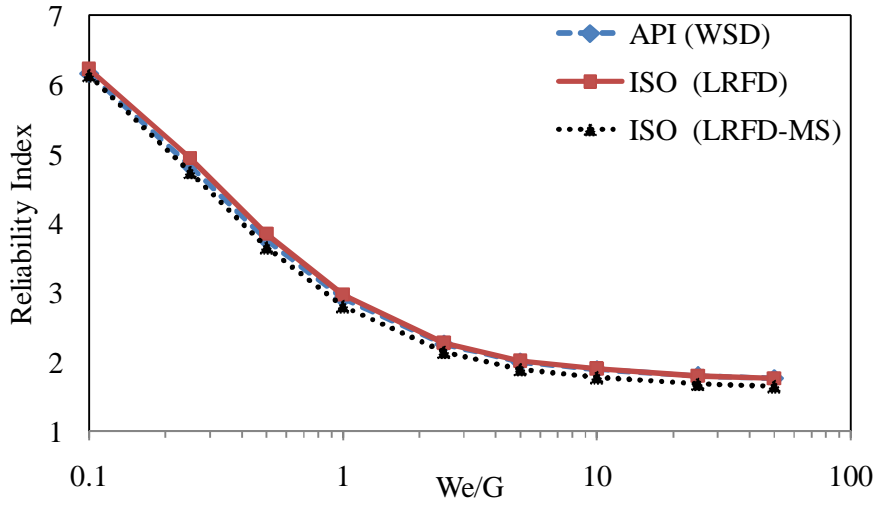


Figure 6.2: Variation of W_e/G ratio Vs Reliability Index for K-Joint- IPB for API WSD, ISO-MS and ISO LRFD Codes at SKO1

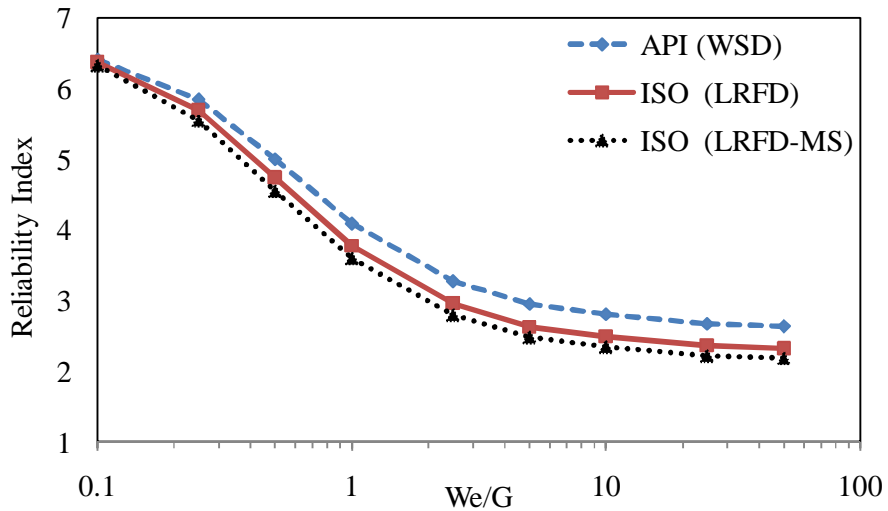


Figure 6.3: Variation of W_e/G ratio Vs Reliability Index for K-Joint- OPB for API WSD, ISO-MS and ISO LRFD Codes at SKO1

Table 6.2: ISO Reliability Index for K- Joints

	Reliability Index MS, $\gamma_w=1.25$	Reliability Index MS, $\gamma_w=1.35$	Reliability Index ISO $\gamma_w=1.35$ [69]
Axial tension	3.98	4.16	3.90
Axial Compression	3.98	4.16	3.90
IPB	2.79	3.01	4.10
OPB	3.03	3.25	3.79
Average	3.45	3.66	3.90

6.2.2 T/Y Joints

For axial stresses and in-plane bending ISO LRFD gave higher reliability index values as compared to API WSD. For OPB case it was API WSD which gave higher values. With increase of environmental load the reliability decreased significantly as shown in Figures 6.4 - 6.7. The ISO LRFD value gave higher values of reliability as compared to API WSD values. This study proposed load factor of 1.25. Table 6.3 shows the reliability index for T/Y-joint for one platform. In this study reliability index was found out at environmental load factor of 1.25 and 1.35. Offshore Malaysia values were compared with ISO LRFD code values. The load factor of 1.25 gave good results as compared to ISO code values.

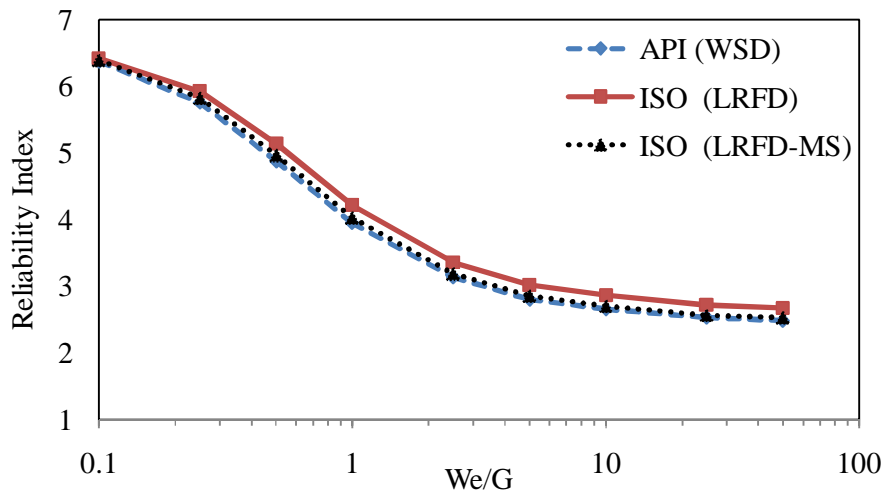


Figure 6.4: Variation of W_e/G ratio Vs Reliability Index for T/Y-Joint in Tension for API WSD, ISO-MS and ISO LRFD Codes at SKO1

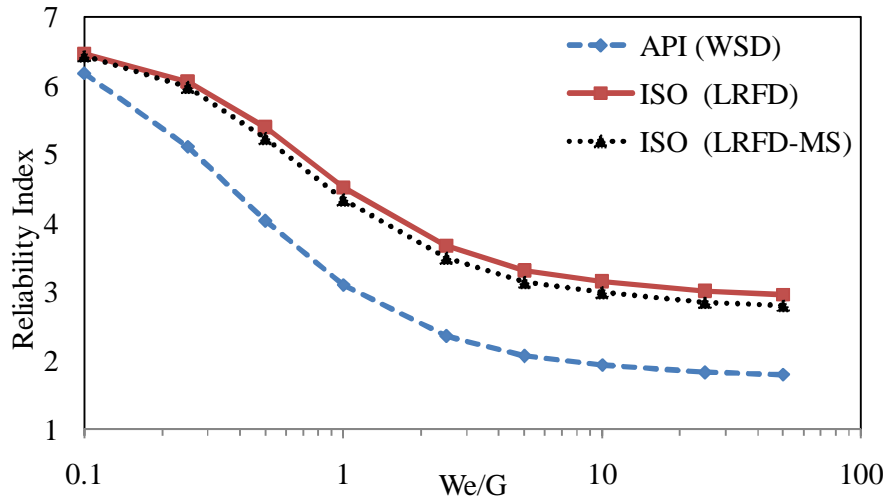


Figure 6.5: Variation of W_e/G ratio Vs Reliability Index for T/Y-Joint in C for API WSD, ISO-MS and ISO LRFD Codes at SKO1

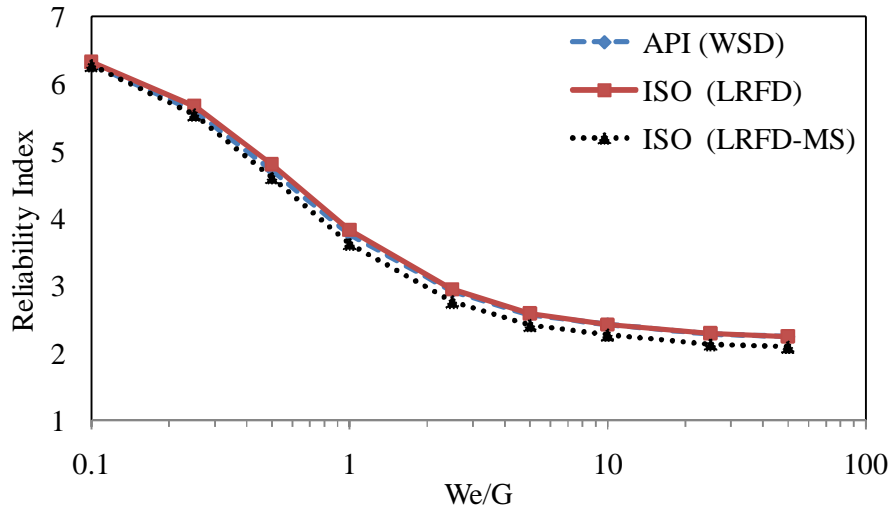


Figure 6.6: Variation of W_e/G ratio Vs Reliability Index for T/Y-Joint in IPB for API WSD, ISO-MS and ISO LRFD Codes at SKO1

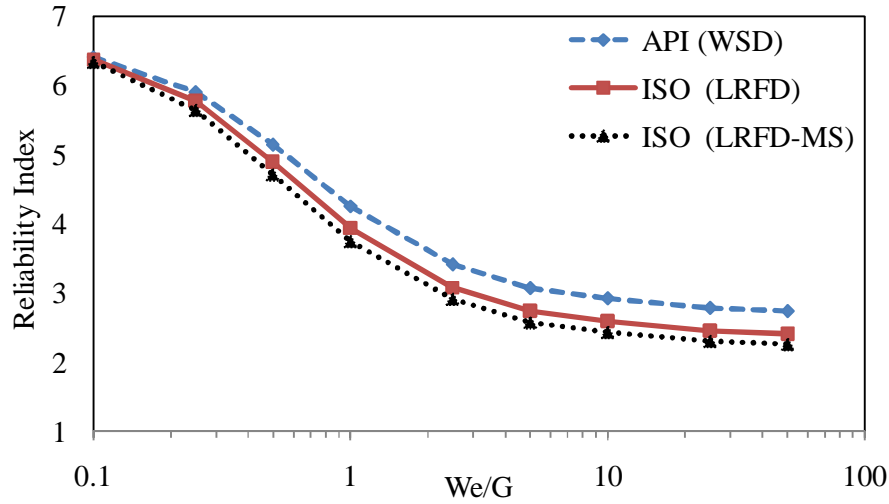


Figure 6.7: Variation of W_e/G ratio Vs Reliability Index for T/Y-Joint in OPB for API WSD, ISO-MS and ISO LRFD Codes at SKO1

Table 6.3: ISO Reliability Index for T/Y- Joints

	Reliability Index MS, $\gamma_w=1.25$	Reliability Index MS, $\gamma_w=1.35$	Reliability Index North Sea $\gamma_w=1.35$ [69]
Axial tension	3.81	4.02	4.13
Axial Compression	3.58	3.78	4.04
IPB	3.37	3.58	4.04
OPB	3.94	4.12	4.11
Average	3.68	3.88	4.06

6.2.3 X- Joints

For axial stresses and IPB, ISO LRFD gave higher reliability index as compared to API WSD. For OPB case it was API which gave higher values. With increase of environmental load the reliability decreased significantly as shown in Figures 6.8 - 6.11. The ISO LRFD gave higher values of reliability as compared to API WSD. This study proposes 1.25 as environmental load factor. Table 6.4 shows the reliability index for X-joint for one platform. In this study reliability index was found at environmental load factor of 1.25 and 1.35. Offshore Malaysia values were compared with ISO code values. The environmental load factor of 1.25 gave good results as compared to ISO code values.

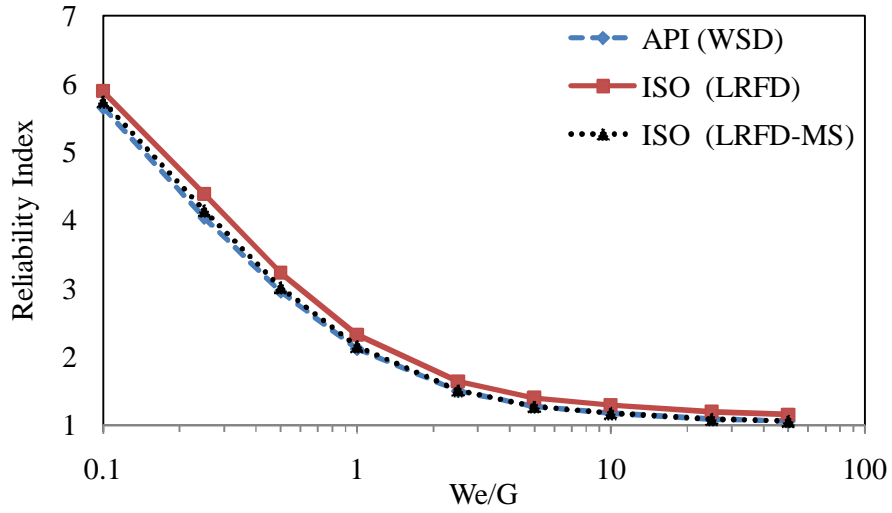


Figure 6.8: Variation of W_e/G ratio Vs Reliability Index for X-Joint in Tension for API WSD, ISO-MS and ISO LRFD Codes at SKO1

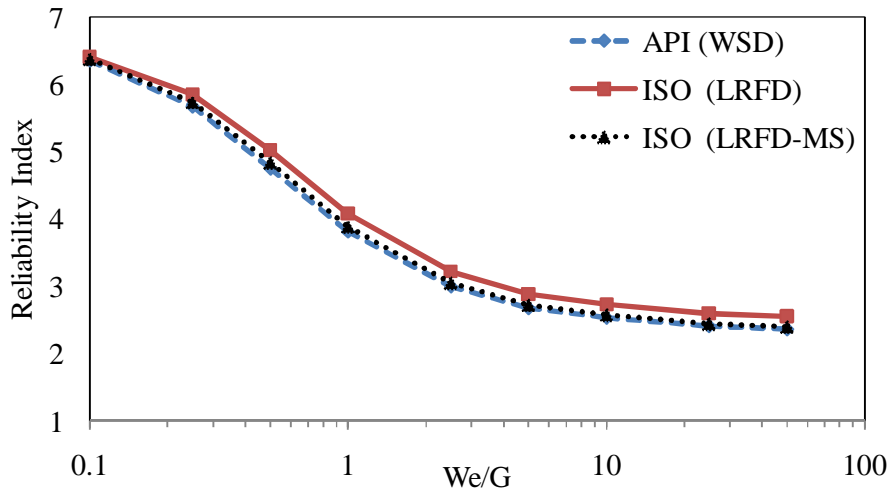


Figure 6.9: Variation of W_e/G ratio Vs Reliability Index for X-Joint in Compression for API WSD, ISO-MS and ISO LRFD Codes at SKO1

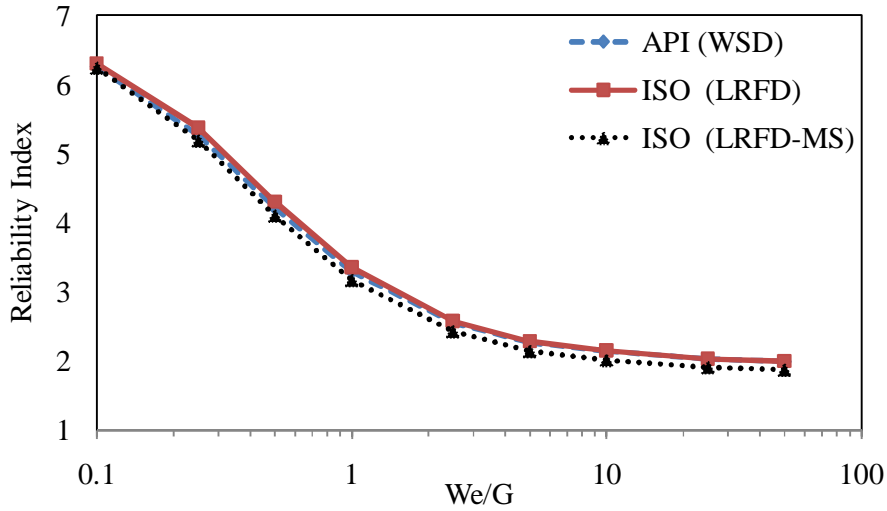


Figure 6.10: W_e Variation of W_e/G ratio Vs Reliability Index for X-Joint in IPB for API WSD, ISO-MS and ISO LRFD Codes at SKO1

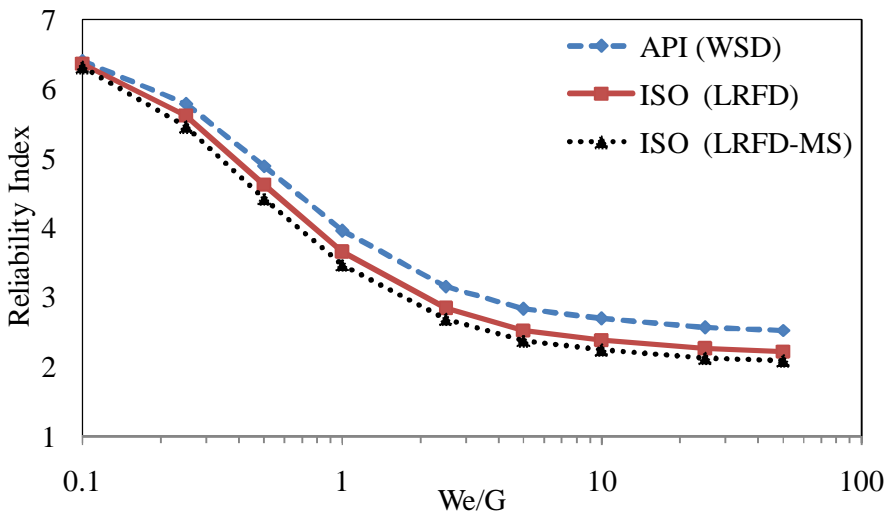


Figure 6.11: Variation of W_e/G ratio Vs Reliability Index for X-Joint in OPB for API WSD, ISO-MS and ISO LRFD Codes at SKO1

Table 6.4: ISO Reliability Index for X- Joints

	Reliability Index MS, $\gamma_w=1.25$	Reliability Index MS, $\gamma_w=1.35$	Reliability Index North Sea $\gamma_w=1.35$ [69]
Axial tension	4.28	4.45	4.07
Axial Compression	4.38	4.52	3.98
IPB	4.61	4.75	4.20
OPB	4.29	4.45	4.00
Average	4.39	4.54	4.03

6.3 Beta Factor (β) Effects (d/D) on Reliability Index

Here brace diameter (d) to chord diameter (D) were varied and all other parameters were made constant, to evaluate the effect of beta factor. The results are shown below:

6.3.1 K- Joints

For ISO LRFD code except OPB stresses gave same reliability index thus the variation has significant effect on OPB Equation only as shown in Figures 6.12 - 6.14. The API WSD code is very sensitive to the beta ratio as the reliability varied much with respect to this ratio. Except in the case of axial stresses (up to β ratio =0.4), the reliability of ISO was higher compared to API WSD code.

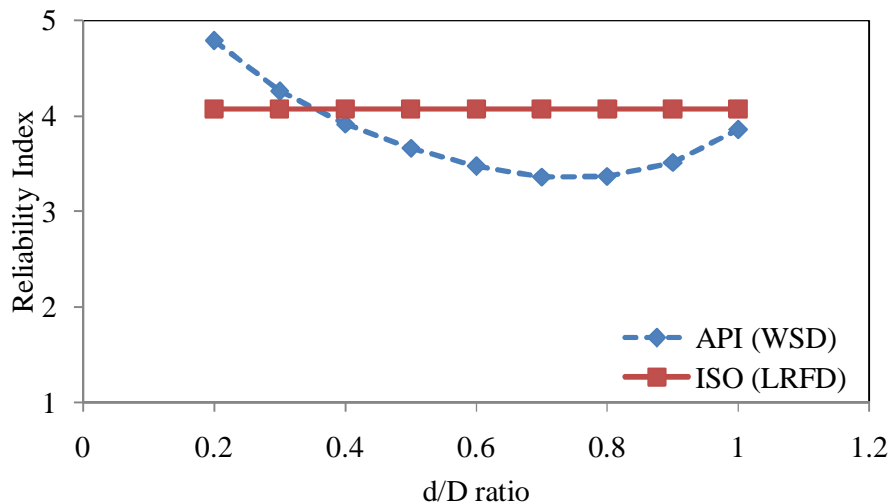


Figure 6.12: Effect of β ratio on Reliability Index, K-Joint in Tension / Compression at SKO1

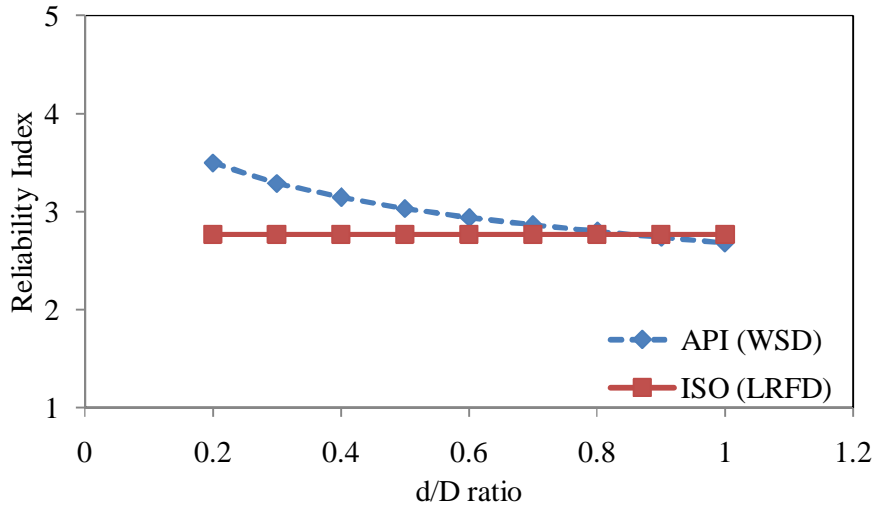


Figure 6.13: Effect of β on Reliability Index of K-Joint in IPB at SKO1

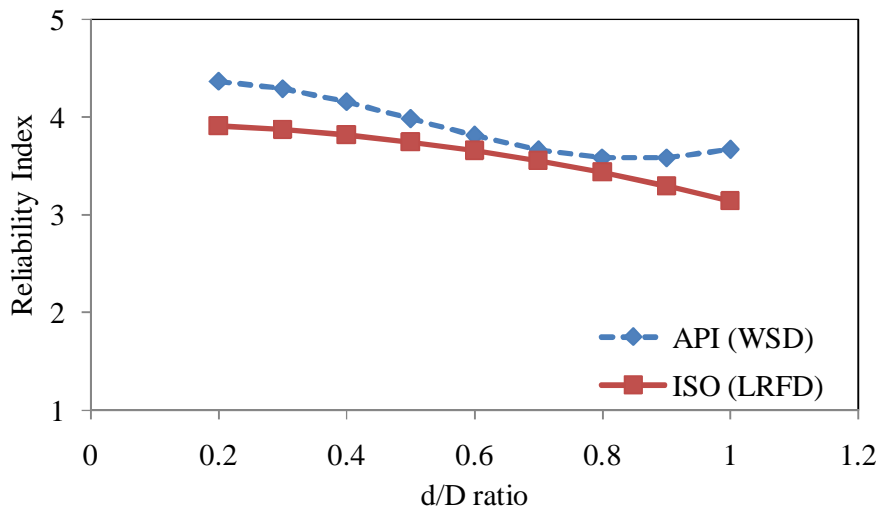


Figure 6.14: Effect of β on reliability index of K-Joint in OPB at SKO1

6.3.2 T/Y Joints

Except OPB, ISO LRFD code was not sensitive to beta ratios and maintained constant reliability as shown in Figures 6.15 - 6.18. For axial stresses alone, ISO LRFD gave higher reliability index always, but when combined with bending, it gave lower values. API WSD was always sensitive to beta ratios except for axial tension case.

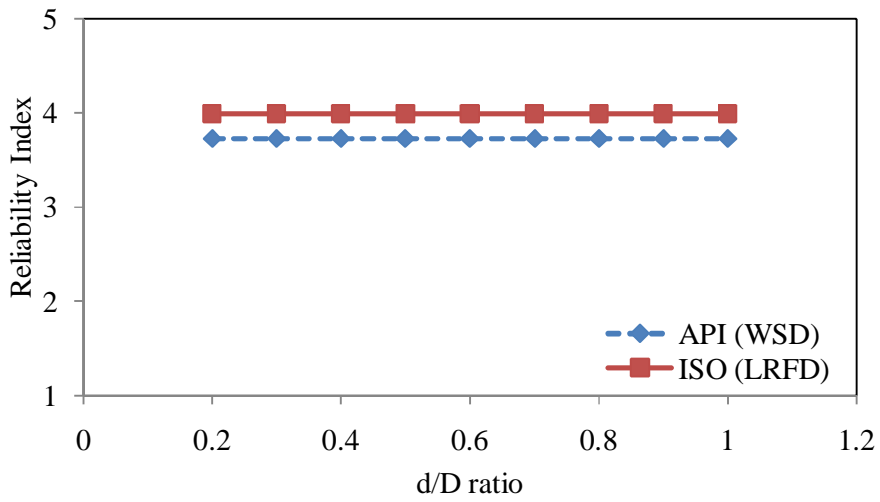


Figure 6.15: Effect of β on Reliability Index of T/Y Joint in Tension at SKO1

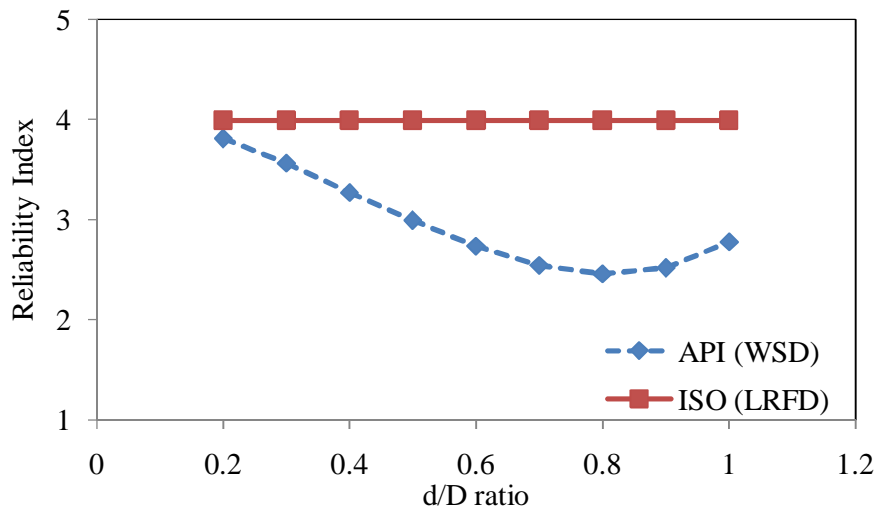


Figure 6.16: Effect of β on Reliability Index of T/Y Joint in Compression at SKO1

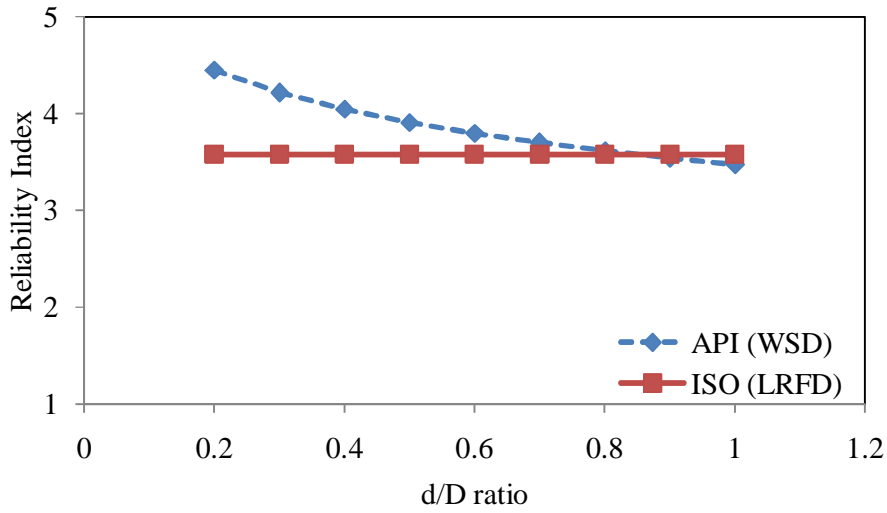


Figure 6.17: Effect of β on Reliability Index of T/Y Joint in IPB at SKO1

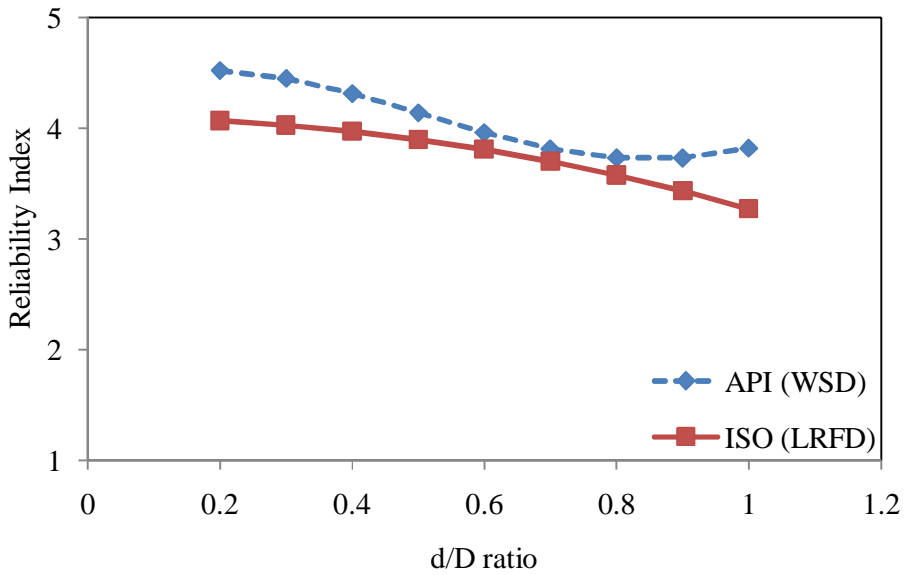


Figure 6.18: Effect of β on Reliability Index of T/Y Joint in OPB at SKO1

6.3.3 X- Joints

Except OPB, ISO LRFD code was not sensitive to beta ratios and maintained constant reliability as shown in Figures 6.19 - 6.22. For axial stresses ISO gave always higher

reliability index but low when bending was involved. API WSD was always sensitive to beta ratios except axial stresses case.

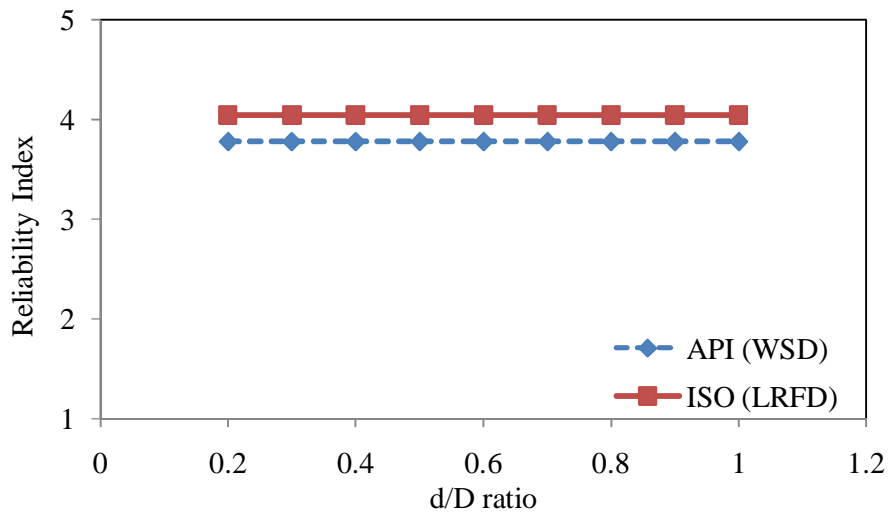


Figure 6.19: Effect of β on Reliability Index of X Joint Tension at SKO1

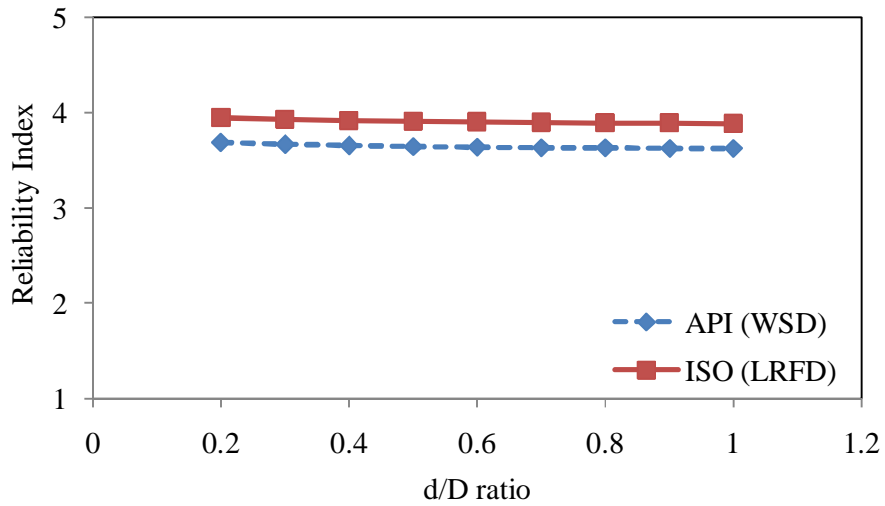


Figure 6.20: Effect of β on Reliability Index of X Joint in Compression at SKO1

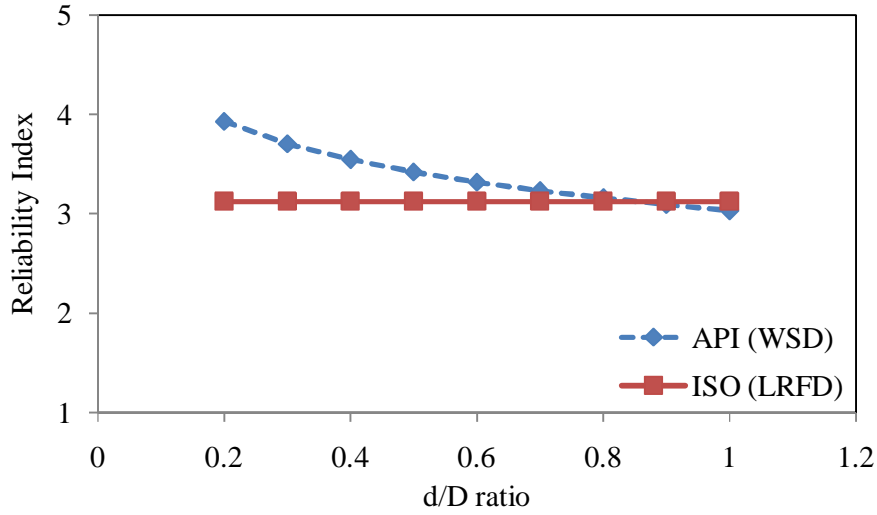


Figure 6.21: Effect of β on Reliability Index of X Joint in IPB at SKO1

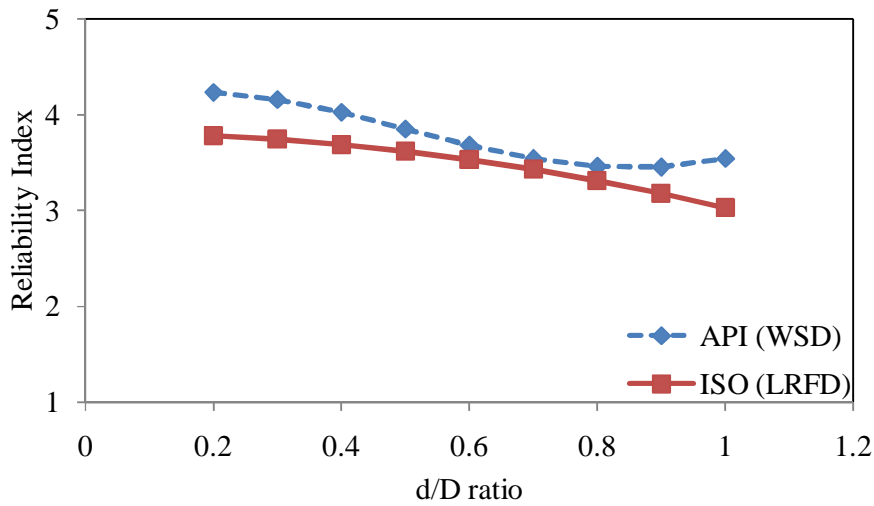


Figure 6.22: Effect of β on Reliability Index of X Joint in OPB at SKO1

6.4 Gamma Factor (γ) Effects (D/2T)

The variation of Gamma factor (D/2T) was checked to find its effect on reliability analysis.

6.4.1 K- Joints: Tension / Compression

Figures 6.23 - 6.25 shows the variability of gamma effect on reliability. It can be seen that ISO LRFD code maintains almost constant reliability except in the case of OPB where it gave minor variability. Thus ISO LRFD is not sensitive to gamma ratios. The API WSD code shows large variability for all three stresses and thus it can be concluded that it has sensitiveness to the gamma ratio. ISO LRFD code shows higher reliability except for OPB stresses.

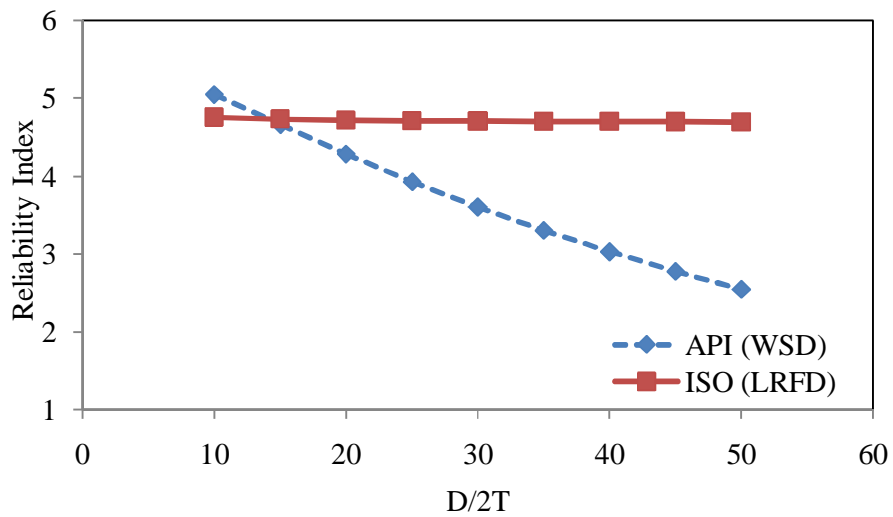


Figure 6.23: Effect of γ on Reliability Index, K Joint Tension and Compression at SKO1

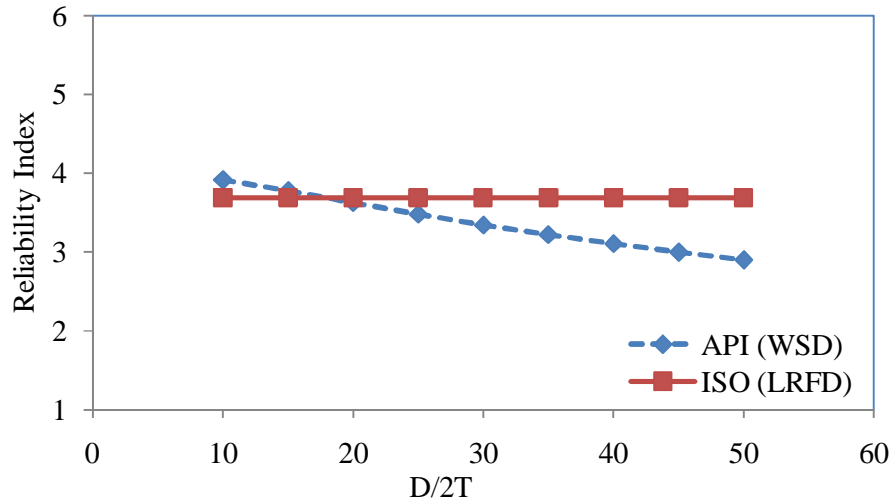


Figure 6.24: Effect of γ on Reliability Index of K Joint in IPB at SKO1

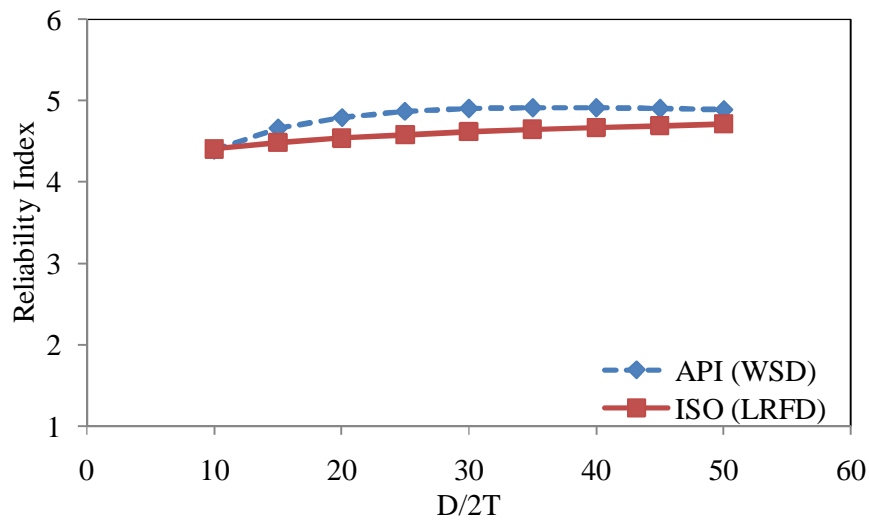


Figure 6.25: Effect of γ on Reliability Index of K Joint in OPB at SKO1

6.4.2 T/Y Joints

The gamma effect on ISO LRFD code was again not susceptible to changes in gamma ratio except the case of OPB as shown in Figures 6.26 - 6.29. The API WSD code shows its sensitiveness to the gamma factor except for axial tension. ISO LRFD code shows higher reliability except for OPB stresses.

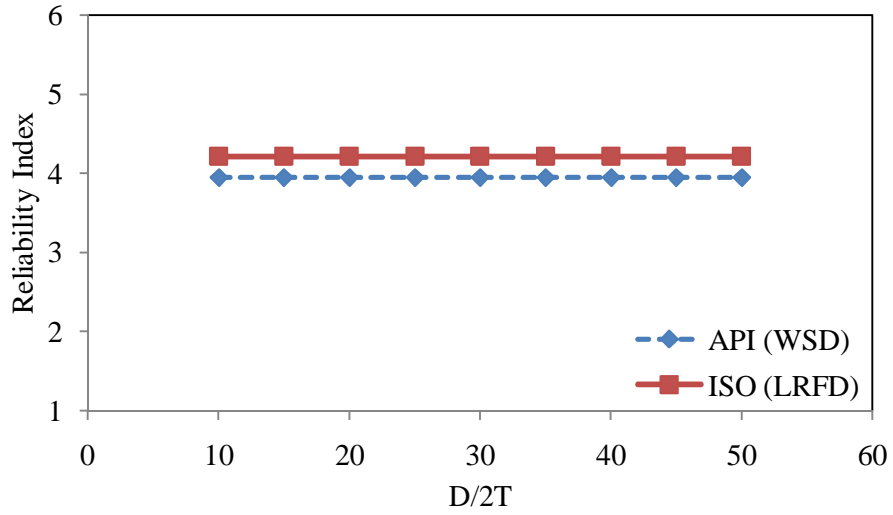


Figure 6.26: Effect of γ on Reliability Index of T/Y Joint in Tension at SKO1

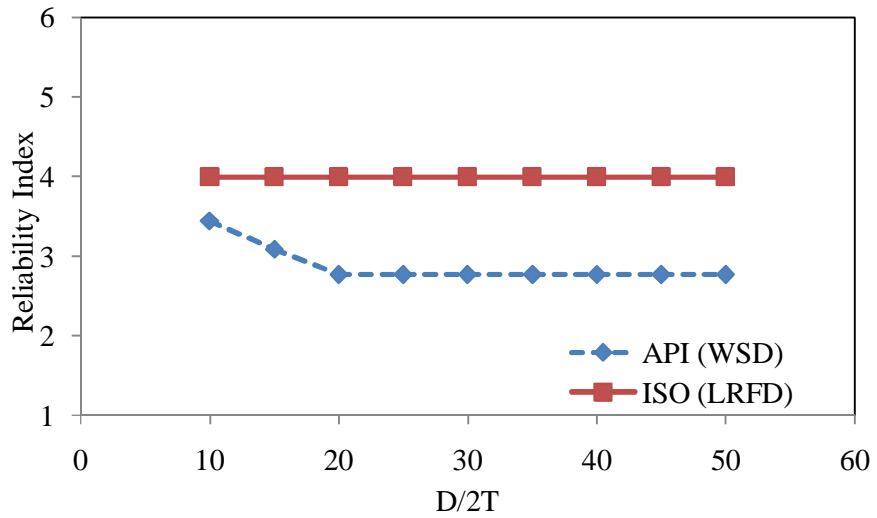


Figure 6.27: Effect of γ on Reliability Index of T/Y Joint in Compression at SKO1

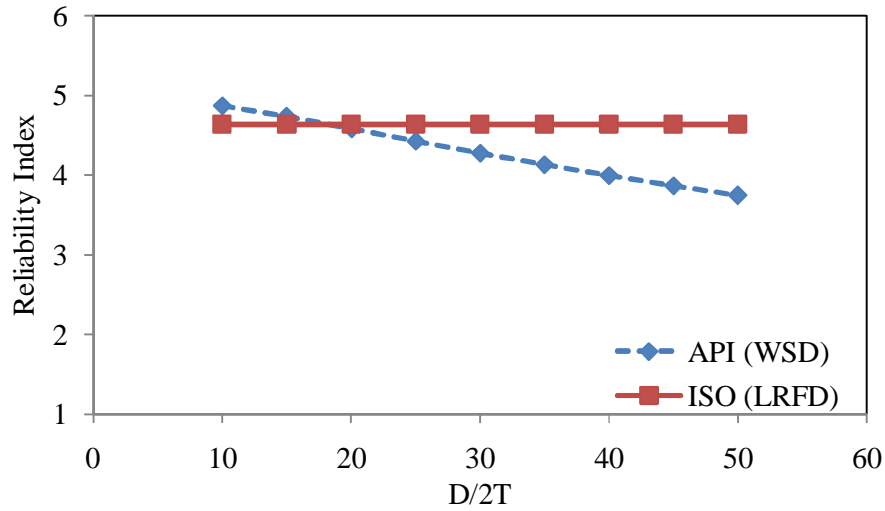


Figure 6.28: Effect of γ on Reliability Index of T/Y Joint in IPB at SKO1

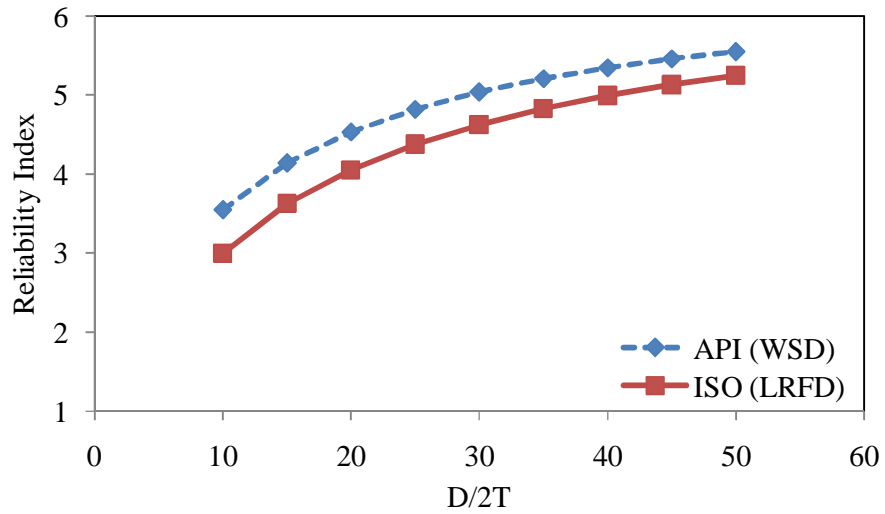


Figure 6.29: Effect of γ on Reliability Index of T/Y Joint in OPB at SKO1

6.4.3 X- Joints

Here both codes show sensitiveness in case of IPB and OPB, otherwise they maintained constant reliability as shown in Figures 6.30 - 6.33. In all cases, ISO shows higher reliability except in the case of OPB stresses.

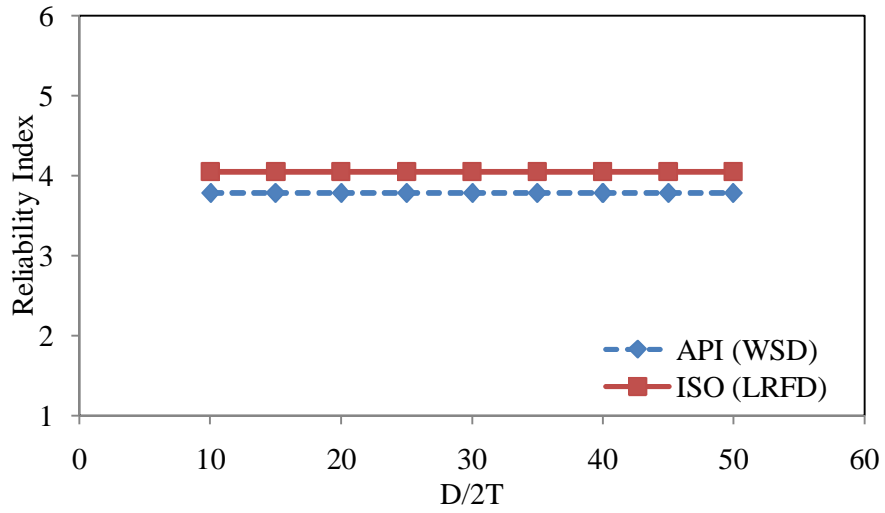


Figure 6.30: Effect of γ on Reliability Index of X Joint in Tension at SKO1

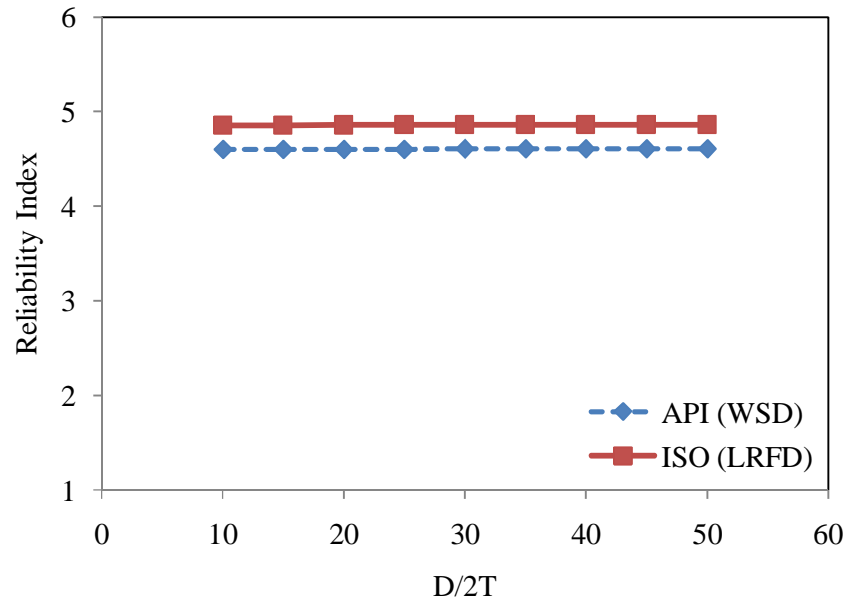


Figure 6.31: Effect of γ on Reliability Index of X Joint in Compression at SKO1

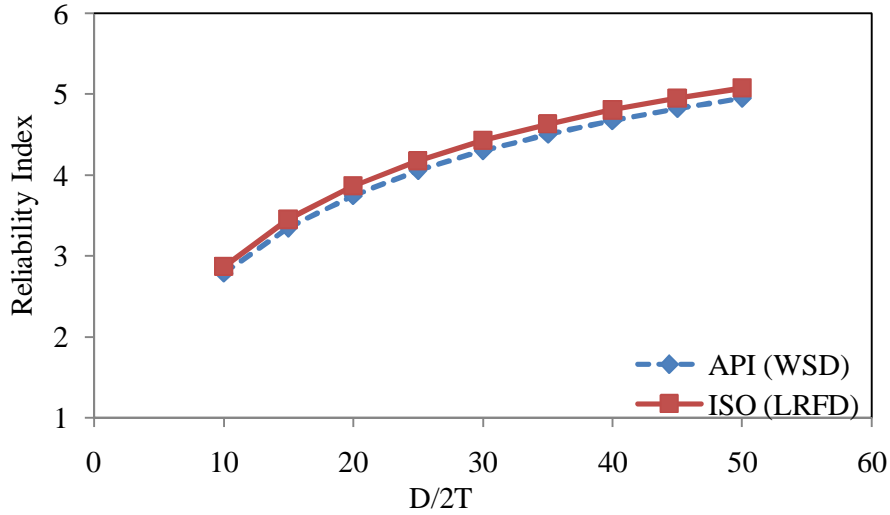


Figure 6.32: Effect of γ on Reliability Index of X Joint in IPB at SKO1

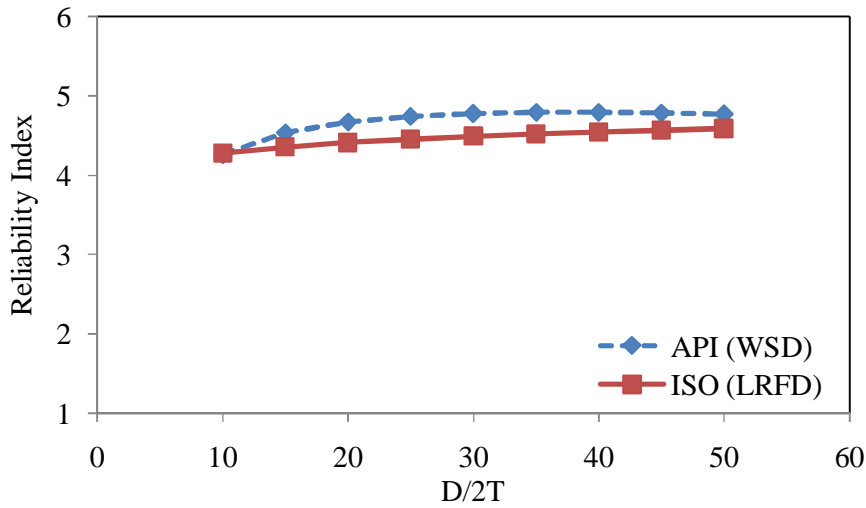


Figure 6.33: Effect of γ on Reliability Index of X Joint in OPB at SKO1

6.5 Variation of Environmental Load Factor

Figures 6.34 - 6.36 show environmental load variation for K, T/Y and X joints. There is large variation with respect to We/G ratios. When dead load ratio governs, it gives higher reliability index as compared to the case when environmental load ratio is governing. The reliability continued to decrease with increase of environmental load factors as was observed by [69]. The same effects were observed during as component reliability analysis.

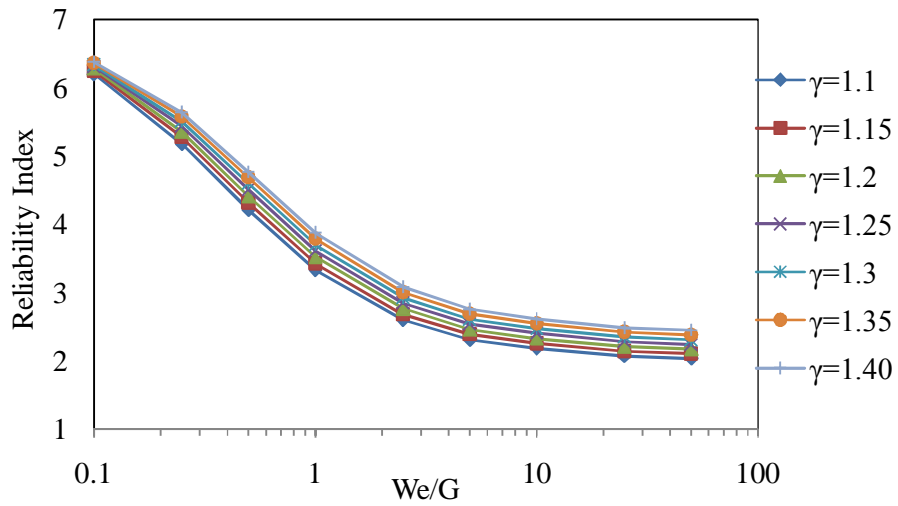


Figure 6.34: Variation of Reliability Index Vs W_e/G for K Joint Using ISO code for Different Values of Environmental Load Factor (γ)

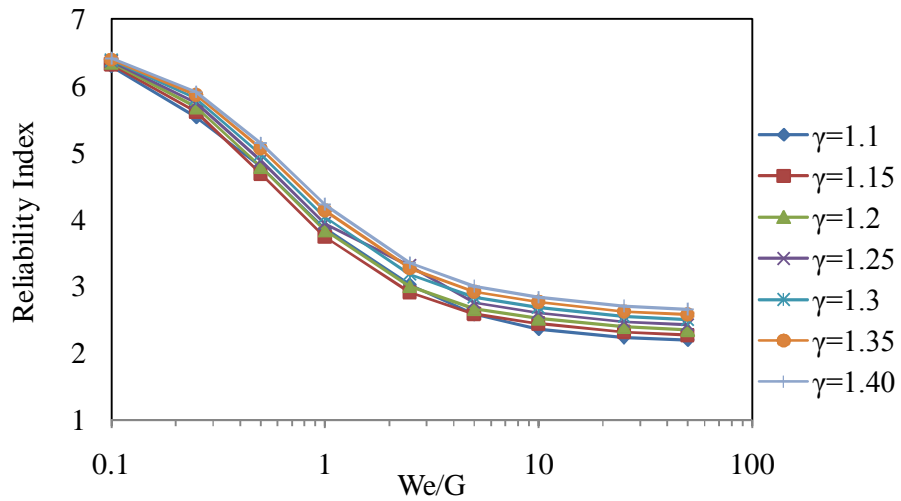


Figure 6.35: Variation of Reliability Index Vs W_e/G for T/Y Joint Using ISO code for Different Values of Environmental Load Factor (γ)

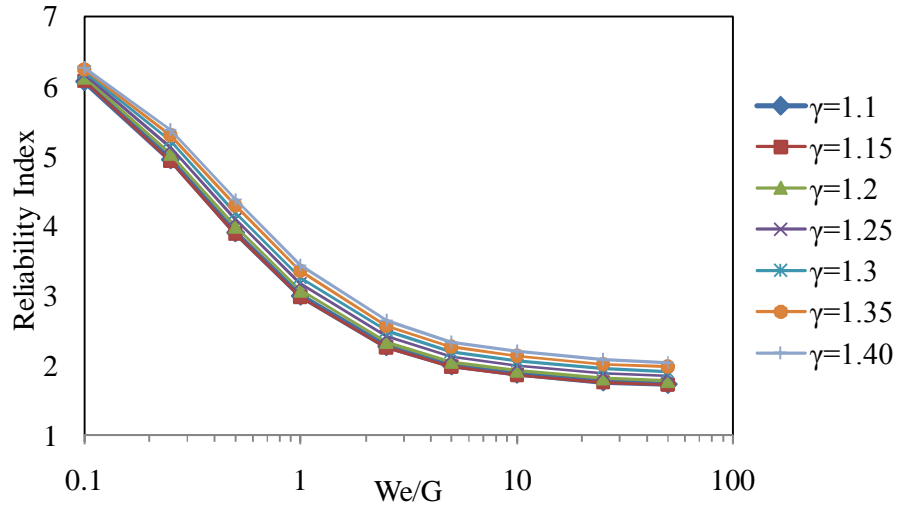


Figure 6.36: Variation of Reliability Index Vs W_e/G for X Joint Using ISO code for Different Values of Environmental Load Factor (γ)

6.6 Calibration of API (WSD) and ISO (LRFD) Reliability Index

To evaluate the effects of both codes on reliability analysis of joints the calibration points in ISO LRFD and API WSD codes were evaluated, as shown in Table 6.5 - 6.6. It was seen that both codes give results which are consistent and not much dispersion was observed. The calibration of reliability index for IPB and OPB in Figures 6.37 - 6.38 showed that the ISO (LRFD) has less variance as compared to API (WSD).

Table 6.5: Joints Reliability Index Under Stresses - ISO 19902 Code [69]

ISO				
	K- Joints	T- Joints	X- Joints	Average
Compression	4.60	4.52	4.08	4.40
Tension	4.60	4.22	2.32	3.71
IPB	2.97	3.83	3.35	3.38
OPB	3.78	3.94	3.66	3.79
Average	3.99	4.13	3.35	3.82

Table 6.6: Joints Reliability Index Under Stresses - API RP2A WSD Code [69]

API WSD				
	K- Joints	T- Joints	X- Joints	Average
Compression	4.12	3.10	3.81	3.68
Tension	4.12	3.95	2.12	3.40
IPB	2.92	3.76	3.29	3.32
OPB	4.09	4.25	3.96	4.10
Average	3.81	3.77	3.30	3.63

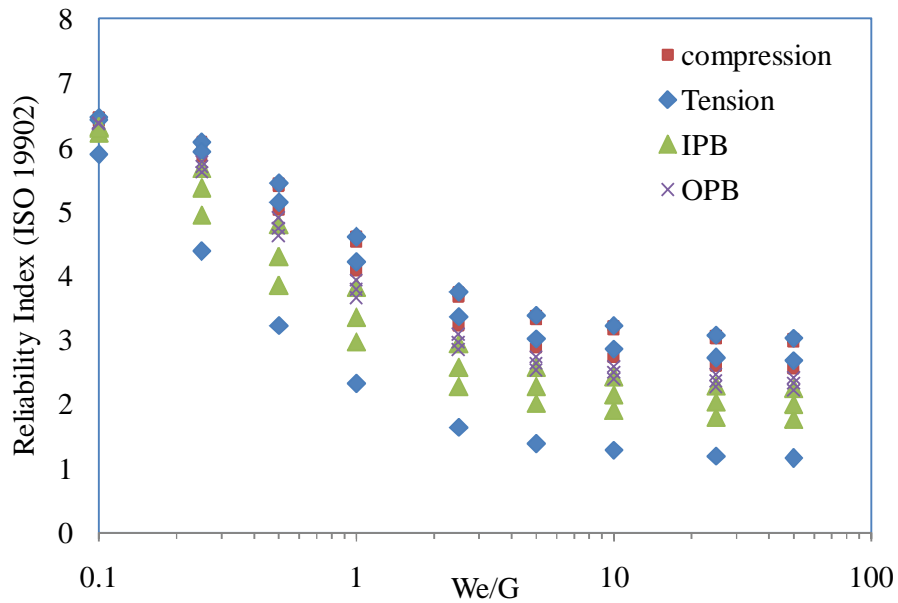


Figure 6.37: Calibration of Jacket Joint Under ISO for all Types of Model Stresses with W_e/G ratios Vs ISO Reliability Indices

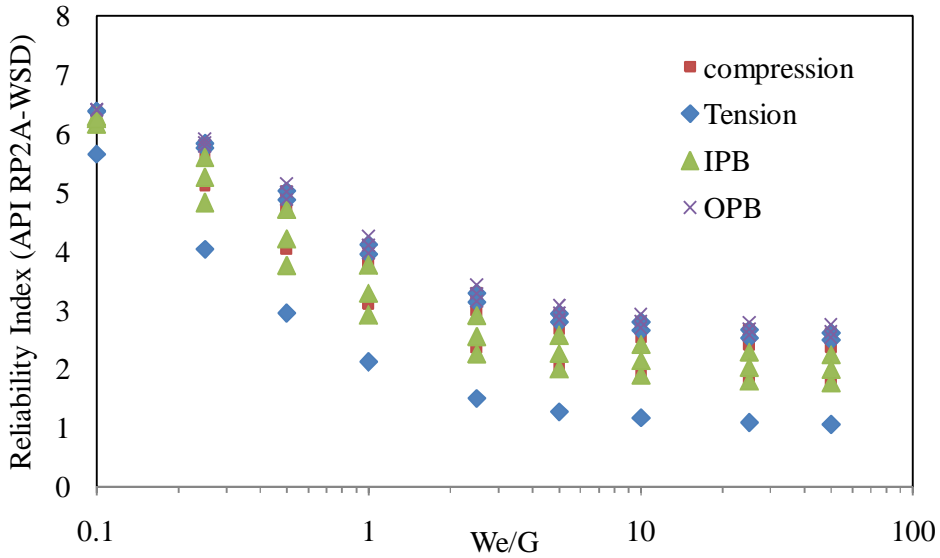


Figure 6.38: Calibration of Jacket Joint Under API WSD for all Types of Model Stresses with W_e/G ratios Vs API WSD Reliability Indices

6.7 Environmental Load Factor

The target reliabilities for Jacket platforms in Malaysia are based on calibration of API (WSD). Environmental load was calibrated so that the one near to target reliability was recommended for future platforms in Malaysia. For GOM and Mediterranean Sea, the load factors and reliability index are shown in Figures 2.8 and 2.9. The environmental load factor for joint of three regions were derived and presented in following sections.

6.7.1 PMO Region Platform

Figures 6.39 - 6.42 show the environmental load factors for the PMO region Jacket, for all three types of joints of Jacket. Figure 6.39 show the load factor for K-joint as 1.30. T/Y joints load factor of 1.20 is shown in Figure 6.40. Figure 6.41 show X-joint load factor of 1.30. The averaged load factor for this region, shown in Figure 6.42 was 1.25. The target reliability was 3.92 for PMO region.

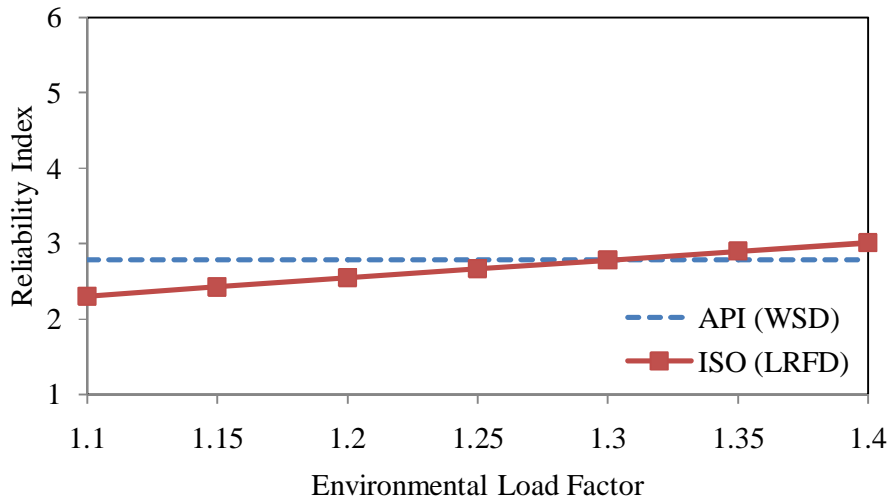


Figure 6.39: Reliability Index Vs Environmental Load Factor for K Joint at PMO Using ISO 19902 and API WSD

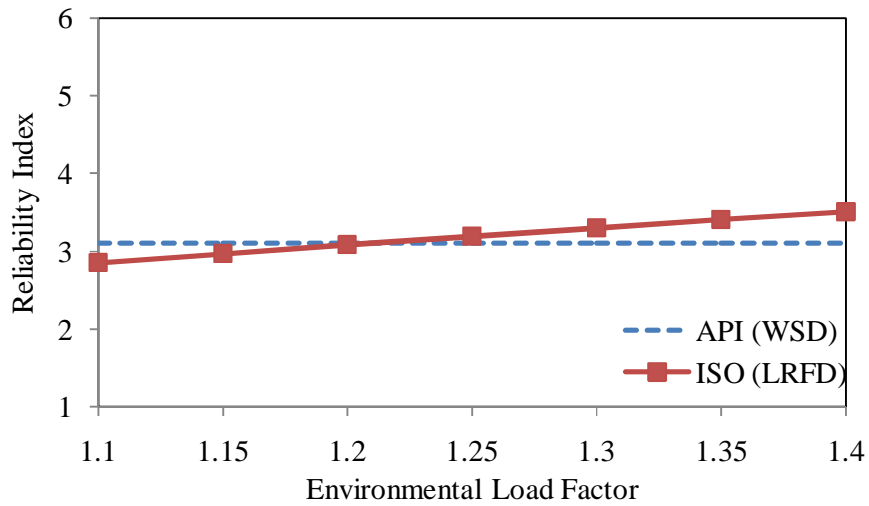


Figure 6.40: Reliability Index Vs Environmental Load Factor for T/Y Joint at PMO Using ISO 19902 and API WSD

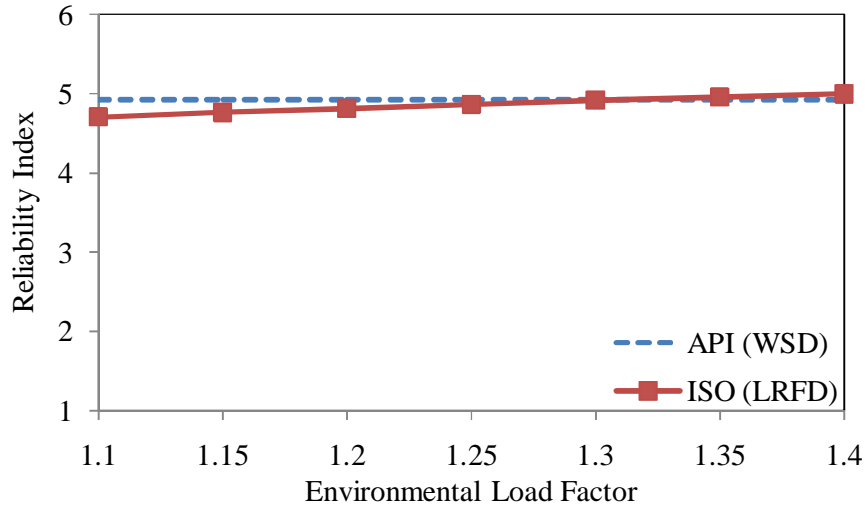


Figure 6.41: Reliability Index Vs Environmental Load Factor for X Joint at PMO Using ISO 19902 and API WSD

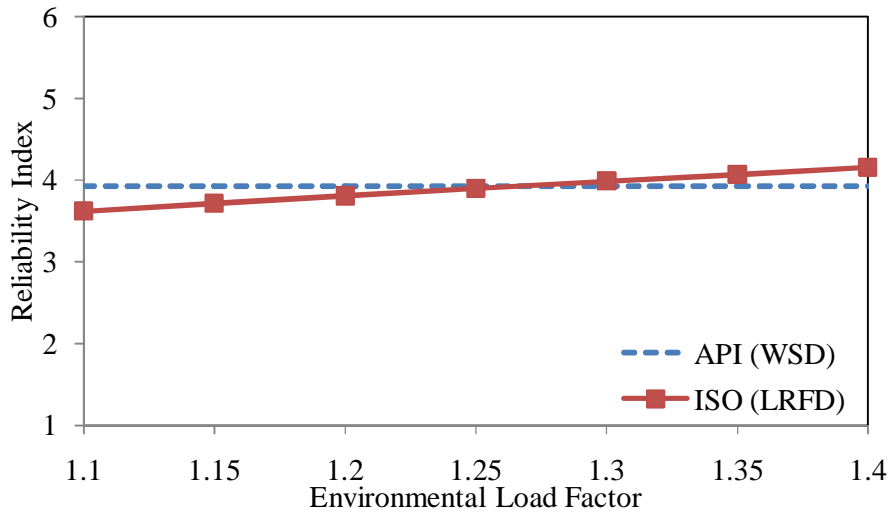


Figure 6.42: Reliability Index Vs Environmental Load Factor for All Joints at PMO Using ISO 19902 and API WSD

In PMO region, it can be seen that X and K joint were most stressed. The target reliability of for X joint was 4.95, the highest among other types. Nowadays, the codes prefer X joints for Jackets due to ductility. This shows that the platform designed was using maximum capacity of this joint.

6.7.2 SBO Region Platform

Figures 6.43 - 6.46 show the environmental load factor for the SBO region Jacket, for all three types of joints of Jacket. Figure 6.43 shows the load factor for K-joint as 1.25. T/Y joints load factor of 1.25 is shown in Figure 6.44. Figure 6.45 shows X-joint load factor of 1.35. The averaged load factor for this region shown in Figure 6.46 was 1.25. The target reliability index was 3.11 for SBO region. In SBO region, it can be seen that X joints were the most stressed. The target reliability for X joint was 3.05 and for K-joint it was 3.4. It was highest target reliability among other types of joints at this platform.

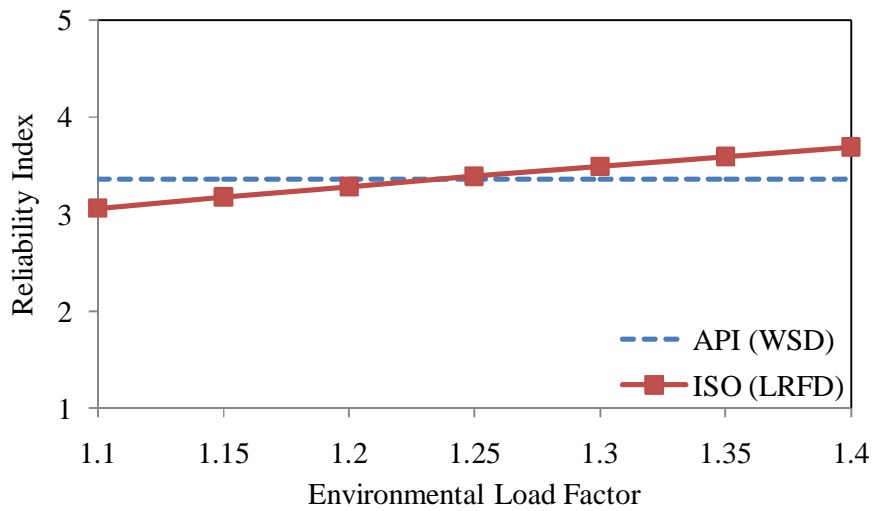


Figure 6.43: Reliability Index Vs Environmental Load Factor for K Joint at SBO Using ISO 19902 and API WSD

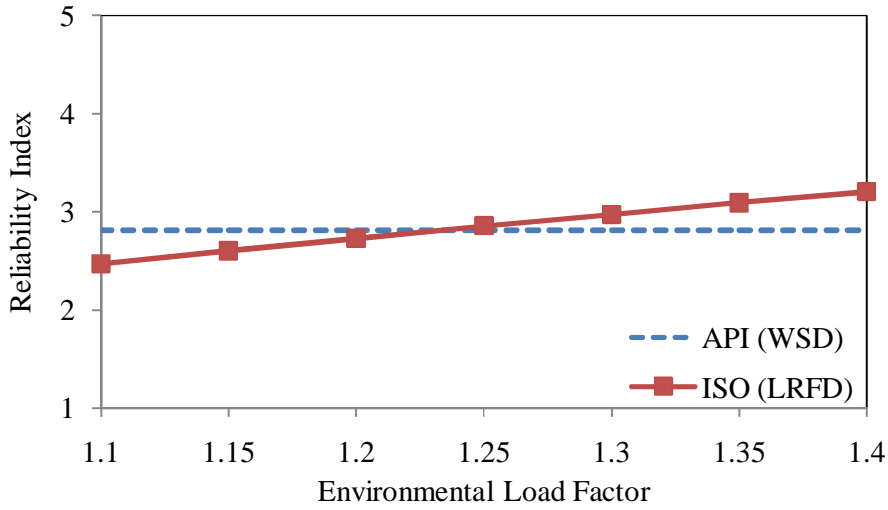


Figure 6.44: Reliability Index Vs Environmental Load Factor for T/Y Joint at SBO Using ISO 19902 and API WSD

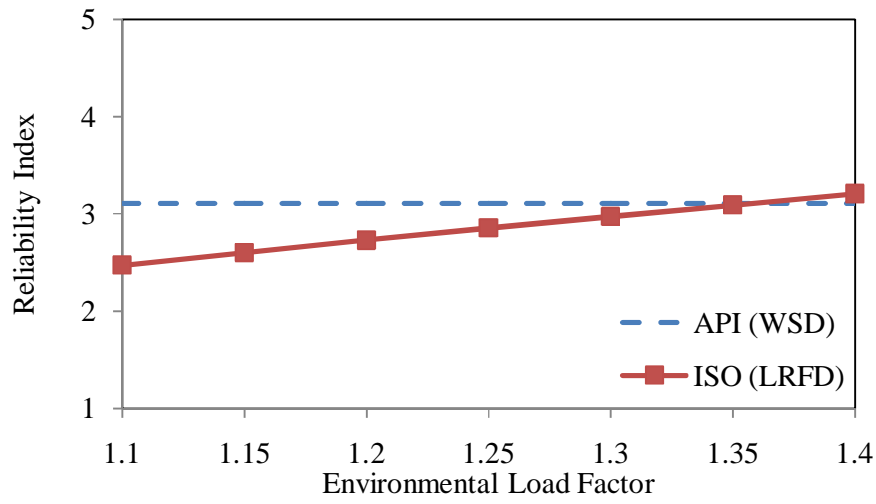


Figure 6.45: Reliability Index Vs Environmental Load Factor for X Joint at SBO Using ISO 19902 and API WSD

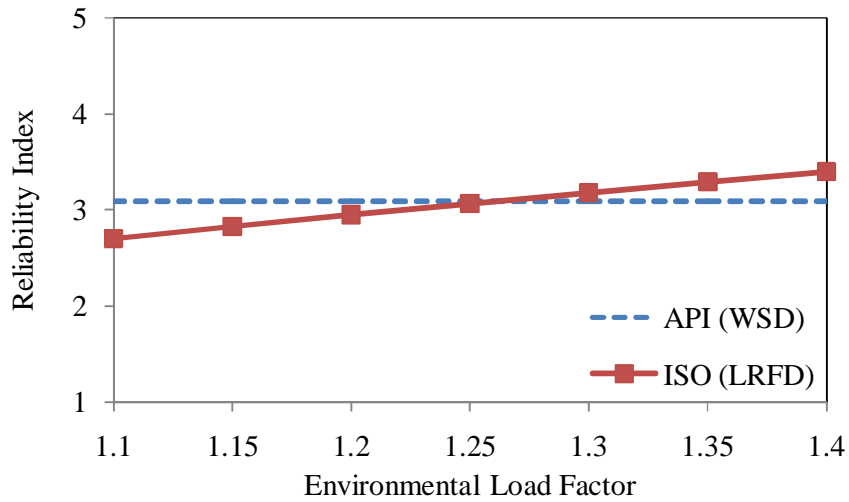


Figure 6.46: Reliability Index Vs Environmental Load Factor for All Joints at SBO Using ISO 19902 and API WSD

6.7.3 SKO Region

From SKO region, two Jackets were selected for analysis and results are produced below:

6.7.3.1 SKO1 Platform

Figure 6.47 - 6.50 shows the environmental load factor for the SKO region with SKO1 Jacket, for all three types of joints of Jacket. Figure 6.47 shows the load factor for K- joint as 1.25. T/Y- joints load factor of 1.20 is shown in Figure 6.48. Figure 6.49 shows X- joint load factor of 1.30. Averaged load factor for this region shown in Figure 6.50 is 1.25. The target reliability index was 3.64 for this platform in SKO region. In SKO1 region, it can be seen that again, X- joints were the most stressed and its target reliability was 3.40. For K- joint, target reliability was 3.95, the highest among other types at this platform.

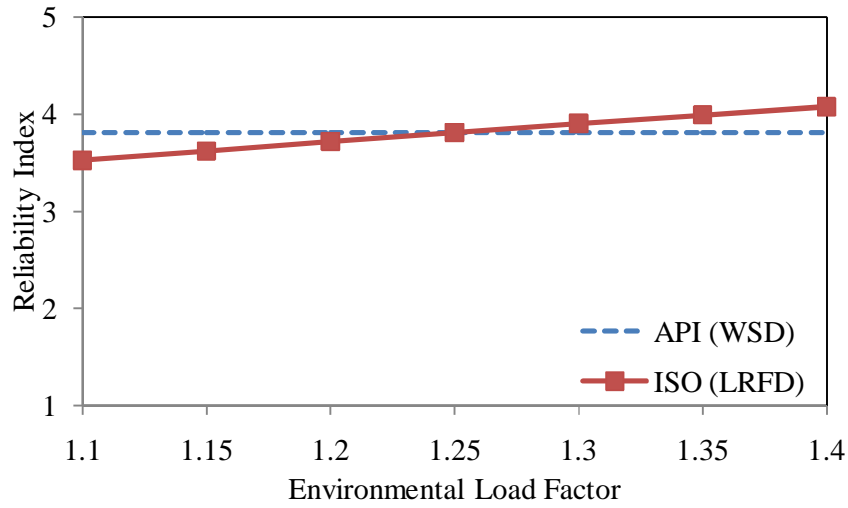


Figure 6.47: Reliability Index Vs Environmental Load Factor for K Joint at SKO1 Using ISO 19902 and API WSD

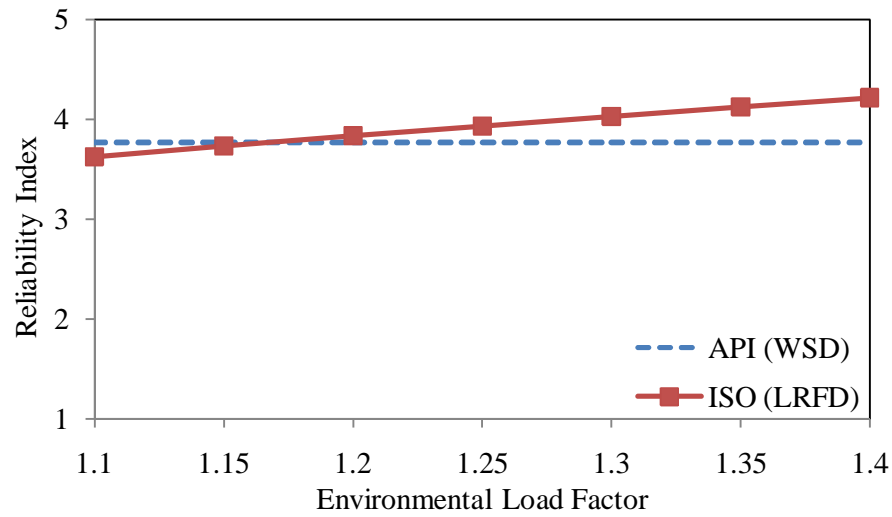


Figure 6.48: Reliability Index Vs Environmental Load Factor for T/Y Joint at SKO1 Using ISO 19902 and API WSD

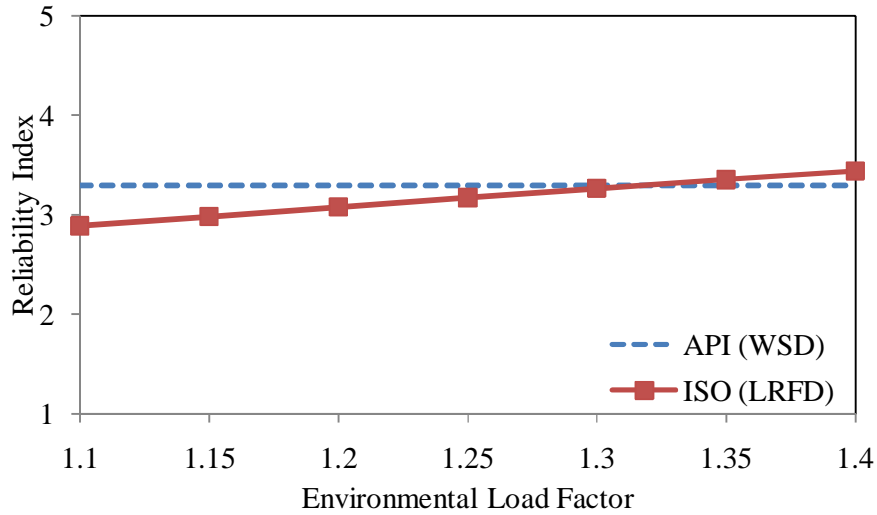


Figure 6.49: Reliability Index Vs Environmental Load Factor for X Joint at SKO1 Using ISO 19902 and API WSD

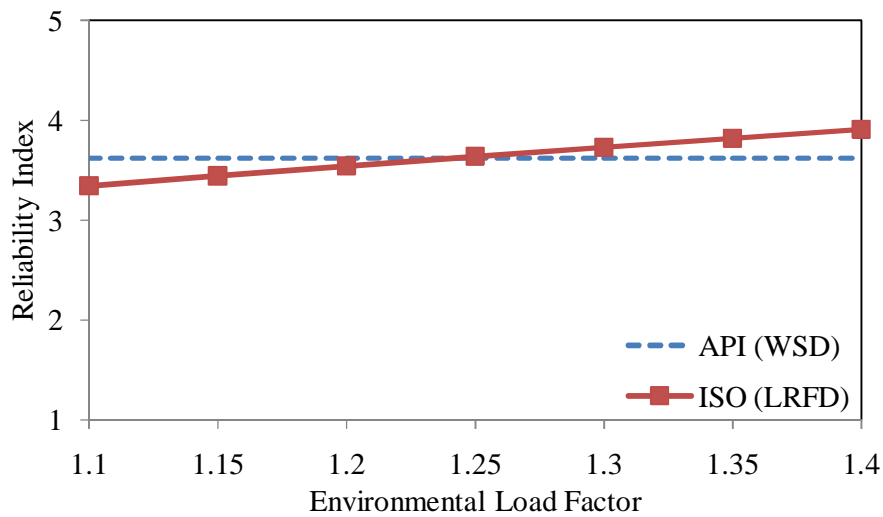


Figure 6.50: Reliability Index Vs Environmental Load Factor for All Joints at SKO1 Using ISO 19902 and API WSD

6.7.3.2 SKO 2 Platform

Figures 6.51 - 6.54 show the environmental load factor for the SKO region at SKO2 Jacket, for all three joints of Jacket. Figure 6.51 show the load factor for K- joint 1.30. T/Y- joints load factor of 1.25 is shown in Figure 6.52. Figure 6.53 shows X- joint load factor of 1.25. Averaged load factor for this region shown in 6.54 is 1.30. The target reliability index was 4.73 for this platform in SKO region. In SKO2

region, it can be seen that again K and X joint were the most stressed and their target reliability was almost equal to 5.0.

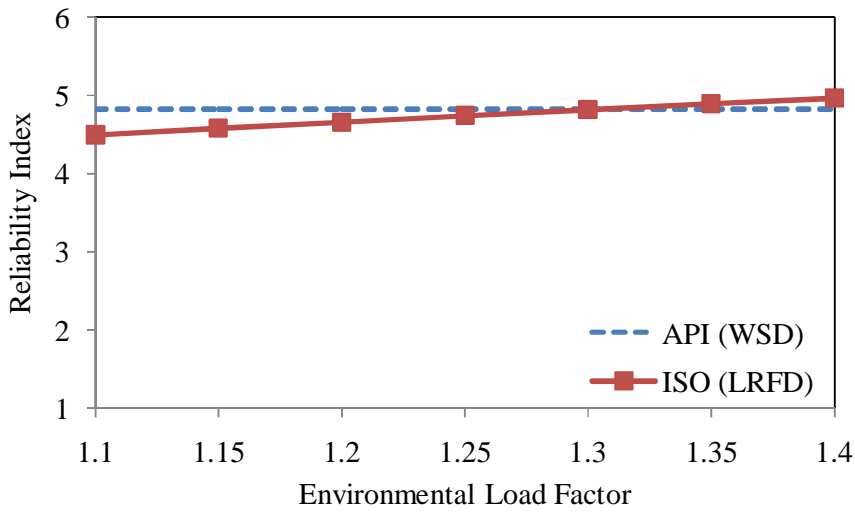


Figure 6.51: Reliability Index Vs Environmental Load Factor for K Joint at SKO2 Using ISO 19902 and API WSD

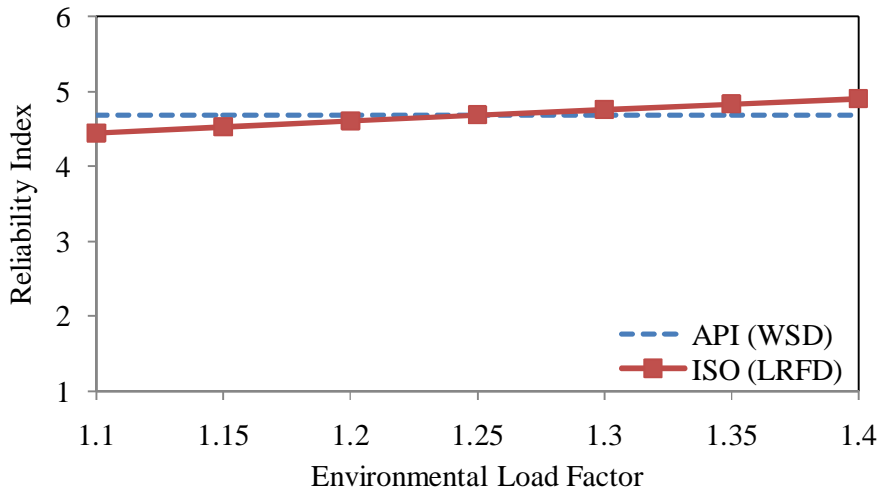


Figure 6.52: Reliability Index Vs Environmental Load Factor for T/Y Joint at SKO2 Using ISO 19902 and API WSD

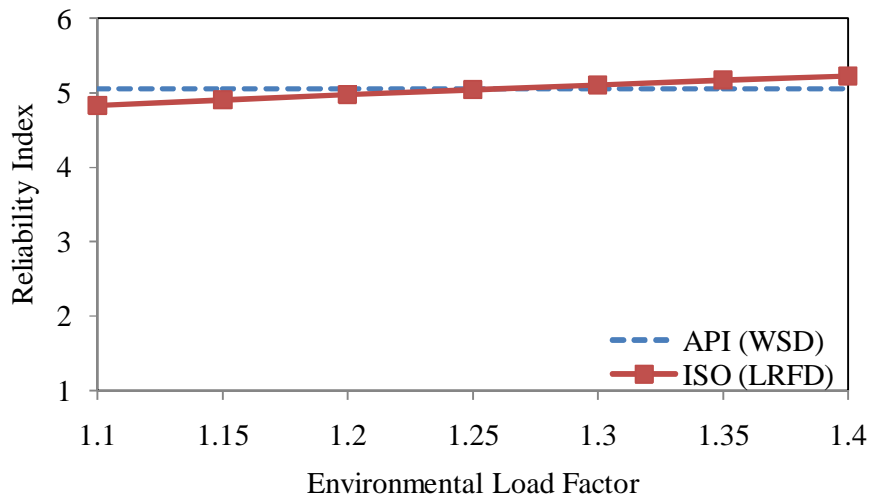


Figure 6.53: Reliability Index Vs Environmental Load Factor for X Joint at SKO2 Using ISO 19902 and API WSD

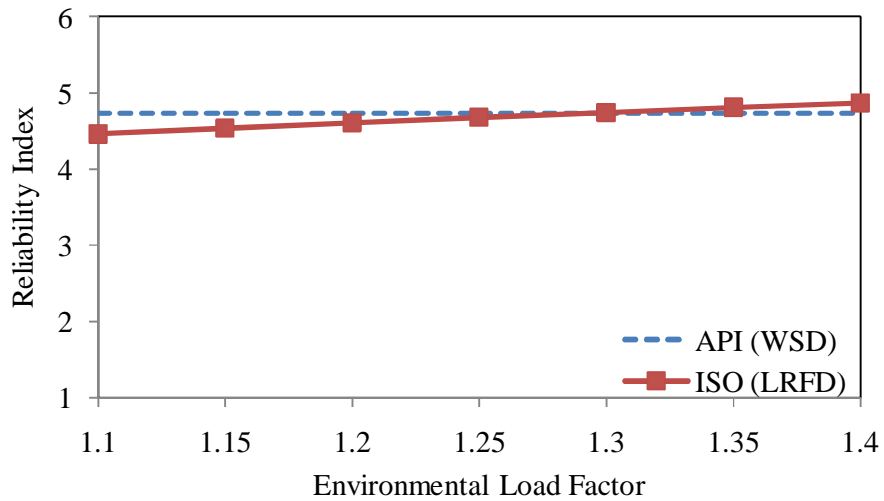


Figure 6.54: Reliability Index Vs Environmental Load Factor for All Joint at SKO2 Using ISO 19902 and API WSD

6.8 All Regions and all Joints Combined Result

The reliability index for API WSD came out to be 3.96 and it was 3.94 when load factor was 1.25 as shown in Table 6.7 and Figure 6.55. When all conditions and

regions are added and averaged together the environmental load factor for Jacket platform joints in Malaysia is proposed to be 1.25. The values have been compared with ISO LRFD values are also shown in the Table 6.7. The high values of reliability indices show that members are oversized. This may be due to provisions to withstand transportation and installation of Jacket [26].

Table 6.7: (WSD) Target Reliability and ISO (LRFD) Reliability for Joints

Code		Reliability Index Malaysia	Reliability Index North Sea/ GOM [69]
API (WSD)		3.96	3.42
ISO(LRFD)	$\gamma_w=1.10$	3.66	-
	$\gamma_w=1.15$	3.75	-
	$\gamma_w=1.20$	3.85	3.74
	$\gamma_w=1.25$	3.94	3.83
	$\gamma_w=1.30$	4.0	3.92
	$\gamma_w=1.35$	4.12	4.0
	$\gamma_w=1.40$	4.20	4.1

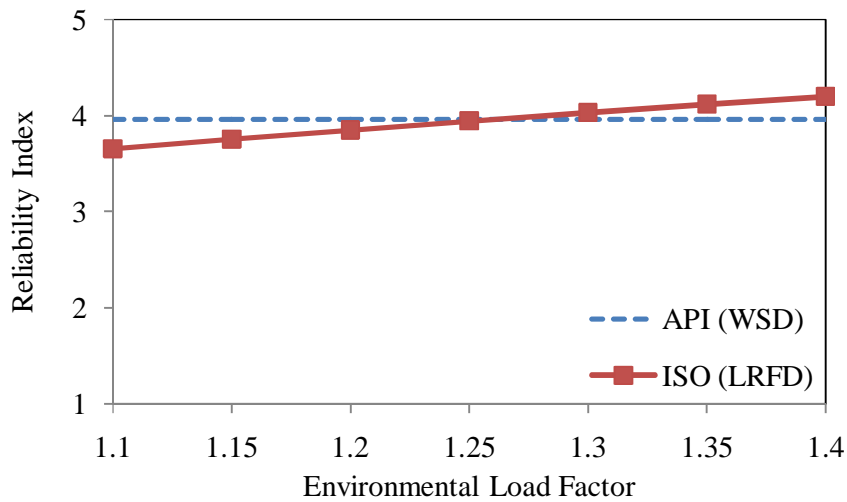


Figure 6.55: Reliability Index Vs Environmental Load Factor for All Joint for All Platforms Using ISO 19902 and API WSD

6.9 Chapter Summary

Environmental load factor for joints used by API RP2A LRFD [107] and ISO is same i.e. 1.35. The wave conditions for 100 year design vary too much for many regions. Therefore applied load were not similar to the conditions in offshore Malaysia. The ISO code reports that joints should be made stronger than the components this makes them safe as compared to component. In this study four platforms were used to find the effect of load factor representing each region of offshore Malaysia. All three types of joints were analysed with four different types of stresses. The environmental load factor results obtained are:

- 1) For the platform in PMO region was in range of 1.2-1.29. The range of target reliability asper API WSD was 2.78-4.93.
- 2) For the platform in SBO region was in range of 1.23-1.33. The range of target reliability asper API WSD was 2.81-3.36.
- 3) For the platform in SKO1 region was in range of 1.17-1.31. The range of target reliability asper API WSD was 3.30-3.81.
- 4) For the platform in SKO2 region was in range of 1.24-1.29. The range of target reliability asper API WSD was 4.69-5.06

The averaged load factor proposed in this research is 1.27.

CHAPTER 7
SYSTEM RELIABILITY BASED ENVIRONMENTAL LOADING AND
EXTENSION OF LIFE OF JACKET PLATFORMS

7.1 Introduction

ISO 19902 and API RP2A codes are calibrated based on North Sea environment or Gulf of Mexico. Codes applicable to Jacket platforms such as API WSD, API LRFD and ISO 19902, are based on component and joint design. If Design codes are followed properly, the strength of member will always exceed the load effect as utility ratio is always maintained less than one while designing the Jacket. Codes consider overall structural integrity, redundancy and multiple failure paths only indirectly by using structural integrity assessment methods. When analysing overall system, the first or initial failure cannot represent the strength of platform. Thus failure of a single component does not mean that the capacity of platform has reached the strength limit. Thus reassessment of old platforms using component based approach becomes unviable. So instead of component reliability, system strength analysis method is used to check the reserve strength of the platform and find its redundancy. In previous chapters environmental load factor was determined based on component and joint reliability this chapter deals with environmental load factor based on system reliability. The next step was to find wave properties through base shear. Wave height was increased so that a wave height which gives RSR of 1.0 could be evaluated. This wave height was used for Bayesian updating of Jacket platform.

Jacket platforms are frequently checked when loading and resistance parameters are changed or at the end of design life and if hydrocarbon reserves are still there to be extracted, it must be checked for extension of life. Therefore the probability of failure was used to check its strength at all the stages. Bayesian updating is a technique

to be used for updating probability of failure taking into consideration probability of failure.

7.2 System Strength Reliability

System reliability is defined as probability that when using given environmental conditions, the system will perform its intended function satisfactorily for a given period of time [119]. It has been proved that without incurring weight penalty, Jacket can be designed not only to achieve governing elastic design criteria but also to provide reserve strength beyond the design requirements. This reserve strength will act as insurance against extreme events or unforeseen operational changes which arise during its life [166]. System strength of Jacket is evaluated using collapse analysis module of SACS. Wave loads are the major loads faced by the Jacket platform during its life and here wave height is increased to find the RSR. Probability of exceedance is ascertained for the design /assessment of Jacket. Existing Jacket platform after surviving severe loading environment for some years/storm events are considered safe for such type of storms if ever they recur. This theory has already been applied on land based structures, such as proof loading used against existing structures to gauge the strength of structure through measurement of deflection. This method has been recommended by ISO for the reassessment of structure [73].

7.2.1 Wave and Current

Here in this study four platforms were analysed for collapse analysis, one from PMO one from SBO and two from SKO. In SKO itself, the platform SKO2 was analysed for two conditions i.e. one with legs fixed at mud line and other with pile soil interaction. For a given sea state wave height and current profile are kept fixed [97]. Topside deck comes under wave attack as wave height increases. The results of four platforms are shown in Figures 7.1-7.5 using the API WSD code. This shows that there is significant increase of load at higher wave heights. This was achieved for platform at PMO with 16 m, at SBO with 11.6 m, with SKO1 with 17.5 m and SKO2

with 17.6 m. Same wave height was taken for SKO2a. This is due to waves hitting the deck, which produced higher base shear.

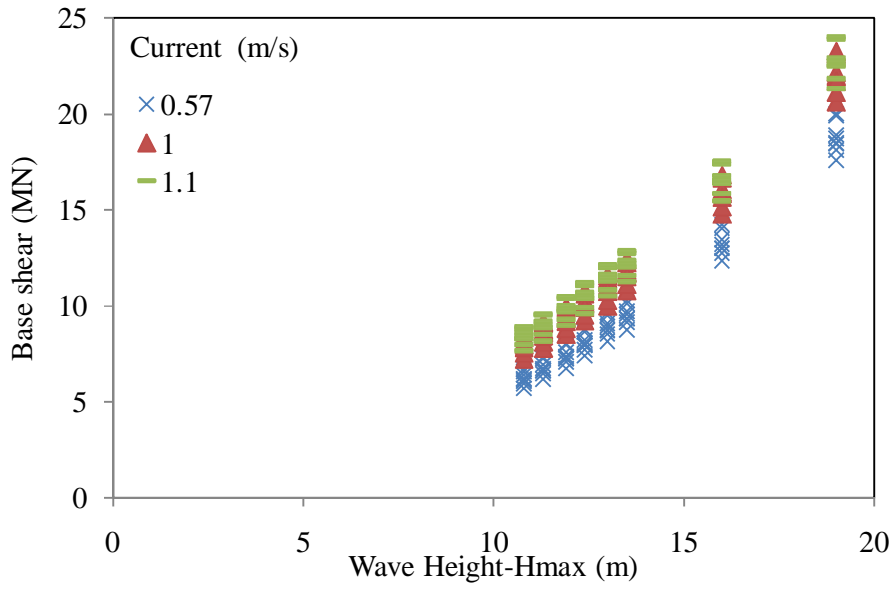


Figure 7.1: Base Shear against Wave Heights and Current Speed at PMO

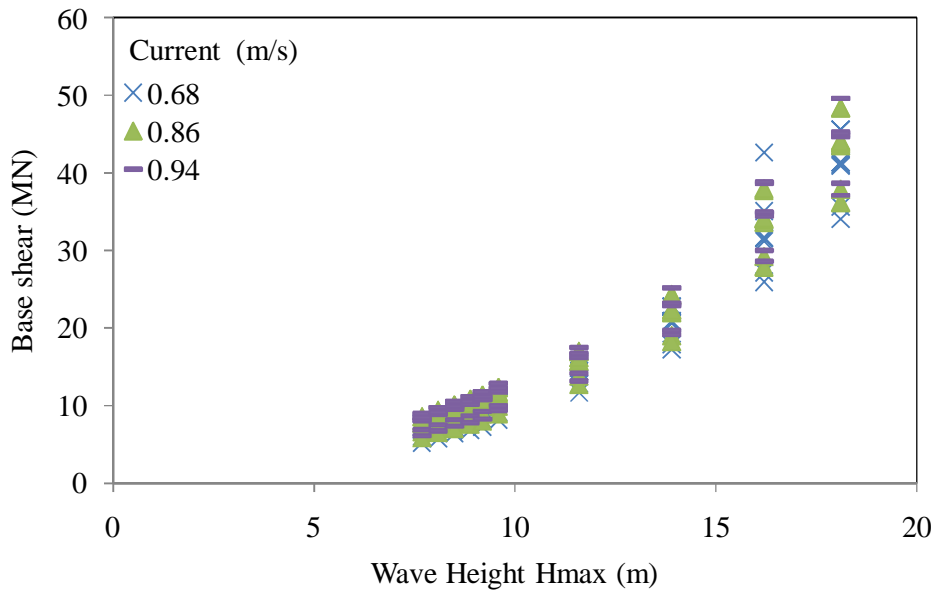


Figure 7.2: Base Shear against Wave Heights and Current Speed at SBO

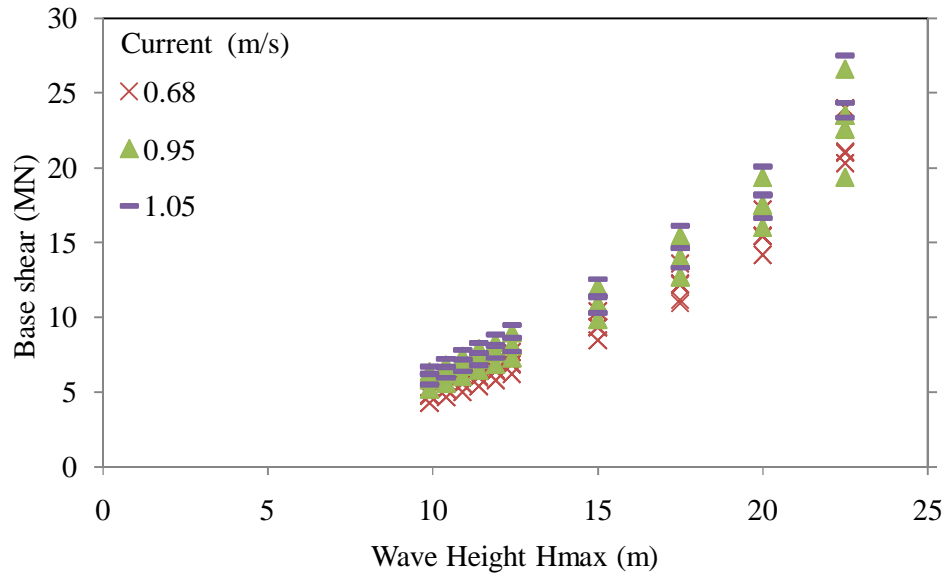


Figure 7.3: Base Shear against Wave Heights and Current Speed at SKO1

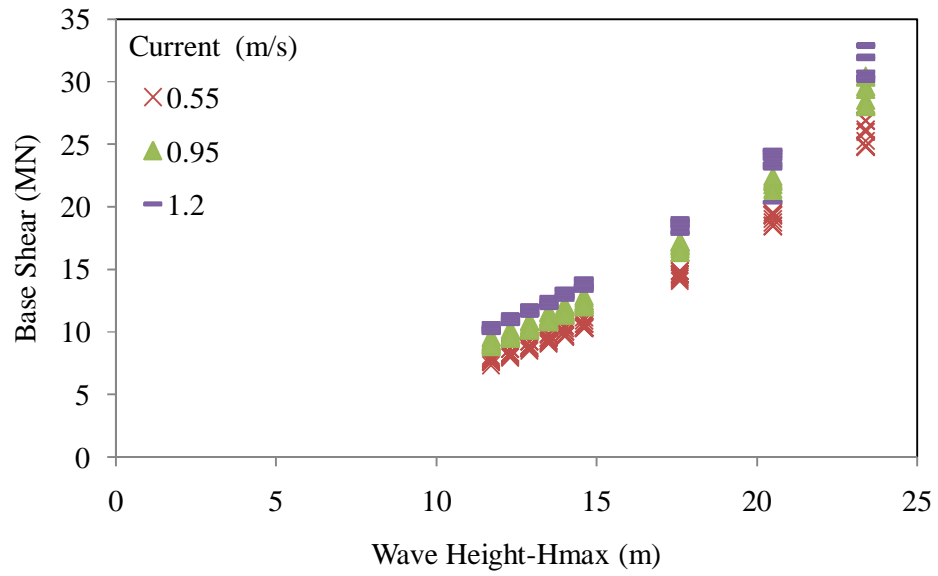


Figure 7.4: Base Shear against Wave Heights and Current Speed at SKO2

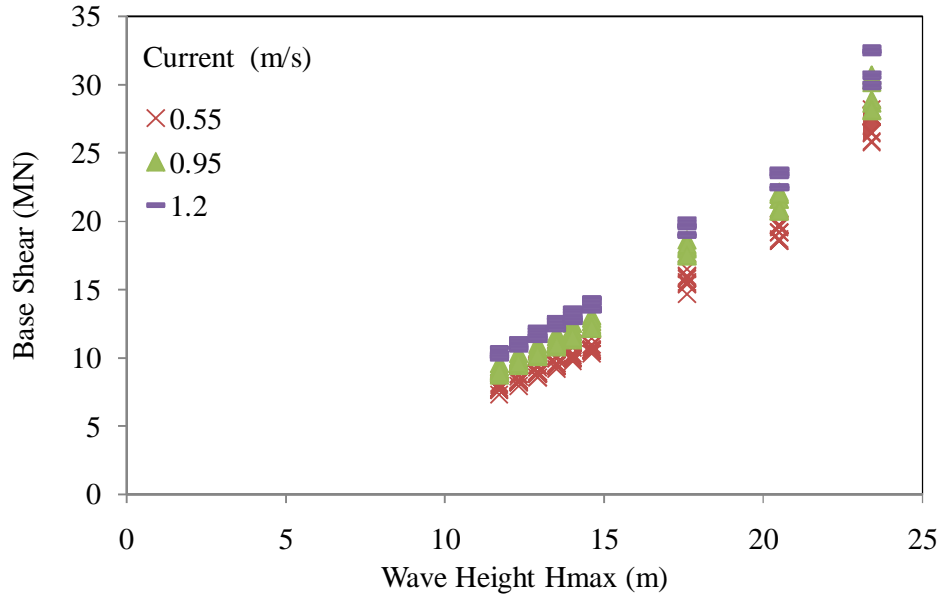


Figure 7.5: Base Shear against Wave Heights and Current Speed at SKO2a

7.2.2 Curve Fitting

Stoke's 5th order wave theory was used by SACS for producing wave loading on the Jacket. During collapse analysis, environmental load increases in steps. To establish the relationship between wave and current load and response of Jacket curve fitting was done to find the coefficients of response surface Equation. This relationship was established by Heideman's Equation (2.15) and which has been used for curve fitting as shown in [167]. Figures 7.6 - 7.10 represent the curve fitting of Jackets. Figure 7.6 shows clearly that the current also plays important part in reliability analysis as the difference in values of base shear is quite high, as compared to 0.57 and 1.0.

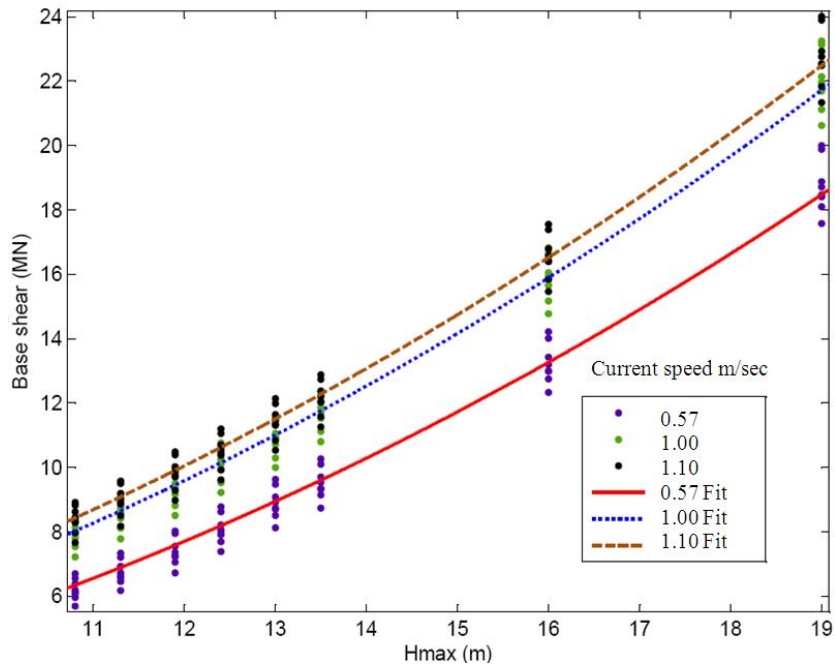


Figure 7.6: Curve Fitting Model for Platform 'PMO'.

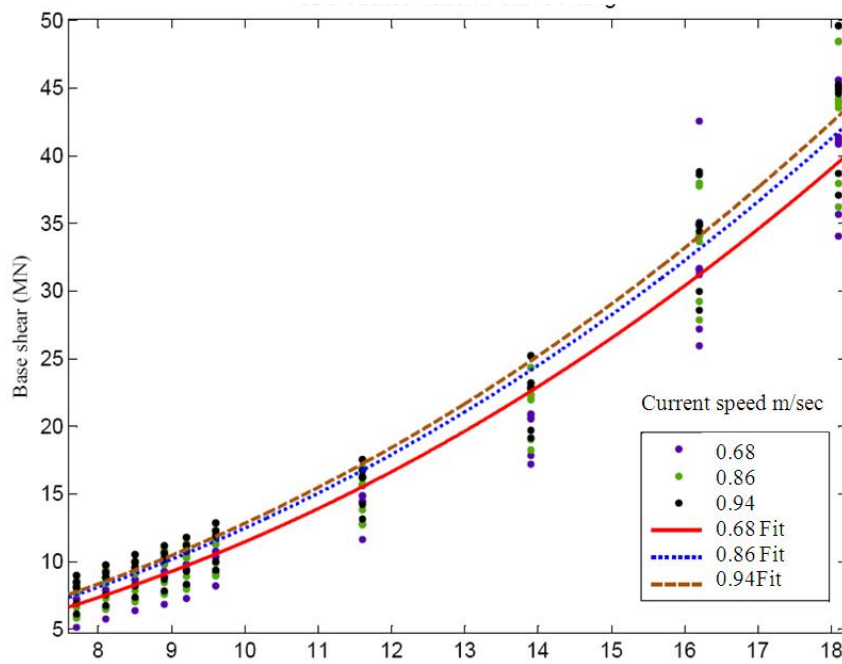


Figure 7.7: Curve Fitting Model for Platform 'SBO'.

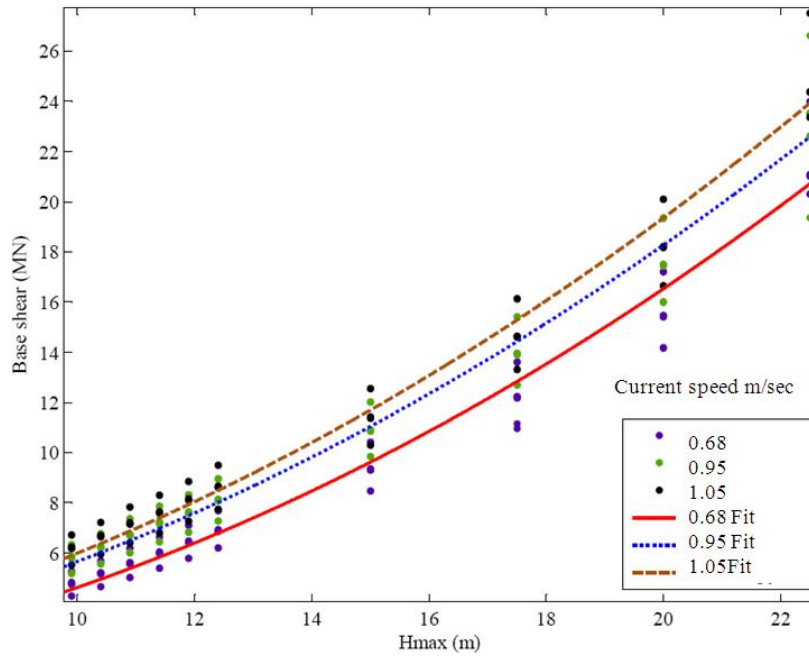


Figure 7.8: Curve Fitting Model for Platform 'SKO1'.

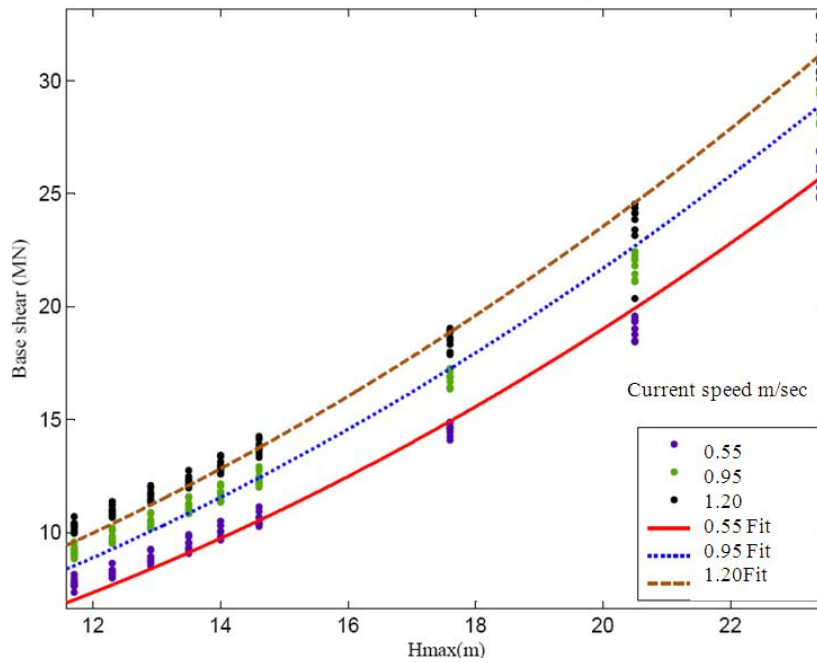


Figure 7.9: Curve Fitting Model for Platform 'SKO2'.

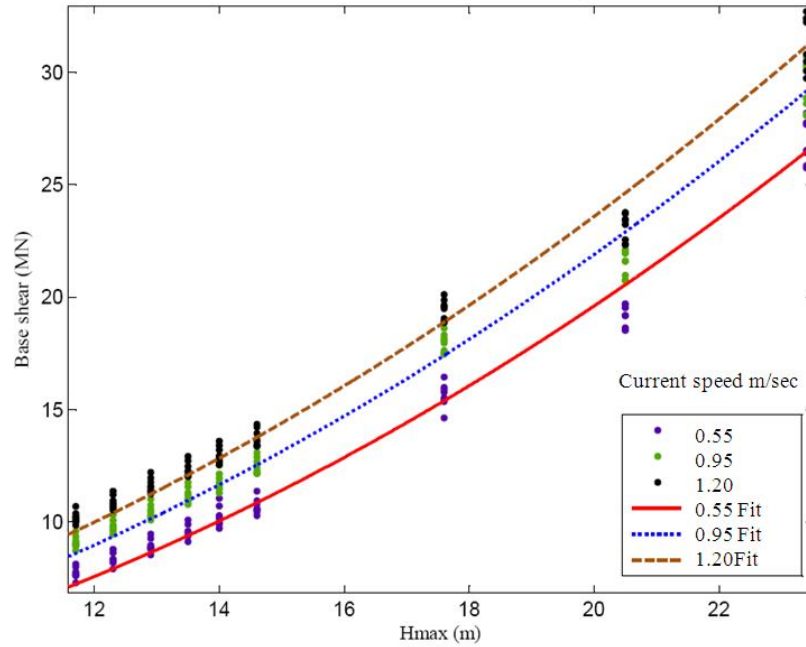


Figure 7.10: Curve Fitting Model for Platform 'SKO2a'.

Table 7.1 provides the parameters for wave and current for the platforms obtained from curve fitting. Separate parameters were obtained for each current speed. Here the design current speed used was based on 100 years as required by ISO/API codes. These values were used to find the probability of failure and reliability index.

Table 7.1: Parameters of Wave and Current for System Reliability

Platform	Current	a_1	a_2	a_3	R^2
PMO	0.57	0.03237	2.7	2.1	0.9831
	1	0.0339	2.7	2.1	0.984
	1.1	0.03419	2.7	2.1	0.9841
SBO	0.68	0.0428	2	2.3	0.956
	0.86	0.04335	2	2.3	0.964
	0.94	0.04459	2	2.3	0.9649
SKO1	0.68	0.026	2.8	2.091	0.9719
	0.95	0.03053	2.8	2.05	0.9703
	1.05	0.03144	2.8	2.05	0.9712
SKO2	0.55	0.03513	2.8	2.05	0.9877
	0.95	0.03614	2.8	2.05	0.9899
	1.2	0.03687	2.8	2.05	0.9856
SKO2a	0.55	0.03624	2.8	2.05	0.9856
	0.95	0.03649	2.8	2.05	0.9864
	1.2	0.03693	2.8	2.05	0.9856

7.2.3 Selection of RSR for Jackets in Malaysia

The collapse analysis was done for the given platforms and results achieved are shown in Tables 7.2 - 7.6. The members which failed initially were diagonal braces, horizontal braces and legs. The base shear varied in each direction. The RSR achieved were on higher sides and minimum RSR achieved was 2.0 at platform in PMO. API WSD and ISO LRFD give minimum RSR of 1.58 and 1.86 respectively for the manned platforms. The range fixed for RSR to find environmental load and probability of failure was 1.5 - 2.25. The probability of failure of 10^{-7} with reliability index of 5.0 was considered practical enough for this study.

Table 7.2: RSR and System Redundancy at Platform PMO

Direction	Member Group	Base Shear (KN)		RSR	Peak Load	100 Year/ Peak Load	System Redundancy
		First Member Failure	100 Year Load		Base Shear (KN)		
0	VD6	19027	9062	2.10	23564	0.385	1.38
45	HD4	26042	10020	2.60	26042	0.385	1.38
90	VF1	30346	10467	2.90	31395	0.333	1.33
135	VB5	33944	10461	3.24	33944	0.308	1.31
180	VD6	29030	9674	3.00	31053	0.312	1.31
225	HD3	30934	10664	2.90	30934	0.345	1.34
270	VE5	25374	10570	2.40	26431	0.400	1.40
315	VB5	20592	10296	2.00	20592	0.500	1.50

Table 7.3: RSR and System Redundancy at Platform SBO

Direction	Member Group	Base shear (KN)		RSR	Peak load	100 year/ Peak Load	System Redundancy
		First Member Failure	100 Year Load		Base Shear (KN)		
0	L13	35162	3702	4.90	46633.97	0.079	1.079
45	L13	42296.38	12818.31	3.30	76867.37	0.167	1.167
90	LG6	39767.77	12428.01	3.20	49707.7	0.250	1.250
135	LG6	39176.36	12243.33	3.20	92806.79	0.132	1.132
180	L19	42919.1	8941.835	4.80	75007.79	0.119	1.119
225	L19	34896.13	12463.53	2.80	84723.34	0.147	1.147
270	XF1	34798.45	12428.34	2.80	84492.46	0.147	1.147
315	L13	35380.36	12636.78	2.80	75810.72	0.167	1.167

Table 7.4: RSR and System Redundancy at Platform SKO1

Direction	Member Group	Base Shear (KN)		RSR	Peak Load	100 Year/ Peak Load	System Redundancy
		First Member Failure	100 Year Load		Base Shear (KN)		
0	LGC	22022	4782	4.61	23937	0.20	1.20
45	LGC	17346	3527	4.92	17718	0.20	1.20
90	V2A	22626	7768	2.91	36448	0.21	1.21
135	LGC	21670	6757	3.21	33882	0.20	1.20
180	LG2	24342	7494	3.25	37472	0.20	1.20
225	LG2	18022	8000	2.25	22054	0.36	1.36
270	LG2	25291	9188	2.75	41652	0.22	1.22
315	LG2	18405	4905	3.75	24573	0.20	1.20

Table 7.5: RSR and System Redundancy at Platform SKO2

Direction	Member Group	Base Shear (KN)		RSR	Peak Load	100 Year/ Peak Load	System Redundancy
		First Member Failure	100 Year Load		Base Shear (KN)		
0	VB9	21215	9752.54	2.18	42222	0.23	1.23
45	VB19	35240	9487	3.71	45500	0.21	1.21
90	VBF	36252	8982	4.04	42012	0.21	1.21
135	VB9	31086	9349	3.33	45050	0.21	1.21
180	VB9	25348	9413	2.69	46903	0.20	1.20
225	VBJ	29666	9191	3.23	42000	0.22	1.22
270	VBJ	22751	9237	2.46	40860	0.23	1.23
315	VB9	22327	9104	2.45	39300	0.23	1.23

Table 7.6: RSR and System Redundancy at Platform SKO2a

Direction	Member Group	Base Shear (KN)		RSR	Peak Load	100 Year/ Peak Load	System Redundancy
		First Member Failure	100 year load		Base Shear (KN)		
0	VB9	20857	8141	2.56	39791	0.20	1.20
45	L32	32056	13017	2.46	36665	0.36	1.36
90	102	29980	8877	3.38	42488	0.21	1.21
135	VAA	30907	9195	3.36	34472	0.27	1.27
180	VB9	26138	9317	2.81	39133	0.24	1.24
225	VBJ	23266	9102	2.56	25768	0.35	1.35
270	VBJ	23544	9190	2.56	32483	0.28	1.28
315	VB9	23141	9096	2.54	31663	0.29	1.29

7.3 System Environmental Load Factor

RSR values were evaluated from existing platforms based on design of API WSD. Here the environmental load factor proposed for all three regions of Malaysia was based on minimum RSR of 2. This was done to build maximum optimised structures which were not only safe as per API but also will economise the cost. It has been suggested that minimum target probability of failure for system reliability should be taken as 3×10^{-5} [106], [157] with a reliability index of 4.0. This reliability index is related to ductile failure of system with reserve capacity and dangerous failure implications for Jacket platforms. Melchers reports that minimum system reliability index should be 3.58. RSR, We/G ratio and system load factor obtained for North Sea have been shown in Figures 2.10 and 2.11. For Figures 7.11 -7.15 reliability index have been determined with respect to different We/G ratios and range of environmental loads. For platforms from three regions, reliability index was high when gravity load was more, but as environmental load increased, the reliability index became stable and curve straightened up. The other influence of higher gravity load was that from 0.1 to 0.5, the spread of difference between load factors was not large but as environmental load increased, spread became more visible. This trend was representative for all regions. The same was also present for ISO code [27]. The curves were steeper between 0.2-0.3 but became flatter after 1.0.

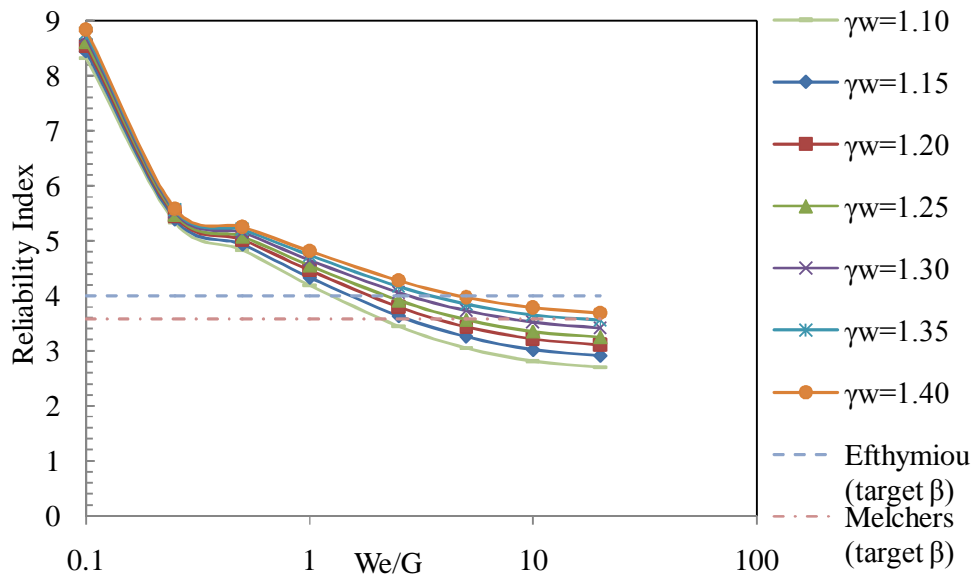


Figure 7.11: Variation of Reliability Index Vs We/G Ratio Using ISO 19902 code for Different Environmental Load Factors (γ_w) at PMO

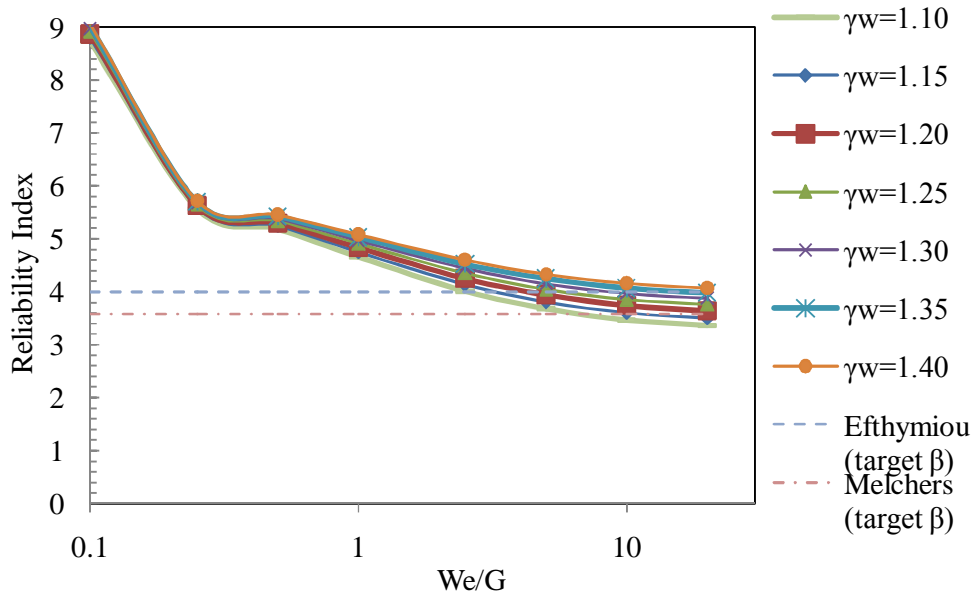


Figure 7.12: Variation of Reliability Index Vs We/G Ratio Using ISO 19902 code for Different Environmental Load Factors (γ_w) at SBO

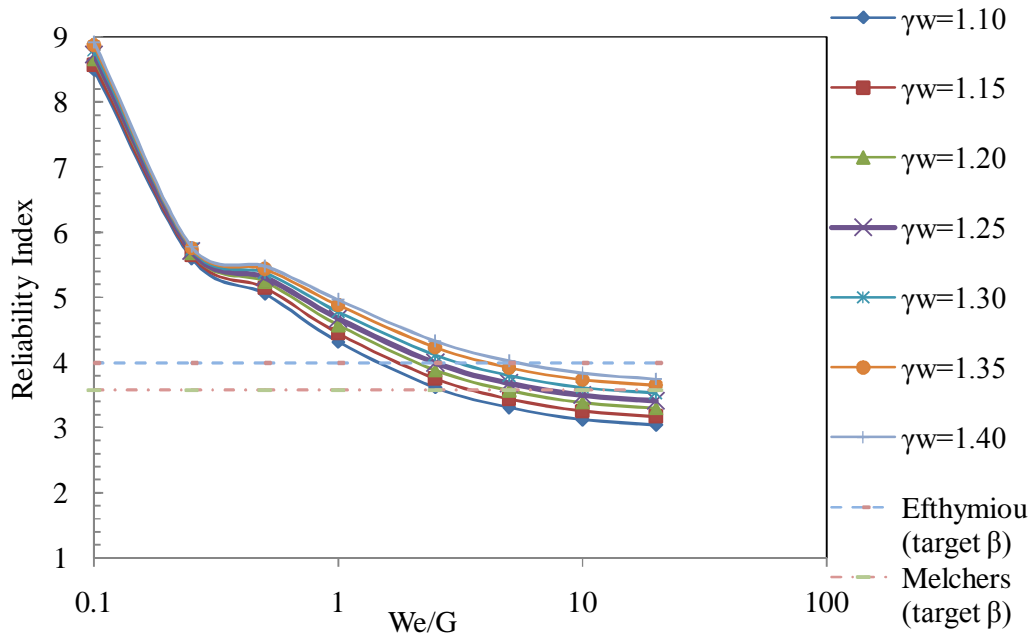


Figure 7.13: Variation of Reliability Index Vs We/G Ratio Using ISO 19902 code for Different Environmental Load Factors (γ_w) at SKO1

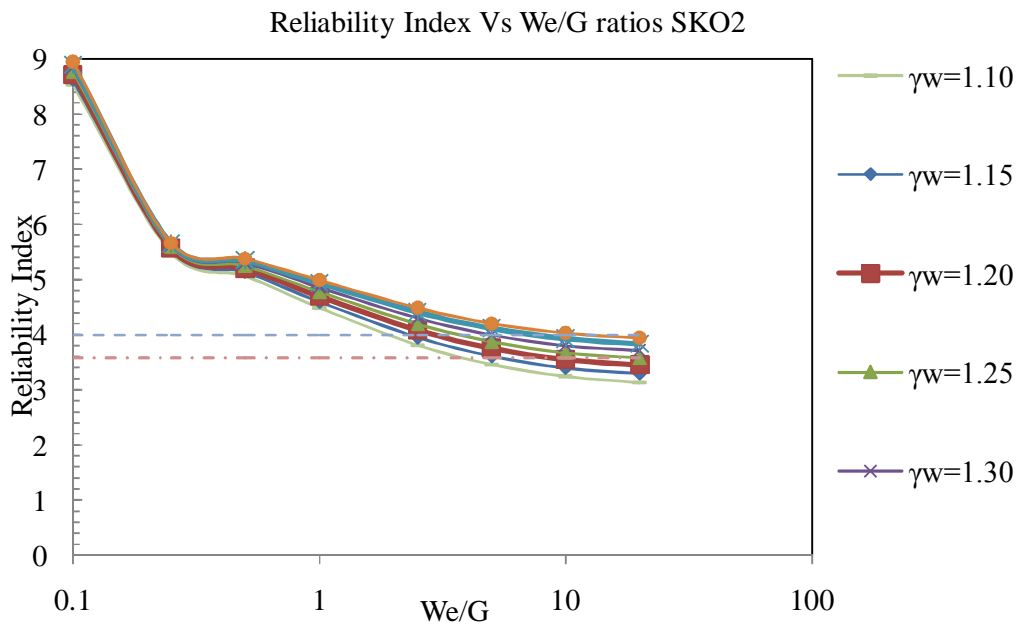


Figure 7.14: Variation of Reliability Index Vs We/G Ratio Using ISO 19902 code for Different Environmental Load Factors (γ_w) at SKO2

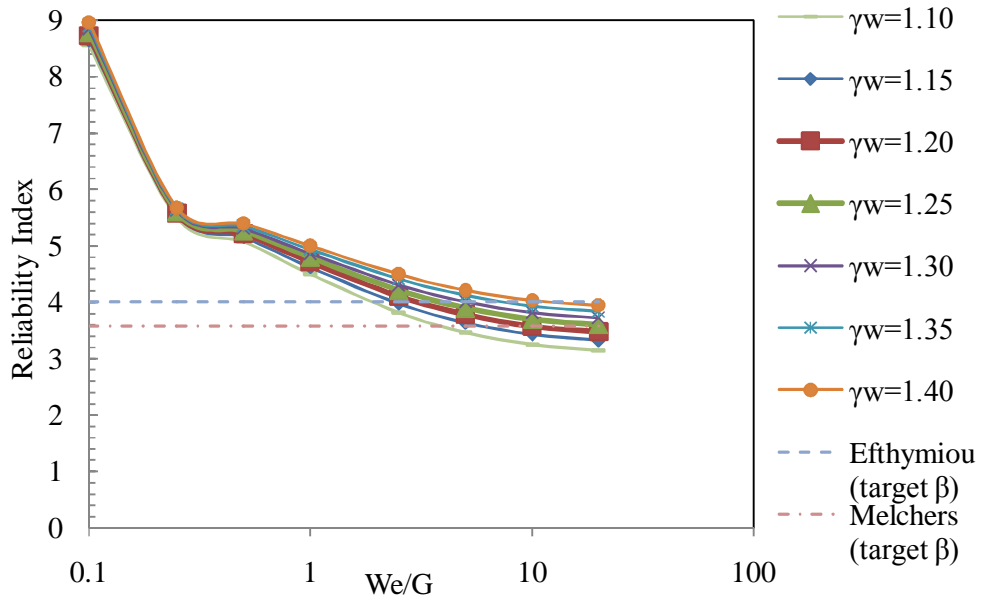


Figure 7.15: Variation of Reliability Index Vs We/G Ratio Using ISO 19902 code for Different Environmental Load Factors (γ_w) at SKO2a

Figures 7.16 - 7.20 show reliability index with respect to different load factors and We/G ratios of 0.5, 1, and 2.5. The Figure shows that except with We/G ratio of 2.5 other ratios were well above the target reliability. When wave load impact increased, the reliability index became lower and vice versa. The reliability index increased with increasing percentage contribution of dead load which were more predictable with less variability [157].

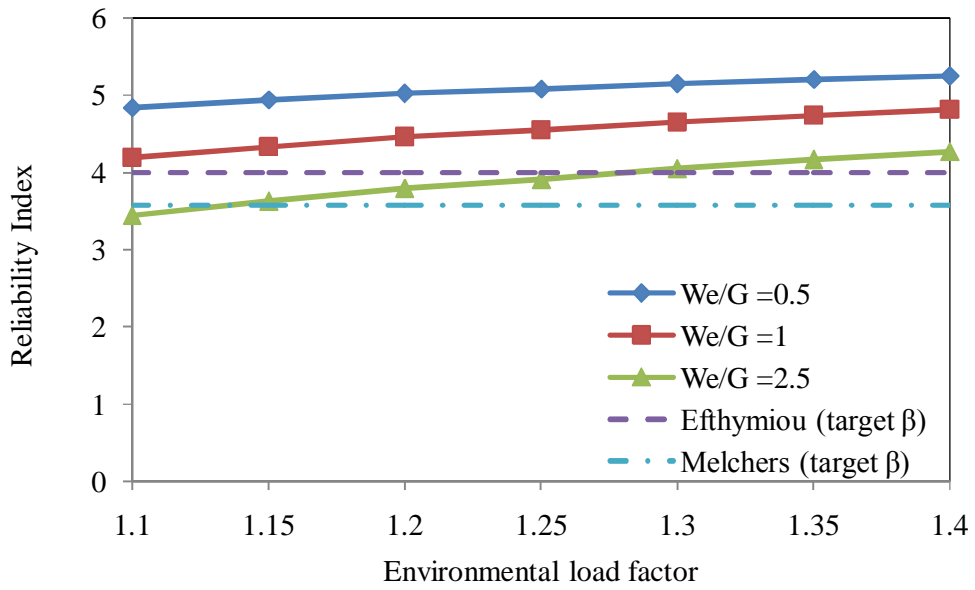


Figure 7.16: Effect of γ_w on Reliability Index against W_e/G ratio of 0.5,1, 2.5 at PMO

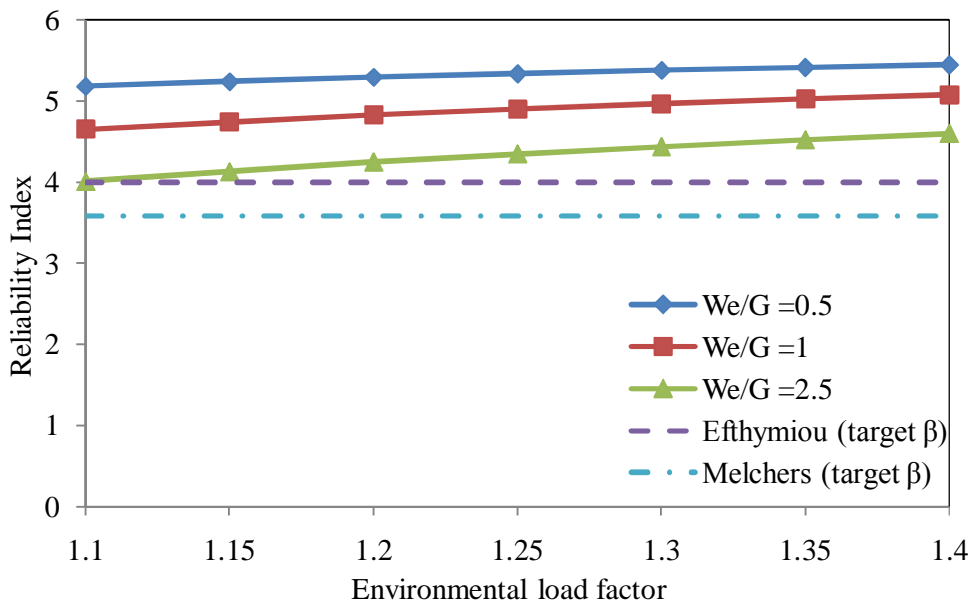


Figure 7.17: Effect Effect of γ_w on Reliability Index against W_e/G ratio of 0.5,1, 2.5 at SBO

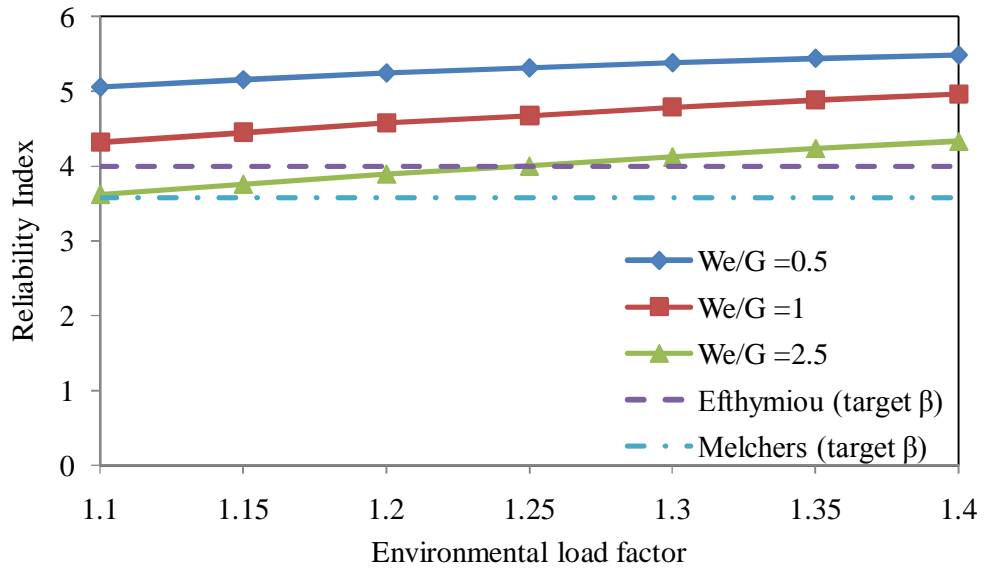


Figure 7.18: Effect of γ_w on Reliability Index against W_e/G ratio of 0.5,1, 2.5 at SKO1

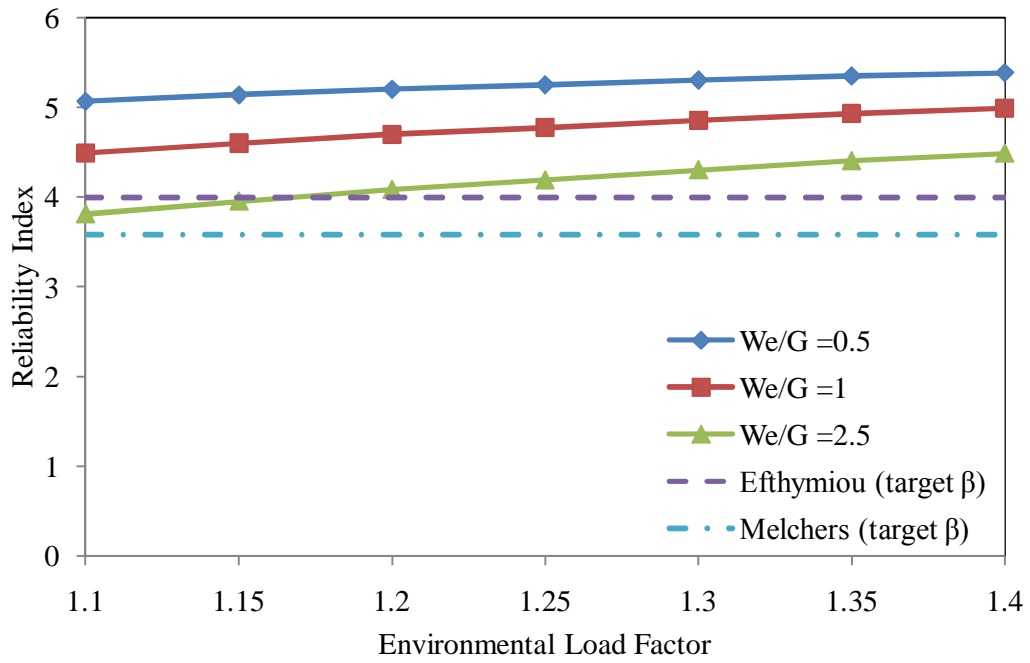


Figure 7.19: Effect of γ_w on Reliability Index against W_e/G ratio of 0.5,1, 2.5 at SKO2

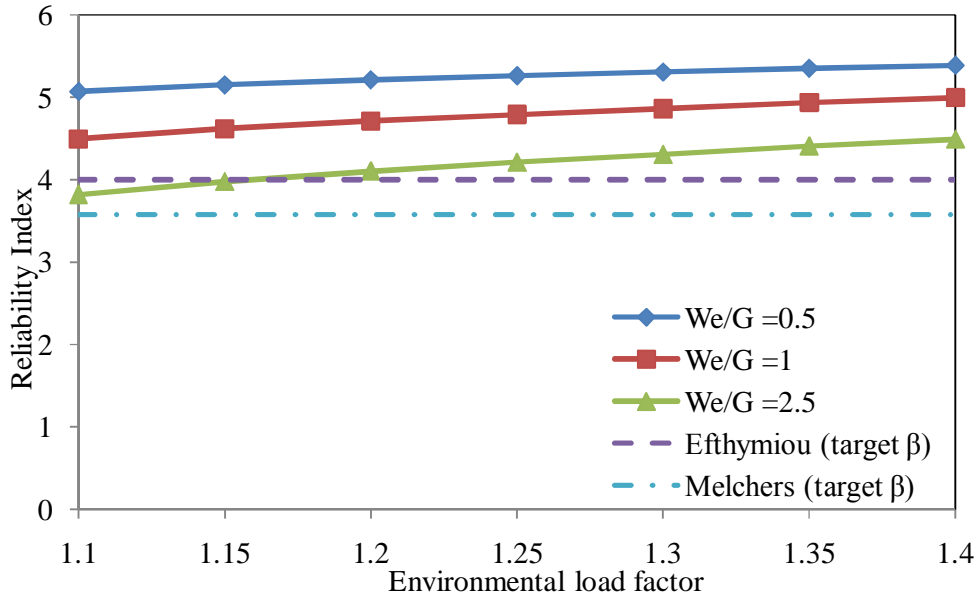


Figure 7.20: Effect of γ_w on Reliability Index against W_e/G ratio of 0.5,1, 2.5 at SKO2a

Figures 7.21 - 7.25 show reliability index with respect to varying W_e/G ratios for the environmental load factor of 1.1. From these Figures, it is clear that load factor of 1.1 is higher than the notional target reliabilities. Thus any reliability above the accepted reliable Jacket will be safe for the Jacket assessed for ductility.

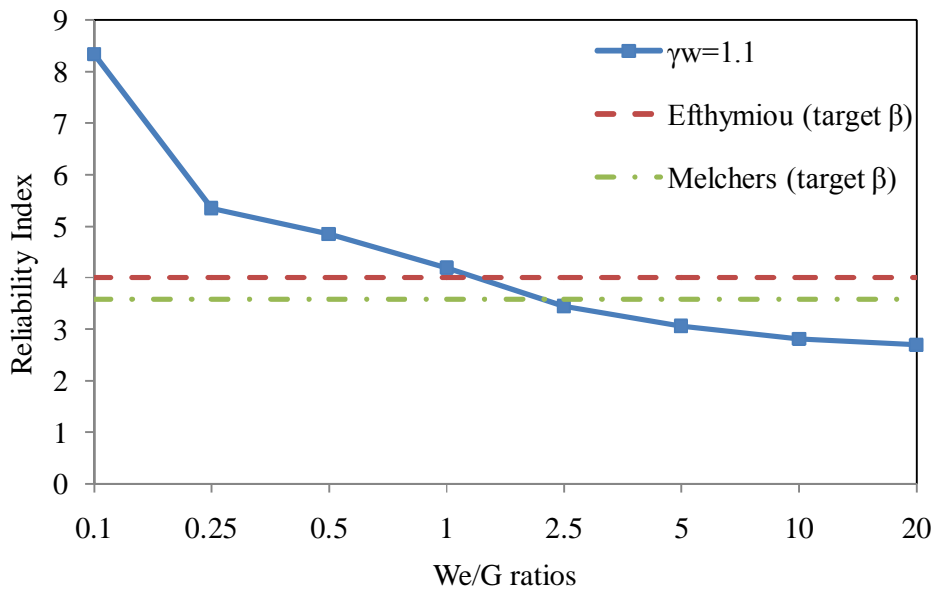


Figure 7.21: Reliability Index Vs W_e/G ratios with $\gamma_w = 1.10$ and Target Reliability at PMO

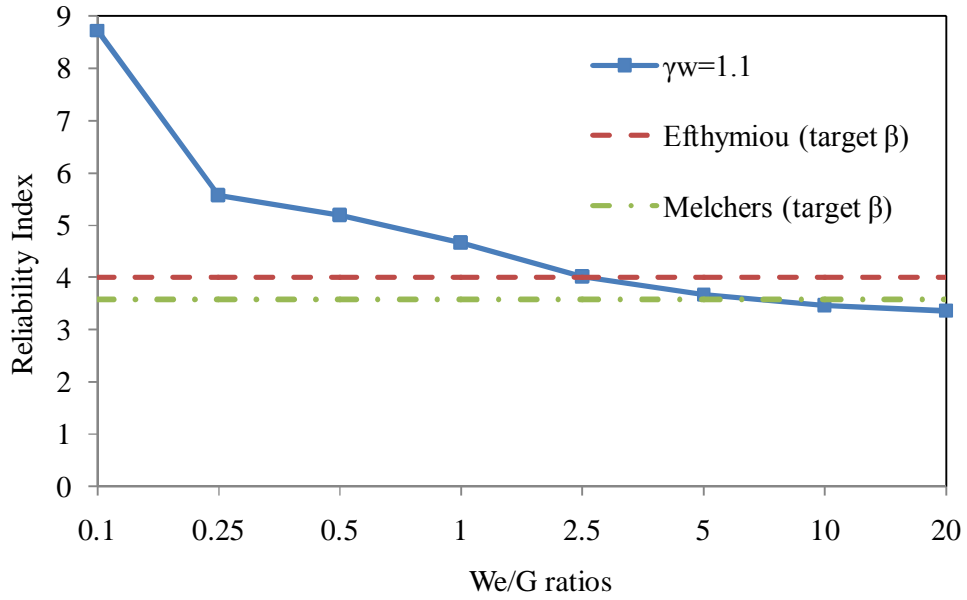


Figure 7.22: Reliability Index Vs We/G ratios with $\gamma_w=1.10$ and Target Reliability at SBO

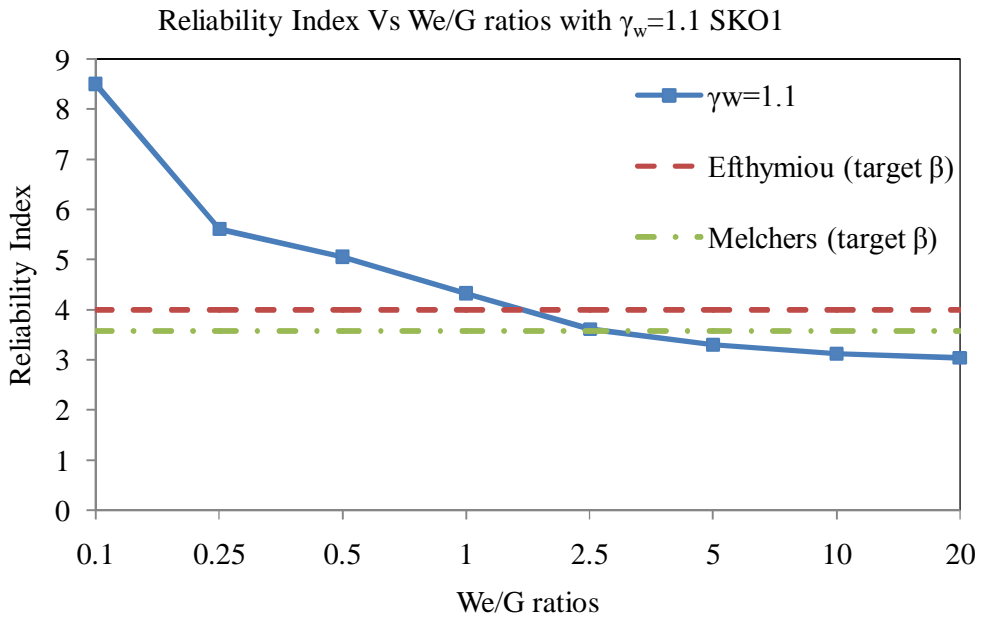


Figure 7.23: Reliability Index Vs We/G ratios with $\gamma_w=1.10$ and Target Reliability at SKO1

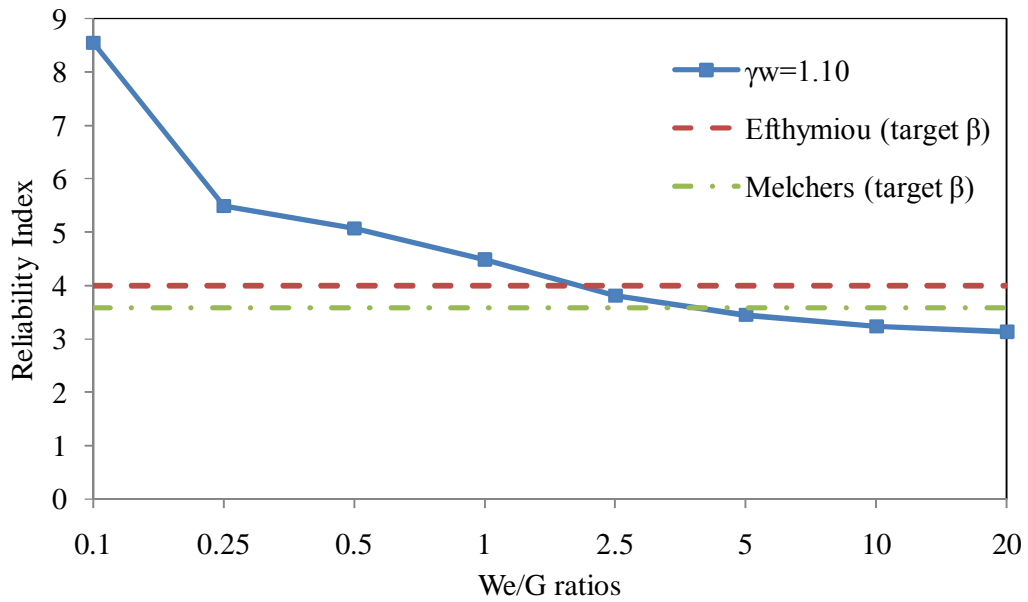


Figure 7.24: Reliability Index Vs We/G ratios with $\gamma_w=1.10$ and Target Reliability at SKO2

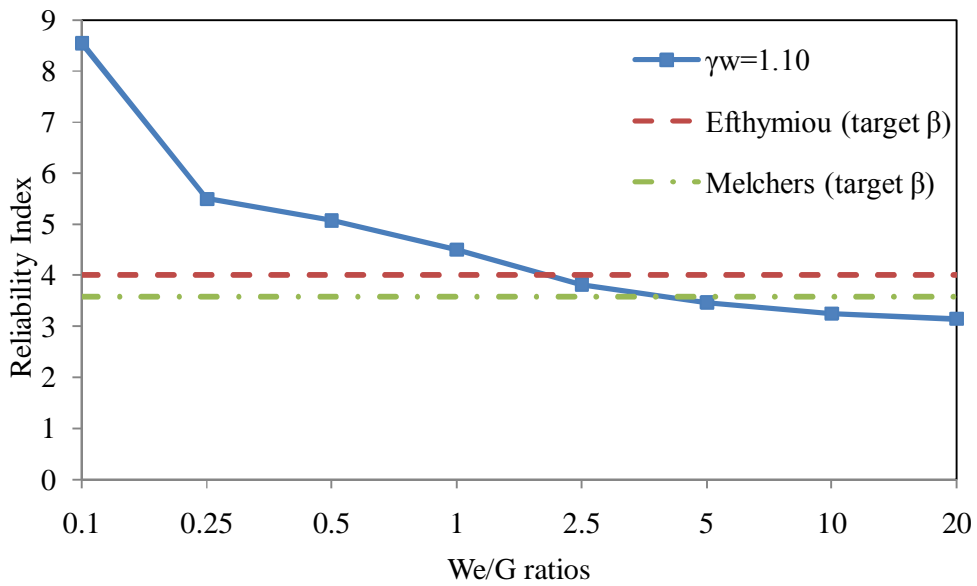


Figure 7.25: Reliability Index Vs We/G ratios with $\gamma_w=1.10$ and Target Reliability at SKO2a

Figures 7.26 - 7.30 show that the proposed load factor for Malaysia of 1.1 was well above the target reliabilities.

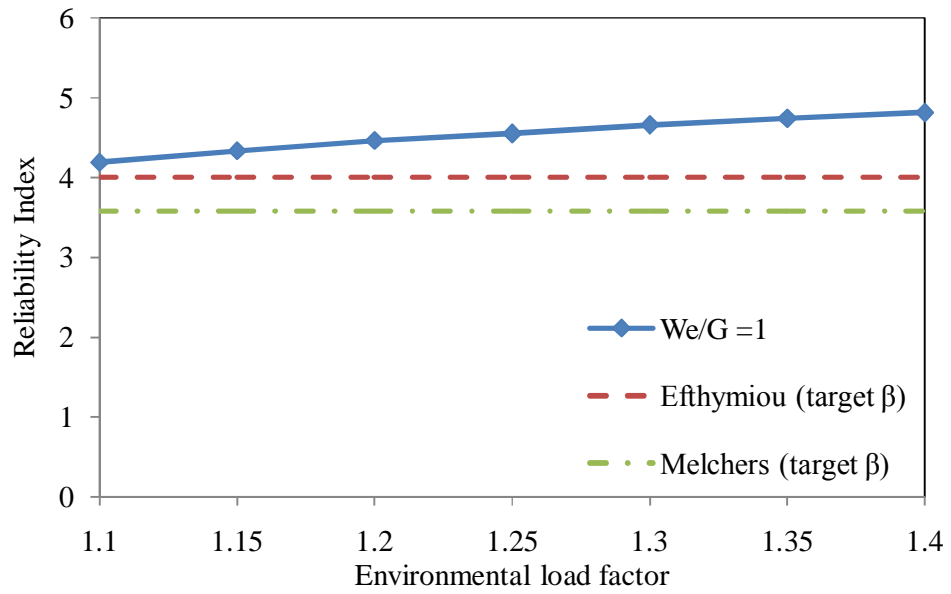


Figure 7.26: Reliability Index Vs Environmental Load Factor, $We/G = 1$ at PMO

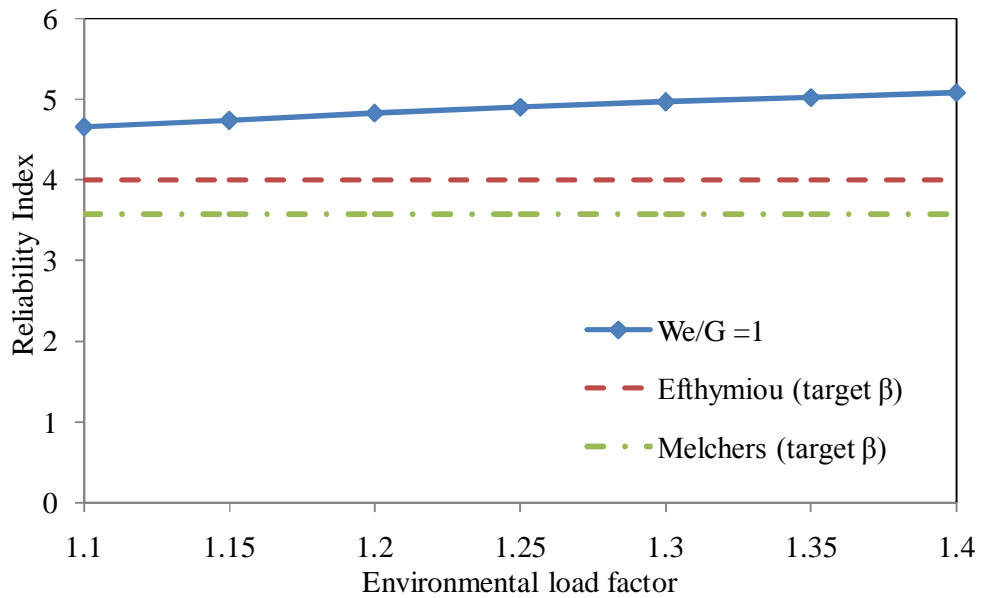


Figure 7.27: Reliability Index Vs Environmental Load Factor, $We/G = 1$ at SBO

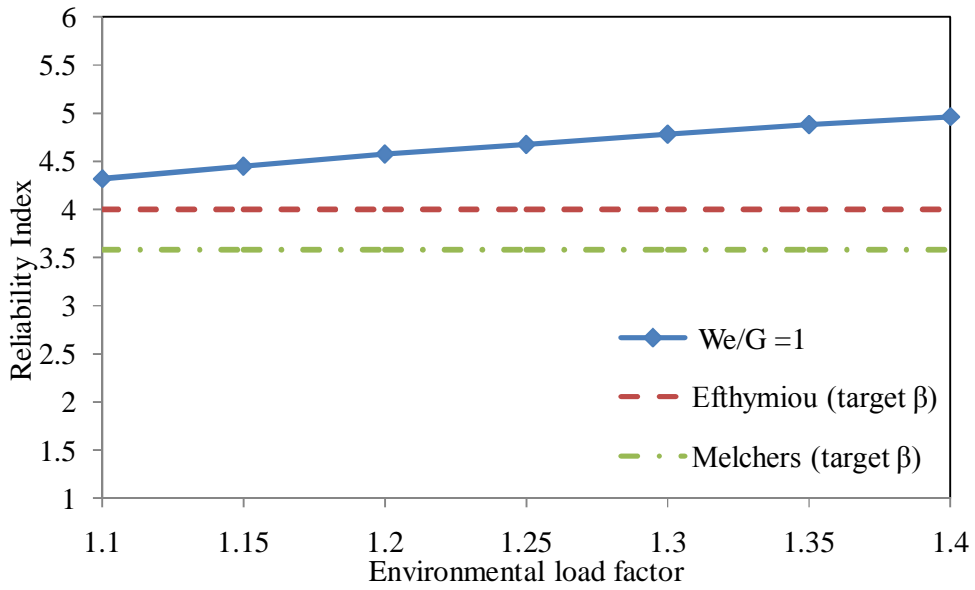


Figure 7.28: Reliability Index Vs Environmental Load Factor, $We/G = 1$ at SKO1

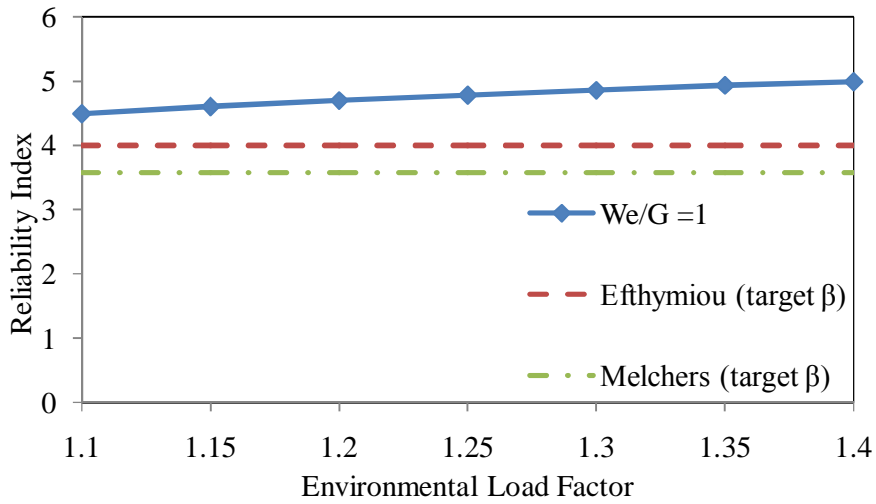


Figure 7.29: Reliability Index Vs Environmental Load Factor, $We/G = 1$ at SKO2

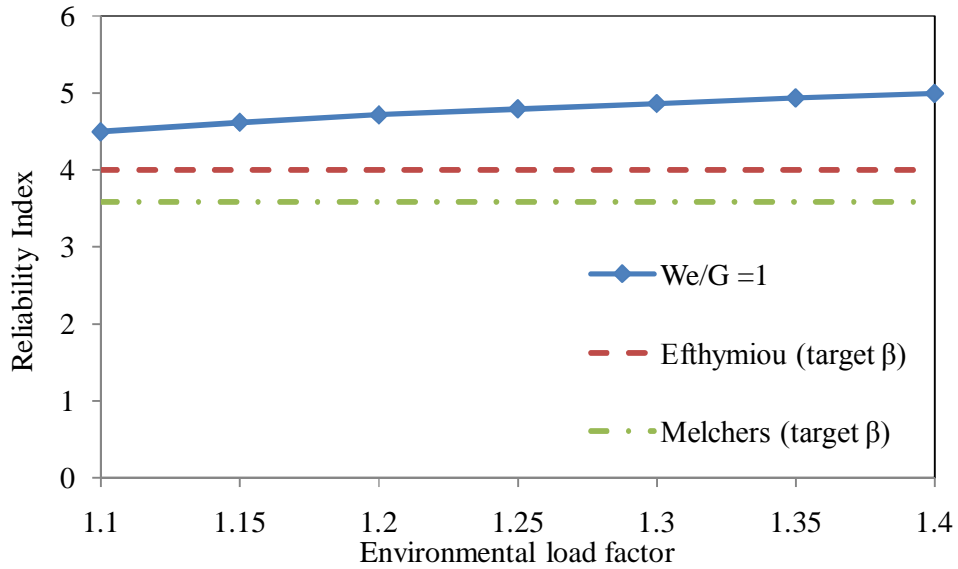


Figure 7.30: Reliability Index Vs Environmental Load Factor, $We/G = 1$ at SKO2a

7.4 Collapse Analysis of Jacket

Failure can be defined as global collapse i.e. loads exceeding the ultimate capacity of Jacket [54]. Appendix G shows the RSR values with respect to applied H_{max} in different ranges starting from design wave. This analysis was done to overload the Jacket and find its response near failure condition. The minimum acceptable safe condition for Jacket was set at RSR of 1.0. The corresponding wave height was further used to find the probability of failure. It can be seen that at low wave height RSR was high but as wave heights increased the RSR reduced. The same trend was observed at all three regions. The wave height details are given in section 3.9.3. The RSR of 1.0 corresponding to the given wave load made us confident about the Jacket strength and ductility.

7.4.1 Wave Effect on Collapse Load

Figures 7.31 - 7.35 show the base shear against wave height effects of Jacket response. The variation in base shear was due to difference of topside weight, Jacket

height, water depth and wave heights. Here each wave height was analysed in eight directions along with three current speeds. Thus there were 24 analyses for each wave. The high variation in base shear was due to increase in wave height. The scatter at different wave heights was due to system redundancy in Jackets for different directions.

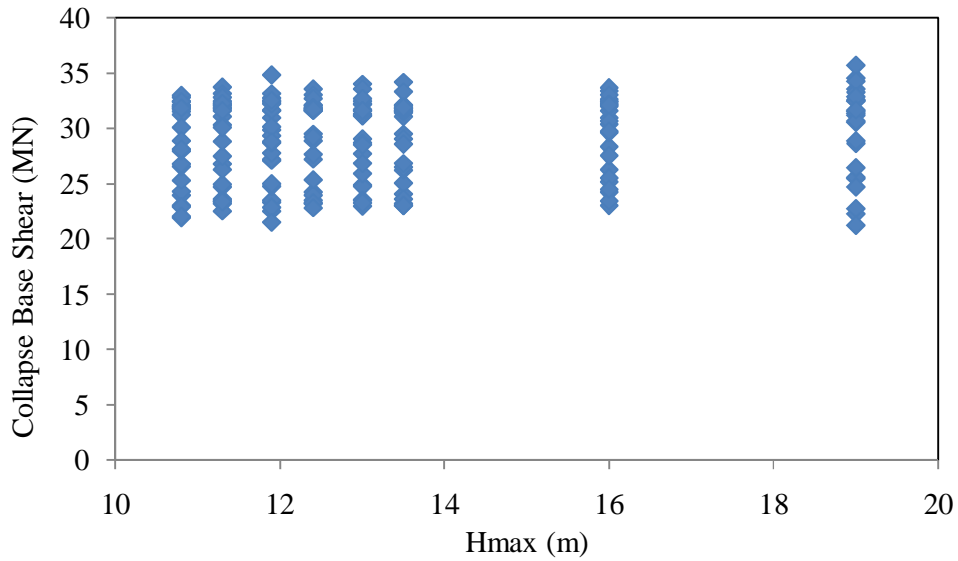


Figure 7.31: Collapse Base Shear against H_{max} for PMO.

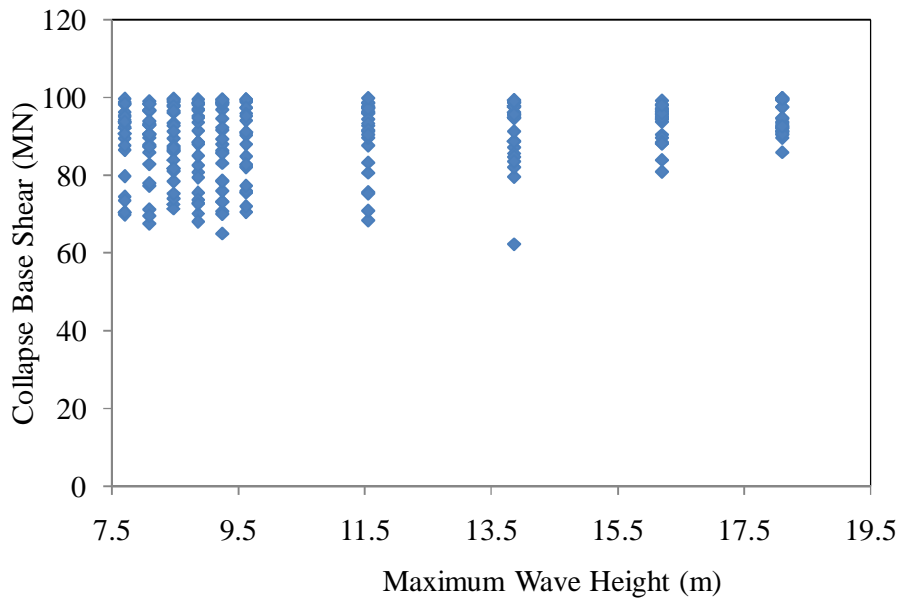


Figure 7.32: Collapse Base Shear against H_{max} for SBO

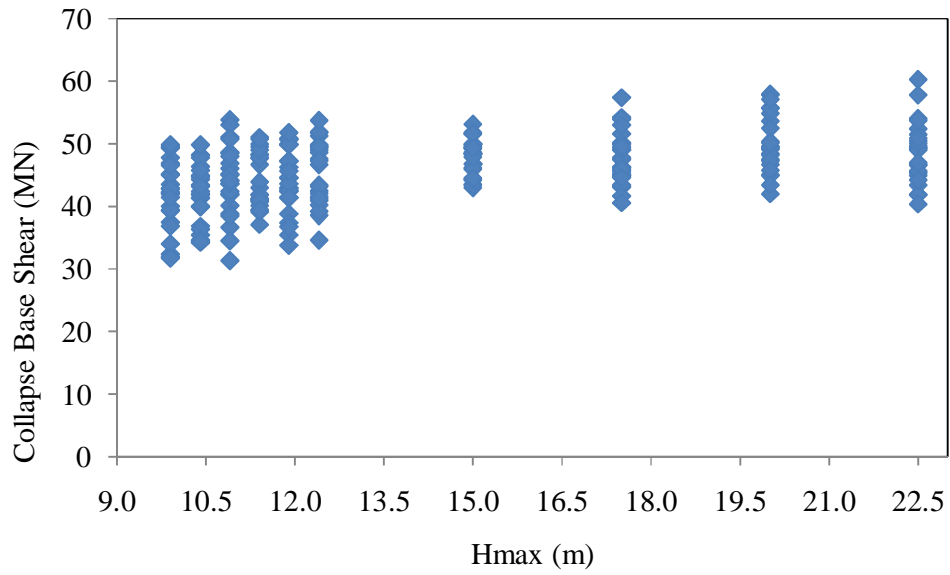


Figure 7.33: Collapse Base Shear against H_{max} for SKO1

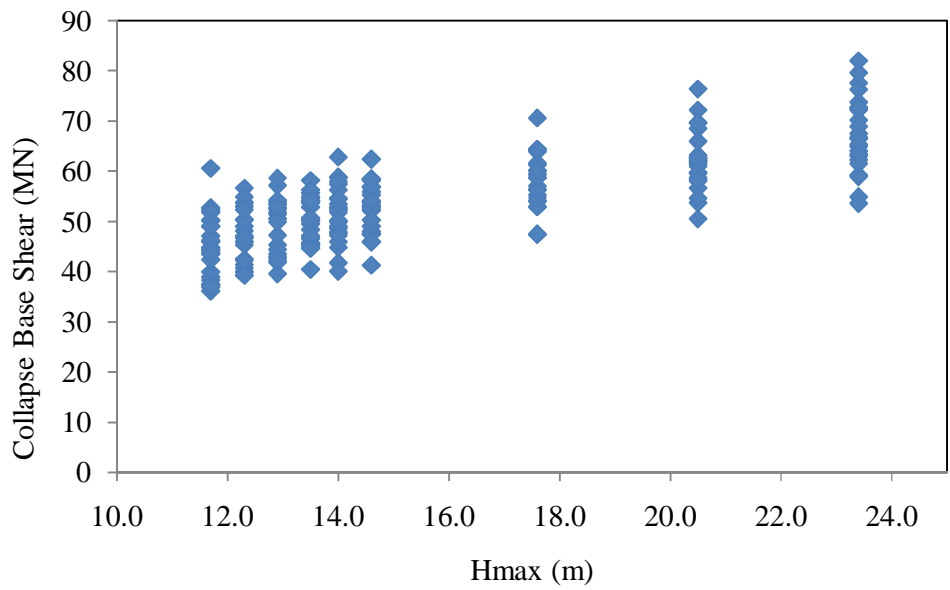


Figure 7.34: Collapse Base Shear against H_{max} for SKO2

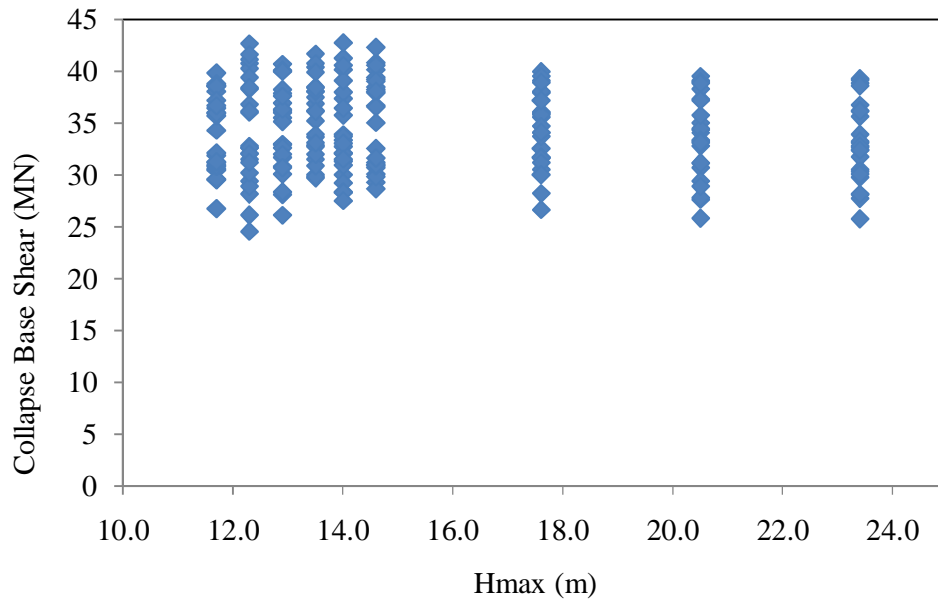


Figure 7.35: Collapse Base Shear against H_{max} for SKO2a

7.4.2 Directional base shear

Figures 7.36 - 7.40 show collapse base shear with eight wave directions. Here Jackets vary in their strength when loads act in different directions. The scatter at PMO was less as compared to other regions.

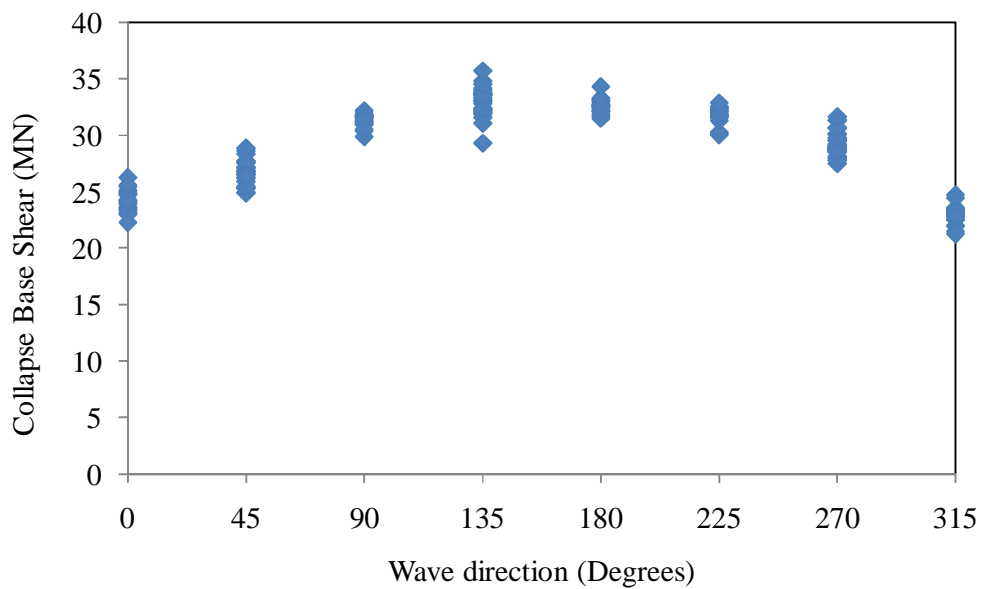


Figure 7.36: Collapse Base Shear against Wave Direction at PMO

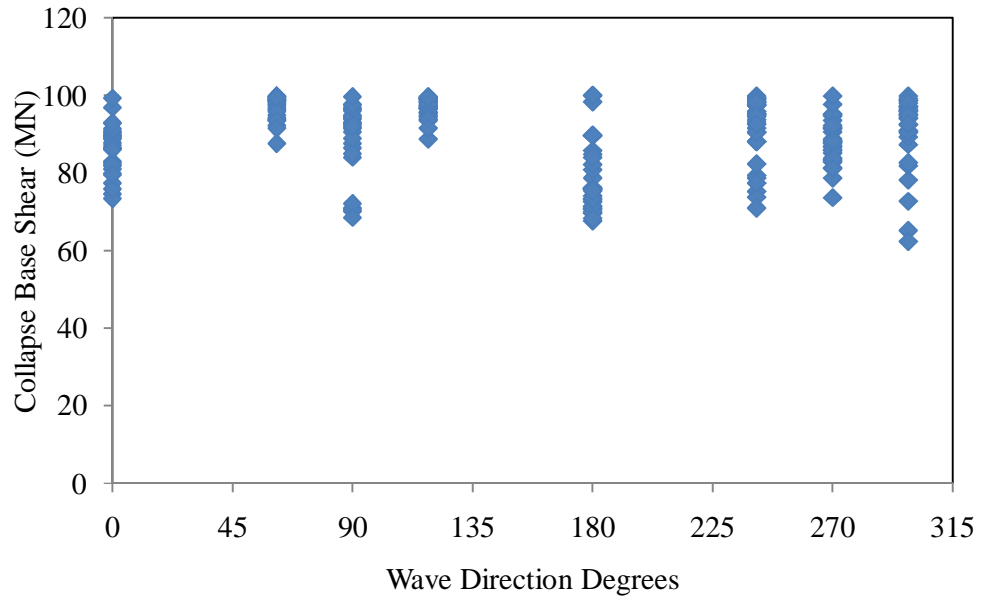


Figure 7.37: Collapse Base Shear against Wave Direction at SBO

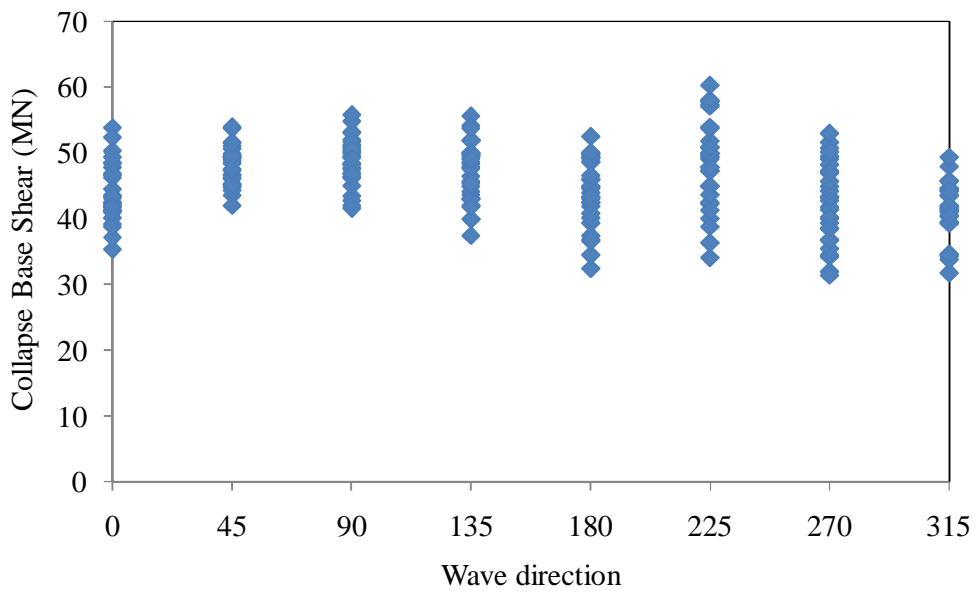


Figure 7.38: Collapse Base Shear against Wave Direction at SKO1

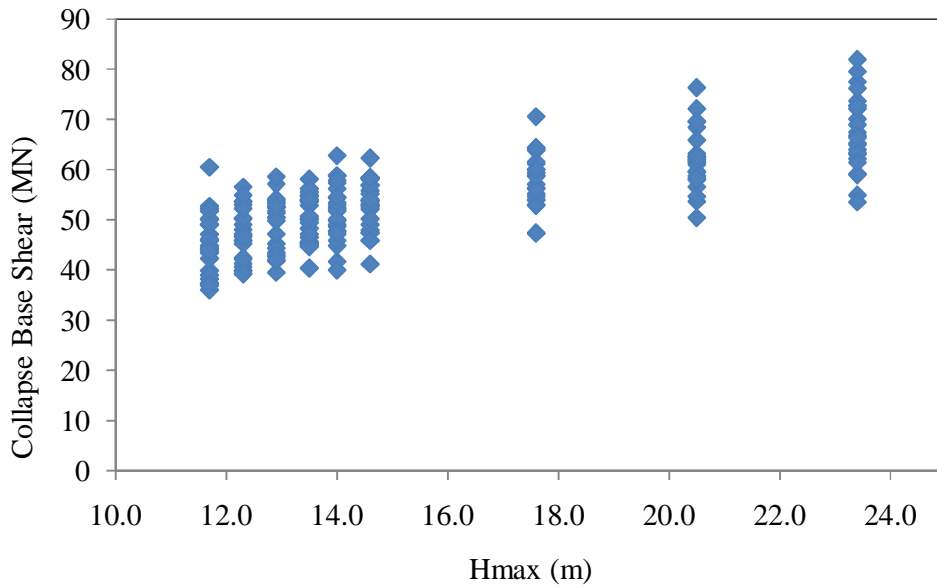


Figure 7.39: Collapse Base Shear against Wave Direction at SKO2

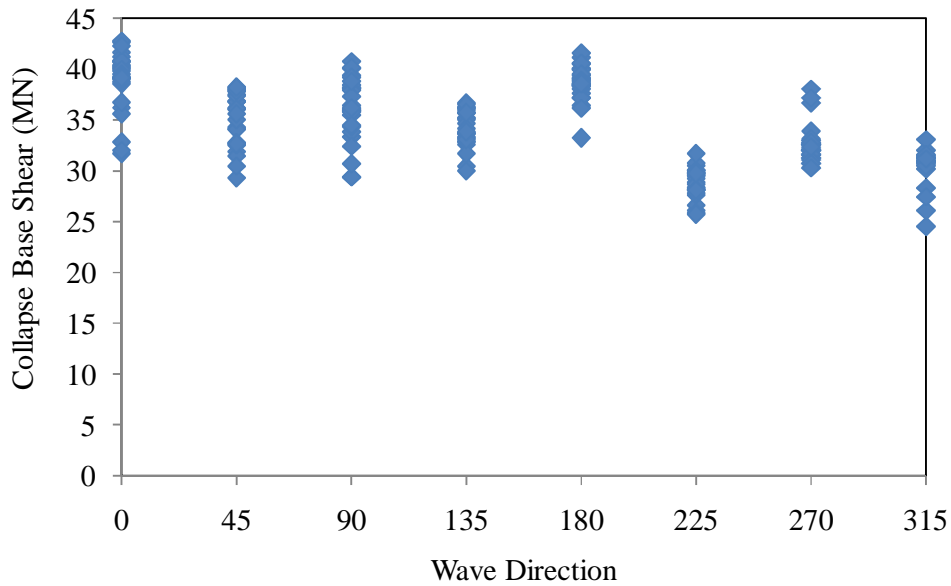


Figure 7.40: Collapse Base Shear against Wave Direction at SKO2a

7.4.3 Wave Directional Effects on Collapse Base Shear

Figures 7.41 - 7.48 show the effect of collapse base shear against H_{max} with varying current speed in eight directions for PMO region. Here effect of each wave height was placed separately. Collapse base shear varied as wave heights increase, due to

system strength of Jacket. The effect of directions was predominant in all cases. Results from SBO, SKO1 and SKO2, SKO2a regions are shown in Appendix C.

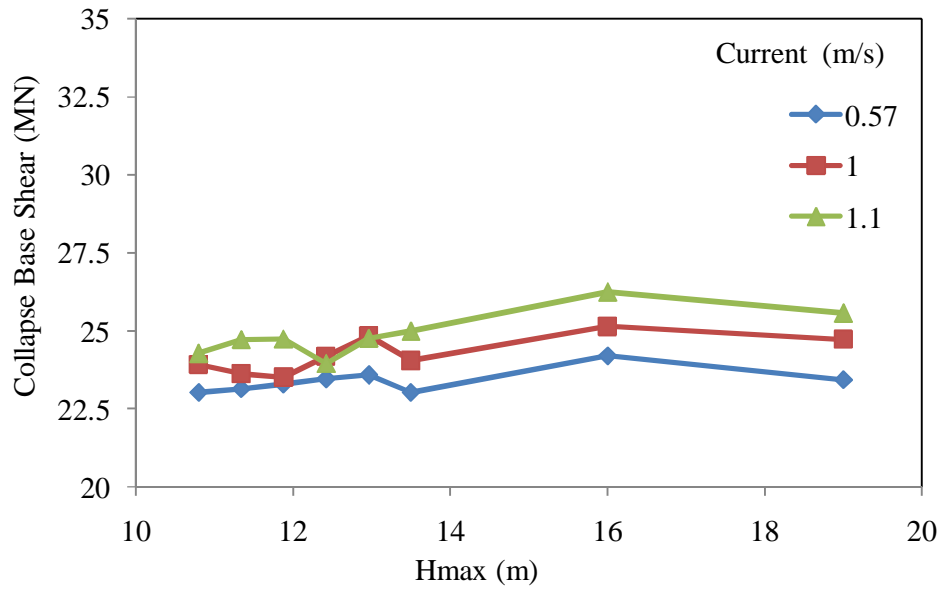


Figure 7.41: Collapse Base Shear against H_{max} Wave with Varying Currents for PMO for 0 Degree

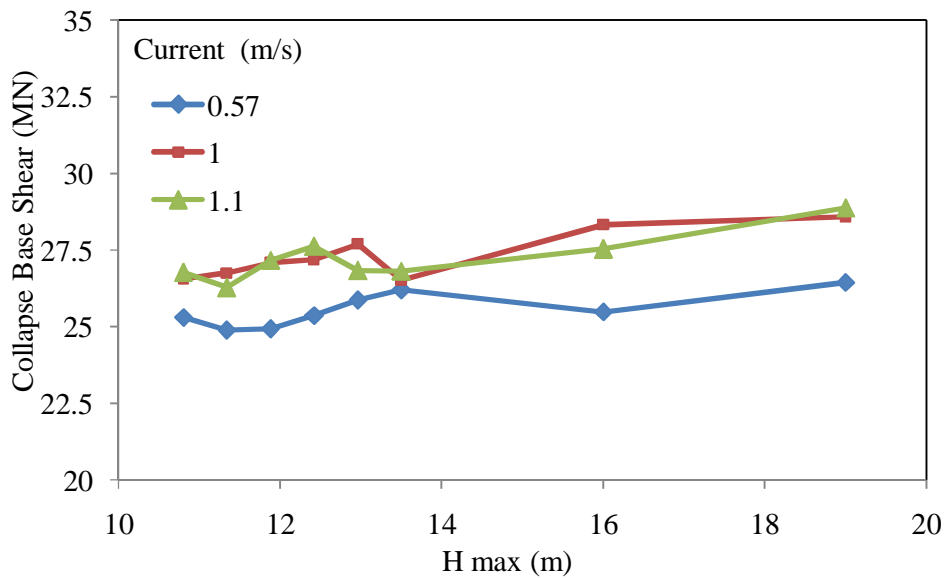


Figure 7.42: Collapse Base Shear against H_{max} Wave with Varying Currents for PMO for 45 Degree

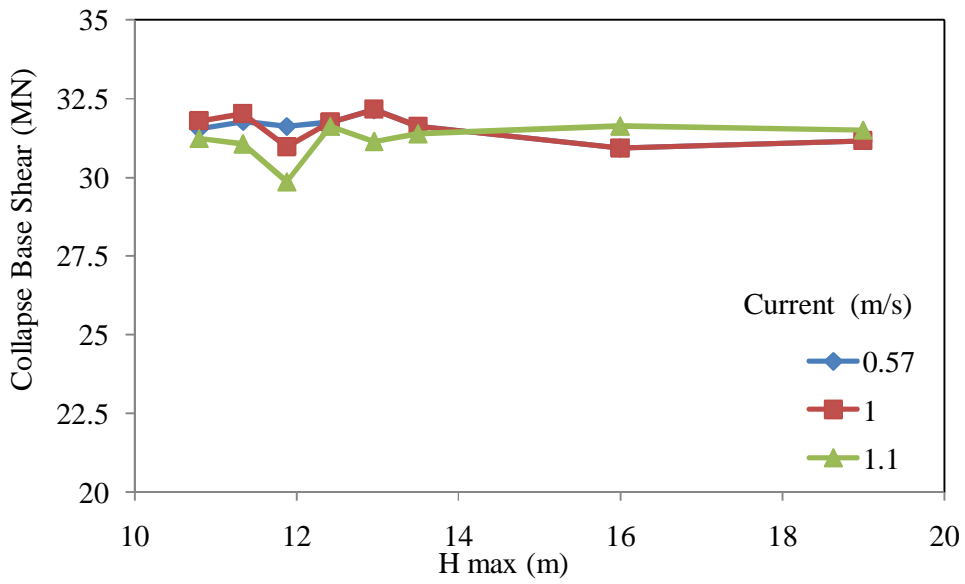


Figure 7.43: Collapse Base Shear against H_{\max} Wave with Varying Currents for PMO for 90 Degree

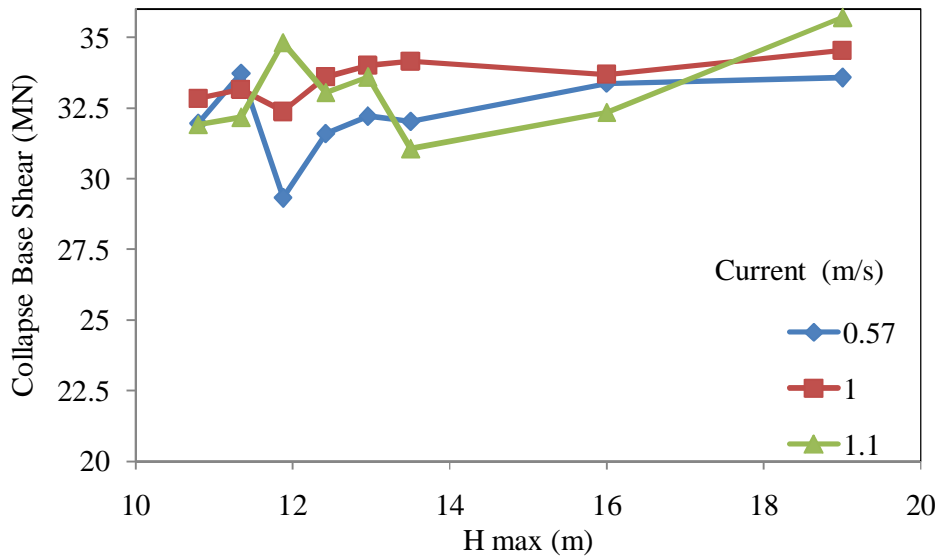


Figure 7.44: Collapse Base Shear against H_{\max} Wave with Varying Currents for PMO for 135 Degree

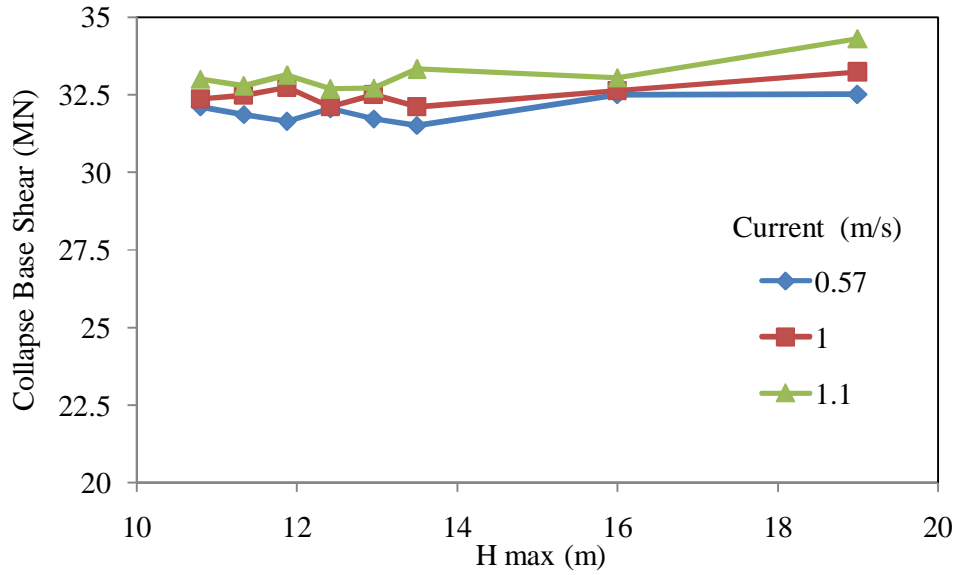


Figure 7.45: Collapse Base Shear against H_{max} Wave with Varying Currents for PMO for 180 Degree

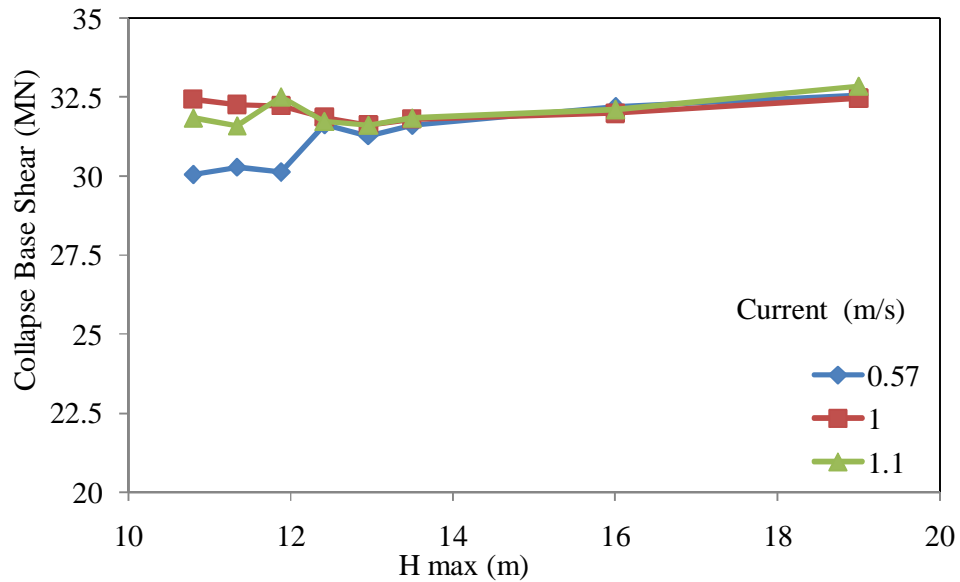


Figure 7.46: Collapse Base Shear against H_{max} Wave with Varying Currents for PMO for 225 Degree

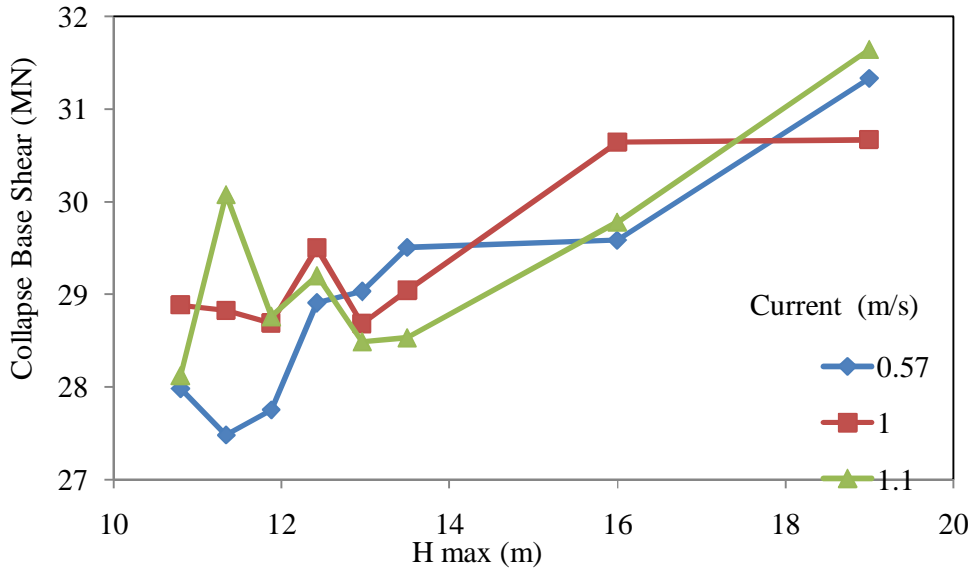


Figure 7.47: Collapse Base Shear against H_{\max} Wave with Varying Currents for PMO for 270 Degree

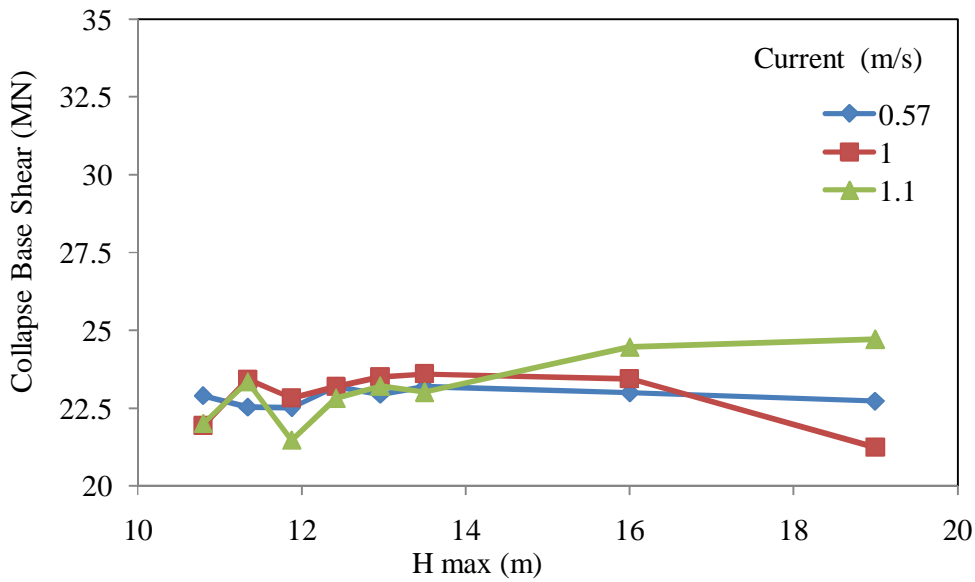


Figure 7.48: Collapse Base Shear against H_{\max} Wave with Varying Currents for PMO for 315 Degree

7.4.4 System Redundancy

Appendix G shows the system redundancy against the wave loads. It shows that system redundancy did not depend on increased wave heights. It was the direction of wave which played important role in this regard.

7.5 Updating the Probability of Failure

Evaluating of probability of failure becomes extremely important in case of any damage to the Jacket, change of loading pattern, application of new loads, routine check-up after some years or when extension of life is required. Most of the existing Jacket platforms in offshore Malaysia have already completed their life and they are constantly being evaluated for extension of life. Here first probability of failure was checked for design and 10,000 year load. The Bayesian updating technique was applied for evaluating of the probability of failure at design load and extremely high load when RSR of Jacket equals to 1.0.

7.5.1 Sensitivity Analysis

The effect of uncertainty has already been seen in Chapter 4 for load and resistance. Here effects of load and resistance model uncertainty on overall system probability of failure are evaluated.

7.5.1.1 Effect of Load Uncertainty Model

Figures 7.49 - 7.53 show the effect on uncertainty model due to load with resistance model uncertainty of 5% and 10% and RSR of 1.5 and 2.0. When RSR was 2, probability of failure was decreasing as compared to RSR of 1.5. The variability in load model uncertainty lies between 10% - 40%. The variability of probability of failure with RSR of 1.5 was 1×10^{-2} to 1×10^{-6} . With RSR of 2.0 this varied from 1×10^{-3} to 1×10^{-8} . Even with resistance model, when variability was kept constant at 10%, the variability at RSR of 1.5 was between 1×10^{-2} to 1×10^{-4} and with RSR of 2.0

this variability reaches to 1×10^{-3} to 1×10^{-7} . This shows that the effects of the parameters of reliability are high and thus fixed target reliability was difficult to achieve for Jacket platforms. Thus it can be said that reliability is always based on personal judgment.

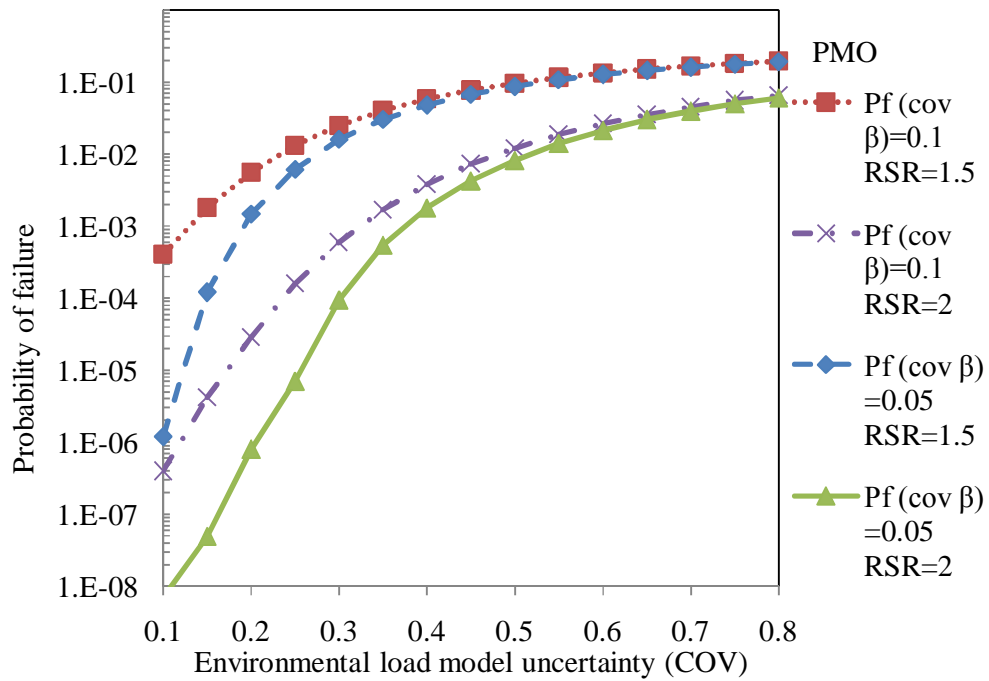


Figure 7.49: Variation of Load Model Uncertainty on Resistance Model Uncertainty at PMO

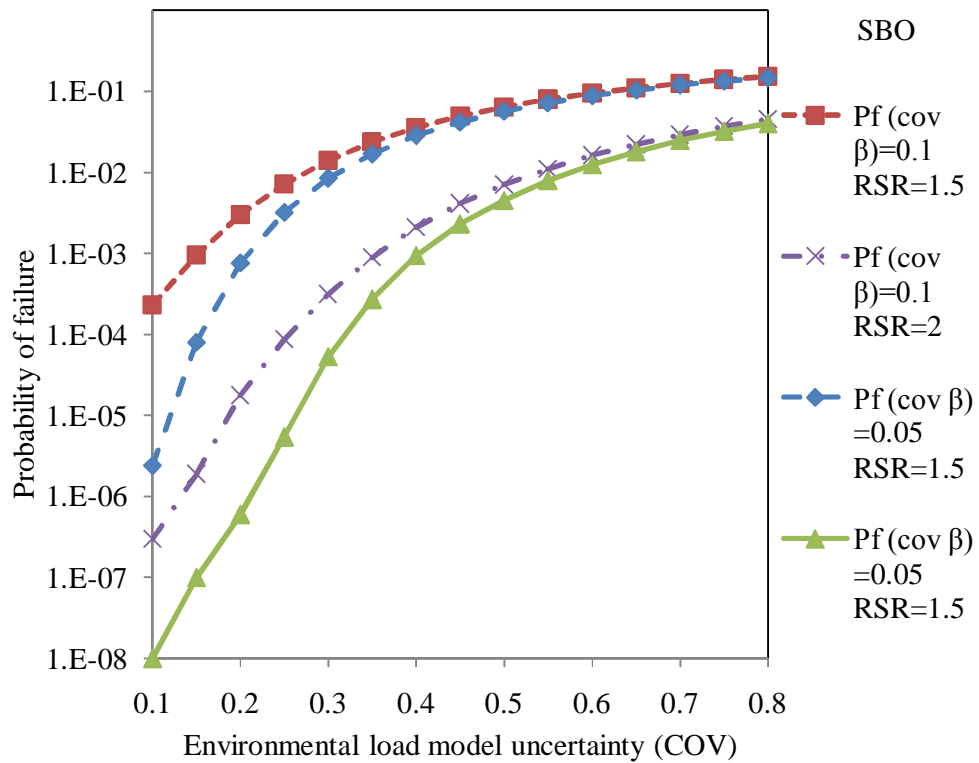


Figure 7.50: Variation of Load Model Uncertainty on Resistance Model Uncertainty at SBO

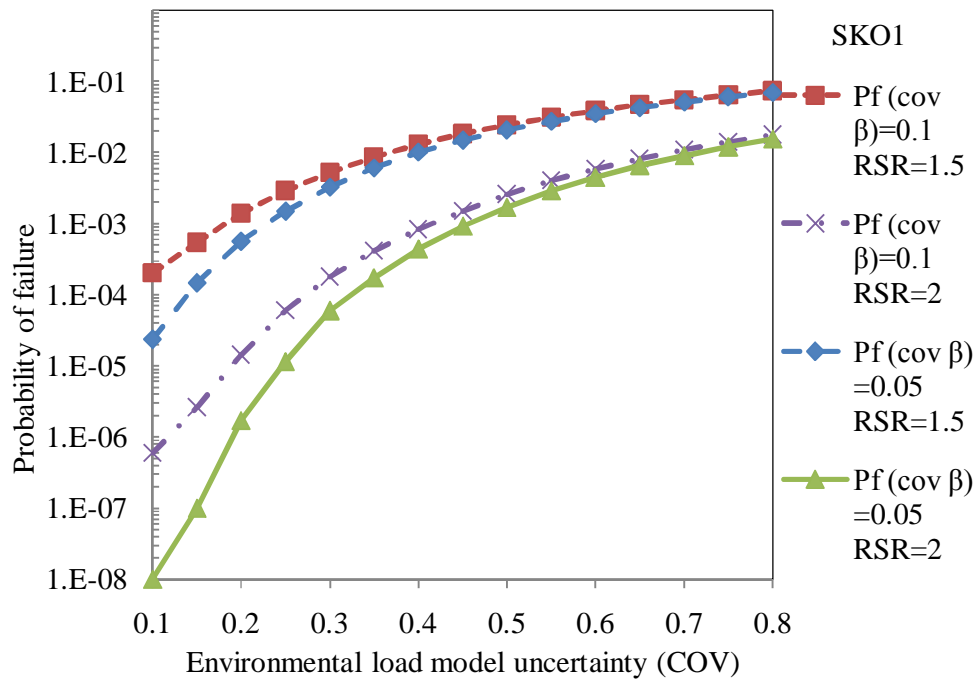


Figure 7.51: Variation of Load Model Uncertainty on Resistance Model Uncertainty at SKO1

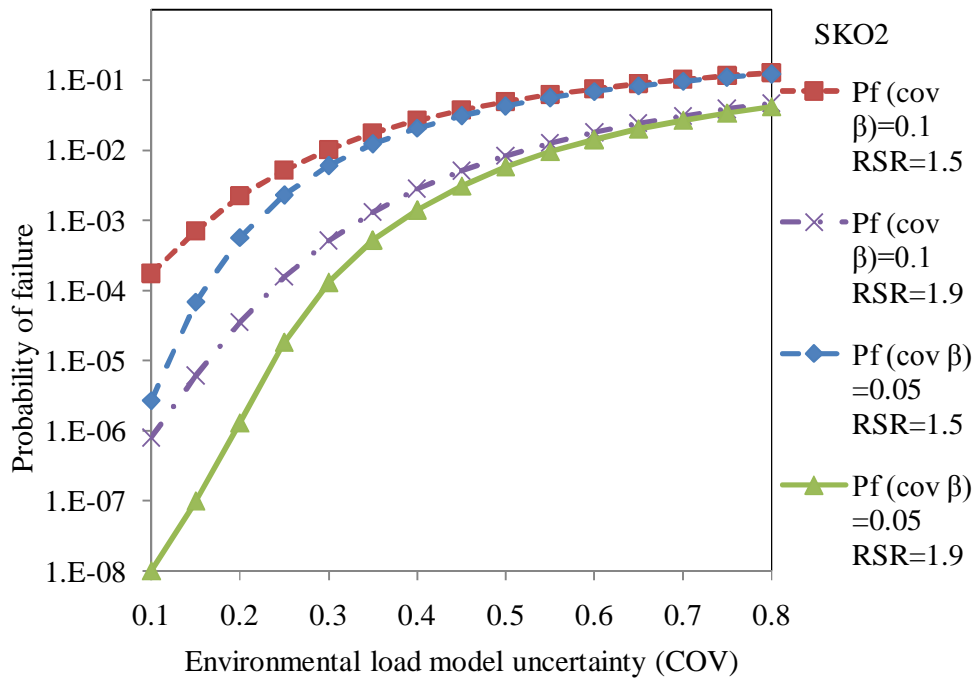


Figure 7.52: Variation of Load Model Uncertainty on Resistance Model Uncertainty at SKO2

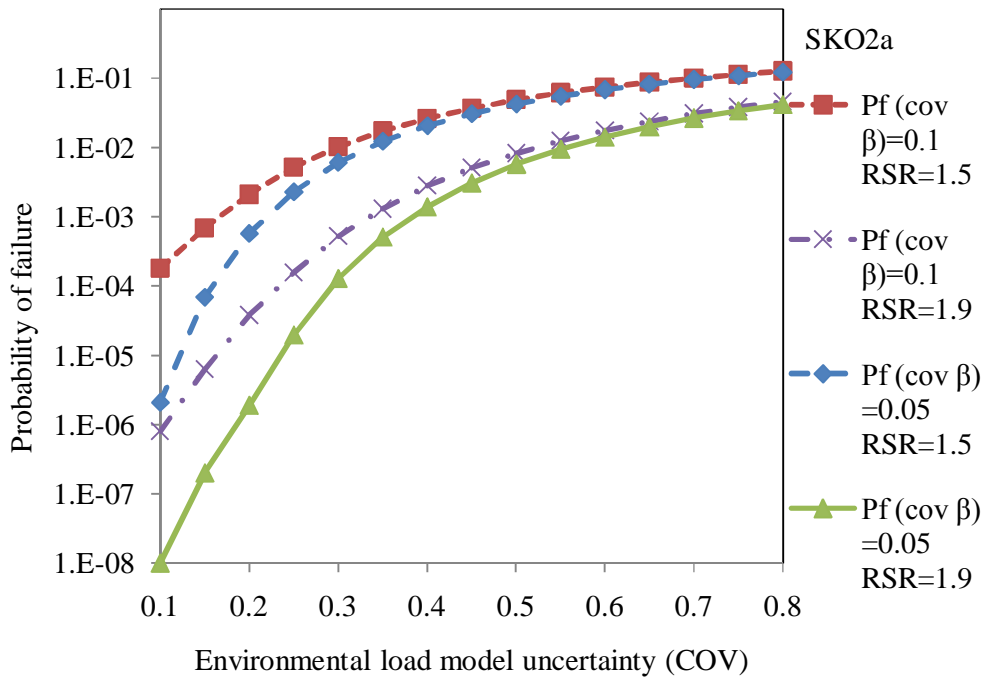


Figure 7.53: Variation of Load Model Uncertainty on Resistance Model Uncertainty at SKO2a

7.5.1.2 Probability of Failure and RSR Sensitivity

Figures 7.54 - 7.58 show the effect of RSR on probability of failure with load model uncertainty in range of 0.15-0.45. The Figures show that the risk increase with reduction in RSR value i.e. probability of failure decreased sharply with increase of RSR. It shows that with RSR value of 2.5, the risk became extremely rare with probability of failure reaching up to 1×10^{-8} for COV of load of 0.15. In case of COV of 0.45, the probability of failure reached up to 1×10^{-4} with RSR of 2.5. Here in this study, COV of 0.15 on load was used and that was the reason why RSR value of 1.5-2.5 was considered safe for analysis. This results in minimum RSR in range of 2.0-2.5 and depends on COV of load model uncertainty.

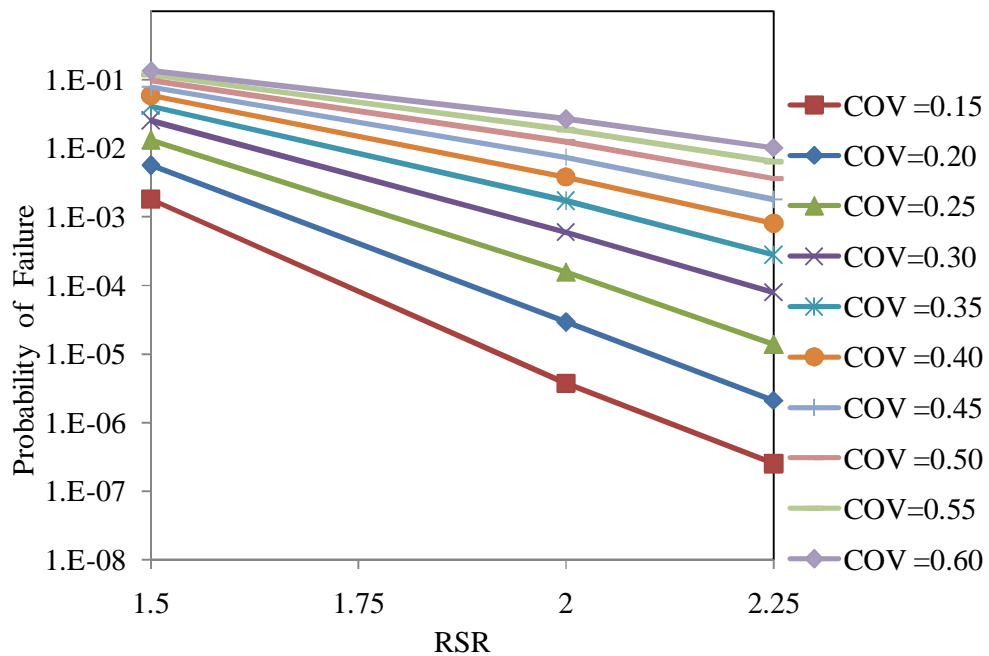


Figure 7.54: Variation of Load Model Uncertainty and RSR on Probability of Failure, with $\beta=0.10$ at PMO

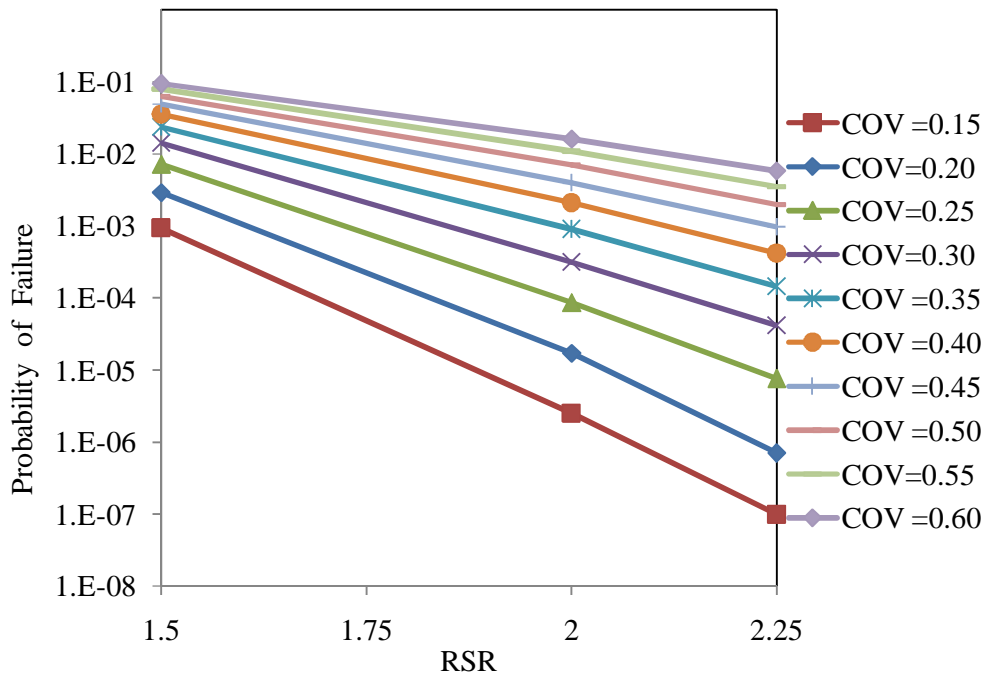


Figure 7.55: Variation of Load Model Uncertainty and RSR on Probability of Failure, with $\beta=0.10$ at SBO

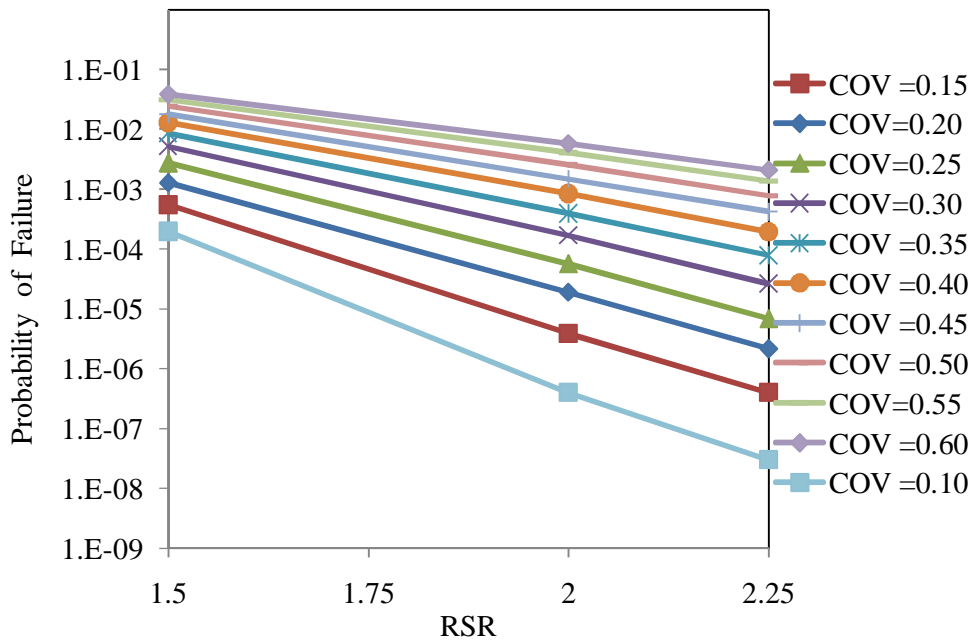


Figure 7.56: Variation of Load Model Uncertainty and RSR on Probability of Failure, with $\beta=0.10$ at SKO1

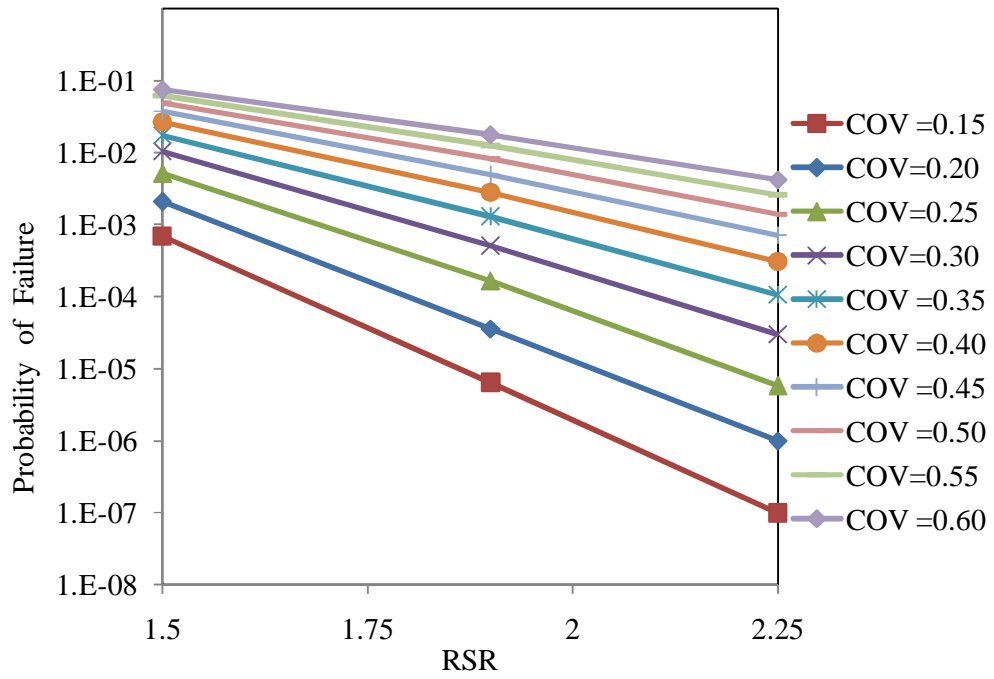


Figure 7.57: Variation of Load Model Uncertainty and RSR on Probability of Failure, with $\beta=0.10$ at SKO2

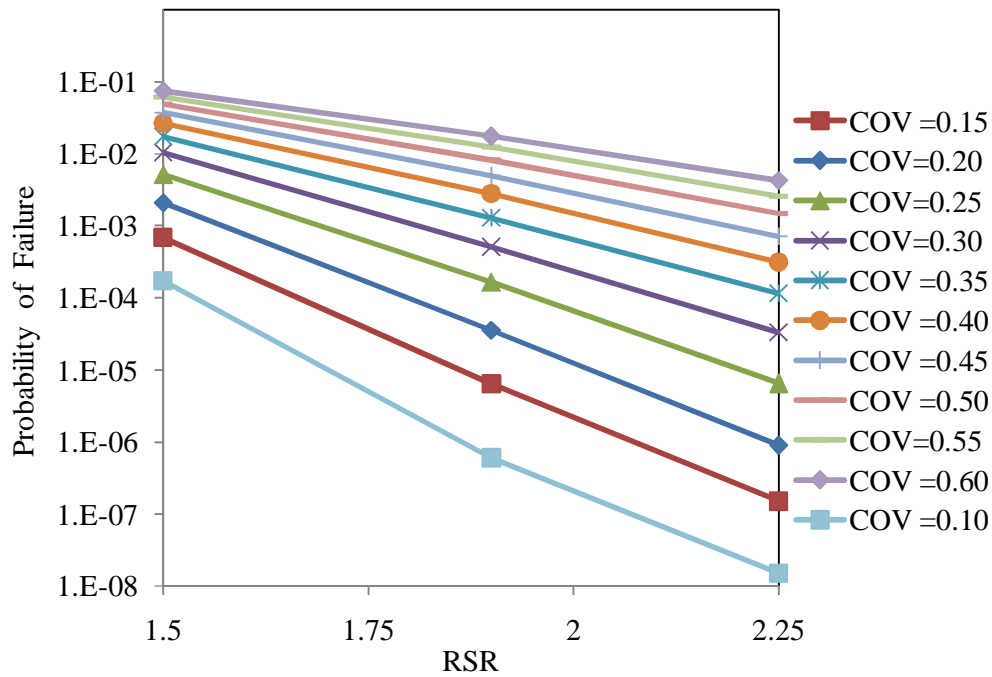


Figure 7.58: Variation of Load Model Uncertainty and RSR on Probability of Failure, with $\beta=0.10$ at SKO2a

7.5.1.3 *Effect of Model Uncertainty of Environmental Load on Probability of Failure*

Figure 7.59 - 7.63 show the effects of experienced waves on probability of failure. The Effect of variation of wave height on probability of failure was significant with variation of COV of load model uncertainty. Failure probability increased with increase in wave height.

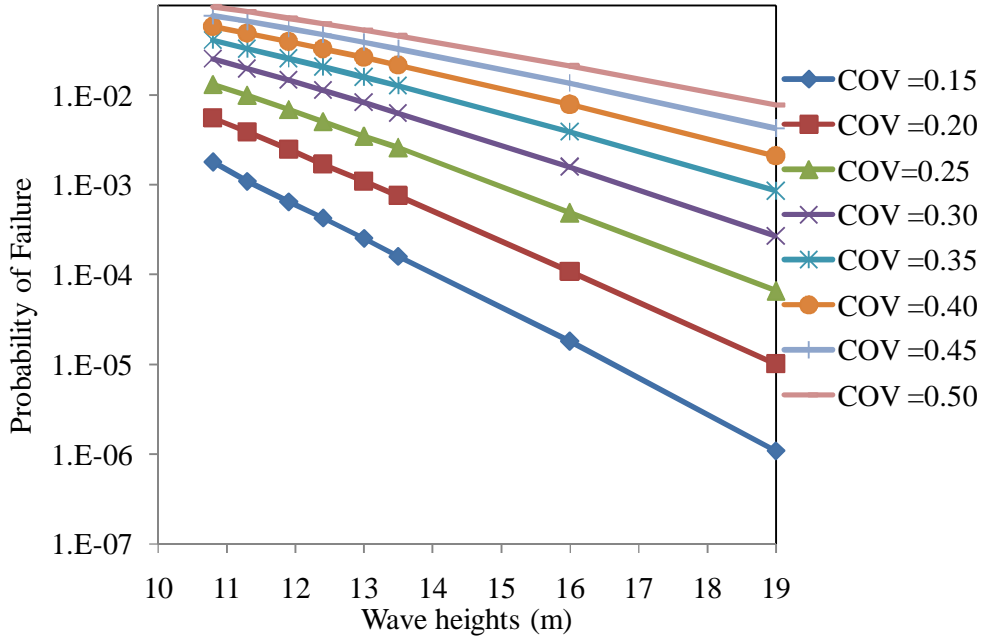


Figure 7.59: Effect of Wave Heights and Load Model Uncertainty on Probability of Failure at PMO

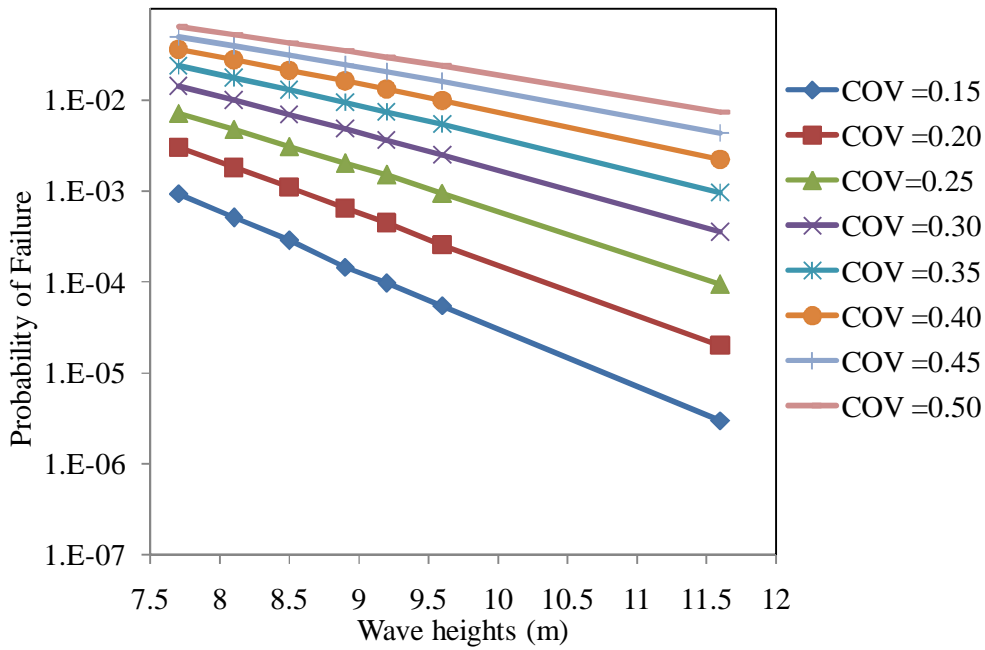


Figure 7.60: Effect of Wave Heights and Load Model Uncertainty on Probability of Failure at SBO

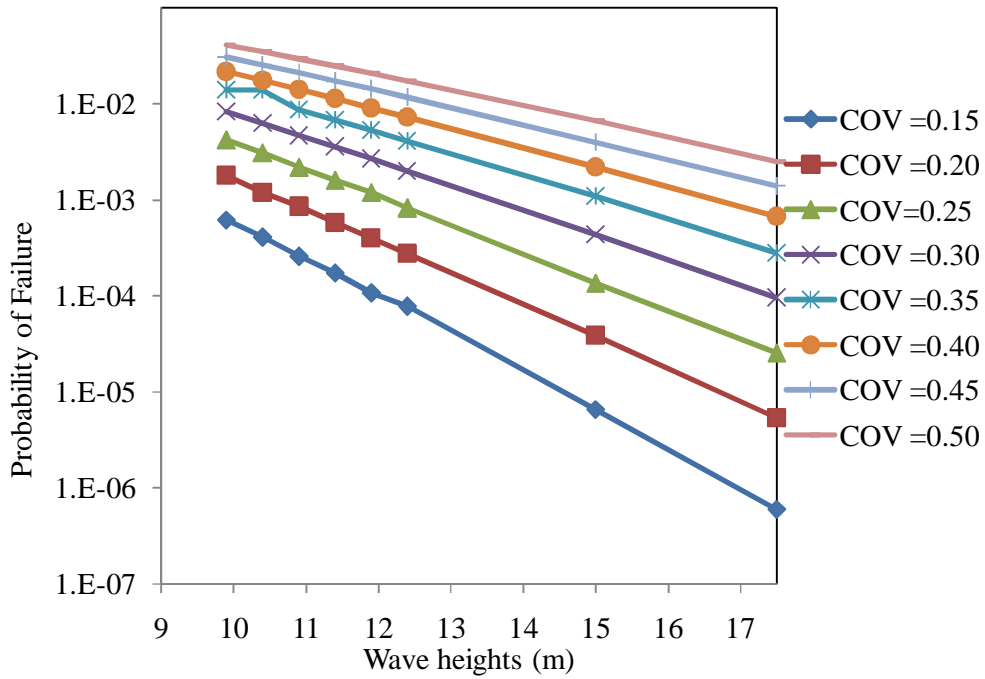


Figure 7.61: Effect of Wave Heights and Load Model Uncertainty on Probability of Failure at SKO1

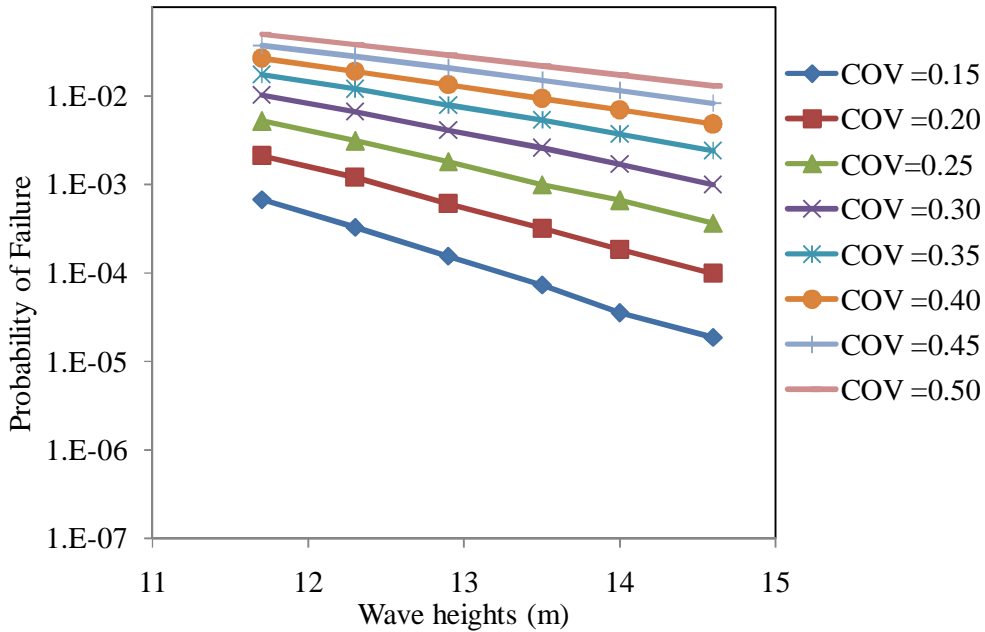


Figure 7.62: Effect of Wave Heights and Load Model Uncertainty on Probability of Failure at SKO2

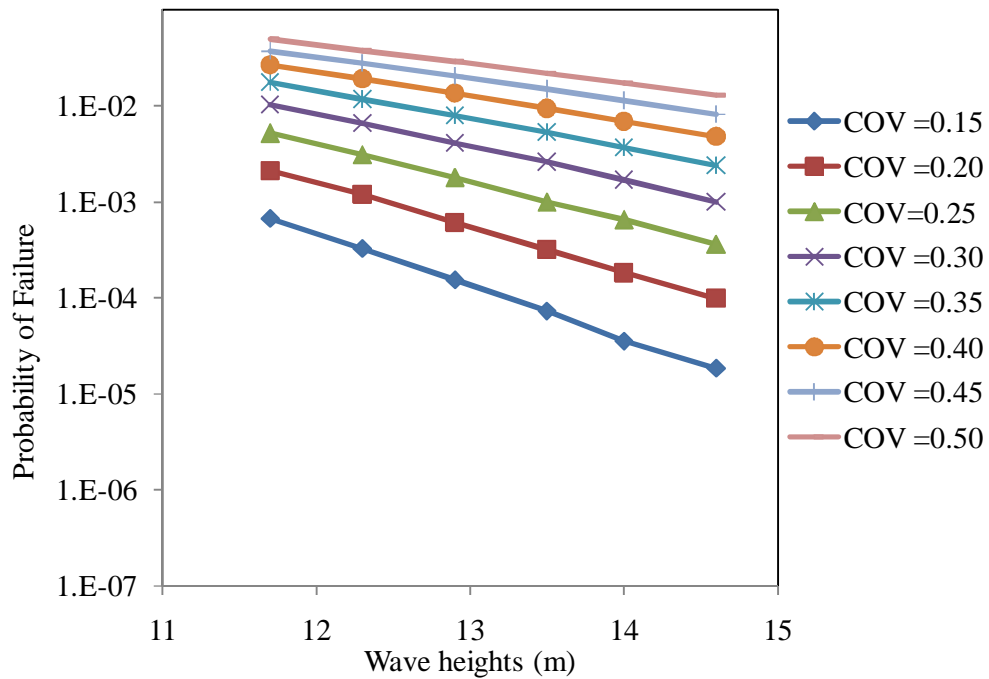


Figure 7.63: Effect of Wave Heights and Load Model Uncertainty on Probability of Failure at SKO2a

7.5.2 Bayesian Updating the Probability of Failure

The probability of failure was evaluated using an RSR value of 1.5 and 2.0. Table 7.7 and Figures 7.64 - 7.68 show the probability of failure with design load and updated probability of failure with increased load. It can be seen that with Bayesian updating, probability of failure decreases. With experienced resistance and load, it could be predicted how much load can be resisted by the Jacket. Thus extension of life as well as assessment of Jacket can be predicted. The main advantage here is that the platform is considered safe against a wave of 10,000 year return period as recommended by ISO, when updating was made. With design probability of failure, an existing Jacket at PMO cannot be recommended for extension of life if it has an RSR of 1.5, but we have seen in Table 7.2 that as it has minimum RSR of 2.0, it can be given extension of life. The same trend was observed in North Sea as shown in Figure 2.12.

Table 7.7: Design and Updated Probability of Failure

	Design Pf (RSR)=1.5	Updated Pf (RSR)=1.5	Design Pf (RSR=2.0)	Updated Pf (RSR)=2.0
PMO	9.20E-03	1.26E-03	3.01E-05	2.04E-05
SBO	9.23E-04	1.14E-04	3.00E-06	1.95E-06
SKO1	6.24E-04	1.80E-04	2.90E-06	2.48E-06
SKO2	6.78E-04	9.94E-05	5.90E-06	3.45E-06
SKO2a	6.78E-04	9.96E-05	6.70E-06	3.92E-06

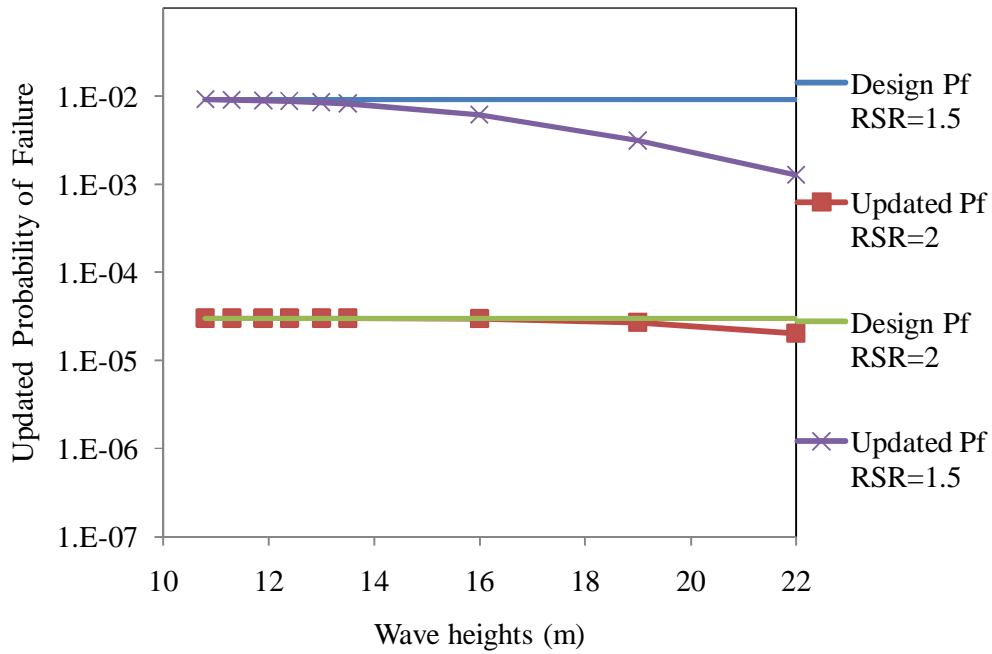


Figure 7.64: Effect Wave Heights and RSR on Updated Probability of Failure at PMO

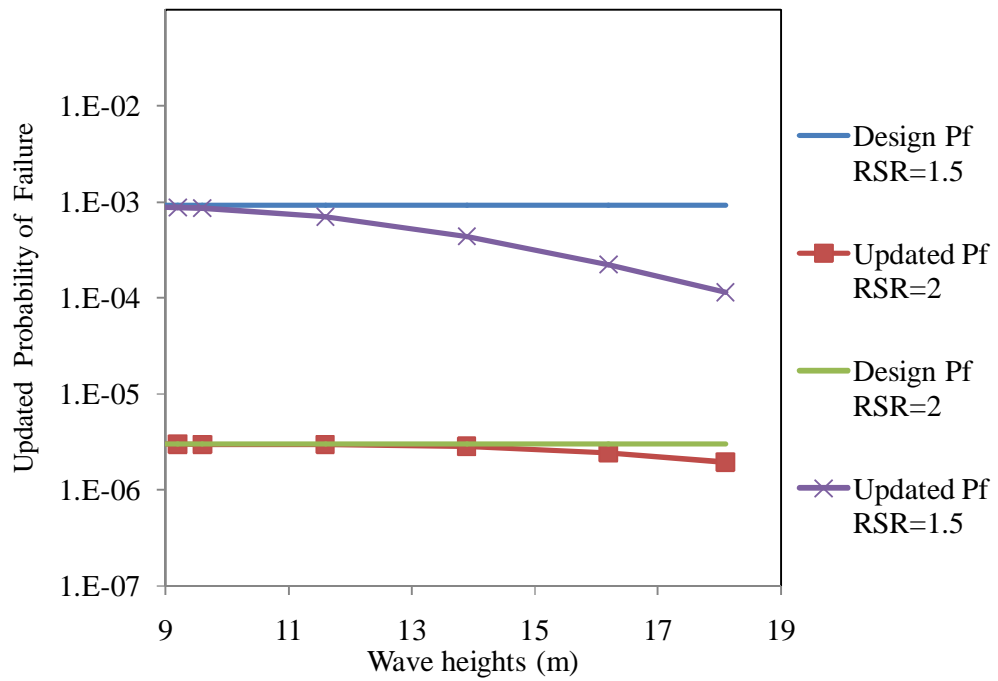


Figure 7.65: Effect Wave Heights and RSR on Updated Probability of Failure at SBO

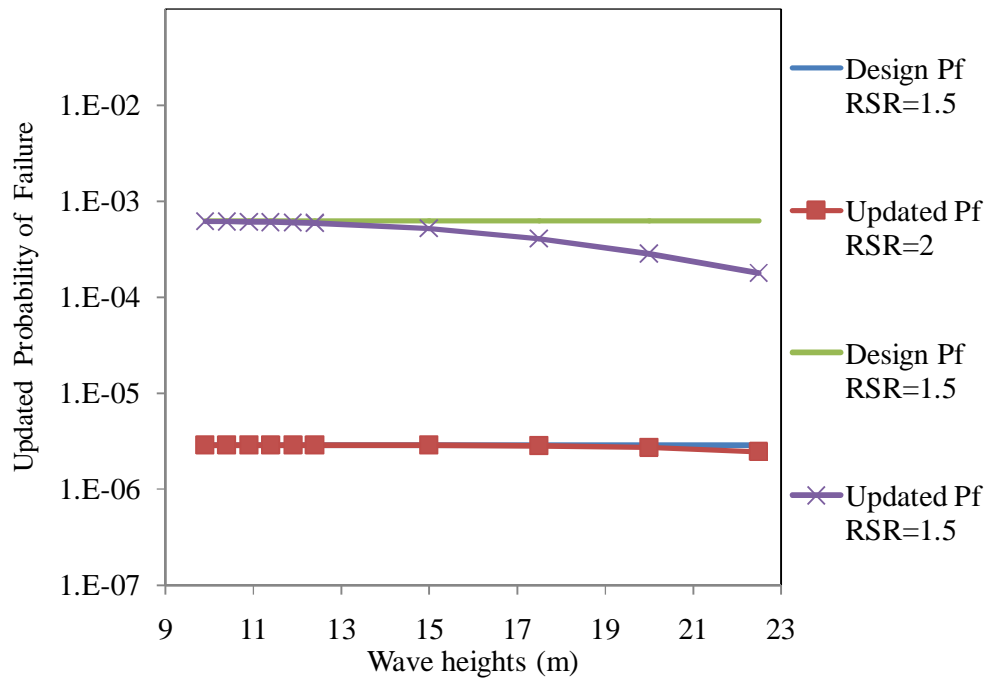


Figure 7.66: Effect Wave Heights and RSR on Updated Probability of Failure at SKO1

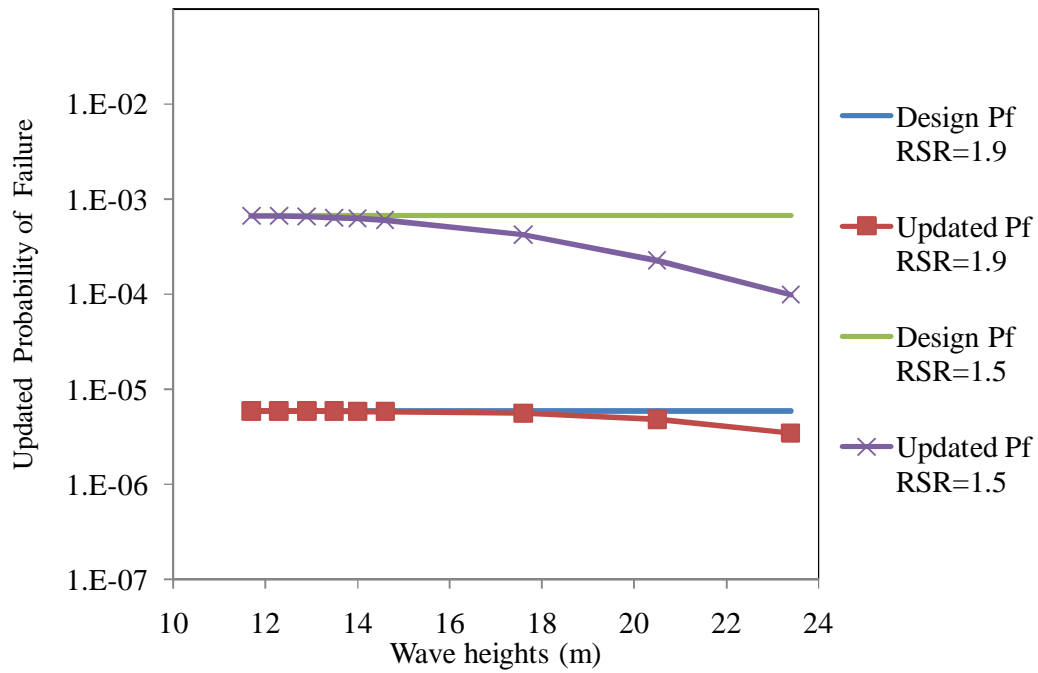


Figure 7.67: Effect Wave Heights and RSR on Updated Probability of Failure at SKO2

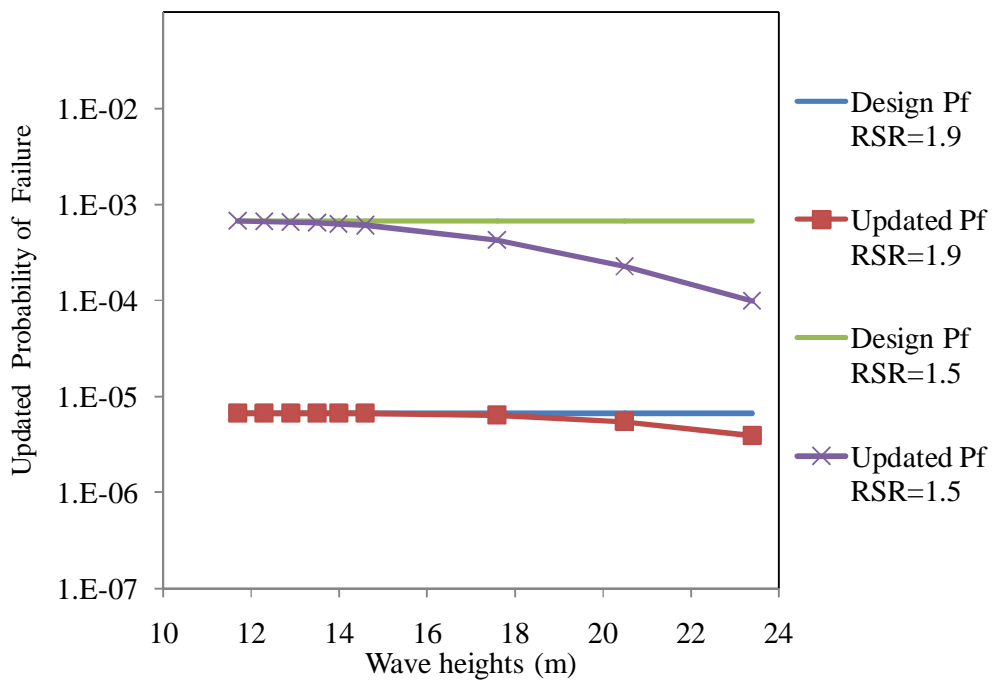


Figure 7.68: Effect Wave Heights and RSR on Updated Probability of Failure at SKO2a

7.5.3 Bayesian Updating Probability of Failure with Damaged Members

When Jacket members fail, the overall capacity of Jacket reduces as shown in Table 7.8 - 7.12. Damaged strength factor was found using Equation 3.68. This reduced capacity was used to find updated probability of failure (UPF) as shown in Figures 7.69 - 7.78. The capacity was reduced about 50% in case of three member failures and therefore probability of failure was determined up to two member failures. Table 7.13 shows that with experienced waves, the probability of failure decreases. Though in all cases probability of failure was very high, with experienced waves it decreased and reached a level where it can sustain 10,000 years load.

Table 7.8: Reduced Capacity for PMO Jacket with Damaged Members

X-Brace	Base Shear at 100 Year Load (KN)	Collapse Base Shear (KN)	Damaged Strength Ratio	Reduced Capacity Factor	Capacity Reduction
Intact	9060.0	20380.0	2.25	1.00	1.00
One Member Removed	9043.0	15822.0	1.75	0.78	0.78
Two Members Removed	9030.0	13548.0	1.50	0.67	0.67

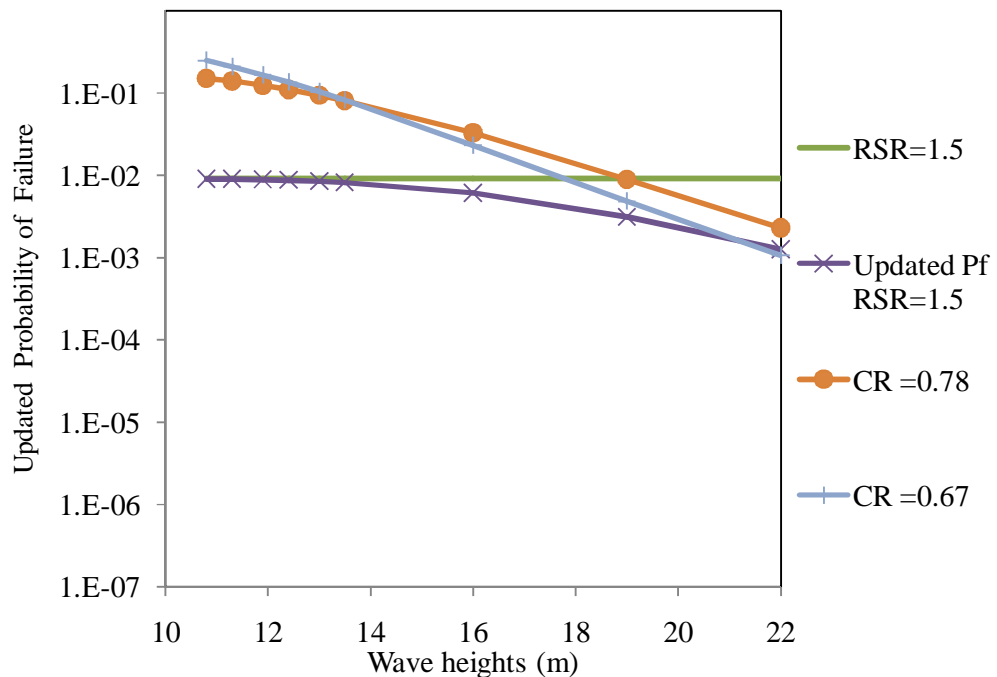


Figure 7.69: Effect of Wave Heights and Collapse Ratio on Updated Probability of Failure with Damaged Members and RSR of 1.5 at PMO

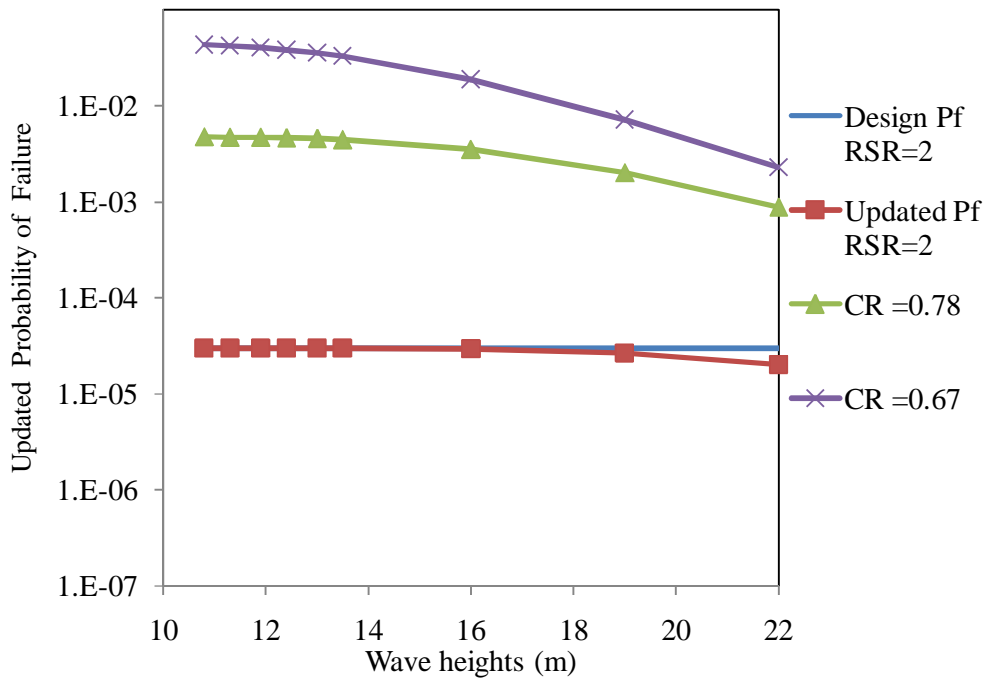


Figure 7.70: Effect of Wave Heights and Collapse Ratio on Updated Probability of Failure with Damaged Members and RSR of 2.0 at PMO

Table 7.9: Reduced Capacity for SBO Jacket with Damaged Members

X-Brace	Base Shear at 100 Year Load (KN)	Collapse Base Shear (KN)	Damaged Strength Ratio	Reduced Capacity Factor	Capacity Reduction
Intact	12636.8	35380.4	2.80	1.00	1
One Member Removed	12555.0	31387.0	2.50	0.89	0.893
Two Members Removed	12494.0	24987.0	2.00	0.80	0.714

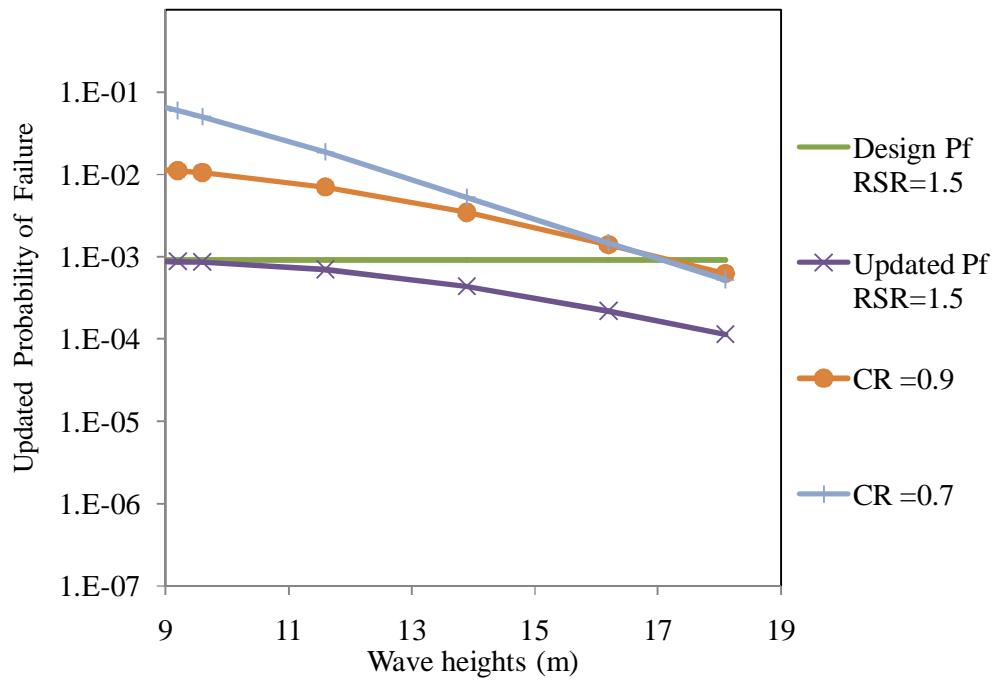


Figure 7.71: Effect of Wave Heights and Collapse Ratio on Updated Probability of Failure with Damaged Members and RSR of 1.5 at SBO

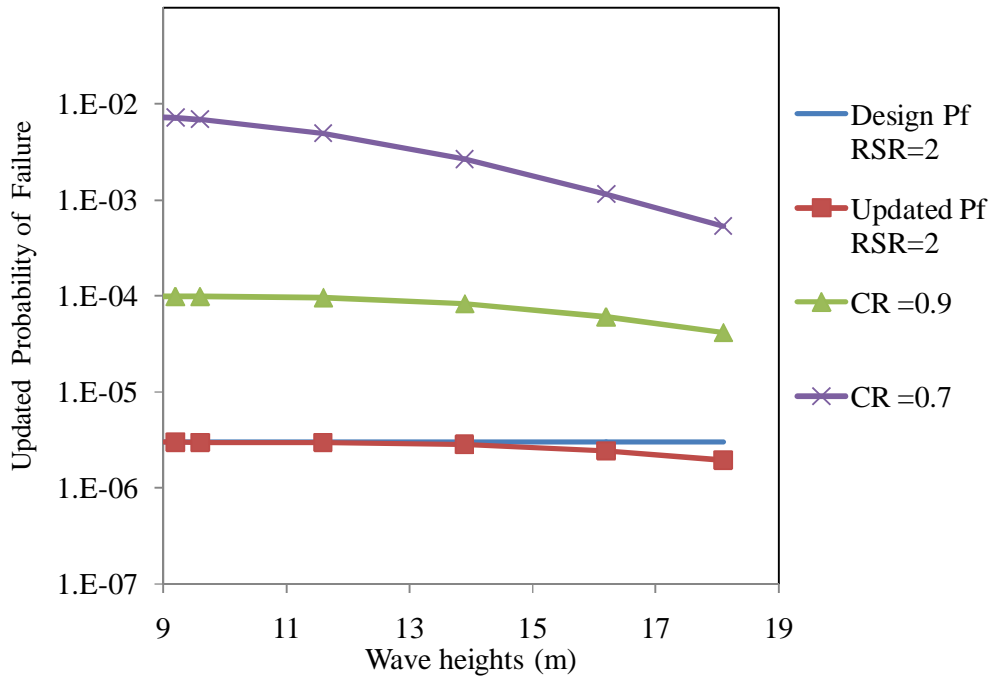


Figure 7.72: Effect of Wave Heights and Collapse Ratio on Updated Probability of Failure with Damaged Members and RSR of 2.0 at SBO

Table 7.10: Reduced Capacity for SKO1 Jacket with Damaged Members

X-Brace	Base Shear at 100 Year Load (KN)	Collapse Base Shear (KN)	Damaged Strength Ratio	Reduced Capacity Factor	Capacity Reduction
Intact	8000	18022	2.25	1.00	1
One Member Removed	7932.0	15904.0	2.01	0.89	0.89
Two Members Removed	7833.0	13714.0	1.75	0.87	0.78

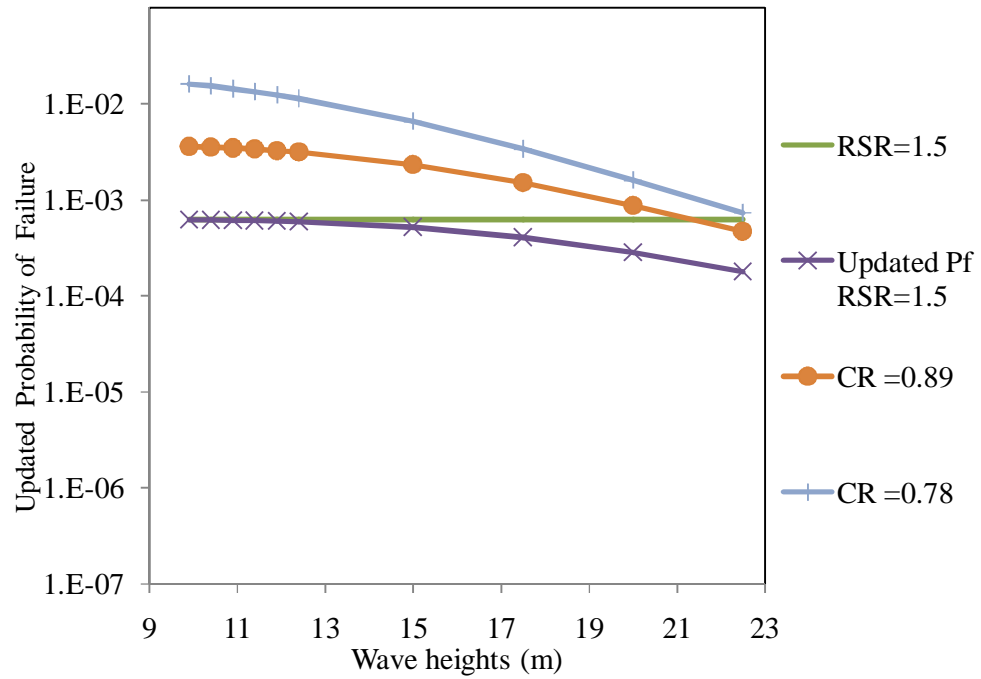


Figure 7.73: Effect of Wave Heights and Collapse Ratio on Updated Probability of Failure with Damaged Members and RSR of 1.5 at SKO1

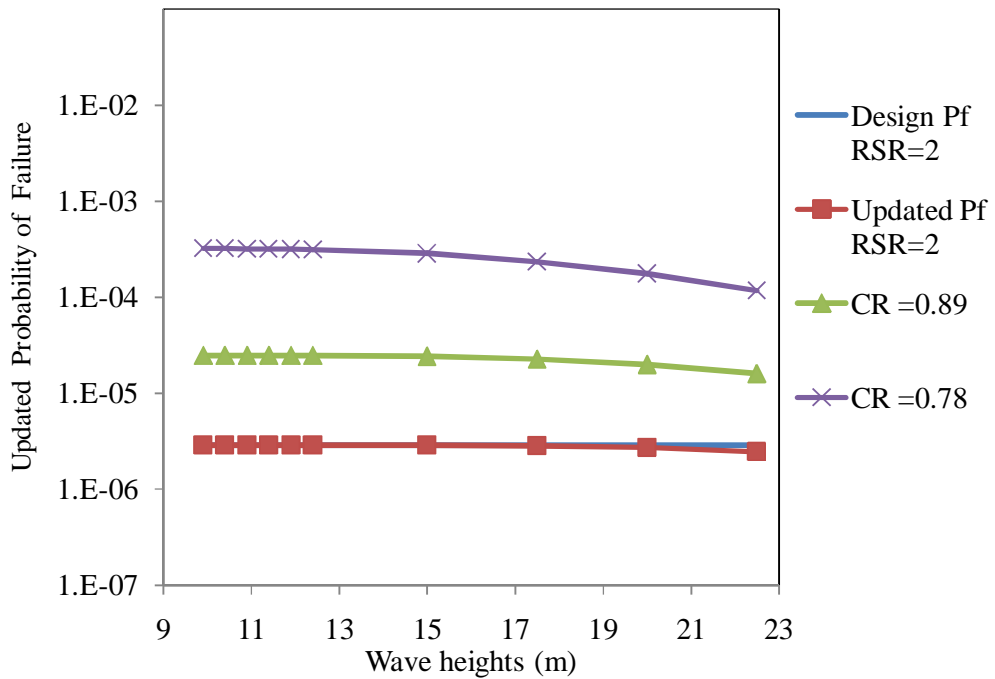


Figure 7.74: Effect of Wave Heights and Collapse Ratio on Updated Probability of Failure with Damaged Members and RSR of 2.0 at SKO1

Table 7.11: Reduced Capacity for SKO2 Jacket with Damaged Members

X-Brace	Base Shear at 100 Year Load (KN)	Collapse Base Shear (KN)	Damaged Strength Ratio	Reduced Capacity Factor	Capacity Reduction
Intact	9752.54	21215	2.18	1.00	1
One Member Removed	9739.0	21660.0	2.22	1.02	1.02
Two Members Removed	9738.0	19253.0	1.98	0.89	0.91

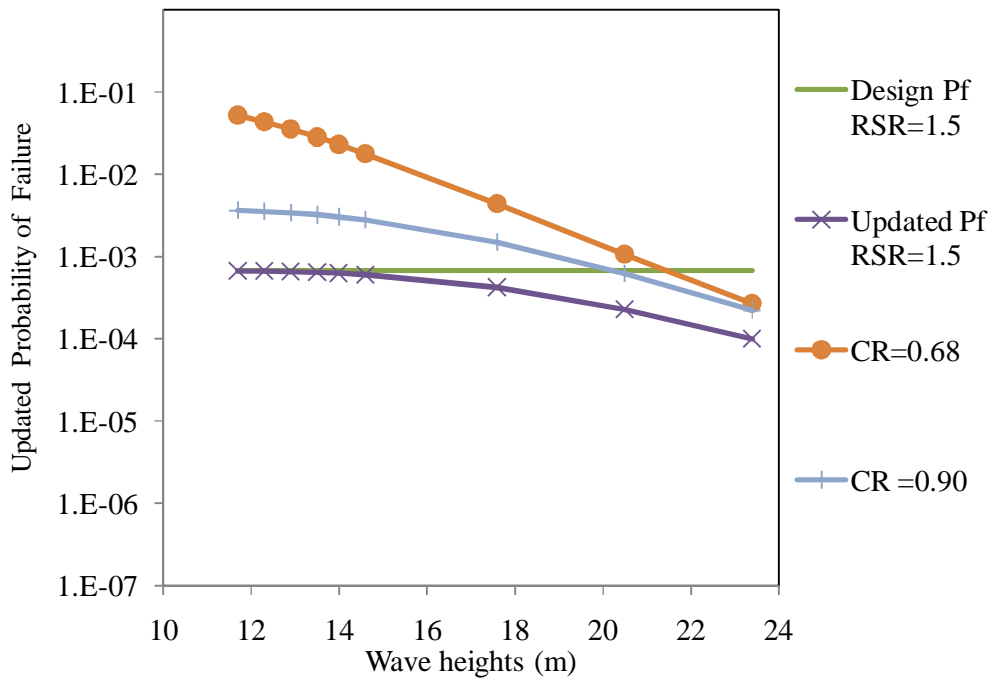


Figure 7.75: Effect of Wave Heights and Collapse Ratio on Updated Probability of Failure with Damaged Members and RSR of 1.5 at SKO2

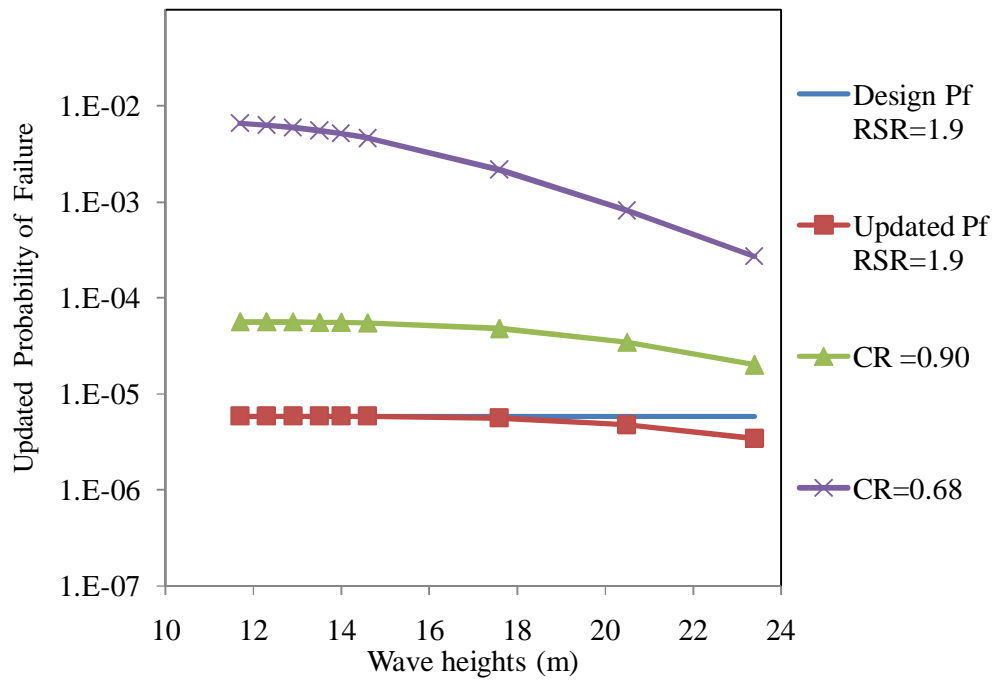


Figure 7.76: Effect of Wave Heights and Collapse Ratio on Updated Probability of Failure with Damaged Members and RSR of 2.0 at SKO2

Table 7.12: Reduced Capacity for SKO2a with Damaged Members

X-Brace	Base Shear at 100 Year Load (KN)	Collapse Base Shear (KN)	Damaged Strength Ratio	Reduced Capacity Factor	Capacity Reduction
Intact	8141	20857	2.56	1.00	1
One Member Removed	9758.0	21650.0	2.22	0.87	0.87
Two Members Removed	9756.0	19271.0	1.98	0.89	0.77

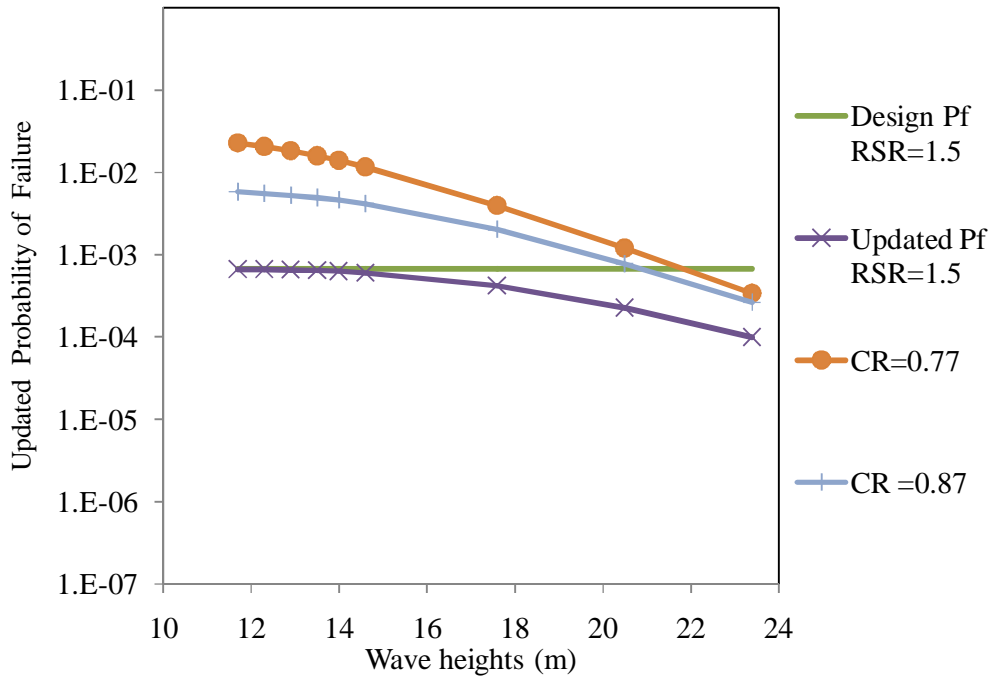


Figure 7.77: Effect of Wave Heights and Collapse Ratio on Updated Probability of Failure with Damaged Members and RSR of 1.5 at SKO2a

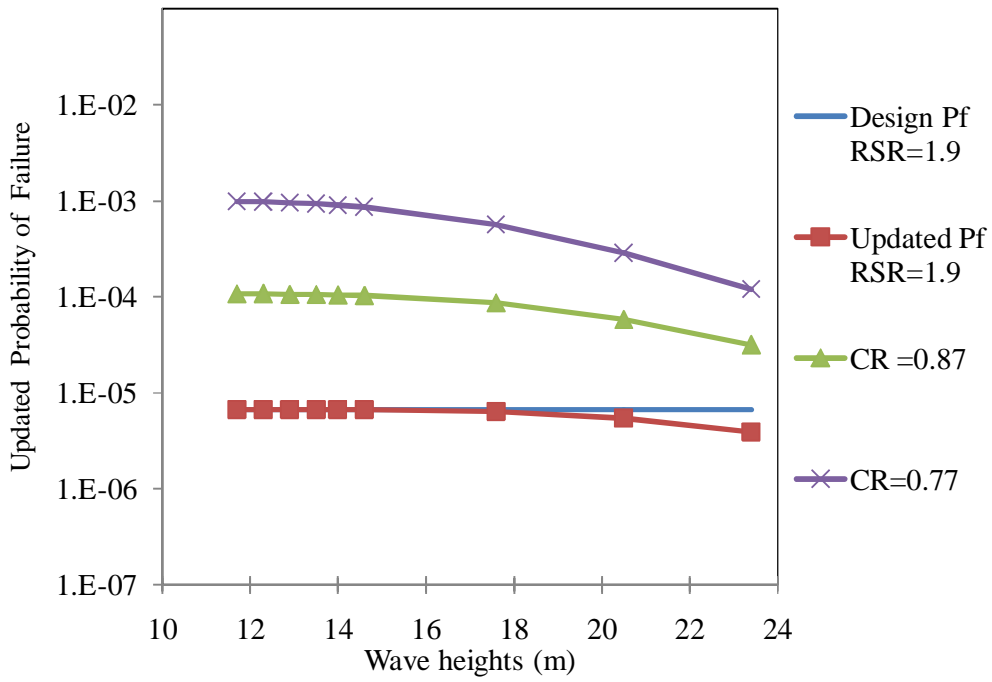


Figure 7.78: Effect of Wave Heights and Collapse Ratio on Updated Probability of Failure with Damaged Members and RSR of 2.0 at SKO2a

Table 7.13: Probability of Failure of Jacket with Damaged Members

Regions	Collapse Ratio	RSR	
		1.5	2.0
PMO	0.78	2.30E-03	8.91E-04
	0.67	1.08E-03	2.30E-03
SBO	0.9	6.25E-04	4.17E-05
	0.7	5.26E-04	5.38E-04
SKO1	0.89	4.70E-04	1.62E-05
	0.78	7.36E-04	1.18E-04
SKO2	0.9	5.90E-06	2.01E-05
	0.68	3.45E-06	2.73E-04
SKO2a	0.87	6.70E-06	3.15E-05
	0.77	3.92E-06	1.20E-04

7.6 Chapter Summary

Once component and joint environmental load has been evaluated it becomes mandatory to assess the load factor for Jacket using system strength and RSR. Here we were interested for minimum RSR as this would give us the most economical Jacket. The minimum RSR specified by API WSD and ISO 19902 is 1.58 and 1.85 respectively. The minimum RSR are compared with return period of load. PMO region has minimum RSR of 2.0, SBO has 2.8, SKO1 has 2.25, SKO2 2.18 and SKO2a 2.54. In this study RSR of 1.5, 2.0 and 2.5 were considered, as higher values will give costly and non-economical Jackets.

The load factor was determined for all three regions and four Jacket platforms. Due to system ductility with given RSR, the environmental load factor was much lower as compared to component and joint. For system, the target reliability index was 4.0 and 3.8 based on notional system reliability index proposed by Efthymiou and Melchers respectively. The load factor evaluated for all regions was found to be 1.1, with W_e/G ratio of 1.0. The same trend of component and joint was present for reliability index of system with regards to W_e/G ratios. The reliability index decreased with increase of environmental load. The load factor of 1.1 can be proposed for offshore Malaysia using the referred target reliability.

Furthermore collapse analysis was made to evaluate the effect of waves against collapse base shear. When Jacket platforms reaches their design age of 30 years, and hydro carbon resources are still there to be extracted, then it becomes mandatory to evaluate the strength of Jacket based on system reliability. The ISO and API have set criteria for checking the system strength integrity assessment of Jacket. Failure of Jacket platforms due to overloading from wave and current action was considered here.

Existing platforms after surviving severe environmental load for some years were found to be very safe against such loads. The increase of load becomes significant after higher wave heights due to wave forces striking the deck of topside. High RSR values show how strong these platforms are designed. The updating of probability of failure showed its advantages over non-updated probability of failure.

CHAPTER 8 CONCLUSIONS AND RECOMMENDATIONS

8.1 Summary

The codes of practice for API WSD and ISO LRFD were used to find the reliability of Jacket platforms in Malaysia. ISO code is based on LRFD methodology and its benefits are shown in Chapter 2, where its advantages were highlighted for design of Jackets in offshore Malaysia. ISO code requires that environmental load factors should be location dependent. This demands that resistance and load uncertainty should be determined first. Then based on this uncertainty, environmental load factors should be ascertained using component, joint and system reliability. To study further, reassessment of Jacket strength was performed using design load probability of failure with 10,000 year return period load. Probability of failure was updated using Bayesian updating technique with higher loads. The main conclusions, findings and achievements are listed as below:

8.1.1 Uncertainty

8.1.1.1 (a) Resistance Uncertainty

Resistance variable played an important role for the reliability analysis specially yield strength which was shown through sensitivity analysis in Chapter 5. Although difference was very little between normal and lognormal distribution, using Anderson-Darling and Kolmogorov-Smirnov fitting tests, the best fit was taken for reliability analysis. Thus the best fit was Gaussian distribution in all cases.

The other variables were thickness, diameter, tensile strength and elongation and their properties have been evaluated. Statistical models were developed using ISO code stress Equations for component and joints resistance. The model Equations were used to find the variability in types of stresses. As the basic distribution was Gaussian, the uncertainty models were also Gaussian.

8.1.1.2 (b) *Environmental Load Uncertainty*

The reliability determination requires that distribution parameters should be used for uncertain random load variables. The main focus of this research was based on extreme values and therefore extreme value distributions were used to fit the data. For this purpose, two types of extreme value distributions i.e. Weibull and Gumbel were used to fit the statistical parameters for wave, wind and current. The data used here was based on 10 and 100 years. Gumbel distribution overestimated the mean value parameters of environmental load. Therefore Weibull two parameter distribution was recommended for the reliability analysis of Jacket platforms in offshore Malaysia.

8.1.2 Load Factors

8.1.2.1 *Component Reliability and Environmental Load Factor*

Component reliability was found for Jacket platforms using API WSD and ISO LRFD codes. Environmental load factor for different regions are shown below:

- For the platform in PMO region were in the range of 1.15 - 1.27.
- For the platform in SBO region were in the range of 1.23 - 1.27.
- For the platform SKO1 in SKO region were in the range of 1.15 - 1.26.
- For the platform SKO2 in SKO region were in the range of 1.14 - 1.24.

The average load factor of 1.25 is recommended for Jacket platforms in offshore Malaysia based on the target reliability index of 3.96. The resistance factor was

checked with proposed load factor of 1.25. It was found that there was no significant effect on resistance factor thus with new environmental load factor the current ISO 19902 resistance factors could be used.

8.1.2.2 *Joint Reliability and Joint based Environmental Load Factor*

ISO LRFD and API LRFD recommend environmental load factors of 1.35, which is considered to be higher even by ISO itself for regions with mild climate is checked in this study for offshore Malaysia. This is due to difference in local ocean geography for each region. In most cases, this could save steel and thus Jacket design would become economical. All three types of joints were analysed with four different types of stresses. Environmental load factor for different regions are shown below:

Environmental load factor for different regions are shown below:

- For the platform in PMO region were in the range of 1.20 - 1.29.
- For the platform in SBO region were in the range of 1.23 - 1.23.
- For the platform SKO1 in SKO region were in the range of 1.17 - 1.31.
- For the platform SKO2 in SKO region were in the range of 1.24 - 1.29.

The average load factor of 1.27 is recommended for Jacket platforms in offshore Malaysia based on the target reliability index of 3.96.

8.1.2.3 *System Based Environmental Load Factor*

System based load factor for Jacket platform was determined using system global strength. Here minimum RSR was used as it would give economical and safe Jacket and the Jacket will be highly utilised. Minimum RSR specified by API WSD and ISO 19902 are 1.58 and 1.85. In this study, RSR of 1.5, 2.0 and 2.5 were considered. The load factor was determined for all three regions and four Jacket platforms. For system, the target reliability index was 4.0 and 3.8 based on notional system reliability index proposed by Efthymiou [27] as reported by BOMEL and Melchers [70] respectively. The reliability index decreased with increase of We/G ratio. The load

factors were determined for W_e/G ratio of 1.0. The load factor of 1.1 was achieved with a target reliability of 4.0. Thus it can be set as load factor for offshore Malaysia based on system reliability.

8.1.3 Bayesian Updating of Probability of Failure for Reassessment

The same methodology was followed here for four platforms by overloading them with wave and current loads. The load increase became significant after higher wave heights due to wave forces striking the deck of topside. With experienced resistance and load, it can be predicted how much load can be resisted by the Jacket with a minimum RSR of 1.0. It can be seen that without Bayesian updating, some Jackets would never have succeeded in getting a probability of failure below 1×10^{-4} , a major requirement for life extension and assessment qualification. Bayesian updating method made SBO and SKO1 platform probability of failure less than 1×10^{-4} which would not have been possible otherwise.

8.2 Future Work

Following are the studies which are suggested for future related work:

8.2.1 Time Variant Reliability

Fatigue and corrosion are the time variant random variables. The fatigue based limit state was not evaluated in this work and should be looked into in future works. This can be based on simulation or with available data. Fatigue crack in joint can cause local member or system failure. Fatigue becomes critical for operating conditions of environmental load. Similarly corrosion variable should also be looked into for reliability analysis of Jacket, TLP, SPAR or any other offshore structure.

8.2.2 Accidental Limit State

Some codes define accidental limit state. The reliability should also be evaluated for this condition. In case of accident, this limit state could play a major role in the stability of Jacket.

8.2.3 Operational Condition Reliability

Due to mild climate Jacket platforms in Malaysia may be governed by operating conditions. The operating loading conditions have not been dealt with in this study and they should be looked into in future works. This will still reduce the environmental load factor for Jacket design in offshore Malaysia for operating load conditions.

8.2.4 Structural Reliability of Floaters

Deep sea platforms have now become necessity due to scarcity of hydrocarbon near continental shelf. Structural reliability analysis for Floaters should be conducted for offshore Malaysia. The data from Kikeh Spar in Malaysia, with water depth of 1300 m, can be obtained and its reliability analysis evaluated.

8.2.5 Environmental Load Parameter Modelling

With more data collected on environmental load parameters and more realistic modelling of wave, wind, current and time period could be used to find accurate reliability for offshore structures in Malaysia.

8.2.6 Reassessment of Jacket

Vortex induced vibrations have not been considered for loading in this study; it is an important aspect and should be checked for assessment of Jacket. Degradation of platform should also be considered in future work for reassessment of strength.

8.2.7 Bayesian Updating due to Change of Conditions

Corrosion, earthquake, marine growth, boat impact and evaluation of pile strength needs to be incorporated in the Bayesian updating of probability of failure.

8.2.8 Reliability of Offshore Mooring Foundations:

Reliability analysis of offshore mooring foundations under operational and extreme environment can be determined. The local geographic environment may have significant effect on foundations.

REFERENCES

- [1] M. C. Ferguson, "A comparative study using API RP2A-LRFD," presented at the Offshore Technology Conference, OTC 6308, Houston, 1990.
- [2] R. O. Snell and D. J. Wisch, "ISO 19900 series: Offshore structures standards," in Offshore Technology Conference, OTC 19605, Houston, 2008.
- [3] F. Moses, "Reliability based design of offshore structures," presented at the American Petroleum Institute, 1981.
- [4] D. J. Wisch, "Fixed Steel Standard: ISO & API Developments - ISO TC 671SC 7NNG 3," presented at the Offshore Technology Conference, OTC 8423, Houston, 1997.
- [5] W. Jin, Q. Hu, Z. Shen, and Z. Shi, "Reliability- based load and resistance factors design for offshore jacket platforms in the Bohai bay: Calibration on target reliability index," *China Ocean Engineering*, vol. 23 (1), pp. 15-26, 2009.
- [6] G. Pradnyana, A. Surahman, and S. Dasbi, "Review on the regional annex of ISO-13819 standard for planning, designing, and constructing fixed offshore platforms in Indonesia," presented at the Sixth AEESEAP Triennial Conference Kuta, Bali, Indonesia, 2000.
- [7] ISO19902, "International Standard Organization 19902", 2007.
- [8] D. J. Wisch, "API Offshore structures standards: changing times," presented at the Offshore Technology Conference, OTC 19606, Houston, 2008.
- [9] A. Theophanatos, R. Cazzulo, I. Berranger, L. Ornaghi, and L. Wittengerg, "Adaptation of API RP2A-LRFD to the Mediterranean Sea," presented at the Offshore Technology Conference, OTC 6932, Houston, 1992.
- [10] J. R. Lloyd and D. I. Karsan, "Development of a reliability-Based alternative to API RP2A," presented at the Offshore Technology Conference, OTC 5882, Houston, 1988.
- [11] A. Mangiavacchi, G. Rodenbusch, A. Radford, and D. Wisch, "API offshore structures standards: RP 2A and much more," presented at the Offshore Technology Conference, OTC 17697, Houston, 2005.
- [12] PTS, "PETRONAS Technical Standard," ed. Malaysia: PETRONAS, 2010.
- [13] S. French, J. Seeto, and P. G. Dominish, "Structural integrity assessment and life extension of platforms in Australia and Southeast Asia," presented at the BOSS 1992.

- [14] J. W. Graff, P. S. Tromans, and M. Efthymiou, "The Reliability of Offshore Structures and its Dependence on Design Code and Environment," presented at the Offshore Technology Conference, OTC 7382, Houston, 1994.
- [15] R. C. Turner, C. P. Ellinas, and G. A. N. Thomas, "Towards the worldwide calibration of API RP2A-LRFD " in Offshore Technology Conference, OTC 6930, Houston, 1992.
- [16] A. Theophanatos and A. H. S. Wickham, "Modelling of environmental loading for adaptation of API RP 2A-Load and Resistance Factor Design in UK offshore structural design practice," in Proceedings of Institution of Civil Engineers, pp. 195-204, 1993,.
- [17] R. C. Turner, "Partial safety factor calibration for North Sea adaptation of API RP2A-LRFD," presented at the Institution of Civil Engineers, 1993.
- [18] A. H. Ang and W. H. Tang, Probability Concepts in Engineering vol. 1, 2007.
- [19] A. S. Nowak and K. Collins, Reliability of Structures, Second Edition: CRC Press, Taylor & Francis Group, 2013.
- [20] E. Gerhard, "Assessment of existing offshore structures for life extension," Doctor of Philosophy, Department of Mechanical and Structural Engineering and Material Science, University of Stavanger, Stavanger, Norway, 2005.
- [21] DNV and TA&R, "Comparison of API, ISO, and NORSOK offshore structural standards," Bureau of ocean energy management, regulation, and enforcement, Washington, D.C., 2012.
- [22] Z. D. Duan, D. C. Zhou, and J. P. Ou, "Calibration of LRFD Format for Steel Jacket Offshore Platform in China Offshore Area (1): Statistical Parameters of Load and Resistances " China Ocean Engineering, vol. 20 (1), pp. 1-14, 2005.
- [23] C. Sakrit, "Safety and reliability of a fixed offshore platform in the gulf of Thailand," MSc, Offshore Technology and Management., AIT, Bangkok, 2010.
- [24] D. C. Leng, "A reliability analysis of Malaysia jacket platform," Master of Science, UTM, 2005.
- [25] C. Tan, "A numerical analysis of fixed offshore structure subjected to environmental loading in Malaysian water," Master of Science, Faculty of Mechanical Engineering., UTM, 2005.
- [26] M. Birades, C. A. Cornell, and B. Ledoigt, "Load Factor Calibration for the Gulf of Guinea Adaptation of API RP2A-LRFD," in Behaviour of Offshore Structures, London, 2003.
- [27] BOMEL(b), "System-based calibration of North West European annex environmental load factors for the ISO fixed steel offshore structures code 19902," 2003.

- [28] G. A. N. Thomas and R. O. Snell, "Application of API RP2A-LRFD to a North Sea Platform Structure," in OTC 6931, Houston, 1992.
- [29] L. Manuel, "A study of the nonlinearities, dynamics and reliability of a drag dominated marine structure," Doctor of philosophy Civil Engineering Stanford university, 1992.
- [30] A. C. Morandi, P. A. Frieze, M. Birkinshaw, D. Smith, and A. T. Dixon, "Jack-up and Jacket platforms: a comparison of system strength and reliability " *Marine Structures*, vol. 12 (4), pp. 311-325, 1999.
- [31] M. Mortazavi, "A probabilistic screening methodology for use in assessment & requalification of steel, template type offshore platforms," Doctor of Philosophy, Civil engineering, University of California at Berkeley 1991.
- [32] P. M. Aagaard and C. P. Besse, "A Review of the Offshore Environment-25 Years of Progress," Society of Petroleum Engineering, pp. 1355-1360, 1973.
- [33] M. Efthymiou and C. G. Graham, "Environmental Loading on Fixed Offshore Platforms," Society for Underwater Technology vol. 26, pp. 293-320, 1990.
- [34] S. K. Chakrabarti, Hydrodynamics of Offshore Structures: WIT Press, 1987.
- [35] R. A. Phani, "Robust Estimation of Reliability in the Presence of Multiple Failure Modes," Doctor of Philosophy, Mechanical and Materials Engineering, Wright State University, 2006.
- [36] A. S. Nowak, "Calibration of LRFD Bridge Code," Journal of Structural Engineering, vol. 121 (8), 1995.
- [37] W. Wang, "Structural system reliability: A study of several important issues," Doctor of Philosophy, The Johns Hopkins, 1994.
- [38] F. Moses and B. Stahl, "Calibration issues in development of ISO standards for fixed steel offshore structures," Journal of OMAE, Transactions of the ASME, vol. 122 (1), pp. 52-56, 2000.
- [39] Shell, "Sarawak-Shell, Design of fixed offshore structures (10.1)," 2005.
- [40] D. J. Wisch, "Fixed Steel Offshore Structure Design-Past, Present and Future," in Offshore Technologi Conference, OTC8822, Houston, 1998.
- [41] G. B. Baecher and J. T. Christian, Reliability and Statistics in Geotechnical Engineering, 2003.
- [42] B. R. Ellingwood, "LRFD: implementing structural reliability in professional practice," Engineering Structures, vol. 22(2), pp. 106-115, 2000.
- [43] AME, "Buckling of offshore structures: assessment of code limitations'," Offshore Technology Report, OTO 97049 (Advance mechanics & Engineering), Health Safety Executive, UK1997.

- [44] T.V.Galambos, "Load Factor Design of Steel Buildings," AISC Engineering Journal, 1972.
- [45] P. R. Brand, W. S. Whitney, and D. B. Lewis, "Load and Resistance Factor Design Case Histories," presented in OTC 7937, Houston 1995.
- [46] M. A. Bilal, "Development of Reliability-based load and resistance factor design (LRFD) methods for piping," ASME, New York, 2007.
- [47] H. O. Madsen, "Integrity and reliability of offshore structures," Veritas Research, Norway, 1987.
- [48] K. V. Raaij, "Dynamic behaviour of jackets exposed to wave-in-deck forces," Doctor of Philosophy (DR. ING.), Department of Mechanical & Structural Engineering & Materials Science, University of Stavanger, Norway, 2005.
- [49] Y. F. Guenard, "Application of structural system reliability analysis to offshore structures " Doctor of Philosophy, Civil Engineering, Stanford University, 1984.
- [50] F. Moses, " Application of Reliability to Formulation of Fixed Offshore Design Codes," presented at the Marine structural reliability symposium, 1995.
- [51] S. K. Choi, R. V. Grandhi, and R. A. Canfield, Reliability-based Structural Design: Springer-Verlag London Limited, 2007.
- [52] R. Thomas, R. Wartelle, and C. L. Griff, "Fixed Platform Design for South East Asia," Society of Petroleum Engineering, 1976.
- [53] M. A. Bilal and A. Haldar, "Practical structural reliability techniques," Journal of Structural Engineering, vol. 110 (8), 1984.
- [54] M. Marley, B. Etterdal, and H. Grigorian, "Structural Reliability Assessment of Ekofisk Jacket Under Extreme Loading," presented at OTC 13190, Houston, 2001.
- [55] Y. Guenard, J. Goyet, B. Remy, and J. Labeyrie, "Structural Safety Evaluation of Steel Jacket Platforms," presented at the Marine Structural Reliability Symposium, Virginia, 1987.
- [56] P. P. Anthony, K. Y. Paul, and R. C. Paul, "Effect of design, Fabrication and installation on the structural reliability of offshore platforms," presented at O, OTC 3026, Houston, 1977.
- [57] R. G. Bea, "Reliability characteristics of a platform in the Mississippi River Delta," Journal of Geotechnical and Geoenvironmental Engineering, ASCE, vol. 124 (8), pp. 779-786, 1998.

- [58] N. J. T. Johansen, "Partial Safety Factors and Characteristics Values for Combined Extreme Wind and Wave Load Effects," *Journal of Solar Energy Engineering*, ASME, vol. 127 (2), pp. 242-252, 2005.
- [59] B. Chakrabarty and A. Bhar, "Sensitivity analysis in structural reliability of Marine structures " presented at the 3rd international ASRANet Colloquium, Glasgow, UK, 2006.
- [60] ENERGO, "Reliability vs. consequences of failure for API RP 2A fixed platforms using API bulletin 2INT-MET," 2009.
- [61] DNV, "Classification Note 30.6 "Structural Reliability Analysis of Marine Structures"," 1992.
- [62] I. Holland, "Norwegian Regulations for Design of Offshore Structures," presented at, OTC 2863, Houston 1977.
- [63] P. A. Frieze, T. M. Hsu, J. T. Loh, and Lotsberg, "Back ground to Draft ISO provisions on Intact and damaged Members," BOSS 1997.
- [64] M. A. Shama, "Marine structural safety and economy," presented at the The society of naval architecture and marine engineers, USA, 1991.
- [65] Z. Hassan, "Calibration of deterministic parameters for reassessment of offshore platforms in the Arabian Gulf using reliability based methods," Doctor of Philosophy, Mechanical engineering University of Western Australia, 2008.
- [66] H. Gulvanessian, J. A. Calgaro, and M. Holicky, "Designers' Guide to EN 1990 Eurocode: Basis of structural design", 2002.
- [67] JCSS, "Joint Committee on Structural Safety (JCSS) Model Code," 2001.
- [68] P. E. Hess, D. Bruchman, I. A. Assakkaf, and B. M. Ayyub, "Uncertainties in Material Strength, Geometric and Load Variables," presented at the American Society of Naval Engineers, 2002.
- [69] BOMEL(a), "Component based calibration of North western European annex environmental load factors for the ISO Fixed Steel offshore structures code 19902" 2003.
- [70] R. E. Melchers, *Structural Reliability Analysis and Prediction: Second ed.:* John Wiley & Sons, 2002.
- [71] B. R. Ellingwood, "Probability-based codified design: past accomplishments and future challenges," *Structural Safety*, vol. 13 (3), pp. 159-176, 1994.
- [72] C. J. Billington and I. F. Tebbett, "The basis for new design formula of grouted Jacket to pile connections," presented at OTC3788, Houston, 1980.

- [73] ISO-2394, "General Principles on reliability for structures, ISO-2394," in ISO, 1998.
- [74] DNV, "Design of offshore steel structures, general (LRFD) method," in DNV-OS-C101, 2008.
- [75] BOMEL, "Comparison of tubular member strength provisions in codes and standards," 2001.
- [76] D. Elms, *Safety Concepts and Risk Management*, "Structural Safety and its Quality Assurance": ASCE, 2005.
- [77] J. Kunda, Load Modelling, "Structural Safety and its Quality Assurance": ASCE, 2005.
- [78] J. D. Sorensen and M. J. Sterndorff, "Stochastic model for Loads on offshore structures from wave, wind, current and water elevation," presented at the Structural safety and reliability, 2001.
- [79] C. Petruskas and P. M. Aagaard, "Extrapolation of historical storm data for estimating design-wave heights," in Society of Petroleum Engineers, 1971.
- [80] E. M. Bitner-Gregersen and E. H. Cramer, "Uncertainties of Load Characteristics and Fatigue Damage of Ships Structures," *Marine Structures*, 8(2), pp. 97-117, 1995.
- [81] P. S. Tromans and G. Z. Forristall, "What is Appropriate Wind Gust Averaging Period for Extreme Force Calculations?," presented at the Offshore Technology Conference, OTC 8908, Houston, 1998.
- [82] P. Tromans, "Extreme environmental load statistics in UK waters," 2001.
- [83] D. B. Driver, L. E. Borgman, and J. B. Bole, "Typhoon Wind, Wave and Current Directionality in the South China Sea," presented at the Offshore Technology Conference, OTC 7416, Huston, 1994.
- [84] C. J. Turkstra, Design Load Combination Factors, "Structural Safety Series", 1985.
- [85] K. Bury, Statistical Distributions in Engineering: University of Cambridge, 1999.
- [86] P. S. Tromans and L. Vanderschuren, "Response Based Design Conditions in the North Sea: Application of a New Method," presented at the Offshore Technology Conference, OTC 7683, Huoston, 1995.
- [87] API, "American Petroleum Institute RP2A (WSD)" 2008.
- [88] Y. K. Wen and H. Banaon, "Development of Environmental Combaion Design Criteria for Fixed Platforms in the Gulf of Mexico," presented at OTC6540, Houston, 1991.

- [89] C. K. Grant, R. C. Dyer, and I. M. Leggett, "Development of a New Metocean Design Basis for the NW Shelf of Europe," presented at, OTC 7685, Houston, 1995.
- [90] H. O. Jahns and J. D. Wheeler, "Long-Term Wave Probabilities Based on Hindcasting of Severe Storms," presented at the Society of Petroleum Engineers 3934, 1973.
- [91] Surrey, "A review of reliability considerations for fixed offshore platforms, Surrey University, Offshore Technology Report-OTO 2000 037, Health and Safety Executive, UK," Offshore Technology Report-OTO 2000 037, Health and Safety Executive, UK, 2000.
- [92] J. C. Heideman, O. Hagen, C. Cooper, and F. E. Dahl, "Joint probability of extreme waves and currents on Norwegian Shelf," *Journal of waterway, Port, Coastal and Ocean Engineering*, vol. 115, pp. 534-546, 1989.
- [93] T. H. Dawson, *Offshore structural engineering*. New Jersey, USA: Prentice-Hall Inc, 1993.
- [94] E. Gerhard, J. D. Sorensen, and I. Langen, "Updating of Structural Failure Probability Based on Experienced Wave Loading," presented at the International Offshore and Polar Engineering Conference Honolulu, Hawaii, USA, 2003.
- [95] O. T. Gudmestad and G. Moe, "Hydrodynamic coefficients for calculation of hydrodynamic loads on offshore truss structures," *Marine Structures*, vol. 9 (8), pp. 745-758, 1996.
- [96] J. T. Gierlinski and E. Yarmier, "Integrity of fixed offshore structures: a case study using RASOS software," in 12th International conference on Offshore Mechanics and Arctic Engineering (OMAE), Glasgow 1993.
- [97] G. Sigurdsson, B. Skallerud, R. Skjong, and J. Amdahl, "Probabilistic collapse analysis of Jackets," presented at the OMAE, Houston, 1994.
- [98] C. Petrauskas, D. L. R. Botelho, W. F. Krieger, and J. J. Griffin, "A Reliability Model for Offshore Platforms and its Application to ST151"H" & "K" Platforms During Hurricane Andrew" 1992.
- [99] Fugro, "Wind and wave frequency distributions for sites around the British Isles," (Fugro-GEOS) Offshore Technology Report 2001/030, Health and Safety Executive, UK, 2001.
- [100] K. Johannessen, T. S. Meling, and S. Haver, "Joint Distribution for wind and Waves in The Northern North Sea," *International Journal of Offshore and Polar Engineers*, vol. 12 (1), 2002.
- [101] R. Bea, "Selection of environmental criteria for offshore platform design " *Journal of petroleum technology, SPE 4452*, 1974.

- [102] M. J. Baker and K. Ramachandran, "Reliability Analysis as a Tool in the Design of Fixed Offshore Platforms," *Integrity of Offshore Structures*, 1981.
- [103] P. A. Frieze, A. C. Morandi, M. Birkinshaw, D. Smith, and A. T. Dixon, "Fixed and Jack-up Platforms: Basis for Reliability Assessment," *Marine Structures*, vol. 10 (2), pp. 263-284, 1997.
- [104] B. F. Renolds, D. J. Trench, and R. Pinna, "On the relationship between platform topology, topside weight and structural reliability under storm overload," *Journal of constructional steel research*, vol. 63 (8), pp. 1016-1023, 2007.
- [105] B. Stahl, S. Aune, J. M. Gebara, and C. A. Cornell, "Acceptance criteria for Offshore Platforms," *Journal of Offshore Mechanics and Arctic Engineering*, vol. 122 (3), pp. 153-156, 1998.
- [106] M. Efthymiou, G. W. Graaf, P. S. Tromans, and I. M. Hines, "Reliability based criteria for fixed steel offshore platforms," *Journal of Offshore Mechanics and Arctic Engineering OMAE*, vol. 119 (2), pp. 120-124, 1997.
- [107] API, "American Petroleum Institute RP2A LRFD," 2003.
- [108] D. C. Zhou, Z. D. Duan, and J. P. OU, "Calibration of LRFD for Steel Jacket Offshore Platform in China Offshore Area (2); Load, Resistance and Load Combination Factors " *China Ocean Engineering*, vol. 20 (2), pp. 199-212, 2006.
- [109] B. Skallerud and J. Amdahl, *Nonlinear Analysis of Offshore Structures: Research Studies Press LTD*, 2002.
- [110] Y. Xiaoming, "Reliability and Durability based Design Sensitivity Analysis and Optimization," *Doctor of Philosophy, Mechanical Engineering, The University of Iowa*, 1996.
- [111] A. S. Nowak and J. T. Raymond, "Reliability-based design criteria for timber bridges in Ontario," *Canadian Journal of Civil Engineering*, vol. 13 (1), pp. 1-7, 1986.
- [112] F. Moses and R. D. Larrabee, "Calibration of the draft RP2A-LRFD for Fixed Platforms," in *OTC 5699, Houston 1988*.
- [113] M. C. Bourinet, J.M, Dubourg, V, "A Review of Recent Features and Improvements Added to Ferum Software," *Safety, Reliability and Risk of Structures, Infrastructures and Engineering Systems*, 2010.
- [114] M. T. Allen, A. S. Nowak, and R. J. Bathurst, "Calibration to determine load and resistance factors for geotechnical and structural design," *Transportation Research Board, Washington D.C*, 2005.

- [115] M. Biagi and F. D. Medico, "Reliability-based knockdown factors for composite cylindrical shells under axial compression, vol 46 (12)," *Thin-walled Structures*, pp. 1351-1358, 2008.
- [116] O. T. Gudmestad, "Challenges in Requalification and Rehabilitation of Offshore Platforms-On the Experience and Developments of a Norwegian Operator," *Journal of offshore Mechanics and Arctic Engineering*, vol. 122 (1), pp. 3-6, 1999.
- [117] G. Sigurdsson, "Guidelines for Offshore Structural Reliability Analysis: Application to Jacket Platforms, DNV Report no. 95-3203," 1996.
- [118] Chapter 5. Probabilistic design tools and applications [Online].
- [119] O. Furnes and A. Sele, "Offshore Structures-Implementation of Reliability," in *Extreme Loads Response Symposium, Integrity of offshore structures*, Society of Naval Architects and Marine Engineers, 1982.
- [120] L. Manuel, D. G. Schmucker, C. A. Cornell, and J. E. Carballo, "A reliability-based Design Format for Jacket Platforms under Wave Loads," *Marine Structures*, vol. 11 (10), pp. 413-428, 1998.
- [121] Eurocode, "Euro Code 1," 1993.
- [122] M. Mark, E. Birger, and G. Henrik, "Structural Reliability Assessment of Ekofisk Jacket Under Extreme Loading," in *Offshore Technology Conference, OTC 13190.*, Houston, 2001.
- [123] M. H. Faber, "Basics of structural reliability " 2002.
- [124] J. T. Gierlinski, Reliability analysis system for offshore structures, *RASOS: BOSS 92*, 1992.
- [125] T. Onoufriou and V. J. Forbes, "Developments in structural system reliability assessments of fixed steel offshore platforms," *Reliability Engineering & System Safety*, vol. 71 (2), pp. 189-199, 2001.
- [126] H. M. Bolt, "Results from Large Scale Ultimate Strength Tests of K-Braced Jacket Frame Structures," presented at OTC 7783, Houston, 1995.
- [127] PAFA, "Implications for the assessment of existing fixed steel structures of proposed ISO 13819-2 member strength formulations," PAFA consulting engineers for Health Safety and Executive, UK, 2000.
- [128] D. I. Karsan, P. W. Marshall, D. A. Pecknold, W. C. Mohr, and J. Bucknell, "The new API RP2A, 22nd edition tubular joint design practice," in OTC 17236, Houston, USA, 2005.
- [129] D. Pecknold, P. W. Marshall, and J. Bucknell, "New API RP2A Tubular joint strength design provisions," in OTC 17310, Houston, USA, 2005.

- [130] T. S. Thandavamoorthy, "Finite Element modelling of the behaviour of internally ring stiffened T-Joints of Offshore Platforms, *Journal of Offshore Mechanics and Arctic Engineering*, OMAE, vol 131 (4) " 2002.
- [131] R. Rackwitz and H. Streicher, "Optimization and target reliabilities," presented at the JCSS Workshop on Reliability Based Code Calibration, Zurich, Switzerland, 2002.
- [132] Ø. Hellan, T. Moan, and S. O. Drange, "Use of nonlinear pushover analyses in ultimate limit state design and integrity assessment of jacket structures," presented at the Behaviour of Offshore Structures Conference, Massachusetts, 1994.
- [133] Ø. Hellan, "Nonlinear pushover and cyclic analysis in ultimate limit state design and reassessment of tubular steel offshore structures.," Norwegian Institute of Technology, University in Trondheim, Norway, 1995.
- [134] J. I. Dalane, "System reliability in design and maintenance of fixed offshore structures.," Norwegian Institute of Technology, University in Trondheim, Norway., 1993.
- [135] R. Bea, "Developments in the assessment and requalification of offshore platforms," presented at OTC 7138, 1993.
- [136] DNV2018, "Guidelines for Offshore Structural Reliability Analysis-General, appendix B. ", 1995.
- [137] T. Moan, "Target levels for structural reliability and risk analysis of offshore structures, *Risk and Reliability in Marine Techonology*," 1998.
- [138] V. D. Graaf, J. W. Efthymiou, and P. S. Tromans, "Implied Reliability levels for RP 2A-LRFD from Studies of North Sea Platforms," presented at the Society for Underwater Technology International Conference, London, 1993.
- [139] A. Kvitrud, G. Ersdal, and R. L. Leonardsen, "On the Risk of Structural failure on Norwegian Offshore Installations," presented at the Proceedings of ISOPE 2001, 11th International Offshore and Polar Engineering Conference, Stavanger, Norway, 2001.
- [140] A. M. Haldar, *Probability Reliability and Statistical Methods in Engineering Design*: John Wiley & Sons, 2000.
- [141] H. O. Ditlevsen, *Structural Reliability Methods*, 2007.
- [142] J. Fatemeh, L. Iervolino, and G. Manfredi, "Structural modeling uncertainties and their influence on seismic assessment of existing RC structures," *Structural Safety*, vol. 32 (3), pp. 220-228, 2010.
- [143] M. Enright and D. Frangopol, "Condition prediction of deteriorating concrete bridges using bayesian updating," *Journal of Structural Engineering*, vol. 126 (10), pp. 1118-1125, 1999.

- [144] F. J. Puskar, A. P. Ku, and R. E. Sheppard, "Hurricane Lili's impact on Fixed Platforms and Calibration of Platform Performance to API RP2A," presented at OTC 16802, Houston, 2004.
- [145] H. M. Bolt, C. J. Billington, and J. K. Ward, "Results From Large-Scale Ultimate Load Tests on Tubular Jacket Frame Structures," presented at the Offshore Technology Conference, OTC 7451, Houston, 1994.
- [146] AME, "API RP2A-LRFD - Its consequences for and adaptation to North Sea Offshore Design Practice," Advanced Mechanics & Engineering, Ltd. for Health Safety Executive, UK, 1991.
- [147] ISO19901-1, "Metoccean design and operating considerations", 2005.
- [148] R. G. Standing, "The sensitivity of Structure Load and Responses to Environmental Modelling," in Advances in Underwater Technology, Ocean Science and Offshore Engineering, Modelling the Offshore Environment, Society of Underwater Technology, 1987.
- [149] Q. Yiquan, Z. Zhizu, and S. Ping, "Extreme Wind, Wave and Current in Deep Water of South China Sea," International Journal of Offshore and Polar Engineers, vol. 20 (1), pp. 18-23, 2010.
- [150] R. Bea, "Gulf of Mexico hurricane wave heights," Journal of Petroleum technology, SPE 5317, 1975.
- [151] R. C. Turner, C. P. Ellinas, and G. A. N. Thomas, "Worldwide calibration of API RP2A-LRFD " Journal of Waterway, Port, Coastal, and Ocean Engineering,, vol. 120 (5), p. 11, 1992.
- [152] A. H. Monahan, "The Probability Distribution of Sea Surface Wind Speeds. Part I: Theory and SeaWinds Observations," Journal of Climate, vol. 19 (4), 2006.
- [153] A. S. Nowak and M. S. Maria, "Structural reliability as applied to highway bridges," Structural Engineering Material, John Wiley & Sons, Ltd., vol. 2 (2), pp. 218-224, 2000.
- [154] J. M. Bourinet, "FERUM 4.1 User's Guide (Online)," 2010.
- [155] W. D. Gifford, "Risk analysis and the acceptable probability of failure " Risk analysis, 2004.
- [156] M. K. Ochi, "Probabilistic Extreme values and their implication for Offshore Structure Design," in OTC 3161, Houston, 1978.
- [157] T. Ingebrigtsen, O. Loset, and S. G. Nielsen, "Fatigue design and overall safety of grouted pile sleeve connections," in OTC 6344, Houston, 1990.
- [158] A. J. Adams, A. V. R. Warren, and P. C. Masson, "On the development of Reliability-Based Design Rules for Casing Collapse," *SPE 48331*, 1998.

- [159] J. Niels, H. Peter, and F. Sten, "Calibration of Partial Safety Factors for Extreme Loads in Wind Turbines, European Wind Energy Conference and Exhibition, Spain," 2003.
- [160] MSL, "Load factor calibration for ISO 13819 Regional Annex: Component resistance", Offshore Technology Report, 2000/072, Health and Safety Executive, UK, 2000.
- [161] S. Neelamani, K. Salem, and K. Rakha, "Extreme Waves in the Arabian Gulf," presented at the Proceedings of the 9th International Coastal Symposium, Australia, 2007.
- [162] R. L. Prior-Jones and F. L. Beiboer, "Use of Joint Probability in Deriving Environmental Design Criteria," presented at the Environmental Forces on Offshore Structures and their Prediction Netherlands, 1990.
- [163] G. C. Soares and M. Scotto, "Modelling Uncertainty in Long-term Predictions of significant wave height," Ocean Engineering, vol 28 (3), pp. 329-342, 2001.
- [164] V. G. Panchang and D. C. Li, "Large Waves in the Gulf of Mexico Caused by Hurricane Ivan," American Meteorological Society, vol. 87 (4), 2006.
- [165] N. C. Lind, "Target Reliability levels from social indicators " in Proceedings of the sixth International Conference of Structural Safety and Reliability, ICOSSAR-93, Rotterdam, Netherlands, 1994,.
- [166] P. G. Titus and H. Banon, "Reserve strength analysis of offshore platforms, Paper 88179," presented at the 7th Offshore Southeast Asia Conference, Singapore, 1988.
- [167] J. Heideman, "Parametric Response Model for Wave/current Joint Probability," Report Submitted to API TAC 88-20 for API LRFD1980.

LIST OF PUBLICATIONS

C.1 PUBLICATIONS

1. V.J. Kurian, **Z. Nizamani** and M.S. Liew, “Probability of Failure updating Using Bayesian Technique for the Jacket Platforms in Offshore Malaysia”. Journal of Offshore Mechanics and Arctic Engineering, ASME Publication (Paper under review)
2. V.J. Kurian, **Z. Nizamani** and M.S. Liew, “Determination of Environmental Load Factors for ISO 19902 Code in Offshore Malaysia using FORM Structural Reliability Method”. Journal of Ocean Engineering, Elsevier Publication (Paper under review)
3. V.J. Kurian, **Z. Nizamani** and M.S. Liew, “Modelling for Uncertainties in Resistance for Jacket Platforms in Malaysia”, Research Journal of Applied Sciences, Engineering and Technology. Vol. 5, Issue 3, Published January 21, 2013, ISSN: 2040-7459
4. Nelson J. Cossa, Narayanan S. Potty, Arazi B. Idrus, Mohd Foad Abdul Hamid and **Zafarullah Nizamani** “Reliability Analysis of Jacket Platforms in Malaysia-Environmental Load Factors”, Research Journal of Applied Sciences, Engineering and Technology, Vol. 4, Issue: 19, Published October 01, 2012, ISSN: 2040-7467
5. Arazi B. Idrus, Narayanan Sambu Potty, **Z. Nizamani**, "Tubular Strength Comparison of Offshore Jacket Structures under APIRP 2A and ISO 19902," Journal of the Institute of Engineers, Malaysia, Vol. 72, No. 3, Sept. 2011 (Awarded best technical paper for year 2011).

C.2. CONFERENCE PROCEEDINGS

1. V.J. Kurian, **Z. Nizamani** and M.S. Liew, “Component, Joint and System based Environmental Load Factor for Jacket Platforms in Malaysia” The International Society of Offshore and Polar Engineers, (ISOPE, USA, 2013).

2. V.J. Kurian, **Z. Nizamani** and M.S. Liew, “Bayesian updating for Probability of Failure of Jacket Platforms in Malaysia”, IEEE Business Engineering and Industrial Applications Colloquium 2013, (BEIAC 2013).
3. V.J. Kurian, **Z. Nizamani** and M.S. Liew, “Statistical Modelling of Environmental Load Uncertainty for Jacket Platforms in Malaysia”, IEEE Colloquium on Humanities, Science and Engineering, (CHUSER 2012)
4. V.J. Kurian, **Z. Nizamani** and M.S. Liew, M.M.A. Wahab., “System Reliability for Jacket Platform Subjected to Wave and Current Loads”, International Conference on Civil, Offshore & Environmental Engineering (ICCOEE-2012)
5. A.B. Idrus, Narayanan S. P., M. F. A. Hamid, **Z. Nizamani**, N. J. Cossa., “Selection of Environmental Parameters for Offshore Jacket Platform Design in Malaysia”, International Conference on Steel & Aluminium Structures (ICSAS 2011)
6. A.B. Idrus, Narayanan S. P., M. F. A. Hamid, N. J. Cossa., **Z. Nizamani**, “Statistical Parameters of Steel Tubular Member Design for Offshore Platforms in Malaysia”, International Conference on Steel & Aluminium Structures (ICSAS 2011)
7. A.B. Idrus, Narayanan S. P., M. F. A. Hamid, N. J. Cossa., **Z. Nizamani**, “Resistance Parameters Statistics for Jacket Platforms in Offshore Malaysia”, The International Society of Offshore and Polar Engineers (ISOPE) USA, 2011
8. N. S. Potty, **Z. Nizamani**, A. B. Idrus, “Strength of Tubular Members– Numerical Comparison of API RP2A to ISO Codes” ISOPE Pacific/Asia Offshore Mechanics Symposium Busan, Korea, November 14-17, 2010 (ISOPE 2010) (Paper citation listed below).
9. Narayanan Sambu Potty, Cossa N.J., **Z. Nizamani**, Arazi B. Idrus., “Tubular Joint Strength Models in API RP2A WSD, API RP2A LRFD and ISO 19902”, World Engineering Congress, Sarawak-Malaysia (WEC 2010)
10. Arazi B. Idrus, Narayanan Sambu Potty, Mohd Foad Abdul Hamid, **Z. Nizamani** “Hydrodynamic Load Models for Offshore Jacket Platforms:

Comparison of API and ISO codes”, The Asia-Pacific Offshore Conference –Kuala Lumpur, APOC 2010,

11. Arazi B. Idrus, Narayanan Sambu Potty, Mohd Foad Abdul Hamid, **Z. Nizamani** “Comparison of Foundation Strength Modelling of Jacket Platforms in API RP2A codes and ISO 19902”, The Asia-Pacific Offshore Conference –Kuala Lumpur, APOC 2010,
12. Narayanan Sambu Potty, **Z. Nizamani**, Arazi B. Idrus “Tubular Strength Modelling -Comparison of API RP2A WSD and LRFD and ISO 19902”, International Conference on Sustainable Building and Infrastructure, Kuala Lumpur-Malaysia (ICSBI 2010)
13. Narayanan Sambu Potty, **Z. Nizamani**, Arazi B. Idrus “Pile-Sleeve Strength Modelling in API RP2A WSD,LRFD and ISO 19902”, International Conference on Sustainable Building and Infrastructure, Kuala Lumpur-Malaysia (ICSBI 2010).
14. Narayanan Sambu Potty, **Z. Nizamani**, Arazi B. Idrus “Sustainable Infrastructure through Rational Codes using Reliability and Code Calibration”, International Conference on Sustainable Building and Infrastructure, Kuala Lumpur-Malaysia (ICSBI 2010).
15. Narayanan Sambu Potty, **Z. Nizamani**, Arazi B. Idrus “Offshore Jacket Platforms – LRFD Code Calibration”, International Conference on Sustainable Building and Infrastructure, Kuala Lumpur-Malaysia (ICSBI 2010)
16. Narayanan Sambu Potty, **Z. Nizamani**, Arazi B. Idrus “Load and Resistance Factor Calibration Methodology for Offshore Jacket Platforms in Malaysia”, Proceedings of the First Makassar International Conference on Civil Engineering (MICCE2010)

C.3 BEST TECHNICAL PAPER AWARDS

Institute of Engineers Malaysia for year 2011

C.4 CITATION

DNV report 2012 “Bureau of Ocean Energy Management”, U.S. Department of the Interior

[http://www.bsee.gov/uploadedFiles/BSEE/Research_and_Training/Technology Assessment and Research/AA%20%20TAR%20677%20Code%20Comparison.pdf](http://www.bsee.gov/uploadedFiles/BSEE/Research_and_Training/Technology_Assessment_and_Research/AA%20%20TAR%20677%20Code%20Comparison.pdf)

APPENDIX A

Strength of tubular members– Numerical Comparison of API RP2A to ISO Codes

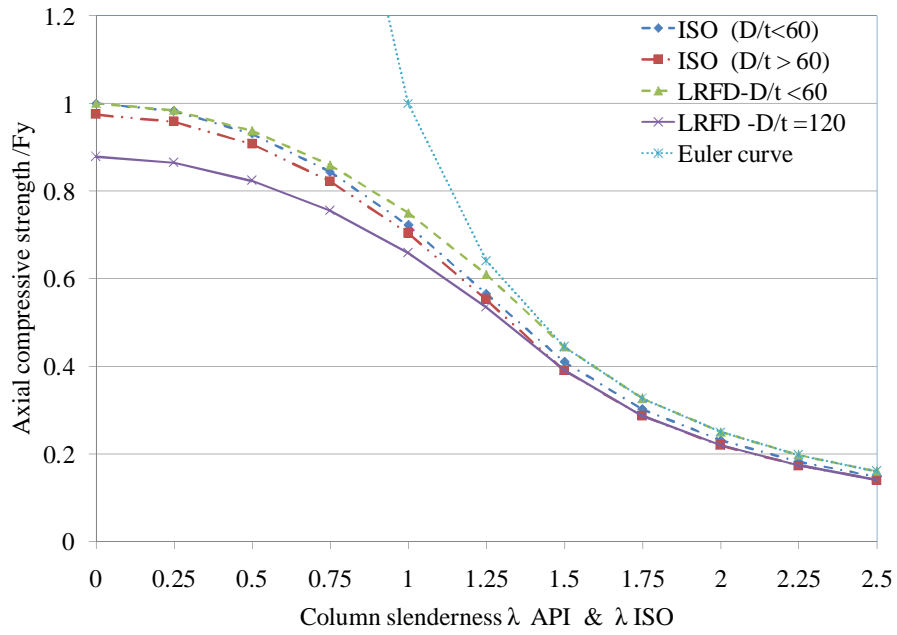


Figure A1: Comparison of Characteristic Column Curves Strength of ISO 19902 and API LRFD

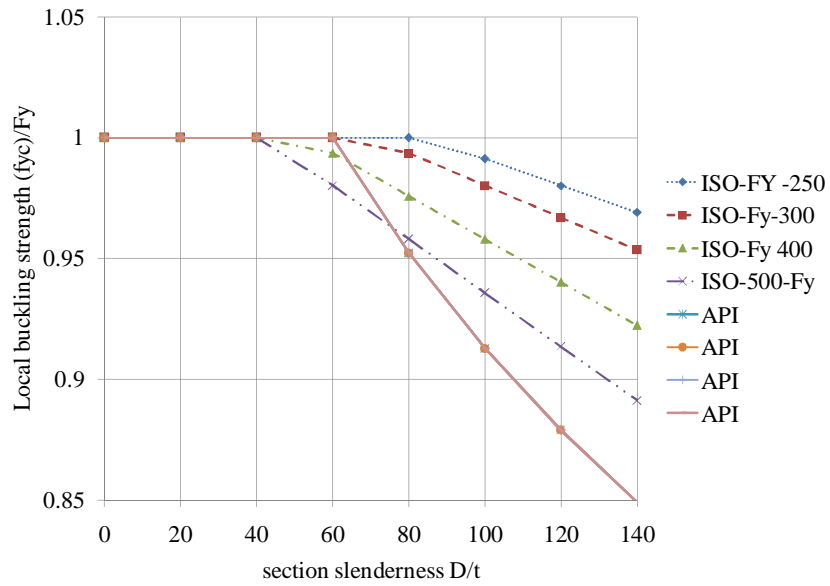


Figure A2: Comparison of API and ISO Local Buckling Strength

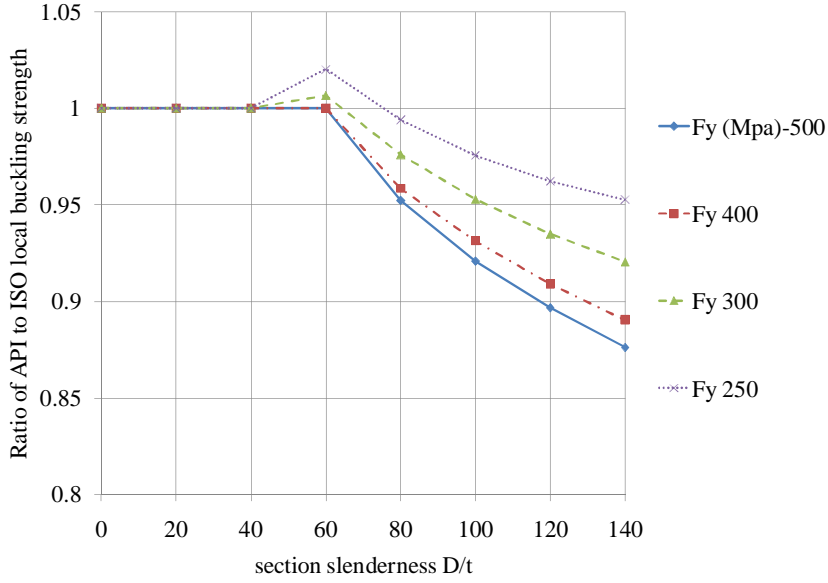


Figure A3: Comparison of ISO and API (LRFD or WSD) Local Buckling Strengths

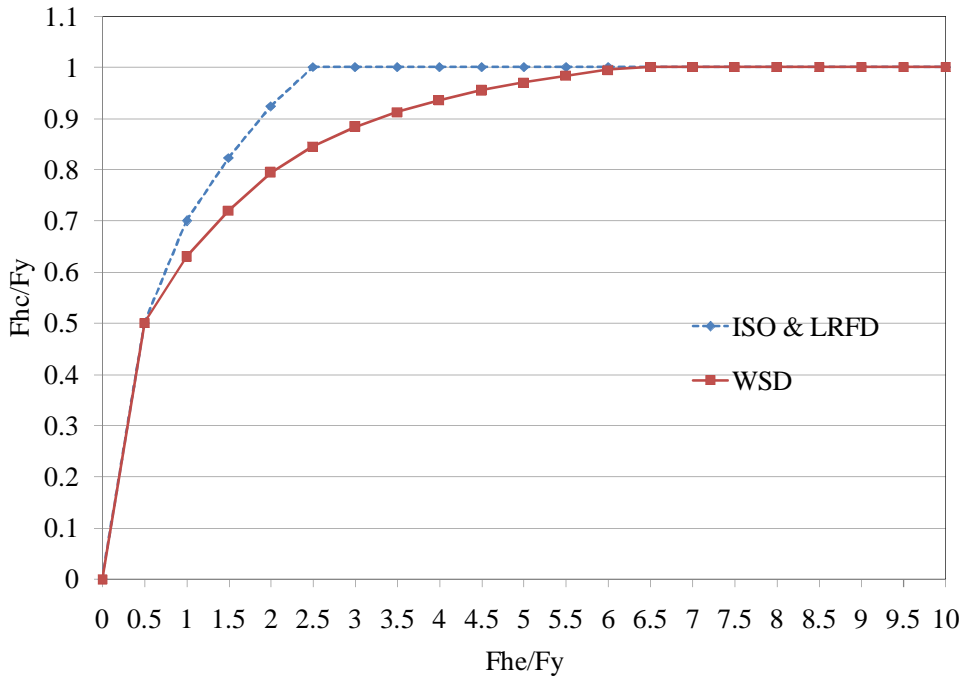


Figure A4: Hoop Buckling Strength as a Function of Elastic Buckling Stress

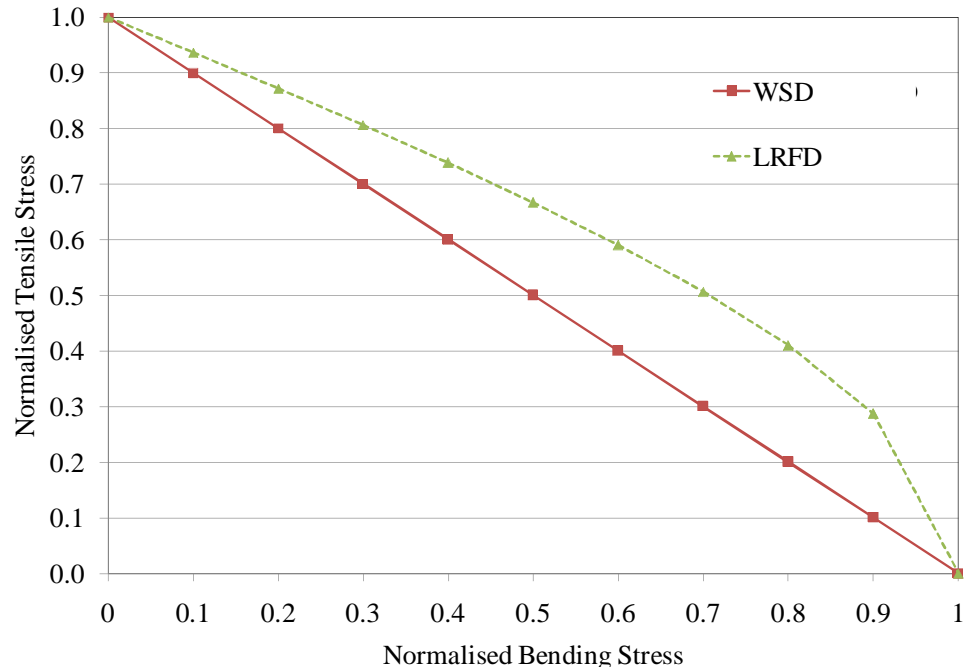


Figure A5: Normalised Interaction Curve for Combined Axial Tension and Bending

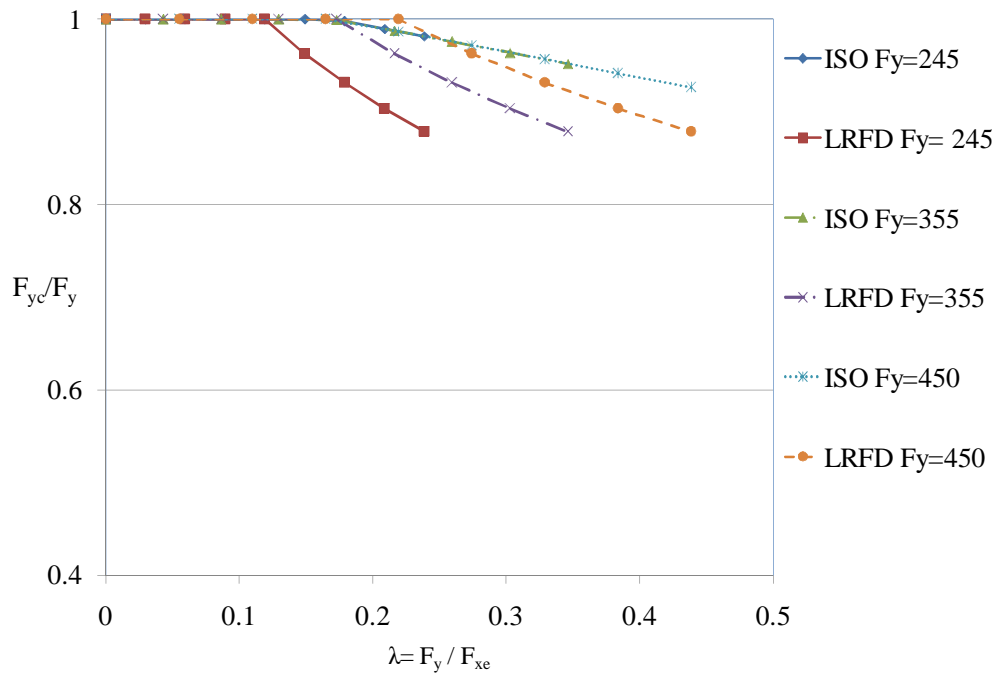


Figure A6: Comparison of API and ISO Local Buckling Strength

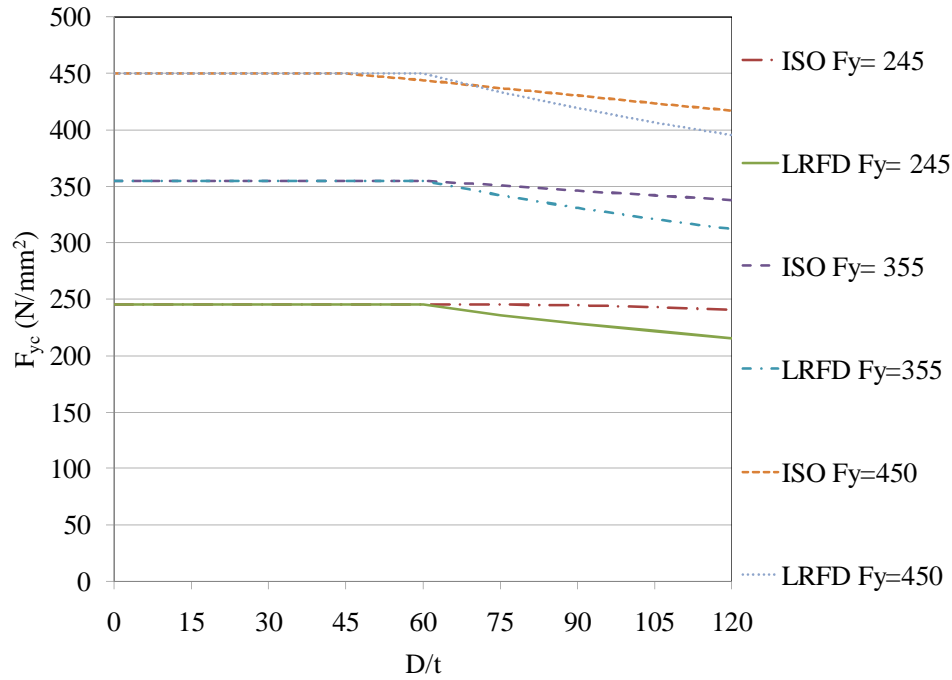


Figure A7: Comparison of API and ISO Local Buckling Strength

APPENDIX B

Load Ratios

Develop w , d , l ratios for given condition of $\frac{w_e}{G} = 0.1$

$$w + d + l = 1.0$$

Assuming dead and live ratio is same

$$w + 2d = 1.0 \tag{1}$$

Case study: given ratio of $\frac{w_e}{G} = 0.1$

It can be shown by,

$$\frac{w}{2d} = 0.1$$

$$w = 0.2d$$

Using Equation (1) and putting value of w ,

$$0.2d + 2d = 1.0$$

$$d = \frac{1}{2.2}$$

Now again putting value of d in Equation (1),

$$w + 2 * \left(\frac{1}{2.2}\right) = 1.0$$

$$w = 0.0909$$

Now the given ratio is $\frac{w}{d+l} = 0.1$

$$\frac{0.0909}{d+l} = 0.1$$

$$0.1(d+l) = 0.0909$$

$$G = d + l = 0.909$$

$$70\% \text{ of } d = 0.7 * 0.909 = 0.64$$

$$30\% \text{ of } l = 0.3 * 0.909 = 0.27$$

APPENDIX C

Wave load against corresponding base shear in 8 directions at SBO, SKO1, SKO2 and SKO2a Jacket platforms.

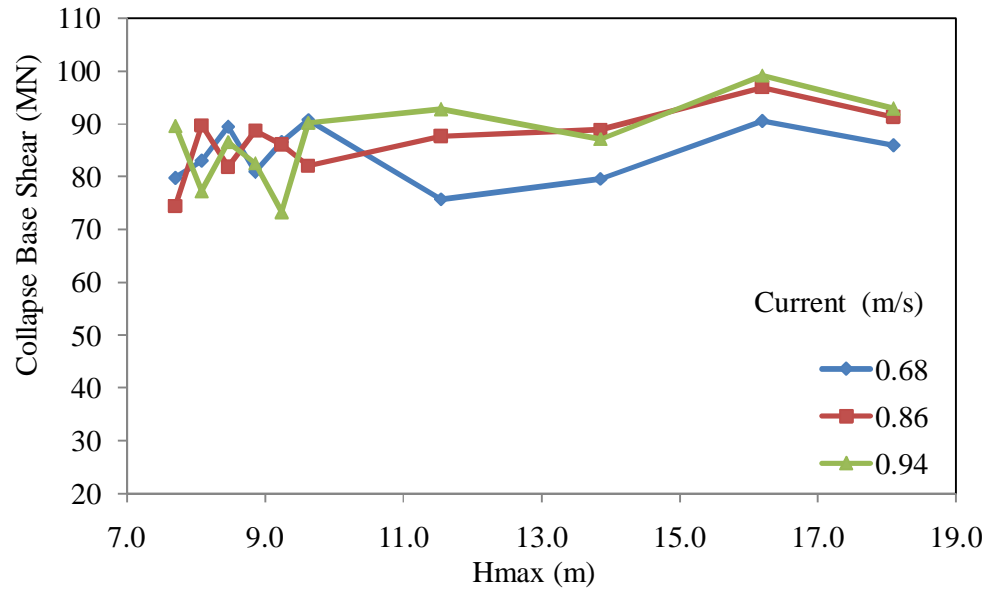


Figure C1: Collapse Base Shear against H_{max} Wave with Varying Currents at SBO for 0 Degree

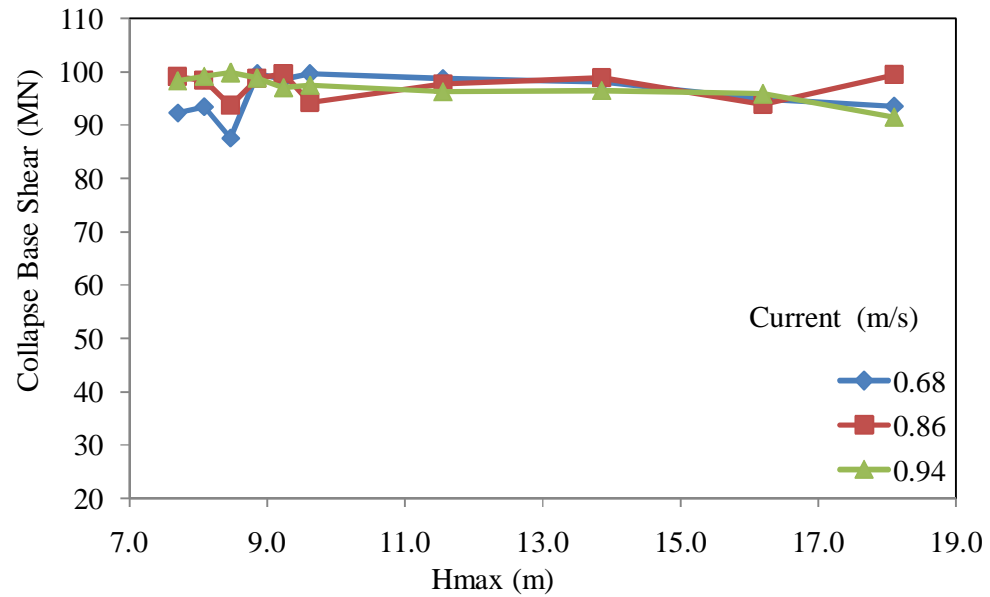


Figure C2: Collapse Base Shear against H_{max} Wave with Varying Currents at SBO for 61.59 Degree

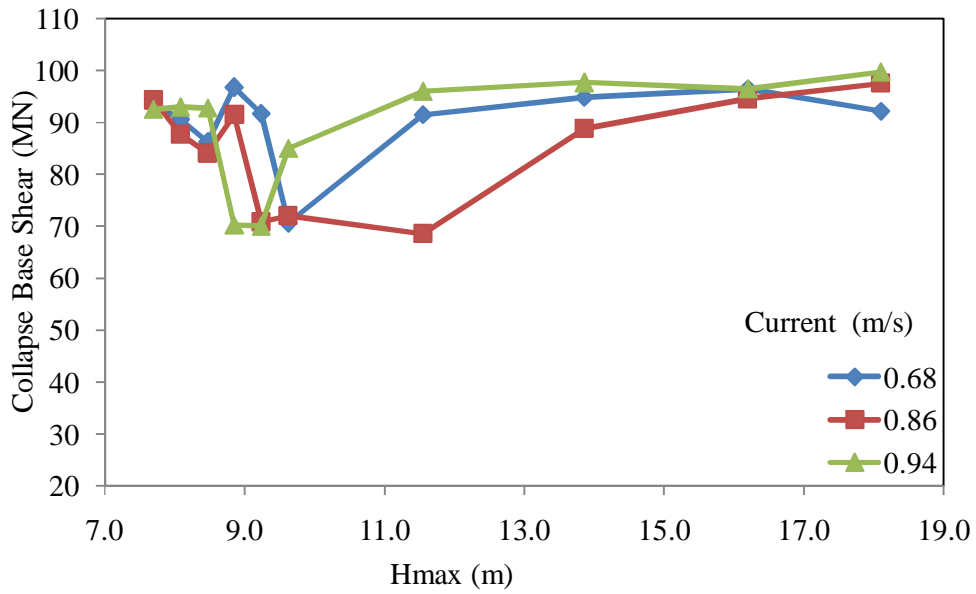


Figure C3: Collapse Base Shear against H_{max} Wave with Varying Currents at SBO for 90 Degree

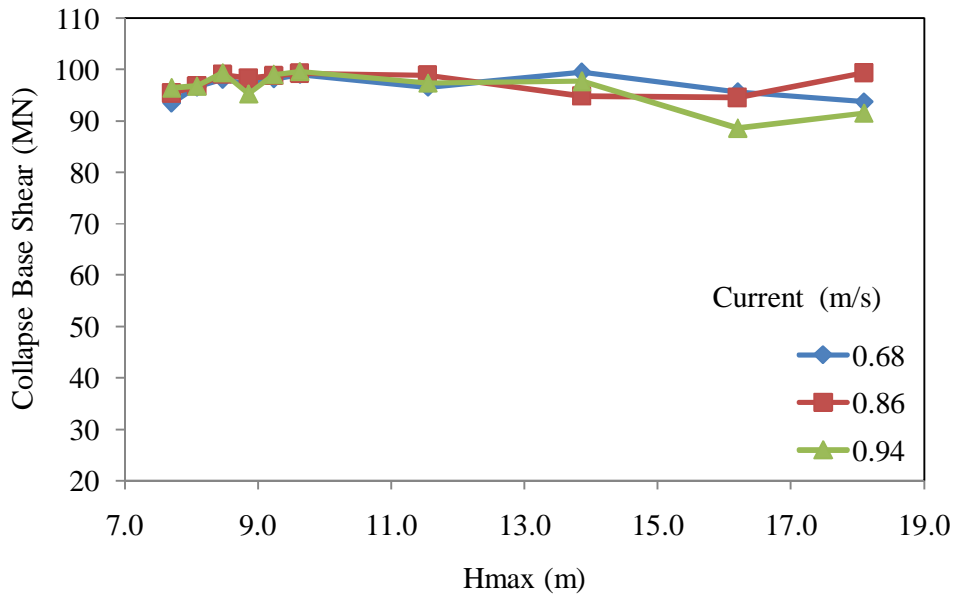


Figure C4: Collapse Base Shear against H_{max} Wave with Varying Currents at SBO for 118.41 Degree

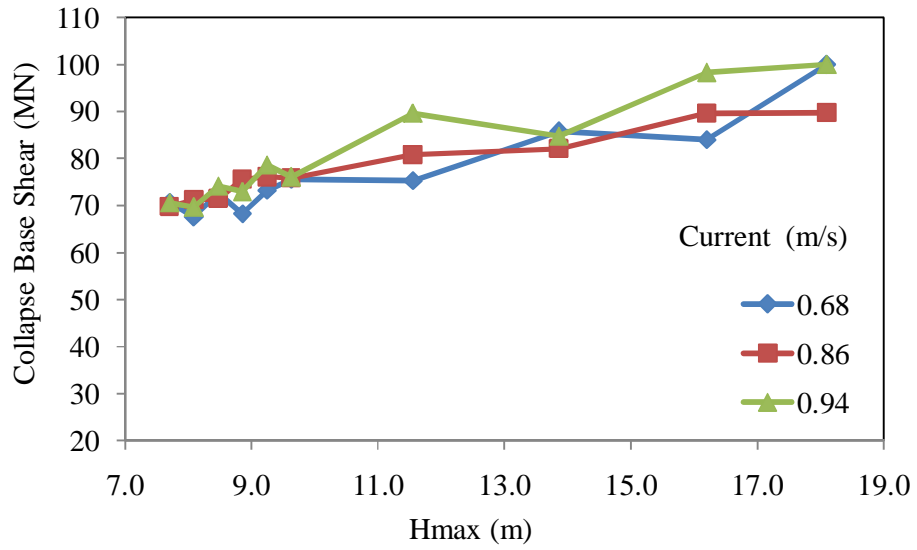


Figure C5: Collapse Base Shear against H_{max} Wave with Varying Currents at SBO for 180 Degree

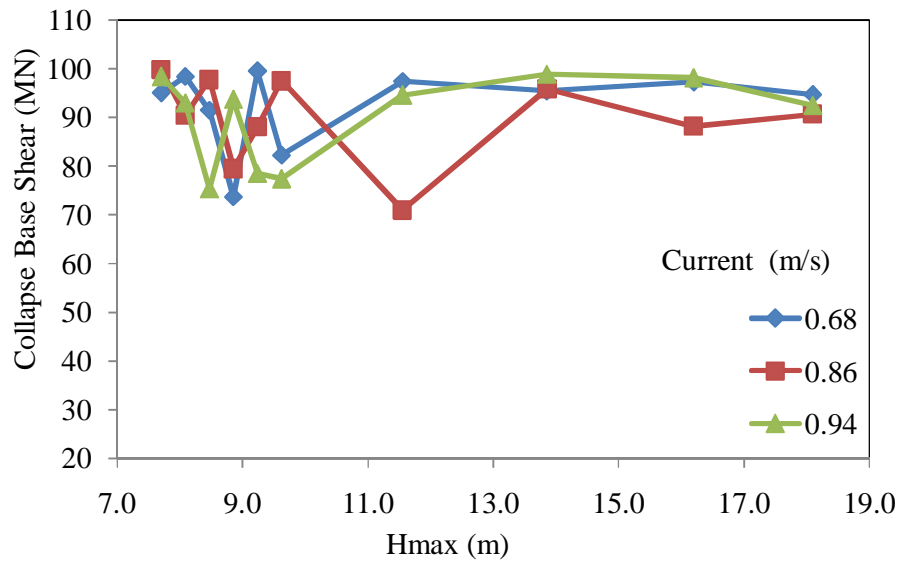


Figure C6: Collapse Base Shear against H_{max} Wave with Varying Currents at SBO for 241.59 Degree

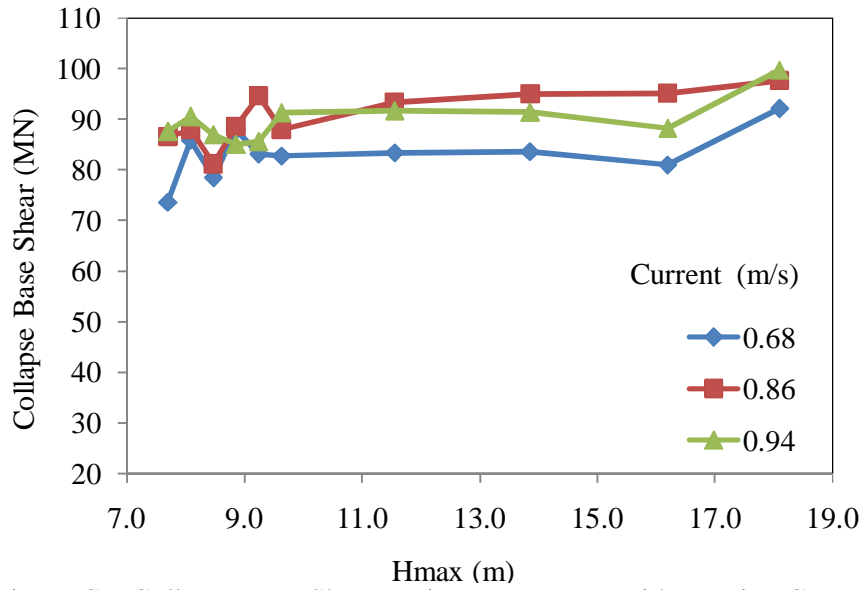


Figure C7: Collapse Base Shear against H_{max} Wave with Varying Currents at SBO for 270 Degree

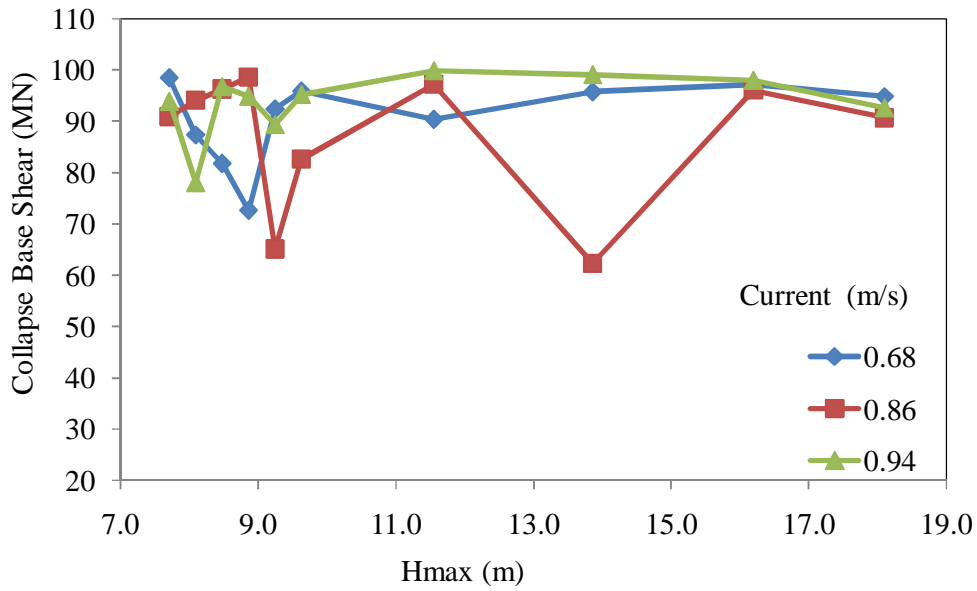


Figure C8: Collapse Base Shear against H_{max} Wave with Varying Currents at SBO for 298.41 Degree

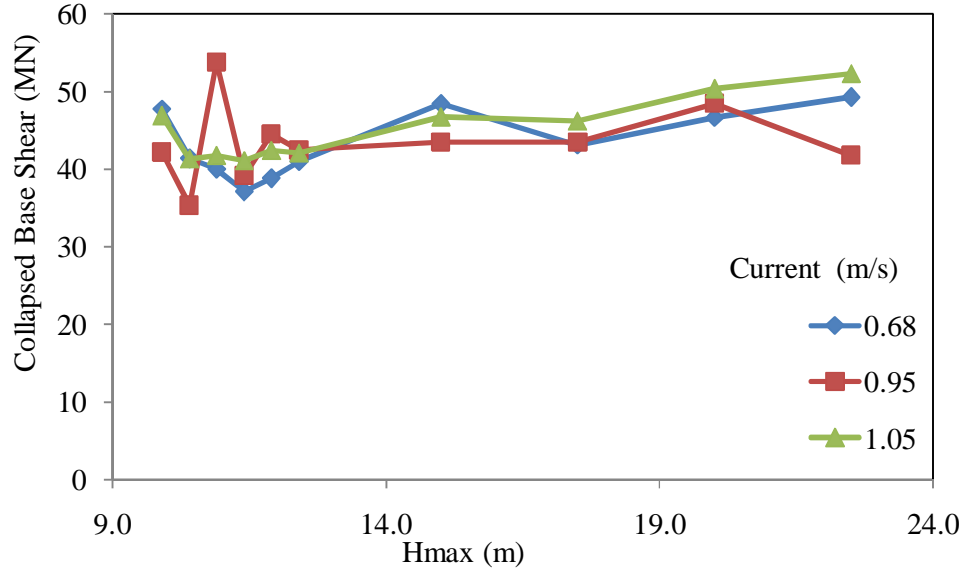


Figure C9: Collapse Base Shear against H_{max} Wave with Varying Currents at SKO1 for 0 Degree

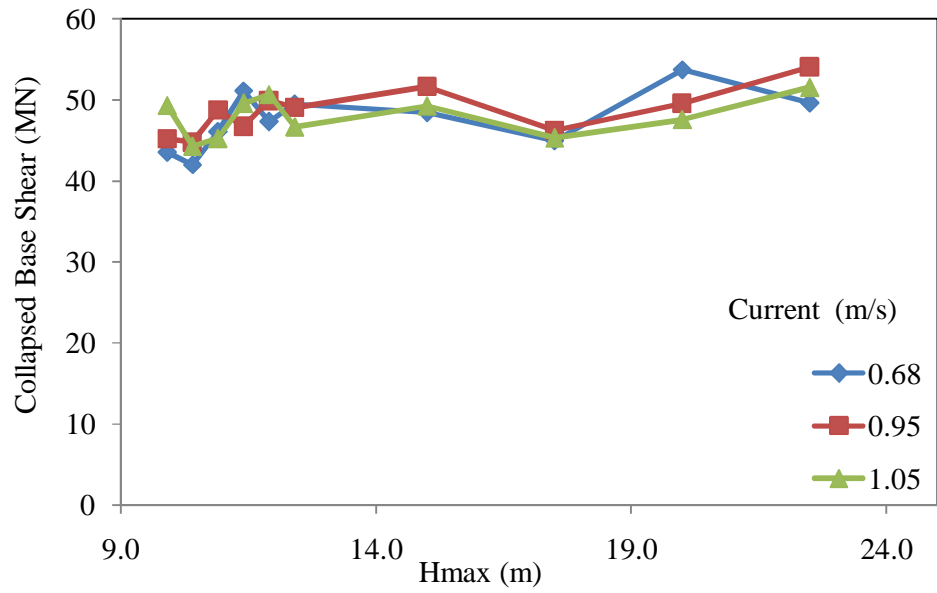


Figure C10: Collapse Base Shear against H_{max} Wave with Varying Currents at SKO1 for 45 Degree

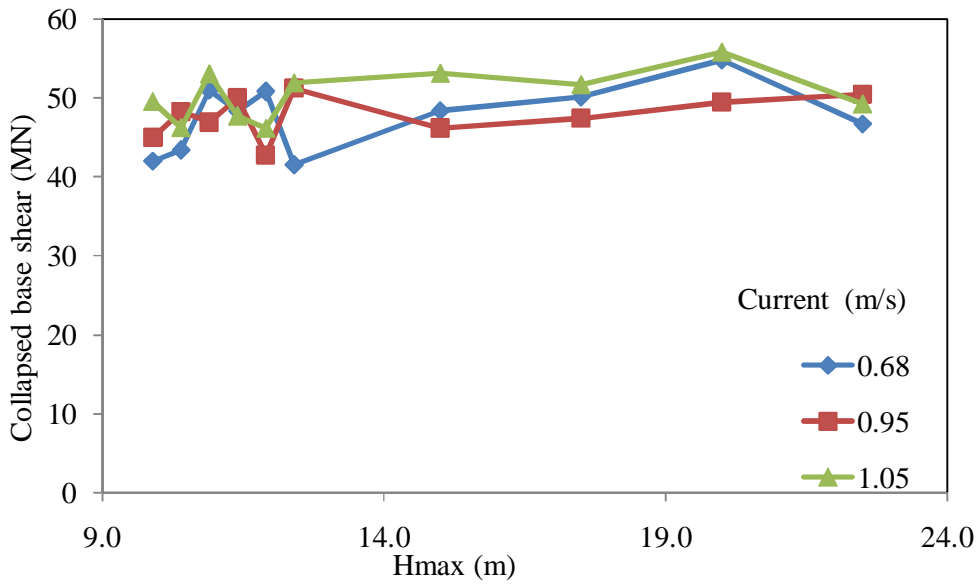


Figure C11: Collapse Base Shear against H_{max} Wave with Varying Currents at SKO1 for 90 Degree

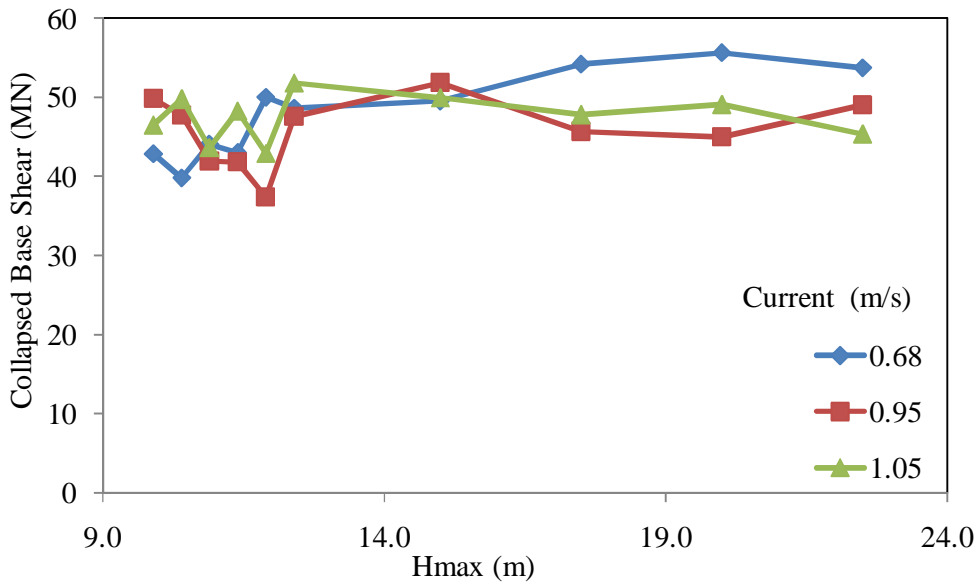


Figure C12: Collapse Base Shear against H_{max} Wave with Varying Currents at SKO1 for 135 Degree

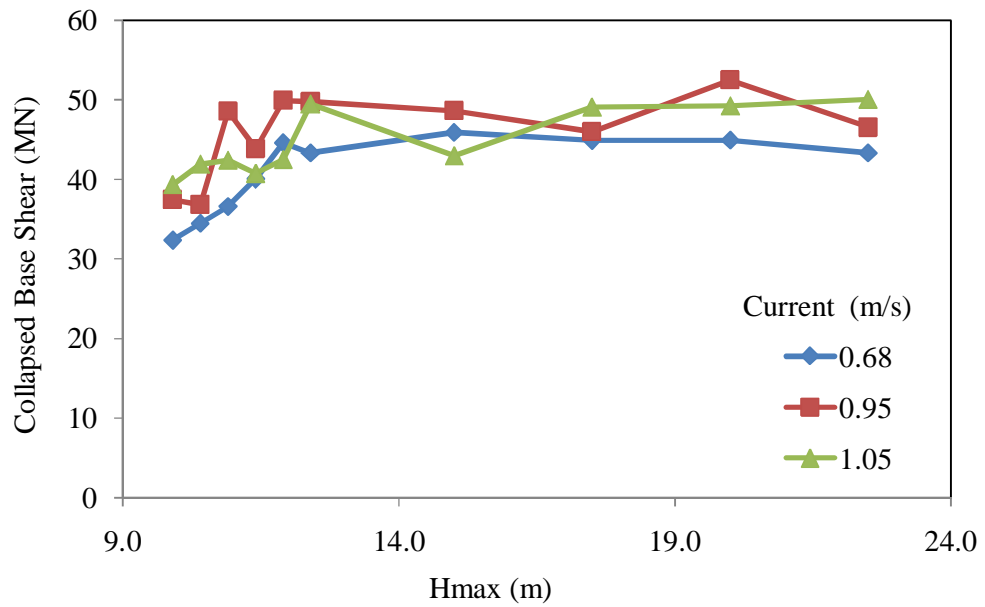


Figure C13: Collapse Base Shear against H_{max} Wave with Varying Currents at SKO1 for 180 Degree

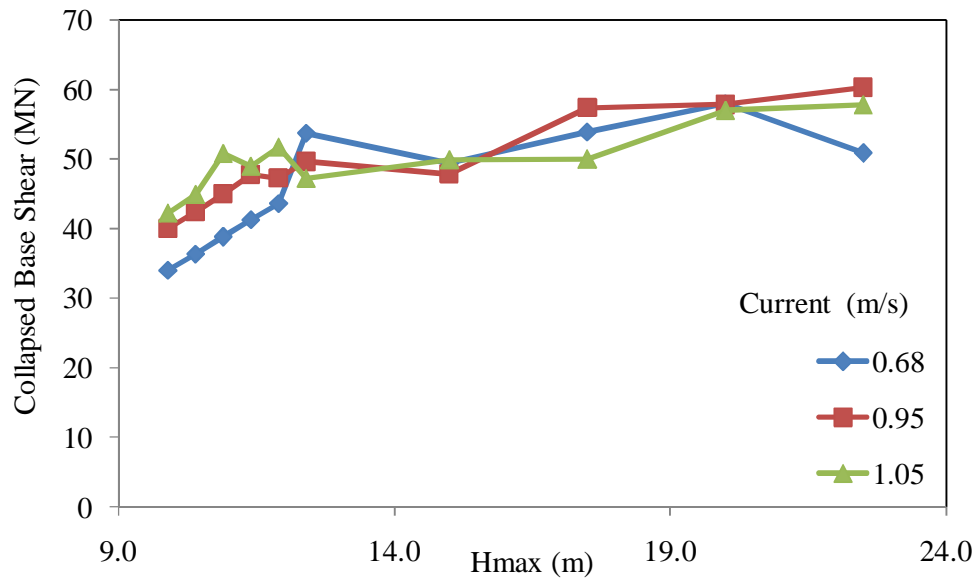


Figure C14: Collapse Base Shear against H_{max} Wave with Varying Currents at SKO1 for 225 Degree

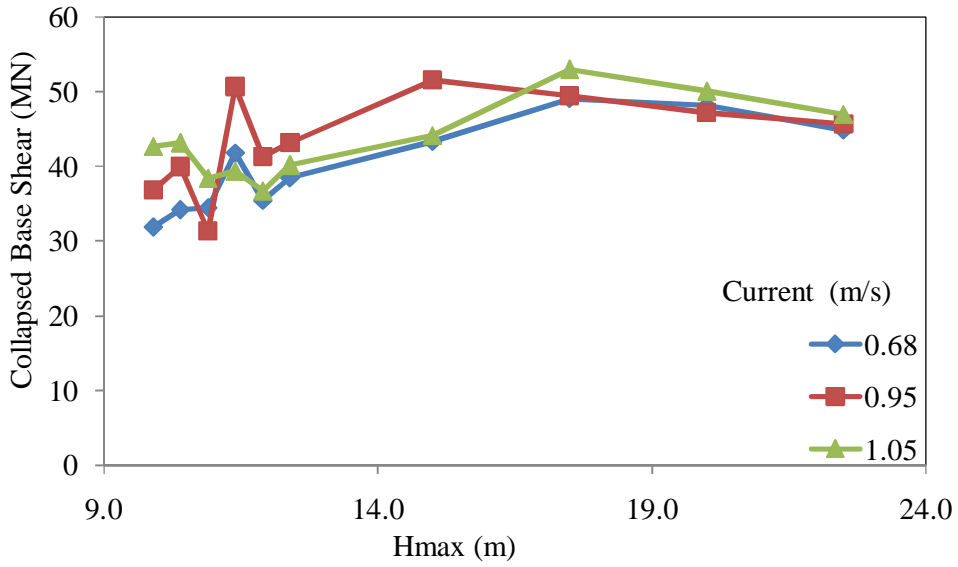


Figure C15: Collapse Base Shear against H_{max} Wave with Varying Currents at SKO1 for 270 Degree

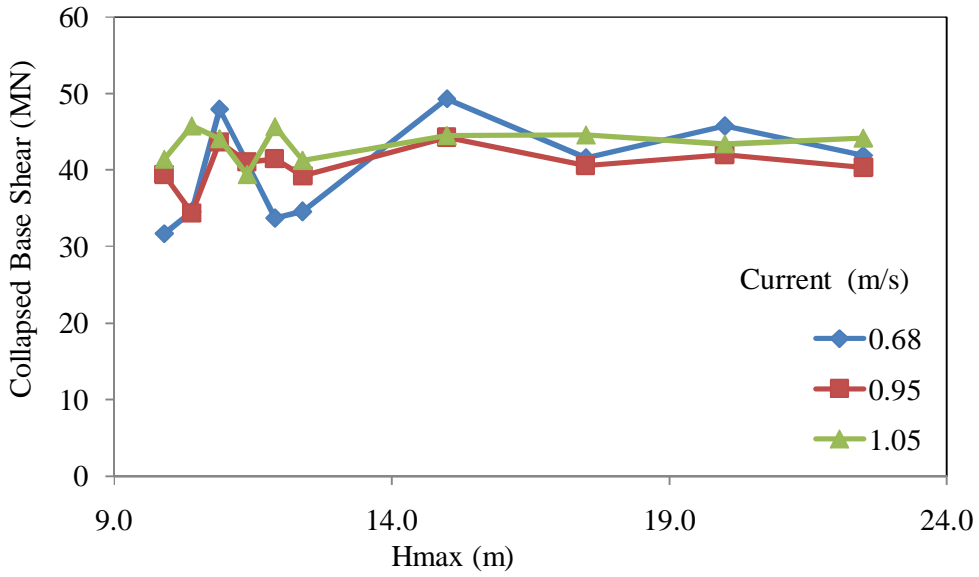


Figure C16: Collapse Base Shear against H_{max} Wave with Varying Currents at SKO1 for 315 Degree

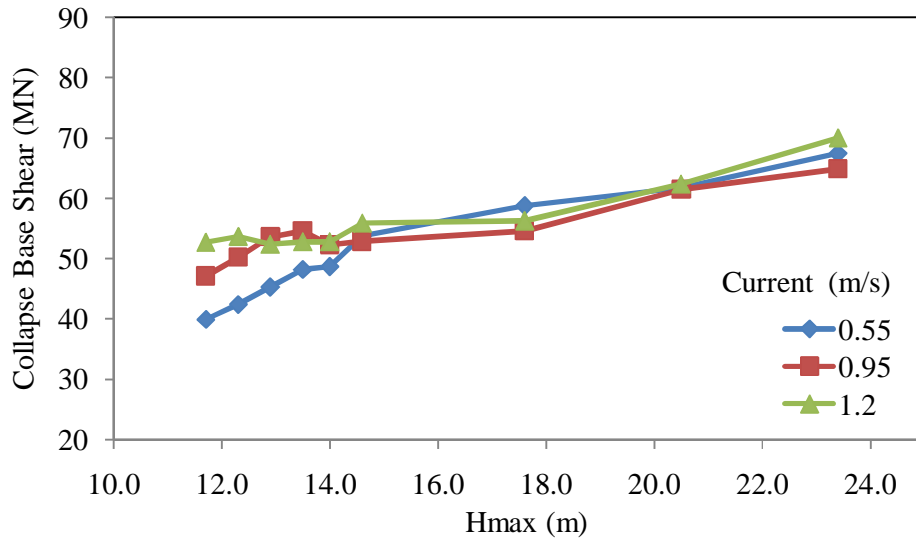


Figure C17: Collapse Base Shear against H_{max} Wave with Varying Currents at SKO2 for 0 Degree

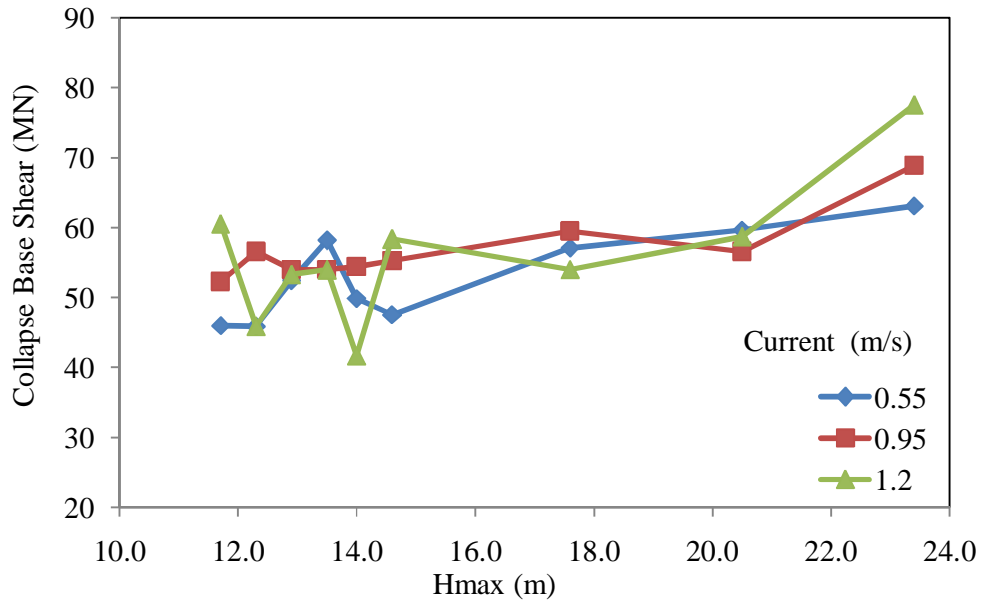


Figure C18: Collapse Base Shear against H_{max} Wave with Varying Currents at SKO2 for 45 Degree

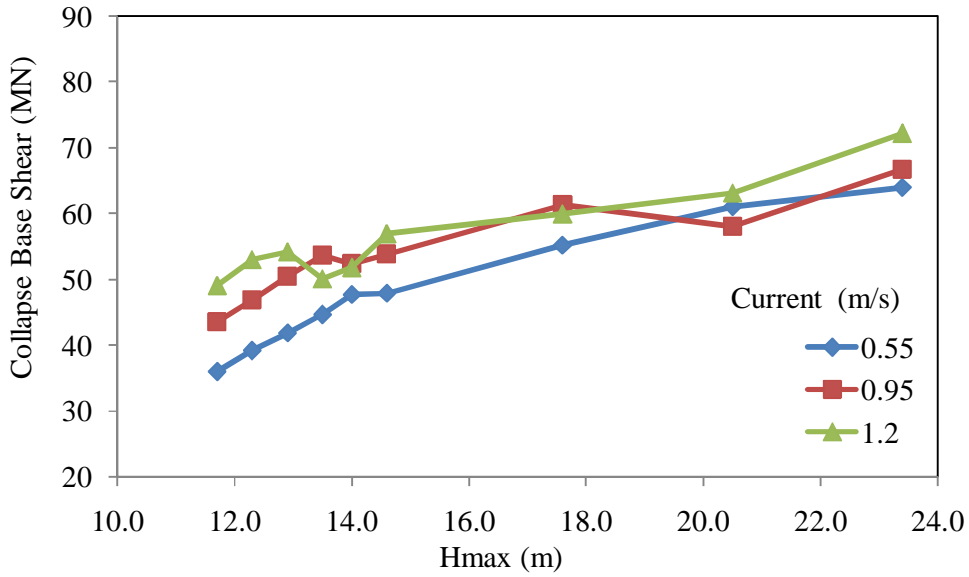


Figure C19: Collapse Base Shear against H_{max} Wave with Varying Currents at SKO2 for 90 Degree

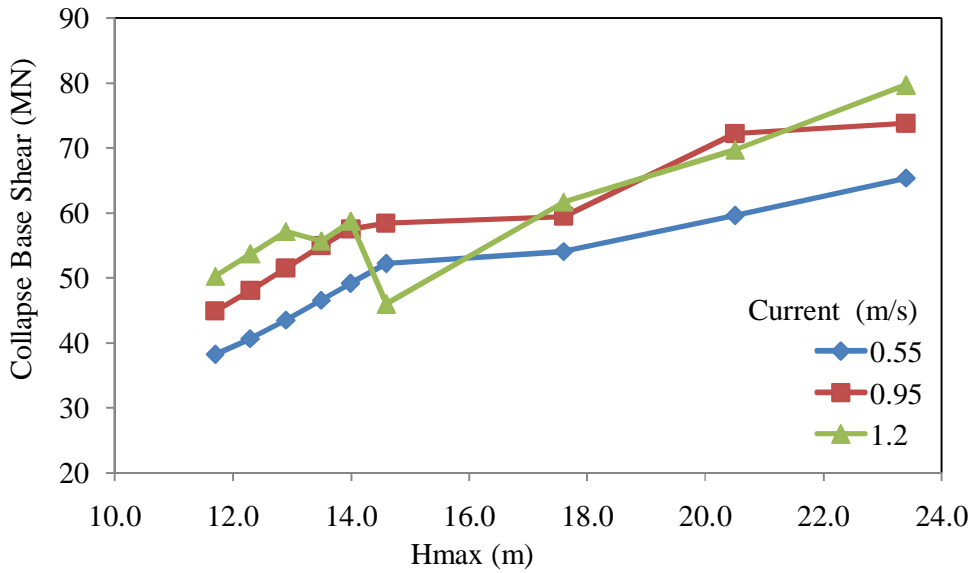


Figure C20: Collapse Base Shear against H_{max} Wave with Varying Currents at SKO2 for 135 Degree

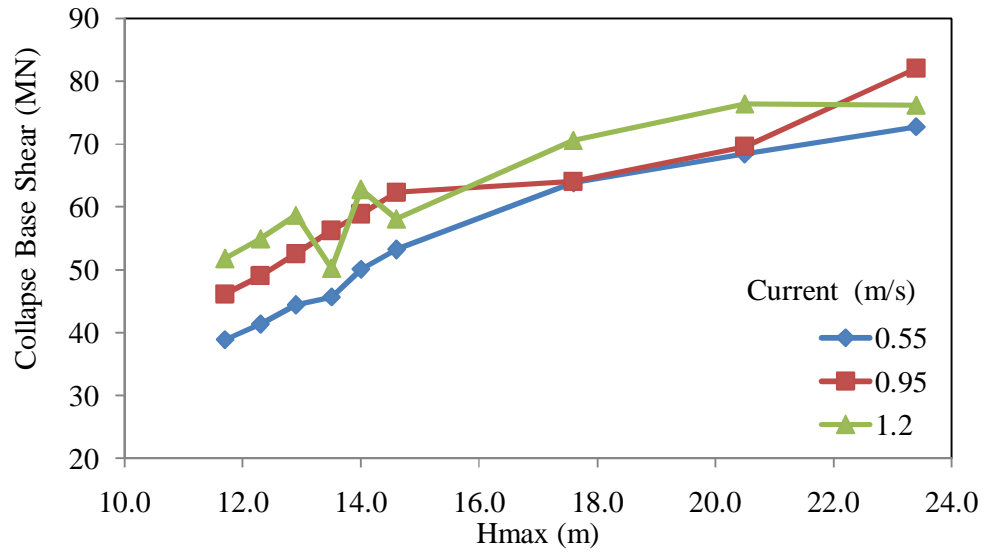


Figure C21: Collapse Base Shear against H_{max} Wave with Varying Currents at SKO2 for 180 Degree

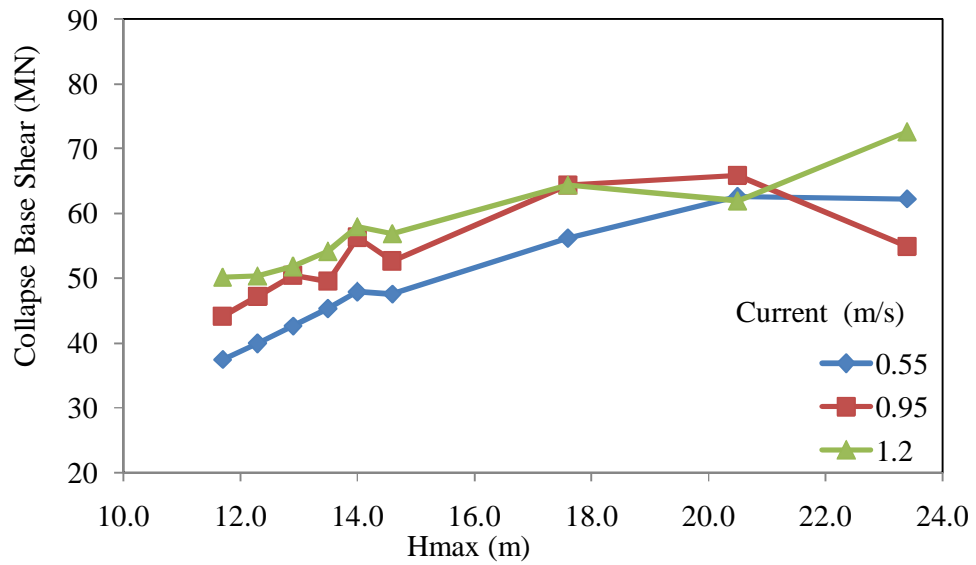


Figure C22: Collapse Base Shear against H_{max} Wave with Varying Currents at SKO2 for 225 Degree

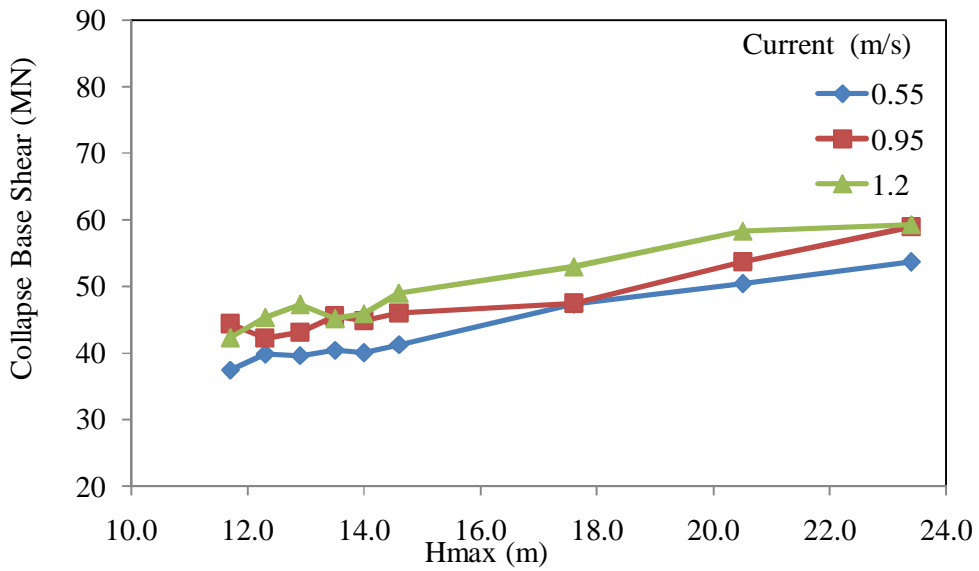


Figure C23: Collapse Base Shear against H_{max} Wave with Varying Currents at SKO2 for 270 Degree

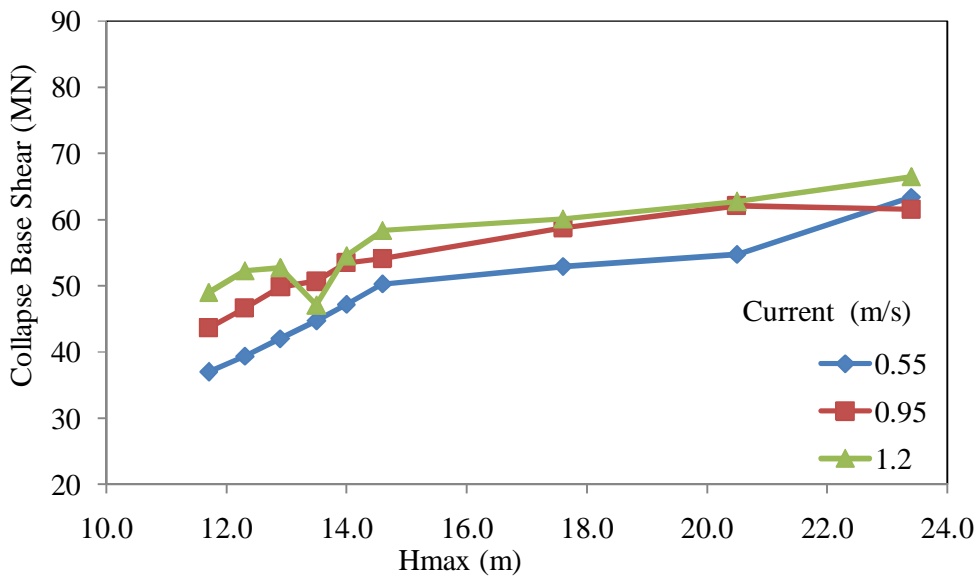


Figure C24: Collapse Base Shear against H_{max} Wave with Varying Currents at SKO2 for 315 Degree

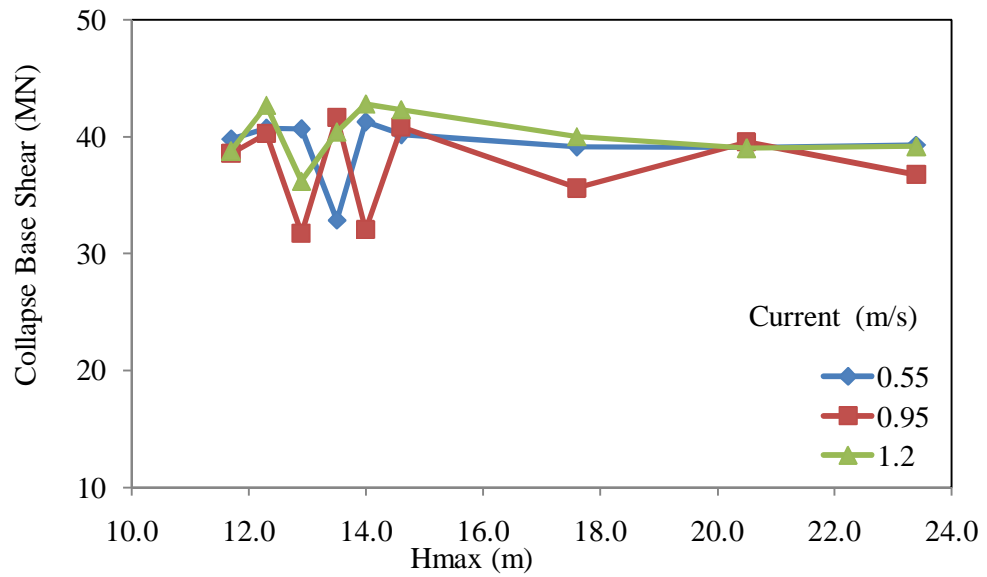


Figure C25: Collapse Base Shear against H_{max} Wave with Varying Currents at SKO2a for 0 Degree

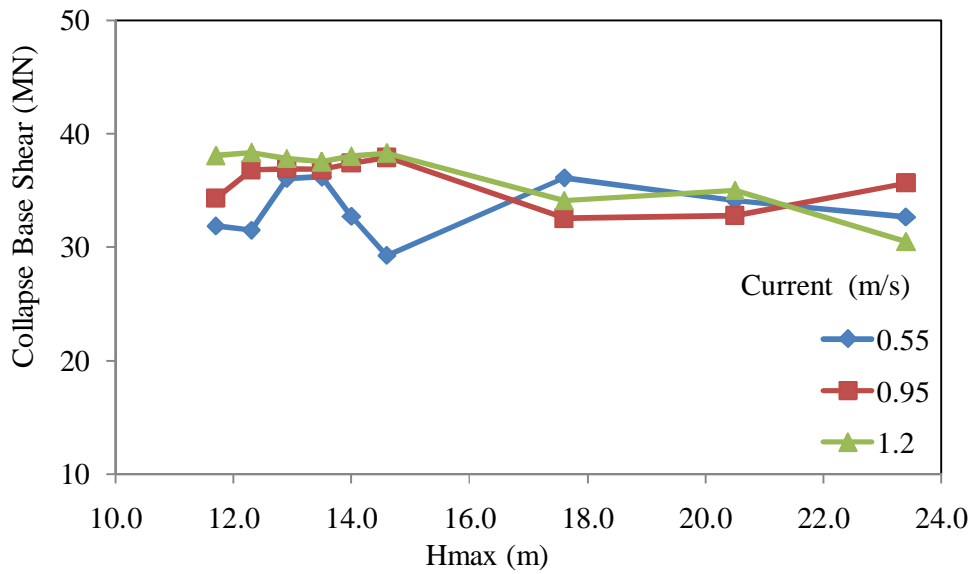


Figure C26: Collapse Base Shear against H_{max} Wave with Varying Currents at SKO2a for 45 Degree

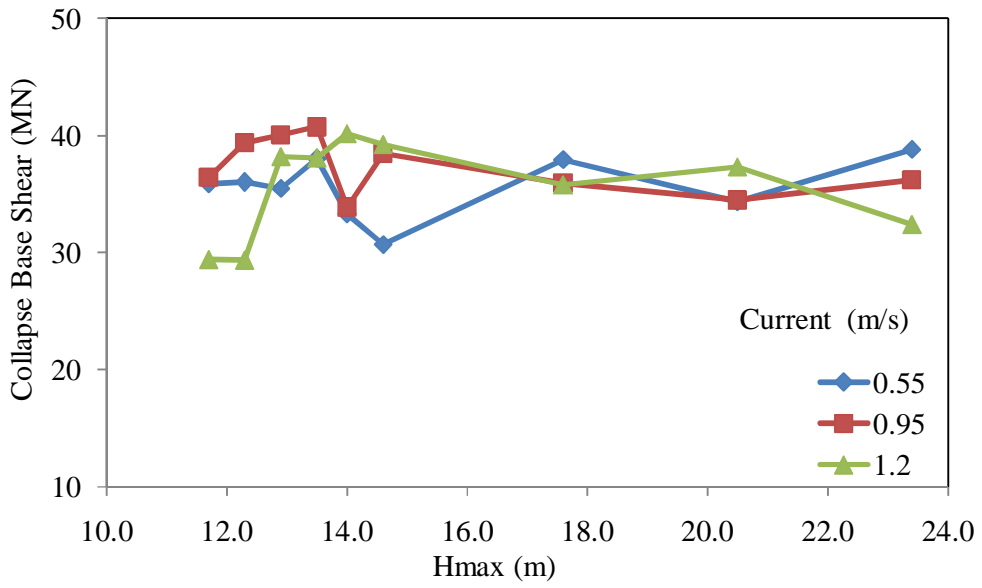


Figure C27: Collapse Base Shear against H_{max} Wave with Varying Currents at SKO2a for 90 Degree

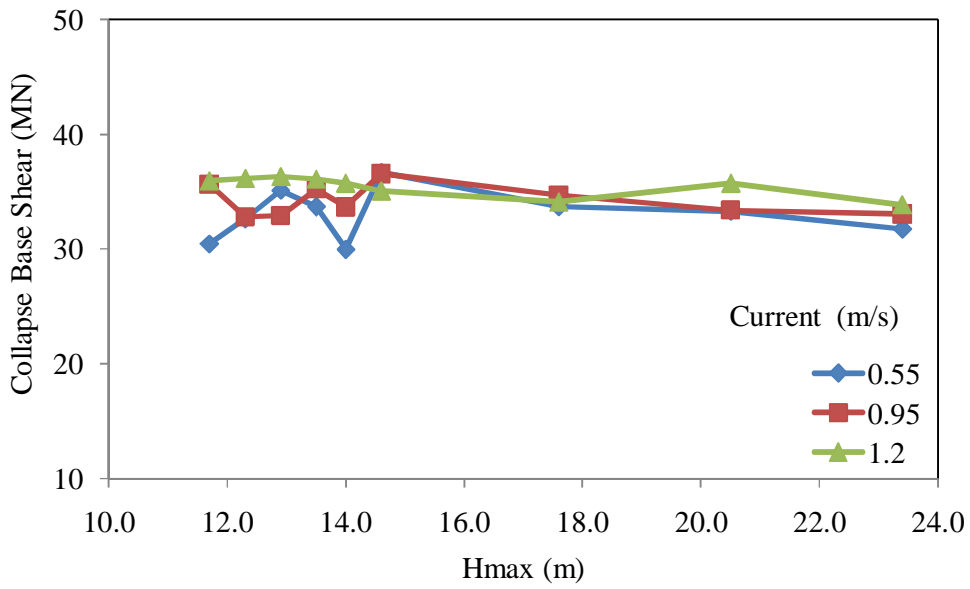


Figure C28: Collapse Base Shear against H_{max} Wave with Varying Currents at SKO2a for 135 Degree

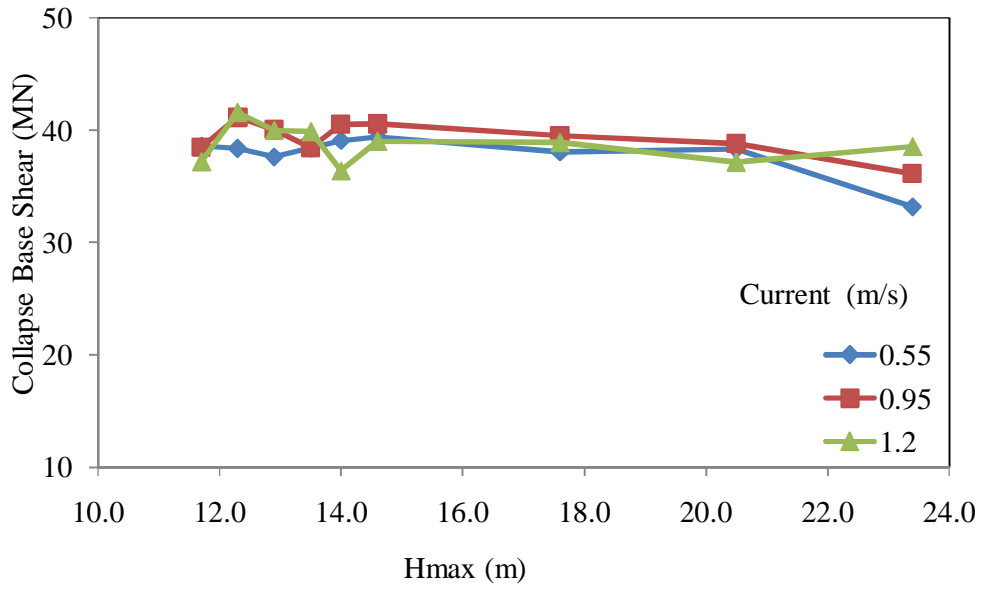


Figure C29: Collapse Base Shear against H_{max} Wave with Varying Currents at SKO2a for 180 Degree

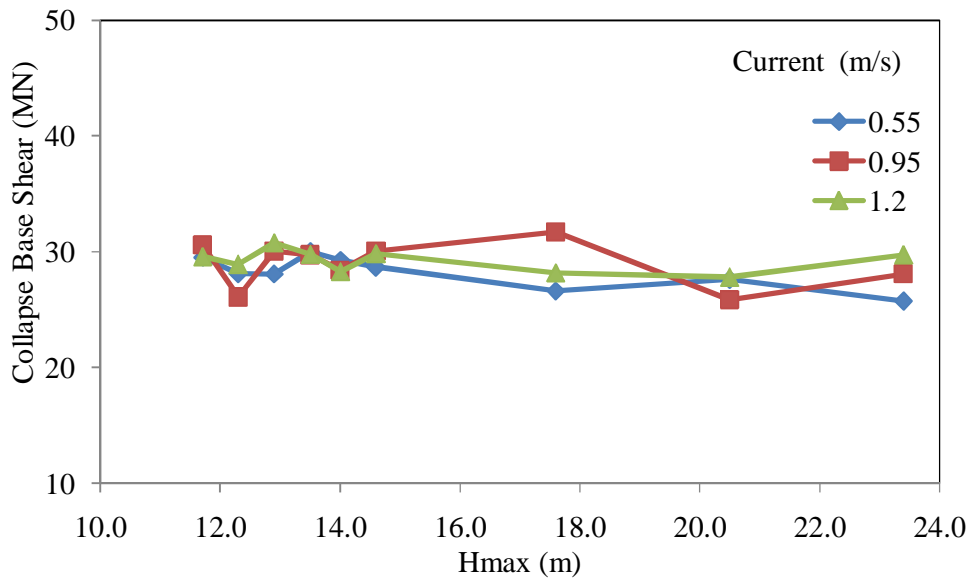


Figure C30: Collapse Base Shear against H_{max} Wave with Varying Currents at SKO2a for 225 Degree

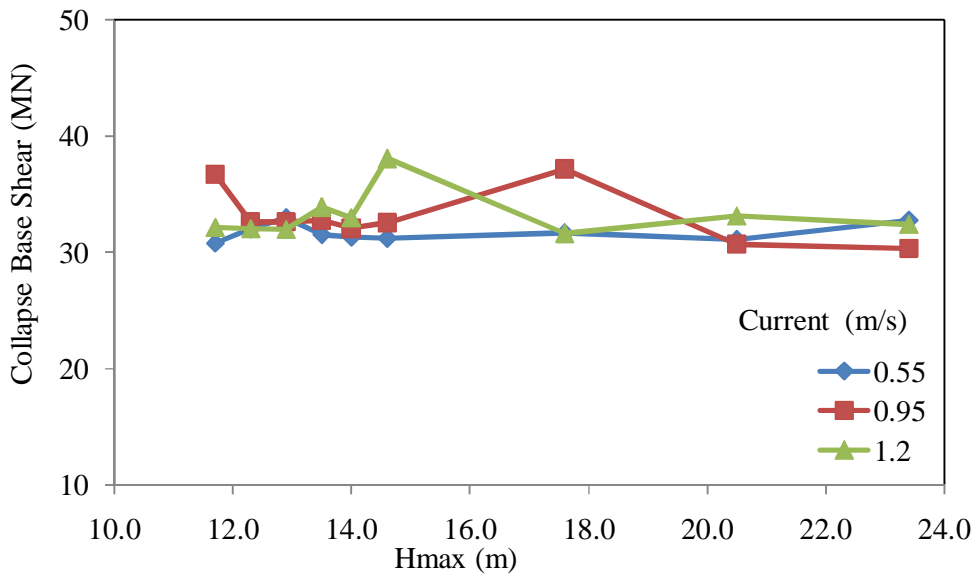


Figure C31: Collapse Base Shear against H_{max} Wave with Varying Currents at SKO2a for 270 Degree

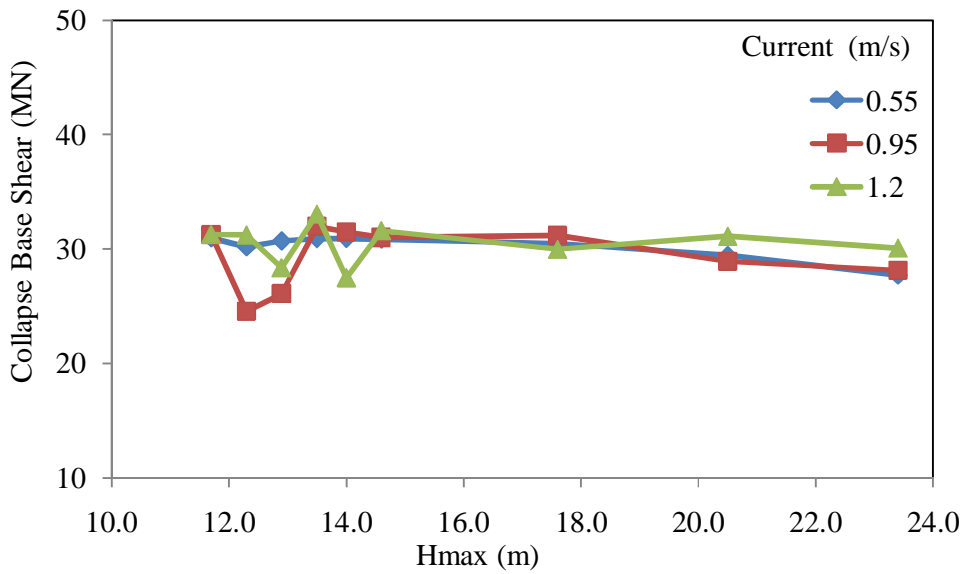


Figure C32: Collapse Base Shear against H_{max} Wave with Varying Currents at SKO2a for 315 Degree

APPENDIX D

Offshore Regions of Malaysia

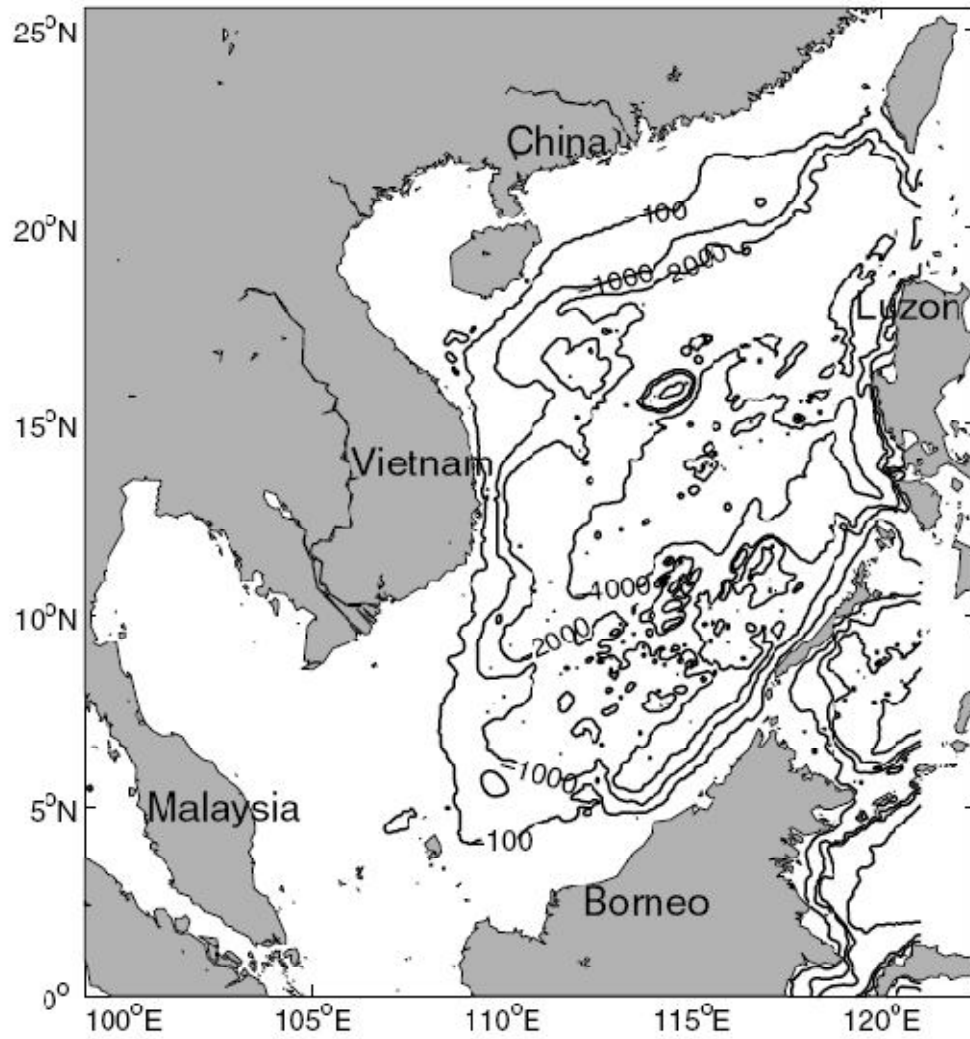


Figure D1: Offshore Malaysia [149]

APPENDIX E

Tubular Member API WSD and ISO 19902 Code Provisions

(a) Single Stresses

Table E1: API WSD and ISO Code Equations for Single Stress Component

API RP2A-WSD	ISO 19902
<p style="text-align: center;">Axial Tension</p> $F_t = 0.6F_y$	<p style="text-align: center;">Axial Tension</p> $\sigma_t \leq \frac{f_t}{\gamma_{R,t}}, \quad \gamma_{R,t} = 1.05$
<p style="text-align: center;">Axial Compression</p> <p style="text-align: center;">Column Buckling</p> $F_a = \frac{\left[1 - \frac{(Kl/r)^2}{2C_c^2}\right] F_y}{5/3 + \frac{3(Kl/r)}{8C_c} - \frac{(Kl/r)^3}{8C_c^3}} \quad \text{for } \frac{Kl}{r} < C_c$ $F_a = \frac{12\pi^2 E}{23(Kl/r)^2} \quad \text{for } \frac{Kl}{r} \geq C_c$ $C_c = \left[\frac{2\pi^2 E}{F_y}\right]^{1/2}$ <p style="text-align: center;">Local buckling</p> $F_{xe} = 2CE t/D, \quad C=0.3$ $F_{xc} = F_y \left[1.64 - 0.23 \left(\frac{D}{t}\right)^{\frac{1}{4}}\right] \leq F_{xe}, \quad \frac{D}{t} > 60$	<p style="text-align: center;">Axial Compression</p> $\sigma_c \leq \frac{f_c}{\gamma_{R,c}}, \quad \gamma_{R,c} = 1.18$ <p style="text-align: center;">Column Buckling</p> $f_c = (1 - 0.278\lambda^2) f_{yc} \quad \text{for } \lambda \leq 1.34$ $f_c = \frac{0.9}{\lambda^2} f_{yc} \quad \text{for } \lambda > 1.34$ $\lambda = \sqrt{\frac{f_{yc}}{f_e}} = \frac{KL}{\pi r} \sqrt{\frac{f_{yc}}{E}}$ <p style="text-align: center;">Local Buckling</p> $F_{yc} = F_y \quad \text{for } \frac{f_y}{f_{xe}} \leq 0.170$

$F_{xe} = F_y, \text{ for } (D/t) \leq 60$	$f_{yc} = \begin{cases} 1.047 \\ - 0.274 \frac{f_y}{f_{xe}} \end{cases} f_y, \text{ for } 0.170 < \frac{f_y}{f_{xe}} < \frac{f_y}{f_{xe}}$ $F_{xe} = 2C_x Et/D$ $C_x = 0.3$
<p style="text-align: center;">Bending</p> $F_b = 0.75 F_y \quad D/t \leq \frac{10340}{F_y}$ $F_b = \left[0.84 - 1.74 \frac{F_y D}{Et} \right] F_y, \frac{10340}{F_y} < \frac{D}{t} \leq 20680/F_y$ $F_b = \left[0.72 - 0.58 \frac{F_y D}{Et} \right] F_y, \text{ for } 3000/F_y < D/t \leq 300$	<p style="text-align: center;">Bending</p> $\sigma_b = \frac{M}{Z_e} \leq \frac{f_b}{\gamma_{R,b}}, \quad \gamma_{R,b} = 1.05$ $f_b = \left(\frac{Z_p}{Z_e} \right) f_y \quad \text{for } \frac{f_y D}{Et} \leq 0.0517$ $f_b = \left[1.13 - 2.58 \left(\frac{f_y D}{Et} \right) \right] \left(\frac{Z_p}{Z_e} \right) f_y, \text{ for } 0.0517 < \frac{f_y D}{Et} \leq 0.1034$ $f_b = \begin{cases} 0.94 \\ - 0.76 \left(\frac{f_y D}{Et} \right) \end{cases} \left(\frac{Z_p}{Z_e} \right) f_y, \text{ for } 0.1034 < \frac{f_y D}{Et} \leq 120 \frac{f_y}{E}$

(b) Combined Stresses

Table E2: API WSD and ISO Code Equations for Combined Stress Component

API RP2A-WSD	ISO 19902
<p>Tension and Bending</p> $\frac{f_a}{0.6F_{xc}} + \frac{\sqrt{f_{bx}^2 + f_{by}^2}}{F_b} \leq 1.0$	<p>Tension and Bending</p> $\frac{\gamma_{R,t}\sigma_t}{f_t} + \frac{\gamma_{R,b}\sqrt{\sigma_{b,y}^2 + \sigma_{b,z}^2}}{f_b} \leq 1.0$
<p>Compression and Bending</p> $\frac{f_a}{F_b} + \frac{C_m \sqrt{f_{bx}^2 + f_{by}^2}}{\left(1 - \frac{f_a}{F_e}\right) F_b} \leq 1.0$ $\frac{f_a}{F_a} + \frac{\sqrt{\left[\frac{C_{mx}f_{bx}}{1 - \frac{f_a}{F_{ex}}}\right] + \left[\frac{C_{my}f_{by}}{1 - \frac{f_a}{F_{ey}}}\right]}}{F_b} \leq 1.0$ $\frac{f_a}{0.6F_a} + \frac{\sqrt{f_{bx}^2 + f_{by}^2}}{F_b} \leq 1.0$ <p>Hydrostatic Pressure (hoop buckling)</p> $f_h \leq F_{hc}/SF_{hc}$ <p>Critical hoop buckling stress</p>	<p>Compression and Bending</p> $\frac{\gamma_{R,c}\sigma_c}{f_c} + \frac{\gamma_{R,b}}{f_b} \left[\left(\frac{C_{m,y}\sigma_{b,y}}{1 - \sigma_c/f_{e,y}} \right)^2 + \left(\frac{C_{m,z}\sigma_{b,z}}{1 - \sigma_c/f_{e,z}} \right)^2 \right]^{0.5} \leq 1.0$ $\frac{\gamma_{R,c}\sigma_c}{f_{yc}} + \frac{\gamma_{R,b}\sqrt{\sigma_{b,y}^2 + \sigma_{b,z}^2}}{f_b} \leq 1.0$ $f_{e,y} = \frac{\pi^2 E}{(K_y L_y / r)^2}$ $f_{e,z} = \frac{\pi^2 E}{(K_z L_z / r)^2}$ <p>Hydrostatic Pressure (hoop buckling)</p> $\sigma_h = \frac{pD}{2t} \leq \frac{f_h}{\gamma_{R,h}}, \quad \sigma_h = 1.25$

$$F_{hc} = F_{he} \quad , \quad F_{he} \leq 0.55 F_y$$

$$F_{hc} = 0.45F_y + 0.18 F_{he} \quad , \quad 0.55 < F_{he} \leq 1.6F_y$$

$$F_{hc} = \frac{1.31F_y}{1.15 + (F_y/F_{hc})} \quad 1.6F_y < F_{he} < 6.2F_y$$

$$F_{hc} = F_y \quad , \quad F_{he} > 6.2 F_y$$

Elastic hoop buckling stress

$$F_{he} = 2C_h Et/D$$

$$C_h = 0.44t/D$$

$$C_h = 0.44(t/D) + \frac{0.21\left(\frac{D}{t}\right)^3}{M^4} \quad , \quad 0.825 \frac{D}{t} \leq M < \frac{1.6D}{t}$$

$$C_h = 0.736/(M - 0.636) \quad , \quad 3.5 \leq M < 0.825 D/t$$

$$C_h = 0.755(M - 0.559) \quad , \quad 1.5 \leq M < 3.5$$

$$C_h = 0.8 \quad M < 1.5$$

$$M = \frac{L}{D} (2D/t)^{1/2}$$

$$f_h = f_y \quad \text{for } f_{he} > 2.44f_y$$

$$f_h = 0.7 \left(\frac{f_{he}}{f_y} \right)^{0.4} f_y \leq f_y$$

$$\text{for } 0.55f_y < f_{he} \leq 2.44f_y$$

$$f_h = f_{he} \quad \text{for } f_{he} \leq 0.55f_y$$

$$f_{he} = 2C_h Et/D,$$

$$C_h = \frac{0.44t}{D} \quad \text{for } \mu \geq 1.6 D/t$$

$$C_h = 0.44 t/D + 0.21(D/t)^3 \mu^4 \quad \text{for } 0.825 D/t \leq \mu < 1.6 D/t$$

$$C_h = \frac{0.737}{(\mu - 0.579)} \quad \text{for } 1.5 \leq \mu < 0.825 D/t$$

$$C_h = 0.80 \quad \text{for } \mu < 1.5$$

$$\mu = \frac{L_r}{D} \sqrt{\frac{2D}{t}}$$

APPENDIX F

Tubular Joints API WSD and ISO 19902 Code Provisions

(a) ISO 19902 Code Provisions

Table F1: ISO 19902 Code Equations for Joints

Axial Tension	Axial Compression	In-Plane Bending	Out-Plane Bending
K-Joint			
$(1.9 + 19\beta)Q_\beta^{0.5}Q_g$	$(1.9 + 19\beta)Q_\beta^{0.5}Q_g$	$4.5 \beta \gamma^{0.5}$	$3.2 \gamma^{(0.5 \beta^2)}$
T/Y Joint			
30β	$(1.9 + 19\beta)Q_\beta^{0.5}$	$4.5 \beta \gamma^{0.5}$	$3.2 \gamma^{(0.5 \beta^2)}$
X-Joint			
23β for $\beta \leq 0.9$ $20.7 + (\beta - 0.9)(17\gamma - 220)$ for $\beta > 0.9$	$[2.8 + (12 + 0.1\gamma)\beta]Q_\beta$	$4.5 \beta \gamma^{0.5}$	$3.2 \gamma^{(0.5 \beta^2)}$

Table F2: ISO 19902 Code Equations for Geometrical and Gap Factor

$Q_\beta =$ Geometrical Factor	$Q_g =$ Gap factor
$Q_\beta = \frac{0.3}{\beta(1-0.833\beta)}$ for $\beta > 0.6$	$Q_g = 1.9 - 0.7 \gamma^{-0.5} (g/T)^{0.5}$ for $(g/T) \geq 2.0$ but $Q_g \geq 1.0$
$Q_\beta = 1.0$ for $\beta \leq 0.6$	$Q_g = 0.13 + 0.65 \phi \gamma^{0.5} (g/T)^{0.5}$ for $(g/T) \leq -2.0$
	$\phi = \frac{t * f_{yb}}{(T * f_y)}$

$$Q_f = 1 - \lambda q_A^2$$

Where $\lambda=0.03$ (brace axial force), 0.045 (brace IPB), 0.021 (brace OPB)

$$q_A = \left[C_1 \left(\frac{P_c}{P_y} \right)^2 + C_2 \left(\frac{M_c}{M_p} \right)_{ipb}^2 + C_2 \left(\frac{M_c}{M_p} \right)_{opb}^2 \right]^{0.5} \gamma_{Rq}$$

Table F3: Coefficients C_1 and C_2

Joint Type	C_1	C_2
Y-Joint	25	11
X-Joint	20	22
K-Joint	14	43

(b) API WSD Code Provisions

Table F4: API WSD Code Equations for Joints

Axial Tension	Axial Compression	In-Plane Bending	Out-Plane Bending
K-joint			
$(16 + 1.2\gamma)\beta^{1.2}Q_g$ but $\leq 40 \beta^{1.2}Q_g$	$(16 + 1.2\gamma)\beta^{1.2}Q_g$ but $\leq 40 \beta^{1.2}Q_g$	$(5 + 0.7 \gamma)\beta^{1.2}$	$2.5 + (4.5 + 0.2 \gamma)\beta^{2.6}$
T/Y joint			
30β	$2.8 + (20 + 0.8 \gamma)\beta^{1.6}$ but $\leq 2.8 + 36 \beta^{1.6}$	$(5 + 0.7 \gamma)\beta^{1.2}$	$2.5 + (4.5 + 0.2 \gamma)\beta^{2.6}$
X-joint			
23β for $\beta \leq 0.9$ $20.7 + (\beta - 0.917\gamma - 220)$ for $\beta > 0.9$	$[2.8 + (12 + 0.1\gamma)\beta]Q_\beta$	$(5 + 0.7 \gamma)\beta^{1.2}$	$2.5 + (4.5 + 0.2 \gamma)\beta^{2.6}$

Table F5: API WSD Code Equations for Geometrical and Gap Factor

$Q_\beta = \text{Geometrical Factor}$	$Q_g = \text{Gap factor}$
$Q_\beta = \frac{0.3}{\beta(1-0.833\beta)}$ for $\beta > 0.6$	$Q_g = 1 + 0.2[1 - 2.8 g/D]^3$ for $g/D \geq 0.05$ but ≥ 1.0
$Q_\beta = 1.0$ for $\beta \leq 0.6$	$Q_g = 0.13 + 0.65 \phi \gamma^{0.5} (g/T)^{0.5}$ for $(g/T) \leq -2.0$ $\phi = \frac{t * f_{yb}}{(T * f_y)}$

$$Q_f = \left[1 + C_1 \left(\frac{FS P_c}{P_y} \right) - C_2 \left(\frac{FS M_{ipb}}{M_p} \right) - C_3 A^2 \right]$$

$$A = \left[\left(\frac{FS P_c}{P_y} \right)^2 + \left(\frac{FS M_c}{M_p} \right)^2 \right]^{0.5}, \text{ FS}=1.2$$

Table F6: Coefficients C_1, C_2 and C_3

Joint Type	C_1	C_2	C_3
K-Joint	0.2	0.2	0.3
T/Y-Joint	0.3	0	0.8
X-Joint			
$\beta \leq 0.9$	0.2	0	0.5
$\beta = 1.0$	-0.2	0	0.2

APPENDIX G

Evaluation of RSR of 1.0 and system redundancy

a) PMO Jacket:

Direction	Wave Period (Sec)	Wave Height (m)	Current (cm/s)	Base shear (KN)		RSR	Peak Load (KN)	100 Year/ Peak Load	System Redundancy
				Collapse Load (KN)	100 Year Load (KN)				
0	10	10.8	0.57	19305	7427	2.60	23023	0.32	1.32
0	10	10.8	1	20233	9199	2.20	23919	0.38	1.38
0	10	10.8	1.1	20385	9709	2.10	24274	0.40	1.40
0	10.1	11.3	0.57	19153	7982	2.40	23149	0.34	1.34
0	10.1	11.3	1	20669	9844	2.10	23628	0.42	1.42
0	10.1	11.3	1.1	20596	10300	2.00	24722	0.42	1.42
0	10.3	11.9	0.57	19846	8630	2.30	23303	0.37	1.37
0	10.3	11.9	1	21375	10689	2.00	23519	0.45	1.45
0	10.3	11.9	1.1	21370	11249	1.90	24751	0.45	1.45
0	10.5	12.4	0.57	20650	9388	2.20	23472	0.40	1.40
0	10.5	12.4	1	21875	11515	1.90	24184	0.48	1.48
0	10.5	12.4	1.1	21556	11977	1.80	23958	0.50	1.50
0	10.7	13.0	0.57	21523	10250	2.10	23579	0.43	1.43
0	10.7	13.0	1	22346	12416	1.80	24836	0.50	1.50
0	10.7	13.0	1.1	22156	13034	1.70	24769	0.53	1.53
0	10.9	13.5	0.57	29834	10967	2.72	23035	0.48	1.48
0	10.9	13.5	1	22700	13354	1.70	24042	0.56	1.56
0	10.9	13.5	1.1	22221	13887	1.60	25001	0.56	1.56
0	11.8	16	0.57	22681	15122	1.50	24201	0.62	1.62
0	11.8	16	1	23340	17954	1.30	25141	0.71	1.71
0	11.8	16	1.1	24366	18744	1.30	26253	0.71	1.71
0	12.8	19	0.57	23439	21194	1.11	23439	0.90	1.90
0	12.8	19	1	24728	24728	1.00	24728	1.00	2.00
0	12.8	19	1.1	25565	25565	1.00	25565	1.00	2.00
45	10	10.8	0.57	25301	8437	3.00	25301	0.33	1.33
45	10	10.8	1	26557	10418	2.55	26557	0.39	1.39
45	10	10.8	1.1	26784	10935	2.45	26784	0.41	1.41
45	10.1	11.3	0.57	23986	9055	2.65	24893	0.36	1.36
45	10.1	11.3	1	25648	11154	2.30	26765	0.42	1.42
45	10.1	11.3	1.1	26282	11684	2.25	26282	0.44	1.44
45	10.3	11.9	0.57	23964	9784	2.45	24943	0.39	1.39
45	10.3	11.9	1	25287	12045	2.10	27094	0.44	1.44
45	10.3	11.9	1.1	25913	12643	2.05	27179	0.47	1.47
45	10.5	12.4	0.57	23782	10573	2.25	25368	0.42	1.42

45	10.5	12.4	1	25890	12948	2.00	27187	0.48	1.48
45	10.5	12.4	1.1	26281	13480	1.95	27630	0.49	1.49
45	10.7	13	0.57	24727	11504	2.15	25877	0.44	1.44
45	10.7	13	1	26315	13853	1.90	27701	0.50	1.50
45	10.7	13	1.1	26831	14506	1.85	26831	0.54	1.54
45	10.9	13.5	0.57	25000	12198	2.05	26220	0.47	1.47
45	10.9	13.5	1	26517	14734	1.80	26517	0.56	1.56
45	10.9	13.5	1.1	26818	15327	1.75	26818	0.57	1.57
45	11.8	16	0.57	27959	16448	1.70	25490	0.65	1.65
45	11.8	16	1	26861	19537	1.37	28330	0.69	1.69
45	11.8	16	1.1	27537	20399	1.35	27537	0.74	1.74
45	12.8	19	0.57	26176	22762	1.15	26453	0.86	1.86
45	12.8	19	1	28591	26594	1.08	28591	0.93	1.93
45	12.8	19	1.1	27509	27509	1.00	28887	0.95	1.95
90	10	10.8	0.57	29607	8585	3.45	31542	0.27	1.27
90	10	10.8	1	31786	10597	3.00	31786	0.33	1.33
90	10	10.8	1.1	31237	11158	2.80	31237	0.36	1.36
90	10.1	11.3	0.57	29903	9348	3.20	31774	0.29	1.29
90	10.1	11.3	1	32030	11441	2.80	32030	0.36	1.36
90	10.1	11.3	1.1	31067	11951	2.60	31067	0.38	1.38
90	10.3	11.9	0.57	30605	10205	3.00	31628	0.32	1.32
90	10.3	11.9	1	30975	12392	2.50	30975	0.40	1.40
90	10.3	11.9	1.1	29862	12986	2.30	29862	0.43	1.43
90	10.5	12.4	0.57	29561	10951	2.70	31752	0.34	1.34
90	10.5	12.4	1	31809	13255	2.40	31809	0.42	1.42
90	10.5	12.4	1.1	31625	13751	2.30	31625	0.43	1.43
90	10.7	13	0.57	30970	11914	2.60	32163	0.37	1.37
90	10.7	13	1	31182	14175	2.20	31182	0.45	1.45
90	10.7	13	1.1	31142	14831	2.10	31142	0.48	1.48
90	10.9	13.5	0.57	30347	12647	2.40	31613	0.40	1.40
90	10.9	13.5	1	31755	15123	2.10	31755	0.48	1.48
90	10.9	13.5	1.1	31388	15695	2.00	31388	0.50	1.50
90	11.8	16	0.57	30926	17182	1.80	30926	0.56	1.56
90	11.8	16	1	30357	20238	1.50	30357	0.67	1.67
90	11.8	16	1.1	31631	21087	1.50	31631	0.67	1.67
90	12.8	19	0.57	31163	23971	1.30	31163	0.77	1.77
90	12.8	19	1	30526	27750	1.10	30526	0.91	1.91
90	12.8	19	1.1	31501	28636	1.10	31501	0.91	1.91
135	10	10.8	0.57	31963	8606	3.71	31963	0.27	1.27
135	10	10.8	1	32826	10608	3.09	32826	0.32	1.32
135	10	10.8	1.1	31916	11170	2.86	31916	0.35	1.35
135	10.1	11.3	0.57	33718	11321	2.98	33718	0.34	1.34
135	10.1	11.3	1	33138	11853	2.80	33138	0.36	1.36
135	10.1	11.3	1.1	32175	11854	2.71	32175	0.37	1.37

135	10.3	11.9	0.57	29304	9947	2.95	29304	0.34	1.34
135	10.3	11.9	1	32371	12197	2.65	32371	0.38	1.38
135	10.3	11.9	1.1	34801	12822	2.71	34801	0.37	1.37
135	10.5	12.4	0.57	31596	10747	2.94	31596	0.34	1.34
135	10.5	12.4	1	33590	13080	2.57	33590	0.39	1.39
135	10.5	12.4	1.1	33037	13604	2.43	33037	0.41	1.41
135	10.7	13	0.57	32200	11709	2.75	32200	0.36	1.36
135	10.7	13	1	34005	14020	2.43	34005	0.41	1.41
135	10.7	13	1.1	33582	14692	2.29	33582	0.44	1.44
135	10.9	13.5	0.57	32016	12450	2.57	32016	0.39	1.39
135	10.9	13.5	1	34153	14941	2.29	34153	0.44	1.44
135	10.9	13.5	1.1	31048	15524	2.00	31048	0.50	1.50
135	11.8	16	0.57	33351	16675	2.00	33351	0.50	1.50
135	11.8	16	1	33676	19748	1.71	33676	0.59	1.59
135	11.8	16	1.1	32343	20581	1.57	32343	0.64	1.64
135	12.8	19	0.57	33560	22526	1.49	33560	0.67	1.67
135	12.8	19	1	34526	26852	1.29	34526	0.78	1.78
135	12.8	19	1.1	35700	27763	1.29	35700	0.78	1.78
180	10	10.8	0.57	29680	8019	3.70	32101	0.25	1.25
180	10	10.8	1	29401	9798	3.00	32358	0.30	1.30
180	10	10.8	1.1	29888	10304	2.90	32991	0.31	1.31
180	10.1	11.3	0.57	30118	8602	3.50	31852	0.27	1.27
180	10.1	11.3	1	28269	10468	2.70	32472	0.32	1.32
180	10.1	11.3	1.1	28399	10920	2.60	32782	0.33	1.33
180	10.3	11.9	0.57	29773	9301	3.20	31644	0.29	1.29
180	10.3	11.9	1	28208	11281	2.50	32730	0.34	1.34
180	10.3	11.9	1.1	28393	11828	2.40	33132	0.36	1.36
180	10.5	12.4	0.57	29036	10010	2.90	32053	0.31	1.31
180	10.5	12.4	1	28471	12113	2.35	32113	0.38	1.38
180	10.5	12.4	1.1	28901	12563	2.30	32677	0.38	1.38
180	10.7	13	0.57	29522	10932	2.70	31727	0.34	1.34
180	10.7	13	1	28585	12991	2.20	32494	0.40	1.40
180	10.7	13	1.1	27934	13624	2.05	32711	0.42	1.42
180	10.9	13.5	0.57	28000	11665	2.40	31506	0.37	1.37
180	10.9	13.5	1	29312	13956	2.10	32110	0.43	1.43
180	10.9	13.5	1.1	28965	14480	2.00	33317	0.43	1.43
180	11.8	16	0.57	30102	15841	1.90	32490	0.49	1.49
180	11.8	16	1	29824	18638	1.60	32627	0.57	1.57
180	11.8	16	1.1	31083	19425	1.60	33031	0.59	1.59
180	12.8	19	0.57	30846	22031	1.40	32505	0.68	1.68
180	12.8	19	1	30655	25544	1.20	33219	0.77	1.77
180	12.8	19	1.1	31644	26369	1.20	34292	0.77	1.77
225	10	10.8	0.57	30055	8836	3.40	30055	0.29	1.29
225	10	10.8	1	32438	10808	3.00	32438	0.33	1.33

225	10	10.8	1.1	31846	11369	2.80	31846	0.36	1.36
225	10.1	11.3	0.57	30284	9459	3.20	30284	0.31	1.31
225	10.1	11.3	1	32272	11522	2.80	32272	0.36	1.36
225	10.1	11.3	1.1	31607	12038	2.63	31607	0.38	1.38
225	10.3	11.9	0.57	30123	10207	2.95	30123	0.34	1.34
225	10.3	11.9	1	32224	12391	2.60	32224	0.38	1.38
225	10.3	11.9	1.1	32517	13003	2.50	32517	0.40	1.40
225	10.5	12.4	0.57	31643	10907	2.90	31643	0.34	1.34
225	10.5	12.4	1	31860	13272	2.40	31860	0.42	1.42
225	10.5	12.4	1.1	31733	13793	2.30	31733	0.43	1.43
225	10.7	13	0.57	31271	11909	2.63	31271	0.38	1.38
225	10.7	13	1	31618	14207	2.23	31618	0.45	1.45
225	10.7	13	1.1	31622	14878	2.13	31622	0.47	1.47
225	10.9	13.5	0.57	31619	12644	2.50	31619	0.40	1.40
225	10.9	13.5	1	31810	15144	2.10	31810	0.48	1.48
225	10.9	13.5	1.1	31851	15726	2.03	31851	0.49	1.49
225	11.8	16	0.57	32206	16946	1.90	32206	0.53	1.53
225	11.8	16	1	31991	19993	1.60	31991	0.62	1.62
225	11.8	16	1.1	32106	16675	1.93	32106	0.52	1.52
225	12.8	19	0.57	32565	23258	1.40	32565	0.71	1.71
225	12.8	19	1	32466	27053	1.20	32466	0.83	1.83
225	12.8	19	1.1	32857	27961	1.18	32857	0.85	1.85
270	10	10.8	0.57	26235	8743	3.00	27986	0.31	1.31
270	10	10.8	1	26747	10697	2.50	28887	0.37	1.37
270	10	10.8	1.1	27000	11248	2.40	28126	0.40	1.40
270	10.1	11.3	0.57	25586	9474	2.70	27483	0.34	1.34
270	10.1	11.3	1	26521	11529	2.30	28829	0.40	1.40
270	10.1	11.3	1.1	27671	12029	2.30	30078	0.40	1.40
270	10.3	11.9	0.57	26726	10277	2.60	27756	0.37	1.37
270	10.3	11.9	1	27443	12472	2.20	28692	0.43	1.43
270	10.3	11.9	1.1	27450	13070	2.10	28759	0.45	1.45
270	10.5	12.4	0.57	26683	11116	2.40	28908	0.38	1.38
270	10.5	12.4	1	26821	13409	2.00	29504	0.45	1.45
270	10.5	12.4	1.1	27811	13904	2.00	29204	0.48	1.48
270	10.7	13	0.57	26611	12095	2.20	29032	0.42	1.42
270	10.7	13	1	27247	14339	1.90	28682	0.50	1.50
270	10.7	13	1.1	26987	14991	1.80	28488	0.53	1.53
270	10.9	13.5	0.57	26941	12827	2.10	29509	0.43	1.43
270	10.9	13.5	1	27514	15284	1.80	29044	0.53	1.53
270	10.9	13.5	1.1	26946	15849	1.70	28533	0.56	1.56
270	11.8	16	0.57	27845	17402	1.60	29587	0.59	1.59
270	11.8	16	1	28600	20427	1.40	30643	0.67	1.67
270	11.8	16	1.1	27654	21271	1.30	29782	0.71	1.71
270	12.8	19	0.57	28919	24099	1.20	31330	0.77	1.77

270	12.8	19	1	30668	27879	1.10	30668	0.91	1.91
270	12.8	19	1.1	28766	28766	1.00	31645	0.91	1.91
315	10	10.8	0.57	22910	8480	2.70	22910	0.37	1.37
315	10	10.8	1	21941	10447	2.10	21941	0.48	1.48
315	10	10.8	1.1	22021	11010	2.00	22021	0.50	1.50
315	10.1	11.3	0.57	22545	9017	2.50	22545	0.40	1.40
315	10.1	11.3	1	22293	11145	2.00	23421	0.48	1.48
315	10.1	11.3	1.1	22166	11665	1.90	23346	0.50	1.50
315	10.3	11.9	0.57	22519	9785	2.30	22519	0.43	1.43
315	10.3	11.9	1	21607	12003	1.80	22820	0.53	1.53
315	10.3	11.9	1.1	21472	12629	1.70	21472	0.59	1.59
315	10.5	12.4	0.57	22119	10531	2.10	23185	0.45	1.45
315	10.5	12.4	1	21902	12882	1.70	23203	0.56	1.56
315	10.5	12.4	1.1	22817	13413	1.70	22817	0.59	1.59
315	10.7	13	0.57	21787	11466	1.90	22947	0.50	1.50
315	10.7	13	1	22106	13815	1.60	23501	0.59	1.59
315	10.7	13	1.1	21742	14493	1.50	23204	0.62	1.62
315	10.9	13.5	0.57	21960	12199	1.80	23194	0.53	1.53
315	10.9	13.5	1	22118	14744	1.50	23605	0.62	1.62
315	10.9	13.5	1.1	21464	15330	1.40	23010	0.67	1.67
315	11.8	16	0.57	21354	16425	1.30	23009	0.71	1.71
315	11.8	16	1	21482	19527	1.10	23447	0.83	1.83
315	11.8	16	1.1	22424	20384	1.10	24476	0.83	1.83
315	12.8	19	0.57	22725	22725	1.00	22725	1.00	2.00
315	12.8	19	1	21236	21236	1.00	21236	1.00	2.00
315	12.8	19	1.1	24712	24712	1.00	24712	1.00	2.00

b) SBO Jacket

Direction	Wave (m)	Wave Period (Sec)	Current (cm/s)	Base Shear (KN)		RSR	Peak Load Base Shear (KN)	100 Year/ Peak Load	System Redundancy
				Collapse Load (KN)	100 Year Load (KN)				
0	7.7	9.6	0.68	43156	7993	5.40	79804	0.10	1.10
0	7.7	9.6	0.86	45096	8673	5.20	74514	0.12	1.12
0	7.7	9.6	0.94	45053	9011	5.00	89585	0.10	1.10
0	8.1	9.9	0.68	45135	8680	5.20	82968	0.10	1.10
0	8.1	9.9	0.86	43212	9394	4.60	89780	0.10	1.10
0	8.1	9.9	0.94	44511	9677	4.60	77304	0.13	1.13
0	8.5	10.1	0.68	43053	9360	4.60	89488	0.10	1.10
0	8.5	10.1	0.86	43950	9989	4.40	81870	0.12	1.12
0	8.5	10.1	0.94	43426	10340	4.20	86547	0.12	1.12

0	8.9	10.2	0.68	43480	9883	4.40	80949	0.12	1.12
0	8.9	10.2	0.86	44611	10622	4.20	88679	0.12	1.12
0	8.9	10.2	0.94	45738	10891	4.20	82579	0.13	1.13
0	9.2	10.3	0.68	43518	10362	4.20	86508	0.12	1.12
0	9.2	10.3	0.86	44372	11094	4.00	86046	0.13	1.13
0	9.2	10.3	0.94	45922	11481	4.00	73369	0.16	1.16
0	9.6	10.9	0.68	43233	11378	3.80	90719	0.13	1.13
0	9.6	10.9	0.86	46117	12137	3.80	82148	0.15	1.15
0	9.6	10.9	0.94	45247	12569	3.60	90249	0.14	1.14
0	11.6	11.4	0.68	42478	15171	2.80	75764	0.20	1.20
0	11.6	11.4	0.86	45431	16226	2.80	87717	0.18	1.18
0	11.6	11.4	0.94	43286	16649	2.60	92795	0.18	1.18
0	13.9	11.9	0.68	46103	20957	2.20	79574	0.26	1.26
0	13.9	11.9	0.86	44562	22282	2.00	88984	0.25	1.25
0	13.9	11.9	0.94	46022	23012	2.00	87160	0.26	1.26
0	16.2	13.3	0.68	48389	30244	1.60	90540	0.33	1.33
0	16.2	13.3	0.86	45336	32384	1.40	96932	0.33	1.33
0	16.2	13.3	0.94	46455	33183	1.40	99238	0.33	1.33
0	18.1	14.1	0.68	46953	39128	1.20	85988	0.46	1.46
0	18.1	14.1	0.86	49840	41535	1.20	91301	0.45	1.45
0	18.1	14.1	0.94	50795	42330	1.20	92916	0.46	1.46
61.59	7.7	9.6	0.68	43881	10971	4.00	92254	0.12	1.12
61.59	7.7	9.6	0.86	45003	11844	3.80	98998	0.12	1.12
61.59	7.7	9.6	0.94	44263	12297	3.60	98237	0.13	1.13
61.59	8.1	9.9	0.68	44331	11667	3.80	93425	0.12	1.12
61.59	8.1	9.9	0.86	45551	12654	3.60	98405	0.13	1.13
61.59	8.1	9.9	0.94	47042	13069	3.60	99135	0.13	1.13
61.59	8.5	10.1	0.68	45002	12502	3.60	87516	0.14	1.14
61.59	8.5	10.1	0.86	45516	13388	3.40	93601	0.14	1.14
61.59	8.5	10.1	0.94	47190	13881	3.40	99765	0.14	1.14
61.59	8.9	10.2	0.68	44632	13128	3.40	99613	0.13	1.13
61.59	8.9	10.2	0.86	45278	14151	3.20	98682	0.14	1.14
61.59	8.9	10.2	0.94	46516	14538	3.20	98787	0.15	1.15
61.59	9.2	10.3	0.68	46589	13704	3.40	98524	0.14	1.14
61.59	9.2	10.3	0.86	46915	14662	3.20	99596	0.15	1.15
61.59	9.2	10.3	0.94	48557	15175	3.20	96998	0.16	1.16
61.59	9.6	10.9	0.68	47056	14706	3.20	99614	0.15	1.15
61.59	9.6	10.9	0.86	47104	15703	3.00	94140	0.17	1.17
61.59	9.6	10.9	0.94	48772	16259	3.00	97440	0.17	1.17
61.59	11.6	11.4	0.68	49467	19027	2.60	98694	0.19	1.19
61.59	11.6	11.4	0.86	48894	20375	2.40	97703	0.21	1.21
61.59	11.6	11.4	0.94	46107	20959	2.20	96242	0.22	1.22
61.59	13.9	11.9	0.68	46468	25817	1.80	97984	0.26	1.26
61.59	13.9	11.9	0.86	49454	27477	1.80	98799	0.28	1.28

61.59	13.9	11.9	0.94	45406	28380	1.60	96433	0.29	1.29
61.59	16.2	13.3	0.68	51077	36488	1.40	94817	0.38	1.38
61.59	16.2	13.3	0.86	46946	39124	1.20	93862	0.42	1.42
61.59	16.2	13.3	0.94	47932	39946	1.20	95817	0.42	1.42
61.59	18.1	14.1	0.68	46784	46784	1.00	93540	0.50	1.50
61.59	18.1	14.1	0.86	49754	49754	1.00	99397	0.50	1.50
61.59	18.1	14.1	0.94	50829	50829	1.00	91469	0.56	1.56
90	7.7	9.6	0.68	45971	11494	4.00	93756	0.12	1.12
90	7.7	9.6	0.86	47306	12450	3.80	94316	0.13	1.13
90	7.7	9.6	0.94	49074	12915	3.80	92512	0.14	1.14
90	8.1	9.9	0.68	46772	12309	3.80	90558	0.14	1.14
90	8.1	9.9	0.86	47937	13317	3.60	87608	0.15	1.15
90	8.1	9.9	0.94	49424	13730	3.60	92997	0.15	1.15
90	8.5	10.1	0.68	47215	13116	3.60	86282	0.15	1.15
90	8.5	10.1	0.86	47699	14031	3.40	84047	0.17	1.17
90	8.5	10.1	0.94	49402	14531	3.40	92784	0.16	1.16
90	8.9	10.2	0.68	49595	13778	3.60	96755	0.14	1.14
90	8.9	10.2	0.86	50364	14814	3.40	91520	0.16	1.16
90	8.9	10.2	0.94	48695	15219	3.20	70229	0.22	1.22
90	9.2	10.3	0.68	48840	14366	3.40	91710	0.16	1.16
90	9.2	10.3	0.86	49138	15358	3.20	70822	0.22	1.22
90	9.2	10.3	0.94	50794	15874	3.20	70023	0.23	1.23
90	9.6	10.9	0.68	49139	15358	3.20	70617	0.22	1.22
90	9.6	10.9	0.86	49157	16388	3.00	72045	0.23	1.23
90	9.6	10.9	0.94	50860	16955	3.00	84944	0.20	1.20
90	11.6	11.4	0.68	51702	19887	2.60	91472	0.22	1.22
90	11.6	11.4	0.86	51023	21261	2.40	68493	0.31	1.31
90	11.6	11.4	0.94	52473	21866	2.40	95983	0.23	1.23
90	13.9	11.9	0.68	50254	27920	1.80	94795	0.29	1.29
90	13.9	11.9	0.86	53351	29641	1.80	88828	0.33	1.33
90	13.9	11.9	0.94	55022	30570	1.80	97676	0.31	1.31
90	16.2	13.3	0.68	48297	40249	1.20	96453	0.42	1.42
90	16.2	13.3	0.86	51688	43078	1.20	94556	0.46	1.46
90	16.2	13.3	0.94	52726	43943	1.20	96451	0.46	1.46
90	18.1	14.1	0.68	51277	51277	1.00	92157	0.56	1.56
90	18.1	14.1	0.86	54251	54251	1.00	97526	0.56	1.56
90	18.1	14.1	0.94	55486	55486	1.00	99665	0.56	1.56
118.41	7.7	9.6	0.68	38797	11412	3.40	93523	0.12	1.12
118.41	7.7	9.6	0.86	39259	12269	3.20	95435	0.13	1.13
118.41	7.7	9.6	0.94	40716	12725	3.20	96410	0.13	1.13
118.41	8.1	9.9	0.68	38818	12131	3.20	96634	0.13	1.13
118.41	8.1	9.9	0.86	41911	13098	3.20	96835	0.14	1.14
118.41	8.1	9.9	0.94	40506	13503	3.00	96796	0.14	1.14
118.41	8.5	10.1	0.68	41360	12926	3.20	98063	0.13	1.13

118.41	8.5	10.1	0.86	41373	13792	3.00	98992	0.14	1.14
118.41	8.5	10.1	0.94	42749	14251	3.00	99386	0.14	1.14
118.41	8.9	10.2	0.68	40546	13516	3.00	97195	0.14	1.14
118.41	8.9	10.2	0.86	43496	14500	3.00	98277	0.15	1.15
118.41	8.9	10.2	0.94	41712	14898	2.80	95331	0.16	1.16
118.41	9.2	10.3	0.68	42236	14080	3.00	98230	0.14	1.14
118.41	9.2	10.3	0.86	42033	15013	2.80	98768	0.15	1.15
118.41	9.2	10.3	0.94	43450	15519	2.80	98967	0.16	1.16
118.41	9.6	10.9	0.68	42162	15059	2.80	98996	0.15	1.15
118.41	9.6	10.9	0.86	44977	16065	2.80	99271	0.16	1.16
118.41	9.6	10.9	0.94	43204	16619	2.60	99626	0.17	1.17
118.41	11.6	11.4	0.68	46460	19360	2.40	96534	0.20	1.20
118.41	11.6	11.4	0.86	45406	20641	2.20	98852	0.21	1.21
118.41	11.6	11.4	0.94	46670	21218	2.20	97386	0.22	1.22
118.41	13.9	11.9	0.68	47254	26255	1.80	99513	0.26	1.26
118.41	13.9	11.9	0.86	50216	27902	1.80	94772	0.29	1.29
118.41	13.9	11.9	0.94	46064	28793	1.60	97686	0.29	1.29
118.41	16.2	13.3	0.68	44250	36877	1.20	95601	0.39	1.39
118.41	16.2	13.3	0.86	47331	39448	1.20	94516	0.42	1.42
118.41	16.2	13.3	0.94	48298	40251	1.20	88640	0.45	1.45
118.41	18.1	14.1	0.68	46984	46984	1.00	93811	0.50	1.50
118.41	18.1	14.1	0.86	49775	49775	1.00	99419	0.50	1.50
118.41	18.1	14.1	0.94	50882	50882	1.00	91530	0.56	1.56
180	7.7	9.6	0.68	41265	8253	5.00	70695	0.12	1.12
180	7.7	9.6	0.86	43081	8975	4.80	69846	0.13	1.13
180	7.7	9.6	0.94	42837	9313	4.60	70586	0.13	1.13
180	8.1	9.9	0.68	42793	8915	4.80	67621	0.13	1.13
180	8.1	9.9	0.86	42545	9670	4.40	71246	0.14	1.14
180	8.1	9.9	0.94	43882	9973	4.40	69603	0.14	1.14
180	8.5	10.1	0.68	42153	9580	4.40	72585	0.13	1.13
180	8.5	10.1	0.86	43052	10250	4.20	71494	0.14	1.14
180	8.5	10.1	0.94	44552	10608	4.20	74111	0.14	1.14
180	8.9	10.2	0.68	44248	10056	4.40	68210	0.15	1.15
180	8.9	10.2	0.86	45480	19829	2.29	75589	0.26	1.26
180	8.9	10.2	0.94	44414	11104	4.00	72956	0.15	1.15
180	9.2	10.3	0.68	44129	10507	4.20	73277	0.14	1.14
180	9.2	10.3	0.86	44196	11229	3.94	76130	0.15	1.15
180	9.2	10.3	0.94	46471	11618	4.00	78669	0.15	1.15
180	9.6	10.9	0.68	45907	11477	4.00	75590	0.15	1.15
180	9.6	10.9	0.86	46570	12256	3.80	75780	0.16	1.16
180	9.6	10.9	0.94	45737	12705	3.60	76007	0.17	1.17
180	11.6	11.4	0.68	48259	15082	3.20	75252	0.20	1.20
180	11.6	11.4	0.86	48579	16193	3.00	80790	0.20	1.20
180	11.6	11.4	0.94	49985	16662	3.00	89652	0.19	1.19

180	13.9	11.9	0.68	47268	21487	2.20	85719	0.25	1.25
180	13.9	11.9	0.86	50293	22862	2.20	82101	0.28	1.28
180	13.9	11.9	0.94	51938	23610	2.20	84729	0.28	1.28
180	16.2	13.3	0.68	48126	30081	1.60	84039	0.36	1.36
180	16.2	13.3	0.86	51367	32107	1.60	89669	0.36	1.36
180	16.2	13.3	0.94	52566	32856	1.60	98258	0.33	1.33
180	18.1	14.1	0.68	54033	38599	1.40	99923	0.39	1.39
180	18.1	14.1	0.86	49040	40870	1.20	89713	0.46	1.46
180	18.1	14.1	0.94	50120	41770	1.20	99947	0.42	1.42
241.59	7.7	9.6	0.68	32476	11599	2.80	95054	0.12	1.12
241.59	7.7	9.6	0.86	34964	12490	2.80	99770	0.13	1.13
241.59	7.7	9.6	0.94	33673	12952	2.60	98329	0.13	1.13
241.59	8.1	9.9	0.68	34484	12319	2.80	98371	0.13	1.13
241.59	8.1	9.9	0.86	34592	13308	2.60	90404	0.15	1.15
241.59	8.1	9.9	0.94	35615	13701	2.60	92951	0.15	1.15
241.59	8.5	10.1	0.68	33996	13077	2.60	91441	0.14	1.14
241.59	8.5	10.1	0.86	36337	13977	2.60	97703	0.14	1.14
241.59	8.5	10.1	0.94	34756	14482	2.40	75247	0.19	1.19
241.59	8.9	10.2	0.68	35521	13666	2.60	73724	0.19	1.19
241.59	8.9	10.2	0.86	35319	14720	2.40	79422	0.19	1.19
241.59	8.9	10.2	0.94	36219	15095	2.40	93679	0.16	1.16
241.59	9.2	10.3	0.68	36991	14230	2.60	99435	0.14	1.14
241.59	9.2	10.3	0.86	36456	15193	2.40	88003	0.17	1.17
241.59	9.2	10.3	0.94	37725	15721	2.40	78538	0.20	1.20
241.59	9.6	10.9	0.68	36595	15250	2.40	82256	0.19	1.19
241.59	9.6	10.9	0.86	39001	16253	2.40	97447	0.17	1.17
241.59	9.6	10.9	0.94	37009	16826	2.20	77324	0.22	1.22
241.59	11.6	11.4	0.68	39005	19506	2.00	97432	0.20	1.20
241.59	11.6	11.4	0.86	41743	20873	2.00	70911	0.29	1.29
241.59	11.6	11.4	0.94	38631	21467	1.80	94496	0.23	1.23
241.59	13.9	11.9	0.68	42404	26508	1.60	95399	0.28	1.28
241.59	13.9	11.9	0.86	39445	28178	1.40	95778	0.29	1.29
241.59	13.9	11.9	0.94	40725	29091	1.40	98874	0.29	1.29
241.59	16.2	13.3	0.68	44928	37446	1.20	97316	0.38	1.38
241.59	16.2	13.3	0.86	40062	40062	1.00	88089	0.45	1.45
241.59	16.2	13.3	0.94	40892	40892	1.00	98126	0.42	1.42
241.59	18.1	14.1	0.68	37906	47382	0.80	94691	0.50	1.50
241.59	18.1	14.1	0.86	40246	50309	0.80	90554	0.56	1.56
241.59	18.1	14.1	0.94	41110	51389	0.80	92489	0.56	1.56
270	7.7	9.6	0.68	32181	11494	2.80	73594	0.16	1.16
270	7.7	9.6	0.86	32350	12443	2.60	86600	0.14	1.14
270	7.7	9.6	0.94	33563	12909	2.60	87642	0.15	1.15
270	8.1	9.9	0.68	31987	12304	2.60	85932	0.14	1.14
270	8.1	9.9	0.86	34590	13305	2.60	87858	0.15	1.15

270	8.1	9.9	0.94	35665	13718	2.60	90577	0.15	1.15
270	8.5	10.1	0.68	34075	13106	2.60	78547	0.17	1.17
270	8.5	10.1	0.86	33645	14019	2.40	81191	0.17	1.17
270	8.5	10.1	0.94	34853	14523	2.40	87001	0.17	1.17
270	8.9	10.2	0.68	33044	13769	2.40	87971	0.16	1.16
270	8.9	10.2	0.86	35530	14805	2.40	88641	0.17	1.17
270	8.9	10.2	0.94	36507	15211	2.40	85069	0.18	1.18
270	9.2	10.3	0.68	34453	14356	2.40	83150	0.17	1.17
270	9.2	10.3	0.86	36837	15349	2.40	94689	0.16	1.16
270	9.2	10.3	0.94	34903	15866	2.20	85666	0.19	1.19
270	9.6	10.9	0.68	36828	15345	2.40	82759	0.19	1.19
270	9.6	10.9	0.86	36026	16375	2.20	87973	0.19	1.19
270	9.6	10.9	0.94	37274	16942	2.20	91317	0.19	1.19
270	11.6	11.4	0.68	35762	19869	1.80	83352	0.24	1.24
270	11.6	11.4	0.86	38261	21256	1.80	93418	0.23	1.23
270	11.6	11.4	0.94	39345	21860	1.80	91745	0.24	1.24
270	13.9	11.9	0.68	39013	27868	1.40	83628	0.33	1.33
270	13.9	11.9	0.86	41424	29590	1.40	95037	0.31	1.31
270	13.9	11.9	0.94	36621	30518	1.20	91427	0.33	1.33
270	16.2	13.3	0.68	40576	40576	1.00	81044	0.50	1.50
270	16.2	13.3	0.86	34649	43311	0.80	95153	0.46	1.46
270	16.2	13.3	0.94	35344	44181	0.98	88241	0.50	1.50
270	18.1	14.1	0.68	41039	51299	0.80	92228	0.56	1.56
270	18.1	14.1	0.86	43442	54304	0.80	97648	0.56	1.56
270	18.1	14.1	0.94	44405	55506	0.80	99816	0.56	1.56
298.41	7.7	9.6	0.68	32998	11786	2.80	98537	0.12	1.12
298.41	7.7	9.6	0.86	32898	12654	2.60	90845	0.14	1.14
298.41	7.7	9.6	0.94	34064	13105	2.60	93946	0.14	1.14
298.41	8.1	9.9	0.68	32518	12509	2.60	87314	0.14	1.14
298.41	8.1	9.9	0.86	35069	13488	2.60	94097	0.14	1.14
298.41	8.1	9.9	0.94	33359	13902	2.40	78078	0.18	1.18
298.41	8.5	10.1	0.68	34614	13315	2.60	81791	0.16	1.16
298.41	8.5	10.1	0.86	34092	14207	2.40	96224	0.15	1.15
298.41	8.5	10.1	0.94	35286	14704	2.40	96718	0.15	1.15
298.41	8.9	10.2	0.68	33500	13960	2.40	72680	0.19	1.19
298.41	8.9	10.2	0.86	35932	14973	2.40	98648	0.15	1.15
298.41	8.9	10.2	0.94	33783	15358	2.20	94872	0.16	1.16
298.41	9.2	10.3	0.68	34843	14519	2.40	92405	0.16	1.16
298.41	9.2	10.3	0.86	34089	15496	2.20	65021	0.24	1.24
298.41	9.2	10.3	0.94	35217	16009	2.20	89347	0.18	1.18
298.41	9.6	10.9	0.68	34148	15523	2.20	95904	0.16	1.16
298.41	9.6	10.9	0.86	36351	16524	2.20	82682	0.20	1.20
298.41	9.6	10.9	0.94	34168	17085	2.00	95231	0.18	1.18
298.41	11.6	11.4	0.68	35731	19852	1.80	90425	0.22	1.22

298.41	11.6	11.4	0.86	38155	21197	1.80	97231	0.22	1.22
298.41	11.6	11.4	0.94	34854	21785	1.60	99877	0.22	1.22
298.41	13.9	11.9	0.68	37323	26659	1.40	95747	0.28	1.28
298.41	13.9	11.9	0.86	39654	28324	1.40	62262	0.45	1.45
298.41	13.9	11.9	0.94	35071	29228	1.20	99102	0.29	1.29
298.41	16.2	13.3	0.68	37462	37462	1.00	97208	0.39	1.39
298.41	16.2	13.3	0.86	40089	40089	1.00	96024	0.42	1.42
298.41	16.2	13.3	0.94	40919	40919	1.00	98020	0.42	1.42
298.41	18.1	14.1	0.68	37999	47502	0.80	94846	0.50	1.50
298.41	18.1	14.1	0.86	50464	40371	1.25	90708	0.45	1.45
298.41	18.1	14.1	0.94	51534	41227	1.25	92613	0.45	1.45

C) SKO1 Jacket

Direction	Wave (m)	Wave Period (Sec)	Current (cm/s)	Base Shear (KN)		RSR	Peak Load Base Shear (KN)	100 Year/ Peak Load	System Redundancy
				Collapse Load (KN)	100 Year Load (KN)				
0	9.9	10.2	0.68	21509	6935	3.10	47775	0.15	1.15
0	9.9	10.2	0.95	22237	8083	2.75	42212	0.19	1.19
0	9.9	10.2	1.05	23389	8500	2.75	46859	0.18	1.18
0	10.4	10.5	0.68	22221	7402	3.00	41360	0.18	1.18
0	10.4	10.5	0.95	23563	8564	2.75	35319	0.24	1.24
0	10.4	10.5	1.05	22636	9051	2.50	41304	0.22	1.22
0	10.9	10.7	0.68	21678	7880	2.75	40036	0.20	1.20
0	10.9	10.7	0.95	22853	9135	2.50	53785	0.17	1.17
0	10.9	10.7	1.05	24123	9644	2.50	41781	0.23	1.23
0	11.4	10.9	0.68	22987	8354	2.75	37111	0.23	1.23
0	11.4	10.9	0.95	24210	9680	2.50	39152	0.25	1.25
0	11.4	10.9	1.05	22822	10141	2.25	41098	0.25	1.25
0	11.9	11.1	0.68	22169	8865	2.50	38805	0.23	1.23
0	11.9	11.1	0.95	22875	10164	2.25	44497	0.23	1.23
0	11.9	11.1	1.05	24150	13411	1.80	42425	0.32	1.32
0	12.4	11.3	0.68	23489	9391	2.50	40986	0.23	1.23
0	12.4	11.3	0.95	24197	10749	2.25	42454	0.25	1.25
0	12.4	11.3	1.05	22667	11331	2.00	42101	0.27	1.27
0	15.0	12.3	0.68	24540	12267	2.00	48441	0.25	1.25
0	15.0	12.3	0.95	24506	13998	1.75	43525	0.32	1.32
0	15.0	12.3	1.05	25499	14568	1.75	46769	0.31	1.31
0	17.5	13.2	0.68	23516	15670	1.50	43100	0.36	1.36
0	17.5	13.2	0.95	26406	17602	1.50	43480	0.40	1.40
0	17.5	13.2	1.05	22970	18374	1.25	46225	0.40	1.40

0	20.0	14.0	0.68	24382	19500	1.25	46692	0.42	1.42
0	20.0	14.0	0.95	27244	21793	1.25	48429	0.45	1.45
0	20.0	14.0	1.05	28252	22599	1.25	50345	0.45	1.45
0	22.5	14.7	0.68	27406	27406	1.00	49263	0.56	1.56
0	22.5	14.7	0.95	24252	30318	0.80	41824	0.72	1.72
0	22.5	14.7	1.05	25018	31278	0.80	52340	0.60	1.60
45	9.9	10.2	0.68	16025	9139	1.75	43518	0.21	1.21
45	9.9	10.2	0.95	16303	10832	1.51	45168	0.24	1.24
45	9.9	10.2	1.05	17211	11452	1.50	49285	0.23	1.23
45	10.4	10.5	0.68	17166	9788	1.75	41981	0.23	1.23
45	10.4	10.5	0.95	17282	11499	1.50	44731	0.26	1.26
45	10.4	10.5	1.05	18358	12215	1.50	44261	0.28	1.28
45	10.9	10.7	0.68	18351	10462	1.75	46023	0.23	1.23
45	10.9	10.7	0.95	18497	12307	1.50	48676	0.25	1.25
45	10.9	10.7	1.05	16367	13053	1.25	45198	0.29	1.29
45	11.4	10.9	0.68	16766	11153	1.50	51070	0.22	1.22
45	11.4	10.9	0.95	16420	13094	1.25	46665	0.28	1.28
45	11.4	10.9	1.05	17254	13776	1.25	49476	0.28	1.28
45	11.9	11.1	0.68	17848	11875	1.50	47257	0.25	1.25
45	11.9	11.1	0.95	17284	13783	1.25	49843	0.28	1.28
45	11.9	11.1	1.05	18293	14609	1.25	50615	0.29	1.29
45	12.4	11.3	0.68	18927	12611	1.50	49417	0.26	1.26
45	12.4	11.3	0.95	18283	14601	1.25	49018	0.30	1.30
45	12.4	11.3	1.05	19355	15452	1.25	46621	0.33	1.33
45	15.0	12.3	0.68	16671	16671	1.00	48394	0.34	1.34
45	15.0	12.3	0.95	19170	19170	1.00	51601	0.37	1.37
45	15.0	12.3	1.05	19988	19988	1.00	49207	0.41	1.41
45	17.5	13.2	0.68	17120	21402	0.80	44908	0.48	1.48
45	17.5	13.2	0.95	18132	24881	0.73	46192	0.54	1.54
45	17.5	13.2	1.05	18973	25332	0.75	45300	0.56	1.56
45	20.0	14.0	0.68	19983	26695	0.75	53650	0.50	1.50
45	20.0	14.0	0.95	17989	30065	0.60	49474	0.61	1.61
45	20.0	14.0	1.05	18686	31219	0.60	47488	0.66	1.66
45	22.5	14.7	0.68	17998	36061	0.50	49573	0.73	1.73
45	22.5	14.7	0.95	19965	40011	0.50	53997	0.74	1.74
45	22.5	14.7	1.05	20656	41380	0.50	51528	0.80	1.80
90	9.9	10.2	0.68	23197	10294	2.25	42023	0.24	1.24
90	9.9	10.2	0.95	24145	12049	2.00	44982	0.27	1.27
90	9.9	10.2	1.05	22210	12686	1.75	49528	0.26	1.26
90	10.4	10.5	0.68	22060	10997	2.01	43420	0.25	1.25
90	10.4	10.5	0.95	22355	12769	1.75	48229	0.26	1.26
90	10.4	10.5	1.05	23689	13509	1.75	46287	0.29	1.29
90	10.9	10.7	0.68	23723	11838	2.00	51007	0.23	1.23
90	10.9	10.7	0.95	24101	13746	1.75	46923	0.29	1.29

90	10.9	10.7	1.05	21798	14521	1.50	53080	0.27	1.27
90	11.4	10.9	0.68	22055	12566	1.76	48326	0.26	1.26
90	11.4	10.9	0.95	21901	14590	1.50	49983	0.29	1.29
90	11.4	10.9	1.05	22982	15294	1.50	47676	0.32	1.32
90	11.9	11.1	0.68	23419	13359	1.75	50807	0.26	1.26
90	11.9	11.1	0.95	23055	15341	1.50	42749	0.36	1.36
90	11.9	11.1	1.05	24344	16201	1.50	46224	0.35	1.35
90	12.4	11.3	0.68	21492	14317	1.50	41518	0.34	1.34
90	12.4	11.3	0.95	24632	16396	1.50	51216	0.32	1.32
90	12.4	11.3	1.05	21676	17284	1.25	51922	0.33	1.33
90	15.0	12.3	0.68	23557	18818	1.25	48421	0.39	1.39
90	15.0	12.3	0.95	26846	21461	1.25	46156	0.46	1.46
90	15.0	12.3	1.05	22344	22344	1.00	53155	0.42	1.42
90	17.5	13.2	0.68	24133	24133	1.00	50153	0.48	1.48
90	17.5	13.2	0.95	27062	27062	1.00	47429	0.57	1.57
90	17.5	13.2	1.05	28242	28242	1.00	51653	0.55	1.55
90	20.0	14.0	0.68	22541	30091	0.75	54827	0.55	1.55
90	20.0	14.0	0.95	25183	33618	0.75	49499	0.68	1.68
90	20.0	14.0	1.05	26086	34811	0.75	55760	0.62	1.62
90	22.5	14.7	0.68	24805	41569	0.60	46733	0.89	1.89
90	22.5	14.7	0.95	27372	46121	0.59	50433	0.91	1.91
90	22.5	14.7	1.05	23554	49254	0.48	49254	1.00	2.00
135	9.9	10.2	0.68	20344	9026	2.25	42885	0.21	1.21
135	9.9	10.2	0.95	18804	10727	1.75	49880	0.22	1.22
135	9.9	10.2	1.05	19896	11351	1.75	46482	0.24	1.24
135	10.4	10.5	0.68	19458	9713	2.00	39854	0.24	1.24
135	10.4	10.5	0.95	19993	11406	1.75	47752	0.24	1.24
135	10.4	10.5	1.05	21259	12125	1.75	49738	0.24	1.24
135	10.9	10.7	0.68	20747	10356	2.00	44110	0.23	1.23
135	10.9	10.7	0.95	19564	12208	1.60	41953	0.29	1.29
135	10.9	10.7	1.05	19466	12957	1.50	43639	0.30	1.30
135	11.4	10.9	0.68	19369	11050	1.75	42992	0.26	1.26
135	11.4	10.9	0.95	19529	12999	1.50	41778	0.31	1.31
135	11.4	10.9	1.05	20559	13684	1.50	48277	0.28	1.28
135	11.9	11.1	0.68	20641	11775	1.75	50003	0.24	1.24
135	11.9	11.1	0.95	20569	13691	1.50	37415	0.37	1.37
135	11.9	11.1	1.05	21792	14520	1.50	42959	0.34	1.34
135	12.4	11.3	0.68	18801	12515	1.50	48611	0.26	1.26
135	12.4	11.3	0.95	21780	14512	1.50	47592	0.30	1.30
135	12.4	11.3	1.05	19237	15367	1.25	51826	0.30	1.30
135	15.0	12.3	0.68	20709	16540	1.25	49532	0.33	1.33
135	15.0	12.3	0.95	19099	19099	1.00	51819	0.37	1.37
135	15.0	12.3	1.05	19941	19941	1.00	49903	0.40	1.40

135	17.5	13.2	0.68	21293	21293	1.00	54176	0.39	1.39
135	17.5	13.2	0.95	19308	24161	0.80	45647	0.53	1.53
135	17.5	13.2	1.05	20206	25265	0.80	47765	0.53	1.53
135	20.0	14.0	0.68	19975	26644	0.75	55610	0.48	1.48
135	20.0	14.0	0.95	22451	29957	0.75	44959	0.67	1.67
135	20.0	14.0	1.05	23335	31138	0.75	49110	0.63	1.63
135	22.5	14.7	0.68	21532	35981	0.60	53714	0.67	1.67
135	22.5	14.7	0.95	19995	39956	0.50	49045	0.81	1.81
135	22.5	14.7	1.05	20667	41355	0.50	45398	0.91	1.91
180	9.9	10.2	0.68	24271	6476	3.75	32370	0.20	1.20
180	9.9	10.2	0.95	24354	7479	3.26	37445	0.20	1.20
180	9.9	10.2	1.05	25600	7880	3.25	39295	0.20	1.20
180	10.4	10.5	0.68	24108	6892	3.50	34458	0.20	1.20
180	10.4	10.5	0.95	23804	7938	3.00	36819	0.22	1.22
180	10.4	10.5	1.05	25142	8384	3.00	41871	0.20	1.20
180	10.9	10.7	0.68	23747	7310	3.25	36572	0.20	1.20
180	10.9	10.7	0.95	25376	8461	3.00	48530	0.17	1.17
180	10.9	10.7	1.05	24539	8927	2.75	42408	0.21	1.21
180	11.4	10.9	0.68	23230	7746	3.00	40046	0.19	1.19
180	11.4	10.9	0.95	24632	8960	2.75	43873	0.20	1.20
180	11.4	10.9	1.05	25795	9382	2.75	40785	0.23	1.23
180	11.9	11.1	0.68	24631	8214	3.00	44588	0.18	1.18
180	11.9	11.1	0.95	25856	9404	2.75	49885	0.19	1.19
180	11.9	11.1	1.05	24795	9921	2.50	42479	0.23	1.23
180	12.4	11.3	0.68	23907	8697	2.75	43308	0.20	1.20
180	12.4	11.3	0.95	24843	9940	2.50	49774	0.20	1.20
180	12.4	11.3	1.05	26180	10474	2.50	49428	0.21	1.21
180	15.0	12.3	0.68	25494	11333	2.25	45921	0.25	1.25
180	15.0	12.3	0.95	25835	12919	2.00	48650	0.27	1.27
180	15.0	12.3	1.05	26879	13440	2.00	42980	0.31	1.31
180	17.5	13.2	0.68	25289	14453	1.75	44879	0.32	1.32
180	17.5	13.2	0.95	28386	16220	1.75	45955	0.35	1.35
180	17.5	13.2	1.05	25389	16928	1.50	49076	0.34	1.34
180	20.0	14.0	0.68	26945	17963	1.50	44915	0.40	1.40
180	20.0	14.0	0.95	25075	20061	1.25	52487	0.38	1.38
180	20.0	14.0	1.05	25999	20798	1.25	49262	0.42	1.42
180	22.5	14.7	0.68	27637	25119	1.10	43331	0.58	1.58
180	22.5	14.7	0.95	27748	27748	1.00	46543	0.60	1.60
180	22.5	14.7	1.05	28637	28637	1.00	50049	0.57	1.57
225	9.9	10.2	0.68	18677	6783	2.75	34020	0.20	1.20
225	9.9	10.2	0.95	17985	7984	2.25	39954	0.20	1.20
225	9.9	10.2	1.05	18979	8423	2.25	42250	0.20	1.20
225	10.4	10.5	0.68	18151	7252	2.50	36326	0.20	1.20
225	10.4	10.5	0.95	19054	8456	2.25	42409	0.20	1.20

225	10.4	10.5	1.05	17952	8964	2.00	44913	0.20	1.20
225	10.9	10.7	0.68	17392	7720	2.25	38825	0.20	1.20
225	10.9	10.7	0.95	18082	9029	2.00	45032	0.20	1.20
225	10.9	10.7	1.05	19144	9558	2.00	50758	0.19	1.19
225	11.4	10.9	0.68	18497	8210	2.25	41265	0.20	1.20
225	11.4	10.9	0.95	19203	9586	2.00	47751	0.20	1.20
225	11.4	10.9	1.05	20139	10070	2.00	48987	0.21	1.21
225	11.9	11.1	0.68	17467	8722	2.00	43610	0.20	1.20
225	11.9	11.1	0.95	17645	10075	1.75	47220	0.21	1.21
225	11.9	11.1	1.05	18682	10661	1.75	51766	0.21	1.21
225	12.4	11.3	0.68	18514	9243	2.00	53695	0.17	1.17
225	12.4	11.3	0.95	18674	10655	1.75	49623	0.21	1.21
225	12.4	11.3	1.05	19736	11258	1.75	47273	0.24	1.24
225	15.0	12.3	0.68	18157	12085	1.50	49378	0.24	1.24
225	15.0	12.3	0.95	20809	13870	1.50	47864	0.29	1.29
225	15.0	12.3	1.05	18100	14465	1.25	49934	0.29	1.29
225	17.5	13.2	0.68	19323	15430	1.25	53870	0.29	1.29
225	17.5	13.2	0.95	21794	17419	1.25	57378	0.30	1.30
225	17.5	13.2	1.05	18267	18267	1.00	49971	0.37	1.37
225	20.0	14.0	0.68	19219	19219	1.00	57947	0.33	1.33
225	20.0	14.0	0.95	21542	21542	1.00	57842	0.37	1.37
225	20.0	14.0	1.05	22383	22383	1.00	57041	0.39	1.39
225	22.5	14.7	0.68	19297	25737	0.75	50835	0.51	1.51
225	22.5	14.7	0.95	21436	28622	0.75	60259	0.47	1.47
225	22.5	14.7	1.05	22179	29633	0.75	57779	0.51	1.51
270	9.9	10.2	0.68	25781	7925	3.25	31892	0.25	1.25
270	9.9	10.2	0.95	24764	9166	2.70	36800	0.25	1.25
270	9.9	10.2	1.05	26477	9617	2.75	42722	0.23	1.23
270	10.4	10.5	0.68	25288	8421	3.00	34215	0.25	1.25
270	10.4	10.5	0.95	26639	9675	2.75	40002	0.24	1.24
270	10.4	10.5	1.05	25522	10199	2.50	43149	0.24	1.24
270	10.9	10.7	0.68	24798	9007	2.75	34495	0.26	1.26
270	10.9	10.7	0.95	25942	10365	2.50	31374	0.33	1.33
270	10.9	10.7	1.05	24595	10913	2.25	38447	0.28	1.28
270	11.4	10.9	0.68	26238	9529	2.75	41832	0.23	1.23
270	11.4	10.9	0.95	24671	10961	2.25	50704	0.22	1.22
270	11.4	10.9	1.05	25813	11459	2.25	39382	0.29	1.29
270	11.9	11.1	0.68	25251	10089	2.50	35445	0.28	1.28
270	11.9	11.1	0.95	25888	11492	2.25	41357	0.28	1.28
270	11.9	11.1	1.05	27264	12100	2.25	36721	0.33	1.33
270	12.4	11.3	0.68	24266	10767	2.25	38498	0.28	1.28
270	12.4	11.3	0.95	24514	12237	2.00	43159	0.28	1.28
270	12.4	11.3	1.05	24483	12866	1.90	40172	0.32	1.32
270	15.0	12.3	0.68	24450	13947	1.75	43328	0.32	1.32

270	15.0	12.3	0.95	27726	15818	1.75	51589	0.31	1.31
270	15.0	12.3	1.05	24692	16435	1.50	44187	0.37	1.37
270	17.5	13.2	0.68	26541	17681	1.50	49056	0.36	1.36
270	17.5	13.2	0.95	24746	19766	1.25	49496	0.40	1.40
270	17.5	13.2	1.05	25785	20597	1.25	52976	0.39	1.39
270	20.0	14.0	0.68	27398	21883	1.25	48175	0.45	1.45
270	20.0	14.0	0.95	26808	24350	1.10	47242	0.52	1.52
270	20.0	14.0	1.05	25256	25256	1.00	50126	0.50	1.50
270	22.5	14.7	0.68	26901	29901	0.90	44886	0.67	1.67
270	22.5	14.7	0.95	26352	32994	0.80	45691	0.72	1.72
270	22.5	14.7	1.05	25485	34031	0.75	46958	0.72	1.72
315	9.9	10.2	0.68	18864	7252	2.60	31718	0.23	1.23
315	9.9	10.2	0.95	19290	8567	2.25	39418	0.22	1.22
315	9.9	10.2	1.05	20369	9047	2.25	41437	0.22	1.22
315	10.4	10.5	0.68	19429	7767	2.50	34564	0.22	1.22
315	10.4	10.5	0.95	20475	9094	2.25	34345	0.26	1.26
315	10.4	10.5	1.05	19310	9650	2.00	45768	0.21	1.21
315	10.9	10.7	0.68	19062	8281	2.30	47973	0.17	1.17
315	10.9	10.7	0.95	19444	9714	2.00	43645	0.22	1.22
315	10.9	10.7	1.05	20601	10294	2.00	44147	0.23	1.23
315	11.4	10.9	0.68	19851	8818	2.25	40973	0.22	1.22
315	11.4	10.9	0.95	20664	10325	2.00	41037	0.25	1.25
315	11.4	10.9	1.05	19011	10855	1.75	39429	0.28	1.28
315	11.9	11.1	0.68	18770	9377	2.00	33748	0.28	1.28
315	11.9	11.1	0.95	19019	10859	1.75	41412	0.26	1.26
315	11.9	11.1	1.05	20139	11501	1.75	45686	0.25	1.25
315	12.4	11.3	0.68	18918	9949	1.90	34569	0.29	1.29
315	12.4	11.3	0.95	19556	11494	1.70	39256	0.29	1.29
315	12.4	11.3	1.05	19481	12155	1.60	41261	0.29	1.29
315	15.0	12.3	0.68	19604	13059	1.50	49319	0.26	1.26
315	15.0	12.3	0.95	22544	15016	1.50	44292	0.34	1.34
315	15.0	12.3	1.05	20386	15668	1.30	44531	0.35	1.35
315	17.5	13.2	0.68	20917	16722	1.25	41588	0.40	1.40
315	17.5	13.2	0.95	20807	18903	1.10	40571	0.47	1.47
315	17.5	13.2	1.05	19791	19791	1.00	44582	0.44	1.44
315	20.0	14.0	0.68	20844	20844	1.00	45765	0.46	1.46
315	20.0	14.0	0.95	21076	23435	0.90	41996	0.56	1.56
315	20.0	14.0	1.05	21897	24345	0.90	43435	0.56	1.56
315	22.5	14.7	0.68	22517	28156	0.80	41898	0.67	1.67
315	22.5	14.7	0.95	21860	31273	0.70	40360	0.77	1.77
315	22.5	14.7	1.05	22624	32342	0.70	44195	0.73	1.73

d) SKO2 Jacket

Direction	Wave (m)	Wave Period (Sec)	Current (cm/s)	Base Shear (KN)		RSR	Peak Load Base Shear (KN)	100 year/ Peak Load	System Redundancy
				Collapse Load (KN)	100 Year Load (KN)				
0	11.7	10.6	0.55	20870	8151	2.56	39946	0.20	1.20
0	11.7	10.6	0.95	22738	9592	2.37	47147	0.20	1.20
0	11.7	10.6	1.2	23332	10715	2.18	52713	0.20	1.20
0	12.3	11.0	0.55	22163	8649	2.56	42433	0.20	1.20
0	12.3	11.0	0.95	22213	10207	2.18	50222	0.20	1.20
0	12.3	11.0	1.2	24799	11382	2.18	53735	0.21	1.21
0	12.9	11.2	0.55	21859	9226	2.37	45317	0.20	1.20
0	12.9	11.2	0.95	23695	10880	2.18	53585	0.20	1.20
0	12.9	11.2	1.2	23978	12090	1.98	52459	0.23	1.23
0	13.5	11.4	0.55	21357	9818	2.18	48277	0.20	1.20
0	13.5	11.4	0.95	22893	11547	1.98	54639	0.21	1.21
0	13.5	11.4	1.2	25293	12747	1.98	52831	0.24	1.24
0	14.0	11.7	0.55	22438	10309	2.18	48726	0.21	1.21
0	14.0	11.7	0.95	23912	12057	1.98	52320	0.23	1.23
0	14.0	11.7	1.2	23898	13366	1.79	52813	0.25	1.25
0	14.6	11.9	0.55	23818	10937	2.18	53843	0.20	1.20
0	14.6	11.9	0.95	25309	12755	1.98	52868	0.24	1.24
0	14.6	11.9	1.2	25276	14132	1.79	55879	0.25	1.25
0	17.6	13.0	0.55	26607	14871	1.79	58779	0.25	1.25
0	17.6	13.0	0.95	27423	17215	1.59	54610	0.32	1.32
0	17.6	13.0	1.2	30159	18925	1.59	56352	0.34	1.34
0	20.5	14.0	0.55	26984	19332	1.40	61746	0.31	1.31
0	20.5	14.0	0.95	30873	22110	1.40	61480	0.36	1.36
0	20.5	14.0	1.2	28937	24148	1.20	62424	0.39	1.39
0	23.4	14.9	0.55	31391	26193	1.20	67509	0.39	1.39
0	23.4	14.9	0.95	35515	29630	1.20	64917	0.46	1.46
0	23.4	14.9	1.2	32009	32009	1.00	70071	0.46	1.46
45	11.7	10.6	0.55	32084	15121	2.12	45965	0.33	1.33
45	11.7	10.6	0.95	34157	17835	1.92	52289	0.34	1.34
45	11.7	10.6	1.2	36184	19968	1.81	60525	0.33	1.33
45	12.3	11.0	0.55	36436	16398	2.22	45871	0.36	1.36
45	12.3	11.0	0.95	36938	19299	1.91	56571	0.34	1.34
45	12.3	11.0	1.2	39032	21551	1.81	45925	0.47	1.47
45	12.9	11.2	0.55	37396	17650	2.12	52450	0.34	1.34
45	12.9	11.2	0.95	37594	20751	1.81	53971	0.38	1.38
45	12.9	11.2	1.2	39449	23081	1.71	53287	0.43	1.43
45	13.5	11.4	0.55	38192	18946	2.02	58146	0.33	1.33

45	13.5	11.4	0.95	40398	22298	1.81	53962	0.41	1.41
45	13.5	11.4	1.2	42051	24611	1.71	53933	0.46	1.46
45	14.0	11.7	0.55	40596	20147	2.01	49885	0.40	1.40
45	14.0	11.7	0.95	40066	23442	1.71	54434	0.43	1.43
45	14.0	11.7	1.2	41708	25955	1.61	41708	0.62	1.62
45	14.6	11.9	0.55	38760	21400	1.81	47517	0.45	1.45
45	14.6	11.9	0.95	42621	24948	1.71	55249	0.45	1.45
45	14.6	11.9	1.2	41590	27625	1.51	58323	0.47	1.47
45	17.6	13.0	0.55	42812	28440	1.51	57046	0.50	1.50
45	17.6	13.0	0.95	42849	32892	1.30	59452	0.55	1.55
45	17.6	13.0	1.2	43428	36138	1.20	54002	0.67	1.67
45	20.5	14.0	0.55	41791	37963	1.10	59644	0.64	1.64
45	20.5	14.0	0.95	43242	43242	1.00	56594	0.76	1.76
45	20.5	14.0	1.2	42612	47386	0.90	58709	0.81	1.81
45	23.4	14.9	0.55	43927	48845	0.90	63110	0.77	1.77
45	23.4	14.9	0.95	44129	55233	0.80	68883	0.80	1.80
45	23.4	14.9	1.2	47360	59274	0.80	77536	0.76	1.76
90	11.7	10.6	0.55	36066	7361	4.90	36066	0.20	1.20
90	11.7	10.6	0.95	38307	8849	4.33	43507	0.20	1.20
90	11.7	10.6	1.2	37348	9965	3.75	49075	0.20	1.20
90	12.3	11.0	0.55	36069	7986	4.52	39188	0.20	1.20
90	12.3	11.0	0.95	37536	9523	3.94	46870	0.20	1.20
90	12.3	11.0	1.2	38074	10710	3.55	53003	0.20	1.20
90	12.9	11.2	0.55	36875	8524	4.33	41878	0.20	1.20
90	12.9	11.2	0.95	38231	10197	3.75	50494	0.20	1.20
90	12.9	11.2	1.2	38385	11421	3.36	54231	0.21	1.21
90	13.5	11.4	0.55	37547	9082	4.13	44672	0.20	1.20
90	13.5	11.4	0.95	38650	10870	3.56	53646	0.20	1.20
90	13.5	11.4	1.2	38311	12100	3.17	50101	0.24	1.24
90	14.0	11.7	0.55	38190	9687	3.94	47692	0.20	1.20
90	14.0	11.7	0.95	38639	11495	3.36	52379	0.22	1.22
90	14.0	11.7	1.2	38107	12826	2.97	51792	0.25	1.25
90	14.6	11.9	0.55	38865	10365	3.75	47923	0.22	1.22
90	14.6	11.9	0.95	38673	12213	3.17	53851	0.23	1.23
90	14.6	11.9	1.2	37779	13612	2.78	56986	0.24	1.24
90	17.6	13.0	0.55	37866	14678	2.58	55245	0.27	1.27
90	17.6	13.0	0.95	40798	17108	2.38	61286	0.28	1.28
90	17.6	13.0	1.2	41282	18866	2.19	59999	0.31	1.31
90	20.5	14.0	0.55	38594	19390	1.99	61050	0.32	1.32
90	20.5	14.0	0.95	39926	22266	1.79	58064	0.38	1.38
90	20.5	14.0	1.2	38887	24374	1.60	63194	0.39	1.39
90	23.4	14.9	0.55	42861	26858	1.60	63998	0.42	1.42
90	23.4	14.9	0.95	42485	30402	1.40	66737	0.46	1.46
90	23.4	14.9	1.2	39388	32855	1.20	72155	0.46	1.46

135	11.7	10.6	0.55	30627	7875	3.89	38213	0.21	1.21
135	11.7	10.6	0.95	32366	9201	3.52	44844	0.21	1.21
135	11.7	10.6	1.2	34237	10275	3.33	50216	0.20	1.20
135	12.3	11.0	0.55	30936	8356	3.70	40618	0.21	1.21
135	12.3	11.0	0.95	32766	9843	3.33	48054	0.20	1.20
135	12.3	11.0	1.2	34451	10966	3.14	53675	0.20	1.20
135	12.9	11.2	0.55	31402	8933	3.52	43504	0.21	1.21
135	12.9	11.2	0.95	33019	10518	3.14	51435	0.20	1.20
135	12.9	11.2	1.2	34449	11677	2.95	57139	0.20	1.20
135	13.5	11.4	0.55	31726	9537	3.33	46525	0.20	1.20
135	13.5	11.4	0.95	33015	11199	2.95	54850	0.20	1.20
135	13.5	11.4	1.2	34050	12348	2.76	55638	0.22	1.22
135	14.0	11.7	0.55	33466	10048	3.33	49086	0.20	1.20
135	14.0	11.7	0.95	34589	11723	2.95	57462	0.20	1.20
135	14.0	11.7	1.2	35820	12980	2.76	58706	0.22	1.22
135	14.6	11.9	0.55	33463	10657	3.14	52142	0.20	1.20
135	14.6	11.9	0.95	34189	12398	2.76	58370	0.21	1.21
135	14.6	11.9	1.2	35201	13718	2.57	45942	0.30	1.30
135	17.6	13.0	0.55	37070	14437	2.57	54043	0.27	1.27
135	17.6	13.0	0.95	39652	16692	2.38	59389	0.28	1.28
135	17.6	13.0	1.2	39994	18338	2.18	61661	0.30	1.30
135	20.5	14.0	0.55	40962	18776	2.18	59587	0.32	1.32
135	20.5	14.0	0.95	42606	21448	1.99	72203	0.30	1.30
135	20.5	14.0	1.2	41912	23413	1.79	69680	0.34	1.34
135	23.4	14.9	0.55	40272	25279	1.59	65366	0.39	1.39
135	23.4	14.9	0.95	39837	28538	1.40	73755	0.39	1.39
135	23.4	14.9	1.2	43001	30798	1.40	79654	0.39	1.39
180	11.7	10.6	0.55	24913	7812	3.19	38904	0.20	1.20
180	11.7	10.6	0.95	27693	9257	2.99	46127	0.20	1.20
180	11.7	10.6	1.2	28999	10382	2.79	51752	0.20	1.20
180	12.3	11.0	0.55	26508	8310	3.19	41395	0.20	1.20
180	12.3	11.0	0.95	27475	9838	2.79	49029	0.20	1.20
180	12.3	11.0	1.2	28615	11030	2.59	54946	0.20	1.20
180	12.9	11.2	0.55	26651	8910	2.99	44390	0.20	1.20
180	12.9	11.2	0.95	27336	10538	2.59	52530	0.20	1.20
180	12.9	11.2	1.2	28185	11767	2.40	58660	0.20	1.20
180	13.5	11.4	0.55	26638	9539	2.79	45696	0.21	1.21
180	13.5	11.4	0.95	29276	11284	2.59	56254	0.20	1.20
180	13.5	11.4	1.2	29924	12491	2.40	50239	0.25	1.25
180	14.0	11.7	0.55	28056	10045	2.79	50067	0.20	1.20
180	14.0	11.7	0.95	28289	11810	2.40	58881	0.20	1.20
180	14.0	11.7	1.2	31454	13128	2.40	62816	0.21	1.21
180	14.6	11.9	0.55	27684	10672	2.59	53198	0.20	1.20
180	14.6	11.9	0.95	29965	12508	2.40	62290	0.20	1.20

180	14.6	11.9	1.2	30520	13894	2.20	58113	0.24	1.24
180	17.6	13.0	0.55	31971	14554	2.20	63836	0.23	1.23
180	17.6	13.0	0.95	33785	16912	2.00	64084	0.26	1.26
180	17.6	13.0	1.2	33502	18630	1.80	70569	0.26	1.26
180	20.5	14.0	0.55	34200	19017	1.80	68425	0.28	1.28
180	20.5	14.0	0.95	34879	21814	1.60	69598	0.31	1.31
180	20.5	14.0	1.2	38161	23865	1.60	76404	0.31	1.31
180	23.4	14.9	0.55	41590	26009	1.60	72775	0.36	1.36
180	23.4	14.9	0.95	41189	29432	1.40	82031	0.36	1.36
180	23.4	14.9	1.2	44509	31804	1.40	76218	0.42	1.42
225	11.7	10.6	0.55	30000	7716	3.89	37429	0.21	1.21
225	11.7	10.6	0.95	31819	9047	3.52	44083	0.21	1.21
225	11.7	10.6	1.2	31781	10130	3.14	50137	0.20	1.20
225	12.3	11.0	0.55	30383	8208	3.70	39889	0.21	1.21
225	12.3	11.0	0.95	32152	9660	3.33	47153	0.20	1.20
225	12.3	11.0	1.2	33896	10791	3.14	50318	0.21	1.21
225	12.9	11.2	0.55	30790	8761	3.51	42652	0.21	1.21
225	12.9	11.2	0.95	32347	10306	3.14	50432	0.20	1.20
225	12.9	11.2	1.2	33838	11471	2.95	51780	0.22	1.22
225	13.5	11.4	0.55	30903	9293	3.33	45316	0.21	1.21
225	13.5	11.4	0.95	32319	10965	2.95	49491	0.22	1.22
225	13.5	11.4	1.2	33418	12120	2.76	54103	0.22	1.22
225	14.0	11.7	0.55	30664	9780	3.14	47869	0.20	1.20
225	14.0	11.7	0.95	31595	11469	2.75	56275	0.20	1.20
225	14.0	11.7	1.2	35132	12732	2.76	57957	0.22	1.22
225	14.6	11.9	0.55	30588	10388	2.94	47514	0.22	1.22
225	14.6	11.9	0.95	33489	12145	2.76	52609	0.23	1.23
225	14.6	11.9	1.2	34580	13477	2.57	56813	0.24	1.24
225	17.6	13.0	0.55	33797	14251	2.37	56215	0.25	1.25
225	17.6	13.0	0.95	35798	16429	2.18	64356	0.26	1.26
225	17.6	13.0	1.2	35870	10879	3.30	64386	0.17	1.17
225	20.5	14.0	0.55	33058	18494	1.79	62548	0.30	1.30
225	20.5	14.0	0.95	33715	21180	1.59	65873	0.32	1.32
225	20.5	14.0	1.2	36872	23153	1.59	61930	0.37	1.37
225	23.4	14.9	0.55	34734	24892	1.40	62226	0.40	1.40
225	23.4	14.9	0.95	33742	28166	1.20	54856	0.51	1.51
225	23.4	14.9	1.2	36466	30436	1.20	72658	0.42	1.42
270	11.7	10.6	0.55	22518	7658	2.94	37440	0.20	1.20
270	11.7	10.6	0.95	23324	9111	2.56	44355	0.21	1.21
270	11.7	10.6	1.2	24272	10246	2.37	42289	0.24	1.24
270	12.3	11.0	0.55	22460	8168	2.75	39892	0.20	1.20
270	12.3	11.0	0.95	24962	9742	2.56	42226	0.23	1.23
270	12.3	11.0	1.2	25909	10928	2.37	45344	0.24	1.24
270	12.9	11.2	0.55	24020	8725	2.75	39595	0.22	1.22

270	12.9	11.2	0.95	24633	10397	2.37	43073	0.24	1.24
270	12.9	11.2	1.2	25285	11618	2.18	47211	0.25	1.25
270	13.5	11.4	0.55	23851	9314	2.56	40400	0.23	1.23
270	13.5	11.4	0.95	24066	11063	2.18	45501	0.24	1.24
270	13.5	11.4	1.2	26721	12270	2.18	45206	0.27	1.27
270	14.0	11.7	0.55	23259	9824	2.37	40012	0.25	1.25
270	14.0	11.7	0.95	25198	11578	2.18	44840	0.26	1.26
270	14.0	11.7	1.2	25614	12921	1.98	45902	0.28	1.28
270	14.6	11.9	0.55	24758	10449	2.37	41217	0.25	1.25
270	14.6	11.9	0.95	26841	12325	2.18	45968	0.27	1.27
270	14.6	11.9	1.2	27245	13736	1.98	49006	0.28	1.28
270	17.6	13.0	0.55	26632	14897	1.79	47368	0.31	1.31
270	17.6	13.0	0.95	27482	17262	1.59	47474	0.36	1.36
270	17.6	13.0	1.2	26562	19037	1.40	52972	0.36	1.36
270	20.5	14.0	0.55	27328	19585	1.40	50440	0.39	1.39
270	20.5	14.0	0.95	26898	22453	1.20	53694	0.42	1.42
270	20.5	14.0	1.2	29422	24556	1.20	58264	0.42	1.42
270	23.4	14.9	0.55	26915	26915	1.00	53635	0.50	1.50
270	23.4	14.9	0.95	30477	30477	1.00	58929	0.52	1.52
270	23.4	14.9	1.2	32941	32941	1.00	59242	0.56	1.56
315	11.7	10.6	0.55	22300	7625	2.92	36977	0.21	1.21
315	11.7	10.6	0.95	24565	8958	2.74	43643	0.21	1.21
315	11.7	10.6	1.2	25635	10037	2.55	49052	0.20	1.20
315	12.3	11.0	0.55	23738	8104	2.93	39374	0.21	1.21
315	12.3	11.0	0.95	24379	9553	2.55	46624	0.20	1.20
315	12.3	11.0	1.2	27303	10678	2.56	52250	0.20	1.20
315	12.9	11.2	0.55	23671	8639	2.74	42048	0.21	1.21
315	12.9	11.2	0.95	26028	10188	2.55	49812	0.20	1.20
315	12.9	11.2	1.2	26824	11344	2.36	52746	0.22	1.22
315	13.5	11.4	0.55	23411	9181	2.55	44767	0.21	1.21
315	13.5	11.4	0.95	25606	10837	2.36	50704	0.21	1.21
315	13.5	11.4	1.2	28357	11983	2.37	47072	0.25	1.25
315	14.0	11.7	0.55	24684	9671	2.55	47234	0.20	1.20
315	14.0	11.7	0.95	26820	11343	2.36	53486	0.21	1.21
315	14.0	11.7	1.2	27369	12597	2.17	54593	0.23	1.23
315	14.6	11.9	0.55	26258	10276	2.56	50257	0.20	1.20
315	14.6	11.9	0.95	26091	12016	2.17	54122	0.22	1.22
315	14.6	11.9	1.2	28994	13336	2.17	58380	0.23	1.23
315	17.6	13.0	0.55	27920	14104	1.98	52910	0.27	1.27
315	17.6	13.0	0.95	29209	16355	1.79	58718	0.28	1.28
315	17.6	13.0	1.2	32167	17998	1.79	60102	0.30	1.30
315	20.5	14.0	0.55	32965	18442	1.79	54704	0.34	1.34
315	20.5	14.0	0.95	33604	21110	1.59	62072	0.34	1.34
315	20.5	14.0	1.2	32186	20372	1.58	62696	0.32	1.32

315	23.4	14.9	0.55	34588	24788	1.40	63404	0.39	1.39
315	23.4	14.9	0.95	33632	28075	1.20	61557	0.46	1.46
315	23.4	14.9	1.2	36365	30352	1.20	66438	0.46	1.46

e) SKO2a Jacket

Direction	Wave (m)	Wave Period (Sec)	Current (cm/s)	Base Shear (KN)		RSR	Peak Load (KN)	100 year/ Peak load	System Redundancy
				Collapse Load (KN)	100 Year Load (KN)				
0	11.7	10.6	0.55	20857	8140	2.56	39790	0.20	1.20
0	11.7	10.6	0.95	22723	9597	2.37	38571	0.25	1.25
0	11.7	10.6	1.2	23318	10694	2.18	38740	0.28	1.28
0	12.3	11.0	0.55	20808	8802	2.36	40736	0.22	1.22
0	12.3	11.0	0.95	22477	10325	2.18	40274	0.26	1.26
0	12.3	11.0	1.2	22601	11382	1.99	42670	0.27	1.27
0	12.9	11.2	0.55	20543	9466	2.17	40684	0.23	1.23
0	12.9	11.2	0.95	21791	11018	1.98	31697	0.35	1.35
0	12.9	11.2	1.2	24192	12218	1.98	36192	0.34	1.34
0	13.5	11.4	0.55	19989	10097	1.98	32829	0.31	1.31
0	13.5	11.4	0.95	20995	11771	1.78	41668	0.28	1.28
0	13.5	11.4	1.2	23071	12925	1.78	40418	0.32	1.32
0	14.0	11.7	0.55	21174	10709	1.98	41265	0.26	1.26
0	14.0	11.7	0.95	22034	12528	1.76	32034	0.39	1.39
0	14.0	11.7	1.2	24290	13602	1.79	42784	0.32	1.32
0	14.6	11.9	0.55	20285	11378	1.78	40183	0.28	1.28
0	14.6	11.9	0.95	20801	13091	1.59	40846	0.32	1.32
0	14.6	11.9	1.2	22819	14351	1.59	42323	0.34	1.34
0	17.6	13.0	0.55	22955	16459	1.39	39115	0.42	1.42
0	17.6	13.0	0.95	22326	18631	1.20	35600	0.52	1.52
0	17.6	13.0	1.2	24119	20118	1.20	39991	0.50	1.50
0	20.5	14.0	0.55	23633	19711	1.20	39096	0.50	1.50
0	20.5	14.0	0.95	26501	22126	1.20	39536	0.56	1.56
0	20.5	14.0	1.2	23785	23785	1.00	39000	0.61	1.61
0	23.4	14.9	0.55	28195	28195	1.00	39275	0.72	1.72
0	23.4	14.9	0.95	30687	30687	1.00	36750	0.84	1.84
0	23.4	14.9	1.2	26238	32726	0.80	39154	0.84	1.84
45	11.7	10.6	0.55	31418	8001	3.93	31878	0.25	1.25
45	11.7	10.6	0.95	31934	9360	3.41	34302	0.27	1.27
45	11.7	10.6	1.2	33130	10382	3.19	38053	0.27	1.27
45	12.3	11.0	0.55	31506	8640	3.65	31506	0.27	1.27

45	12.3	11.0	0.95	32048	10070	3.18	36801	0.27	1.27
45	12.3	11.0	1.2	35666	11208	3.18	38310	0.29	1.29
45	12.9	11.2	0.55	29976	9274	3.23	36037	0.26	1.26
45	12.9	11.2	0.95	31781	10751	2.96	36889	0.29	1.29
45	12.9	11.2	1.2	32353	11971	2.70	37827	0.32	1.32
45	13.5	11.4	0.55	31471	9900	3.18	36189	0.27	1.27
45	13.5	11.4	0.95	34084	11580	2.94	36825	0.31	1.31
45	13.5	11.4	1.2	34444	12732	2.71	37517	0.34	1.34
45	14.0	11.7	0.55	32741	11059	2.96	32741	0.34	1.34
45	14.0	11.7	0.95	32844	12150	2.70	37377	0.33	1.33
45	14.0	11.7	1.2	33022	13401	2.46	37991	0.35	1.35
45	14.6	11.9	0.55	28326	10453	2.71	29285	0.36	1.36
45	14.6	11.9	0.95	31766	12900	2.46	37885	0.34	1.34
45	14.6	11.9	1.2	31628	14235	2.22	38252	0.37	1.37
45	17.6	13.0	0.55	32535	14640	2.22	36098	0.41	1.41
45	17.6	13.0	0.95	31568	18165	1.74	32532	0.56	1.56
45	17.6	13.0	1.2	34083	19648	1.73	34083	0.58	1.58
45	20.5	14.0	0.55	34089	19679	1.73	34089	0.58	1.58
45	20.5	14.0	0.95	32772	21962	1.49	32772	0.67	1.67
45	20.5	14.0	1.2	35012	23468	1.49	35012	0.67	1.67
45	23.4	14.9	0.55	32654	26432	1.24	32654	0.81	1.81
45	23.4	14.9	0.95	35643	28633	1.24	35643	0.80	1.80
45	23.4	14.9	1.2	30500	30500	1.00	30500	1.00	2.00
90	11.7	10.6	0.55	28777	7296	3.94	35903	0.20	1.20
90	11.7	10.6	0.95	29536	8745	3.38	36432	0.24	1.24
90	11.7	10.6	1.2	29422	9869	2.98	29422	0.34	1.34
90	12.3	11.0	0.55	29829	7929	3.76	36031	0.22	1.22
90	12.3	11.0	0.95	30113	9472	3.18	39395	0.24	1.24
90	12.3	11.0	1.2	29399	10537	2.79	29399	0.36	1.36
90	12.9	11.2	0.55	28803	8543	3.37	35489	0.24	1.24
90	12.9	11.2	0.95	30116	10100	2.98	40045	0.25	1.25
90	12.9	11.2	1.2	29284	11252	2.60	38219	0.29	1.29
90	13.5	11.4	0.55	29058	9140	3.18	38078	0.24	1.24
90	13.5	11.4	0.95	30135	10790	2.79	40759	0.26	1.26
90	13.5	11.4	1.2	28649	12038	2.38	38089	0.32	1.32
90	14.0	11.7	0.55	28941	9712	2.98	33352	0.29	1.29
90	14.0	11.7	0.95	29396	11304	2.60	33873	0.33	1.33
90	14.0	11.7	1.2	30249	12562	2.41	40159	0.31	1.31
90	14.6	11.9	0.55	30702	10289	2.98	30702	0.34	1.34
90	14.6	11.9	0.95	28977	12172	2.38	38485	0.32	1.32
90	14.6	11.9	1.2	29337	13426	2.19	39228	0.34	1.34
90	17.6	13.0	0.55	31384	15771	1.99	37948	0.42	1.42
90	17.6	13.0	0.95	28808	18069	1.59	35941	0.50	1.50
90	17.6	13.0	1.2	31269	19597	1.60	35799	0.55	1.55

90	20.5	14.0	0.55	30598	19174	1.60	34353	0.56	1.56
90	20.5	14.0	0.95	30243	21629	1.40	34496	0.63	1.63
90	20.5	14.0	1.2	32697	23420	1.40	37337	0.63	1.63
90	23.4	14.9	0.55	33226	27725	1.20	38814	0.71	1.71
90	23.4	14.9	0.95	30327	30327	1.00	36199	0.84	1.84
90	23.4	14.9	1.2	32429	32429	1.00	32429	1.00	2.00
135	11.7	10.6	0.55	30452	7778	3.92	30452	0.26	1.26
135	11.7	10.6	0.95	32196	9045	3.56	35665	0.25	1.25
135	11.7	10.6	1.2	32069	10109	3.17	35954	0.28	1.28
135	12.3	11.0	0.55	31056	8313	3.74	32635	0.25	1.25
135	12.3	11.0	0.95	32815	9754	3.36	32815	0.30	1.30
135	12.3	11.0	1.2	32041	10787	2.97	36159	0.30	1.30
135	12.9	11.2	0.55	29955	8924	3.36	35147	0.25	1.25
135	12.9	11.2	0.95	32928	10462	3.15	32928	0.32	1.32
135	12.9	11.2	1.2	31973	11577	2.76	36326	0.32	1.32
135	13.5	11.4	0.55	30167	9539	3.16	33681	0.28	1.28
135	13.5	11.4	0.95	30884	11192	2.76	35233	0.32	1.32
135	13.5	11.4	1.2	31454	12262	2.57	36132	0.34	1.34
135	14.0	11.7	0.55	30003	10168	2.95	30003	0.34	1.34
135	14.0	11.7	0.95	32424	11743	2.76	33689	0.35	1.35
135	14.0	11.7	1.2	33258	12947	2.57	35767	0.36	1.36
135	14.6	11.9	0.55	29792	10801	2.76	36698	0.29	1.29
135	14.6	11.9	0.95	31929	12447	2.57	36568	0.34	1.34
135	14.6	11.9	1.2	32440	13658	2.38	35053	0.39	1.39
135	17.6	13.0	0.55	30814	15531	1.98	33719	0.46	1.46
135	17.6	13.0	0.95	31538	17625	1.79	34688	0.51	1.51
135	17.6	13.0	1.2	34114	19051	1.79	34114	0.56	1.56
135	20.5	14.0	0.55	29725	18656	1.59	33279	0.56	1.56
135	20.5	14.0	0.95	33390	20978	1.59	33390	0.63	1.63
135	20.5	14.0	1.2	31468	22560	1.39	35750	0.63	1.63
135	23.4	14.9	0.55	31741	26539	1.20	31741	0.84	1.84
135	23.4	14.9	0.95	31710	28875	1.10	33052	0.87	1.87
135	23.4	14.9	1.2	32352	30826	1.05	33863	0.91	1.91
180	11.7	10.6	0.55	24769	7717	3.21	38621	0.20	1.20
180	11.7	10.6	0.95	25708	9160	2.81	38511	0.24	1.24
180	11.7	10.6	1.2	26789	10251	2.61	37207	0.28	1.28
180	12.3	11.0	0.55	25094	8348	3.01	38418	0.22	1.22
180	12.3	11.0	0.95	25675	9862	2.60	41158	0.24	1.24
180	12.3	11.0	1.2	26309	10949	2.40	41597	0.26	1.26
180	12.9	11.2	0.55	25164	8976	2.80	37634	0.24	1.24
180	12.9	11.2	0.95	25358	10554	2.40	40077	0.26	1.26
180	12.9	11.2	1.2	28273	11767	2.40	39991	0.29	1.29
180	13.5	11.4	0.55	25036	9602	2.61	38450	0.25	1.25
180	13.5	11.4	0.95	27170	11308	2.40	38435	0.29	1.29

180	13.5	11.4	1.2	27487	12481	2.20	39917	0.31	1.31
180	14.0	11.7	0.55	24730	10293	2.40	39088	0.26	1.26
180	14.0	11.7	0.95	26307	11945	2.20	40558	0.29	1.29
180	14.0	11.7	1.2	26437	13205	2.00	36437	0.36	1.36
180	14.6	11.9	0.55	24133	10957	2.20	39414	0.28	1.28
180	14.6	11.9	0.95	25392	12683	2.00	40570	0.31	1.31
180	14.6	11.9	1.2	27927	13950	2.00	39059	0.36	1.36
180	17.6	13.0	0.55	25447	15888	1.60	38066	0.42	1.42
180	17.6	13.0	0.95	28792	17973	1.60	39517	0.45	1.45
180	17.6	13.0	1.2	27305	19500	1.40	38938	0.50	1.50
180	20.5	14.0	0.55	26895	19207	1.40	38331	0.50	1.50
180	20.5	14.0	0.95	30251	21603	1.40	38833	0.56	1.56
180	20.5	14.0	1.2	27913	23249	1.20	37181	0.63	1.63
180	23.4	14.9	0.55	33227	27692	1.20	33227	0.83	1.83
180	23.4	14.9	0.95	30158	30158	1.00	36161	0.83	1.83
180	23.4	14.9	1.2	32242	32242	1.00	38571	0.84	1.84
225	11.7	10.6	0.55	22393	7632	2.93	29516	0.26	1.26
225	11.7	10.6	0.95	22013	8957	2.46	30561	0.29	1.29
225	11.7	10.6	1.2	24722	10037	2.46	29586	0.34	1.34
225	12.3	11.0	0.55	22184	8220	2.70	28115	0.29	1.29
225	12.3	11.0	0.95	23745	9645	2.46	26085	0.37	1.37
225	12.3	11.0	1.2	23720	10674	2.22	28888	0.37	1.37
225	12.9	11.2	0.55	21714	8829	2.46	28098	0.31	1.31
225	12.9	11.2	0.95	22795	10263	2.22	30072	0.34	1.34
225	12.9	11.2	1.2	25377	11416	2.22	30799	0.37	1.37
225	13.5	11.4	0.55	23210	9431	2.46	30021	0.31	1.31
225	13.5	11.4	0.95	24389	10977	2.22	29715	0.37	1.37
225	13.5	11.4	1.2	23931	12083	1.98	29805	0.41	1.41
225	14.0	11.7	0.55	24586	9984	2.46	29258	0.34	1.34
225	14.0	11.7	0.95	22800	11516	1.98	28398	0.41	1.41
225	14.0	11.7	1.2	25202	12719	1.98	28302	0.45	1.45
225	14.6	11.9	0.55	23540	10598	2.22	28680	0.37	1.37
225	14.6	11.9	0.95	24158	12199	1.98	30071	0.41	1.41
225	14.6	11.9	1.2	23315	13414	1.74	29837	0.45	1.45
225	17.6	13.0	0.55	22903	15362	1.49	26641	0.58	1.58
225	17.6	13.0	0.95	26052	17470	1.49	31700	0.55	1.55
225	17.6	13.0	1.2	23559	18906	1.25	28191	0.67	1.67
225	20.5	14.0	0.55	23093	18535	1.25	27633	0.67	1.67
225	20.5	14.0	0.95	25837	20743	1.25	25837	0.80	1.80
225	20.5	14.0	1.2	27812	22333	1.25	27812	0.80	1.80
225	23.4	14.9	0.55	19408	25758	0.75	25758	1.00	2.00
225	23.4	14.9	0.95	21172	28099	0.75	28099	1.00	2.00
225	23.4	14.9	1.2	22636	29754	0.76	29754	1.00	2.00
270	11.7	10.6	0.55	24117	7616	3.17	30796	0.25	1.25

270	11.7	10.6	0.95	23221	9066	2.56	36697	0.25	1.25
270	11.7	10.6	1.2	22173	10198	2.17	32130	0.32	1.32
270	12.3	11.0	0.55	22562	8197	2.75	32021	0.26	1.26
270	12.3	11.0	0.95	23094	9750	2.37	32593	0.30	1.30
270	12.3	11.0	1.2	23565	10831	2.18	32035	0.34	1.34
270	12.9	11.2	0.55	22661	8849	2.56	32956	0.27	1.27
270	12.9	11.2	0.95	22523	10360	2.17	32619	0.32	1.32
270	12.9	11.2	1.2	22914	11570	1.98	31982	0.36	1.36
270	13.5	11.4	0.55	22337	9433	2.37	31533	0.30	1.30
270	13.5	11.4	0.95	24091	11070	2.18	32744	0.34	1.34
270	13.5	11.4	1.2	24240	12230	1.98	33878	0.36	1.36
270	14.0	11.7	0.55	21625	9949	2.17	31322	0.32	1.32
270	14.0	11.7	0.95	22999	11608	1.98	32074	0.36	1.36
270	14.0	11.7	1.2	22993	12875	1.79	32993	0.39	1.39
270	14.6	11.9	0.55	22990	10568	2.18	31236	0.34	1.34
270	14.6	11.9	0.95	24379	12299	1.98	32540	0.38	1.38
270	14.6	11.9	1.2	24262	13578	1.79	38070	0.36	1.36
270	17.6	13.0	0.55	22304	15995	1.39	31661	0.51	1.51
270	17.6	13.0	0.95	25550	18320	1.39	37172	0.49	1.49
270	17.6	13.0	1.2	23800	19873	1.20	31637	0.63	1.63
270	20.5	14.0	0.55	23404	19541	1.20	31094	0.63	1.63
270	20.5	14.0	0.95	22007	22007	1.00	30708	0.72	1.72
270	20.5	14.0	1.2	23717	23717	1.00	33111	0.72	1.72
270	23.4	14.9	0.55	22278	27778	0.80	32778	0.85	1.85
270	23.4	14.9	0.95	24322	30323	0.80	30323	1.00	2.00
270	23.4	14.9	1.2	25963	32398	0.80	32398	1.00	2.00
315	11.7	10.6	0.55	22236	7624	2.92	30951	0.25	1.25
315	11.7	10.6	0.95	22768	8954	2.54	31240	0.29	1.29
315	11.7	10.6	1.2	25563	10028	2.55	31282	0.32	1.32
315	12.3	11.0	0.55	22385	8199	2.73	30188	0.27	1.27
315	12.3	11.0	0.95	22650	9623	2.35	24542	0.39	1.39
315	12.3	11.0	1.2	25109	10647	2.36	31219	0.34	1.34
315	12.9	11.2	0.55	22359	8795	2.54	30695	0.29	1.29
315	12.9	11.2	0.95	24107	10232	2.36	26107	0.39	1.39
315	12.9	11.2	1.2	24652	11378	2.17	28366	0.40	1.40
315	13.5	11.4	0.55	22064	9379	2.35	30897	0.30	1.30
315	13.5	11.4	0.95	23684	10938	2.17	31987	0.34	1.34
315	13.5	11.4	1.2	23762	12039	1.97	33074	0.36	1.36
315	14.0	11.7	0.55	21413	9907	2.16	30937	0.32	1.32
315	14.0	11.7	0.95	22637	11478	1.97	31509	0.36	1.36
315	14.0	11.7	1.2	25039	12678	1.97	27486	0.46	1.46
315	14.6	11.9	0.55	22778	10527	2.16	30886	0.34	1.34
315	14.6	11.9	0.95	24019	12168	1.97	31002	0.39	1.39
315	14.6	11.9	1.2	23828	13376	1.78	31614	0.42	1.42

315	17.6	13.0	0.55	24518	15435	1.59	30514	0.51	1.51
315	17.6	13.0	0.95	24370	17502	1.39	31187	0.56	1.56
315	17.6	13.0	1.2	26307	18887	1.39	29976	0.63	1.63
315	20.5	14.0	0.55	25828	18544	1.39	29442	0.63	1.63
315	20.5	14.0	0.95	24853	20763	1.20	28922	0.72	1.72
315	20.5	14.0	1.2	26770	22365	1.20	31136	0.72	1.72
315	23.4	14.9	0.55	25868	25868	1.00	27709	0.93	1.93
315	23.4	14.9	0.95	28126	28126	1.00	28126	1.00	2.00
315	23.4	14.9	1.2	30072	30072	1.00	30072	1.00	2.00